CUK-H03722-42-P024747

42

VOLUME 106 — OCTOBER 1997
Number 10, Part 1 (Issued in 2 Parts)

— Founded in 1892 —

ANNALS

OF OTOLOGY, RHINOLOGY & LARYNGOLOGY

Official Organ of the
AMERICAN LARYNGOLOGICAL ASSOCIATION
AMERICAN BRONCHO-ESOPHAGOLOGICAL ASSOCIATIO

MENIERE'S SYNDROME AND MIGRAINE: INCIDENCE IN ONE FAMILY

QT INTERVAL CHANGES FOLLOWING NECK DISSECTION. A STRATIFIED PROSPECTIVE STUDY

EFFECT OF IMMUNOTHERAPY ON SERUM LEVELS OF EOSINOPHIL CATIONIC PROTEIN IN PERENNIAL ALLERGIC RHINITIS

PERILYMPHATIC FISTULA: A WASHINGTON, DC, EXPERIENCE

ANNALS
PUBLISHING CO.
ST. LOUIS

P24747 -1

LEVAQUIN

Overpowers

key gram-positive, gram-negative, and atypical pathogens

Proven Effective in Mild-to-Severe Community-Acquired Pneumonia, Acute Maxillary Sinusitis, and Acute Bacterial Exacerbations of Chronic Bronchitis*

In an In Vitro Study, 100% of *Streptococcus pneumoniae* Isolates Were Susceptible to LEVAQUIN

	% Susceptible
S pneumoniae (n=209)	**100%**

- The first once-a-day anti-infective indicated for all three common atypical pathogens *Mycoplasma pneumoniae, Chlamydia pneumoniae,* and *Legionella pneumophila* in community-acquired pneumonia
- 96% eradication rate of gram-negative and gram-positive pathogens in patients with mild-to-severe community-acquired pneumonia

The safety and efficacy of levofloxacin in children, adolescents (under 18), pregnant women, and nursing mothers have not been established. Levofloxacin is contraindicated in persons with a history of hypersensitivity to levofloxacin, quinolone antimicrobial agents, or any other components of this product. Serious and occasionally fatal hypersensitivity and/or anaphylactic reactions have been reported in patients receiving therapy with quinolones. These reactions often occur following the first dose. The drug should be discontinued at the first appearance of a skin rash or any other sign of hypersensitivity.

Antacids containing magnesium or aluminum, as well as sucralfate, metal cations such as iron, and multivitamin preparations with zinc should be taken at least 2 hours before or 2 hours after levofloxacin administration.

For information on Warnings, Precautions, and additional Adverse Reactions that may occur, regardless of drug relationship, please see full Prescribing Information.

Please see brief summary of Prescribing Information at the end of this advertisement.

ANNALS OF OTOLOGY, RHINOLOGY & LARYNGOLOGY

VOLUME 106 OCTOBER 1997 NUMBER 10

CONTENTS

PART 1

ANNALS CLASSIC AND A PERSPECTIVE

A Syndrome of Ear and Sinus Symptoms Dependent Upon Disturbed Function of the Temporomandibular Joint
James B. Costen, MD 805

Jaws Revisited: Costen's Syndrome
Ludwig A. Michael, MD 820

OTOLOGY AND AUDITORY SYSTEM

Meniere's Syndrome and Migraine: Incidence in One Family
Carlos A. Oliveira, MD, PhD; Roberta L. Bezerra, MD; Mercedes F. Araújo, MD; Vanessa F. Almeida; Christiane I. Messias, MD 823

Perilymphatic Fistula: A Washington, DC, Experience
Dennis C. Fitzgerald, MD; Pamela Getson, PhD; Cynthia O. Brasseux, MA 830

Vestibular and Optokinetic Function in the Normal Guinea Pig
James C. Andrews, MD; June Li, PhD; Sumiko Koyama, MD; Larry F. Hoffman, PhD 838

RHINOLOGY AND UPPER DIGESTIVE TRACT

Effect of Immunotherapy on Serum Levels of Eosinophil Cationic Protein in Perennial Allergic Rhinitis
Yoshihiro Ohashi, MD; Yoshiaki Nakai, MD; Yasushi Kakinoki, MD; Yoshiharu Ohno, MD; Hirokazu Sakamoto, MD; Akifumi Kato, MD; Ayaki Tanaka, MD 848

Incidence of Primary Ciliary Dyskinesia in Children With Recurrent Respiratory Diseases
Catherine Chapelin; André Coste, MD; Philippe Reinert, MD; Michel Boucherat, MD; Marie-Claude Millepied; Françoise Poron; Estelle Escudier, MD, PhD 854

In Vivo Measurement of Human Nasal Mucociliary Motility Using a Laser Light Scattering Instrument
Yoav Paltieli, MD, DSc; Milo Fradis, MD; Jacob Ben-David, MD; Ludwig Podoshin, MD; Hala Shiti, BSc; Zvi Kam, DSc 859

LARYNGOLOGY AND HEAD AND NECK

Effects of Anesthetic Technique on the Hemodynamic Response to Microlaryngeal Surgery
Angeles Ayuso, MD; Mercedes Luis, MD; Xavier Sala, MD; Jesús Sánchez, MD; José Traserra, MD 863

QT Interval Changes Following Neck Dissection. A Stratified Prospective Study
Christopher H. Rassekh, MD; Kevin C. Dellsperger, MD, PhD; James A. Hokanson, PhD; Carl H. Snyderman, MD; Jonas T. Johnson, MD; Bruce A. Bollen, MD; Henry T. Hoffman, MD ... 869

IMAGING CASE STUDIES OF THE MONTH

Intracranial Complications of Otitis Media
Daniel Saah, MD; J. Elidan, MD; M. Gomori, MD 873

Calcified Mucor Fungus Ball of Sphenoid Sinus: An Unusual Presentation of Sinoorbital Mucormycosis
Levent Saydam, MD; Gökhan Erpek, MD; Ahmet Kizilay, MD 875

CLINICOPATHOLOGICAL CONSULTATION

Syndrome of Inappropriate Antidiuretic Hormone Secretion Associated With Head and Neck Cancers: Review of the Literature
Alfio Ferlito, MD; Alessandra Rinaldo, MD; Kenneth O. Devaney, MD 878

MISCELLANEOUS

Letters to the Editor 884

Book Reviews 886

Information for Subscribers 3a

Index to Advertisers 14a

PART 2

Measurement of Airway Patency. A Manual for Users of the Toronto Systems and Others Interested in Nasal Patency Measurement
Philip Cole, MD, FRCSC; Renato Roithmann, MD; Yehudah Roth, MD; and by invitation, J. S. Chapnik, MD, FRCSC .... Supplement 171

PEDIATRIC OTOLARYNGOLOGY FELLOWSHIP

July 1, 1999

Children's Hospital and Medical Center
University of Washington
Seattle, Washington

This fellowship emphasizes clinical pediatric otolaryngology with exposure to a full spectrum of pathophysiology, including airway reconstruction, bronchoesophagology, chronic ear disease, sinus surgery, velopharyngeal insufficiency surgery, and microtia repair.

Basic or clinical research utilizing the resources at the University of Washington and Children's Hospital is emphasized during the latter portion of the fellowship.

Direct inquiries to:

Scott C. Manning, MD
Division of Pediatric Otolaryngology
Children's Hospital and Medical Center
4800 Sand Point Way NE
PO Box 5371, CH-62
Seattle, WA 98105-0371
(206) 526-2100 ext 5264
fax: (206) 527-3955

A128

FACULTY POSITION PEDIATRIC OTOLARYNGOLOGY

Children's National Medical Center
George Washington University

The Department of Otolaryngology at Children's National Medical Center is seeking candidates for a faculty position at the Assistant Professor level. Candidates should be Board Certified and Fellowship trained in Pediatric Otolaryngology.

Children's National Medical Center is an equal opportunity employer. Women and minorities are encouraged to apply.

If interested send Curriculum Vitae to:

George H. Zalzal, M.D.
Professor & Chairman
Department of Otolaryngology
Children's National Medical Center
111 Michigan Avenue, NW
Washington, DC 20010

Children's
National Medical Center.

FELLOWSHIP IN PEDIATRIC OTOLARYNGOLOGY

CHILDREN'S HOSPITAL OF PITTSBURGH
UNIVERSITY OF PITTSBURGH
SCHOOL OF MEDICINE

JULY 1, 1999 — JUNE 30, 2001

A two- or three-year fellowship program; the first half is devoted to clinical activities, and the second half is devoted to research activities. The fellowship is under the direction of Drs Margaretha L. Casselbrant and Charles D. Bluestone.

Clinical Part — Intensive experience in all phases of ear, nose, and throat diseases in children, including otology, rhinology, bronchoesophagology, head and neck reconstructive surgery, and training in cleft palate–related problems.

Research Part — National Institutes of Health (NIDCD)–sponsored fellowship to train fellows to develop skills in clinical and laboratory research which will be used in an academic career. Requirements: US citizen or permanent resident.

Direct inquiries to:

Margaretha L. Casselbrant, MD, PhD
Department of Pediatric Otolaryngology
Children's Hospital of Pittsburgh
3705 Fifth Avenue
Pittsburgh, PA 15213
(412) 692-8577

An Equal Opportunity/Affirmative Action Employer.
Qualified minority and female applicants are encouraged to apply.

A45

MANHATTAN EYE, EAR & THROAT HOSPITAL
DEPARTMENT OF
OTOLARYNGOLOGY
HEAD & NECK SURGERY

CME COURSE FALL 1997

TEMPORAL BONE SURGICAL DISSECTION
November 5-7, 1997

Course Director: Simon C. Parisier, M.D.

Featured Guests: Richard Bellucci, M.D., Richard Dynia, M.D., David Edelstein, M.D., Milton Ingerman, M.D., Charles Kimmelman, M.D., Mark Levenson, M.D., Samuel Selesnick, M.D., Eric Smouha, M.D.

Description: Contemporary otologic surgery is based on an understanding of the surgical anatomy of the temporal bone. The goal of this intensive three day course is to enhance the surgeon's ability to perform the exacting procedures required for the treatment of common otologic disorders. Emphasis is on surgical dissection of the cadaveric human temporal bones with the presentation of selected clinical subjects.

Course Objectives: 1) have an in-depth knowledge of the anatomy of the human temporal bone demonstrated through dissection under the observation of experienced faculty, 2) gain skill in the use of the state-of-the-art equipment used in common otologic procedures, including the Zeiss microscope, Xomed high speed drill and suction irrigation, 3) understand the pathophysiology and surgical treatment of common otologic disorders, including vertigo, otosclerosis, cholesteatoma and conductive hearing loss.

FOR FURTHER INFORMATION, CONTACT:
Kathleen Thompson, Administrator
Department of Otolaryngology
Manhattan Eye, Ear & Throat Hospital
210 East 64th Street, New York, NY 10021
Tel: (212) 838-9200, ext 2432 • Fax (212) 838-6239
Manhattan Eye, Ear & Throat Hospital is an Equal Opportunity Employer

ANNALS OF OTOLOGY, RHINOLOGY & LARYNGOLOGY

— Founded in 1892 —

Editor

BRIAN F. McCABE, MD
Iowa City, Iowa

Associate Editors

CHARLES D. BLUESTONE, MD
Pittsburgh, Pa

GEORGE A. GATES, MD
Seattle, Wash

LAWRENCE W. DeSANTO, MD
Scottsdale, Ariz

LEE A. HARKER, MD
Omaha, Neb

Board of Editors

JOHN G. BATSAKIS, MD	Kalkaska, Mich
POUL BRETLAU, MD, DMSc	Copenhagen, Denmark
RICHARD A. BUCKINGHAM, MD	Park Ridge, Ill
JACK D. CLEMIS, MD	Chicago, Ill
CHARLES W. CUMMINGS, MD	Baltimore, Md
PATRICK J. DOYLE, MD	Vancouver, Canada
ALFIO FERLITO, MD	Padua, Italy
UGO FISCH, MD	Zurich, Switzerland
BRUCE GANTZ, MD	Iowa City, Iowa
JEFFREY P. HARRIS, MD, PhD	San Diego, Calif
GERALD B. HEALY, MD	Boston, Mass
WILLIAM F. HOUSE, MD	Los Angeles, Calif
STEVEN K. JUHN, MD	Minneapolis, Minn
TIMOTHY T. K. JUNG, MD, PhD	Loma Linda, Calif
JEROME O. KLEIN, MD	Boston, Mass
FRANK E. LUCENTE, MD	New York, NY
JOSEF MILLER, PhD	Ann Arbor, Mich
WILLIAM W. MONTGOMERY, MD	Boston, Mass
EUGENE N. MYERS, MD	Pittsburgh, Pa
YASUYA NOMURA, MD	Tokyo, Japan
LORNE S. PARNES, MD	London, Canada
FRANK N. RITTER, MD	Ann Arbor, Mich
ROBERT J. RUBEN, MD	Bronx, NY
JAI H. RYU, PhD	Winston-Salem, NC
JACOB SADÉ, MD	Tel Aviv, Israel
ISAMU SANDO, MD	Pittsburgh, Pa
CLARENCE T. SASAKI, MD	New Haven, Conn
RICHARD J. H. SMITH, MD	Iowa City, Iowa
JAN E. VELDMAN, MD, PhD	Utrecht, The Netherlands
T. J. YOO, MD	Memphis, Tenn

Software Review and Computer Applications Editor

KEVIN T. KAVANAGH, MS, MD .... Somerset, Ky

Imaging Editor

YUTAKA SATO, MD .... Iowa City, Iowa

Book Review Editor

DENNIS G. PAPPAS, MD .... Birmingham, Ala

Emeritus Board Members

WESLEY H. BRADLEY, MD	Albany, NY
D. THANE CODY, MD	Jacksonville, Fla
SEYMOUR COHEN, MD	Los Angeles, Calif
ARNDT J. DUVALL III, MD	Minneapolis, Minn
JOHN M. FREDRICKSON, MD	St Louis, Mo
RICHARD R. GACEK, MD	Syracuse, NY
JEROME C. GOLDSTEIN, MD	Alexandria, Va
SIR DONALD F. N. HARRISON, MD PhD	London, England
SAM E. KINNEY, MD	Cleveland, Ohio
JOHN A. KIRCHNER, MD	New Haven, Conn
DAVID J. LIM, MD	Los Angeles, Calif
FRED H. LINTHICUM, Jr, MD	Los Angeles, Calif
MICHEL PORTMANN, MD	Bordeaux, France
LORING W. PRATT, MD	Waterville, Me
GUNNER O. PROUD, MD	Kansas City, Kan
WILLIAM H. SAUNDERS, MD	Columbus, Ohio
F. BLAIR SIMMONS, MD	Palo Alto, Calif
RUEDIGER THALMANN, MD	St Louis, Mo
HARVEY M. TUCKER, MD	Cleveland, Ohio
PAUL H. WARD, MD	Los Angeles, Calif

This article originally appeared in March 1934, Volume 43, No. 1, pages 1-15, and is reproduced here in its entirety.

A SYNDROME OF EAR AND SINUS SYMPTOMS DEPENDENT UPON DISTURBED FUNCTION OF THE TEMPOROMANDIBULAR JOINT.*

James B. Costen, M. D.,

St. Louis.

The problem of temporomandibular joint function and occlusion being a major dental issue, it appears almost entirely in the dental literature. The following group of symptoms may be observed frequently in patients with endentulous mouths and a marked overbite; the syndrome is classic for lesions of the sinuses or ears; yet overbite and disturbance of the joint are so easily overlooked as etiologic factors that it becomes a source of error in analyzing cases in otolaryngology.

Conditions that have been given most attention in the medical literature are anterior dislocations, fracture of the neck of the mandible and ankylosis of the joint after chronic irritation or infection. These have received prolific comment, and appropriate surgical treatment has been carefully worked out.

Each of these symptoms may be ascribed to some evident disturbance in anatomic function of the joint, its ligaments and muscular attachments. The ear symptoms depend upon actual involvement of the eustachian tube and tympanic structures. The "sinus" symptoms are more apparent than real. The actual source of this group of complaints was confirmed by the marked improvement which followed correction of the overbite, renewal of molar support to take pressure off the condyle, and establishment of proper articulation of the condyle within the fossa.

---

*Read before the Texas Ophthalmological and Otolaryngological Society, Dallas, Texas, December 8, 1933.

From the Department of Otolaryngology, Washington University School of Medicine, and the Oscar Johnson Institute.

The ear symptoms observed were:

Impaired hearing, continuously, or with intervals of improvement.

Stopping, or "stuffy" sensation in ears, marked about meal time.

Tinnitus, usually "low buzz" in type; less often, a snapping noise while chewing.

Pain, dull type, within and about ears.

Dizziness, mild; again, attacks of prostrating severity, definitely relieved by inflation of eustachian tubes.

Alleged "sinus" symptoms:

Headache, severe and constant, localized to vertex and occiput, and behind the ears—typical site of posterior sinus pain, but increasing toward the end of day (atypical sinus history, and suggestive of eye headache).

Burning sensation in throat, tongue and side of nose.

The diagnosis of this condition is established by:

1. The lack of molar teeth, or badly fitting dental plates, permitting overbite;

2. Mild catarrhal deafness, improved at once by inflation of eustachian tubes;

3. Dizzy spells, relieved by inflation of tubes;

4. Tenderness to palpation of mandibular joints;

5. Marked comfort to patient from interposing a flat object between the jaws.

6. Presence of the typical headache after sinus or eye involvement has been corrected; presence of the typical headache when sinuses or eyes are found to be negative.

Eleven cases in which disturbance of mandibular joint function was the chief etiologic factor of abnormal ear and head conditions:

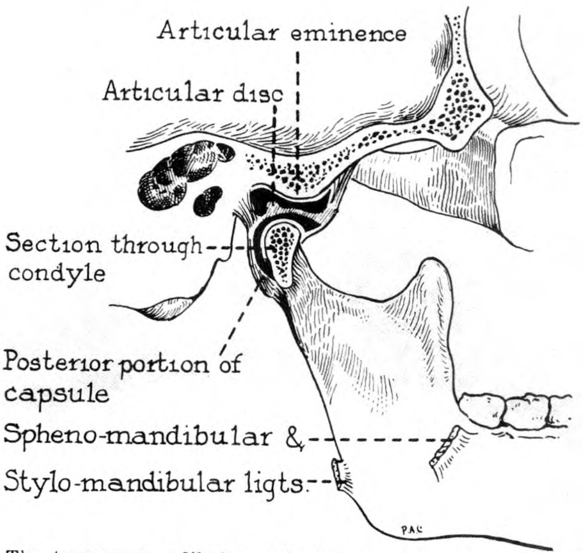

Fig. 1. The temporo-mandibular articulation. Schematic drawing to show position assumed by articular structures when full molar support is afforded (mesial aspect). No pressure is exerted on the meniscus by the condyle.

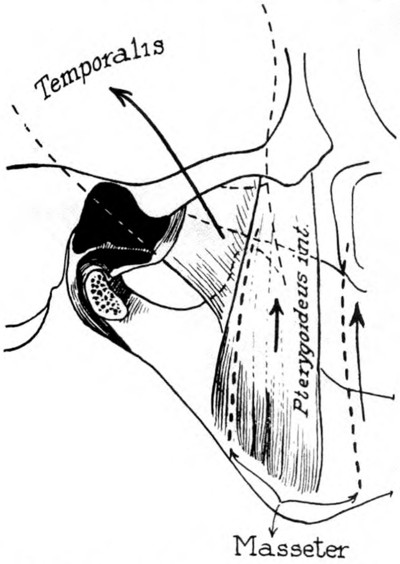

Fig. 2. Variety of movements increased in the pathological temporo-mandibular joint. With molar support gone, condyle is brought upward against meniscus, forward against articular eminence, or backward against tympanic plate.

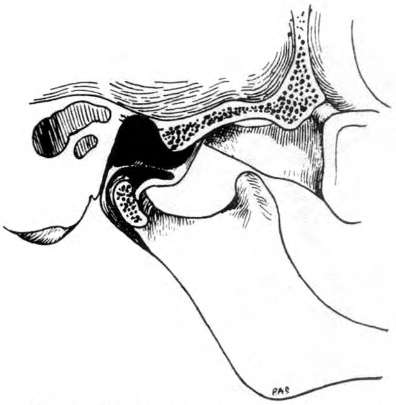

Fig. 3. Sketch of section through mandibular joint in a cadaver specimen. It demonstrated the effect of uncontrolled movement of the condyle in the edentulous mouth. The bone has undergone pressure (?) atrophy, excavating the glenoid cavity.

Case 1.—Mrs. P. F. N., 61. The past history of this patient was unimportant, the only events being concerned with the ears. The hearing was gradually impaired for a few years, with tinnitus of low buzzing type. The relatives noted her to be more deaf, or inattentive, at meal time; an hour later she seemed responsive and heard much better, denying stoutly any hearing difficulty. The object of examination was to prove whether or not she could hear, and consult a neurologist if necessary. No headache, or respiratory infection of importance. Occasional dizzy spell, attributed to "biliousness." Dental plates 20 years old.

Examination, September 27, 1927: The patient has a good structural nose with no evidence of chronic infection about sinuses or pharynx. Tonsils are small, atrophic. The ear drums are perfect, somewhat dull, slightly retracted. Inflation of eustachian tubes show the left patent, admitting air with normal sound. The right tube is tightly adherent, admitting no air.

Hearing distance is 30 feet on left, WV and CV. On the right, CV is heard at one foot, WV not at all. Weber to right. Diminished positive Rinne, both sides. Bone conduction slightly prolonged over examiners. C1 and C4 reduced on right. Marked overbite of the lower jaw, folding the lower lip over the upper.

Diagnosis: O. M. C. C., right; overbite with eustachian tube compression.

Proper dental plates were advised. No treatment of the ears was possible, as the patient lived in a small town at some distance.

On October 25, 1927, one month after opening of the bite with well-fitted plates, she returned for inspection. CV was increased from one foot to fifteen, and WV from 0 to ten feet. There were no further dizzy spells.

Case 2.—Mrs. A. K., 62. For many years this patient has had a "raw" feeling in the right side of the throat. She has frequent headache, daily, over the right eye, behind the right ear, and into occiput. There is a burning sensation, at the end of the day, in the right side of the nose and tongue, which extends at times to the right ear. No deafness or dizzy spells.

Examination, July 24, 1928: The nasal spaces are clear of infection. The lower turbinates are enlarged, but not occluding. In the nasopharynx, the right eustachian tube is set forward by a smooth mass, mucosa not broken on surface, and about 0.5 cm. in diameter. Palpation shows it soft in texture. The pharynx is otherwise normal. Upper and lower molars absent on right.

Hearing tests show normal hearing, bone conduction slightly prolonged.

Biopsy of the mass was suggested and refused.

Diagnosis: Sphenoiditis, chronic; right; pharyngitis, chronic, secondary; nasopharyngeal tumor, right (?).

October 2, 1933. The patient returned after five years' absence. Biopsy was made and sections reported as chronic inflammation, lymphadenoid tissue. Palpation of the mass showed it still soft, not increased in size.

All molars, upper and lower, missing on the right. The right temporomandibular joint is quite tender to firm pressure, and bite closes with slipping of jaw to left, and wrenching of right joint. Observed through nasopharyngoscope, the soft mass in the nasopharynx is seen to bulge markedly on closure of bite.

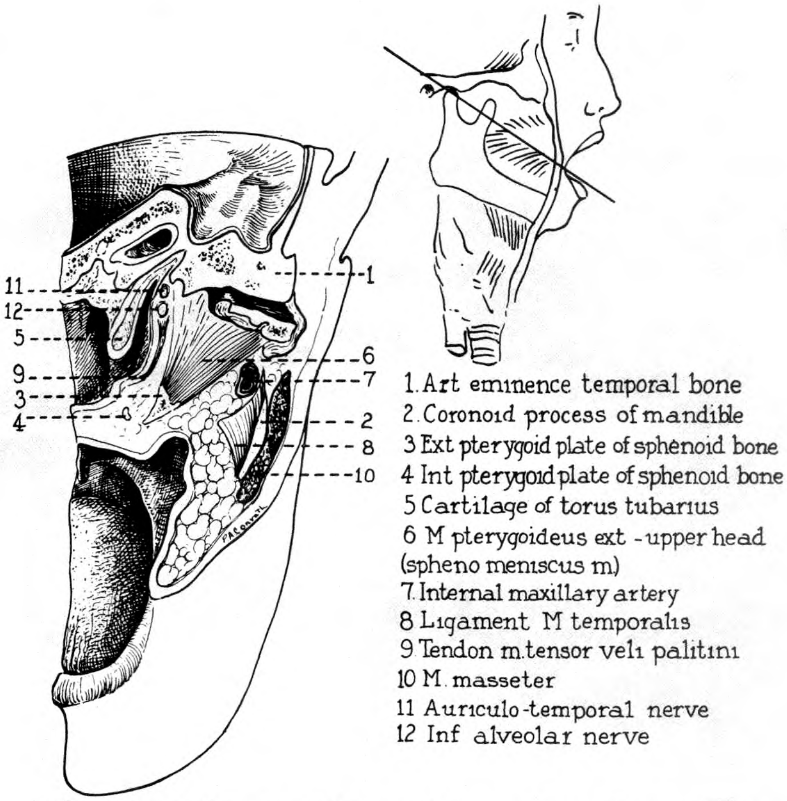
11
12
5
9
3
4
1
6
7
2
8
10
1. Art eminence temporal bone
2. Coronoid process of mandible
3 Ext pterygoid plate of sphenoid bone
4 Int pterygoid plate of sphenoid bone
5 Cartilage of torus tubarius
6 M pterygoideus ext - upper head (spheno meniscus m)
7. Internal maxillary artery
8 Ligament M temporalis
9 Tendon m. tensor veli palitini
10 M. masseter
11 Auriculo-temporal nerve
12 Inf alveolar nerve

Fig. 4. This section was made in a cadaver specimen with mouth open, and the condyle well forward on the articular eminence of the temporal bone. In this position the sphenomeniscus muscle is taut. When the jaw is brought upward, as in a marked overbite, this muscle and associated structures, are seen to relax, and the bulging tissues compress the membranous part of the eustachian tube.

The patient was sent to her dentist, and upper and lower denture fitted in the molar spaces on the right. The last report from her was three weeks after, and there was marked relief from the headache and burning sensation.

Case 3.—Mrs. W. H. B., 33. Patient is just beginning her allergic reaction to the fall grasses. In addition to the usual symptoms of sneezing, watery discharge, and obstruction of the nose, she has had a regular dull headache, localized about the ears and radiating to the cheek bones. The pain is daily and becomes severe by the end of the day. A burning sensation radiates to the right ear. Onset corresponds with extraction of lower molar teeth six months before.

Examination, July 30, 1932: Nasal spaces show allergic reaction, throat negative. Tonsils removed. Much dental work. Lower molars missing on both sides, and the lower incisors close behind the uppers with an extreme overbite.

Diagnosis: Headache from mandible joint overaction; overbite of jaws—extreme.

On May 20, 1933, patient returned with previous headache symptoms more severe. No trace of her seasonal allergy may be seen in the nose. Complains of "full feeling" in right ear; examination negative—tube normal. She was again urged to have proper fitting of jaw teeth, and this time did so.

On July 2, 1933, about one month later, she reported that all of her headache had disappeared. It did not return with her hay fever in the late summer.

Case 4.—Mrs. B. B., 63. For past two years there has been a noticeable impairment for whispered voice, with middle and low tones heard well. No tinnitus. No severe illness, or quinine medication. No headache or dizzy spells. All upper teeth have been extracted and an upper plate worn about nine years.

Examination, August 15, 1932: The nasal spaces are of fair structure, except for a low spur forward on the left. Ear drums perfect. Tonsils removed, small fragment in the left lower pole. The upper teeth are replaced by a plate, lower teeth in good repair. There is a forward overbite of almost one-half inch, and the upper incisor teeth edges cover the lower gums.

Hearing distance, CV is thirty feet, both ears. WV is heard at one foot on left, not at all on right. Weber not lateralized. Rinne normal. Schwabach, bone conduction time approximates that of examiners for normal, 40 seconds.

On June 19, 1933, patient reported, after wearing new upper plate for six months. Whispered voice increased to five feet, both ears. There was great difficulty in making a proper plate, and occlusion is still obviously very bad.

Case 5.—Mrs. J. S. M., 55. This remarkable case has been an invalid with paralysis agitans symptoms for four years. The tremor was confined to the hands, weakness and gait difficulty prevented any effort at walking, and attacks of mild dizziness made the patient refuse to sit up in bed. The hearing was impaired, with sensation of "stopped ears." There was a dull temporal and occipital headache, daily. The presence of occasional infection about the posterior sinuses seemed to prove this the source of the headache, and in view of the tendency to become worse, a resection of the posterior sinuses was considered. The gravity of this procedure brought in consulting advice.

Examination, November 15, 1932: The nasal spaces were entirely normal except for some hyperplasia about the posterior sinuses. The pharynx was negative. Ear drums perfect, slightly dull and retracted. Very flat and poorly fitting plates, 22 years old, permitted an extensive overbite of the jaw. Palpation of the mandibular joint showed marked tenderness, both sides.

Hearing distance for spoken voice was thirty feet, both ears, whispered voice not heard. C4 and C gross forks not heard, middle C heard well. Weber not lateralized. Bone conduction prolonged to sixty seconds. Rinne

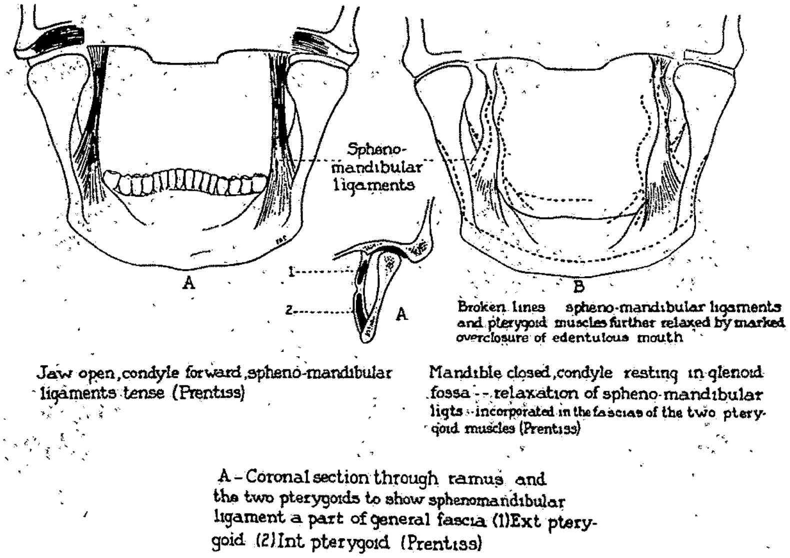
Spheno-mandibular ligaments
A
1
2
A
B
Broken lines spheno-mandibular ligaments and pterygoid muscles further relaxed by marked overclosure of edentulous mouth
Jaw open, condyle forward, spheno-mandibular ligaments tense (Prentiss)
Mandible closed, condyle resting in glenoid fossa -- relaxation of spheno-mandibular ligts -- incorporated in the fascias of the two pterygoid muscles (Prentiss)
A - Coronal section through ramus and the two pterygoids to show sphenomandibular ligament a part of general fascia (1) Ext pterygoid (2) Int pterygoid (Prentiss)

Fig. 5. Sketch of a study by Prentiss, showing the manner of tensing the spheno-mandibular ligaments, and their behavior in a closed bite. Movement of the pterygoid muscles is uniform with the ligaments, being controlled by them.

positive. Eustachian tubes were tightly stopped when inflation was attempted.

New dental plates were fitted, and the eustachian tubes inflated weekly for one month. The dizzy spells disappeared at once, the headache was completely relieved by the end of the month's period. This report is one year later, at which time the paralysis agitans symptoms have gradually increased. The patient sits up in bed or wheel chair without dizziness; there is no further headache; the hearing is improved.

Case 6.—Mrs. L. W., 66. The patient notices impairment of hearing, which is gradually worse, and is more marked at meal times. No tinnitus or "stopped" sensation of ears. In spite of good general condition, she has had dizzy spells, requiring support during an attack. Dental plates 15 years old.

Examination, November 29, 1932: There is a good structural nose, with a small spur on the septum. No infection in any sinus group. Drums are dull, somewhat retracted. Fork tests show all tones heard well except C gross, which is lost in both ears. No change from normal bone conduction, Rinne, or Schwabach. Weber to the right.

Diagnosis: O. M. C. C. bilateral. Dental plates fitted loosely, and in addition to a wide overbite, allow the jaw to slip over one side in occlusion. New plates were advised, but patient could not buy them. She refused to obtain them at a charity clinic.

June 15, 1933, while having a dizzy spell, the patient fell, fracturing right femur; recovery after seven weeks.

September 3, 1933. On this date she fell, breaking several ribs.

The hearing is improved and the dizziness disappears as long as she can report weekly for inflation of the eustachian tubes. After explaining the condition to her, she has had marked relief, also, from holding a small pad of gauze between the jaw teeth.

Case 7.—Mrs. S. L., 55. This patient was admitted on the neurological service at Barnes Hospital on April 18, 1933. Routine examination was entirely negative. She had a history of headache, covering a period of ten years. The pain was dull, distributed over eyes, in the parietal region, and around the ears. It had become more severe the past winter. No hearing impairment or ear symptoms. She was referred for sinus study.

Examination, April 19, 1933: The sinus groups were negative except for a small amount of mucopus in the middle meati. Throat negative, ears normal. X-ray study showed maxillary involvement on both sides, and clouding of the left frontal.

The 18-year-old dental plates showed a wide overbite, with a ludicrous weaving of the lower jaw during attempted occlusion. Tenderness may be elicited on palpation of each mandibular joint.

She was advised to have the mouth refitted with proper dentures, before attempt to correct the rather inactive sinus condition. This was promptly done. She reported by letter after four months, that all of her headache symptoms had entirely gone.

Case 8.—Mrs. O. J. K., 64: For several years this patient has had a pain or ache which is occipital, worse on the right side, and during the daily attack has a low buzz in the ears. No history of nasal infection. Family notice hearing impairment, but she is not aware of it.

Examination, April 30, 1933: Shows good structural nose, no trace of infection observed. The pharynx is normal, tonsils small. Ear drums are dull, slightly retracted. The lower plate, which is ill fitting (10 years old), allows a marked overbite. Two tongue depressors held flat between the jaw teeth is a noticeable comfort to the patient. (The patient then remarked that holding the mouth open at night always prevented headache. She reasoned that this kept the "cold air" out of her nose and helped the headache.)

Fork tests were within normal range, except for hearing C4 and C gross poorly. Hearing distance normal for CV, reduced to 10 feet for WV.

Diagnosis: O. M. C. C., mild; overbite with pathological joints.

On May 13, 1933, patient reports wearing a new lower plate one week, with complete relief of her symptoms, and improvement in hearing.

On August 1, 1933, a further report from the patient, that she has had no further symptoms, and hearing is improved.

Case 9.—Mr. J. W. T., 47. The patient complains of recurrent attacks of "stuffiness" in ears for several years, with muffling of sounds. He has been treated by an otologist for one year with transient improvement. During the year he had a nasal operation—resection of right sphenoid. He still has an occasional occipital headache. The hearing involvement corresponds roughly with the extraction of all his molar teeth for arthritis five years ago.

Examination, June 2, 1933: The ear drums are normal except for slight retraction. Nasal spaces show sphenoid resection, right side, thin mucopus pouring from all posterior sinus groups. Pharynx is negative. There is

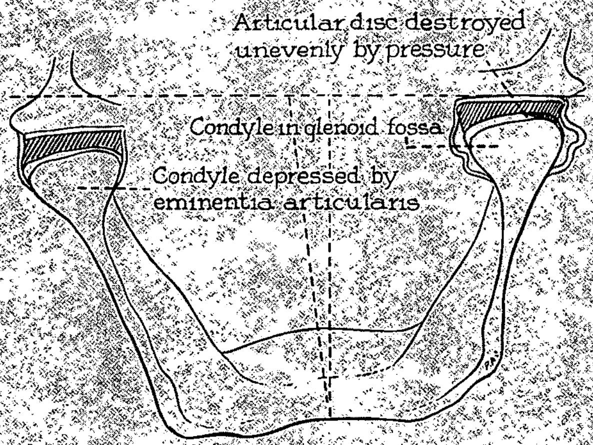
Articular disc destroyed unevenly by pressure
Condyle in glenoid fossa
Condyle depressed by eminentia articularis

Fig. 6. Asymmetric position of condyles due to uneven support of molars or lack of support on one side. (Prentiss.)

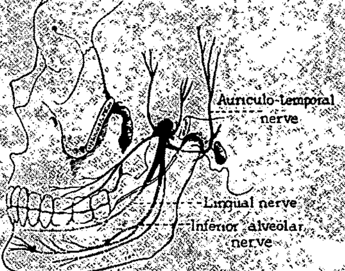

Fig. 7. Sketch showing the distribution of the mandibular nerve and the course of the auriculo-temporal nerve. (Henle.)

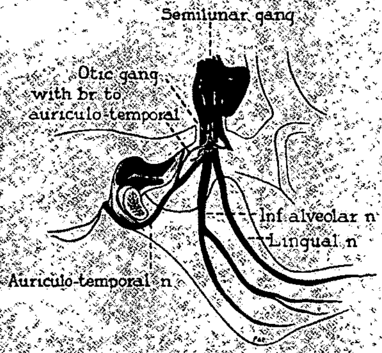

Fig. 8. Diagram of mesial view of mandibular nerve showing auriculo-temporal nerve and its connections with the otic ganglion. (After Spalteholz).

marked malocclusion of the remaining teeth, and, with all molars extracted, the lower incisors rest on the hard palate, one-half inch behind the upper.

Fork tests within normal limits. Hearing distance reduced for WV to ten feet on right, and for SV to six feet. Both are normal at thirty feet on left. The distance is improved by inflation of the right tube to fifteen feet, both SV and WV.

On October 5, 1933, after wearing inlays of molar teeth three months, hearing tests show the same improvement as obtained on the first inflation. He has had no further "stuffy" sensation in ears, and no further headache. The dentist has had extreme difficulty because of his badly deformed jaw.

Case 10.—Mrs. C. F. G., 55. Fifteen years ago this patient had a severe influenza, with nasal trouble ever since. She definitely associated the nasal infections with loss of her upper teeth. Any severe cold seemed to localize in one sinus or other. All teeth were extracted six years ago. This attack dates from a severe cold one month before examination, with daily supraorbital headache, and profuse nasal discharge.

Examination, September 19, 1933: Generally the nose is somewhat crowded, but of good structure. Heavy mucopus in both middle meati. Ears normal. All teeth are extracted, and on first examination it was not noted that there was any abnormal jaw position.

The antra were irrigated several times, with prompt improvement in nasal infection. In spite of this, her headache persisted, and when she returned in one month X-ray study was made, and operative treatment of sinuses considered. Before proceeding, however, she was sent to a prosthetic dentist, who reported retrusion of the condyles on chewing, due to improperly fitted plates. These were changed, and all remaining headache symptoms improved. Sinus operation is still advised, in view of her serious handicap of chronic sinus infection.

Case 11.—Mr. E. A. F., 73. This patient has a remarkably negative past history, and is still in perfect health. He recently had a thorough routine physical examination because of dizzy spells, which were increasing in frequency and severity. All findings being essentially negative, he was referred for the question of toxic labyrinthitis.

He stated that the attacks were brief, severe enough only to occasionally reach for support. There has been some stopping of ears, and impaired hearing. Tinnitus, a low crackle, only when he yawns widely to open ears.

Examination, November 15, 1933: The nasal spaces are free of infection, structures good except for broad septal spur on the left. Pharynx negative. Ear drums normal.

Fork tests show reduction for C4 and C gross, hearing distance reduced to twenty feet for both CV and WV, both ears. No spontaneous nystagmus.

Diagnosis: O. M. C. C., bilateral, mild.

There is a marked overbite of his badly fitting plates, the jaw instantly feeling more comfortable when resting the molar teeth on three tongue depressors, equal to about one cm. in thickness.

Inflation of the eustachian tubes entirely relieved the dizzy attacks and he proceeded to replace the old plates. All his symptoms are improved with the new jaw position effective a few days.

Wright[1] and later Decker[2] reported cases demonstrating compression of the cartilaginous canal by habitual retrusion of the condyles of the mandible. These authors ascribe deafness in those individuals to: (1) Compression of external canals to point of closure, (2) trauma to tympanitic structures and irritation from the continued click and pound as the condyles slip backward with each closure of the mouth.

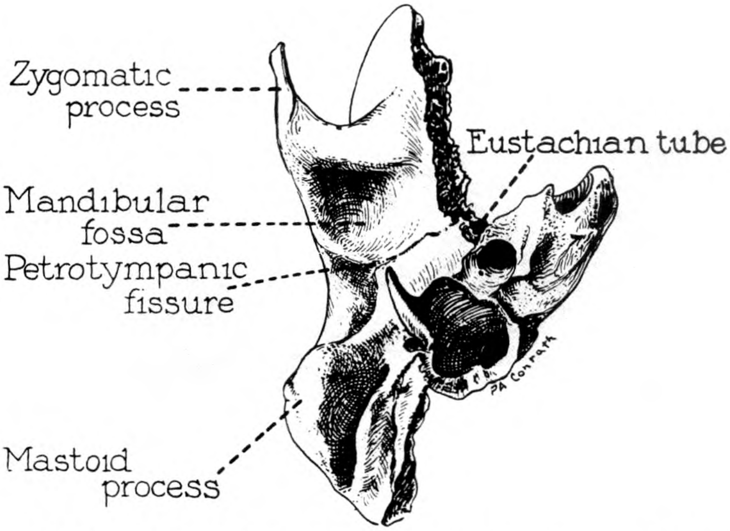

Fig. 9. Lower aspect of temporal bone, showing the petrotympanic fissure quite high, within the depression of the mandibular fossa. In such relation as this, the chorda tympani nerve emerging at the mesial end of the petrotympanic fissure, is subject to irritation from the movements of the condyle in a pathological mandibular joint. (Drawn from a specimen in the anatomical collection of Dr. R. J. Terry, Washington University School of Medicine.)

If these deductions are accepted, it would be on the basis of some type of concussion of labyrinthine structure or injury to the eighth nerve, in which case the recovery of hearing after correcting the joint function would be very slow. Their cases, as well as most of the present series, promptly improved in hearing within a few days or weeks after restoration of proper occlusion. The temporary nature of such deafness seems clear. The symptoms of dizziness in cases 1, 5, 6, 8 and 11 temporarily disappeared with the first inflation of the eustachian tubes and hearing distance was improved during the test. The rôle of compression of the eustachian tubes and a resultant conduction deafness was quite evident; and the association of dizziness with improper regulation of the intratympanic pressure was repeatedly demonstrated. Cases 5, 6 and 11 habitually practiced opening the mouth as in a yawn to relieve dizziness and coincident "stopped" feeling in the ears.

Looking to anatomic reasons for such a pressure effect, we find a definite basis for compression of the tubes. A section (Fig. 4) made through the articular eminence close to the glenoid fossa, passes through the attachment of the sphenomeniscus muscle to the articular disc, and through the lumen of the eustachian tube; it embraces all soft structures adjacent to the tube. With the joint in normal position, the external pterygoid muscle is taut (Fig. 5-A), and the tensor veli palatini muscle borders the tube anteriorly on an almost straight line (Fig. 4-9). Between these lie only connective and adipose tissue, and posteriorly, close to the tube, are the auriculotemporal nerve and the inferior alveolar nerve. If the jaw is brought upward into a position of marked overbite, the upper head of the external pterygoid muscle (called the sphenomeniscus muscle by Prentiss[4]) is relaxed and a bundle of soft tissue piles against the tube. (Fig. 4.) The tensor veli palatini muscle appears loose, preventing its function in tightening the soft palate and opening the eustachian tube during deglutition. Especially during the act of swallowing, when the tensor palatini muscle usually opens the eustachian tubes, the compressing effect of the tissues on the tube from the overbite is present and prevents it.

The very looseness of the capsule of the mandibular joint and its restraining ligaments now works to further exaggerate the pushing of tissues toward the tube. (Figs. 5-B.) With each overacting closure of the mandible by the masseters the internal pterygoid and temporal muscles, the condyle is shoved upward against or through the atrophic or perforated meniscus, or it moves backward to the tympanic plate and pushes mesially on one side or the other through the loose capsule. This happens countless times with each meal, when the patient retrudes the jaw to occlude his poorly fitting plates.

Prentiss[3] observed with wide variations of thinning of the meniscus that perforations were produced on various areas. Its location would depend upon the angle at which the condyle was forced against the meniscus; such an uneven pressure follows the unilateral loss of molar support. (Fig. 6.)

The overbite with atrophy of the joint structure occurs at once if the dental plates are poorly fitted and allow it. It develops slowly if the same plates are worn for many years, and shrinkage of the bone in the dental ridges is marked.

Goodfriend[5] recently gave exhaustive reports on the symptomatology and treatment of abnormalities of mandibular articulation, with emphasis on the mechanics of repositioning the mandible and establishing the proper dental occlusion. His analysis of ninety-one cases shows only 12 per cent of the group are aware of the joint symptoms and that the majority of them seek treatment for the associated reflex symptoms. Deafness leads the list of primary complaints, and then come, in order of frequency, bite anomalies, speech defects, snapping of joints, tinnitus and eczema of ear canals, facial deformities, pyorrhea, malocclusions, and lastly, vertigo. Audiometric examinations were made in an otolaryngologic clinic and these showed 13.3 per cent loss of hearing for the abnormal group, but the type of deafness was not reported.

This important investigation demonstrates the following points:

(a) That the patient mentions deafness most frequently as a primary complaint, vertigo last, and headache not at all. (This means that the patient does not associate the two symptoms, and that the vertigo is mild and recurrent over a long onset period. In my group, cases 6 and 11 were referred by internists suspecting toxic labyrinthitis.)

(b) That treatment is sought by the majority of patients for headache and referred pains, the result rather than the unsuspected mandibular joint disease.

The anatomic explanation of pain in connection with disturbed joint function is fairly simple, if recognized: (1) deep erosion of the bone (Fig. 3) of the glenoid cavity leaves only a thin plate between the condyles and the dura—practically nil (Prentiss[3]). Each closure of the jaw impacts this evacuated area with the condyle, which thus rocks in the glenoid fossa, barely separated by the remaining thin bone from the dura and its rich nerve supply. (2) With some of the chewing movements and closures of the jaw, the condyle exerts pressure on or near the auriculotemporal nerve which passes intimate to the mesial side of the capsule and between the condyle and the tympanic plate to distribute over the temporal region. (Fig. 7.) (3) Further, in the type of pathologic joint in which the condyle snaps backward over the articular disc, impacting and eroding the tympanic plate, the chorda tympani nerve passes this spot through the iter chordæ anterius at the medial end of the Glasserian (petrotympanic) fissure. (Fig. 9.) It is therefore quite evident that dull vertex pain from this source may be of dural origin, that pain over the temporal region originates in irritation of the auriculotemporal nerve, and that the pains referred to the side of the tongue may be attributed to pressure on the chorda tympani nerve.

SUMMARY.

Headache and ear symptoms directly dependent upon disturbed function of the mandibular joint frequently occur in cases showing sufficient pathology about the sinuses to otherwise account for them. There are so many medical, rhinologic and ophthalmologic reasons for headache distributed about the ears, vertex and occiput; and there are so many nasal changes to account for eustachian tube obstruction, that evulsion of the condyle of the mandible from overbite is not considered.

Hearing tests show a mild type of catarrhal otitis with eustachian tube involvement, usually simple obstruction. This is due to pressure on its anterior membranous wall, transmitted through soft tissue from the relaxation of pterygoid muscles and associated sphenomandibular ligaments during overbite.

The promptness with which the ears improve seems to controvert the idea that the ear condition is due to trauma or concussion of the labyrinth or tympanic structures from the condyle of the mandible. Cases of shock to the labyrinth from a blow on the chin are not within the scope of this paper.

Attacks of dizziness in these cases are obviously due to changes in intratympanic pressure affecting the labyrinth. The effect is transient and recurrent, relieved by inflation of the eustachian tube, and not the picture seen in toxic labyrinthitis.

The areas involved in the headache cases are typical of headache of posterior sinus origin and are easily taken for such. Persistence of the headache after indicated sinus surgery is sometimes due to mandibular joint pathology.

The symptoms arise as a result of overaction of the joint at first, and later adds the regional effect of a loose, pathologic joint,

produced by absorption of the meniscus, condyles and surrounding bone.

The prognosis in a given case depends on these factors: (a) the accuracy with which refitted dentures relieve abnormal pressure on the joint; (b) the extent of injury to the tube and to the condyle, the meniscus, and the joint capsule.

The mechanics of occlusion and dental problems are not included here. Only sufficient reference to the anatomy of the mandible and joint is made to clarify the ear or sinus diagnosis.

Anatomic reasons are advanced to account for abnormal conditions of the eustachian tube, and for the distribution of pain toward the vertex, occiput, pharynx and tongue. It is barely possible that mandibular joint pathology may be an etiologic factor in glossopharyngeal neuralgia, the association of chorda tympani and auriculotemporal nerves with the ninth occurring via sensory connections to the otic ganglion.

722 Beaumont Medical Building.

BIBLIOGRAPHY.

1. Wright, W. H.: Deafness as Influenced by Malposition of the Jaws. Journal of the National Dental Assoc., Dec., 1920, p. 979-92.

2. Decker, J. C.: Traumatic Deafness as a Result of Retrusion of the Condyles of the Mandible. Annals of Otology, Rhinology and Laryngology, 34:519-27, 1925.

3. Prentiss, H. J.: A Preliminary Report Upon the Temporomandibular Articulation in the Human Type. Dental Cosmos, 60:505-14, 1918.

4. Prentiss, H. J.: Regional Anatomy, Emphasizing Mandibular Movements With Specific Reference to Full Denture Construction. Jour. of Am. Dental Assoc., 10:1085-99, 1923.

5. Goodfriend, D. J.: Symptomatology and Treatment of Abnormalities of the Mandibular Articulation. Dental Cosmos, 75:844-52, 1933.
Ibid. 75:947-57, 1933.
Ibid. 75:1106-11, 1933.

Ann Otol Rhinol Laryngol 106:1997

A PERSPECTIVE

JAWS REVISITED: COSTEN'S SYNDROME

LUDWIG A. MICHAEL, MD
DALLAS, TEXAS

Although James Costen was not the first to ascribe ear pain, tinnitus, impaired hearing, and even dizziness to temporomandibular joint dysfunction, he developed an integrated and systematic approach ascribing the symptoms to dental malocclusion. He wrote extensively on it, and a few years after his original article, the term Costen's syndrome came into general use. Recently, the use of the eponym has decreased, as dental malocclusion has assumed a lesser role in explaining many of the symptoms formerly ascribed to it.

KEY WORDS — Costen's syndrome, temporomandibular joint.

Listed in the *Quarterly Cumulative Index Medicus (QCIM)* for 1939, under "Jaws, diseases," is the first article with "Costen's syndrome" in the title.[1] Costen's original article, which appeared in 1934, also listed under "Jaws, diseases," was titled "A Syndrome of Ear and Sinus Symptoms Dependent Upon Disturbed Function of the Temporomandibular Joint."[2] He included ear symptoms such as impaired hearing, stuffy sensation in the ears, tinnitus, ear pain, and sometimes severe dizziness relieved by eustachian tube inflation, "sinus" symptoms such as headache at the vertex and occiput, and burning sensations in the throat and tongue. When causes in the sinuses and ears could be ruled out, he attributed all these symptoms to dental malocclusion. He followed up his 1934 publication in the next 5 years with 11 other articles on the same subject.[3-13]

Costen was not the first to point out otolaryngological symptoms of abnormalities of mandibular articulation,[14] but he made an impact in his 1934 article "with its directness and unequivocation,"[15(p113)] in spite of its anatomic naivete. He had become interested in referred pain after seeing many patients for head pain that had been unrelieved by ethmoid or sphenoid sinus surgery. Costen thought the pain was probably related to the temporomandibular joint (TMJ). His work focused attention on pain in the region of the ear and the TMJ. Stressing occlusal derangement with consequent disturbance in the function of the joint, he publicized to his fellow otolaryngologists an important diagnostic advance: to look beyond the sinuses for a source of head pain. (Costen's son [William S. Costen, MD, an orthopedic surgeon] recalls his father laying out charts in his study at home when he began collecting data on the TMJ and on pain fibers in the chorda tympani. In 1957 William noted a description of the possible anatomic basis for referred pain in Hilton's *On Rest and Pain*[16] [1879] and brought it to his father's attention. Subsequently, his father wrote a monograph giving Hilton credit for describing the anatomic basis for pain referral.) It is interesting to follow the history of the eponym Costen's syndrome over the past 60 years and to know something of the man it honors.

James ("Jimmy") B. Costen (see Figure) was born

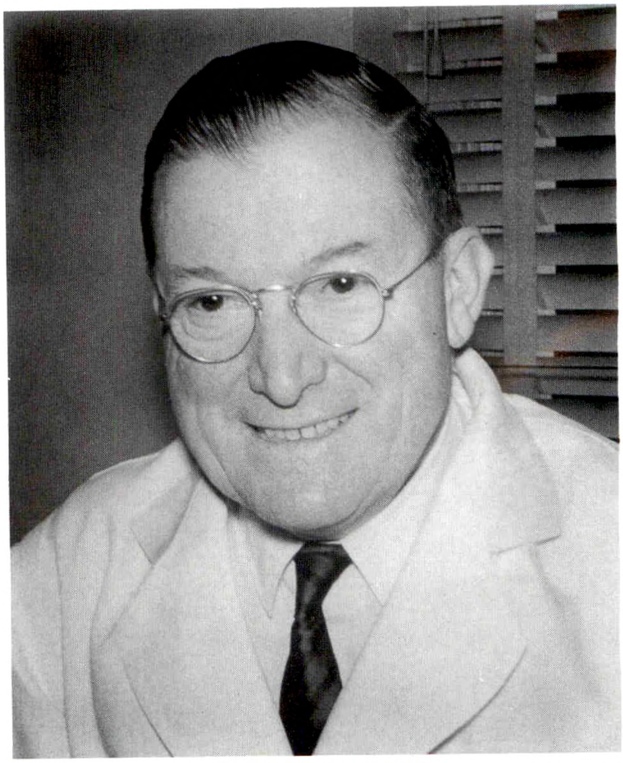

James B. Costen in 1961.

From the Department of Otolaryngology, University of Texas Southwestern Medical Center at Dallas and Baylor University Medical Center, Dallas, Texas.

CORRESPONDENCE — Ludwig A. Michael, MD, Texas Medical and Surgical Associates, 8440 Walnut Hill Lane, #500, Dallas, TX 75231.

in Tennessee in 1895, the younger of two sons. His father worked for Bell Telephone Company in promoting telephone service in small communities. Once service was established, he moved on. In 1900 the family, consisting of Jimmy, his parents, and an older brother, moved to Paragould, Arkansas, where Jimmy grew up, and which he always considered home. At one time his father was asked to move to Tulsa, Oklahoma, but after witnessing a gunfight in the street outside his hotel, he decided that this was not the place to bring up his two sons and returned to Arkansas.

While he was in high school, Jimmy was apprenticed to a local physician who taught him to give open drop anesthesia for office procedures and dressing changes. After high school, he went to Virginia Military Institute, but returned to Arkansas 1 year later when his father became ill. He then attended the University of Arkansas, graduating from the Department of Chemistry. His older brother was a student at Vanderbilt Medical School, and Jimmy, also interested in medicine, decided to go to Washington University in St Louis, Missouri, which was affiliated with St Louis Medical College. When classes began in September 1917, World War I was under way and Barnes Hospital Unit 21 was being organized to go to France. The dean of the medical school informed the students that if they volunteered and left their class they would not be readmitted on their return. However, Dr Robert Terry, Professor of Anatomy, announced before a lecture that he would personally see to it that any volunteer would be readmitted on his return. Jimmy later told his son William that army life "saved his life." He weighed 114 lb (51 kg) when he left, but returned to medical school at 150 lb (66 kg). He ascribed this gain to army food and regular exercise. After completing medical school he went to Vienna to study at the world-famous Krankenhaus and then to Basel, Switzerland, where he concentrated on the mastoid bone and its dissection. On his return to St Louis, he married Carolyn Thompson, also from Paragould. They had one son and three daughters. After about 1 year practicing with another otolaryngologist, he moved to the Beaumont Building in midtown St Louis, and remained there in solo practice throughout his career.

Almost as soon as the term Costen's syndrome came into general use, questions as to its validity began to surface. Over the years, various authors have disagreed with the idea that this sweeping panoply of symptoms could be attributable to such a simple cause as malocclusion. Sicher,[17] in 1948, wrote that Costen's syndrome should be replaced by the diagnosis "temporomandibular deforming arthritis from mandibular overclosure or displacement." He rejected Costen's anatomic explanations for the pain in this symptom complex, but seemed to accept the grouping of symptoms. As early as 1943, Shapiro and Truex[18] were doubtful that TMJ problems could be responsible for deafness, except for possible eustachian tube impingement, and even this was considered unlikely. Questions were also raised about tinnitus, vertigo, neuralgias similar to trigeminal, and headaches as being of TMJ dysfunction origin. On the other hand, writers defending the use of Costen's syndrome as a diagnosis suggested that not all the symptoms listed in Costen's original work were required to be present to make the diagnosis.[19] In more than one study, tinnitus and vertigo were found to be statistically more frequent in TMJ disorder patients than in normal controls.[20]

Of a group of dentists and physicians,[21] both general and specialized, surveyed as to whether a group of symptoms (namely, TMJ pain, cracking or popping TMJs, and limitation of mandibular movement) constituted a distinct clinical syndrome, 88% of the dentists responded positively, while only 51% of the physicians did so. Asked about causation, those surveyed frequently cited both "bite problems" and "Costen's syndrome." In the details of this survey, confusion about TMJ pain dysfunction is apparent, both as to diagnosis and therapy.[22]

Even after "Costen's" syndrome became a widely used term, the *QCIM* continued listing it under "TMJ syndrome." By 1966, however, it was listed as a separate entry. In 1969, there were 59 entries in the category "Costen's syndrome," and "TMJ syndrome" was listed *under* "Costen's syndrome." However, just 4 years later, "Costen's syndrome" was back under "TMJ syndrome."

This rise and subsequent fall in the use of the term Costen's syndrome to classify all TMJ syndrome references can be attributed to several factors. Although universally acclaimed for bringing the significant role of the TMJ into the realm of awareness of physicians and dentists alike, Costen was judged by many to have been naive in his espousal of the range of symptoms arising from TMJ disorders, in his anatomic explanations, and especially in his view of the pivotal role of malocclusion. Some authors recommended that the term Costen's syndrome be dropped, as it was too inclusive, and replaced with "osteoarthritis of the temporomandibular joint." Others began using "myofascial pain," by definition a muscular pain in numerous body regions produced by pressure on trigger points, with TMJ syndrome being the prime example. Proponents viewed the TMJ syndrome as a cascade of events, from psychologic stress to clenching and bruxism, resulting in occlusal problems, spasm, and pain.[23] "Myofascial pain syndrome" has gradually become the more popular diagnosis. Nowadays, it is more acceptable in medical diagnosis to include the etiologic effects of tension and anxiety. Nevertheless, many cases of TMJ disorders have continued to be reported as "Costen's syndrome," even in recent times.

The etiology and treatment offered by Costen were not always correct, yet the term Costen's syndrome may still be useful, perhaps with a new, more inclusive etiology.[19] Costen rendered a great service in pointing out the relationship between malocclusion, TMJ dysfunction, and facial pain. Otolaryngology owes a debt to Costen for bringing out these points.[24] References to his work continue appearing in the literature, and he is still cited with some frequency in the *Science Citation Index*.

James B. Costen died in 1962. His son remembers that for 10 years after his death not a week would go by without someone's mentioning him with fondness. Although with the years these remembrances have diminished to one or two a month, even now, more than 30 years after his death, some of his old patients remember nostalgically that he worked on Saturdays until 5 PM. For those of us who came in contact with him during our residencies at Washington University–Barnes Hospital, his memory is a pleasant one. He gave of himself unstintingly. He was always cheerful, came to the teaching clinics regularly, and never dashed out early. Listening to him and learning from him are memories that we treasure.

REFERENCES

1. Emenhiser LK. Temporomandibular syndrome (Costen syndrome). J Okla Med Assoc 1939;32:256-60.
2. Costen JB. A syndrome of ear and sinus symptoms dependent upon disturbed function of the temporomandibular joint. Ann Otol Rhinol Laryngol 1934;43:1-15.
3. Costen JB. Group of symptoms frequently involved in general diagnosis, typical of sinus and ear disease and of mandibular joint pathology. J Mo Med Assoc 1935;32:184-90.
4. Costen JB. Neuralgias and ear symptoms involved in general diagnosis due to mandibular joint pathology. J Kans Med Soc 1935;36:315-21.
5. Costen JB. Glossodynia; reflex irritation from mandibular joint as principal etiologic factor; study of 10 cases. Arch Otolaryngol 1935;22:554-64.
6. Costen JB. Neuralgias and ear symptoms associated with disturbed function of temporomandibular joint. JAMA 1936; 107:252-5.
7. Costen JB. Some features of mandibular articulation as it pertains to otolaryngology. Int J Orthodontia 1936;22:1011-7.
8. Costen JB. Neuralgias and ear symptoms associated with mandibular joint. Trans Sec Laryngol Otol Rhinol AMA 1936:72-83.
9. Costen JB. Summary of neuralgias and ear symptoms associated with mandibular joint. Miss Doct 1937;15:33-41.
10. Costen JB. Some features of mandibular articulation as it pertains to medical diagnosis, especially in otolaryngology. J Am Dent Assoc 1937;24:1507-11.
11. Ernst EC, Costen JB. X-ray study in relation to mandibular joint syndrome. Radiology 1938;30:68-75.
12. Costen JB. Correlation of x-ray findings in mandibular joint with clinical signs, especially trismus. J Am Dent Assoc 1939;26:405-7.
13. Costen JB. Mechanism of trismus and its occurrence in mandibular joint dysfunction. Ann Otol Rhinol Laryngol 1939; 48:499-514.
14. Goodfriend DJ. Abnormalities of mandibular articulation. J Am Dent Assoc 1934;21:204-18.
15. Roydhouse N. In defence of Costen's syndrome. J Otolaryngol Soc Aust 1970;3:106-14.
16. Hilton J. On rest and pain. 2nd ed. New York, NY: William Wood, 1879:44.
17. Sicher H. Temporomandibular articulation in mandibular overclosure. J Am Dent Assoc 1948;36:131-9.
18. Shapiro HH, Truex RC. Temporomandibular joint and auditory function. J Am Dent Assoc 1943;30:1147-68.
19. Freese AS. Costen's syndrome: a reinterpretation. AMA Arch Otolaryngol 1959;70:309-14.
20. Chole RA, Parker WS. Tinnitus and vertigo in patients with temporomandibular disorder. Arch Otolaryngol Head Neck Surg 1992;118:817-21.
21. Greene CS. A survey of current professional concepts and opinions about the myofascial pain-dysfunction (MPD) syndrome. J Am Dent Assoc 1973;86:128-36.
22. Greene CS. The temporomandibular syndrome. JAMA 1973;224:622.
23. Lerman MD. A unifying concept of the TMJ pain-dysfunction syndrome. J Am Dent Assoc 1973;86:833-41.
24. Hankey GT. Some observations on Costen's mandibular syndrome: including a review of 100 out of 500 cases. Proc R Soc Med 1957;51:225-8.

Ann Otol Rhinol Laryngol 106:1997

MENIERE'S SYNDROME AND MIGRAINE: INCIDENCE IN ONE FAMILY

CARLOS A. OLIVEIRA, MD, PHD

ROBERTA L. BEZERRA, MD
MERCEDES F. ARAÚJO, MD
VANESSA F. ALMEIDA
CHRISTIANE I. MESSIAS, MD

BRASÍLIA, BRAZIL

Since 1992, we have applied a standard questionnaire to all our Meniere's syndrome patients. We ask about other family members affected by the symptoms and about the presence of the usual migraine symptoms. Through this questionnaire we have identified a family that has some members affected by Meniere's syndrome alone, some others with associated migraine, and still others with migraine alone. Two members of this family started out with migraine and later in life developed Meniere's syndrome. The genetic transmission follows an autosomal dominant pattern for both Meniere's syndrome and migraine. We have interviewed and studied 19 affected persons from several generations of this family, who form the basis of this report. The possibility of a common autosomal dominant genetic determinant for Meniere's syndrome and migraine and its implications for the causation of Meniere's disease are discussed.

KEY WORDS — central etiology, genetic determinant, Meniere's syndrome, migraine.

The familial incidence of Meniere's syndrome was described by Brown in 1941[1] and 1949.[2] Bernstein,[3] in 1965, also described affected families. The genetic transmission in all families studied was autosomal dominant. However, there were 3 affected siblings who were products of a consanguineous marriage in one of the families described by Brown.[2] These reports were summarized by Konigsmark and Gorlin,[4] who accepted the existence of two mechanisms of genetic transmission for Meniere's syndrome: autosomal dominant and autosomal recessive. They also stated that the hereditary syndrome is different from the idiopathic one (Meniere's disease).

Paroxysmal headaches have been associated with both hereditary[1-3] and idiopathic Meniere's syndrome[5] or Meniere's disease. However, these headaches were never documented as true migraine. Since migraine has a strong familial incidence and is believed to be caused by microvascular changes in the central nervous system (central causation), it is important to know whether the headaches associated with Meniere's syndrome are true migraine or not.

In 1992, Oliveira and Braga[6] described another family with Meniere's syndrome transmitted in an autosomal dominant pattern. Again, "migraine-like" headaches were present in several affected members of this family. The index patient had an endolymphatic sac drainage procedure done on the affected ear; his vertiginous symptoms improved markedly and hearing remained stable for a long time in the operated ear. Because of this excellent response to the endolymphatic sac drainage procedure, Oliveira and Braga stated that there seemed to be no difference between idiopathic (Meniere's disease) and hereditary Meniere's syndrome. They also speculated that a sporadic genetic determinant may be the cause of idiopathic Meniere's syndrome (Meniere's disease).

In order to test the possibility of a genetic determinant in idiopathic Meniere's syndrome (Meniere's disease), as well as a possible association between migraine and Meniere's syndrome, we have applied a standard questionnaire to all patients with this syndrome seen at the Department of Otolaryngology of Brasília University Medical School since 1992. Questions about the presence of the syndrome in other members of the family, as well as regarding the incidence of the common migraine symptoms in all members affected, were included. We have found that when asked to do so, the Meniere's syndrome patients frequently report on other family members affected by the symptoms. The high incidence of true migraine associated with Meniere's syndrome also is becoming apparent. We intend to report the numbers on these questions separately.

In this communication we describe a family that was identified through the standard questionnaire described above. Typical Meniere's syndrome is present in some members, migraine associated with Meniere's syndrome in others, and migraine symptoms alone in still others. Of interest, 2 members of this family started out early in life with migraine symptoms only, and developed Meniere's syndrome later in life. The mode of genetic transmission for both Meniere's syndrome and

---

From the Department of Otolaryngology, Brasília University Medical School, Brasília, Brazil.

CORRESPONDENCE — Carlos A. Oliveira, MD, PhD, SHIS, QL-22, Conjunto 04, Casa 09, Brasília, DF, 71650-245, Brazil.

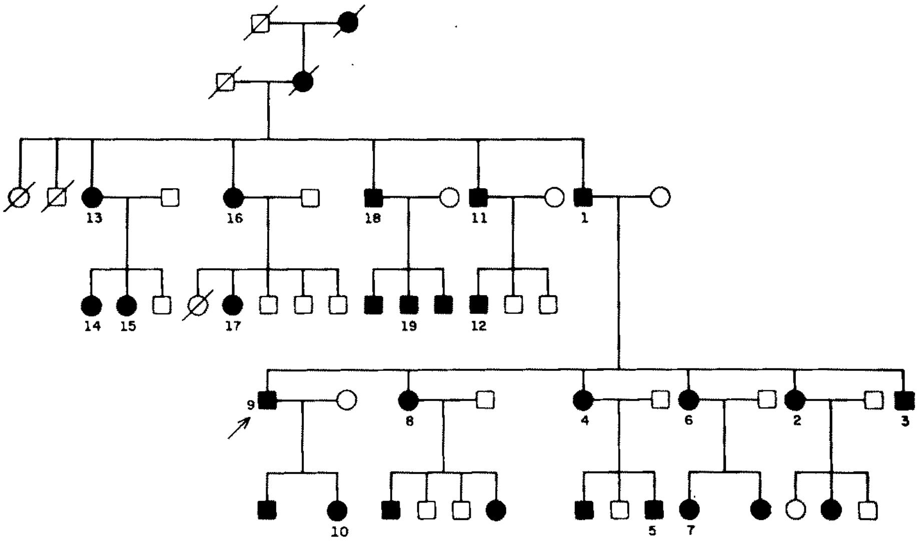

Fig 1. Pedigree. Light circle — nonaffected female; light square — nonaffected male; dark circle — affected female; dark square — affected male; arrow — index patient; crossed circle — deceased female; crossed square — deceased male. Numbers indicate position of affected member in Table. Affected members without numbers were not available for documentation, and therefore are not listed in Table.

migraine is autosomal dominant.

The intimate association between migraine and Meniere's syndrome in this family points to a common autosomal dominant genetic determinant. The evolution of migraine symptoms early in life to Meniere's syndrome later in 2 patients suggests a continuum disease process. The implications of these findings will be discussed.

DESCRIPTION OF THE FAMILY

Figure 1 shows the pedigree of this family for several generations. It was obtained by carefully interviewing the index patient and all 18 of the other affected members. The autosomal dominant mode of genetic transmission is borne out by the pedigree.

The Table summarizes the data obtained by the application of our standard questionnaire to all affected members of the family. A complete otolaryngological physical examination was performed on all of them and the results were uniformly negative. Laboratory tests (blood urea nitrogen, blood sugar, serum creatinine, complete blood count, cholesterol, and triglycerides) were performed on 7 of them, audiometry with speech discrimination tests was performed on 10 of them, tympanometry was performed on 9, and electronystagmography (ENG) was performed on 10. The results of all these tests are included in the Table. Speech discrimination results are omitted because they were all normal.

The numbers in Fig 1 indicate each affected patient in the Table. Because the symptoms were bilateral in all patients, with occasional predominance of one side in a few patients, laterality was omitted from the Table.

From the Table we can see that headache was present in 17 of the 19 patients (95%), and associated migraine symptoms in 11 (58%). Scotomas were present in 12 (63%), and several degrees of anopsia during the crisis in 6 (31%). Paresthesias during the crisis were present in 4 (21%). Three patients (16%) had scotomas without headache, 2 patients (10%) had anopsia without headache, and 2 others (10%) had paresthesias alone associated with the Meniere's symptoms. Tinnitus, hearing loss, and vertigo (Meniere's triad) were present in 12 patients (63%), and in another 3 cases (16%) only tinnitus and vertigo were present. In 2 patients (patients 5 and 7) only migraine symptoms were present. Finally, in 2 patients (patients 4 and 12) the migraine symptoms were present early in life, but later disappeared, and the typical Meniere's syndrome started. These 2 patients will be described in Case Reports, along with the index patient.

Laboratory test results were normal on the 7 patients in whom they were performed. Audiometry showed bilateral moderate sensorineural hearing loss with a down-sloping curve in 5 cases. Three cases showed sensorineural hearing losses in the lower frequencies, and 2 were bilateral. One case showed sensorineural hearing loss with a flat curve in the left ear, and another case showed mixed moderate hearing loss with a flat curve, worse on the left. Tympanometric results were all normal. Results of ENG were normal in 3 patients. Four patients showed a hyperactive labyrinth on one side, and 3 showed a hyperactive labyrinth on both sides.

CASE REPORTS

The index patient (patient 9 on Table) and 2 other patients (patients 4 and 12) who first had migraine symptoms and later developed Meniere's syndrome are described in this section.

The index patient (patient 9) was a 58-year-old man. When first seen by the senior author (C.A.O.), he complained of bilateral tinnitus, worse in the left ear, vertigo with nausea and vomiting, hearing loss in both

SUMMARY OF CLINICAL, LABORATORY, AUDIOMETRIC, AND ELECTRONYSTAGMOGRAPHIC FINDINGS IN 19 AFFECTED MEMBERS OF FAMILY STUDIED

Patient	*Age*	*Sex*	*Tinnitus*	*Hearing Loss*	*Vertigo*	*Headache*	*Vomiting*	*Nausea*	*Scotomas*
1	22	M	+	+	+	–	+	+	–
2	41	F	+	+	+	+*	+	+	+
3	50	M	+	+	+	+*	+	+	+
4	46	F	+	+	+	+*	+	+	+
5	17	M	–	–	–	+*	+	+	+
6	41	F	+	+	+	+	+	+	+
7	19	F	–	–	–	+*	+	+	+
8	56	F	+	–	+	+	–	+	+
9	58	M	+	+	+	+*	+	+	+
10	15	F	+	–	+	+*	+	+	+
11	77	M	+	+	+	–	+	+	–
12	51	M	+	+	+	+*	–	–	+
13	71	F	+	+	+	+	+	+	–
14	49	F	–	–	–	+*	–	–	–
15	47	F	+	+	+	+	–	–	–
16	80	F	+	–	+	+	–	–	–
17	59	F	+	+	+	+*	–	+	+
18	75	M	+	+	+	+	+	+	+
19	45	M	–	–	–	+*	–	–	–

ENG — electronystagmography, N — normal, SNHL — sensorineural hearing loss, ND — not done, MS — Meniere's syndrome, HL — hyperactive labyrinth.

*Headache was described by patient as typical migraine.

ears, but worse in the left, and pressure sensation in both ears, again worse on the left side. He had a long history of migrainelike headaches and scotomas preceding the vertiginous attacks described above. The symptoms tended to occur when he was stressed or overworked. He was a dentist and had been exposed to the noise of a high-speed hand drill for many years. Findings on physical examination were normal. Audiometry showed a bilateral sensorineural hearing loss that was moderate and down-sloping (Fig 2A). A presumptive diagnosis of Meniere's disease was made and the patient was medicated accordingly. He improved considerably. Eight years later he returned with the same complaints. He had been free of symptoms for the last 2 years. One month before he was seen, he again experienced a strong migraine crisis that was followed by Meniere's syndrome. Audiometry done during this visit showed the high-frequency sensorineural hearing loss seen before, but this time also a low-frequency sensorineural hearing loss, bilateral and worse in the left ear (Fig 2B). This time he was questioned about the presence of the symptoms in other members of his family, because we

TABLE CONTINUED

Patient	Anopsia	Pares- thesia	Age (y) at Which Symptoms Appeared	Time Sequence of Headache and Vertigo	Blood Tests	Audiometry	Tympa- nometry	ENG
1	+	–	30		N	SNHL, bilateral, down-sloping	N	ND
2	+	–	10	Headache precedes vertigo	ND	ND	ND	ND
3	–	–	10	Variable	ND	ND	ND	ND
4	–	+	13 migraine, 30 MS	Migraine only for 17 years, MS only afterward	N	Mild SNHL, bilateral, 500 and 1,000 Hz	N	N
5	+	–	15		ND	Mild SNHL, bilateral, 500 and 1,000 Hz	ND	N
6	–	+	14	Headache precedes vertigo	N	Bilateral moderate SNHL, down-sloping	N	HL left side
7	–	–	10		ND	ND	N	N
8	+	+	9	Headache and scotomas precede vertigo	N	Mild SNHL, 500 and 1,000 Hz, right	N	HL left side
9	–	–	39	Headache precedes vertigo	N	Bilateral moderate SNHL, down-sloping	N	HL left side
10	–	–	7	Headache precedes vertigo	ND	ND	ND	ND
11	–	–	18		ND	Bilateral moderate SNHL, down-sloping	N	HL left side
12	+	–	17 migraine, 25 MS	Migraine only for 8 years, then MS only	ND	Bilateral moderate SNHL, down-sloping	N	HL bilateral
13	–	–	30	Variable	N	Bilateral mixed hearing loss, worse on left	ND	HL bilateral
14	–	–	20		ND	ND	ND	ND
15	–	–	35	Variable	N	Mild SNHL, left	N	HL bilateral
16	–	–	21	Variable	ND	ND	ND	ND
17	+	+	43	Variable	ND	ND	ND	ND
18	–	–	15	Headache precedes vertigo	ND	ND	ND	ND
19	–	–	20		ND	ND	ND	ND

ENG — electronystagmography, N — normal, SNHL — sensorineural hearing loss, ND — not done, MS — Meniere's syndrome, HL — hyperactive labyrinth.

*Headache was described by patient as typical migraine.

were asking these questions of all our Meniere's syndrome patients. Numerous members of his family turned out to have the symptoms, were individually studied, and are being reported in this communication. One should note that even though this patient was well educated, he did not mention the presence of the symptoms in other members of his family until he was directly questioned. The workup outlined in the Table was then applied to him, and a diagnosis of hereditary Meniere's syndrome was established based on history, audiometric results, ENG results (bilateral hyperactive labyrinth worse on the left), and negative laboratory tests. A glycerol test was also performed, and fluctuation of his hearing in the low frequencies was demonstrated between the first and second hours after glycerol intake.

Patient 4 was a 46-year-old woman. She was a younger sister of the index patient. She started having migraine-like headaches, scotomas, and paresthesias when she was 13 years old. When she was 30 years old, she began to have bilateral tinnitus, vertigo, and nausea

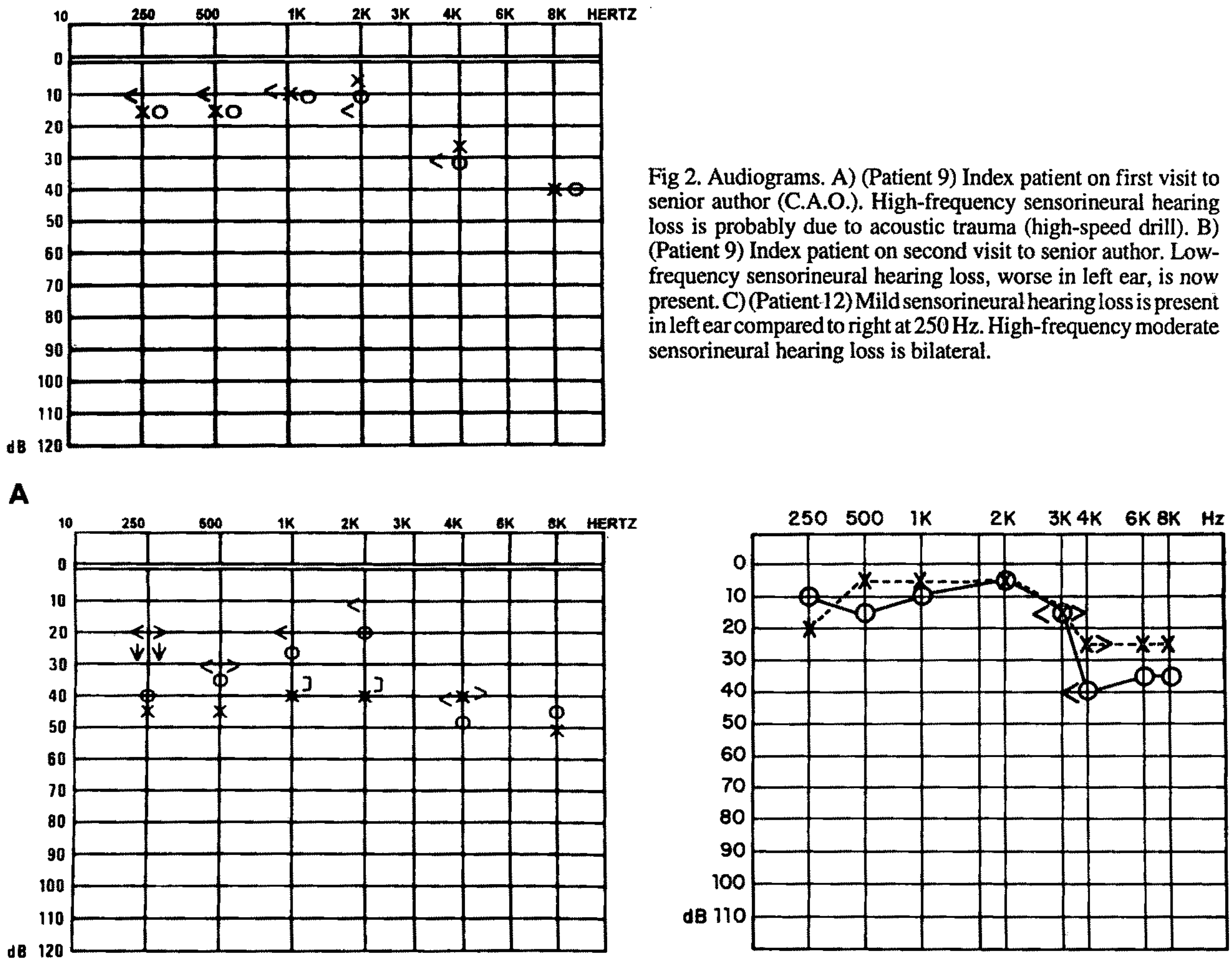

Fig 2. Audiograms. A) (Patient 9) Index patient on first visit to senior author (C.A.O.). High-frequency sensorineural hearing loss is probably due to acoustic trauma (high-speed drill). B) (Patient 9) Index patient on second visit to senior author. Low-frequency sensorineural hearing loss, worse in left ear, is now present. C) (Patient 12) Mild sensorineural hearing loss is present in left ear compared to right at 250 Hz. High-frequency moderate sensorineural hearing loss is bilateral.

A

B

C

associated with the migraine symptoms, which became milder. Her physical examination findings were normal and the results of her workup are summarized in the Table. There was a mild bilateral sensorineural hearing loss at 500 and 1,000 Hz. Results of ENG were normal.

Patient 12 was a 51-year-old man who was a first-degree cousin of the index patient. When he was 17 years old, he started having migraine symptoms (headache, scotomas, hemianopsia). When he was 25 years old, he had bilateral tinnitus, hearing loss, and vertigo associated with the migraine symptoms for the first time. Since then, he has had Meniere's syndrome attacks associated with moderate migraine episodes. His workup is summarized in the Table. He had bilateral moderate sensorineural hearing loss in the high frequencies, associated with a mild sensorineural hearing loss in the lower frequencies in his left ear (Fig 2C). The ENG results showed bilateral hyperactive labyrinths.

DISCUSSION

Meniere's syndrome is a clinical diagnosis based on the presence of the classic Meniere's triad. This triad was present in 12 of the 19 patients (63%) studied in this family. Findings on ENG were compatible with the clinical diagnosis in 7 of the 10 patients who were tested (hyperactive labyrinth unilaterally or bilaterally). Audiometry showed high-frequency sensorineural hearing loss in the index patient and several other members of the family. This is probably due to associated presbycusis and acoustic trauma (high-speed drill used by the index patient). In 3 cases, low-frequency sensorineural hearing losses were demonstrated, and they are compatible with the diagnosis of Meniere's syndrome. Since most audiometric tests were performed when the patients were asymptomatic, the low incidence of low-frequency sensorineural hearing loss is acceptable. The glycerol test was positive in the index patient and further contributes to documenting the diagnosis of Meniere's syndrome. Ideally, all the patients should have had the glycerol test and electrocochleography in order to establish the diagnosis of Meniere's syndrome definitively. However, these patients were asked to participate in the study, and many of them would not consent to an invasive procedure (electrocochleography) or would not take the time for a long glycerol test to be performed. We do believe, however, that it is reasonable to accept the diagnosis of Meniere's syndrome on the basis of the workup performed. The laboratory test findings were all normal, and these results contribute to ruling out metabolic causes for the symptoms.

Figure 1 shows the pedigree of this family. This Figure makes clear the autosomal dominant pattern of genetic transmission for both the Meniere's syndrome and the migraine symptoms. As in the families described before,[1-3,6] most cases are bilateral, with some patients having worse symptoms on one side. The high incidence of headache associated with Meniere's syndrome has been noted before,[1,2,5,6] but never before has this headache been clearly characterized as migrainous. We specifically sought this characterization with our standard questionnaire. There were scotomas associated with headache in 12 of 19 cases (63%), and several degrees of anopsia in 6 of 19 cases (31%). Paresthesias were present in 4 of 19 patients (21%). The characteristics of the headache described by the patients were also compatible with migraine. It is therefore reasonable to accept that this family has Meniere's syndrome and migraine transmitted as autosomal dominant traits.

Two patients (patients 5 and 7) had migraine symptoms only. Two patients (14 and 19) had headache that was clinically categorized as migraine without other migraine symptoms. Two others started out early in life with migraine symptoms and later developed Meniere's syndrome (patients 4 and 12). They were described in detail to demonstrate the evolution of migraine (of central origin) to Meniere's syndrome (peripheral origin). The presence of both migraine and Meniere's syndrome in all but 4 patients, as well as the progress of migraine to Meniere's syndrome in 2 patients, strongly suggests a common autosomal dominant genetic determinant for both conditions in this family.

While the association of Meniere's syndrome and migraine is clearly established in this large family, the pathophysiologic mechanism for this association is unclear at this time. However, the following hypothesis deserves further investigation.

Some authors have postulated a central cause for idiopathic Meniere's syndrome (Meniere's disease).[5,7-9] An initial vascular change in the central nervous system would cause migraine initially and later affect the microcirculation of the inner ear by means of the autonomic nervous system. In this way, the inner ear fluid balance would be disturbed, provoking endolymphatic hydrops and the peripheral symptoms (Meniere's syndrome). The occurrence in this family of migraine that was associated with vascular dysfunction in the central nervous system and Meniere's syndrome with a common autosomal dominant genetic determinant certainly favors this line of thinking. In 2 patients (patients 4 and 12), migraine was present for some years before the Meniere's syndrome manifested itself. A continuum process from migraine (central cause) to Meniere's syndrome (peripheral cause) is certainly suggested by these cases.

If, as Oliveira and Braga[6] suggested in 1992, idiopathic Meniere's syndrome (Meniere's disease) is no different from its hereditary counterpart and has a sporadic genetic determinant, then the above outlined reasoning also applies to Meniere's disease. The final answer to this question will be found at the molecular genetics level.

Recently, Gottslich et al[10] found that 22% of patients with bilateral rapidly progressive sensorineural hearing loss and 30% of Meniere's disease patients had antibodies that reacted with a 68 kd antigen present in bovine inner ear material. Billings et al[11] have provided evidence linking this 68 kd antigen to heat shock protein 70 (HSP 70). Harrison et al[12] demonstrated that functional genes encoding HSP 70 map to human chromosomes 6, 14 (HSPA 2; 140560), and 21 (HSPA 3; 140570) and at least one other chromosome. Sargent et al[13] demonstrated a duplicated HSP 70 locus between the complement and tumor necrosis factor genes within the human major histocompatibility complex 12 kilobase apart from each other and 92 kilobase telomeric of C2 gene. On chromosome 14 the localization was 14q22-q24. Both these regions contained fragile sites. Considering the presence of antibodies that react with HSP 70 antigen in the sera of patients with rapidly progressive (autoimmune) sensorineural hearing loss and Meniere's disease, and the fact that HSP 70–encoding genes are found in the region of the human major histocompatibility complex, the possibility that Meniere's disease is an autoimmune genetically determined disease certainly must be investigated. Furthermore, HSP 70 loci would be good candidates to harbor abnormalities that lead to Meniere's disease.

CONCLUSIONS

1. There is a clear association between migraine and Meniere's syndrome in the family we described. Furthermore, both appear to be transmitted by a common autosomal dominant genetic determinant. How the migraine (central) symptoms are related to Meniere's syndrome (peripheral) is not known at the present time.

2. It is important to determine how often migraine is associated with idiopathic Meniere's syndrome (Meniere's disease) as well. If the headache associated with Meniere's disease[5] is indeed migraine, then a sporadic

genetic determinant is likely to be present in this disease. This can be easily accomplished by asking appropriate questions of all Meniere's disease patients. Most of them will not give this information spontaneously.

REFERENCES

1. Brown MR. Meniere's syndrome. Arch Neurol Psychiatry 1941;46:561-5.

2. Brown MR. The factor of heredity in labyrinthine deafness and paroxysmal vertigo (Meniere's syndrome). Ann Otol Rhinol Laryngol 1949;58:665-70.

3. Bernstein JM. Occurrence of episodic vertigo and hearing loss in families. Ann Otol Rhinol Laryngol 1965;74:1011-21.

4. Konigsmark BW, Gorlin RJ. Genetic and metabolic deafness. Philadelphia, Pa: WB Saunders, 1976:7-48.

5. Dolowitz DA. Meniere's — an inner ear seizure. Laryngoscope 1979;89:67-77.

6. Oliveira CA, Braga AM. Meniere's syndrome inherited as an autosomal dominant trait. Ann Otol Rhinol Laryngol 1992; 101:590-4.

7. Williams HL Jr. A review of the literature as to the physiologic dysfunction of Meniere's disease: a new hypothesis as to its fundamental cause. Laryngoscope 1965;75:1661-89.

8. Gelhorn E. Autonomic imbalance and the hypothalamus. Minneapolis, Minn: University of Minnesota Press, 1957:300.

9. Torok N. Etiology as a guide in the management of Meniere's disease. Laryngoscope 1982;92:237-8.

10. Gottslich S, Billings PB, Keithley EM, Weisman MH, Harris JP. Assessment of serum antibodies in patients with rapidly progressive sensorineural hearing loss and Meniere's disease. Laryngoscope 1995;105:1347-52.

11. Billings PB, Keithley EM, Harris JP. Evidence linking the 68 kilodalton antigen identified in progressive sensorineural hearing loss patient sera with heat shock protein 70. Ann Otol Rhinol Laryngol 1995;104:181-8.

12. Harrison GS, Morinoto R, Kao FT, Chu EHY, Drabkin H. Chromosomal location of human genes encoding the major heat shock protein HSP70 [Abstract]. Am J Hum Genet 1986;39:A157.

13. Sargent CA, Dunham I, Trowsdale J, Campbell RD. Human major histocompatibility complex contains genes for the major heat shock protein HSP70. Proc Natl Acad Sci U S A 1989; 86:1968-72.

≈

TWENTIETH ANNUAL MEETING OF THE BÁRÁNY SOCIETY

The Twentieth Annual Meeting of the Bárány Society will be held in Würzburg, Germany, September 20-23, 1998. For more information, contact the Local Organizing Committee, Institute of the 4-G-F, Kurhausstrasse 12, D 97688 Bad Kissingen, Germany; telephone 0049/971-64832; fax 0049/ 971-68637.

Ann Otol Rhinol Laryngol 106:1997

PERILYMPHATIC FISTULA: A WASHINGTON, DC, EXPERIENCE

DENNIS C. FITZGERALD, MD

PAMELA GETSON, PHD   CYNTHIA O. BRASSEUX, MA

WASHINGTON, DC

One hundred ninety-seven patients who underwent surgical repair for a presumed unilateral perilymphatic fistula were reviewed. Of those patients, 87% with vestibular symptoms reported complete or near-complete relief of their symptoms. Forty percent of the patients with sudden hearing loss had an improvement in their hearing levels. An analysis of several diagnostic tests revealed their sensitivity and specificity ratings. A review of the patients' operative records showed a marked disparity between the visual identification of an actual fluid leak during surgery and their postoperative outcome. This review supports the premise that at the present time, the patient's surgical outcome is the best way of documenting a successfully repaired perilymphatic fistula.

KEY WORDS — diagnostic tests, ear surgery, ear trauma, perilymphatic fistula.

INTRODUCTION

Perilymphatic fistulas (PLFs) are abnormal connections between the perilymphatic fluid spaces of the inner ear and another space, most commonly the middle ear. These PLFs are usually either tears in the ligamentous attachments of the stapedial footplate to the bone of the oval window (OW) or in the round window (RW) membrane. Other abnormal connections have been identified, but are much less commonly reported.[1,2] The causes of a PLF are multiple, including stapedectomy,[3,4] head or ear trauma,[5-7] diving,[8] flying,[9] surgery for chronic otitis media,[10] Valsalva-like exertion,[7,11] general anesthesia,[7,12] acoustic trauma,[13] and congenital PLF.[7,14-18]

The diagnostic tests for establishing a PLF were first well outlined and evaluated by Singleton et al[19] in 1978. Their suspicion of a PLF was raised by a history of trauma or exertion with associated hearing loss or positional vertigo. The presence of a mild, nonfatiguing positional nystagmus with the affected ear undermost was closely correlated with a PLF. A positive "objective" fistula test — eye deviation produced by positive and negative pressure applied to the ear — was often not present. When present, it strongly implied the presence of a PLF. In time, tests other than the audiometric examination and electronystagmography (ENG) became available to aid in diagnosing a PLF: the ENG fistula test,[20] the platform fistula test (PFT),[21] and electrocochleography (ECochG).[22-24] Although a treatment of initial bed rest and then surgical repair of the RW and OW if symptoms persist has been relatively well accepted, firm guidelines for the diagnosis of this disorder have been elusive.

This review outlines experience with PLF patients that has evolved over the past 9 years. Much remained the same over this period, but just as much changed. Indications for this relatively simple operation have been enlarged as experiences with certain "outlying" patients proved that too strict a set of indications was causing patients to be sent home with treatable problems. Some tests were dropped, while others were added. This proved somewhat of a problem in an analysis of their specificity and sensitivity, since not all patients had all tests. Sometimes, injuries prevented certain tests, as did financial limitations. Nonetheless, though, we gained certain insights through listening to the patients' problems, treating these patients, and evaluating the outcome of that treatment.

SUBJECTS

A retrospective review was made of 197 patients, seen between August 1982 and June 1991, who underwent a unilateral PLF repair. During this period, 22 bilateral cases were treated. Additionally, 47 patients had a history compatible with typical Meniere's disease as well as a positive fistula test (subjective fistula test [SFT] and/or PFT) or abnormal ECochG results; none of these will be reported here. Subjects ranged in age from 4 to 75 years. The duration of symptoms prior to surgery ranged from 1 day to 40 years, with a median duration of 3.1 years. Of the 197 unilateral cases, 74 (38%) had direct head or ear trauma, 27 (14%) had barotrauma, 26 (13%) had an event of increased intracranial pressure (ICP), and

---

From the Department of Otology/Neurotology, Washington Hospital Center, and the Department of Otolaryngology–Head and Neck Surgery, Georgetown University Medical Center (Fitzgerald), the Department of Pediatrics, George Washington University Medical Center (Getson), and the Department of Biostatistics, Children's National Medical Research Institute (Getson, Brasseux), Washington, DC.

CORRESPONDENCE — Dennis C. Fitzgerald, MD, Washington Hospital Center, POB — 106 Irving St NW, Ste 417, Washington, DC 20010.

TABLE 1. CHIEF COMPLAINT

*Chief Complaint**	*Patients (n = 197)* *No.*	*%*
Sudden hearing loss	48	24
Vertigo or balance disturbance	171	87
Fluctuating hearing	22	11
Tinnitus	50	25
Aural fullness	41	21

*Patients may have presented with more than one chief complaint.

70 (36%) had an undetermined event (patient was unable to remember any specific event or incident prior to onset of symptoms).

METHODS

Patients' symptoms were assessed and categorized by the following chief complaints:

1. Sudden hearing loss (SHL) — A change of hearing of at least 30 dB sensorineural loss in 3 contiguous test frequencies within 3 days. Usually, the patient presents to the physician with a clear understanding that something has happened to the ear, and pre-event audiograms are rarely available for comparison.
2. Fluctuating hearing loss (FHL) — A condition similar to SHL, but audiograms show recurrent recovery and loss patterns on successive tests. This can be evident in both pure tone and speech audiometry. The patient also notices a fluctuation in hearing levels.
3. Balance disturbance — Motion intolerance and disturbance when ambulating.
4. Vertigo — Any disturbance in spatial orientation resulting in the illusion of movement. These patients also may have noted a balance disturbance or motion intolerance.
5. Tinnitus — The perception of sound in the absence of an external stimulus.
6. Meniere's disease symptom complex — The combination of unexplained episodic vertigo, fluctuating hearing, tinnitus, and aural fullness.

A combination of vertigo and balance disturbance (87%) was the most commonly cited chief complaint, followed by tinnitus (25%) and SHL (24%; Table 1).

Indications For Surgery. Patients presenting with vestibular symptoms, SHL, FHL, or progressive hearing loss were all suspects for a PLF. A detailed questionnaire was obtained on all patients presenting with vestibular symptoms. An extensive history of the present illness was taken, with particular emphasis on the circumstances surrounding the 24 hours preceding the onset of the initial symptoms (vestibular and auditory) and the progression of these symptoms. Care was taken to ask for events that exacerbate the symptoms, such as diving, air travel, physical straining, trauma, motion, etc.

An office examination was routinely administered, including an SFT performed as follows: the patient was seated in a chair and a Bruening pneumatic otoscope (Storz-Bruening, Storz Instrument Co, St Louis, Mo) was placed into the ear canal with an airtight seal. The patient was asked to stare at an object on the opposite wall. Erratic increases and decreases in the external canal pressure were applied 6 to 10 times in each ear, never exceeding 120 mm Hg, and the response to the question, "Does that bother you?" was noted. A positive test was recorded if the patient reported the object on the wall moving, a sensation of himself or herself moving, or nausea. A response of pain, pressure, or increased tinnitus was recorded as negative, as was a report of no sensation at all. A tandem Romberg test was routinely performed, with special attention to the side to which the patient fell when the eyes were shut.

All patients suspected of having a PLF had air-bone and speech audiometry, with tympanometry if possible. Most patients also had standard ENG. Some had an ENG fistula test. When the ECochG became available in our testing facility in 1985, this became a standard preoperative test, as did platform posturography with the PFT when it became available. These platform tests were performed in a freestanding vestibular laboratory. The testing was performed on Neurocom Equitest A100100 equipment (Neurocom International, Clackamas, Ore). Software for sensory and motor tests was Equitest 4.03; PFT software was Neurocom Pressure Test V1.12.

The patient was asked to stand on the force-plates with eyes closed. The sway reference gain was set at 1.00. Ten trials of 0 pressure, −300 decapascals (dPa), and +300 dPa were conducted with the nonsuspect ear tested first. Pressure was applied through a hermetically sealed ear tip at a rate of 450 dPa/s. Once the selected pressure was achieved, it was immediately released.

The largest sway amplitude during 0 pressure for anteroposterior and lateral sway was selected, and its own standard deviation was added. The largest amplitude during the positive and negative pressure tests was chosen, and its own standard deviation was subtracted. If the number from the positive or negative test was greater than the control number, the response was scored as positive, since it was greater by more than two standard deviations. Rotational chair testing was rarely used. Computed tomography (CT) scans of the temporal bones were ordered primarily in children and teenagers when a congenital malformation was suspected because of clinical setting or history. Gadolinium magnetic resonance imaging (MRI) of the head became part of the workup in July 1988 and, on occasion, showed interesting enhancement of the inner ear.[25] The only postoperative test performed on every patient was audiometry, but many had postoperative SFTs, especially in the later years of the study.

As would be expected, such problems as tympanic membrane perforations, trauma, and infections, along with financial limitations, precluded some patients from having all diagnostic tests. In the postoperative period, many tests were repeated if the patients' symptoms persisted or recurred.

Following the history, physical examination, and diagnostic tests, the etiology, pathology, and natural history of PLFs were described to the patient, as well as the surgical risks, possible complications, and alternative treatments for PLF. Medical literature on the subject was commonly given to the patient to be read at home. In general, the criteria used in advising a patient to have surgery were as follows: 1) trauma (head, whiplash, barometric, increased ICP) resulting in a persistent vestibular disturbance and/or a nonimproving sudden hearing loss and 2) presence of auditory or vestibular complaints with a positive fistula test (SFT or PFT). Finally, the patient made the decision to have the surgery.

Surgical Procedure. In the absence of medical and psychological contraindications, surgery was performed under general anesthesia, with special attention given to ensuring an atraumatic emergence from the anesthesia. Operations were performed transcanal, unless an endolymphatic shunt was to be done at the same time, in which case the middle ear was approached through the postauricular incision. The initial approach, upon first entering the middle ear, was to spend considerable time inspecting the RW and OW niches. With time and experience, however, it was found that leaks could not be identified until after the lysing of mucosal adhesions and scar tissue. Only twice were "blebs" of fluid seen in a submucosal plane anterior to the OW niche. No "holes" were found in the annular ligament unless the ear had sustained direct trauma with dislocation of the stapes. In one subject, the footplate (congenitally fixed) was found to be cracked following a waterskiing accident. No holes or tears in the RW membrane were ever identified.

Annular bone removal was done with a curette rather than a drill to avoid confusion of the inspection process by irrigation procedures. Special methods to help increase the identification of perilymph leakage were not done. After the inspection process was complete, both windows were routinely packed regardless of the visual identification of a perilymph leak. Tragal perichondrium was used almost exclusively, unless the postauricular approach was used, and then temporalis fascia was used as the graft material. Grafts were covered with plain Gelfoam for the first 127 patients, but fibrin glue was added to the Gelfoam for the last 62 patients. Gelfilm was placed under the tympanic membrane to reduce the chance of adhesions to the ossicles or tissue grafts, and the ear canal was filled with antibiotic ointment.

The patient was kept in the hospital overnight. Upon discharge, he or she was instructed to stay home for 3 days and strictly warned not to do any lifting or undergo physical exertion. After 3 days, patients could go back to school or work, but were advised to lift nothing heavier than 10 lb (4.5 kg), and to avoid engaging in any sports. Flying was permitted after a week. At the 1-month postoperative visit, the ear was cleaned, and an audiogram and an SFT were performed. Patients were advised to avoid contact sports, weight lifting, and diving (water and sky). If symptoms persisted, care was extended for continued observation, revision surgery, or secondary treatment as explained below.

Methods of Determining Surgical Outcome. An individual having a positive surgical outcome for at least one chief complaint was considered to have had a PLF. To demonstrate a positive surgical outcome, an individual had to exhibit at least one of the following conditions.

1. Present with SHL as a chief complaint, and demonstrate improved postoperative hearing meeting the following criteria[26]: improvement greater than 10 dB on pure tone average (500 Hz, 1 kHz, 2 kHz), and improvement greater than 15% on speech discrimination.
2. Present with a balance disturbance or vertigo as a chief complaint and demonstrate a total or near-total postoperative improvement in vestibular disturbance.[15]

Test Results and Sensitivity and Specificity. Results of the vestibular and auditory tests are given in Table 2. Diagnostic tests were evaluated for their sensitivity and specificity according to the following criteria (Table 3).

Sensitivity was defined as percent positivity in the presence of disease.

TABLE 2. RESULTS OF VESTIBULAR AND AUDITORY TESTS

Test	*No. Tested*	*No. Abnormal*	*% Abnormal*
Tandem Romberg	162	123	76
Subjective fistula	185	92	50
ENG	134	76	57
Positional tests and/or reduced vestibular response			
ENG fistula	49	10	20
Turning	19	14	74
Platform posturography	41	10	24
Platform fistula	83	41	49
Audiogram	197	122	62
CT scan	44	2	5

ENG — electronystagmography, CT — computed tomography.

$$\text{Sensitivity} = \frac{\text{true positives}}{\text{all sick subjects}} \times 100$$

where true positives were the number of patients who underwent a PLF repair and had a positive outcome according to criteria presented above and had an abnormal test result, and "all sick subjects" were the number of patients who underwent a PLF repair and had a positive outcome.

Specificity was defined as percent negativity in the absence of disease.

$$\text{Specificity} = \frac{\text{true negatives}}{\text{all subjects free of disease}} \times 100$$

where true negatives were the number of patients who underwent a PLF repair and had a negative outcome and a normal test result, and "all subjects free of disease" were the number of patients who underwent a PLF repair and had a negative outcome.

RESULTS

Only 55 (28%) of the 197 patients who underwent a PLF repair had definite fluid leaks noted during surgery. Those patients who had leaks noted are correlated to surgical outcome in Table 4. Chief complaints and causes correlated to leak sites appear in Tables 5 and 6.

TABLE 3. DIAGNOSTIC TESTS' SENSITIVITY AND SPECIFICITY

Test	*No.**	*Sensitivity %*	*Specificity %*
Tandem Romberg	162	75	19
Subjective fistula	185	53	69
Platform fistula (pressure)	83	51	63
Platform posturography (sensory and motor)	41	61	30
Abnormal ENG	159	45	38
ENG fistula	49	18	50
ECochG	77	21	90

ENG — electronystagmography, ECochG — electrocochleography.

*Number of operated patients who underwent these tests preoperatively.

TABLE 4. LEAK SITE AND SURGICAL OUTCOME

	Oval Window		*Round Window*		*Both*	
	No.	*%*	*No.*	*%*	*No.*	*%*
PLF repairs	32/197	16	18/197	9	5/197	2
Positive surgical outcome	29/32	91	18/18	100	3/5	60

PLF — perilymphatic fistula.

Of the 197 unilateral cases operated on for a suspected PLF, 86% (170/197) demonstrated a positive outcome. Symptoms were alleviated by surgery for 87% (149/171) of those having vertigo or balance disturbance as a chief complaint. Of those with a chief complaint of SHL, 40% (19/48) demonstrated a positive outcome. Those with chief complaints of FHL demonstrated positive outcomes of 100% (22/22). The surgical outcome was the same for those patients with the causes direct trauma, barotrauma, and undetermined cause, but those with increased ICP causes had a lower rate of positive results (Table 7). Follow-up periods for assessing surgical outcomes ranged from 2 to 96 months with a median of 12 months. (See Table 8 for duration of hearing loss in SHL patients compared to surgical outcome.)

Complications included 4 cases (2%) of mild conductive hearing loss and 5 (3%) of mild sensorineural hearing loss. Twenty-six patients had a positive postoperative SFT; of those, 88% (23/26) had a positive outcome. Of 79 patients with a positive preoperative SFT, 29% (23/79) had a positive postoperative SFT, and 71% (56/79) had a negative postoperative SFT.

DISCUSSION

Most important to this discussion is the fact that contrary to most reports on PLF, *our* definition of the presence of a proven PLF was based on a positive surgical outcome — not on the visual or chemical identification of a perilymph leak during surgery. This decision was prompted by the fact that only 28% (55/197) of patients with unilateral problems

TABLE 5. CHIEF COMPLAINT AND LEAK SITE

		OW		*RW*		*Both*	
	No.	*No.*	*%*	*No.*	*%*	*No.*	*%*
Sudden HL	48	6	13	7	15	2	4
Vertigo or BD	171	30	18	14	8	5	3
Fluctuating HL	22	3	14	4	18	0	0

OW — oval window, RW — round window, HL — hearing loss, BD — balance disturbance.

TABLE 6. LEAK SITE AND CAUSE

	No. With	*OW*		*RW*		*Both*	
Cause	*Leak*	*No.*	*%*	*No.*	*%*	*No.*	*%*
Direct head or ear trauma (n = 74)	18	13	72	4	22	1	6
Barotrauma (n = 28)	8	4	50	3	38	1	13
Increased ICP (n = 26)	8	5	63	2	25	1	13

OW — oval window, RW — round window, ICP — intracranial pressure.

TABLE 7. SURGICAL OUTCOME

Cause	*No.*	*Positive*	*Negative*
Undetermined	70	83%	17%
Trauma	74	93%	7%
Barotrauma	27	96%	4%
ICP	26	69%	31%

ICP — intracranial pressure.

were identified during surgery as having a visible perilymph leak, yet 86% (170/197) of the patients reported a positive outcome (all explored ears had the OW and RW patched). A positive outcome for vestibular symptoms could not be explained on any basis other than a successfully repaired PLF (or possibly a placebo effect). Considering that the median duration of vestibular symptoms was 3 years, spontaneous recovery was highly unlikely. For specifically those patients with a chief complaint of SHL, the median duration of symptoms until surgery was 7½ weeks. It has been the first author's experience in managing hundreds of patients with SHL with causes other than PLF that if it occurs, spontaneous improvement begins within the first 2 weeks after onset. None of these patients had shown any sign of improvement by the 2-week mark and, thus, probably would not have had any spontaneous improvement if they had been left alone and not operated upon. Some patients operated on as late as 5 months postonset still had hearing improvement recorded, but none of the 15 patients operated upon after 5 months' duration showed any hearing improvement. Thus, patients with an SHL more than 5 months earlier have almost no chance of improvement with a PLF repair.

Diagnostic Tests. We used a successful outcome as *the* positive indicator of a PLF to look at the strengths of our diagnostic tests. The ENG fistula tests were proven to be of little value because of their low sensitivity (18%). The tandem Romberg test and platform posturography were high in sensitivity but not very specific for a PLF. The ECochG was relatively low in its sensitivity but high in its specificity for borderline-abnormal results. The ECochG results (from canal electrodes) were either normal or borderline-abnormal, with a summating potential–action potential (SP/AP) ratio of 0.40 to 0.60 used as the criterion for a borderline-abnormal test result. Slightly different parameters have been used in previous studies applying ECochG to the diagnosis of a PLF.[22-24] Rarely did a patient in this group have an SP/AP ratio greater than 0.60. If so, this was interpreted as primary Meniere's disease, or at least as a significant secondary endolymphatic hydrops.[24] This finding placed the patient in the MDSC group not reported here. The SFT was moderately sensitive (53%) and highly specific (69%), and the PFT was equally sensitive and specific. Both fistula tests had a predictive value of a positive test in the range of 80%, according to the definition of predictive value of (+) = true positives/(true positives + false positives) × 100. We continue to perform the audiogram, ECochG, tandem Romberg, SFT, ENG, and PFT on all PLF suspects.

Eighty-two patients had *both* an SFT and a PFT performed preoperatively. Of these 82 patients, 74 (90%) had a positive surgical outcome, implying a PLF. Of these 74 patients with a PLF, 46 (62%) had a positive SFT, and 38 (51%) had a positive PFT, but only 26 (35%) patients had *both* a positive SFT and a positive PFT. Of interest, 14 of 34 (41%) with

TABLE 8. DURATION OF HEARING LOSS IN SUDDEN HEARING LOSS PATIENTS RELATED TO SURGICAL OUTCOME

Duration of Hearing Loss	*Patients With Hearing Improvement*	*Patients Without Hearing Improvement*
2 wk	5	5
3 wk	4	1
4 wk	3	1
5 wk	1	
6 wk	1	
7 wk	1	2
2 mo	1	2
3 mo	2	
4 mo	1	1
5 mo	1	2
6 mo		2
7 mo		1
8 mo		1
9 mo		1
10 mo		1
12 mo		2
18 mo		1
2 y		2
4 y		2
6 y		1

a negative SFT had a positive PFT, and 21 of 41 (51%) with a negative PFT had a positive SFT. This implies that both tests were needed to maximize the identification of patients with a PLF.

In general, there is no absolutely sensitive and specific test for a PLF, as many patients had positive outcomes even when all objective test results were normal.

Surgical Findings. Since the visual identification of a perilymphatic leak is extremely subjective and can be influenced by different adjunctive measures such as Trendelenburg position, forced and/or sustained inspirations, and multiple observers, the "hit rate" of positive visualization will continue to be widely variable even if strictly consistent criteria for surgery are followed.

A national survey showed a median "hit rate" of 50%.[27] For these reasons, a slightly more objective standard is proposed to measure sensitivity and specificity values for diagnostic tests and surgery "hit rates." This standard is the postoperative improvement in vertiginous symptoms (subjective), or improvement in hearing levels after SHL or stabilization of progressive hearing loss and/or FHL (objective). These two parameters could be much more consistently reported than dependence on visualization of a few microliters of clear fluid in a bloody surgical field in the middle ear. Moreover, visualized clear fluid may be serum, mucosal fluids, local anesthetic, or even irrigating fluid used during drilling. Many authors (including ourselves) have observed an impressive rate of improvement in symptoms after both windows were patched, even when a specific leak was not identified. This has been attributed to minute leaks[28] (the most likely cause), intermittent leaks,[29] cochlear membrane leaks with spontaneous healing,[30] and even a placebo effect.[31] The placebo effect in PLF surgery has been discussed, but to date, no published trials exist. The only reference to published statistics involves trials with pain medication, and this has little application to the possible placebo effect of a surgical procedure.

Positive surgical outcomes were interpreted in this study as a successfully repaired PLF, since no other disorder of the inner ear is known to respond positively to patching the OW and RW.

The relationship of a predisposition to development of a PLF to an effaced RW membrane remains questionable. Nomura's[32] thorough article on the variations in the architecture of the RW niche clearly showed effacement to occur in at least 25% of normal temporal bones. In addition, mesenchymal tissue in the niche was very common and could be mistaken for scarring or even holes in the RW membrane. This finding was supported by temporal bone studies of Stewart and Belal.[33]

The issue of mild congenital malformations, given so much prominence by Supance and Bluestone,[16] has yet to be emphasized by any other authors, and so also stands to be corroborated by future articles. Our intraoperative findings relative to site of leak and event showed an interesting correlation. All types of trauma caused more OW leaks (Table 6). Regardless of the leak site, the surgical outcome remained the same (Table 4). The other interesting correlation is between the major symptoms and the leak site. As this series contained many more patients with vertigo than hearing loss, there were more OW leaks than RW leaks. Anatomically, this makes sense, since an OW leak would more likely disturb the contents of the vestibule (ampullae of the semicircular canals and maculae of the utricle and saccule), whereas an RW leak would more likely disturb the contents of the cochlea (Table 5).

Revision Surgery. Of the 197 unilateral cases, only 12 patients (6.1%) underwent revision surgery. Only 1 patient underwent more than one revision on a particular ear, since nearly all revisions brought about a satisfactory resolution of the symptoms. This is not to imply that the postoperative course of the majority of PLF patients was straightforward. On the contrary, there were many different scenarios. The most satisfying situations were in the patients who had been experiencing continuous vertigo preoperatively but who awoke from surgery with immediate, complete relief of their symptoms. This occurred not infrequently, but far from commonly. In fact, a full month was usually required before judgment could be passed on the outcome of the surgery for vertiginous symptoms. There was the rare patient who eventually cleared beyond the 1-month postoperative period.

A few patients had preoperative symptoms typical of the PLF patient, with a balance disturbance and motion intolerance, and then postoperatively developed episodic whirling vertigo typical of Meniere's disease. This was first alluded to by House[4] in 1967 in relation to his poststapedectomy patients, but was elucidated further by Potter and Conner[34] in 1983. They felt that these patients had undergone a successful closure of a PLF, but were then experiencing symptoms of exacerbated secondary Meniere's disease in the postoperative period. In the present series, these few postoperative patients were managed in exactly the same way as a primary Meniere's disease patient would be handled, ie, 3 months of treatment with a diuretic, niacin, and a vestibular suppressant, and if this failed, an endolymphatic shunt. Two patients in this series went on to have shunts performed for control of secondary Meniere's disease vertigo. These were counted not as revisions, but as secondary treatment. One of these patients eventually needed a retrolabyrinthine vestibular nerve section before her symptoms were controlled.

Preoperative Surgical Indicators. Most authors who have written on the subject of PLF have expressed frustration in attempting to establish a set of indications for surgery on suspected PLFs. They have emphasized the entire complex of history, physical examination, diagnostic tests, and the patient's informed consent. Some authors have emphasized certain diagnostic tests, such as the positional tests and eyes-closed turning test,[35] fistula tests (SFT,[15,29,36,37] ENG,[20] PFT[38]), ECochG,[22,24] dehydrating tests,[39] and positional audiometry,[40] as having significant sensitivity and specificity in the diagnosis of PLF. The value of some of these tests is supported in national surveys on the subject[27,41] and in the present series.

After working with these 197 patients and analyzing the data in this report, we developed certain diagnostic maxims that, when followed, lead to a high incidence of positive surgical results:

1. Ask for *specific details* about the 24-hour period prior to the onset of symptoms or exacerbation of chronic or recurrent symptoms (trauma, Valsalva's maneuver, barotrauma).
2. Beware of constant disequilibrium and motion intolerance, especially in younger patients.
3. Beware of SHL or vertigo in patients with preexisting sensorineural hearing loss or congenital temporal bone malformations.
4. Remember that PLFs can mimic primary Meniere's disease.
5. Trust a positive fistula test of any kind (SFT, objective fistula test, ENG, PFT).
6. Note that ECochG SP/AP ratios may be mildly abnormal secondary to PLFs.
7. Repair both OW and RW membranes in all explored ears.
8. Use the entire set of information (history, physical examination, and diagnostic tests) to decide on the appropriateness of a PLF repair, and involve the patient in the decision-making process.

CONCLUSION

With the described approach to recommending exploration and grafting of PLFs, 87% of patients improved, with minimal complications; this rate indicates that this approach was beneficial in this patient population. Diagnosis of PLF has not been perfected. Given the relatively safe nature of the surgery, exploration and grafting should be recommended when a complete evaluation has ruled out other causes of the patient's problem and tests and history point to a PLF diagnosis.

The situation should be carefully reviewed with patients so that they understand the basis of the recommendation and the risks and benefits of the procedure. Each surgeon should be aware of his or her outcomes, as they provide the best evidence of the accuracy of the particular approach to the problem. Further studies on both preoperative and intraoperative diagnostic techniques are required to increase the accuracy of diagnosis. Even with the present state of the diagnostic art, however, 87% of patients operated on in this series improved. Because outcome analysis is a potent tool for developing strategies to use with patients who present with the types of complaints described in this paper, surgeons should analyze these cases carefully and follow them closely to determine their outcomes, irrespective of whether the patient undergoes surgery.

REFERENCES

1. Kohut RI, Hinojosa R, Budetti JA. Perilymphatic fistula: a histopathologic study. Ann Otol Rhinol Laryngol 1986;95: 466-71.

2. Kamerer DB, Sando I, Hirsch B, Takagi A. Perilymph fistula resulting from microfissures. Am J Otolaryngol 1987; 8:489-94.

3. Hemenway WG, Hildyard VH, Black FO. Post stapedectomy perilymph fistulas in the Rocky Mountain area. Laryngoscope 1968;78:1687-715.

4. House PH. The fistula problem in otosclerosis surgery. Laryngoscope 1967;77:1410-26.

5. Grimm RJ, Hemenway WG, LeBray PR, Black FO. The perilymph fistula syndrome defined in mild head trauma. Acta Otolaryngol Suppl (Stockh) 1989(suppl 464):1-40.

6. Fee GA. Traumatic perilymphatic fistulas. Arch Otolaryngol 1968;88:477-80.

7. Strohm M. Trauma of the middle ear. Adv Otorhinolaryngol 1986;35:177-247.

8. Pullen FW. Perilymphatic fistula induced by barotrauma. Am J Otolaryngol 1992;13:270-2.

9. Pullen FW, Rosenberg GJ, Cabeza CH. Sudden hearing loss in divers and fliers. Laryngoscope 1979;89:1373-7.

10. Smyth GDL. Sensorineural hearing loss in chronic ear surgery. Ann Otol Rhinol Laryngol 1977;86:3-8.

11. Schuknecht HF, Witt RL. Suppressed sneezing as a cause of hearing loss and vertigo. Am J Otolaryngol 1985;6:468-70.

12. Segal S, Man A, Winerman I. Labyrinthine membrane

rupture caused by elevated intratympanic pressure during general anesthesia. Am J Otolaryngol 1984;5:308-10.

13. Narula A, Marks NJ. Acoustic trauma and perilymph fistula. J Laryngol Otol 1985;99:909-11.

14. Althaus SR. Spontaneous and traumatic perilymph fistulas. Laryngoscope 1977;87:364-70.

15. Seltzer S, McCabe BF. Perilymph fistula: the Iowa experience. Laryngoscope 1986;96:37-49.

16. Supance JS, Bluestone CD. Perilymph fistulas in infants and children. Otolaryngol Head Neck Surg 1983;91:663-71.

17. Pappas DG, Simpson LC, Godwin GH. Perilymphatic fistula in children with pre-existing sensorineural hearing loss. Laryngoscope 1988;98:507-10.

18. Phelps PD. Congenital cerebrospinal fluid fistulae of the petrous temporal bone. Clin Otolaryngol 1986;11:79-92.

19. Singleton GT, Post KN, Karlan MS, Bock DG. Perilymph fistulas. Diagnostic criteria and therapy. Ann Otol Rhinol Laryngol 1978;87:797-803.

20. Daspit CP, Churchill D, Linthicum FH. Diagnosis of perilymph fistula using ENG and impedance. Laryngoscope 1980; 90:217-23.

21. Black FO, Lilly DJ, Nashner LM, Peterka RJ, Pesznecker SC. Quantitative diagnostic test for perilymph fistulas. Otolaryngol Head Neck Surg 1987;96:125-34.

22. Arenberg IK, Ackley RS, Ferraro J, Muchnik C. ECOG results in perilymphatic fistula: clinical and experimental studies. Otolaryngol Head Neck Surg 1988;99:435-43.

23. Meyerhoff WL, Yellin MW. Summating potential/action potential ratio in perilymph fistula. Otolaryngol Head Neck Surg 1990;102:678-82.

24. Gibson WPR. Vertigo associated with trauma. In: Dix MR, Hood JD, eds. Vertigo. New York, NY: John Wiley & Sons, Ltd, 1984:373-89.

25. Mark AS, Fitzgerald DC. Segmental enhancement of the cochlea on contrast-enhanced MR: correlation with the frequency of hearing loss and possible signs of perilymphatic fistula and autoimmune labyrinthitis. AJNR Am J Neuroradiol 1993;14:991-6.

26. Pearson BW, Brackmann DE. Committee on Hearing and Equilibrium guidelines for reporting treatment results in Meniere's disease. Otolaryngol Head Neck Surg 1985;93:579-81.

27. House JW, Morris MS, Kramer SJ, Shasky GL, Coggan BB, Putter JS. Perilymphatic fistula: surgical experience in the United States. Otolaryngol Head Neck Surg 1991;105:51-61.

28. Kohut RI, Waldorf RA, Haenel JL, Thompson JN. Minute perilymph fistulas: vertigo and Hennebert's sign without hearing loss. Ann Otol Rhinol Laryngol 1979;88:153-9.

29. Shelton C, Simmons FB. Perilymph fistula: the Stanford experience. Ann Otol Rhinol Laryngol 1988;97:105-8.

30. Simmons FB. Theory of membrane breaks in sudden hearing loss. Arch Otolaryngol 1968;88:41-8.

31. Rizer FM, House JW. Perilymph fistulas: the House Ear Clinic experience. Otolaryngol Head Neck Surg 1991;104: 239-43.

32. Nomura Y. Otological significance of the round window. Adv Otorhinolaryngol 1984;33:1-155.

33. Stewart TJ, Belal A. Surgical anatomy and pathology of the round window. Clin Otolaryngol 1981;6:45-62.

34. Potter CR, Conner GH. Hydrops following perilymphatic fistula repair. Laryngoscope 1983;93:810-2.

35. Singleton GT. Diagnosis and treatment of perilymph fistulas without hearing loss. Otolaryngol Head Neck Surg 1984; 94:426-9.

36. Thompson JN, Kohut RJ. Perilymph fistulae: variability of symptoms and results of surgery. Otolaryngol Head Neck Surg 1979;87:898-903.

37. Love JT Jr, Waguespack RW. Perilymphatic fistulas. Laryngoscope 1981;91:1118-28.

38. Black FO, Pesznecker S, Norton T, et al. Surgical management of perilymph fistulas. Arch Otolaryngol Head Neck Surg 1991;117:641-8.

39. Lehrer JF, Poole DC, Sigal B. Use of glycerin test in the diagnosis of post-traumatic perilymphatic fistulas. Am J Otolaryngol 1980;1:207-10.

40. Flood LM, Fraser JG, Hazell JW, Rothera MP. Perilymph fistula: four year experience with a new audiometric test. J Laryngol Otol 1985;99:671-6.

41. Hughes GB, Sismanis A, House JW. Is there consensus in perilymphatic fistula management? Otolaryngol Head Neck Surg 1990;102:111-7.

Ann Otol Rhinol Laryngol 106:1997

VESTIBULAR AND OPTOKINETIC FUNCTION IN THE NORMAL GUINEA PIG

JAMES C. ANDREWS, MD
LOS ANGELES, CALIFORNIA
SUMIKO KOYAMA, MD
TOKYO, JAPAN

JUNE LI, PHD
LOS ANGELES, CALIFORNIA
LARRY F. HOFFMAN, PHD
LOS ANGELES, CALIFORNIA

Vestibular and optokinetic function was quantitatively studied in the normal guinea pig through investigation of the vestibulo-ocular reflex (VOR), optokinetic nystagmus (OKN), and the visual vestibulo-ocular reflex (VVOR) by means of sinusoidal stimulation with a computer-controlled rate table (VOR and VVOR) or an optokinetic drum. The VOR exhibited high-pass filter characteristics with steady state gain achieved at 0.125 Hz. The maximum gain was 0.55 at a velocity of 60°/s. The VOR was modeled by a transfer function with best fits obtained with an adaptation time constant of 12.5 seconds. The OKN showed low-pass filter characteristics with a decrease in gain for increase in stimulus amplitude. The maximum gain measured was 0.64. A fractional pole model provided a fit of these data. The VVOR exhibited a mean gain of between 0.6 and 0.7 across the stimulus bandwidth and peak velocities. A model based on a linear combination of the actual OKN and VOR gains provided an estimate of the VVOR gain.

KEY WORDS — guinea pig, modeling, optokinetic nystagmus, vestibular function.

INTRODUCTION

The guinea pig has been frequently utilized as a subject for audiologic physiology studies and as a model for inner ear disorders. Although much research has been conducted on the auditory system, there is a paucity of information in this species in regard to its vestibular responses. This study was undertaken to document quantitative vestibulo-ocular reflexes (VORs) and optokinetic nystagmus (OKN) function in the normal guinea pig and as a prelude to parallel measurements to be made in pathologic subjects with experimental endolymphatic hydrops. The data were used to evaluate the horizontal VOR, OKN, and visual vestibulo-ocular reflex (VVOR) and their interactions as described for other species.

METHODS

Normal multicolored guinea pigs (750 to 1,000 g) underwent surgical implantation of a scleral search coil and electrical connector (for monitoring eye movement) and a cranial bolt (for head fixation). A mixture of ketamine hydrochloride (Ketalar, Parke-Davis, Morris Plains, NJ, 40 mg/kg) and xylazine hydrochloride (Rompun, Miles Laboratories, Shawnee, Kan, 8 mg/kg) was administered intramuscularly as an anesthetic and supplemented with lidocaine hydrochloride (Xylocaine, Astra Pharmaceuticals, Westborough, Mass) 1% as an analgesic for the skin incision. The conjunctiva was incised and the extraocular muscles were identified. A Teflon-coated multistranded stainless steel wire (AWG No. 38, Cooner AS632) was inserted between the extraocular muscles and the sclera for two turns around the globe and then brought through a superiorly directed subcutaneous tunnel to the dorsal skull. A sagittal incision was created centrally over the parietal region of the skull. All soft tissue, including the periosteum, was separated from the calvarium. Six stainless steel flat-head machine screws (No. 00-90 × 1/8 in) were inserted into holes created in the parietal bones with care to maintain the integrity of the underlying dura. Dental cement was used to secure a bolt to the previously placed screws to provide head fixation and to secure an electrical connector to which the leads of the scleral search coil were attached. Animals were allowed to recover for 2 weeks prior to the initiation of vestibular and optokinetic testing.

Alert animals were restrained in a custom box that rigidly fixed the head with the implanted bolt. This system of fixation was designed to maintain the horizontal semicircular canals in the yaw plane of rotation without impeding the animals' vision.[1] The

---

From the Division of Head and Neck Surgery, University of California–Los Angeles School of Medicine, Los Angeles, California (Andrews, Li, Hoffman), and the Department of Surgery, Tokyo Medical and Dental University, Tokyo, Japan (Koyama). This work was supported by National Institutes of Health/National Institute on Deafness and Other Communication Disorders grants DC00945 and DC01404. This study was performed in accordance with the PHS Policy on Humane Care and Use of Laboratory Animals, the NIH *Guide for the Care and Use of Laboratory Animals*, and the Animal Welfare Act (7 U.S.C. et seq.); the animal use protocol was approved by the Institutional Animal Care and Use Committee (IACUC) of the University of California–Los Angeles (protocol #95-004).

CORRESPONDENCE — James C. Andrews, MD, Division of Head and Neck Surgery, UCLA School of Medicine, 62-132CHS, 10833 Le Conte Ave, Los Angeles, CA 90095-1624.

NUMBER OF ANIMALS WITH SYMMETRIC RESPONSES TESTED FOR EACH VELOCITY AND FREQUENCY

Velocity (°/s)	*0.0125 Hz*	*0.025 Hz*	*0.05 Hz*	*0.1 Hz*	*0.2 Hz*	*0.4 Hz*	*0.8 Hz*
VOR 3.75	0	0	8	8	8	8	8
7.5	0	7	14	16	17	17	15
15	0	10	14	16	17	17	16
30	5	11	14	16	16	16	16
60	11	15	16	16	16	16	16
120	14	15	15	13	13	13	0
OKN 3.75	17	17	17	17	14	14	6
7.5	17	17	17	16	14	13	6
15	16	16	16	16	13	11	5
VVOR 3.75	15	15	14	14	16	16	16
7.5	16	15	15	14	17	17	17
15	15	15	15	16	17	17	17
30	13	13	13	12	12	13	13
60	14	16	15	15	17	17	17
120	13	14	14	13	13	12	0

VOR — vestibulo-ocular reflex, OKN — optokinetic nystagmus, VVOR — visual vestibulo-ocular reflex.

box was placed on a computer-controlled rate table for oculomotor studies that included VOR (table rotations in the dark, field coils stationary to the table), VVOR (table rotations in the light, field coils stationary to the table), and OKN (table and field coils stationary with a rotating visual field) testing. The VOR and VVOR utilized sinusoidal table rotations at stimulus frequencies between 0.0125 and 0.8 Hz with peak velocities between 3.75°/s and 60°/s. Optokinetic stimuli were provided by a computer-controlled motorized optokinetic drum positioned around the animal. Sinusoidal drum rotations between 0.0125 and 0.8 Hz with peak velocities between 3.75°/s and 15°/s were used.

Prior to any testing, eye movement was calibrated in the dark by physically rotating the restraining box (containing the animal with the head fixed) 10° in each direction from the center within the search coil field. This calibration procedure was utilized because rodents, unperturbed in a quiet and dark environment, maintain center gaze relative to the head. The signal generated by the known displacement of the eye coil within the field coils was then measured (resolution 0.5°) and used to calibrate the eye recordings during testing.

Eye, table, and optokinetic drum movements were monitored through a continuous strip chart recorder and by a laboratory computer with programs for data acquisition, online display and analysis of eye velocity, and table or optokinetic drum velocities.[2] The computer program identified and removed the nystagmus fast component to allow comparison of the stimulus with the slow component of eye velocity. For each of the various VOR, VVOR, and OKN tests performed, plots of the velocity of slow eye movement versus time and versus stimulus velocity (after removal of the phase shift) were generated.[3] The time-domain data were fit by discrete fast Fourier analysis. The magnitude of the fundamental component was used to compute the gain response, ex-

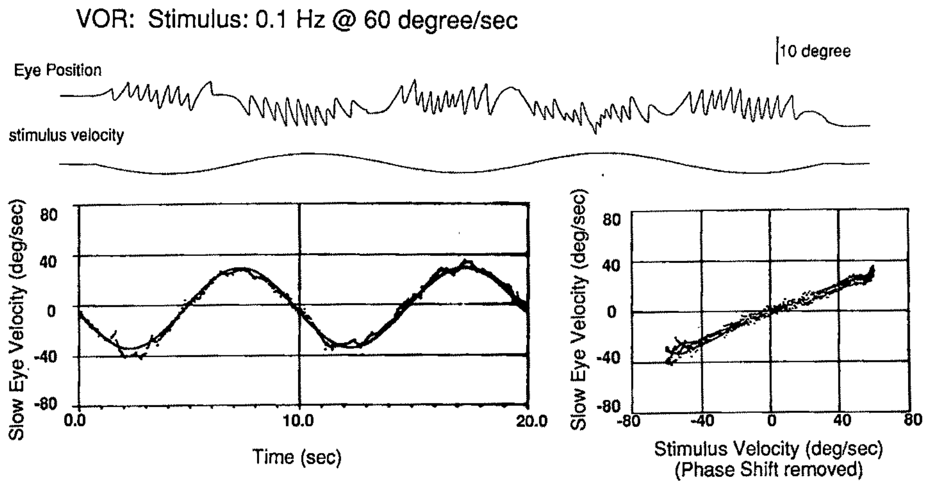

Fig 1. Example of vestibulo-ocular reflex (VOR) recording from guinea pig at stimulus of 0.1 Hz and 60°/s. Upper two tracings illustrate eye position and stimulus velocity relative to time. Bottom left graph shows plot of slow component eye velocity versus time (dots represent actual data). Solid line demonstrates Fourier analysis and curve fitting of data. Bottom right graph shows plot of slow component eye velocity versus stimulus velocity (after phase shift removal).

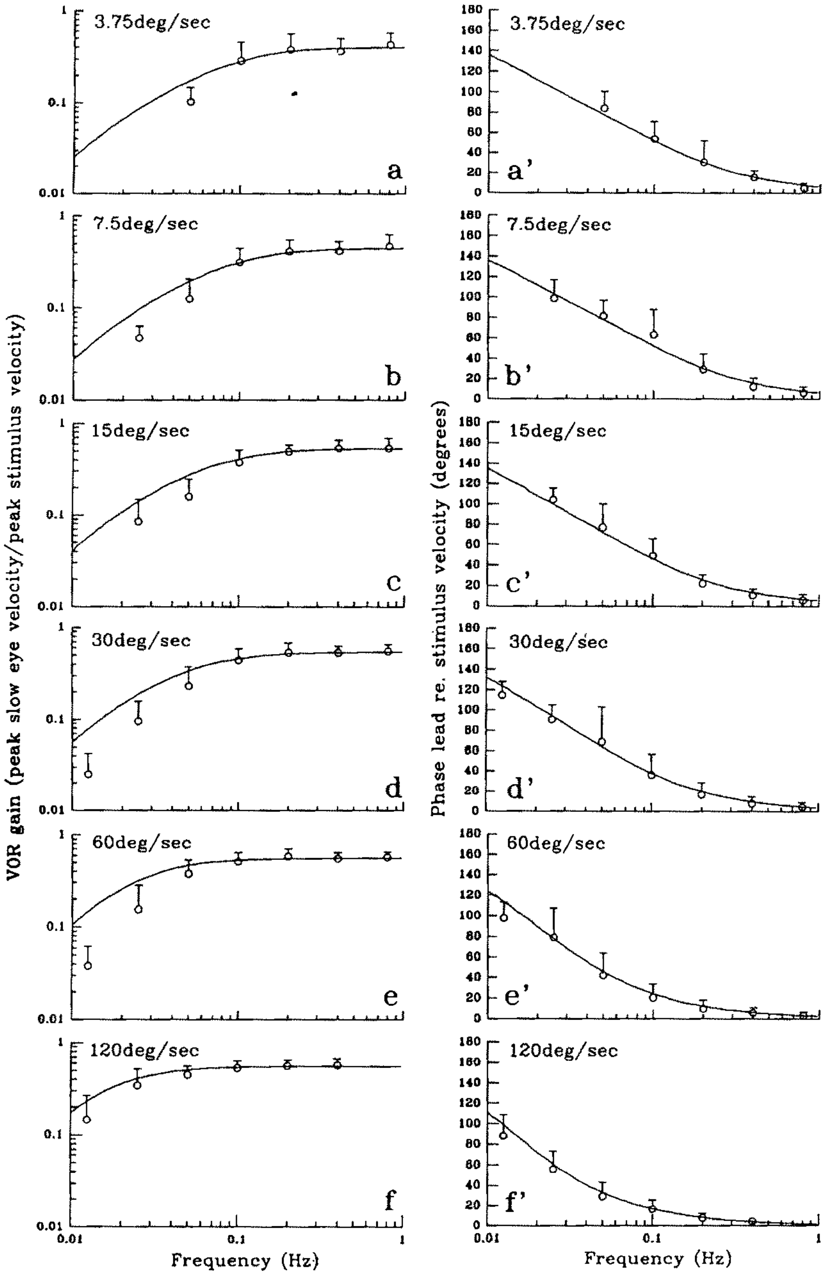

Fig 2. Bode plots of VOR gain (a-f) and phase (a'-f') versus stimulus frequencies for velocities of stimulation tested. Each data point represents average of all animals tested at that particular parameter (see Table), while bar represents positive standard deviation. Solid lines represent modeled fit of data using mathematic model presented in text.

pressed as the ratio of the peak eye velocity to the peak stimulus velocity, and the phase response, described as the difference between the peak eye velocity phase and the peak stimulus velocity phase. For VOR and VVOR, 180° was added to the phase. An assessment of the quality of the animals' response to the various stimuli was performed by visually examining the data plots for symmetry and the tendency for the data to cluster around the fitted curve and by measuring the degree of distortion of the first five harmonics.

Only animals with symmetric and repeatable responses, exhibiting approximately equivalent gains for rotation in each direction and a first harmonic distortion of less than 20%, were included in this study. The number of subjects able to satisfy these criteria for the various parameters tested are shown in the Table. Bode plots were prepared from gain and phase values for each animal and stimulus condition. Best fit transfer functions from these frequency domain data were determined with the aid of a least squares linear control systems fitting algorithm.[4,5]

RESULTS

Vestibulo-ocular Reflex. The VOR data included high-quality eye position recordings from up to 17 animals for the various parameters tested. At the lower peak velocities of stimulation the eye movements were compensatory in nature, demonstrating

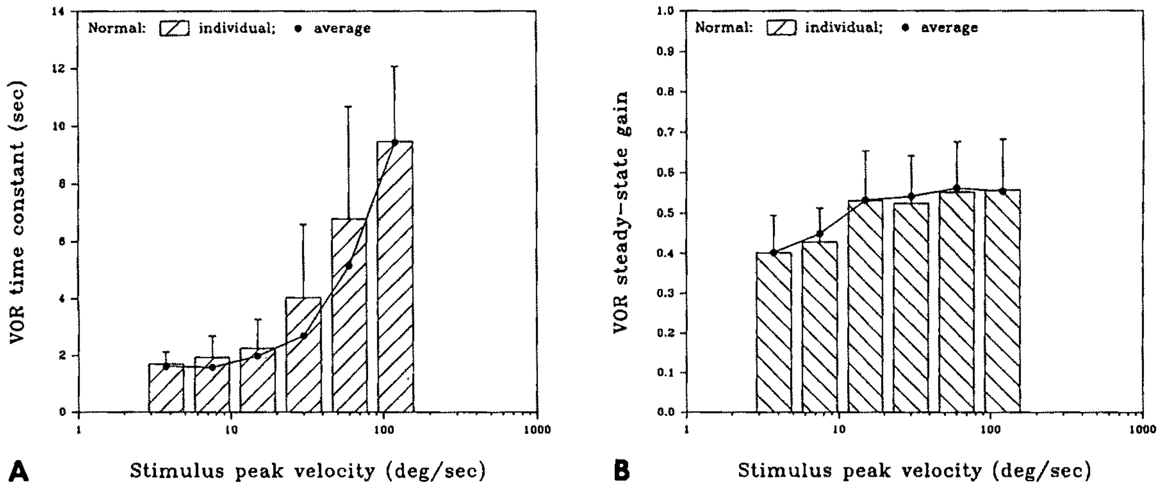

Fig 3. Plot of VOR dominant time constant (A) and steady state gain (B) for each of stimulus peak velocities tested. Closed circles represent model coefficients of equation 1 (in text) calculated for mean gain and phase data of all animals. Bars represent averaged coefficients found by applying model of equation 1 to each individual animal's gain and phase data. Parameter values used in constructing this Figure were τ_v (dominant time constant) and Gv (steady-state gain) obtained through fits of VOR transfer functions that considered all frequencies and phase velocities tested.

an approximate 180° phase shift of the eye position relative to the head. At peak velocities above 7.5°/s, the magnitudes of the VOR stimuli were large enough to produce crisp nystagmus (Fig 1). Plots of the slow component eye velocity versus time demonstrated a sinusoidal curve similar to, but out of phase with, the stimulus velocity. After removal of the phase shift, slow phase eye velocity plotted against stimulus velocity resulted in a scalar plot that was fit to a straight line (utilizing a least squares curve-fitting method) with a slope that represented the gain of the animals' response.

Bode plots of the gain and phase were prepared from the mean and standard deviation data from each peak velocity stimulus (Fig 2). The data demonstrate high-pass filter characteristics with steady state gains achieved at the stimulus frequencies of approximately 0.125 Hz for the various velocities tested. The maximum gain ranged from 0.42 to 0.55 at respective peak velocities of 7.5°/s and 60°/s. The phase response exhibited a lead of greater than 90° for the lower frequencies tested and approached 0° for the higher frequencies.

A model composed of two poles, including an adaptation operator, provided an adequate fit of the data.[6] The form of this transfer function model H(s) is

$$(1) \quad H(s) = G_v \times \frac{\tau_a \tau_v s^2}{(\tau_a s + 1)(\tau_v s + 1)}$$

where Gv is a steady state gain constant, τ_v is the dominant or system time constant, τ_a is the adaptation time constant, and s is the Laplace operator. Based on the best fit of the averaged data, τ_a was estimated at 12.5 seconds. Determination of τ_v and Gv was provided by the curve-fitting software utilizing a best fit transfer function. Although the fitting software determined the values of these parameters with error-

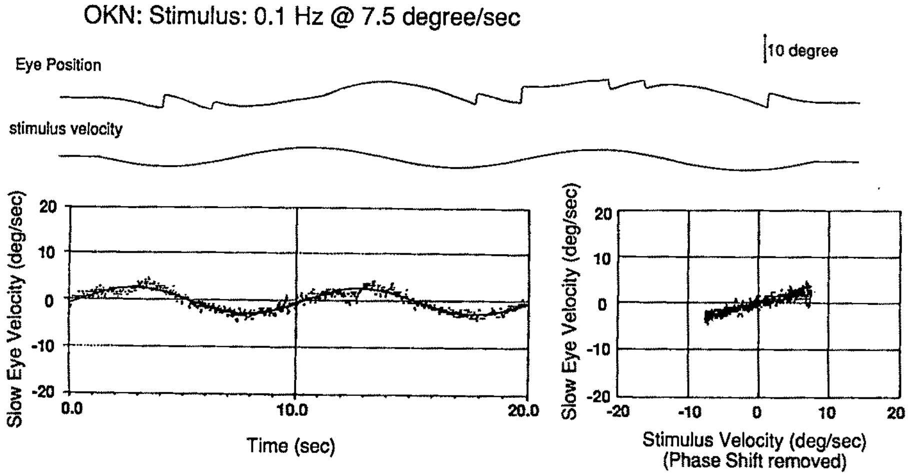

Fig 4. Example of optokinetic nystagmus (OKN) recording from guinea pig at stimulus of 0.1 Hz and 7.5°/s. Illustrations include eye position and stimulus velocity relative to time, plot of slow component eye velocity versus time (dots represent actual data; solid line represents curve fitting of data), and plot of slow component eye velocity versus stimulus velocity (after phase shift removal).

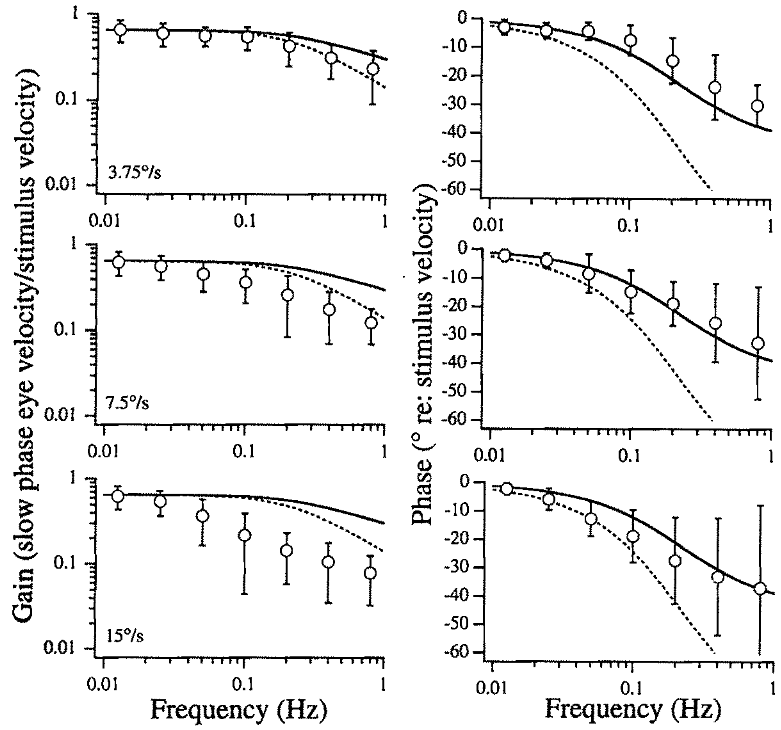

Fig 5. Bode plots of OKN gain and phase versus stimulus frequencies for velocities of stimulation tested. Each data point represents average of all animals tested at that particular parameter (see Table), while bars represent standard deviation. Solid line represents fractional pole model fit (k = 0.5), and dashed line represents first-order modeled fit (k = 1) for transfer function (equation 2, detailed in article).

minimizing criteria, these values were occasionally adjusted and the fits compared so that visually better fits of both the gain and phase data were achieved. The dominant time constant was plotted for each of the stimulus velocities tested in Fig 3. In this graph the closed circles reflect the model coefficients of equation 1 for the mean gain and phase data of all the animals. The bars represent the values found by averaging H(s) coefficients from the data of individual animals. It was noted that τv was velocity-dependent, with an increase in this constant especially at the higher peak velocities.

Optokinetic Nystagmus. The OKN response was recorded from up to 17 animals for the various parameters tested. Recordings of the eye position were of high quality and showed a sinusoidal eye movement response in phase with the target (Fig 4). In those stimuli in which the magnitude was greater than 15°/s, a brisk nystagmus was produced. In some animals an afternystagmus was noted in which nystagmus would continue for a few seconds after ces-

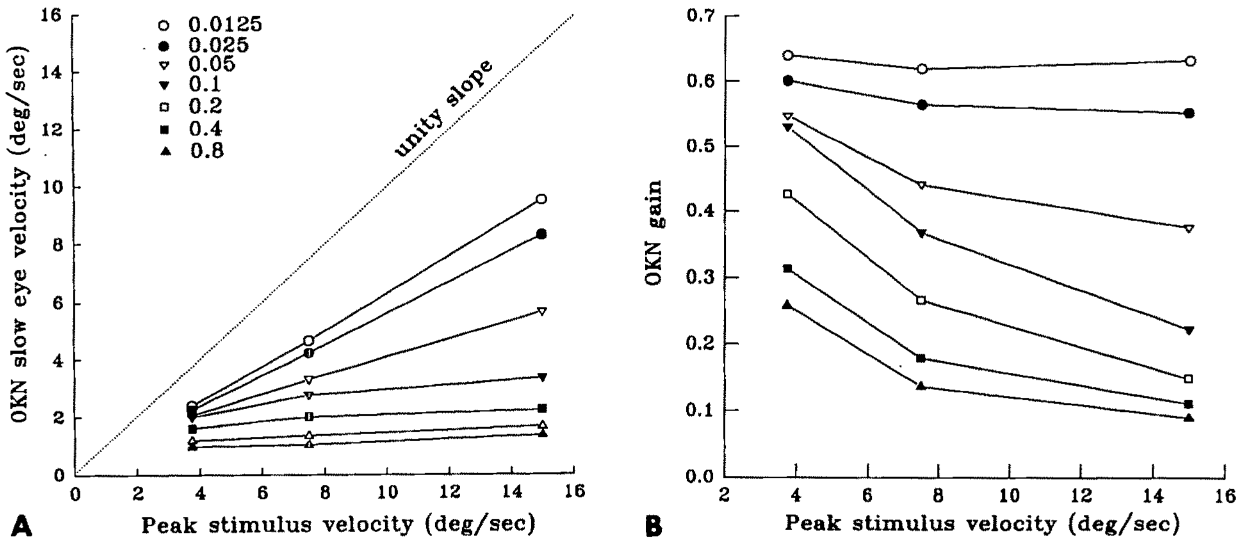

Fig 6. Composite plots of average OKN slow eye velocity (A) and gain (B) versus peak stimulus velocity for various frequencies tested. Note that slope of slow eye velocity response approached unity and highest gains were achieved for lowest frequencies tested, with diminishing response at incrementally greater testing frequencies. Nonlinearities in system are especially evident in OKN gain response at frequencies of 0.05 Hz and greater.

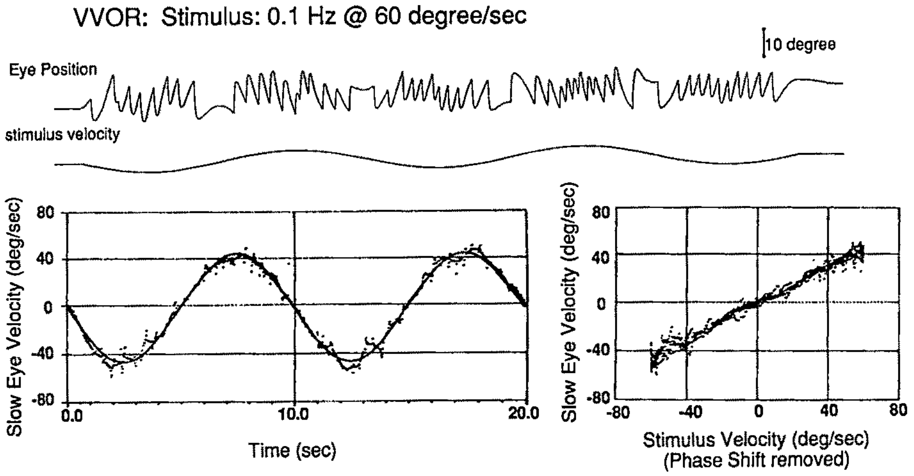

Fig 7. Example of visual vestibulo-ocular reflex (VVOR) recording from guinea pig at stimulus of 0.1 Hz and 60°/s. Illustrations include eye position and stimulus velocity relative to time, plot of slow component eye velocity versus time (dots represent actual data; solid line represents curve fitting of data), and plot of slow component eye velocity versus stimulus velocity (after phase shift removal).

sation of the optokinetic stimuli. Plots of the slow component eye velocity versus time demonstrated a sinusoidal curve similar to and in phase with the stimulus velocity. Plots of the slow eye velocity versus stimulus velocity demonstrated a straight line with a slope representing the gain of the response. Bode plots of the mean (± standard deviation) gain and phase were prepared for each peak velocity stimulus (Fig 5). The data exhibited low-pass filter characteristics, with the highest gains at the lower frequencies of stimulation for all peak velocities tested. At frequencies above 0.1 Hz there was a decrease in gain and phase. The maximum average gain recorded was between 0.62 and 0.64, which decreased to 0.23 ± 0.14 at 3.75°/s and to 0.05 ± 0.08 at 15°/s, both at 0.8 Hz.

The mean closed loop OKN gain and phase data were fit with a transfer function of the form

$$H(s) = \frac{GOK}{(1 + \tau s)^k} \qquad (2)$$

where GOK is the static optokinetic gain (assigned a value of 0.65*)*, τ is the time constant (determined to be 0.48 seconds), and s is the Laplace operator. In an effort to improve the fit to the data, fractional pole exponents (k) were utilized as shown in Fig 5. Whereas the first-order model (eg, k = 1) provides a satisfactory visual fit for the mean OKN gains at 3.75°/s peak stimulus velocity, it overestimates the mean gains at frequencies greater than 0.05 Hz at 7.5°/s and 15°/s peak stimulus velocities. Furthermore, the first-order model underestimates the measures of phase at most frequencies for the tested peak stimulus velocities. The fractional pole model (eg, k = 0.5) appears to provide a better overall fit for the OKN phase measurements, although it overestimates the gain measurements at the various peak stimulus velocities tested.

A comparison of the OKN-stimulated slow eye velocity versus the peak stimulus velocity (Fig 6A) demonstrated a linear response for the various frequencies tested, with a slope closest to 1 for the lowest frequency (0.0125 Hz) and a corresponding decrease in slope for increase in stimulus frequency up to 0.1 Hz. At higher frequencies of stimulation, the slow component eye velocity response remained poor regardless of the stimulus velocity. Plotting the OKN gain versus peak stimulus velocity (Fig 6B) for the frequencies tested showed a relatively constant gain at the lower frequencies tested (0.0125 and 0.025 Hz) and a nonlinear gain reduction with increase in velocity at the higher frequencies tested.

Visual Vestibulo-ocular Reflex. The VVOR was recorded in up to 17 animals for the various parameters tested. Similar to the other reflexes measured, the sinusoidal VVOR stimulus provided a strong ocular movement response (Fig 7). At the lower peak velocities of stimulation, eye movements were sinusoidal and compensatory, with an approximate 180° phase shift relative to the stimulus. At peak velocities above 7.5°/s, a nystagmus response was achieved. Plots of the slow component eye velocity versus time were sinusoidal, but approximately out of phase with the stimulus velocity. After removal of the phase shift, plots of the slow eye velocity versus stimulus velocity demonstrated a curve that was fit with a straight line (by a least squares fitting method) with a slope that reflected the gain of the response. Bode plots showing the average and standard deviation gain and phase responses for the frequencies tested are shown in Figs 8 and 9. The maximum average gains achieved varied between 0.7 at 120°/s and 0.59 at 3.75°/s. For the lower velocities (3.75°/s and 7.5°/s), the gain was relatively constant throughout the frequencies tested; however, the higher velocities tested showed a tendency for a frequency-dependent increase in gain. The phase shift was near zero for the velocities between 3.75°/s and 30°/s, while at the higher velocities tested there was a low-frequency phase lead that approached zero at approximately 0.1

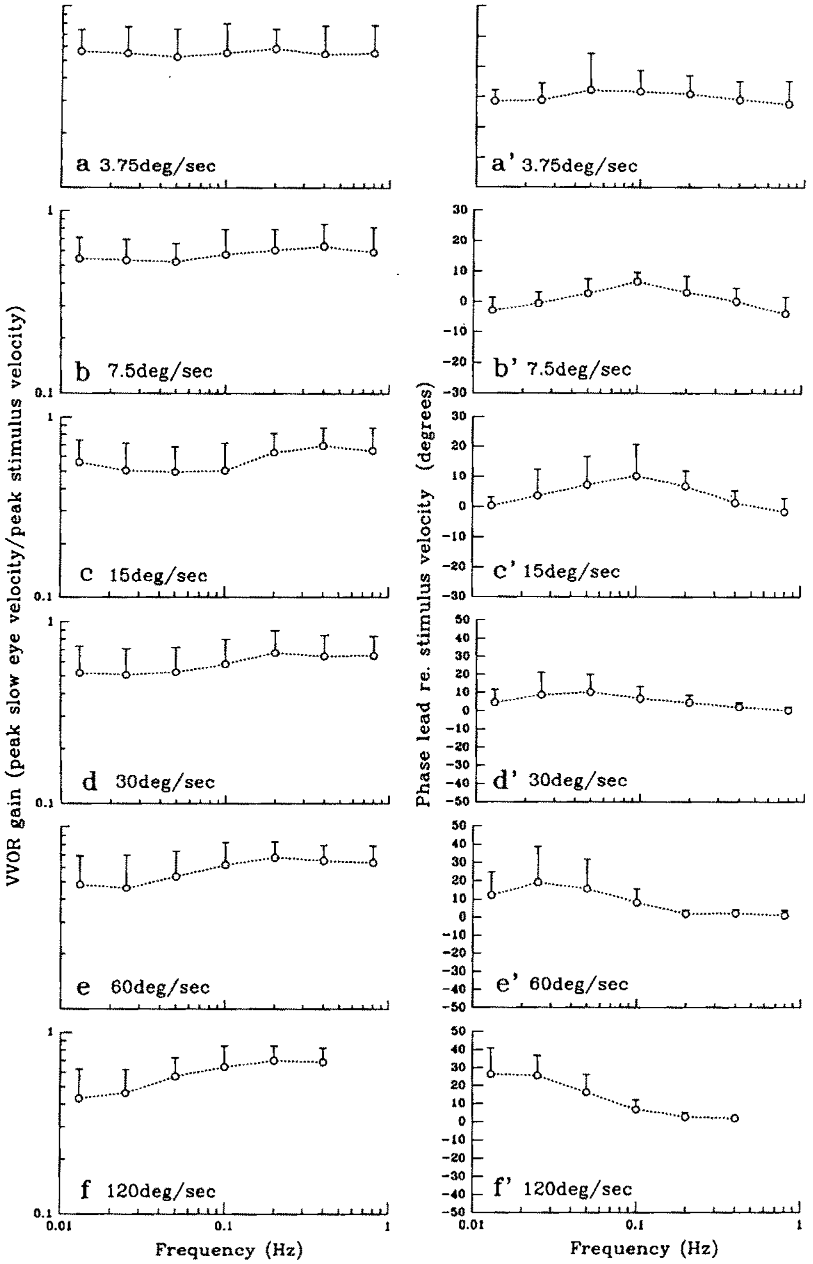

Fig 8. Bode plots of VVOR gain (a-f) and phase (a'-f') versus stimulus frequencies for velocities of stimulation tested. Each data point represents average of all animals tested at that particular parameter (see Table), while bar represents positive standard deviation. Dashed lines merely connect data points and do not represent modeled fit.

Hz.

Paige[7,8] proposed the linear combination of the actual VOR and OKN gain data to estimate VVOR gain utilizing the following relationship:

$$\text{VVOR} = \text{VOR} + \text{OKN}(1 - \text{VOR}) \tag{3}$$

This proposal was studied in 6 animals in which there were complete VOR, OKN, and VVOR data for all the stimuli tested at 0.05, 0.1, 0.2, and 0.4 Hz, including stimulus peak velocities of 3.75°/s, 7.5°/s, and 15°/s. The predicted VVOR was then compared with the measured VVOR data, and a predicted to measured (P/M) ratio was computed for each animal (Fig 10). Optimal modeling of the VVOR would demonstrate a P/M ratio of 1. Statistical evaluation with a two-factor repeated-measures analysis of variance did not show the P/M ratios for our overall data to be different from 1 ($p > .05$). In addition, the P/M ratios were not affected by stimulus velocity ($p > .5$); however, there was a main effect of frequency, with lower P/M ratios for the higher stimulation frequencies ($p < .005$). On a t-test, the P/M ratios for 0.05, 0.1, and 0.2 Hz were not different from 1 ($p > .05$), and only the ratio for 0.4 Hz was statistically lower than 1 ($p < .05$).

Lau et al[9,10] proposed a model of the VVOR that incorporates a linear combination of the VOR and OKN for each amplitude and frequency of stimulation in the form of

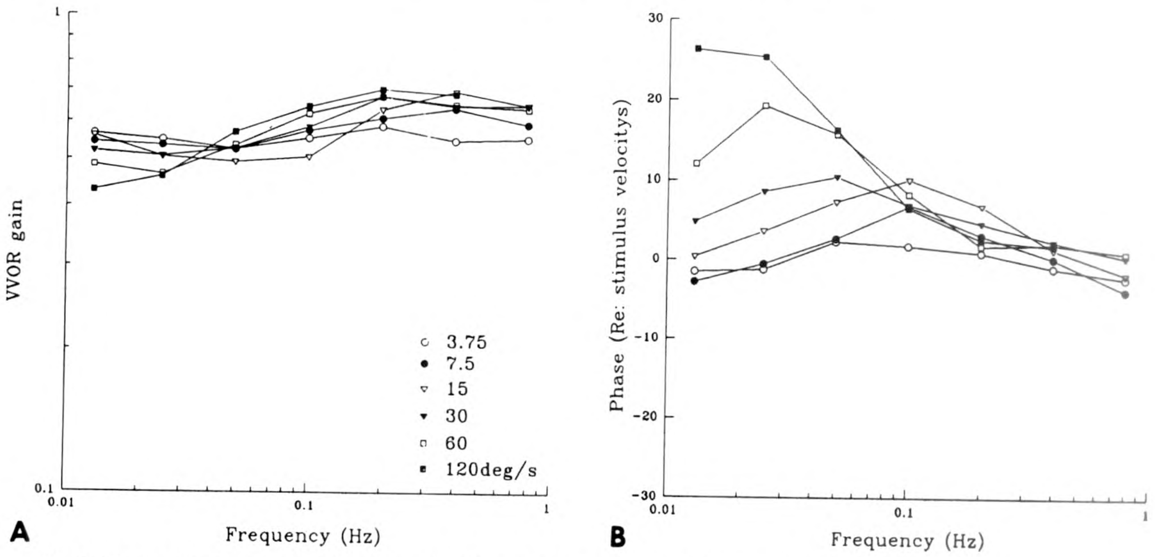

Fig 9. Composite Bode plots of average VVOR gain (A) and phase (B) responses versus stimulus frequencies for various stimulus velocities tested. Note relatively constant VVOR gain response independent of stimulus velocity. Phase response shows phase lead at lower frequencies and higher velocities tested, which approach zero with increase in frequency. At lower velocities tested, phase response remains stable around zero.

$$\text{VVOR} = \text{VOR} - \text{OKN}(1 + \text{VOR}) \tag{4}$$

In this relationship, VOR and OKN represent the respective transfer functions of equations 1 and 2. For the three peak velocities from which OKN data were recorded, we attempted to fit our data utilizing this algebraic summation of transfer functions. Because of computer limitations, we were only able to provide a first-order OKN transfer function ($k = 1$) for analysis of the VVOR model. Although this provided a good fit of the gain data below 0.1 Hz, the high-frequency gain and phase data were inadequately described.

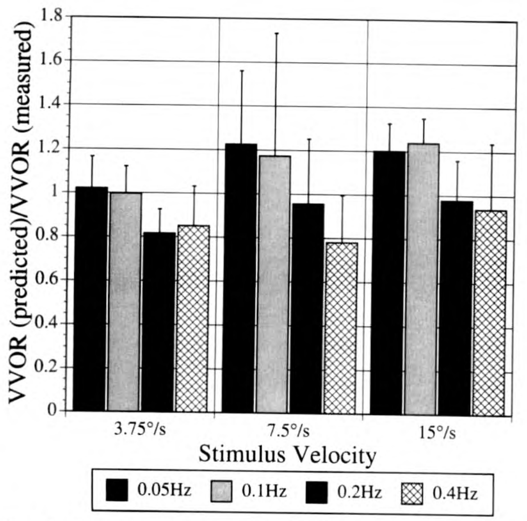

Fig 10. Plot of ratio of VVOR gain predicted (as linear summation of VOR and OKN measured gain data) to VVOR gain measured for various stimulus velocities and frequencies tested. Ratio of 1 demonstrates best possible prediction of data by model.

DISCUSSION

Guinea pigs can provide high-quality vestibulo-ocular data when functionally tested. They demonstrate a robust eye movement response to optokinetic and vestibular stimulation that can be readily recorded. The utility of guinea pigs as models for ear disease can be supplemented by knowledge of their vestibular response. This is especially needed in conditions such as endolymphatic hydrops, in which knowledge of the vestibular interactions is paramount in understanding the disorder.

The tests used for measuring vestibular and optokinetic function in this study represent the lower end of the physiologic range of head movements and visual stimuli in which compensatory eye movements are generated for the guinea pig. In part, this is a limitation of our quantitative vestibular function testing instrumentation. Even with this limitation, the data provide a useful analytic approach to the guinea pig's vestibular system.

The VOR function in the guinea pig is similar to that in other species, such as the rabbit and the chinchilla, with a compensatory nystagmus to stimulation and demonstration of high-pass filter characteristics.[11,12] The average maximum gain achieved for guinea pigs was 0.55 at a peak velocity of 60°/s for the midrange of rotational frequencies tested, as compared to 0.54 to 0.8 for rabbits and 0.6 for chinchillas. These data are comparable with those of other studies of guinea pig vestibulo-ocular function.[13] Adaptation time constants have been calculated at 10.6 seconds for the rabbit and 24 seconds for the chinchilla.[9,10,12] Our data show an estimate of the guinea pig adaptation time constant at 12.5 seconds, which seems consistent with the findings in other species. On a model comprising two poles including an adaptation operator, our phase data fit the model well; however, there was a consistent overestimation of the gain at the lower frequencies.

The OKN response in guinea pigs shows an average maximal gain of between 0.62 and 0.64 achieved at low frequencies of stimulation. Although a first-order model has been utilized for describing closed-loop OKN data in other species, we found response characteristics of the guinea pig that departed from the expected response for a first-order system.[9-11] Primary was the finding that the high-frequency phase response at the three stimulus velocities tested approached an asymptote of –45° (as opposed to a first-order response of –90°). With a fractional pole model, there was much better fit of the phase data. The gain data were in general poorly fit with either model; however, the first-order model was closer to the actual data. Anastasio[14] demonstrated that fractional dynamics of the vestibulo-oculomotor system could result from a "weighted summation" of multiple first-order systems. A similar analysis of our guinea pig OKN data could be adapted by shifting the time constants of multiple summed first-order filters. One physiologic interpretation of the summation of multiple first-order filters could be the distributed integrated activity of premotor neurons at various levels.[14]

The VVOR gain response in guinea pigs was relatively stable between 0.5 and 0.65, with minimal phase shift for the range of frequencies tested in this study. It is notable that a gain of less than 1.0 was achieved. This may be related to our method of testing, which immobilized the head and prevented any cervical musculature interaction (ie, no vestibulo-collic contribution to VVOR).[15-17] Our data indicate that the VVOR gain may in part reflect the linear summation of the actual VOR and OKN gain in this species; however, there is a tendency for this finding to be frequency-dependent. It seems that at the lower frequencies of stimulation the VVOR response may be dominated by the OKN, while at the higher frequencies of stimulation, the response is dominated by the VOR. In the middle frequencies, both the OKN and VOR may contribute to the VVOR.

CONCLUSIONS

1. Guinea pigs can provide reliable vestibular function data and may serve as excellent models for studying vestibular disease.

2. The guinea pig's eye movement response to sinusoidal rotational stimulation shows high-pass filter characteristics at frequencies above 0.1 Hz stimulation, with a stable gain of 0.5 and minimal phase shift.

3. Best fits of the proposed VOR model were achieved with an adaptation time constant for VOR in the guinea pig of 12.5 seconds.

4. A fractional pole model for the OKN was required to provide a reasonable fit of our data.

5. In the guinea pig, VVOR gain may in part be predicted through a linear summation of the actual VOR and OKN gain data. The VVOR appears to reflect a greater OKN influence on the lower frequencies, and a greater VOR influence on the higher frequencies of stimulation.

REFERENCES

1. Curthoys IS, Curthoys EJ, Blanks RHI, Markham CH. The orientation of the semicircular canals in the guinea pig. Acta Otolaryngol (Stockh) 1975;80:197-205.

2. Baloh RW, Langhofer L, Honrubia V, Yee RD. On-line analysis of eye movements using a digital computer. Aviat Space Environ Med 1980;51:563-7.

3. Marco-Algarra J, Honrubia V. Comparative study of the effect of gentamicin on the vestibulo-ocular and visual vestibulo-ocular reflex in the cat. Acta Otolaryngol (Stockh) 1991;111:162-8.

4. Tomko DL, Peterka RJ, Schor RH, O'Leary DP. Response dynamics of horizontal canal afferents in barbiturate-anesthetized cats. J Neurophysiol 1981;45:376-96.

5. Seidel RC. NASA Technical Memorandum TM-X3286, Washington DC, 1975.

6. Fernandez C, Goldberg JM. Physiology of peripheral neurons innervating semicircular canals of the squirrel monkey. II. Response to sinusoidal stimulation and dynamics of peripheral vestibular system. J Neurophysiol 1971;34:661-75.

7. Paige GD. Vestibulo-ocular reflex and its interactions with visual following mechanisms in the squirrel monkey. I. Response characteristics in normal animals. J Neurophysiol 1983;49:134-51.

8. Paige GD. Vestibulo-ocular reflex and its interactions with visual following mechanisms in the squirrel monkey. II. Response characteristics and plasticity following unilateral inactivation of horizontal canal. J Neurophysiol 1983;49:152-68.

9. Lau CGY. Modeling of visual-vestibular interaction and the fast components of nystagmus [Dissertation]. Santa Barbara, Calif: University of California, 1978.

10. Lau CGY, Honrubia V, Baloh RW. A model for visual vestibular interaction. In: Gualtierotti T, ed. The vestibular system: function and morphology. New York, NY: Springer-Verlag, 1981:525-34.

11. Baarsma EA, Collewijn H. Vestibulo-ocular and optokinetic reactions to rotation and their interaction in the rabbit. J Physiol (Lond) 1974;238:603-25.

12. Merwin WH, Wall C, Tomko DL. The chinchilla's vestibulo-ocular reflex. Acta Otolaryngol (Stockh) 1989;108:161-7.

13. Escudero M, de Waele C, Vibert N, Berthoz A, Vidal PP. Saccadic eye movements and the horizontal vestibulo-ocular and vestibulo-collic reflexes in the intact guinea pig. Exp Brain Res 1993;97:254-62.

14. Anastasio TJ. The fractional-order dynamics of brainstem vestibulo-oculomotor neurons. Biol Cybern 1994;72:69-79.

15. Mirenowicz J, Hardy O. Characteristics of saccades induced by neck torsions: a re-examination in the normal guinea pig. Brain Res 1992;592:1-6.

16. Vidal PP, Wang DH, Graf W, de Waele C. Vestibular control of skeletal geometry in the guinea pig: a problem of good trim? Prog Brain Res 1993;97:229-43.

17. Gresty MA. Eye, head and body movements of the guinea pig in response to optokinetic stimulation and sinusoidal oscillation in yaw. Pflugers Arch 1975;353:201-14.

≈

SURGICAL COURSE ON OTOPLASTY

A Surgical Course on Otoplasty will be held in English in Ulm, Germany, March 13-14, 1998. For more information, contact Prof Dr G. Rettinger, Prittwitzstr 43, D-89075 Ulm, Germany; telephone +731-502-7501; fax +49-731-502-6703.

≈

NEONATAL HEARING SCREENING

The European Consensus Development Conference on Neonatal Hearing Screening will be held in Milan, Italy, May 15-16, 1998. For more information, contact Dr F. Grandori, Centre of Biomedical Engineering, Polytechnic of Milan, Piazza Leonardo da Vinci 32, 20133 Milan, Italy; fax +39-2-23993360; email ecdc@elet.polimi.it.

Ann Otol Rhinol Laryngol 106:1997

EFFECT OF IMMUNOTHERAPY ON SERUM LEVELS OF EOSINOPHIL CATIONIC PROTEIN IN PERENNIAL ALLERGIC RHINITIS

YOSHIHIRO OHASHI, MD
YOSHIAKI NAKAI, MD
YASUSHI KAKINOKI, MD
YOSHIHARU OHNO, MD
HIROKAZU SAKAMOTO, MD
AKIFUMI KATO, MD
AYAKI TANAKA, MD
OSAKA, JAPAN

Eosinophil cationic protein (ECP) levels in the serum of clotted blood could reflect the rate of activation of circulating eosinophils. We investigated the serum ECP levels in patients with perennial allergic rhinitis, with special reference to the effect of immunotherapy on the serum ECP levels. Serum ECP levels in untreated patients with perennial allergic rhinitis are significantly higher than those of nonatopic volunteers. Therefore, this elevation in the untreated patients represents an ongoing inflammation occurring in allergic rhinitis. The mean serum ECP level of a 1-year immunotherapy group was significantly higher than that of the nonatopic group, and was not different from that of the untreated group. In contrast, the mean serum ECP level in patients who had more than 2 years of immunotherapy was significantly lower than that of the untreated group, and was not different from that of the nonatopic group. Additionally, serum ECP levels were significantly correlated with the duration of immunotherapy. These findings suggest that activation of circulating eosinophils decreases gradually during immunotherapy, but this inhibition becomes apparent only after 2 years of immunotherapy. The control of circulating eosinophil activation might be one of the important working mechanisms behind the clinical effect of immunotherapy.

KEY WORDS — eosinophil cationic protein, immunotherapy, perennial allergic rhinitis.

INTRODUCTION

The pathogenesis of respiratory allergic diseases, including asthma and allergic rhinitis, is closely linked to the presence of airway chronic inflammation.[1] Activation of eosinophils and eosinophil-derived granule cationic proteins are the causes of the basic histopathologic changes and airway inflammation.[2-4] There are some cationic proteins released from activated eosinophils, such as major basic protein, eosinophil peroxidase, eosinophil cationic protein (ECP), and eosinophil-derived neurotoxin.[5] Among these, ECP is located in the granule matrix around the central core and is toxic to airway epithelia.[6,7] Since ECP may be a major cause of chronic airway inflammation, it may also be an objective parameter of inflammation in respiratory allergic diseases.

Since a sensitive radioimmunosorbent assay as a method of quantitative measurement for ECP was developed by Venge et al,[8] measurements of ECP levels at allergic inflammatory sites, including nasal lavage from patients with allergic rhinitis and bronchoalveolar lavage from asthmatics, have been attempted.[9,10] In nasal lavage as well as in bronchoalveolar lavage, ECP levels are elevated when the patients are symptomatic.[9,10] These data have provided valid information in clinical investigation of allergic diseases. However, harvesting of these fluids cannot be used in large series of patients and may cause increased inconvenience to the patients. The ECP levels in the serum of clotted blood could reflect the rate of activation of circulating eosinophils.[11] Indeed, the serum levels of ECP in allergic asthma and atopic dermatitis are significantly higher.[9,12]

An elevation in the serum ECP is expected in patients with allergic rhinitis, because allergic rhinitis is an allergic inflammatory disease like bronchial asthma. However, serum ECP levels in allergic rhinitis are controversial. It is also unclear whether immunotherapy can reduce serum ECP levels in allergic diseases. We investigated the serum ECP levels in patients with perennial allergic rhinitis, with special reference to the effect of immunotherapy on serum ECP levels.

MATERIALS AND METHODS

Sixty-eight adult patients with perennial allergic rhinitis due to *Dermatophagoides farinae*, 37 women and 31 men, with a mean age of 31.3 ± 8.6 years (range 18 to 50 years) were included in this study. Eighteen of them, the untreated group, had received no treatments for their nasal symptoms for 6 months before blood collection. The remaining 50 patients, the immunotherapy group, had variable periods (mean 2.2 ± 2.6 years) of immunotherapy using Hollister-Stier standardized *D farinae* extracts (Miles Inc, USA) before

---

From the Department of Otolaryngology, Osaka City University Medical School, Osaka, Japan. Supported by a Grant-in-Aid for Scientific Research (07671878) from the Ministry of Education, Science and Culture, Japan.

CORRESPONDENCE — Yoshihiro Ohashi, MD, Dept of Otolaryngology, Osaka City University Medical School, 1-5-7 Asahimachi, Abeno, Osaka 545, Japan.

BACKGROUND OF SUBJECTS

	Age (y)		*Sex (No. of Subjects)*		*Duration of Disease (y)*	
	Mean	*SD*	*Female*	*Male*	*Mean*	*SD*
Untreated group	28.7	8.6	10	8	9.2	4.5
1-year group	31.6	9.2	10	8	8.8	4.4
2-year group	31.1	9.1	6	5	8.6	3.5
≥3-year group	33.4	7.6	11	10	8.9	3.6
Nonatopic group	31.2	9.4	15	9		

blood sampling. The patients of the immunotherapy group were further divided into the following three groups according to their periods of immunotherapy: the 1-year group, 18 patients who had been under immunotherapy for 1 year; the 2-year group, 11 patients who had been under immunotherapy for 2 years; and the ≥3-year group, 21 patients who had been under immunotherapy for 3 or more years.

All the patients satisfied the following criteria: 1) a well-documented history of perennial allergic rhinitis, 2) no history of asthma, 3) no seasonal deterioration during the pollen season, 4) a positive skin test to *D farinae*, 5) a positive nasal provocation test to *D farinae*, and 6) eosinophilia in nasal smears. The patients of the immunotherapy group were allowed to take no concomitant medication affecting nasal symptoms for 6 months before blood collection, with prior informed consent.

Venous blood was collected from each patient in April 1995. Serum ECP levels, blood eosinophil counts, and *D farinae*–specific IgE levels were measured. For determination of serum ECP concentrations, SST tubes were used and clotting was performed at room temperature (20°C) for 70 minutes with a margin of ±10 minutes. Then centrifugation of the blood was carried out (1,200*g*, 10 minutes), and serum samples were frozen at −80°C until they were used in the ECP assay. Serum ECP was assessed by double-antibody radioimmunoassay using an ECP radioimmunoassay kit (Pharmacia, Japan), and all the assays were run in duplicate. Immunoglobulin E antibodies specific to *D farinae* were measured by the use of the Pharmacia immunoCAP system.[13] Blood eosinophil counts were performed in the hospital clinical laboratory and expressed as cells × 10^{-6} per liter.

To serve as controls, 24 nonatopic healthy volunteers (nonatopic group) of the same age range (see Table) were chosen on the basis of the following criteria: 1) a negative history for allergy, 2) no physical findings consistent with atopic diseases, and 3) negativity for serum IgE antibodies specific to the common allergens, including *D farinae*. Venous blood was also collected from these volunteers during the same period, and serum ECP was assessed by the same double-antibody radioimmunoassay.

Data were expressed as mean and standard deviation. Differences between two different groups were statistically analyzed by the use of the Mann-Whitney U-test, and significance was accepted at $p < .01$. Correlation between two different parameters was estimated with Spearman's rank-correlation test, and significance was accepted at $p < .01$.

RESULTS

Background of Subjects. The age, gender, and dura-

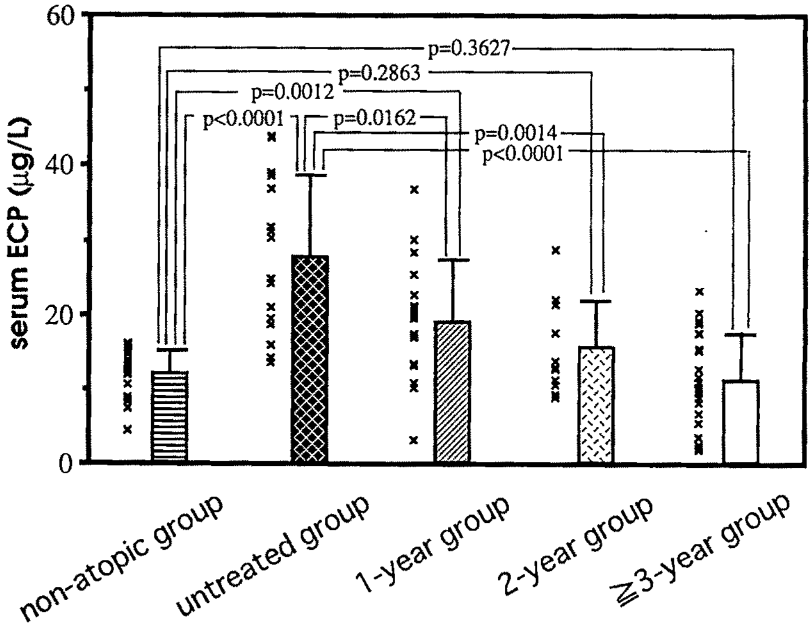

Fig 1. Serum eosinophil cationic protein (ECP) level. Serum ECP levels of untreated group and 1-year group are significantly higher than that of nonatopic group, but those of 2-year group and ≥3-year group are not significantly different from that of nonatopic group. Serum ECP level of 1-year group is not different from that of untreated group, but those of 2-year group and ≥3-year group are significantly lower than that of untreated group.

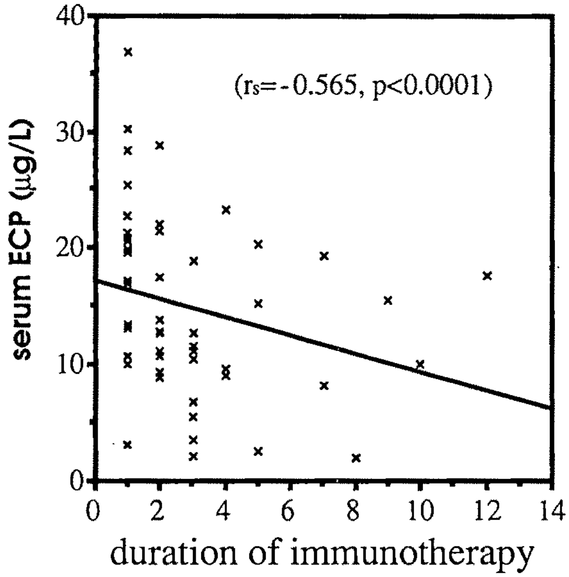

Fig 2. Correlation between serum ECP and duration of immunotherapy. Serum ECP level is significantly correlated with duration of immunotherapy.

tion of disease of the subjects studied are summarized in the Table. No significant differences in these factors were recognized among the groups.

Serum Eosinophil Cationic Protein. The serum ECP level (mean ± standard deviation) of the nonatopic group was 12.17 ± 2.92 µg/L (range 4.5 to 16.2 µg/L). The serum ECP level of the 68 allergic rhinitis patients was 18.38 ± 10.21 µg/L (range 2.0 to 43.9 µg/L). The serum ECP levels of the untreated group, 1-year group, 2-year group, and ≥3-year group were 27.85 ± 10.50 µg/L (range 13.5 to 43.9 µg/L), 19.12 ± 8.07 µg/L (range 3.1 to 36.9 µg/L), 15.39 ± 6.33 µg/L (range 8.9 to 28.8 µg/L), and 11.21 ± 6.36 µg/L (range 2.0 to 23.3 µg/L), respectively (Fig 1). The serum ECP levels of the untreated group and the 1-year group were significantly higher than the serum ECP level of the nonatopic group (untreated group, p < .0001; 1-year group, p = .0012). However, the serum ECP levels of the 2-year group and the ≥3-year group were not significantly different from the serum ECP level of the nonatopic group (2-year group, p = .2863, ≥3-year group, p = .3627). The serum ECP level of the 1-year group was not significantly different from that of the untreated group (p = .0162), but those of the 2-year group and ≥3-year group were significantly lower than that of the untreated group (2-year group, p = .0014; ≥3-year group, p < .0001).

The serum ECP of the 50 patients of the immunotherapy group significantly correlated with the duration of immunotherapy (rs = –.565, p < .0001, Fig 2).

Blood Eosinophil Counts. The blood eosinophil counts were 445.24/L ± 208.89/L (range 89.6/L to 923.4/L) in the untreated group, 384.82/L ± 207.22/L (range 33.0/L to 756.8/L) in the 1-year group, 351.69/L ± 243.29/L (range 110.6/L to 825.0/L) in the 2-year group, and 211.48/L ± 172.23/L (range 19.5/L to 555.0/L) in the ≥3-year group (Fig 3). The blood eosinophil counts of the 1-year group and the 2-year group were not different from that of the untreated group (1-year group, p = .4713; 2-year group, p = .2129), but that of the ≥3-year group was significantly lower than that of the untreated group (p = .0030). The blood eosinophil counts of the 50 patients of the immunotherapy group did not significantly correlate with the duration of immunotherapy (rs = –.335, p = .0541, Fig 4).

Correlation Analysis. A significant correlation was observed between serum ECP levels and blood eosinophil counts in the 68 patients studied (rs = .460, p = .0006). A significant correlation was also observed

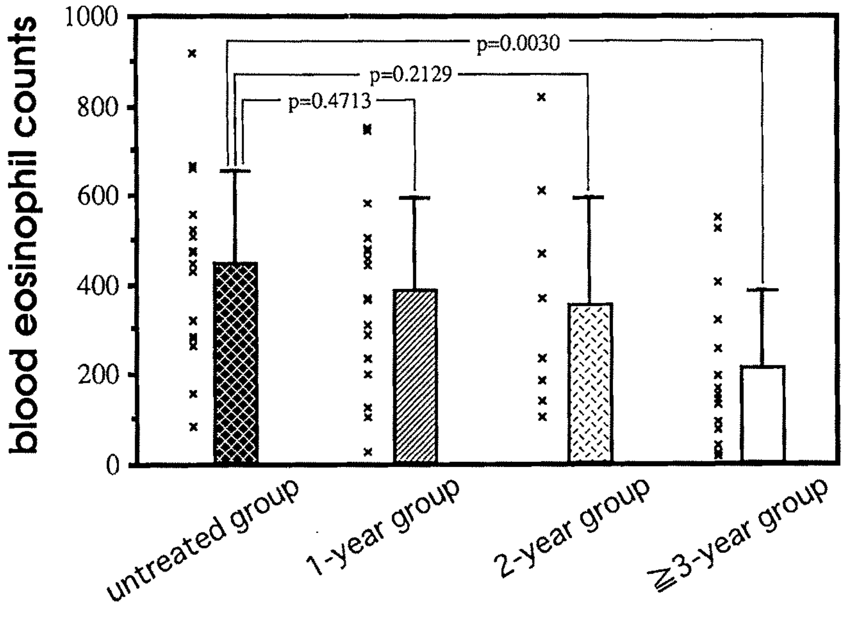

Fig 3. Blood eosinophil counts (per liter). Blood eosinophil counts of 1-year group and 2-year group are not different from that of untreated group, but that of ≥3-year group is significantly smaller than that of untreated group.

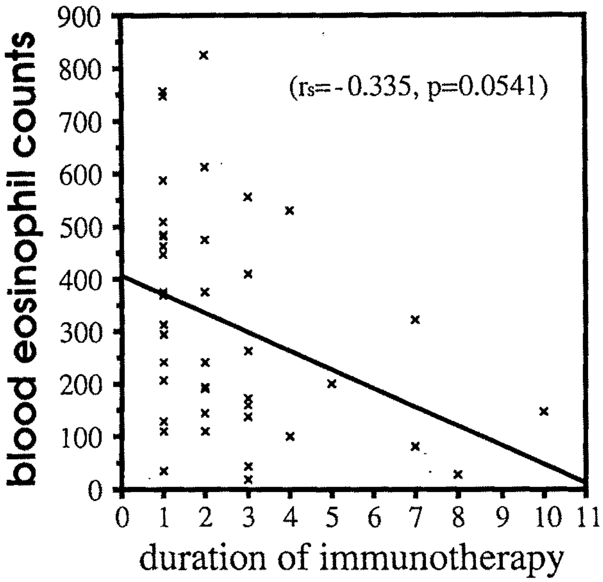

Fig 4. Correlation between blood eosinophil counts (per liter) and duration of immunotherapy (years). Blood eosinophil counts are not significantly correlated with duration of immunotherapy.

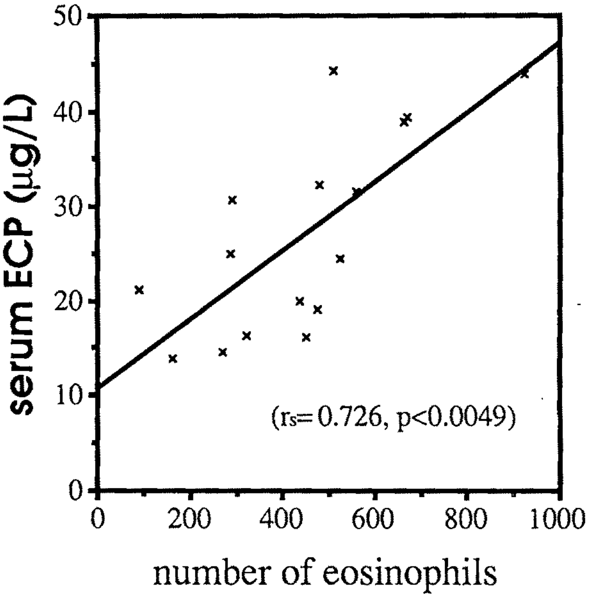

Fig 5. Correlation between serum ECP and blood eosinophil counts (per liter) in untreated group. In untreated group, serum ECP is significantly correlated with blood eosinophil counts.

between serum ECP levels and blood eosinophil counts in the untreated group (rs = .726, p = .0049, Fig 5). However, there was no significant correlation between serum ECP levels and blood eosinophil counts in the 50 immunotherapy patients (rs = .335, p = .0641). Also, there was no significant correlation between serum ECP levels and blood eosinophil counts in the three immunotherapy groups (1-year group, rs = .412, p = .0995; 2-year group, rs = .167, p = .6374; ≥3-year group, rs = .246, p = .3565).

No significant correlation was observed between serum ECP levels and serum IgE antibodies in any patient group (untreated group, rs = .296, p = .2268; 1-year group, rs = .627, p = .0102; 2-year group, rs = .225, p = .4802; ≥3-year group, rs = .128, p = .5758).

DISCUSSION

Serum ECP levels in allergic rhinitis were previously studied by several investigators and still remain controversial. Rak et al[14] demonstrated a significant increase in serum ECP levels in patients with birch pollen-sensitive seasonal allergic rhinitis. More recently, however, an elevation in serum ECP levels in allergic rhinitis was not supported by two investigations.[15,16] Rasp et al[15] examined serum ECP levels in patients with a variety of nasal disorders, including perennial allergic rhinitis and seasonal allergic rhinitis, and compared serum ECP levels in such nasal diseases with those of normal subjects. They failed to find any significant difference among these groups. However, they made no mention of the treatment background of the patients studied. The ECP levels indicate an ongoing inflammation, and some medications such as corticosteroids could modify the serum ECP levels.[11,17-19] If they examined serum ECP levels in patients taking such medications, the insignificant increase might be the result of the medication. Ferguson et al[16] also examined serum levels of ECP in patients with allergic rhinitis, and found them to be in the normal range (less than 16 µg/L). Their study also demonstrated that serum ECP levels in allergic rhinitis were not different from those in symptomatic asthma. Since it is currently accepted that the serum levels of ECP in symptomatic asthma are significantly higher,[11,12,17] their data are confusing.

In this study we examined serum ECP levels in patients with perennial allergic rhinitis. First, we examined whether serum ECP levels were higher in patients with perennial allergic rhinitis than in nonatopic controls. To avoid the possible influence of medications on the serum ECP, we selected 18 untreated patients with perennial allergic rhinitis who were free from seasonal allergic rhinitis or bronchial asthma. Therefore, the serum ECP levels in these patients were considered to be due to environmental *D farinae* exposure alone. We also collected venous blood from each patient for examination of serum ECP and *D farinae*-specific IgE and blood eosinophil counts in April 1995, to avoid the possible influence of seasonal variations in house dust mites. Our study has clearly demonstrated that serum ECP levels in subjects with perennial allergic rhinitis are significantly higher than those of nonatopic healthy volunteers and that serum ECP levels are significantly correlated to blood eosinophil counts. However, we failed to find a significant correlation between specific

IgE antibodies and serum ECP levels. The serum ECP level could reflect the number of activated hypodense eosinophils and the rate of activation of the circulating eosinophils, and the number and activity of primed eosinophils could therefore be linked to an ongoing eosinophil inflammation.[11] Therefore, we interpret this elevation in serum ECP level in the untreated patients as representing an ongoing inflammation process occurring in allergic rhinitis. Additionally, serum concentrations of specific IgE antibodies are independent of allergic inflammation.

The house dust mite, *D farinae*, has been indicated as one of the main sources of house dust allergens and is generally considered to be a major allergen associated with perennial allergic rhinitis.[20] Allergen-specific immunotherapy has been widely used in the treatment of allergic diseases for more than 80 years, but is still controversial. Critics of immunotherapy for perennial allergic rhinitis often claim a lack of documented efficacy. However, three recent double-blind placebo-controlled trials for perennial allergic rhinitis have all clearly shown the efficacy of immunotherapy.[21-23]

In spite of great efforts and diversity of research, the exact mechanisms behind the clinical benefit of immunotherapy have been the subject of much debate and still remain unclear. To date, some possible working mechanisms that have been advocated include a reduction in serum specific IgE antibody level,[24] an increased formation of blocking antibody,[25-27] a decreased sensitivity of basophils to antigen,[28,29] an alteration of T cell function,[30] and an improvement of mucociliary activity.[31] Since the eosinophil inflammatory process could be at least partially involved in allergic rhinitis, immunotherapy might modulate the allergic inflammatory process in allergic rhinitis to reduce the serum levels of ECP. However, this hypothesis has little evidential support.

Thus, the second aim of this study was to elucidate whether immunotherapy is capable of decreasing the increased serum levels of ECP in perennial allergic rhinitis. Rak et al[14] examined the effect of immunotherapy on serum ECP in birch-allergic patients. The levels of serum ECP increased during the season, especially at the end of the pollen season, but not in patients under immunotherapy. In that study, however, the patients were treated with a short course of preseasonal immunotherapy that started 6 months before the pollen season, and were allowed to take topical steroids and antihistamine tablets when they were needed. These medications might have had an influence on the serum ECP.[11,17,19] In the present study, therefore, we selected 50 patients who had exclusively *D farinae*–sensitive allergic rhinitis and had received immunotherapy for at least 1 year before the examination. In addition, the patients were allowed to take no concomitant medication affecting nasal symptoms before the examination. Therefore, their serum ECP levels were modulated exclusively by immunotherapy. The serum ECP level of the 1-year immunotherapy group was significantly higher than that of the nonatopic group, and was not different from that of the untreated group. A year of immunotherapy did not have a favorable effect on the serum ECP levels. In contrast, the serum ECP levels of the 2-year group and the ≥3-year group were significantly lower than that of the untreated group, and were not significantly different from that of the nonatopic group. In addition, serum ECP levels were significantly correlated with the duration of immunotherapy. These findings therefore suggest that serum ECP level or activation in circulating eosinophils decreases gradually during immunotherapy, but this inhibitory effect becomes apparent only after 2 years of immunotherapy. Serum ECP might be a better parameter to represent a favorable action of immunotherapy than eosinophil counts, because there was no significant correlation between serum ECP levels and blood eosinophil counts in the patients who received immunotherapy. This control of serum ECP might be one of the important working mechanisms behind the clinical effect of immunotherapy. However, our present study has not attempted to correlate clinical symptoms and serum ECP levels. Serial determination of serum ECP with special reference to clinical symptom scores in immunotherapy patients as well as untreated patients is necessary to completely explore the clinical role of serum ECP during allergen-specific immunotherapy. Further investigations are needed to establish the therapeutic role of serum ECP in mite-specific immunotherapy for patients with perennial allergic rhinitis.

REFERENCES

1. Smith H. Asthma, inflammation, eosinophils and bronchial hyperresponsiveness. Clin Exp Allergy 1992;22:187-97.

2. Figas E, Gleich GJ. The eosinophil and the pathophysiology of asthma. J Allergy Clin Immunol 1986;77:527-37.

3. Venge P, Dahl R, Fredens K. Epithelial injury by human eosinophils. Am Rev Respir Dis 1988;138:54-7.

4. Togias A, Naclerio RM, Proud D. Studies on the allergic and nonallergic nasal inflammation. J Allergy Clin Immunol 1988; 81:782-90.

5. Venge P, Hakansson L, Peterson CGS. Eosinophil activation in allergic disease. Int Arch Allergy Appl Immunol 1987;82: 333-7.

6. Motojima S, Frigas E, Loegering DA. Toxicity of eosinophil cationic proteins for guinea pig tracheal epithelium in vitro. Am Rev Respir Dis 1988;139:801-5.

7. Gleich GJ, Flavahan NA, Fujisawa T. The eosinophil as a mediator of damage to respiratory epithelium: a model for bronchial hyperreactivity. J Allergy Clin Immunol 1988;81:776-81.

8. Venge P, Roxin LE, Olsson I. Radioimmunoassay of hu-

man eosinophil cationic protein. Br J Haematol 1977;37:331-5.

9. Bousquet J, Chanez P, Lacoste JY. Eosinophilic inflammation in asthma. N Engl J Med 1990;323:1033-9.

10. Klementsson H, Svensson C, Andersson M. Eosinophils, secretory responsiveness and glucocorticoid-induced effects on the nasal mucosa during a weak pollen season. Clin Exp Allergy 1991;21:705-10.

11. Venge P. Serum measurements of eosinophil cationic protein (ECP) in bronchial asthma. Clin Exp Allergy 1993;23(suppl 2):3-7.

12. Sugai T, Sakiyama Y, Matsumoto M. Eosinophil cationic protein in the peripheral blood of pediatric patients with allergic diseases. Clin Exp Allergy 1992;22:275-81.

13. Leimgruber A. Clinical evaluation of a new in vitro assay for specific IgE, the immuno CAP system. Clin Exp Allergy 1991; 21:127-31.

14. Rak S, Lowhagen O, Venge P. The effect of immunotherapy on bronchial hyperresponsiveness and eosinophil cationic protein in pollen-allergic patients. J Allergy Clin Immunol 1988; 82:470-80.

15. Rasp G, Thomas PA, Bujia J. Eosinophil inflammation of the nasal mucosa in allergic and non-allergic rhinitis measured by eosinophil cationic protein levels in native nasal fluid and serum. Clin Exp Allergy 1994;24:1151-6.

16. Ferguson AC, Vaughan R, Brown H. Evaluation of serum eosinophil cationic protein as a marker of disease activity in chronic asthma. J Allergy Clin Immunol 1995;95:23-8.

17. Zimmerman B, Lanner A, Enander I. Total blood eosinophils, serum eosinophil cationic protein and eosinophil protein X in childhood asthma: relation to disease status and therapy. Clin Exp Allergy 1993;23:564-70.

18. Venge P, Dahl R, Peterson CGB. Eosinophil granule proteins in serum after allergen challenge of asthmatic patients and the effects of anti-asthmatic medication. Int Arch Allergy Appl Immunol 1988;87:306-12.

19. Dahl R, Venge P. Blood eosinophil leukocytes and eosinophil cationic protein in vivo study of the influence of beta-2-adrenergic drugs and steroid medication. Scand J Respir Dis 1978; 59:319-22.

20. Nakagawa T, Kudo K, Okudaira H. Characterization of the allergenic components of the house dust mite, *Dermatophagoides farinae*. Int Arch Allergy Appl Immunol 1977;55:47-53.

21. Ewan PW, Alexander MM, Snape C. Effective hyposensitization in allergic rhinitis using a potent partially purified extract of house dust mite. Clin Allergy 1988;18:501-8.

22. Corrado OJ, Pastorello E, Ollier S. A double-blind study of hyposensitization with an alginate conjugated extract of *D pteronyssinus* (Conjuvac) in patients with perennial rhinitis. 1. Clinical aspects. Allergy 1989;44:108-15.

23. McHugh SM, Lavelle B, Kemeny DM. A placebo-controlled trial of immunotherapy with two extracts of *Dermatophagoides pteronyssinus* in allergic rhinitis, comparing clinical outcome with changes in antigen specific IgE, IgG, and IgG subclasses. J Allergy Clin Immunol 1990;86:521-32.

24. Clayton WF, Reisman RE, Georgitis JW, Wypych JI, Arbesman CE. Effect of prolonged venom immunotherapy on serum venom-specific IgE and IgG. Clin Allergy 1983;13:301-7.

25. Ohashi Y, Nakai Y, Kihara S, Nakagawa T, Miyamoto T. House dust mite–specific IgE, IgG1, and IgG4 antibodies in patients with perennial rhinitis. Ann Otol Rhinol Laryngol 1987; 96:434-7.

26. Nakagawa T, Kozeki H, Katagiri J. Changes of house dust mite–specific IgE, IgG and IgG subclass antibodies during immunotherapy with perennial rhinitis. Int Arch Allergy Appl Immunol 1987;82:95-9.

27. Ohashi Y, Nakai Y, Okamoto H, et al. Significant correlation between symptom score and IgG4 antibody titer following long-term immunotherapy for perennial allergic rhinitis. Ann Otol Rhinol Laryngol 1997;106:483-9.

28. Kinura I, Tanizaki Y, Goda Y. Decrease in reactivity of basophils by immunotherapy with house dust extract. Clin Allergy 1985;15:1-7.

29. Uekawa M, Ohashi Y, Esaki Y. Whole blood histamine release rate during immunotherapy for nasal allergy. Acta Otolaryngol Suppl (Stockh) 1991(suppl 486):202-8.

30. Ohashi Y, Nakai Y, Sakamoto H, et al. Serum levels of soluble interleukin-2 receptor in patients with perennial allergic rhinitis before and after immunotherapy. Ann Allergy Asthma Immunol 1996;77:203-8.

31. Ohashi Y, Nakai Y, Ikeoka H, Furuya H, Esaki Y, Kato S. Increased ciliary beating frequency of nasal mucosa following immunotherapy for allergy. Ann Otol Rhinol Laryngol 1989;98: 350-4.

Ann Otol Rhinol Laryngol 106:1997

INCIDENCE OF PRIMARY CILIARY DYSKINESIA IN CHILDREN WITH RECURRENT RESPIRATORY DISEASES

CATHERINE CHAPELIN
CRÉTEIL, FRANCE

ANDRÉ COSTE, MD
CRÉTEIL, FRANCE

PHILIPPE REINERT, MD
CRÉTEIL, FRANCE

MICHEL BOUCHERAT, MD
CRÉTEIL, FRANCE

MARIE-CLAUDE MILLEPIED
CRÉTEIL, FRANCE

FRANÇOISE PORON
CRÉTEIL, FRANCE

ESTELLE ESCUDIER, MD, PHD
PARIS, FRANCE

The goal of the study was to evaluate the incidence of primary ciliary dyskinesia (PCD) in children suffering from recurrent respiratory tract infections (RRIs) by means of a noninvasive method. Respiratory ciliated cells were collected by nasal brushing in 118 children (4.6 ± 2.5 years) with RRIs. The ciliary beat frequency (CBF) was measured with a stroboscopic method, and when the CBF was abnormal, the ciliary ultrastructure was analyzed by a quantitative method.The CBF could be measured in 106 patients (90%) and was abnormal in 15 patients. The ciliary ultrastructure was found to be abnormal in 11 of 15 patients: PCD was diagnosed in 6 cases, and acquired ciliary defects were observed in the remaining 5 patients. Our conclusion, that PCD is rare but not exceptional (5.6%) in children with RRIs, justifies the systematic investigation of ciliated cells in such patients. For this purpose, nasal brushing can be used to sample ciliated cells even in young children.

KEY WORDS — child, ciliary beat frequency, ciliary ultrastructure, recurrent respiratory tract infection.

INTRODUCTION

The upper and lower airways are both lined by respiratory epithelium composed of two main cell types — ciliated and goblet cells — which together ensure efficient mucociliary transport.[1] Failure of ciliary structure and function impairs airway clearance and can be responsible for respiratory tract infections.[2-5] Ciliary insufficiency can be caused by either an inborn error or damage inflicted on the cilia by a noxious agent.[6-10] Congenital defects of ciliary ultrastructure and function correspond to primary ciliary dyskinesia (PCD), including Kartagener's syndrome, which predisposes the patient to upper and lower respiratory tract infections beginning in early childhood.[11-14] These severe and recurrent respiratory infections (RRIs) are different from the normal process of immunization frequently observed in young children and generally lead to a diagnostic evaluation. In the presence of a suggestive clinical pattern (eg, situs inversus, nasal polyposis, bronchiectasis), a two-step protocol with a ciliary beat frequency (CBF) study and then ultrastructural evaluation is classically proposed in order to confirm ciliary abnormalities. Because PCD is considered to be rare, the etiologic survey of RRIs rarely includes ciliary analysis, and in patients with less severe respiratory symptoms, PCD might go undiagnosed. The incidence of this disease appears, therefore, to be underestimated. The aim of this study was to determine the incidence of PCD in children with RRIs by a noninvasive method. For this purpose, ciliary function was systematically included as part of the routine investigations performed in children with RRIs of unknown cause.

MATERIAL AND METHODS

Patients. During 24 months, 118 children (78 boys and 40 girls, mean age 4.6 ± 2.5 years) required etiologic investigations for chronic upper and lower respiratory tract infections in the Pediatric Department of Créteil and entered this study. All these children were considered to have RRIs because of the increased incidence and severity of their respiratory infections, occurring more than once a month over at least 6 consecutive months.

In the study population, RRIs consisted of upper respiratory tract infections (otitis media, rhinosinusitis; 42.4%), lower respiratory tract infections (bronchitis, pneumonitis; 31.3%), or both (26.3%). In 2 siblings, the presence of situs inversus suggested Kartagener's syndrome.

Methods. All the children underwent the same etiologic assessment at the hospital on an outpatient basis. All investigations were performed in the absence of

---

From the Department of Histology, University of Medicine (Paris VI and Paris XII; Chapelin, Poron, Escudier), and the Departments of Otolaryngology (Coste, Boucherat) and Pediatrics (Reinert) and the Laboratory of Electron Microscopy (Millepied), Hôpital Intercommunal, Créteil, France. This study was supported by the Délégation à la Recherche Clinique de l'Assistance Publique-Hôpitaux de Paris, France.

CORRESPONDENCE — Estelle Escudier, MD, PhD, Groupe Hospitalier Pitié-Salpêtrière, Service d'Histologie-Embryologie Cytogénétique, Pr. Jacques Poirier, Pavillon Benjamin Delessert, 83 Bd de l'Hôpital, 75651 Paris Cedex 13, France.

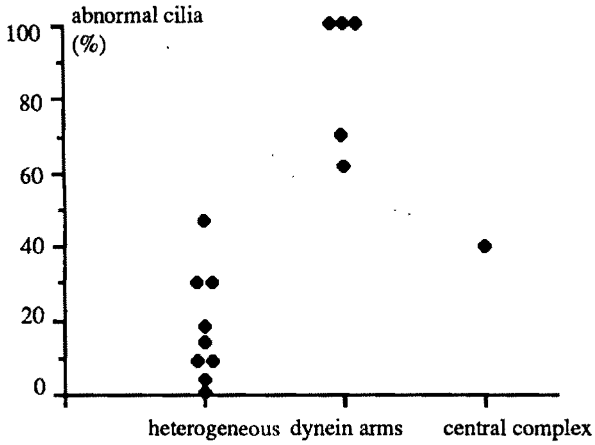

Fig 1. Ultrastructure of respiratory cilia: percentage and type of abnormalities in 15 patients with abnormal ciliary beat frequency.

acute respiratory tract infection. This survey included a complete physical examination with supplementary testing including a chest X-ray and a sweat test. Laboratory tests were performed to determine the immunologic and allergic status. Examination of ciliary function was performed together with the other investigations.

An otolaryngological examination, including sinus films and rhinoscopy with nasal sampling for ciliary study, was performed in the absence of local infection. Upper respiratory tract cells were collected by brushing to study ciliary motion, and a biopsy was performed for ultrastructural analysis of cilia when the CBF was abnormal. In addition, 10 patients with a normal CBF were randomly chosen for ciliary ultrastructural analysis.

Specimens from the nasal mucosa were sampled by brushing or biopsy of the inferior nasal turbinate after local anesthesia (10 minutes with 5% lidocaine hydrochloride–naphazoline hydrochloride, Roger Bellon, France) as previously described.[15-17] A small cytologic brush (Olympus, Rungis, France) with 3-mm-long nylon bristles extending 12 mm from the tip was used for the sampling. When bronchial endoscopy was required because of clinical features or radiologic findings, respiratory cells were obtained during the endoscopic examination.

After nasal or bronchial brushing, respiratory cells were immersed in culture medium (IP 199, Eurobio, France) and incubated at 37°C for 1 hour before the CBF measurements were carried out.[18] Nasal or bronchial biopsy specimens were immersed in 2.5% glutaraldehyde in 0.045 mol/L cacodylate buffer at pH 7.4 and processed as usual for ultrastructural analysis.[19]

Ciliary Beat Frequency. The CBF was measured by a stroboscopic method applied to ciliated epithelial cells maintained in tissue culture medium. The CBF was measured at room temperature on at least three separate areas and expressed in hertz as the mean of the different measurements.[18] In our laboratory, the CBF of normal adults was found to be in the range of 10 to 14 Hz, and a CBF lower than 6 Hz was considered to be clearly abnormal. In all cases, the presence of ciliated cells was confirmed by cytologic analysis after cytocentrifugation (Cytospin Shandon II, 500 rpm for 10 minutes) and staining with May-Grunwald-Giemsa stain.

Ultrastructure of Respiratory Cilia. After fixation, samples for transmission electron microscopy were post-fixed in osmium tetroxide and routinely processed.[19] Ultrathin sections were studied at a final magnification of 60,000. At least 50 transverse sections through the ciliary shafts of different cells were analyzed in each specimen to study the internal axonemal structure according to a quantitative method.[11,18] Briefly, dynein arms, radial spokes, and nexin links were considered to be absent from sections if the structure was missing from at least six of the nine peripheral doublets. In order to facilitate the definition of axonemal abnormalities, the central structures (central microtubules and central sheath) were termed the "central complex." The results of the ciliary ultrastructural study were expressed as a percentage of abnormal cilia among the total number of cilia analyzed, and the main ultrastructural defect was specified. Because, in controls, some 3% to 5% of cilia can exhibit ultrastructural defects,[5,12] a percentage of abnormal cilia higher than 10% was considered to be clearly abnormal.[5,20,21] Ciliary orientation was systematically evaluated by comparing the positions of the central pairs of adjoining cilia. Disorientation was defined as an angle of more than 25°.[22]

RESULTS

No complication (pain or bleeding) occurred in any of the 118 patients. Of the 118 cell samples, 114 were collected from nasal fossae, and 4 were obtained from bronchi.

Ciliary Beat Frequency. A CBF analysis was impossible in 12 cases (10%) due to the absence of ciliated cells in the sample. Only the remaining 106 patients, in whom CBF analysis was possible, were considered for the rest of the study. The CBF was normal (mean ± SEM 10.4 ± 1.7 Hz) in most samples (91/106). In 15 cases, the ciliary beating was abnormal — either slow (<6 Hz) or absent.

Ultrastructure of Respiratory Cilia. A ciliary ultrastructural study was performed in the 15 cases with abnormal CBF. Quantitative and qualitative analyses of ciliary ultrastructure are summarized in Figs 1 and 2. The ciliary ultrastructure was normal for the 10 patients

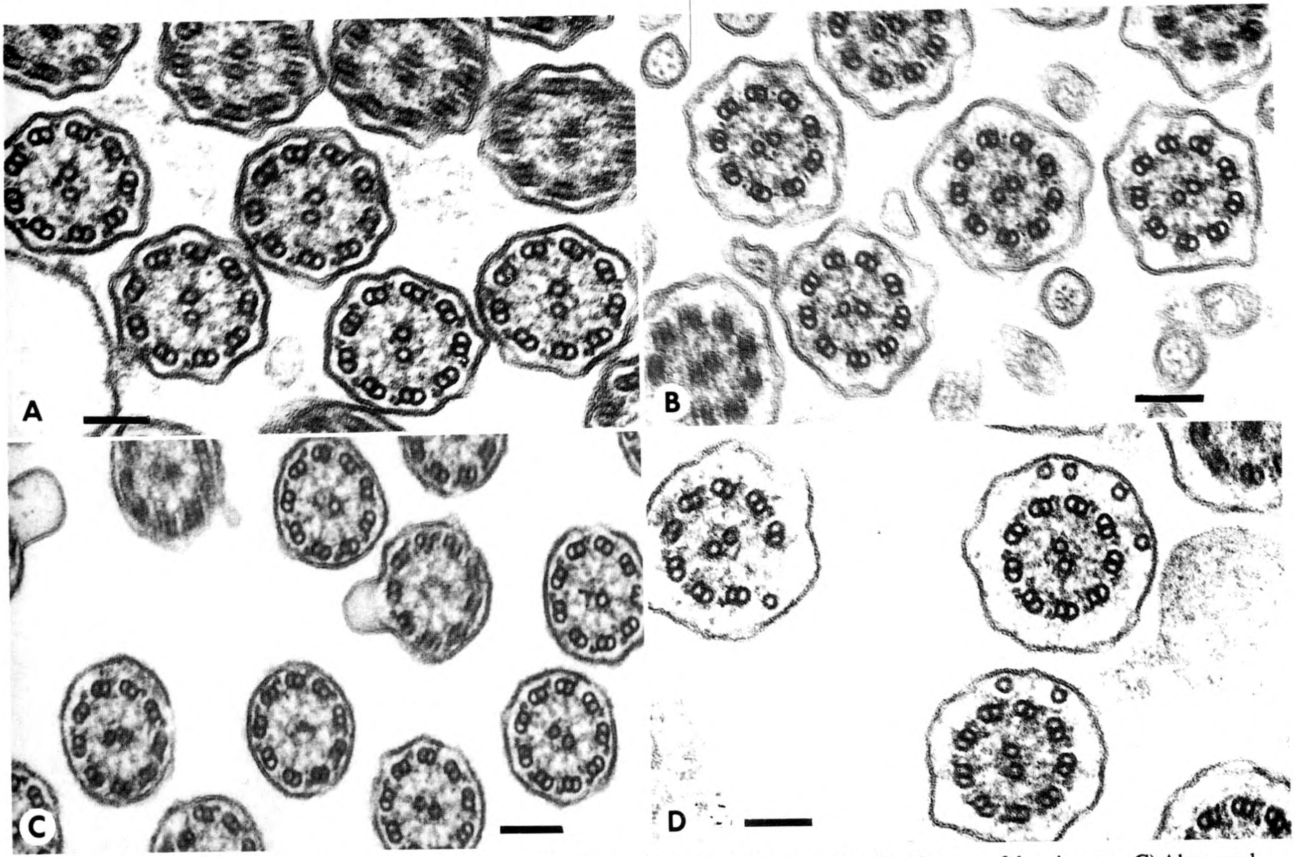

Fig 2. Various ultrastructural patterns of respiratory cilia. Bars — 0.1 μm. A) Normal cilia. B) Absence of dynein arms. C) Abnormal central complex. D) Abnormal number of peripheral microtubules.

with normal CBF selected at random for ultrastructural study of cilia (range of 0.5% to 5% abnormal cilia; Fig 2A).

DISCUSSION

In pediatric departments, RRIs are frequently observed in young children. These RRIs can be due to various causes. Usually, a standardized survey looks for allergies, esophageal reflux, adenoiditis, environmental conditions (pollution or passive smoking), or — less frequently and in the presence of a special clinical context for immunodeficiency — cystic fibrosis and Kartagener's syndrome. Kartagener's syndrome was first described as the clinical association of bronchiectasis, recurrent sinusitis, and situs inversus.[2,3] More recently, this syndrome was considered to be a subgroup of PCD caused by a primary defect of ciliary ultrastructure and function.[4,8] Patients with PCD have virtually no respiratory mucociliary transport, owing to abnormal ciliary ultrastructure and motion, and usually have respiratory symptoms beginning early in life.[2-5] Primary ciliary dyskinesia is considered to be a possible but exceptional cause of RRI and is rarely suspected in the absence of a typical clinical pattern.

As classically proposed,[5,6,9,17,22] CBF measurement constituted the first step of ciliary analysis in the present study. Samples were collected mainly from the nasal fossa, allowing CBF measurement in most cases. In contrast with tracheobronchial sampling requiring endoscopy, nasal brushing is a noninvasive method, usable even in young children. In a previous study,[21] we demonstrated that the diagnosis of PCD can be performed on nasal cilia, since all ciliated cells of the respiratory tract express the same congenital defect. It therefore seems more convenient to start by studying nasal cilia before deciding to perform bronchial sampling.

Most of our patients had normal CBF, and for them the diagnosis of PCD was very unlikely. In the other patients, an abnormal CBF led us to study ciliary ultrastructure. When immotile cilia or a low CBF was associated with a high percentage of abnormal cilia, this suggested the potential role of defective cilia in their respiratory disease. The question was, therefore, to determine whether these ciliary abnormalities had a congenital origin. The diagnosis of PCD is usually established in the presence of a high proportion of abnormal cilia showing the same ultrastructural defect.[3,5,21] According to these criteria, a diagnosis of PCD was accepted for 6 of our patients. As usually reported, the main ciliary defect found in these patients was an absence of dynein arms affecting almost all the

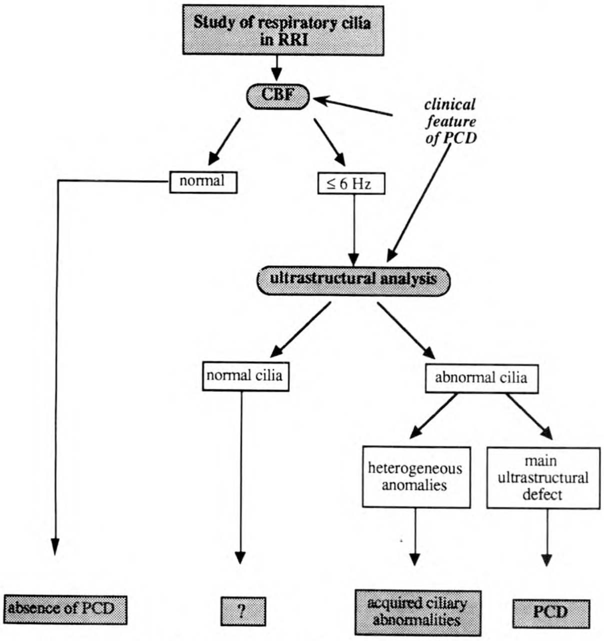

Fig 3. Schedule of functional and ultrastructural ciliary analysis proposed as standardized investigation for primary ciliary dyskinesia (PCD) detection in children with recurrent respiratory infections (RRI). CBF — ciliary beat frequency.

cilia[3-6] (Fig 2B). In only 1 case, the main ultrastructural defect involved the central complex (Fig 2C). The percentage of cilia affected was lower, but this specific ultrastructural defect is described as never involving all cilia, even in PCD.[11]

In the remaining patients with abnormal ciliary motion, numerous cilia with heterogeneous ultrastructural defects were found (Fig 2D). This finding is frequent in patients with chronic respiratory tract infections.[5,9-11] In these patients, it is surprising to note that although most of the cilia were ultrastructurally normal, ciliary beating was abnormal. It is therefore difficult to assert the role of ciliary abnormalities in the respiratory tract infections. In contrast with PCD, acquired ciliary defects are not well characterized. It is generally accepted that the lesions predominantly occur in sites of infection.[6,7,10,22] Acquired ciliary abnormalities detected in the upper respiratory tract of patients with predominant otolaryngological infection therefore cannot predict the existence of the same abnormalities in the lower airways.

Finally, in a few children with abnormal CBF, the ciliary ultrastructure was shown to be normal. In these patients, the absence of ultrastructural defects prevents us from distinguishing between PCD with normal cilia or a technical problem interfering with CBF measurement. Surprisingly, normal ciliary ultrastructure has previously been reported in patients with immotile cilia,[23] suggesting that abnormal ciliary motion could be related to cellular defects not yet detectable by ultrastructural study. Moreover, in a few patients with the clinical triad of Kartagener's syndrome, neither functional nor structural abnormalities of cilia could be detected.[24,25] In all the cases of abnormal ciliary motion and normal ciliary ultrastructure, it would be interesting to perform isotope measurement of mucociliary clearance — unfortunately, not suitable for children.[26]

The schedule of nasal ciliary investigations used in this study (Fig 3) reserves electron microscopic studies for patients with abnormal CBF. The normal ciliary ultrastructure in 10 patients with normal CBF, selected at random, suggests that the possibility of missing the diagnosis of PCD in the absence of specific clinical features and in the absence of abnormal CBF is negligible. Of course, when there is a high clinical suspicion of PCD (ie, familial respiratory tract diseases or Kartagener's syndrome), an ultrastructural analysis should be performed regardless of the CBF. It must be noted that even in the absence of sophisticated equipment for CBF measurement, it is possible, and not expensive, to estimate the ciliary motion with a standard light microscope.

In conclusion, in the child population studied, abnormal ciliary motion was found in 14% of the study patients, and PCD was detected in 5.6% of them. Thus, PCD is rare but seems not exceptional in children with RRIs, justifying the systematic study of ciliary function in this population. Nasal brushing is a noninvasive method that allows us to detect ciliary abnormalities in children with RRIs in whom we suspect the diagnosis of PCD. Because PCD is a genetically determined, lifelong disease, it is especially important to confirm this diagnosis with strict ultrastructural criteria.

REFERENCES

1. Breeze RG, Wheeldon EB. The cells of the pulmonary airways. Am Rev Respir Dis 1977;116:705-77.

2. Afzelius BA. A human syndrome caused by immotile cilia. Science 1976;193:317-9.

3. Afzelius BA. Immotile cilia. Thorax 1980;35:401-4.

4. Rutland J, Cox T, Dewar A, Cole P. Screening for ciliary dyskinesia. A spectrum of defects of motility and structure. Eur J Respir Dis 1983;64(suppl 127):71-7.

5. Rossman CM, Lee RM, Forrest JB, Newhouse MT. Nasal ciliary ultrastructure and function in patients with primary ciliary dyskinesia compared with that in normal subjects and in subjects with various respiratory diseases. Am Rev Respir Dis 1984;129:161-7.

6. Mygind N, Pedersen M, Nielsen MH. Primary and secondary ciliary dyskinesia. Acta Otolaryngol (Stockh) 1983;95:688-94.

7. Afzelius BA, Cammer P, Mossberg B. Acquired ciliary defects compared to those seen in the immotile-cilia syndrome. Eur J Respir Dis 1983;64(suppl 127):5-10.

8. Rossman CM, Forrest JB, Lee RM, Newhouse MT. The dyskinetic cilia syndrome. Ciliary motility in immotile cilia syndrome. Chest 1980;78:580-2.

9. Escalier D, Jouannet P, David G. Abnormalities of the ciliary axonemal complex in children: an ultrastructural and cinetic study in a series of 34 cases. Biol Cell 1982;44:271-82.

10. Lungarella G, Fonzi L, Ermini G. Abnormalities of bronchial cilia in patients with chronic bronchitis. An ultrastructural and quantitative analysis. Lung 1983;161:147-56.

11. Carson JL, Collier AM, Hu SS. Acquired ciliary defects in nasal epithelium of children with acute viral upper respiratory infections. N Engl J Med 1985;312:463-8.

12. Ballenger JJ. Acquired ultrastructural alterations of respiratory cilia and clinical disease. A review. Ann Otol Rhinol Laryngol 1988;97:253-8.

13. Howell JT, Schochet SS, Goldman AS. Ultrastructural defects of respiratory tract cilia associated with chronic infections. Arch Pathol Lab Med 1980;104:52-5.

14. Corbeel L, Cornillie F, Lauweryns J, Boel M, Van den Berghe G. Ultrastructural abnormalities of bronchial cilia in children with recurrent airway infections and bronchiectasis. Arch Dis Child 1981;56:929-33.

15. Cornillie FJ, Lauweryns JM, Corbeel L. Atypical bronchial cilia in children with recurrent respiratory tract infections. A comparative ultrastructural study. Pathol Res Pract 1984;178:595-604.

16. Petruson B, Hansson H-A. Nasal mucosal changes in children with frequent infections. Arch Otolaryngol Head Neck Surg 1987;113:1294-300.

17. Rutland J, Cole P. Non-invasive sampling of nasal cilia for measurement of beat frequency and study of ultrastructure. Lancet 1980;2:564-5.

18. Baum G, Roth T, Teichtahl H, Aharonson E, Priel Z. Ciliary beat frequency of respiratory mucosa cells: comparison of nasal and tracheal sampling sites. Am Rev Respir Dis 1982;125(suppl 211).

19. Pipkorn U, Karlsson G. Methods for obtaining specimens from the nasal mucosa for morphological and biochemical analysis. Eur Respir J 1988;1:856-62.

20. Ehouman A, Pinchon MC, Escudier E, Bernaudin JF. Ultrastructural abnormalities of respiratory cilia. Descriptive and quantitative study of respiratory mucosa in a series of 33 patients. Virchows Arch 1985;48:87-95.

21. Escudier E, Escalier D, Pinchon MC, Boucherat M, Bernaudin JF, Fleury-Feith J. Dissimilar expression of axonemal anomalies in respiratory cilia and sperm flagella in infertile men. Am Rev Respir Dis 1990;142:674-9.

22. Verra F, Fleury-Feith J, Boucherat M, Pinchon MC, Bignon J, Escudier E. Do nasal ciliary changes reflect bronchial changes? An ultrastructural study. Am Rev Respir Dis 1993;147:908-13.

23. Herzon FS, Murphy S. Normal ciliary ultrastructure in children with Kartagener's syndrome. Ann Otol Rhinol Laryngol 1980;89:81-3.

24. Greenstone M, Rutman A, Pavia D, Lawrence D, Cole PJ. Normal axonemal structure and function in Kartagener's syndrome: an explicable paradox. Thorax 1985;40:955-7.

25. Escudier E, Escalier D, Homasson JP, Pinchon MC, Bernaudin JF. Unexpectedly normal cilia and spermatozoa in an infertile man with Kartagener's syndrome. Eur J Respir Dis 1987; 70:180-6.

26. Sleigh MA. Ciliary function in mucus transport. Chest 1981;80:791-5.

≈

ENDOSCOPY DAYS IN PEDIATRIC OTOLARYNGOLOGY

International Pediatric Otolaryngology Endoscopy Days of Lyon: The Pediatric Larynx will be held March 2-3, 1998, in Lyon, France. For more information, contact M. C. Duchez, Secretariat, Departement d'ORL, Hopital Ed. Herriot, 69003 Lyon, France; fax 33 4 72 11 05 34.

Ann Otol Rhinol Laryngol 106:1997

IN VIVO MEASUREMENT OF HUMAN NASAL MUCOCILIARY MOTILITY USING A LASER LIGHT SCATTERING INSTRUMENT

YOAV PALTIELI, MD, DSC
HAIFA, ISRAEL

MILO FRADIS, MD
HAIFA, ISRAEL

JACOB BEN-DAVID, MD
HAIFA, ISRAEL

LUDWIG PODOSHIN, MD
HAIFA, ISRAEL

HALA SHITI, BSC
HAIFA, ISRAEL

ZVI KAM, DSC
REHOVOT, ISRAEL

The mucociliary system is one of the most important airway defense mechanisms, and knowledge of the mucociliary wave frequency (MWF) is important in the understanding of this system. Employing a laser light scattering technique and a thin, flexible fiberoptic probe, we developed and tested a simple and practical device for real-time in vivo measurements of mucociliary activity in the human nose. The laser instrument is user-friendly and does not produce any discomfort to the patient. The mean ± SE of MWF of 36 measurements in 16 normal subjects was 7.7 ± 0.5 Hz. The mean MWF of 17 measurements in 7 patients with allergic rhinitis was 5.5 ± 0.2 Hz ($p < .005$), and the mean MWF of 56 measurements in 17 patients with septum deviation was 5.8 ± 0.2 Hz ($p < .001$). The instrument presented in this study might provide a new and convenient method of studying the mucociliary activity in the respiratory tract.

KEY WORDS — human, in vivo study, laser light scattering instrument, mucociliary motility, nasal ciliary epithelium.

INTRODUCTION

Cilia are tiny, hairlike appendages about 0.25 μm in diameter that contain a bundle of parallel microtubules at their core. They extend from many kinds of cells and are found in most animal species and some lower plants. Their primary function is to move fluid over the surface of a cell or to propel a single cell through a fluid.[1] The mucociliary system is one of the most important airway defense mechanisms. In previous in vitro studies, it was found that drugs,[2,3] allergies,[4] and upper respiratory tract infections[5] affect ciliary motility. Until now, it has not been possible to study mucociliary function in vivo in patients.

Various methods have been used over the past several decades to measure mucociliary transport.[6-12] Some have used saccharine, indigo carmine, or coal powder, which can be detected by a sweet-tasting sensation in the mouth or visual presentation in the pharynx[9-12]; others have used radioactive materials such as technetium sulfur.[6-8] Verdugo and Golborne,[13] Svartengren et al,[14] and Wong and Yeates[15] described the development and validation of the laser light scattering spectroscopy method to measure the movement of cilia in situ, inside the trachea of animals. Lindberg and Runer,[2] using a photoelectric method, described a new means for in vivo measurement of mucociliary activity in the human nose. However, these latter methods have the disadvantage of being sensitive to external movements of the patient and the examiner's hand.

The aims of the present study were to develop a simple and practical instrument for real-time in vivo measurements of mucociliary activity in the human upper airways, and to measure the mucociliary wave frequency (MWF) in the nasal epithelium in normal subjects, as well as in patients suffering from allergic rhinitis or a deviated nasal septum.

MATERIALS AND METHODS

A small portable unit including all the components necessary for laser illumination and optimal detection of the signal was designed and constructed (Fig 1). The light source was a laser diode with a wavelength of 670 nm (FD 6700S, Gerhard Franck Op-

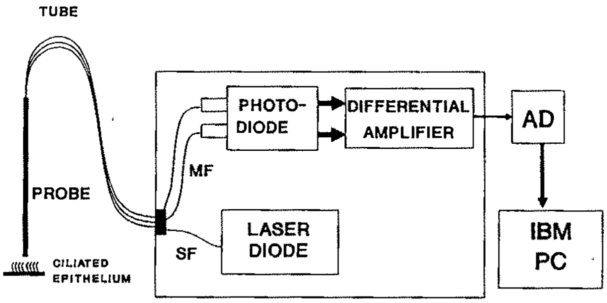

Fig 1. Schematic diagram of mucociliary wave frequency measuring instrument. AD — analog-to-digital acquisition card; MF — multimode fibers; SF — single-mode fiber.

From the Departments of Obstetrics and Gynecology (Paltieli, Shiti) and Otolaryngology (Fradis, Ben-David, Podoshin), Bnai-Zion Medical Center, Faculty of Medicine, Technion-Israel Institute of Technology, Haifa, and the Department of Chemical Immunology, Weizmann Institute of Science, Rehovot (Kam), Israel.

CORRESPONDENCE — Yoav Paltieli, MD, DSc, Dept of Obstetrics and Gynecology, Bnai-Zion Medical Center, 47 Golomb Street, Haifa 31048, Israel.

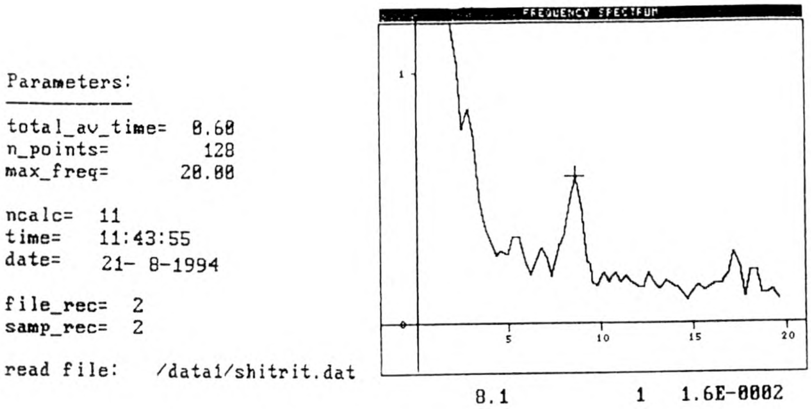

```
Parameters:
-----------
total_av_time=  0.60
n_points=        128
max_freq=      20.00

ncalc=  11
time=   11:43:55
date=   21- 8-1994

file_rec=  2
samp_rec=  2

read file:   /data1/shitrit.dat
```

Fig 2. Computer monitor display during use of instrument for ciliary beat frequency measurement. Power spectrum is displayed on right, and user-chosen parameters are displayed on left. Ciliary beat frequency that was measured was 8.1 Hz. Presence of low-frequency noise spectrum (below 3 Hz) resulted from drifts in detection signal level due to motion.

tronik, Hamburg, Germany). The laser beam was transmitted into a single-mode fiber that was selected in order to avoid speckle pattern fluctuations due to fiber movements. A flexible tube, approximately 1.5 m long, extending from a box, enclosed the single-mode fiber and two multimode fibers guiding the back-scattered light from the probe tip to two photodiode detection units in the recording unit. To collect as much of the scattered light as possible, thick multimode fibers were selected (numerical aperture of 0.316). The two collecting optical fibers enabled differential measurement between the two signals to reduce fluctuations due to relative motion between the sample and the probe. The probe was constructed from a flexible catheter, 1.6 mm in diameter and 50 cm long (Marrs Laparoscopic Catheter, Cook Ob/Gyn, Spencer, Ind), sealed to prevent air leakage during laparoscopy. At the tip of the probe the stripped fibers were joined together, embedded in a special epoxy, and polished. The multimode fibers guided the reflected light from the ciliary epithelium to two detecting photodiodes (DF-670, EG&G Optoelectronics, Lake Forest, Canada). Outputs from the two photodiode preamplifiers were fed into a differential amplifier circuit. A high-pass sharp frequency cutoff at 0.5 Hz was introduced to prevent saturation of amplifiers due to slow movements. A low-pass presampling filter eliminated high frequencies (such as 50-Hz electrical interference). Further amplification with gain ranges between 30× and 350× could be controlled by the user. The spectral analysis of the signal, and the graphic display were carried by a personal computer. An analog-to-digital data acquisition card sampled the output signal according to user-specified sampling parameters and stored the data. On initiation of the program, a parameter menu was displayed. User-chosen parameters were averaging time (in seconds), number of sampling points, and maximum frequency. For each array of N sampled data points, Fourier transformation and squaring yielded the power spectrum for all frequencies up to the maximum frequency. The averaging time determined how many separate power spectra would be averaged in the final power spectrum. The resulting power spectra could be seen on-screen in real time and were stored on disk for later analysis (Fig 2). To establish the sensitivity of ciliary beat measurements and the effects of probe movements, experiments were first performed in vitro on slices of chicken trachea. Photometric microscopy served as a reference to which observations of the laser instrument were compared under well-controlled conditions.

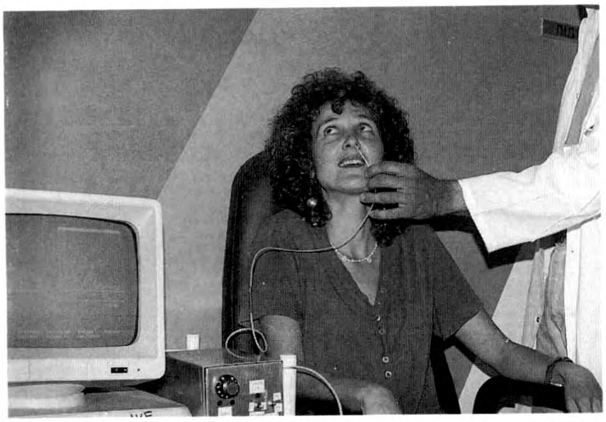

Fig 3. Photograph of mucociliary wave frequency measuring method. Patient is sitting relaxed on upright chair, facing examiner. Probe is introduced in each nostril, sounding anterior border of inferior turbinate.

Description of Measurement Procedure. The patient sat relaxed on a chair, facing the examiner. The probe was introduced in each nostril, sounding the anterior border of the inferior turbinate (Fig 3). Optimal signals were obtained when the probe gently touched the nasal mucosa. The time of each measurement was 30 or 36 seconds.

Patient Groups. The present clinical pilot study included 16 healthy persons, 17 patients with a deviated nasal septum, and 7 patients with allergic rhinitis. Patients who had purulent discharge from the nose, smoked more than 10 cigarettes per day, or used topical nasal medications were excluded.

The clinical study was approved by the Bnai-Zion

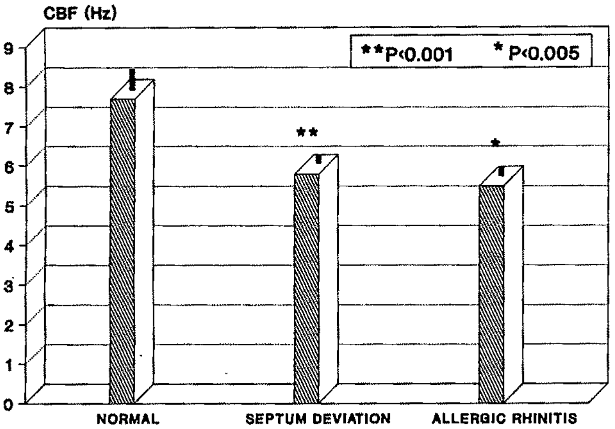

Fig 4. Mean mucociliary wave frequency in normal cases and in patients with allergic rhinitis and septum deviation.

Medical Center Committee on Clinical Investigation, and the patients signed a formal agreement to participate in the study.

Statistical Analysis. The significance of differences between the healthy and the pathologic groups was determined by Student's *t*-test.

RESULTS

The mean ± SE of 36 MWF measurements in normal subjects was 7.7 ± 0.5 Hz (Fig 4). The mean MWF of 17 measurements in patients with allergic rhinitis was 5.5 ± 0.2 Hz ($t = 2.94$, $p < .005$), and of 56 measurements in patients with septum deviation was 5.8 ± 0.2 Hz ($t = 3.59$, $p < .001$) (Fig 4). No significant difference was found between the septal deviation and allergic rhinitis groups ($t = 0.53$).

DISCUSSION

Despite the critical function of the mucociliary epithelium in the respiratory tract, there are not yet conclusive data about the relationship between abnormal mucociliary function and respiratory diseases. A reliable and simple method for investigating the ciliary epithelium could aid in the understanding of the cilia function in the respiratory tract and in diagnosis of impairment of mucociliary activity in various respiratory diseases. Lee and Verdugo[16] described the use of laser light scattering spectroscopy as a reliable technique that presents several important advantages over methods currently used to measure the frequency of ciliary beat. It does not require high-magnification microscopic imaging, and collects the average beat frequency of a large number of cilia. Using this technique as a starting point, we developed a prototype of a compact and easy-to-operate medical instrument capable of real-time in vivo evaluation of MWF.

Previously, Lindberg and Runer[2] reported a method of measurement of MWF in vivo by a rigid probe, 3.2 mm in diameter, containing an optical system; the mucociliary activity was photoelectrically analyzed by a computer. This method has significant limitations. In order to avoid motion artifacts, the lower jaw and forehead of the patient had to be supported by a frame, and the upper jaw was fixed in a plastic cast of the subject's upper teeth, screwed to a stand. This caused most subjects significant discomfort, and is therefore not suitable for routine clinical measurements. In our method, motion artifacts are overcome, and a shorter time is needed for each spot measurement (30 or 36 seconds). It avoids the discomfort of the 30-minute duration, as well as the fixation to the stand utilized by Lindberg and Runer.[2] The nasal probe in our device is thin and flexible, does not produce any discomfort in patients, and can be used in freehand fashion.

In the present study we measured the MWF to be 7.7 ± 0.5 Hz in the nose of normal subjects. This is higher than the MWF we measured in human oviducts using the same instrument (5.4 ± 0.3 Hz in the fimbria and 5.0 ± 0.1 Hz in the ampulla).[17] Lindberg and Runer[2] measured an MWF in the human nose of 11.5 ± 1.6 Hz, whereas Hameister et al[18] obtained a value of 7.2 ± 0.6 Hz in baboon trachea, and Svartengren et al[14] a value of 5 Hz in pig trachea. In the present study, it was found that patients with a deviated nasal septum and patients with allergic rhinitis had an MWF that was significantly lower than that in normal subjects. We assume that the reduced airflow through the nose also reduces the mucociliary activity.

The device described in this study appeared capable of producing an accurate and reliable real-time in vivo analysis of abnormal mucociliary activity. It could provide a new and convenient means for studying mucociliary activity in the respiratory tract. Further clinical studies may substantially contribute to diagnosis of impaired mucociliary function in the nose, as well as in the lower airways, with different respiratory diseases and medical treatments.

ACKNOWLEDGMENTS — We thank Dr Gila Zur, Eng Reuven Deroos, Prof Gadi Eisenstein, and Eng Ron Nagar, whose dedication and competence in the design and construction of instrumentation hardware and software enabled us to bring this project to the level of a functional device in the hospital.

REFERENCES

1. Albert B, Bray D, Lewis J, Raff M, Roberts K, Watson JD, eds. Molecular biology of the cell. New York, NY: Garland Publishing, 1994:1294.

2. Lindberg S, Runer T. Method for in vivo measurement of mucociliary activity in the human nose. Ann Otol Rhinol Laryngol 1994;103:558-66.

3. Dolata J, Lindberg S, Mercke U. Histamine stimulation of mucociliary activity in the rabbit maxillary sinus. Ann Otol Rhinol Laryngol 1990;99:666-71.

4. Hisamatsu K, Ganbo T, Nakatowe T, et al. Cytotoxicity of human eosinophil granule major basic protein to human nasal sinus mucosa in vitro. J Allergy Clin Immunol 1990;86:52-3.

5. Petrusson B, Hansson HA. Nasal mucosa change in children with frequent infections. Arch Otolaryngol Head Neck Surg 1987;113:1294-300.

6. Espana RD, Franch M, Garcia A, Pavia J. Measurement of mucociliary transport in man. Rhinology 1986;24:241-7.

7. Brondeel L, Sonstabo R, Clement P, van Ryckeghem W. Value of the Tc99 particle test and saccharine test in mucociliary examinations. Rhinology 1983;21:135-42.

8. Puchelle E, Aug F, Zahm JM, Bertrand A. Comparison of nasal and bronchial mucociliary clearance in young nonsmokers. Clin Sci (Colch) 1982;62:13-6.

9. Dietmer T. A modification of the saccharine test for nasal mucociliary clearance. Rhinology 1986;24:237-40.

10. Passali D, Bianchini Ciampoli M. Normal values of mucociliary transport times in young subjects. Int J Pediatr Otorhinolaryngol 1985;9:151-6.

11. Duchateau GS, Graamans K, Zuidema J, Merkus FW. Correlation between nasal ciliary beat frequency and mucus transport rate in volunteers. Laryngoscope 1985;95:854-9.

12. Puchelle E, Aug F, Pham QT, Bertrand A. Comparison of three methods for measuring nasal mucociliary clearance in man. Acta Otolaryngol (Stockh) 1981;91:297-303.

13. Verdugo P, Golborne CA. Remote detection of ciliary movement by fiber optic laser-Doppler spectroscopy. IEEE Trans Biomed Eng 1988;35:303-7.

14. Svartengren K, Wiman LG, Thyberg P, Rigler R. Laser light scattering spectroscopy: a new method to measure tracheobronchial mucociliary activity. Thorax 1989;44:539-47.

15. Wong LB, Yeates DB. Stimulation of tracheal ciliary beat frequency by localized tissue incursion. J Appl Physiol 1990; 68:411-6.

16. Lee WI, Verdugo P. Laser light scattering spectroscopy: a new application in the study of ciliary activity. Biophys J 1976; 16:1115-9.

17. Paltieli Y, Weichselbaum A, Hoffman N, Eibschitz I, Kam Z. Laser scattering instrument for real time in-vivo measurement of ciliary activity in human fallopian tubes. Hum Reprod 1995;10:1638-41.

18. Hameister WM, Wong LB, Yeates DB. Tracheal ciliary beat frequency in baboons: effects of peripheral histamine and capsaicin. Agents Actions 1992;35:200-6.

≈

ENDOSCOPIC AND IMAGE GUIDED SINUS SURGERY

Advanced Endoscopic and Image Guided Sinus Surgery — Beyond the Basics will be held in Boston, Massachusetts, November 7-8, 1997. For more information, contact Harvard MEDCME, PO Box 825, Boston, MA 02117-0826; telephone 617-432-1525.

Ann Otol Rhinol Laryngol 106:1997

EFFECTS OF ANESTHETIC TECHNIQUE ON THE HEMODYNAMIC RESPONSE TO MICROLARYNGEAL SURGERY

ANGELES AYUSO, MD
MERCEDES LUIS, MD
XAVIER SALA, MD
JESÚS SÁNCHEZ, MD
JOSÉ TRASERRA, MD
BARCELONA, SPAIN

Our aim was to study the attenuation of the hemodynamic response to microlaryngeal surgery by β-blocking agents used as support drugs to the anesthetic technique. The study was carried out in 30 patients randomly allocated to one of three groups. The control group received only anesthetic drugs. The second group received labetalol hydrochloride 0.3 mg/kg 3 minutes before induction and 0.15 mg/kg 2 minutes prior to the start of suspension of the larynx. The third group received esmolol hydrochloride 500 μg/kg 3 minutes prior to induction and a continuous infusion of 300 μg/kg during the surgical procedure. Hemodynamic data in the three groups were compared by analysis of variance. A statistically significant difference ($p < .05$) was found in hemodynamic data among the two groups treated with blocking agents and the control group. The addition of β-blocking agents to the anesthetic technique attenuates the hemodynamic response to suspension laryngoscopy.

KEY WORDS — alfentanil, esmolol, hemodynamic response, intubation, labetalol, laryngoscopy, microlaryngeal surgery, suspension laryngoscopy.

INTRODUCTION

Suspension laryngoscopy is a most valuable tool for diagnosis and staging of laryngeal tumors. Some surgical procedures, such as laser surgery, can only be performed by this particular technique.

The larynx is always severely stressed when it has been adequately exposed with the operating laryngoscope and placed on the suspension device. This stretching of the laryngeal structures produces maximum stimulation of the deep sensory receptors of the larynx, with this stimulation being further increased by the surgical manipulations of the tissues.[1,2] It is well known that suspension laryngoscopy produces marked increases in heart rate (HR) and blood pressure (BP) that are generally transitory and without sequelae,[3] but in those patients having a preexisting history of cardiovascular disease, an increase in BP may precipitate ischemic changes, arrhythmias, and even myocardial infarction.[4] Perioperative myocardial ischemia has been associated with postoperative myocardial infarction, and a causal relationship has been postulated.[5]

Response to laryngoscopy is associated with the release of large amounts of catecholamines.[6] Attempts to attenuate this response by various techniques or drugs or their combination have had varied success.[7-11] There are many studies about different methods to blunt the hemodynamic response to laryngoscopy and orotracheal intubation[7,9,11]; however, few studies have been carried out on techniques to reduce the response to microlaryngeal surgery,[2] a short surgical procedure that produces an important hyperdynamic response.

We studied the attenuation of the hemodynamic response to suspension laryngoscopy by an α- and β-blocking agent, labetalol hydrochloride, and a selective β-1–blocking agent, esmolol hydrochloride, used as support drugs to the conventional anesthetic technique usually administered in our surgical unit. Both drugs were administered in regimen doses previously reported in the literature to attenuate the hemodynamic response to laryngoscopy and tracheal intubation.[12-15]

MATERIAL AND METHODS

Subjects. Thirty patients (24 men, 6 women) ranging in age from 40 to 62 years, with an American Society of Anesthesiologists risk classification of I or II, and scheduled for microlaryngeal surgery were included in this study. Informed consent was obtained and the study was approved by the ethics committee of the hospital in accordance with the Helsinki II declaration.

Patients with a history of coronary artery disease,

From the Departments of Anesthesiology (Ayuso, Luis, Sala, Sánchez) and Otolaryngology–Head and Neck Surgery (Traserra), Hospital Clinic, University of Barcelona, Barcelona, Spain.

CORRESPONDENCE — Angeles Ayuso, MD, Departamento de Anestesiología y Reanimación, Hospital Clinic i Provincial, Universidad de Barcelona, Villarroel 170, 08036 Barcelona, Spain.

arterial hypertension, preoperative antihypertensive drug therapy, cardiac conduction defects, asthma, or any potential difficulties in airway management — or in whom intubation took longer than 15 seconds — were excluded from the study.

Study Design. Patients studied were randomly allocated into three groups with 10 patients in each group. The control group (CG; n = 10) received only the anesthetic technique. The labetalol group (LG; n = 10) received the same anesthetic technique and 0.3 mg/kg of intravenous (IV) labetalol hydrochloride 3 minutes before anesthesia induction and 0.15 mg/kg 2 minutes prior to placement of the suspension laryngoscope. The esmolol group (EG; n = 10) received the same anesthetic technique as the CG and an esmolol hydrochloride bolus of 500 µg/kg (in 1 minute) 3 minutes prior to induction. After this time, a continuous infusion of 300 µg/kg of esmolol was started and maintained throughout the surgical procedure. The infusion was discontinued on removal of the suspension laryngoscope.

The anesthetic technique used was as follows. Oral premedication with 5 to 10 mg oral diazepam was given the night before. When patients arrived in the operating room, IV premedication with atropine sulfate (0.01 mg/kg), midazolam hydrochloride (0.05 mg/kg), and alfentanil hydrochloride (10 µg/kg) was administered. Breathing of 100% oxygen was performed via mask.

Before IV premedication and after injection of the local anesthetic agent (lidocaine hydrochloride 2%, 1 mL), the radial artery was cannulated for blood gas determinations and continuous monitoring of BP. After this procedure, anesthetic induction was carried out with propofol (1.5 mg/kg), alfentanil hydrochloride (10 µg/kg), and succinylcholine chloride (1 mg/kg). Direct laryngoscopy was attempted with the aid of a standard Macintosh laryngoscope blade, and orotracheal intubation was performed with an insufflating catheter (2.2 mm internal diameter). Laryngoscopy and intubation were always performed by the same anesthesiologist. After return of a single twitch, neuromuscular block was maintained with vecuronium bromide (0.08 mg/kg), and anesthesia was maintained with continuous perfusion of propofol (8 mg/kg per hour). The duration of the propofol perfusion was 22 ± 4 minutes (n = 30).

Patients were ventilated by high-frequency jet ventilation (HFJV) using an Ergojet CVT (control volume time) module of the Ergotronic 3 ventilator (Temel SA Inc, Valencia, Spain). The respiratory frequency was 100 cycles per minute, the percentage inspiratory time was 30%, the inspiratory oxygen fraction (FiO_2) was 80%, or 50%, if it was a carbon dioxide laser procedure, and the driving pressure was regulated to obtain good chest expansion and a hemoglobin saturation (SpO_2) higher than 94%; however, the driving pressure did not exceed 3 bars. A second orotracheal catheter (2.2 mm) was introduced to the level of the carina to measure tracheal pressure. Microlaryngeal surgery was started 10 minutes after orotracheal intubation.

The HR was monitored and an electrocardiographic lead II and V_1 was displayed continuously on a Sirecust 402 Siemens monitor. The BP, systolic BP (SBP), and diastolic BP (DBP) were measured with a Sirecust 402 Siemens pressure transducer.

Arterial blood samples were obtained at baseline (prior to IV premedication) and at 10 minutes and 20 minutes after mechanical ventilation for determining arterial blood gases if the procedure was not finished by then. The SpO_2 was monitored with an Ohmeda oximeter. Serial hemodynamic variables (HR, SBP, DBP) were recorded at baseline (prior to IV premedication), after IV premedication, during direct laryngoscopy prior to tracheal intubation, 1, 2, and 4 minutes after tracheal intubation, 1, 2, 4, and 8 minutes after placement of the suspension laryngoscope, at the end of the procedure, and at 30 and 60 minutes in the recovery room. The rate-pressure product (RPP) was calculated as follows: RPP = HR × SBP.

Hemodynamic values in the LG and EG were compared to those in the CG. The hemodynamic values obtained at the measuring points in each group were compared to those at baseline.

Recorded data were analyzed with the statistics program by Macintosh, Statview II. Variations were compared with respect to baseline values by means of an analysis of variance for repeated measurements. Significance was defined as $p < .05$.

RESULTS

There were no significant differences in age, weight, or sex among the groups. The types of laryngeal disease were similar in the three groups. Likewise, the times employed for the surgical procedure were similar in all groups (Table 1).

The arterial blood samples analyzed at 10 minutes (n = 30) and 20 minutes (n = 23, because of the short duration of the procedure) from the start of HFJV showed no differences among the groups, and they indicated adequate gas exchange (Table 2). No patient developed electrocardiographic changes indicating ischemia. Table 3 shows the hemodynamic values measured in the three groups.

TABLE 1. CLINICAL DATA

	CG (*n = 10*)	*EG* (*n = 10*)	*LG* (*n = 10*)
Age (y)*	53 ± 9	50 ± 13	48 ± 16
Sex (M/F)	7/3	8/2	9/1
Weight (kg)*	70 ± 11	71 ± 11	76 ± 9
Height (cm)*	169 ± 6	166 ± 7	171 ± 7
ASA (I/II)	5/5	7/3	6/4
Surgical indication (No. of patients)			
Polyp	4	3	5
Biopsy	5	4	3
Reinke's edema	1	3	2
Time of SL (min)*	12.3 ± 3.2	11.9 ± 4.5	12.8 ± 3.3

CG — control group, EG — esmolol group, LG — labetalol group, ASA — American Society of Anesthesiologists classification of anesthetic risk, SL — surgical laryngoscopy.

*Data are mean ± SD.

Heart Rate. Changes in HR indicated that laryngoscopy and the subsequent orotracheal intubation produced a statistically significant rise in HR with respect to the baseline for each group: CG ($p < .01$), EG ($p < .05$), and LG ($p < .05$). Significant differences among groups were observed at the first minute after orotracheal intubation ($p < .05$).

The rise of HR persisted during suspension laryngoscopy in all groups. Lower values were observed in the EG and LG, but no significant differences were observed among the three groups.

Thirty minutes after the end of the surgical procedure, the HR was similar to baseline values in the CG and EG. Furthermore, in the LG, the HR was lower than baseline values at 30 minutes after the end of the procedure, but similar to baseline values 60 minutes after the end.

Systolic Blood Pressure. In the CG, the SBP remained stable with respect to baseline during laryngoscopy and intubation, but a significant increase ($p < .01$) was found during suspension laryngoscopy with respect to baseline.

The EG showed a significant decrease during laryngoscopy and intubation with respect to baseline values ($p < .05$). The SBP was restored to baseline values during suspension laryngoscopy.

Values obtained in the LG during laryngoscopy and intubation were similar to baseline. A small increase in SBP was found during suspension laryngoscopy, but this increase was not as great as that observed in the CG.

No significant differences were observed among groups during laryngoscopy and intubation. But a significant difference ($p < .01$) appeared during suspension laryngoscopy.

TABLE 2. ARTERIAL BLOOD SAMPLE VALUES AT BASELINE AND 10 AND 20 MINUTES AFTER STARTING HFJV

	CG (*n = 10*)	*EG* (*n = 10*)	*LG* (*n = 10*)
Baseline (n = 30)			
pH	7.4 ± 0.5	7.4 ± 0.3	7.4 ± 0.4
pO2 (mm Hg)	92 ± 11	95 ± 11	94 ± 9
pCO2 (mm Hg)	43 ± 6	39 ± 7	44 ± 7
SpO2 (%)	98	98	98
10 minutes (n = 30)			
pH	7.4 ± 0.6	7.4 ± 0.3	7.4 ± 0.5
pO2 (mm Hg)	221 ± 111	234 ± 129	244 ± 98
pCO2 (mm Hg)	40 ± 9	38 ± 5	42 ± 7
SpO2 (%)	99	100	100
20 minutes (n = 23)			
pH	7.4 ± 0.5	7.4 ± 0.3	7.4 ± 0.4
pO2 (mm Hg)	264 ± 114	256 ± 118	251 ± 109
pCO2 (mm Hg)	43 ± 6	38 ± 7	40 ± 7
SpO2 (%)	100	100	100

Data are mean ± SD.

HFJV — high-frequency jet ventilation, CG — control group, EG — esmolol group, LG — labetalol group, pO2 — partial pressure of oxygen, pCO2 — partial pressure of carbon dioxide, SpO2 — hemoglobin saturation.

Diastolic Blood Pressure. In the CG, the DBP decreased without significance during laryngoscopy and intubation as compared to baseline. The DBP increased significantly ($p < .01$) with respect to baseline during suspension laryngoscopy.

On the other hand, a significant decrease was observed in the EG during laryngoscopy and intubation. The DBP returned to similar-to-baseline values during suspension laryngoscopy.

In the LG, the DBP decreased without significance during laryngoscopy and intubation. A significant rise ($p < .05$) was obtained as compared to baseline during suspension laryngoscopy.

A significantly lower DBP ($p < .05$) was observed in the EG with respect to the CG during suspension laryngoscopy.

Rate-Pressure Product. Significant differences were observed among groups during laryngoscopy, intubation, and suspension laryngoscopy ($p < .05$). In the EG and LG, the RPP was always below 12,000. But in the CG, the RPP values were higher than 12,000 (see Figure).

DISCUSSION

The strength of reflex response to laryngeal stimulation appears to vary according to many factors: 1)

TABLE 3. HEART RATE AND SYSTOLIC AND DIASTOLIC BLOOD PRESSURES AT SELECTED TIME POINTS IN THREE GROUPS IN RESPONSE TO LARYNGOSCOPY, OROTRACHEAL INTUBATION, AND SUSPENSION LARYNGOSCOPY

	CG (*n* = *10*)	*EG* (*n* = *10*)	*LG* (*n* = *10*)	*p* (*ANOVA*)
Heart rate (beats per minute)				
Baseline	73 ± 12	73 ± 15	73 ± 8	
Postpremedication	80 ± 16	80 ± 20	80 ± 9	
Laryngoscopy	89 ± 8*	77 ± 19	78 ± 9	
OTI-1	101 ± 10*	83 ± 17†	84 ± 12†	<.05
OTI-2	96 ± 17*	82 ± 17†	86 ± 14†	
OTI-4	90 ± 13*	82 ± 20†	84 ± 11†	
SL-1	91 ± 11*	88 ± 21†	81 ± 11†	
SL-2	88 ± 11*	91 ± 17*	80 ± 9	
SL-4	88 ± 11*	86 ± 16†	79 ± 11	
SL-8	86 ± 11*	87 ± 16†	80 ± 11	
End of procedure	82 ± 12†	81 ± 19	79 ± 9	
30 minutes in recovery	75 ± 9	73 ± 11	66 ± 10	
60 minutes in recovery	75 ± 7	79 ± 12	72 ± 12	
Systolic blood pressure (mm Hg)				
Baseline	117 ± 10	128 ± 22	127 ± 28	
Postpremedication	107 ± 12	121 ± 25	120 ± 25	
Laryngoscopy	117 ± 28	92 ± 36†	110 ± 23	
OTI-1	120 ± 33	98 ± 27†	121 ± 29	
OTI-2	110 ± 26	93 ± 24	114 ± 33	
OTI-4	99 ± 14†	83 ± 23*	102 ± 29†	
SL-1	156 ± 21*	113 ± 27	140 ± 34	<.05
SL-2	164 ± 20*	135 ± 19	141 ± 32†	<.05
SL-4	156 ± 18*	129 ± 17	137 ± 24	<.05
SL-8	154 ± 23*	130 ± 16	134 ± 23	
End of procedure	124 ± 16	118 ± 21	119 ± 15	
30 minutes in recovery	115 ± 21	125 ± 27	109 ± 28	
60 minutes in recovery	127 ± 19	121 ± 24	123 ± 20	
Diastolic blood pressure (mm Hg)				
Baseline	73 ± 10	80 ± 13	73 ± 11	
Postpremedication	60 ± 7*	59 ± 17*	66 ± 8†	
Laryngoscopy	66 ± 11	49 ± 24*	66 ± 13	
OTI-1	66 ± 16†	54 ± 19*	68 ± 15	
OTI-2	62 ± 12	48 ± 18*	66 ± 17	
OTI-4	56 ± 7*	44 ± 20*	62 ± 14†	<.05
SL-1	93 ± 10*	64 ± 20†	84 ± 17†	<.01
SL-2	93 ± 7*	76 ± 13	81 ± 14†	<.05
SL-4	90 ± 8*	74 ± 15	82 ± 11†	<.05
SL-8	87 ± 7*	75 ± 15	81 ± 10†	
End of procedure	77 ± 10	67 ± 19	70 ± 11	
30 minutes in recovery	75 ± 9	72 ± 11	68 ± 9	
60 minutes in recovery	73 ± 15	77 ± 21	70 ± 16	

CG — control group, EG — esmolol group, LG — labetalol group, ANOVA — analysis of variance, OTI — orotracheal intubation [and number of minutes after tracheal intubation], SL — suspension laryngoscopy [and number of minutes after placement].

*p < .01 compared with baseline.

†p < .05 compared with baseline.

depth of anesthesia and tracheal intubation difficulties,[11,16] 2) patient-dependent variables such as age and history of cardiovascular disease,[17] and 3) laryngoscopic factors such as any difficulty in suspension laryngoscope placement, the duration of the exploration and surgical procedure, and the maximal forces applied to adequately expose the larynx.[17] The first point depends on the anesthesiologist and the

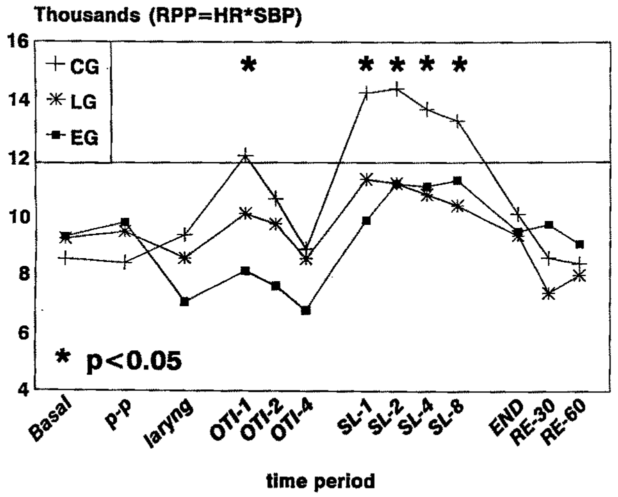

Rate-pressure product (RPP = HR × SBP) at selected points in three groups. HR — heart rate, SBP — systolic blood pressure, CG — control group, EG — esmolol group, LG — labetalol group, Basal — baseline, p-p — post-premedication, Laryng — laryngoscopy, OTI — orotracheal intubation [and number of minutes after tracheal intubation], SL — suspension laryngoscopy [and number of minutes after placement], RE — recovery and number of days after procedure, * — p < .05 over baseline.

anesthetic technique.

In all groups, the values of arterial blood gases were indicative of an appropriate gas exchange throughout the procedure using HFJV with an FiO2 of 50%.

The depth of the anesthesia itself may reduce the hemodynamic response. Methods to deepen anesthesia, such as an increase in inhalation anesthesia or higher doses of narcotic analgesics such as fentanyl or alfentanil, have been used with not-completely-satisfactory results in short surgical procedures.[7,9,18,19] Alfentanil hydrochloride at a dose of 15 μg/kg moderates the hemodynamic response, and it can prevent a rise in BP, although it only partially suppresses the release of epinephrine and norepinephrine following tracheal intubation. A higher dose, 30 μg/kg, is required to prevent increases in HR and prevent any significant increase in endogenous catecholamines after orotracheal intubation.[9] At this dose, depressant effects may persist after conclusion of a short surgical procedure such as microlaryngeal surgery.

In order to use an anesthetic technique appropriate for this short surgical procedure, we have used 20 μg/kg of alfentanil hydrochloride in association with other support drugs such as esmolol or labetalol. The hemodynamic response to suspension laryngoscopy observed in the present study was not found to be completely blocked with the dose of alfentanil used (observed in the CG).

Labetalol is an α- and β-adrenergic blocking agent. The β-adrenergic activity (both β-1 and -2) is evident in the absence of tachycardia and the unchanged cardiac response to a decreased systemic resistance caused by the α-blocking activity. The long half-life (3.5 to 4.5 hours) can maintain the bradycardic effects for 1 to 2 hours after the last dose.[8,12,13,20]

Esmolol is a cardioselective β-1–adrenergic blocking agent with a short duration of action. It has a rapid onset of action and a short half-life (9 minutes).[14,15,21,22]

The results of our study indicate that laryngoscopy, intubation, and suspension laryngoscopy produced a significant increase in HR in all groups, although this increase was not as marked in the EG and LG (no statistical significance). Esmolol and labetalol, at the doses administered, did not entirely block the chronotropic response during the procedure. However, BP remained unchanged in the CG during laryngoscopy and intubation. In the EG, the infusion of esmolol caused an initial decrease in SBP and DBP that can be related to the negative inotropic effect of this drug, which is more evident before surgical aggression. This effect is certainly powered by alfentanil. The BP in the LG remained stable during laryngoscopy and intubation. In all groups, the lack of increase in BP during laryngoscopy and intubation may be related to the lesser laryngotracheal injury (in comparison to conventional intubation) produced by the small uncuffed catheter employed in HFJV.

During persistent stretching of the laryngeal tissues in suspension laryngoscopy, the increase observed in BP was significantly lower in the EG and LG than in the CG. Labetalol seemed to be less effective than esmolol in blunting the hypertensive response during suspension laryngoscopy. The best values of arterial pressure during the surgical procedure were found in the EG. The onset and duration of the effects of esmolol were rapid and transient because of the rapid metabolism of this drug in the blood. No patients demonstrated severe hypotension. On the other hand, the β-effects of labetalol persisted 30 minutes after the surgical procedure. It is known that the α- and β-effects last an average of 30 and 60 minutes, respectively.[23]

The RPP showed decreased values in the EG and LG with statistical significance with respect to the CG. The values obtained in the CG were increased, indicating that myocardial oxygen demand is high enough to be a risk factor in patients with coronary artery disease. In our patients, SBP changes made a greater contribution to the RPP decrease than did HR. In patients with coronary disease, RPP values higher than 12,000 increase the risk of ischemia,[24] and the same risk increases in healthy patients if RPP values are higher than 20,000.[25]

We have demonstrated that the anesthetic technique employed prevents a hyperdynamic response after laryngoscopy and intubation. However, this anesthetic technique cannot completely prevent the hyperdynamic response that occurs when the suspension laryngoscope stretches the laryngeal tissues. We also think that the use of an anesthetic-only technique may fail in patients with hypertension or a risk of cardiac ischemia.[26]

In conclusion, the support of β-blocking agents provides hemodynamic stability during suspension laryngoscopy. These drugs may also help to decrease the hyperdynamic response to laryngoscopy and intubation prior to the surgical procedure. We found that esmolol and labetalol were both effective in limiting increases in HR, BP, and RPP throughout the surgical procedure. Although both drugs can be used in microlaryngeal surgery, the cardioselectivity, rapid onset, and short duration of esmolol make this the drug of first choice in patients scheduled for microlaryngeal surgery, since this is a short surgical procedure with important hyperadrenergic stimulation.

Follow-up studies evaluating the safety and efficacy in higher-risk patients are warranted.

ACKNOWLEDGMENTS — The authors thank the staff of the operating room and recovery room at the otolaryngology surgical unit for their help with this study.

REFERENCES

1. Wenig BL, Raphael N, Stern JR, Shikowitz MJ, Abramson AL. Cardiac complications of suspension laryngoscopy. Arch Otolaryngol Head Neck Surg 1986;112:860-2.
2. Mustola ST, Baer GA, Metsä-Ketelä T, Laippala P. Haemodynamic and plasma catecholamine responses during total intravenous anaesthesia for laryngomicroscopy. Thiopentone compared with propofol. Anaesthesia 1995;50:108-13.
3. Strong MS, Vaughan CHW, Mahler DL, Jaffe DR, Sullivan RC. Cardiac complications of microsurgery of the larynx: etiology, incidence and prevention. Laryngoscope 1974;84:908-20.
4. Leslie JB. Incidence and aetiology of perioperative hypertension. Acta Anaesthesiol Scand Suppl 1993;37(suppl 99):5-9.
5. Kaplan JA, King SB. The precordial electrocardiographic lead (V5) in patients who have coronary artery disease. Anesthesiology 1976;45:570-4.
6. Russell WJ, Morris RG, Frewin DB, Drew SE. Changes in plasma catecholamine concentrations during endotracheal intubation. Br J Anaesth 1981;53:837-9.
7. Kautto UM. Attenuation of the circulatory response to laryngoscopy and intubation by fentanyl. Acta Anaesthesiol Scand 1982;26:217-21.
8. Bruder N, Ortega D, Granthil C. Conséquences et moyens de prévention des modifications hémodynamiques lors de la laryngoscopie et de l'intubation endotrachéale. Ann Fr Anesth Reanim 1992;11:57-71.
9. Miller DR, Martineau RJ, O'Brien H, et al. Effects of alfentanil on the hemodynamic and catecholamine response to tracheal intubation. Anesth Analg 1993;76:1040-6.
10. Achola KJ, Jones MJ, Mitchell RWD, Smith G. Effects of beta-adrenoceptor antagonism on the cardiovascular and catecholamine responses to tracheal intubation. Anaesthesia 1988; 43:433-6.
11. Helfman SM, Gold MI, DeLisser EA, Herrington CA. Which drug prevents tachycardia and hypertension associated with tracheal intubation: lidocaine, fentanyl or esmolol? Anesth Analg 1991;72:482-6.
12. Bernstein JS, Nelson MA, Ebert TJ, Woods MD, Boerig DL. Beat by beat cardiovascular responses to rapid sequence induction in humans: effect of labetalol [Abstract]. Anesthesiology 1987;67:A32.
13. MacCarthy EP, Bloomfield MS. Labetalol: a review of its pharmacology, pharmacokinetics, clinical uses and adverse effects. Pharmacotherapy 1983;3:193-219.
14. Ebert JP, Pearson JD, Gelman S, Harris C, Bradley EL. Circulatory responses to laryngoscopy: the comparative effects of placebo, fentanyl and esmolol. Can J Anaesth 1989;36:301-6.
15. Liu PL, Gatt S, Gugino LD, Mallampati SR, Covino BG. Esmolol for control of increases in heart rate and blood pressure during tracheal intubation after thiopentone and succinylcholine. Can Anaesth Soc J 1986;33:556-62.
16. Angelard B, Debry C, Planquart X, et al. Les intubations difficiles. Une étude prospective. Ann Otolaryngol Chir Cervicofac 1991;108:241-3.
17. Bucx MJL, Van Geel RTM, Scheck PAE, Stijnen T. Cardiovascular effects of forces applied during laryngoscopy. The importance of tracheal intubation. Anaesthesia 1992;47:1029-33.
18. Turner DAB, Shribman AJ, Smith G, Achola KJ. Effect of halothane on cardiovascular and plasma catecholamine responses to tracheal intubation. Br J Anaesth 1986;58:1365-70.
19. Black TE, Kay B, Healy TEJ. Reducing the haemodynamic responses to laryngoscopy and intubation. A comparison of alfentanil with fentanyl. Anaesthesia 1984;39:883-7.
20. Leslie JB, Kalayjian RW, McLoughlin TM, Russell RD, Plachetka JR. Ablation of the hemodynamic responses to tracheal intubation with preinduction intravenous labetalol [Abstract]. Anesthesiology 1987;67:A30.
21. Hall RI. Esmolol — just another beta blocker? Can J Anaesth 1992;39:757-64.
22. Chung KS, Sinatra RS, Halevy JD, Paige D, Silverman DG. A comparison of fentanyl, esmolol, and their combination for blunting the haemodynamic responses during rapid-sequence induction. Can J Anaesth 1992;39:774-9.
23. Cope DH, Crawford MC. Labetalol in controlled hypotension: administration of labetalol when adequate hypotension is difficult to achieve. Br J Anaesth 1979;51:359-65.
24. Kaplan JA. Hemodynamic monitoring. In: Kaplan JA, ed. Cardiac anesthesia. New York, NY: Grune & Stratton, 1979:71-115.
25. Cokkinos DV, Voridis EM. Constancy of pressure-rate product in pacing-induced angina pectoris. Br Heart J 1976;38:39-42.
26. Prys-Roberts C. Anaesthetic considerations for the patient with coronary artery disease. Br J Anaesth 1988;61:85-96.

Ann Otol Rhinol Laryngol 106:1997

QT INTERVAL CHANGES FOLLOWING NECK DISSECTION

A STRATIFIED PROSPECTIVE STUDY

CHRISTOPHER H. RASSEKH, MD
GALVESTON, TEXAS

KEVIN C. DELLSPERGER, MD, PHD
IOWA CITY, IOWA

JAMES A. HOKANSON, PHD
GALVESTON, TEXAS

CARL H. SNYDERMAN, MD
PITTSBURGH, PENNSYLVANIA

JONAS T. JOHNSON, MD
PITTSBURGH, PENNSYLVANIA

BRUCE A. BOLLEN, MD
MISSOULA, MONTANA

HENRY T. HOFFMAN, MD
IOWA CITY, IOWA

Studies from Europe have suggested that neck dissection, especially right radical neck dissection, causes a dangerous prolongation of the QT interval. Sudden cardiac arrest due to QT prolongation has been reported following right radical neck dissection. We investigated the prevalence of QT interval prolongation following neck dissection. Electrocardiogram tracings from 45 patients who underwent different combinations of neck dissection were studied. Preoperative and postoperative tracings were interpreted by a cardiologist blinded to the patient identification of each tracing. There were 28 unilateral neck dissection patients and 17 bilateral neck dissection patients eligible for analysis. There were 7 patients in the classic right radical neck dissection group, and only 3 of these had no neck dissection on the left. Comparisons of preoperative versus postoperative corrected QT interval for all subjects did not indicate a significant change. Stratification by neck dissection type (radical, modified or selective, and carotid artery resection) or by side dissected (left, right, or both) also showed no significant differences. No malignant arrhythmias were encountered. Thus, in contrast to the European experience, our findings show no significant predictable change in the QT interval after any of the combinations of neck dissection. Head and neck surgeons should be aware of the possibility of postoperative QT interval prolongation following neck dissection, although in the absence of other risk factors it appears to be a rare occurrence.

KEY WORDS — arrhythmia, neck dissection, QT interval.

INTRODUCTION

Previous studies in Europe have suggested that there is a significant risk of malignant arrhythmias following right radical neck dissection.[1-3] This has been thought to be associated with altered cervical sympathetic innervation to the heart leading to a delay in ventricular repolarization and prolongation of the QT interval. QT interval prolongation may lead to torsades de pointes and subsequently degenerate into ventricular fibrillation. There have also been reports of prolongation of the QT interval after neck dissection in the United States,[4-6] but no predictable changes specifically related to right radical neck dissection[5] or carotid artery resection[6] have been demonstrated in prospective studies. This study was designed to clarify the effect of various neck dissections and combinations of neck dissections on the QT interval.

PATIENTS AND METHODS

Over the course of 3 years, all patients undergoing neck dissection were enrolled in the study if possible. Patients were excluded if they had postoperative serum electrolyte (potassium, calcium, and magnesium) abnormalities, missing data, or inadequate electrocardiogram (ECG) tracings for evaluation. Patients taking medications known to affect QT interval, with abnormal corrected QT (QTc) intervals preoperatively, or with a history of known cardiac arrhythmias were also excluded. A previously reported prospective group of patients who underwent extended radical neck dissection with carotid resection were also included in the analysis.[6] Preoperative 12-lead ECGs were obtained in all patients and controls with a 12-channel Marquette Electronics unit (Milwaukee, Wis). We chose to perform the ECG at the earliest possible time, when the anesthetic effect was minimal (on the second or third postoperative day). We did not do serial ECGs unless there were abnormalities. Postoperative monitoring of lead II and postoperative ECGs were obtained in the early postoperative period. If any abnormality was noted, serial ECGs were obtained. The tracings were coded and then interpreted by a cardiologist (K.C.D.)

From the Department of Otolaryngology, University of Texas Medical Branch, Galveston, Texas (Rassekh, Hokanson), the Departments of Internal Medicine (Dellsperger [Cardiovascular Division]), Anesthesiology (Bollen), and Otolaryngology (Hoffman), The University of Iowa, Iowa City, Iowa, and the Department of Otolaryngology, University of Pittsburgh, Pittsburgh, Pennsylvania (Snyderman, Johnson).

Presented as a poster at the Association for Research in Otolaryngology research forum at the meeting of the American Association of Otolaryngology–Head and Neck Surgery, New Orleans, Louisiana, September 17, 1995.

CORRESPONDENCE — Christopher H. Rassekh, MD, Dept of Otolaryngology, University of Texas Medical Branch, 301 University, Galveston, TX 77555-0521.

TABLE 1. STRATIFICATION OF SUBSETS

Group	*Neck Dissection Left*	*Neck Dissection Right*	*No. of Patients*
1	None	Radical	3
2	Other	Radical	4
3	Radical	Other or none	3
4	Other	None	5
5	None	Other	11
6	Other	Other	11
7*	Carotid	None	4
8*	None	Carotid	4

*These groups were previously reported.[6]

TABLE 2. MEAN AND STANDARD DEVIATION OF QTc FOR EIGHT NECK DISSECTION GROUPS

Group	*Preop QTc (ms)*	*Postop QTc (ms)*
1	383 ± 29	440 ± 36
2	423 ± 10	430 ± 16
3	413 ± 21	430 ± 46
4	408 ± 23	452 ± 29
5	423 ± 23	422 ± 33
6	431 ± 23	434 ± 41
7	413 ± 17	420 ± 42
8	435 ± 17	427 ± 9

blinded to the patient's identity and the timing of the ECG. QTc was calculated with the following formula[7]:

$$\mathrm{QTc} = \mathrm{QT}/\sqrt{\mathrm{RR}}$$

where QT is the interval in seconds from the onset of the QRS complex to the termination of the T wave, and RR is the interval in seconds between the two QRS complexes prior to the complex at which QT was measured. QT and RR measurements were made from lead II whenever possible. Heart rate was also measured from lead II. A QTc of greater than 0.46 millisecond is considered prolonged in this study. This is the standard in our laboratory. Blood was obtained from the patients to exclude electrolyte abnormalities.

Results were analyzed by comparing preoperative and postoperative results for the entire group of patients, as well as for different subsets after stratification. The differences in mean values were considered statistically significant if $p < .05$ on paired Student's *t*-test and analysis of variance where appropriate. Bonferroni correction for multiple components was used where appropriate. All calculations were performed with a microcomputer implementation of the statistical software package SAS.

RESULTS

A large number of patients were deemed ineligible due to exclusion criteria. We eliminated these patients to purify our groups as much as possible from any effect other than the specific surgery performed. Many of the patients who were excluded from the study did have transient changes in QTc, some over the normal limit, but all changes were felt to be due to exclusion criteria. To date, 45 patients have adequate data for analysis. They are stratified in Table 1.[6] Modified and selective neck dissection are grouped together in this study as "other," by convention. The groups were comparable in terms of age, duration of anesthesia, and anesthetic techniques.

Mean preoperative and postoperative QTc for each group are summarized in Table 2. Comparison of postoperative QTc for all patients is shown in the Figure, A, and comparison of right radical neck dissection groups (groups 1 and 2) to all other patients is in the Figure, B. Comparison of the change in QTc for all right-only neck dissections (groups 1, 5, and 8) to that for all other neck dissections is in the Figure, C. Analysis of variance comparing preoperative versus postoperative intervals for all patients shows no significant change. The mean value of QTc was not considered prolonged in any of the groups. Although there was a prolongation of the QTc interval in some patients, there were no significant differences between groups, and no clear pattern emerged to suggest that any of the groups are at higher risk of such changes. In the right radical neck dissection–only group, 1 patient out of 3 had a significant prolongation of the QT interval, from 0.35 to 0.48 milliseconds, but this did not result in any arrhythmia. The preoperative QTc value caused the low mean QTc value in group 1. There were 5 other patients who had a postoperative QTc above the normal range: 1 in group 3, 1 in group 4, 1 in group 5, and 2 in group 6 (in addition to the previously reported transient increases in QTc for 1 patient in group 7 and 2 patients in group 8[6]). None of these patients had further abnormalities on serial ECGs.

DISCUSSION

Hugenholtz[1] first reported a case of prolonged QT interval after right radical neck dissection in 1967. Otteni et al,[2] in 1983, studied 60 patients who underwent radical neck dissection. They found a consistent and apparently permanent prolongation of the QT interval in the majority of patients who underwent right radical neck dissection, but this effect did not occur after left radical neck dissection. Three of their 32 patients who underwent right radical neck dissection developed extremely long QT prolongation with subsequent torsades de pointes and ventricular fibrillation.[2] One of the patients died, possibly due to this phenomenon. A study in the German literature[3] appears to support the concept raised by the French study[2] of right radical neck dissection leading to a prolonged QT interval. In 1993, Strickland et al[4] reported a case of prolonged QT interval and cardiac arrest in a young woman who underwent a right supraomohyoid selective neck dissection. The arrest

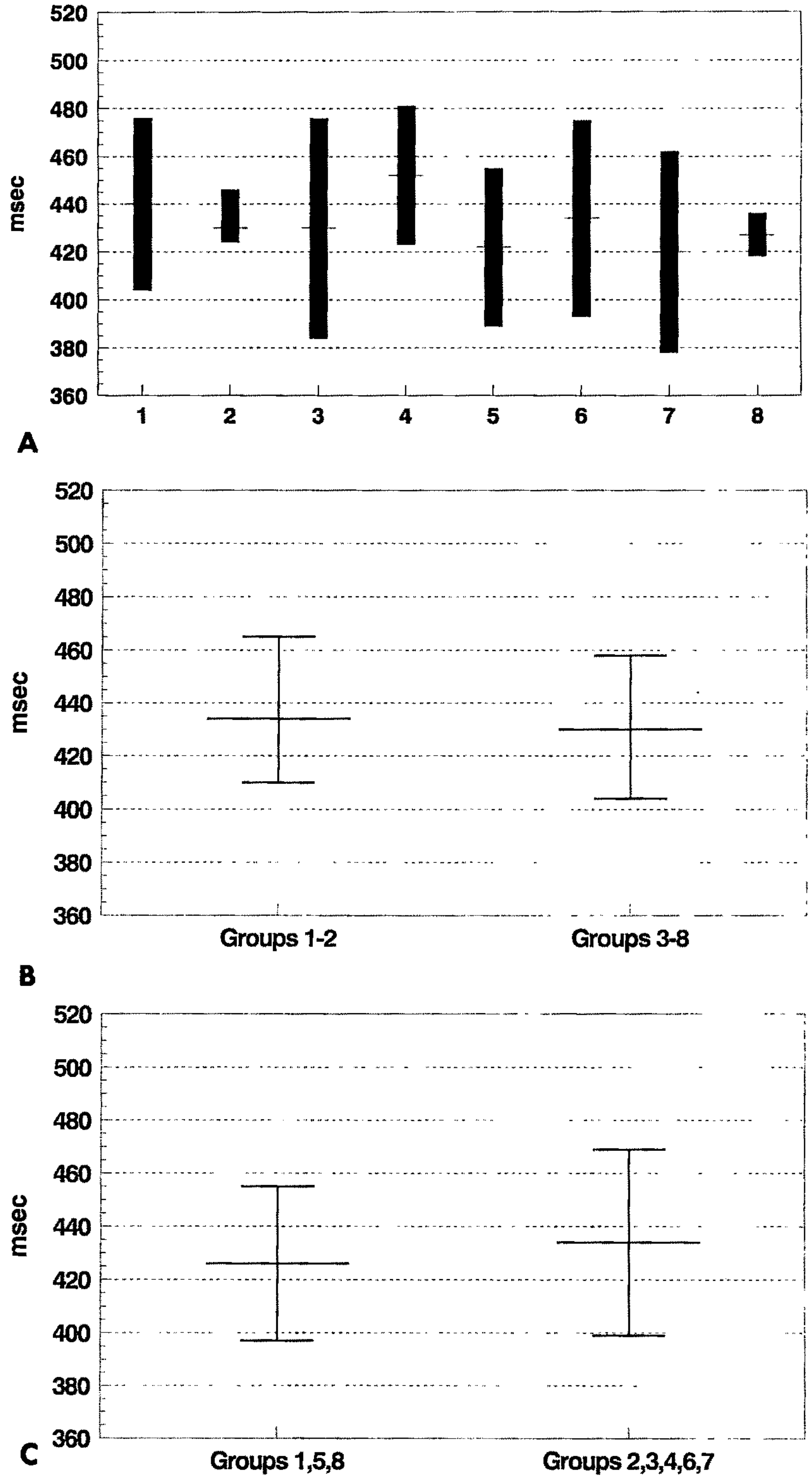

Comparisons of postoperative corrected QT intervals (p values were not significant). A) For all patients. B) For groups 1 and 2 combined versus all other groups combined. C) For groups 1, 5, and 8 combined versus all other groups combined.

was felt to be secondary to a congenital QT prolongation. Although the authors did not conclude that the arrhythmia was related to the neck dissection, this case raises the question of whether even a selective right-sided neck dissection may result in arrhythmia in a high-risk patient. A prospective trial was conducted by Acquadro et al,[5] dividing patients who underwent "extensive" neck surgery into three groups (right, left, and no neck dissection). Although they did note a significant change in the QT interval in all three groups and in the entire population, no differences between groups were found to suggest that right-sided neck dissection is any riskier than left neck dissection or neck surgery without neck dissection. They concluded that acquired long QT syndrome is unlikely to trigger malignant arrhythmias following radical neck dissection in the absence of other risk factors such as congenital, metabolic, or pharmacologic disturbances. We now have a small group of prospectively studied patients in several representative groups. We cannot find any difference between these groups, comparing any combinations of these groups. No malignant arrhythmias have occurred in the 3 years that the study has been open. We believe that the strict exclusion criteria are necessary, but they have made accrual slow.

We speculate that our exclusion criteria have allowed us to analyze a more homogeneous group of patients, and that is why our results differ from those of the European study. Although the Acquadro et al[5] study did find a significant prolongation of the QT interval after neck dissection and we did not, their overall clinical conclusion is the same as ours: that neck dissection is unlikely to trigger malignant arrhythmias. Both our study and the Acquadro et al study differ from those of the European literature. One possible explanation for the differences between our data and those of the Acquadro et al study is that the ECGs were done at 1 to 3 hours postoperatively in the Acquadro et al study, when anesthetic effects may still have been present. A much larger number of patients would be necessary to definitively quantitate the relative risk for each of our neck dissection groups, but such a study would be labor-intensive, expensive, and very difficult to control for nonsurgical factors. Even if these were controlled for, the large number of surgical variables would seem to make the task virtually impossible.

We still believe that the operating head and neck surgeon must be aware of prolonged QT syndrome and its possible relationship to cervical sympathetic nerves and neck dissection. The association of long QT syndrome with deafness has been established,[8] but no anatomic connection is known to link this type of QT prolongation with the type that occurs after neck dissection. However, Jackman et al[9] have classified congenital long QT and neck dissection–induced long QT together in the "adrenergic dependent" group of long QT syndromes. A number of factors such as hypocalcemia,[10] hypokalemia,[11] drugs and anesthetic agents,[12] and genetic alterations[13] have all been associated with long QT syndrome. Yanowitz et al,[14] in 1966, demonstrated that right and left stellate ganglion lesions prolong and shorten the QT interval, respectively, in dogs; and left stellate ganglionectomy has been effective as a therapeutic maneuver in long QT syndrome.[15-17] Although the effect is rare, this might explain why right neck dissections could have a prolonging effect on the QT interval. Theoretically, left neck dissection might have the opposite effect. Left stellate ganglionectomy is often effective when pharmacologic management including β-adrenergic blockers, other supportive measures for metabolic disturbances, and cardiac pacing fail.[16] Therapy for long QT syndrome should be individualized.[16] Anatomic and neurophysiologic studies to date have been limited to animal models. Further studies are warranted to clarify the precise cervicothoracic neuroanatomic and neurophysiologic sympathetic pathways to the ventricles of the human heart.

REFERENCES

1. Hugenholtz PG. Electrocardiographic changes typical for central nervous system disease after right radical neck dissection. Am Heart J 1967;74:438-41.
2. Otteni JC, Pettecher T, Bronner C, Flesch H, Diebolt JR. Prolongation of the QT interval and sudden cardiac arrest following right radical neck dissection. Anesthesiology 1983;59:358-61.
3. Behne M, Hermann R, Lischke V, Lorz M. Prolongation of the QT interval in the ECG following surgery of the neck (neck dissection). HNO 1989;37:449-53.
4. Strickland RA, Stanton MS, Olsen KD. Prolonged QT syndrome: perioperative management. Mayo Clin Proc 1993;68: 1016-20.
5. Acquadro MA, Nghiem TX, Beach TP, Donlon JV, Joseph MP, Ahern DK. Acquired QT interval changes and neck dissections. J Clin Anesth 1995;7:54-7.
6. Rassekh CH, Dellsperger KC, Bollen BA, Hoffman HT, Ricks-McGillin J. The QT interval following carotid artery resection. Head Neck 1995;17:242-6.
7. Bazett HC. An analysis of the time-relations of the electrocardiograms. Heart 1920;7:353-70.
8. Jervell A. The surdo-cardiac syndrome. Eur Heart J 1985; 6(suppl D):97-102.
9. Jackman WM, Friday KJ, Anderson JL, Aliot EM, Clark M, Lazzara R. The long QT syndromes: a critical review, new clinical observations and a unifying hypothesis. Prog Cardiovasc Dis 1988;31:115-72.
10. Zane EA, Eisencraft JB, Haimov M. Hypocalcemia and prolonged QT interval following carotid artery surgery. Anesthesiology 1987;67:998-1000.
11. Weaver WF, Burchell HB. Serum potassium and the electrocardiogram in hypokalemia. Circulation 1960;21:505-21.
12. McConachie I, Keaveny JP, Healy TEJ, Vohra S, Million L. Effect of anaesthesia on the QT interval. Br J Anaesth 1989;63: 558-650.
13. Curran ME, Splawski I, Timothy KW, Vincent GM, Green ED, Keating MT. A molecular basis for cardiac arrhythmia: HERG mutations cause long QT syndrome. Cell 1995;80:795-803.
14. Yanowitz F, Preston JB, Abildskov JA. Functional distribution of right and left stellate innervation to the ventricles: production of neurogenic electrocardiographic changes by alteration of sympathetic tone. Circ Res 1966;18:416-28.
15. Moss AJ, McDonald J. Unilateral cervicothoracic sympathetic ganglionectomy for the treatment of long QT interval syndrome. N Engl J Med 1971;285:903-4.
16. Moss AJ, Robinson J. Clinical features of the idiopathic long QT syndrome. Circulation 1992;85(suppl 1):1140-4.
17. Moss AJ, Schwartz PJ, Crampton RS, Locati E, Carleen E. The long QT syndrome: a prospective international study. Circulation 1985;71:17-21.

Ann Otol Rhinol Laryngol 106:1997

IMAGING CASE STUDY OF THE MONTH

INTRACRANIAL COMPLICATIONS OF OTITIS MEDIA

DANIEL SAAH, MD
J. ELIDAN, MD
M. GOMORI, MD
JERUSALEM, ISRAEL

INTRODUCTION

Central nervous system (CNS) complications of otitis media are rare today because of the development of effective antimicrobial agents. A case of simultaneous multiple intracranial abscesses is presented. A high index of suspicion should be maintained in the early detection and treatment of otitis media and its complications.

CASE REPORT

A 15-year-old girl was admitted because of a 2-week history of fever, headache, vomiting, and grand mal seizures. She had an 8-year history of chronic otitis media with symptoms of purulent otorrhea, otalgia, and hearing loss. She had been previously treated with systemic antibiotics and ear drops.

On admission, she was febrile (39°C) and had a right-sided facial palsy with spontaneous nystagmus, papilledema, severe cerebellar ataxia, fluctuating retroauricular swelling, and a right-sided purulent, malodorous otorrhea. She also showed signs of meningeal irritation. Computed tomography (CT) of the brain and temporal bones revealed a right posterior temporal abscess and a posterior parafalcial subdural empyema. There was also a right cerebellar abscess and thrombosis of the right sigmoid sinus. The right mastoid was opacified, with an associated dural enhancement and granulation tissue (Figs 1 and 2). She was started on gentamicin sulfate (60 mg every 12 hours), metronidazole hydrochloride (500 mg every

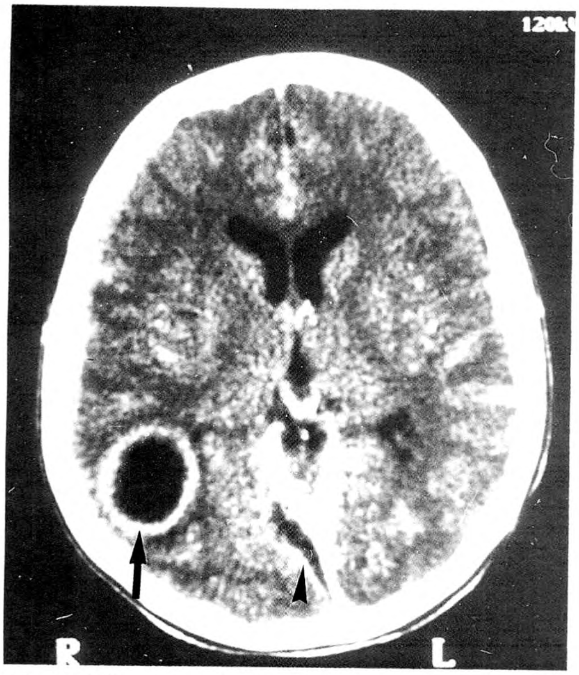

Fig 1. Brain computed tomogram with contrast showing right posterior temporal abscess (arrow) and posterior parafalcial subdural empyema (arrowhead).

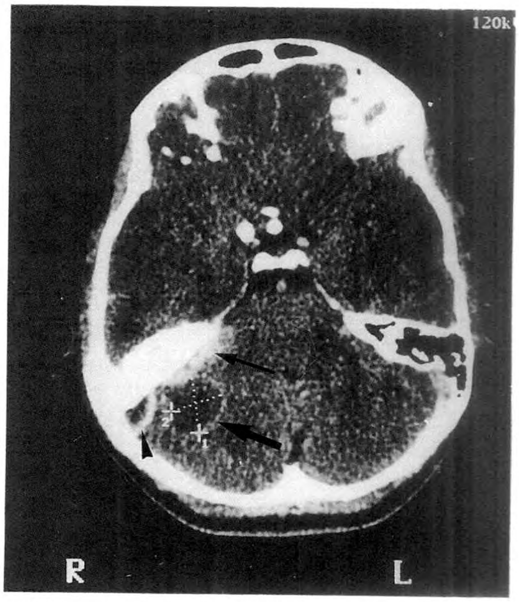

Fig 2. Computed tomogram of brain and temporal bone with contrast showing opacification of right mastoid with associated dural enhancement (small arrow) and right sigmoid vein thrombosis (arrowhead). There is also right cerebellar abscess (large arrow).

From the Departments of Otolaryngology–Head and Neck Surgery (Saah, Elidan) and Radiology (Gomori), Hadassah University Hospital, Jerusalem, Israel.

CORRESPONDENCE — Daniel Saah, MD, Dept of Otolaryngology–Head and Neck Surgery, Hadassah University Hospital, Jerusalem, Israel.

8 hours), and ampicillin sodium (2 g every 6 hours). The patient underwent surgery. The brain abscesses were drained through a right parieto-occipital craniotomy, and a right cortical mastoidectomy was performed with removal of antral granulations. The posterior fossa bone was dehiscent, and the sigmoid sinus was not thrombosed. The patient defervesced postoperatively and remained stable. Cultures of the aural discharge and abscess material grew *Proteus mirabilis* and *Pseudomonas aeruginosa.*

Two months later, the right temporal lobe abscess re-collected and was drained again. The patient improved gradually, with recovery of her neurologic status, but retained a right sensorineural hearing loss. The patient was, however, lost to follow-up in the outpatient clinic.

DISCUSSION

Today, only infrequent reports of CNS complications of ear disease appear.[1,2] Multiple brain abscesses are uncommon and, when present, usually result from meningitis occurring in neonates or infants.[3] However, although rare, CNS complications of ear disease continue to cause a significant morbidity and mortality. While the mortality is much lower than in the preantibiotic era, it is still alarmingly high, being approximately 10% overall.[4] Continued vigilance must therefore be kept up in order to detect complications of otitis media early in their course. Familiarity with the early signs and symptoms of complications of middle ear disease is essential to early diagnosis. These include fever associated with a chronic perforation, retro-orbital pain on the side of the infected ear (petrositis), and vertigo and nystagmus. Other signs include facial paralysis on the side of an infected ear, headache and/or lethargy, papilledema, meningismus, focal neurologic signs and/or seizures, and other catastrophic neurologic signs such as loss of consciousness or rapidly progressive neurologic signs and symptoms in a patient with otitis media. The intracranial complications range from meningitis to otitic hydrocephalus and include subdural abscess, extradural abscess and granulation, labyrinthitis, sigmoid sinus thrombosis, and brain abscesses, especially temporal and cerebellar. It is interesting to note that our patient presented with all of the above complications.

The traditional pathways of infections spreading from the ear centrally remain the present avenues for CNS complications. These pathways are either direct extension through bone by cholesteatoma or osteomyelitis, spread by thrombophlebitis, extension through preformed pathways, or a combination of these. The pathology and pathogenesis of these complications is extensively covered in the literature. Management of complications includes drainage of abscesses, cortical mastoidectomy, and antibiotic therapy. Prevention, however, of these complications is the best cure. As stated by Gower and McGuirt,[4] whereas the care of acute ear disease is generally antibiotic therapy, local drainage procedures should never be avoided, since they hasten resolution of the focus of CNS complications and provide material for comparative cultures. The clinical course of a patient with acute otitis media should be continuously monitored to allow further surgical intervention if improvement fails even with appropriate antibiotherapy, or more significantly, if the patient's condition deteriorates following the original surgical drainage procedure.

Computed tomography has expanded our ability to identify early bony destructive lesions in the mastoid. However, CNS complications may occur with little or no CT evidence of bone destruction. Magnetic resonance imaging with gadolinium may be useful in detecting early extradural abscess formation and sigmoid sinus thrombosis, though we did not use this method of imaging in this case.

Despite the availability of these modern diagnostic tools, these complications still occur, and the clinician should be familiar with the early signs and symptoms of complications of otitis media in order to render early diagnosis and treatment.

REFERENCES

1. Teichgraeber JF, Per-Lee JH, Turner JS. Lateral sinus thrombosis: a modern perspective. Laryngoscope 1982;92:744-51.

2. Wolfowitz B. Otogenic intracranial complications. Arch Otolaryngol 1972;96:220-2.

3. Hirsch JF, Roux FX, Sainte Rose C, Renier D, Pierre Kahn A. Brain abscess in childhood: a study of 34 cases treated by puncture and antibiotics. Childs Brain 1983;10:251-65.

4. Gower D, McGuirt FW. Intracranial complications of acute and chronic infectious ear disease: a problem still with us. Laryngoscope 1983;93:1028-33.

Ann Otol Rhinol Laryngol 106:1997

IMAGING CASE STUDY OF THE MONTH

CALCIFIED MUCOR FUNGUS BALL OF SPHENOID SINUS: AN UNUSUAL PRESENTATION OF SINOORBITAL MUCORMYCOSIS

LEVENT SAYDAM, MD
GÖKHAN ERPEK, MD
AHMET KIZILAY, MD
MALATYA, TURKEY

INTRODUCTION

Mucormycosis is an uncommon and potentially fatal fungal infection of paranasal sinuses and neighboring structures. Usually, affected patients are uncontrolled diabetics and those immunologically compromised. The causative organisms are Mucorales, which are one of the subgroups of Phycomycetes. *Absidia, Rhizopus*, and *Mucor* are the most common members of this family that cause disease in humans.[1]

Mucormycosis may occur in several locations in the body. Classically, the rhinocerebral form is encountered most often in uncontrolled diabetics, while the pulmonary and disseminated forms occur in nondiabetic immunosuppressed patients.[2] The most common presentations are rhinoorbital or rhinoorbitocerebral forms. Once the sinonasal tract is involved, the organism first attacks the arteries and, following this, the vascular pathways, and reaches to the orbital and intracranial structures. Facial swelling, facial pain, proptosis, and ophthalmoplegia are common alerting symptoms and signs reflecting the progression of the disease in uncontrolled diabetics or immunocompromised patients.

While the definitive diagnosis is achieved by histopathologic examination of the affected tissue and demonstration of nonseptate hyphae with right-angle branching, computed tomography (CT) scanning is the best imaging procedure either in early diagnosis or in assessing the extent of the disease. It must be performed in every patient with a suspicion of mucormycosis.

In this article, we present an uncommon CT appearance of a sinoorbital mucormycosis case and discuss the CT findings in light of the literature.

CASE REPORT

A 70-year-old diabetic woman was referred to our department with facial swelling and loss of vision in the right eye that had developed in the last 15 days. The patient had been judged to have periorbital cellulitis and treated with antibiotics and steroids in another hospital during this period. At the time of

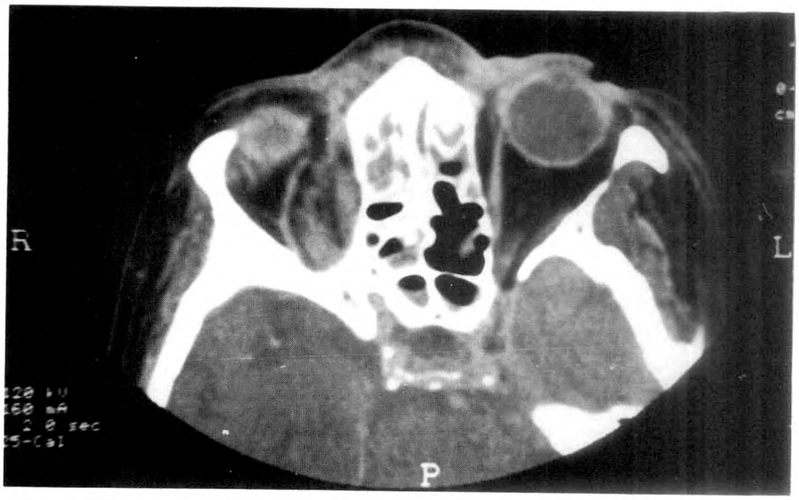

Fig 1. Preoperative computed tomography scan at level of orbits and ethmoid sinuses. Note soft tissue density infiltrating retroorbital space and orbital apex.

From the Department of Otolaryngology, Inonu University, School of Medicine, Malatya, Turkey.
CORRESPONDENCE — Levent Saydam, MD, Dept of Otolaryngology, Inonu University, School of Medicine, Malatya 43100, Turkey.

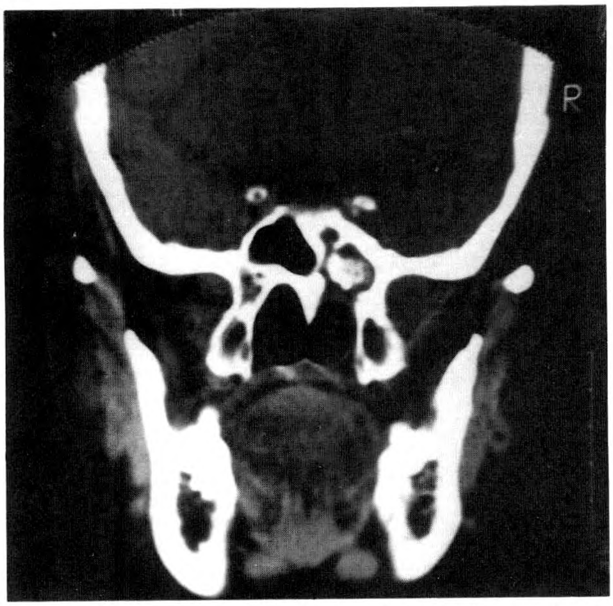

Fig 2. Coronal computed tomography scan shows calcified mass in right sphenoid sinus.

referral, the patient was in ketoacidotic coma. A right-sided total ophthalmoplegia, proptosis, facial swelling, and black crusting of the ipsilateral nasal vestibule were also noted. Computed tomography revealed pansinusitis and granulation tissue infiltrating the medial half of the right orbit (Fig 1). With a presumptive diagnosis of rhinoorbital mucormycosis, a transnasal biopsy of the right inferior concha was performed. The pathologic examination revealed nonseptate hyphae and necrotizing vasculitis, confirming the clinical diagnosis.

In addition to a right Caldwell-Luc procedure and ethmoidectomy, a sphenoid sinusotomy and a right orbital exenteration were performed. The sphenoid sinus mucosa was found to be intact at surgical exploration. Postoperatively, amphotericin B was given until a total cumulative dose of 2.0 g was reached. The patient was discharged upon completion of this treatment. On the first-month follow-up CT examination, a calcified mass in the right sphenoid sinus and some erosion of the posterior sinus wall were noted (Fig 2). The patient was reexplored and a calcified fungus ball and thickened mucosa were removed from the right sphenoid sinus. The final pathologic diagnosis was reported as fungal mycetoma consistent with mucormycosis.

DISCUSSION

In the presence of sinusitis-like symptoms, in every case of diabetes mellitus and every patient with immunosuppression, rhinocerebral mucormycosis should be suspected until disproven. It has been postulated that decreased polymorphonuclear leukocyte phagocytic activity and myeloperoxidase activity in diabetic patients are responsible for development of this destructive process.[1] Survival rates are 60% and 20% in diabetic and immunosuppressed patients, respectively. Due to its rapidly progressive and destructive nature, rhinocerebral mucormycosis represents one of the true rhinitis emergencies.[3] Prognosis is directly related to a high index of suspicion, prompt diagnosis, and treatment of the underlying medical condition. Once a Mucorales infection is confirmed histopathologically, amphotericin B and aggressive surgical debridement should be administered without hesitancy.

While histopathologic examination yields the definitive diagnosis in mucormycosis, CT examination gives the best results in early diagnosis and defining the extent of the disease.[1] Despite this fact, in the early stages of disease, CT findings may be considered as nonspecific.[4] Mucosal thickening, which is the most common early CT finding, is similar to that caused by other inflammatory conditions. The differentiation between CT findings of *Mucor* mucositis and common inflammatory sinus disease is clinically based on the presence of diabetic ketoacidosis, signs of orbital involvement, and infiltration of deep facial tissues by an inflammatory process.

Involvement of orbital contents is an intermediate stage that exists before the disease becomes intracranial. Intraorbital fungus foci easily penetrate into the retroorbital space, cavernous sinus, and cerebrum by following certain vascular pathways. Preseptal edema, proptosis, infiltration of the orbital fat, and thickening of the extraocular muscles constitute common CT appearances of orbital involvement. In our case, the presence of cavernous sinus opacification in addition to the orbital infiltration revealed by the first preoperative CT examination clearly defined the vascular pathways (Fig 1). Bone destruction is usually considered to be a late sign.[5] As reported by Zinreich et al,[6] CT yields very critical information for distinguishing fungal sinusitis from bacterial sinusitis and sinonasal neoplasms. The most important finding is scattered areas of increased attenuation, which are believed to be caused by ferromagnetic material produced by fungi.

In this case, the postoperative CT examination revealed a calcified mass in the right sphenoid sinus without any sign of further clinical exacerbation of the disease. At surgical exploration, the mass was easily removed via a previously created sphenoid sinusotomy. The sinus mucosa seemed to be grossly intact, but was removed for histopathologic examination. The pathologic diagnosis was reported as a calcified mucor fungus ball and normal sinus mucosa. Fungus balls or "mycetomas" consist of cheesy, thick or solid material.[7] These structures consist of fungal foci that also produce macromolecular proteins, carbohydrates, and ferromagnetic elements.[6] Principles of successful treatment of a noninvasive mucor sinus ball are removal of the fungal mass and establishment of adequate sinus drainage and also close follow-up of the patient's underlying medical condition. Additionally, the innovative amphotericin B treatment places mucormycosis into the classification of less-dreaded diseases today. Also, having sophisticated diagnostic tools, such as CT and magnetic resonance imaging, helps us to make a definite preoperative or postoperative diagnosis even in very circumscribed cases, such as that described in this article.

REFERENCES

1. Emanuelli JL. Infectious granulomatous diseases of the head and neck. Am J Otolaryngol 1993;14:155-67.
2. Pillsbury HC, Fischer ND. Rhinocerebral mucormycosis. Arch Otolaryngol 1977;103:600-4.
3. Kopke RD, Jackson RL. Rhinitis. In: Bailey BJ, ed. Head and neck surgery–otolaryngology. Vol 1. Philadelphia, Pa: JB Lippincott, 1993:269-89.
4. Goodnight J, Dulgerov P, Abemayor E. Calcified mucor fungus ball of the maxillary sinus. Am J Otolaryngol 1993;14:209-10.
5. Gamba JL, Woodruff WW, Djang WT, Yeates AE. Craniofacial mucormycosis: assessment with CT. Radiology 1986;160:207-12.
6. Zinreich SJ, Kennedy DW, Malat J, et al. Fungal sinusitis: diagnosis with CT and MR imaging. Radiology 1988;169:439-44.
7. Som PM, Dillon WP, Curtin HD, Fullerton GD, Lidov M. Hypointense paranasal sinus foci: differential diagnosis with MR imaging and relation to CT findings. Radiology 1990;176:777-81.

≈

HEAD-NECK SURGERY AND ONCOLOGY

The Second Israeli International Symposium on Head-Neck Surgery and Oncology will be held in Jerusalem, Israel, November 1-5, 1998. For more information, please contact the Symposium Secretariat, PO Box 1931, Ramat-Gan 52118, Israel; telephone 972-3-6133340; fax 972-3-6133341.

Ann Otol Rhinol Laryngol 106:1997

CLINICOPATHOLOGICAL CONSULTATION

SYNDROME OF INAPPROPRIATE ANTIDIURETIC HORMONE SECRETION ASSOCIATED WITH HEAD AND NECK CANCERS: REVIEW OF THE LITERATURE

ALFIO FERLITO, MD
PADUA, ITALY

ALESSANDRA RINALDO, MD
PADUA, ITALY

KENNETH O. DEVANEY, MD
ANN ARBOR, MICHIGAN

In a minority of patients with malignant tumors, signs and symptoms develop that cannot be explained on the basis of the mass effect produced by the primary tumor or its metastases, or production of a hormone normally associated with the tissue type that has given rise to the malignant tumor; these peculiar symptom complexes are known as paraneoplastic syndromes, and may be divided into endocrinologic, dermatologic, hematologic, neurologic, and osteoarticular manifestations. In the head and neck region in particular, the syndrome of inappropriate antidiuretic hormone production (SIADH, or Schwartz-Bartter syndrome) is a well-recognized form of paraneoplastic syndrome that may accompany head and neck malignancies. Most of such tumors are squamous carcinomas, with lesser numbers of olfactory neuroblastomas, small cell neuroendocrine carcinomas, adenoid cystic carcinomas, and undifferentiated carcinomas; sarcoma was reported in only a single instance. The lesions associated with the development of SIADH have most often been located in the oral cavity, and less often in the larynx, nasopharynx, hypopharynx, nasal cavity, maxillary sinus, parapharyngeal space, salivary glands, and oropharynx. Key features of SIADH include serum hypo-osmolality; an unexpectedly high urinary specific gravity; an absence of edema or dehydration; normal adrenal, thyroid, and renal function; hyponatremia; and an elevation of plasma vasopressin.

Paraneoplastic syndromes are systemic and nonmetastatic manifestations associated with a variety of malignant neoplasms and develop in a minority of cancer patients. Specifically, many forms of primary and metastatic malignancies in the head and neck area may on occasion cause a variety of metabolic and other disturbances that are important causes of symptoms. These "paraneoplastic symptoms" are produced as a result of secretion of hormones by tumor or by ill-understood mechanisms that give rise to different syndromes (cutaneous, endocrine, hematologic, neurologic, osteoarticular; Table 1). As a rule, paraneoplastic symptoms develop at sites remote from the primary tumor and so are not due to metastases. Different terms such as paraneoplastic syndromes, paraneoplastic effects, nonmetastatic syndromes, paraneoplastic phenomena, paraneoplastic disturbances, and remote effects have all been employed at one time or another to refer to development of symptoms that are not referable to either the primary mass lesion or any metastases, but rather appear to be associated with the tumor on the basis of some other mechanism. Lung carcinomas, especially oat cell carcinoma and squamous cell carcinoma, are the most common tumors causing paraneoplastic syndromes.

Ectopic or inappropriate hormone secretion causing clinically manifest syndromes is uncommon in patients with cancer of the head and neck. The most important of these is the syndrome of inappropriate secretion of arginine vasopressin, known as Schwartz-Bartter syndrome or as the syndrome of inappropriate secretion of antidiuretic hormone (SIADH). Antidiuretic hormone (ADH) or its biologically active form in humans, ie, arginine vasopressin, is normally synthesized in the hypothalamus (supraoptic nucleus) and then transported through the hypothalamic-neurohypophyseal stalk to the posterior pituitary, where it is stored and finally released. Antidiuretic hormone physiologically participates in maintaining a constant serum osmolality and intravascular volume, acting on the renal tubular apparatus by retaining water and concentrating urine. This syndrome is associated with a large variety of neoplastic and nonneoplastic processes, including central nervous system lesions, pulmonary diseases, trauma, and drugs (including those used to treat malignancies; Table 2[1]) and may be experimentally induced in dogs by increasing cerebral venous pressure.[2]

Schwartz et al[3] first described SIADH in 1957, in patients with bronchogenic cancer. Although small

---

From the Department of Otolaryngology, University of Padua, Padua, Italy (Ferlito, Rinaldo), and the Department of Pathology, University of Michigan, Ann Arbor, Michigan (Devaney). Supported by The Laryngeal Cancer Association, Italy.

CORRESPONDENCE — Alfio Ferlito, MD, Dept of Otolaryngology, University of Padua, Nuovo Policlinico, Via Giustiniani 2, 35128 Padua, Italy.

TABLE 1. CLASSIFICATION OF PARANEOPLASTIC SYNDROMES OBSERVED IN HEAD AND NECK MALIGNANCIES

- Paraneoplastic cutaneous or dermatologic syndromes
  - Acanthosis nigricans
  - Bazex's syndrome (paraneoplastic acrokeratosis)
  - Bowen's disease
  - Bullous pemphigoid
  - Dermatomyositis
  - Sweet's syndrome
  - Tripe palms
  - Yellow nail syndrome
- Paraneoplastic endocrine syndromes
  - Calcitonin
  - Carcinoid syndrome
  - Cushing's syndrome or ectopic adrenocorticotrophic hormone syndrome
  - Nonmetastatic hypercalcemia
  - Schwartz-Bartter syndrome or syndrome of inappropriate secretion of antidiuretic hormone (SIADH)
- Paraneoplastic hematologic syndromes
  - Thrombophlebitis migrans or migratory thrombophlebitis or Trousseau's syndrome
  - Consumption coagulopathies
  - Leukocytosis
- Paraneoplastic neurologic syndromes
  - Eaton-Lambert myasthenic syndrome
- Paraneoplastic osteoarticular syndromes
  - Hypertrophic osteoarthropathy

cell lung cancer is the most common cause of SIADH, the syndrome has been associated with many different types of tumors, including pancreatic carcinoma, duodenal carcinoma, prostatic carcinoma, bladder carcinoma, mesothelioma, lymphomas, Hodgkin's disease, acute myelogenous leukemia, thymoma, and adrenocortical carcinoma. The present article describes cancers of the head and neck associated with SIADH.

The syndrome (SIADH) is characterized by excessive blood levels or actions of vasopressin associated with hyponatremia without edema. The inability to excrete a dilute urine implies a subsequent retention of the ingested fluids with expansion of the extracellular fluid volume without edema. Hyponatremia is due to both sodium dilution in a larger extracellular fluid volume, and its higher urinary excretion caused by a decreased reabsorption in the proximal renal tubular tract because of the increased extracellular fluid volume.

The syndrome is more commonly associated with cancers of the head and neck than previously thought,[4] and in a review of the literature we collected 70 cases of SIADH-associated malignancies of these areas (Table 3[4-26]). Only in 1976, 19 years after the first description of SIADH, was it found in association with a head and neck cancer.[5] Between then and 1991, only 19 cases were detected.[6-20] It was in 1992

TABLE 2. CAUSES OF SIADH

- Malignant neoplasms with autonomous arginine vasopressin release
  - Small cell lung cancer
  - Cancers of head and neck
  - Other types of tumors in different sites of body
    - Olfactory neuroblastoma
    - Pancreatic carcinoma
    - Mesothelioma
    - Lymphomas, Hodgkin's disease
    - Duodenal carcinoma
    - Thymoma
    - Adrenocortical carcinoma
- Pulmonary diseases
  - Tuberculosis
  - Lung abscess
  - Pneumonia
  - Viral pneumonitis
  - Empyema
  - Chronic obstructive airway disease
- Central nervous system disorders
  - Trauma
    - Skull fracture
    - Subdural hematoma
    - Subarachnoid hemorrhage
    - Cerebral vascular thrombosis
  - Cerebral atrophy
  - Intracranial space-occupying lesions
    - Primary and metastatic tumor
  - Infections
    - Acute encephalitis
    - Tuberculous meningitis
    - Purulent meningitis
    - Lues
  - Guillain-Barré syndrome
  - Vasculitis
    - Lupus erythematosus
  - Acute intermittent porphyria
  - Pain and emotional stress
- Drugs
  - Chlorpropamide
  - Vincristine sulfate
  - Vinblastine sulfate
  - Cyclophosphamide
  - Carbamazepine
  - Oxytocin
  - General anesthesia
  - Narcotics
  - Tricyclic antidepressants
- Miscellaneous causes
  - Hypothyroidism
  - Positive-pressure respiration

Modified from Moses and Streeten.[1]

TABLE 3. SIADH ASSOCIATED WITH MALIGNANCIES OF HEAD AND NECK

Authors	*Year*	*No. of Cases*	*Location*	*Tumor Type*
Moses et al[5]	1976	2	Larynx	SCC
Forrest et al[6]	1978	1	Tongue	SCC
Robertson[7]	1978	1	Tongue	SCC
Trotoux et al[8]	1979	1	Larynx	SCNC
Singh et al[9]	1980	1	Nasal cavity	ON
Yokokawa et al[10]	1981	1	Nasopharynx	Sarcoma
Srigley et al[11]	1983	1	Nasal cavity	ON
Cullen et al[12]	1986	1	Nasal cavity	ON
Hayes et al[13]	1986	2	Oropharynx, oral cavity	SCC
Osterman et al[14]	1986	1	Nasal cavity	ON
Kandylis et al[15]	1986	1	Pyriform sinus	SCC
Okutomi et al[16]	1987	1	Floor of mouth	SCC
Abdi and Bishop[17]	1988	1	Tongue	SCC
Tatemoto et al[18]	1989	1	Nasal cavity	ACC
Takeuchi et al[19]	1989	1	Larynx	SCNC
Zohar et al[20]	1991	4	Larynx (3), pyriform sinus (1)	SCC
Kavanagh et al[21]	1992	1	Nasopharynx	UC
Talmi et al[4]	1992	43	Oral cavity (24)	SCC
			Hypopharynx (5)	SCC
			Nasopharynx (6)	SCC (5), ACC (1)
			Larynx (4)	SCC
			Salivary glands (2)	SCC (1), ACC (1)
			Parapharyngeal space (2)	SCC
Al Ahwal et al[22]	1994	1	Maxillary sinus	ON
Kokatsu and Tsukuda[23]	1994	1	Nasopharynx	UC
Pierce et al[24]	1994	1	Maxillary sinus	SCNC*
Roth et al[25]	1994	1	Larynx	SCC
Myers and Kessimian[26]	1995	1	Larynx	SCNC

SCC — squamous cell carcinoma, SCNC — small cell neuroendocrine carcinoma, ON — olfactory neuroblastoma, ACC — adenoid cystic carcinoma, UC — undifferentiated carcinoma.

*In article, neoplasm was generically indicated as extrapulmonary small cell cancer.

that Talmi et al[4] presented the largest series to date of head and neck cancer patients with SIADH, a report of 43 patients drawn from a review of the University of Iowa Tumor Registry. This retrospective review identified a 3% incidence of SIADH among 1,436 patients with head and neck cancers and included an examination of relevant laboratory values and exclusion of other causes of hypo-osmolality and hyponatremia for each patient.

The most common site of occurrence was the oral cavity, with 29 detected cases (29 of 70 or 41.43%). In 13 patients the larynx was involved (13 of 70 or 18.57%), while nasopharyngeal malignancies were found in 9 cases (9 of 70 or 12.86%). In 7 cases (7 of 70 or 10.00%) the cancer was localized in the hypopharyngeal area, and in 5 cases (5 of 70 or 7.14%) the lesion involved the nasal cavity. Other regions of involvement were the maxillary sinus (2 cases), parapharyngeal space (2), salivary glands (2), and oropharynx (1; Table 4[4-26]). The case reported by Kundaje and Shenoy[27] was not included in Table 4, because the authors reported a case of SIADH due to a metastatic squamous cell carcinoma (from a probable primary lung carcinoma) diagnosed in a supraclavicular lymph node biopsy.

The histologic tumor type most frequently present was squamous cell carcinoma, with 55 of 70 cases (78.57%); however, other tumor types, such as olfactory neuroblastoma, adenoid cystic carcinoma, small cell neuroendocrine carcinoma, undifferentiated carcinoma, and sarcoma, were found (Table 5[4-26]).

The syndrome has been observed after induction chemotherapy for advanced squamous cell carcinomas of the head and neck,[13] in patients with recurrent neoplasms,[4] and after neck dissection.[28,29]

The syndrome may precede the presentation of the cancer by a few weeks or months.[8,22] In 1979, Trotoux

TABLE 4. LOCATION OF TUMORS OF HEAD AND NECK ASSOCIATED WITH SIADH

Site	*No. of Cases*
Oral cavity	29
Larynx	13
Nasopharynx	9
Hypopharynx	7
Nasal cavity	5
Maxillary sinus	2
Parapharyngeal space	2
Salivary glands	2
Oropharynx	1
Total	70

Information from references 4-26.

et al[8] described Schwartz-Bartter syndrome in a 61-year-old man that led to the detection of a small cell carcinoma of the subglottic region. The patient presented with initial headache, confusion, temporo-spatial disorientation, hyperreflexia, hyponatremia, hypochloremia, serum hypo-osmolarity, reduced hematocrit, negative free water clearance, and high plasma levels of ADH. The diagnosis of the subglottic tumor was only made 3 months later. In 1994, Al Ahwal et al[22] reported a case of olfactory neuroblastoma in a 27-year-old man who initially presented with SIADH manifesting as nausea, vomiting, hyponatremia, and a serum osmolality of 225 mmol/kg. No lower limb edema was present. After a few weeks, a neoplastic lesion of the right maxillary sinus was discovered.

Clinically, water retention causes weight gain, but the symptomatology is mainly characterized by neurologic signs due to cerebral edema caused by water passage from the hypotonic extracellular fluid volume to the nerve cells. For these reasons, the manifestations of SIADH depend on its grade. In mild SIADH (serum sodium concentration 130 to 135 mmol/L, or gradual development over several weeks) symptoms may be absent or limited to nausea, anorexia, and vomiting. When hyponatremia is severe or acute, the most important symptoms are body weight increases, weakness, lethargy, confusion, convulsions, and coma.

TABLE 5. HISTOLOGY OF TUMORS OF HEAD AND NECK ASSOCIATED WITH SIADH

Histotype	*No. of Cases*
Squamous cell carcinoma	55
Olfactory neuroblastoma	5
Small cell neuroendocrine carcinoma	4*
Adenoid cystic carcinoma	3
Undifferentiated carcinoma	2
Sarcoma	1
Total	70

Information from references 4-26.

*In 1 case, neoplasm was generically indicated as extrapulmonary small cell cancer.

A diagnosis of SIADH should be considered in patients initially presenting with hyponatremia (<135 mEq/L) and a urine concentration (urine osmolality) or a urine specific gravity greater than expected for serum osmolality (urine osmolality > 300 mmol/kg; urine specific gravity > 1.015; serum osmolality < 280 mOsm/kg; Table 6). A urinary sodium concentration of >20 mEq/L is suggestive of the syndrome. These signs are associated with lethargy and an absence of edema, orthostatic hypotension and the appearance of dehydration.

The syndrome has to be distinguished from other diseases causing a similar clinical picture. It is necessary to exclude other causes of hyponatremia: dilutional hyponatremias, hyponatremic edema states, hypertensive states, primary polydipsia, pseudohyponatremia, and essential hyponatremia (sick-cell syndrome). Dilutional hyponatremias are present in patients with adrenal insufficiency, excessive fluid loss (from vomiting, diarrhea, drug-induced diuresis, and excessive sweating), fluid deprivation, and, probably, positive-pressure respiration. In adrenocortical insufficiency, orthostatic hypotension with tachycardia and an elevated or high-normal blood urea nitrogen are characteristic. Hyponatremic edematous states are caused by congestive heart failure, cirrhosis with ascites, nephrosis, orthostatic edema, myxedema (hypothyroidism), and treatment with sodium-retaining drugs (fludrocortisone acetate, nonsteroidal anti-inflammatory agents, and others). Hypertensive states associated with hyponatremia are present in patients with renovascular stenosis or diuretic therapy. Primary polydipsia is always associated with a dilute urine (osmolality > 150 mmol/kg). Pseudohyponatremia is combined with excessive plasma glucose, triglyceride, or protein concentrations. Sick-cell syn-

TABLE 6. PARAMETERS THAT HAVE TO BE MET TO MAKE DIAGNOSIS OF SIADH

Serum hypo-osmolality (usually <280 mOsm/kg)

Urine concentration or specific gravity greater than expected for serum osmolality: continued urinary excretion of sodium; urine osmolality of ≥500 mOsm/kg or >300 mmol/kg; urinary concentration of sodium of >20 mEq/L

No edema, orthostatic hypotension, or features of dehydration

No evidence of volume depletion

Normal adrenal, thyroid, and renal function

Usually, elevated plasma concentrations of vasopressin

Hypouricemia due to increased renal clearance, hypocreatininemia, and hypoalbuminemia

Hyponatremia (<135 mEq/L)

Low-normal or subnormal range of blood urea nitrogen drome is characterized by hyponatremia due to a subnormal setting of the hypothalamic osmoreceptors, associated usually with a chronic, debilitating disease.[1]

The symptoms of SIADH are frequently treatable. Treatment comprises limiting fluid intake in less serious cases. In severe cases this syndrome should be treated with a hypertonic saline solution (3% saline) and furosemide. The treatment of choice in tumor relapse and recurrent SIADH is demeclocycline (600 to 1,200 mg/d in divided doses).[30] The prognosis depends on the underlying malignancy and its treatment.

REFERENCES

1. Moses AM, Streeten DHP. Disorders of the neurohypophysis. In: Isselbacher KJ, Martin JB, Braunwald E, Fauci AS, Wilson JD, Kasper DL, eds. Harrison's principles of internal medicine. 13th ed. Vol 2. New York, NY: McGraw-Hill, 1994: 1921-30.

2. McQuarrie DG, Mayberg M, Ferguson M, Shons AR. A physiologic approach to the problem of simultaneous bilateral neck dissection. Am J Surg 1977;134:455-60.

3. Schwartz WB, Warren B, Curelop S, Bartter FC. A syndrome of renal sodium loss and hyponatremia probably resulting from inappropriate secretion of antidiuretic hormone. Am J Med 1957;23:529-42.

4. Talmi YP, Hoffman HT, McCabe BF. Syndrome of inappropriate secretion of arginine vasopressin in patients with cancer of the head and neck. Ann Otol Rhinol Laryngol 1992;101: 946-9.

5. Moses AM, Miller M, Streeten DHP. Pathophysiologic and pharmacologic alterations in the release and action of ADH. Metabolism 1976;25:697-721.

6. Forrest JN, Cox M, Hong C, Morrison G, Bia M, Singer I. Superiority of demeclocycline over lithium in the treatment of chronic syndrome of inappropriate secretion of antidiuretic hormone. N Engl J Med 1978;298:173-7.

7. Robertson GL. Cancer and inappropriate antidiuresis. In: Ruddon RW, ed. Biological markers of neoplasia: basic and applied aspects. New York, NY: Elsevier, North-Holland, 1978: 277-93.

8. Trotoux J, Glickmanas M, Sterkers O, Trousset M, Pinel J. Syndrome de Schwartz-Bartter: révélateur d'un cancer laryngé sousglottique à petites cellules. Ann Otolaryngol Chir Cervicofac 1979;96:349-58.

9. Singh W, Ramage C, Best P, Angus B. Nasal neuroblastoma secreting vasopressin. Cancer 1980;45:961-6.

10. Yokokawa T, Shigetomi S, Takahashi S, Ogawa S, Fukuchi S, Miura T. A case of epipharyngeal sarcoma associated with the syndrome of inappropriate secretion of antidiuretic hormone (SIADH). Nippon Naika Gakkai Zasshi 1981;70:410-6.

11. Srigley JR, Dayal VS, Gregor RT, Love R, van Nostrand AWP. Hyponatremia secondary to olfactory neuroblastoma. Arch Otolaryngol 1983;109:559-62.

12. Cullen MJ, Cusack DA, O'Briain DS, Devlin JB, Kehely A, Lyons TA. Neurosecretion of arginine vasopressin by an olfactory neuroblastoma causing reversible syndrome of antidiuresis. Am J Med 1986;81:911-6.

13. Hayes DF, Lechan RM, Posner MR, Weichselbaum RR, Miller D, Ervin TJ. The syndrome of inappropriate antidiuretic hormone secretion associated with induction chemotherapy for squamous cell carcinoma of the head and neck. J Surg Oncol 1986;32:150-2.

14. Osterman M, Calhoun A, Dunham M, et al. Chronic syndrome of inappropriate antidiuretic hormone secretion and hypertension in a patient with olfactory neuroblastoma. Arch Intern Med 1986;146:1731-5.

15. Kandylis KV, Vasilomanolakis M, Efremides AD. Syndrome of inappropriate antidiuretic hormone secretion in pyriform sinus squamous cell carcinoma [Letter]. Am J Med 1986; 81:946.

16. Okutomi T, Sakata S, Tatematsu N, Oka N. Squamous cell carcinoma of tongue and floor of mouth associated with syndrome of inappropriate secretion of antidiuretic hormone. J Oral Maxillofac Surg 1987;45:447-9.

17. Abdi EA, Bishop S. The syndrome of inappropriate antidiuretic hormone secretion with carcinoma of the tongue. Med Pediatr Oncol 1988;16:210-5.

18. Tatemoto K, Goto K, Uno T, et al. A case of adenocarcinoma of the nasal cavity associated with syndrome of inappropriate secretion of antidiuretic hormone (SIADH). Gan No Rinsho 1989;35:1153-9.

19. Takeuchi K, Nishii S, Jin CS, Ukai K, Sakakura Y. Anaplastic small cell carcinoma of the larynx. Auris Nasus Larynx 1989;16:127-32.

20. Zohar Y, Talmi YP, Finkelstein Y, Nobel M, Gafter U. Syndrome of inappropriate antidiuretic hormone secretion in cancer of the head and neck. Ann Otol Rhinol Laryngol 1991; 100:341-4.

21. Kavanagh BD, Halperin EC, Rosenbaum LC, Shannon EM, Nilaver G. Syndrome of inappropriate secretion of antidiuretic hormone in a patient with carcinoma of the nasopharynx. Cancer 1992;69:1315-9.

22. Al Ahwal M, Jha N, Nabholtz JM, Hugh J, Birchall I, Nguyen GK. Olfactory neuroblastoma: report of a case associated with inappropriate antidiuretic hormone secretion. J Otolaryngol 1994;23:437-9.

23. Kokatsu T, Tsukuda M. Hypopituitarism and hyponatremia in a case with nasopharyngeal carcinoma. ORL J Otorhinolaryngol Relat Spec 1994;56:347-51.

24. Pierce ST, Cibull ML, Metcalfe MS, Sloan D. Bone marrow metastases from small cell cancer of the head and neck. Head Neck 1994;16:266-71.

25. Roth Y, Lightman SL, Kronenberg J. Hyponatremia associated with laryngeal squamous cell carcinoma. Eur Arch Otorhinolaryngol 1994;251:183-5.

26. Myers TJ, Kessimian N. Small cell carcinoma of the larynx and ectopic antidiuretic hormone secretion. Otolaryngol Head Neck Surg 1995;113:301-4.

27. Kundaje GN, Shenoy P. A case of syndrome of inappropriate antidiuretic hormone (SIADH) secretion due to a metastatic squamous cell carcinoma. J Assoc Physicians India 1982; 30:253-4.

28. Wenig BL, Heller KS. The syndrome of inappropriate secretion of antidiuretic hormone (SIADH) following neck dis-

section. Laryngoscope 1987;97:467-70.

29. Mesko TW, Garcia O, Yee LD, Villar M, Chan H. The syndrome of inappropriate secretion of antidiuretic hormone (SIADH) as a consequence of neck dissection. J Laryngol Otol 1997;111:449-53.

30. Deleu D, De Geeter F. Neurological manifestations of neuroendocrine neoplasms of the larynx. ORL J Otorhinolaryngol Relat Spec 1991;53:250-8.

≈

FIRST WORLD CONGRESS OF OTORHINOLARYNGOLOGIC ALLERGY, ENDOSCOPY AND LASER SURGERY

The First World Congress of Otorhinolaryngologic Allergy, Endoscopy and Laser Surgery will be held in Athens, Greece, June 25-27, 1998. For more information, contact Nereus Tours, Congress & Conference Department, 2 Afentouli Street, 185 36 Piraeus, Greece; telephone 1-4524842; fax 1-4182308.

≈

GERIATRIC LARYNGOLOGY — EVALUATION AND MANAGEMENT OF THE AGING VOICE

Geriatric Laryngology — Evaluation and Management of the Aging Voice will be held November 13, 1997, in New York, NY. For information, contact Julia Baumgarten, Manager, Institute for Continuing Medical Education, The New York Eye & Ear Infirmary, 310 E 14th St, New York, NY 10003; telephone (212) 979-4430; fax (212) 979-4441.

LETTERS TO THE EDITOR

To the Editor:

I am writing concerning the article by Laszig et al called "Nucleus 20-Channel and 21-Channel Auditory Brain Stem Implants: First European Experiences" (*Ann Otol Rhinol Laryngol Suppl* 1995;104[suppl 166]:28-30) and other papers related to electrical stimulation of the central hearing structures published in the same supplement. Implantation of electrodes on the brain surface for the purpose of generating auditory sensation in deaf patients has been performed by a number of teams over the past 20 years.[1-3] The early electrode consisted of two platinum plates mounted on insulating material. This and later types of electrodes were placed until the early 1990s, such that "three quarters of its length was positioned medial and one quarter was lateral to the taenia."[3] However, almost the entire cochlear nucleus is covered by the fourth ventricle velum and the taenia. The latter must be cut through to place the prosthesis.[4,5] Therefore, the electrode's medial (distal) part is obviously separated from the cochlear nucleus surface by the choroid plexus and the taenia, as well as by the cerebrospinal fluid. Our studies[6] have also demonstrated that the root of the cochlear nerve is mostly located under the taenia. Therefore, the lateral (proximal) part of the electrode would seem to be positioned over the root or even more proximally, ie, on the adjacent segment of the cochlear nerve.

Thus, one can assume that the electrode can produce stimulation of the central auditory structures without being in direct contact with the cochlear nucleus surface. Even if the cochlear nerve is completely degenerated following acoustic tumor removal, the propagation of the electrical current through it, as well as other structures, is a possibility. It has been recently demonstrated that electrical stimulation of the lateral hypothalamus causes activation of cells of the dorsal and ventral cochlear nuclei.[7]

It has been reported that the entire electrode array is now placed within the lateral recess through the foramen of Luschka.[3] Our unpublished observations show that the choroid plexus that protrudes through the foramen occupies virtually the entire foramen. In addition, the lateral recess has the shape of a bent tube, the diameter of which is close to the width of the electrode array. These anatomic peculiarities should interfere with the technique and suggest the need for more research.

In conclusion, the probability exists that auditory sensation obtained by electrical stimulation may be due to stimulation of the tissues adjacent to the cochlear nucleus structures, including the remaining segment of the cochlear nerve, or simply their ability to conduct electrical current toward the cochlear nucleus or other structures of the auditory brain stem, rather than to direct stimulation of the cochlear nucleus. Further studies in the neuroanatomy and anatomic neurosurgery of the brain area involved would be beneficial. This could result in development of specialized techniques of electrode placement and design of various types of electrodes that would be adapted to the size, shape, and intrinsic structure of the areas selected for implantation.

Leonid I. Terr, PhD
12144 Miranda St
North Hollywood, CA 91607

REFERENCES

1. Edgerton BJ, House WF, Hitselberger W. Hearing by cochlear nucleus stimulation in humans. Ann Otol Rhinol Laryngol Suppl 1982; 91(suppl 91):117-24.

2. Luetje CM, Whittaker CK, Geier L, Mediavilla SJ, Shallop JK. Feasibility of multichannel human cochlear nucleus stimulation. Laryngoscope 1992;102:23-5.

3. Brackmann DE, Hitselberger WE, Nelson RA, et al. Auditory brainstem implant: I. Issues in surgical implantation. Otolaryngol Head Neck Surg 1993;108:624-33.

4. Terr LI, Edgerton BJ. Surface topography of the cochlear nuclei in humans: two- and three-dimensional analysis. Hear Res 1985;17:51-9.

5. Terr LI, Edgerton BJ. Three-dimensional reconstruction of the cochlear nuclear complex in humans. Arch Otolaryngol 1985;111:495-501.

6. Sinha UK, Terr LI, Galey FR, Linthicum FH Jr. Computer-aided three-dimensional reconstruction of the cochlear nerve root. Arch Otolaryngol Head Neck Surg 1987;113:651-5.

7. Woody CD, Chen AC, Gruen E. Activation of cells of cochlear nucleus by electrical stimulation of lateral hypothalamus. Neuroreport 1996;7:758-60.

To the Editor:

I contacted all authors who have been working with the European auditory brain stem prosthesis and were mentioned as coauthors in the paper Dr Terr writes about (*Ann Otol Rhinol Laryngol Suppl* 1995;104[suppl 166]:28-30).

Obviously, it is true that we do not yet have the optimal stimulation electrode at the moment, and that further studies, anatomical as well, are required. In other words, the use of needle electrodes has to be checked, too. The results of the American, as well as the European, research does show sufficiently the direct electrical stimulation of the nucleus cochlearis. For this reason, we in Europe are using as many electrodes as possible, ie, 21, which also seems to be an advantage over the 8 electrodes used in the United States so far. On May 11, 1997, we met with the most important American users and researchers, together with Cochlear Corp Denver, in Scottsdale, Arizona, and agreed to exclusively use the European prosthesis with 21 electrodes, slightly modified in regard to the fixation mode.

In the mostly large tumors of neurofibromatosis 2 patients, the foramen of Luschka often is so enlarged that we do not find normal anatomic conditions. It is not quite comprehensible that complex stimulation only with acoustic sensations, indirectly via the stump of the auditory nerve or other structures, should have been constant over 5 years. Here the stimulation has to be direct — even more so as the choroid plexus is dissected.

We know that the hypothalamus of the healthy human possesses a complete neuronal circuit. If this had any impact on the function of electrical stimulation of the nucleus cochlearis, a perceptible side effect should be registered with each single electrode. However, this is not the case with the 25 patients implanted in Europe with the 21-electrode auditory brain stem implant since 1992.

Ongoing stimulation via the nerve stump will not have any long-lasting success, as the axons will degenerate. Our experience might show this degeneration as we register auditory sensations and responses with the middle and lower electrodes; however, there has not been sensation registered with the distal ones near the end of the cochlear nerve. Therefore, it is our endeavour to place the electrode array as deep as possible in the lateral recess. We are of the opinion that theoretical considerations, even though perfectly justified, have in this instance been contradicted by clinical experience to date.

Prof Dr Roland Laszig
ENT Department
University of Freiburg
Killianstr 5
D-79106 Freiburg
Germany

To the Editor:

The discussion below is in regard to the article by Deguine et al "Criteria for Selecting the Side for Cochlear Implantation" (*Ann Otol Rhinol Laryngol Suppl* 1995;104(suppl 166): 403-6). The assessment of individual cerebral dominance for speech is not easy, but it is important for selecting the side of cochlear implantation.

Deguine et al described in their article the criterion of hemispheric dominance, indirectly measured by handedness, for deciding on the side of cochlear implantation. Laterality of handedness is a very rough sign of cerebral dominance. Are there other meaningful signs? Eyedness and footedness are two simple possible tests. One problem is the interpretation of handedness. In the case of right-handedness, there are clear relationships: 95% of right-handers have a dominance of the left hemisphere for speech, and the remaining 5% a dominance of the right side. In the case of left-handedness, there are not such clear relationships.[1] Of course, we know little about speech dominance in deaf people, especially in congenitally deaf children.[2] In the population there is only 7% left-handedness. The assessment of this handedness type must be especially careful. Not only preference tests, but also performance tests are important. If we know that the patient is a left-hander, the question of the dominant hemisphere for speech is not easy. About 60% to 70% of left-handers show a dominance of the left hemisphere, and about 30% to 40% show a dominance of the right hemisphere. These distributions are the results of several studies using 1) patients with an aphasia and 2) patients undergoing several invasive tests: Wada's test (intracarotid amobarbital sodium) and unilateral electroconvulsive therapy.[1] Noninvasive tests are not as valid, eg, the dichotic listening test, visual field asymmetries, and tests using perfusion or oxygenation of the brain (single photon emission computed tomography or positron emission tomography). Also, so-called latent handedness is impracticable to test.[3] The assessment of the individual dominant hemisphere is very complex, with accurate results possible only with the above-described invasive tests. So, we proposed at least testing hand performance and hand preference,[4] along with foot and eye dominance.[5] These tests will give better markers of an atypical noncrossed dominance for speech and, so, a better indication for deciding the better or dominant side for cochlear implantation. The question concerning "former" earedness is also meaningful.

Michael Reiss, MD
Dept of Ear, Nose and Throat
Universitätsklinikum Dresden
Technische Universität
Fetscherst. 74
D-01307 Dresden
Germany

REFERENCES

1. Beaumont JG. Methods for studying cerebral hemispheric function. In: Young AW, ed. Functions of the right hemisphere. London, England: Academic Press, 1983:113-46.
2. Sanders G, Wright HV, Ellis C. Cerebral lateralization of language in deaf and hearing people. Brain Lang 1989;36:555-79.
3. Reiss M. Leg-crossing: incidence and inheritance. Neuropsychologia 1994;32:747-50.
4. Tapley SM, Bryden MP. A group test for the assessment of performance between the hands. Neuropsychologia 1985;23:215-21.
5. Strauss E. Hand, foot, eye and ear preference and performance on a dichotic listening test. Cortex 1986;22:475-82.

Editor's Reply:

Regarding auditory "cortical dominance" in choice of the side of an implant, if there is equal anatomy peripherally, what would be necessary would be evidence that speech is better understood when put into one ear as opposed to the other. There is no research evidence to support this from functional magnetic resonance imaging or positron emission tomography scanning. The only time any advantage is seen is when competing and different signals are put into both ears simultaneously; then, an advantage of about 3% is seen for the ear on the nondominant side.

However, when speech is put into only one ear at a time, as would be the case for a unilateral cochlear implant, no advantage is seen for either ear. It appears to be clear that the crossed and uncrossed pathways are equally efficient, except under very special circumstances.

Thus, selection of ears on the basis of "auditory sidedness" is a nonissue. The side of greater neural survival is the prime consideration.

Brian F. McCabe, MD
Christopher W. Turner, PhD
The University of Iowa
Iowa City, IA 52242

BOOK REVIEWS

Lasers in Otorhinolaryngology and in Head and Neck Surgery

Volume 49 of *Advances in Oto-Rhino-Laryngology*, W. Arnold, editor. H. Rudert and J. A. Werner, editors. Hard cover, illustrated, indexed, 264 pages, 56 figures, 1995. S. Karger AG, Basel, Switzerland, $215.75.

Laser technology has been in a constant state of change since its induction in the 1970s, and numerous books have been written on the subject. This is an up-to-date volume on lasers for head and neck surgeons. Dermatologists and plastic surgeons may also reap benefits from the book. Individual chapters are results of papers of the 4th Laser Congress, though every aspect of laser treatment is not included.

Overviews of laser treatment are preserved for middle and inner ear, vascular malformation, diseases of the nasal cavity and the paranasal sinuses, and benign and malignant tumors of the larynx and skin. Valuable information is shared relating to transoral laser therapy in the treatment of carcinoma — a controversial subject despite the fact that long-term results are now becoming available that may or may not justify transoral laser therapy. Only four chapters discuss the use of laser in otology: two chapters show why specific lasers are used for stapedotomy; the other two chapters are experimental and convey rather poor results of combined low-power laser therapy and extracts of *Ginkgo biloba* in cases of tinnitus.

The merits of laser types are discussed. Pertinent information is circulated. Included in the volume are 56 figures (1 in color) and 38 tables. Each chapter is concise and organized into five sections: Introduction, Material and Methods, Results, Discussion, and Conclusion.

This volume is recommended for updated information for those that utilize laser technology in their practice. It is not intended for the practitioner or reader who typically wants to be informed about which laser to use for a certain procedure or how efficacious is the laser in tonsillectomy and stapedotomy.

DENNIS G. PAPPAS, MD
Birmingham, Alabama

Otologic Surgery

Derald E. Brackmann, Clough Shelton, and Moises A. Arriaga, editors. Hard cover, illustrated, indexed, 828 pages, 1994. WB Saunders, Philadelphia, Pa, $150.

This is a textbook of otologic, neurotologic, and skull base surgery that emphasizes surgical indications, techniques, and postoperative management. Derald Brackmann, the senior editor, sets as his goal the creation of "a ready resource for residents wishing to learn the various techniques as well as a reference for clinicians in practice..." He and his coeditors and authors have succeeded to a remarkable degree. They have produced an outstanding resource volume.

Chapters on specific surgical procedures outline the indications for surgery, any necessary preoperative preparation, significant detail of surgical technique, including necessary instrumentation, and potential postoperative problems and management. Separate chapters are devoted to the complications of more commonly performed procedures such as chronic ear surgery and stapedectomy. Surgical topics range from the basic, such as external canalplasty for exostoses, to the most complex, such as middle fossa surgery, infratemporal fossa surgery, and the auditory brain stem implant. This text is inclusive and covers every imaginable operative circumstance. No subject is overlooked.

A highlight is the detailed presentation of differing surgical approaches to a common problem. The editors have chosen knowledgeable and well-respected proponents of differing views. For example, Sam Kinney argues persuasively for limited temporal bone resection for malignancy. In the subsequent chapter, Prasad and Janecka give their equally erudite justification for radical temporal bone resection. Sheehy supports canal wall up tympanomastoidectomy, Smyth and Toner canal wall down. In sequential chapters, Sheehy makes a case for the outer surface grafting technique of tympanoplasty, M. Coyle Shea the transcanal underlay technique, Glasscock and Strasnick the postauricular approach to the underlay technique, and Wehrs the use of the homograft tympanic membrane. The variations in stapes surgery are given similar treatment with chapters on total stapedectomy, partial stapedectomy, and stapedotomy. In presenting these contrasting views of surgical approach, this text is at its very best. Controversial issues are addressed forthrightly and with remarkable objectivity.

What, then, are the limitations of *Otologic Surgery*? I can find none worthy of note. Brackmann, Shelton, and Arriaga have produced a textbook of rare excellence that, in this reviewer's opinion, is second to none. It is a must for the resident in training, the otology fellow, and any otolaryngologist who performs otologic surgery.

RONALD A. HOFFMAN, MD
New York, New York

NOTE

The following is a corrected version of the article that appeared on pages 93-96 of Supplement 166 from September 1995 (Volume 104, Number 9, Part 2). The text and figure legends are nearly unchanged, but the figures have been replaced. The revised figures failed to reach our production offices in time for publication. These pages have been designed to replace those in the Supplement.

WAVEFORMS OF COCHLEAR IMPLANT–EVOKED AUDITORY BRAIN STEM RESPONSES IN ANESTHETIZED YOUNG CHILDREN, RECORDED WITH A NEW PREAMPLIFIER

C. J. A. GAME, MBBS, PHD; H. SANLI, M ENG, PHD

From the Royal Alexandra Hospital for Children, Sydney, Australia. Supported by the Elizabeth Scott Fellowship in Hearing Research (C.J.A.G.).

An ultra–low-noise preamplifier has been specifically designed for the conditions in lightly anesthetized young children, to record cochlear implant–evoked auditory brain stem responses (impEABRs). The preamplifier linearly filters out the signal from the radio-frequency implant-driver. The preamplifier provides simultaneous accurate records of the stimulus-current artifact and impEABR, both ipsilaterally and contralaterally. It is convenient to label electrically evoked vertex-positive peaks, eg, eII, on probable analogy with acoustically evoked potentials. In order to label all the commonly observed peaks with latency less than 5 milliseconds, it is necessary at times to use labels eIIa, eIIb, eIIIa, eIIIb, eIVa, eIVb, eVa, and eVb. The records also show two distinct nadirs, with latencies about 2.5 milliseconds and about 6 milliseconds. The details of the waveforms are preserved as the stimulus strength descends towards threshold.

INTRODUCTION

In young children, electrical measurements of Melbourne cochlear implant–stimulated electrically evoked auditory brain stem responses (impEABRs)[1,2] call for light general anesthesia and paralysis and an ultra–low-noise, wide–dynamic range, frequency-selective differential preamplifier, with a very high common mode rejection.

The implant is driven by a coil that emits a radio-frequency signal, which has a strong component at 2.5 MHz and a magnitude of about 1 V at the usual surface recording sites for brain stem auditory potentials. For impEABR, it is desirable not to switch or cut this signal out, but instead to accurately and linearly filter it out, because it is superimposed on the useful artifact from the implant stimulus current. This artifact allows one to check that the headset is correctly located, to measure the stimulus current pulse duration, and to measure the voltage produced by the stimulus current. A crite-

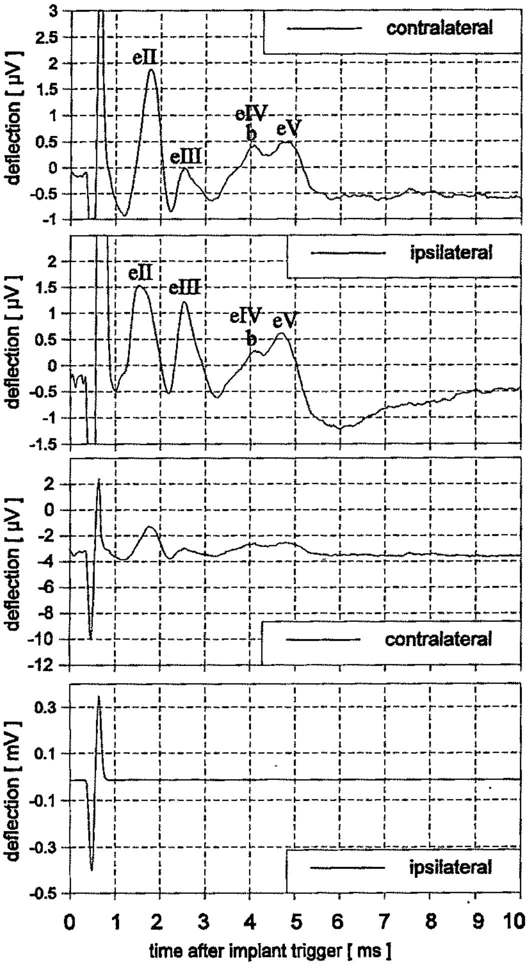

Fig 1. Simultaneous records of ipsilateral and contralateral impEABR and stimulus current artifact. Stimulus mode level 192, pulse duration 206 µs, amplitude 993 µA per phase, channel 22. Low-frequency band edge 100 Hz.

rion of accurate linear filtering is that the stimulus current artifact record is of skew-symmetric shape, like the stimulus waveform.

A third superimposed component of electrical stimulus artifact is neither of utility to the operator, nor susceptible of being selectively filtered out by any preamplifier. This component is usually negligible in the contralateral record, but is quite significantly large in the ipsilateral record. We call it the polarization artifact, because we believe it represents the electric currents which flow between the electrodes through the tissues, outside the nominal stimulus time interval, because of polarization of the electrodes. In the ipsilateral record, the polarization artifact makes it difficult to see the earliest components of the impEABR.

Accordingly, we have designed and built a new preamplifier, following sound principles,[3] but also with a new circuit topology. With colleagues in our team, we have recorded some features of the impEABR that are seen with the new preamplifier.

METHODS

The two recording channels are from the vertex (vertex-positive), with respect to the ipsilateral and contralateral earlobes. Stimuli are from a computer-driven Melbourne cochlear implant, in stimulus mode, with the common ground electrode configuration. In stimulus mode, pulse duration and stimulus current (small variations for individual implants) vary with stimulus level, as tabulated by Cochlear Pty Limited; stimulus timing is visible in records with the new preamplifier. While the implant provides reliable stimulus current control, it is observed that the stimulus voltage, in common ground mode, varies with stimulus repetition, probably because of variable distribution of stimulus current among the various electrodes; the new preamplifier shows these variations. The stimulus repetition rate is 21 Hz. The records are triggered by the speech processor interface to the implant; delay from trigger to start of stimulus varies slightly about 300 microseconds. The high-frequency band edge of the recorded signal is 5 kHz.

As noted in legends to Figs 1-4, the low-frequency band edge is set at various values, and various numbers of sweeps are averaged. The subjects were young children, lightly anes-

Fig 2. Two pairs of simultaneous averages made with a prototype preamplifier, with 256 sweeps per trace, showing difference between ipsilateral and contralateral waves eIIIa and eIIIb. Stimulation was in current mode (level 192), pulse duration 205 µs, amplitude 1,005 µA per phase, channel 20, mode CG. Low-frequency band edge 7 Hz.

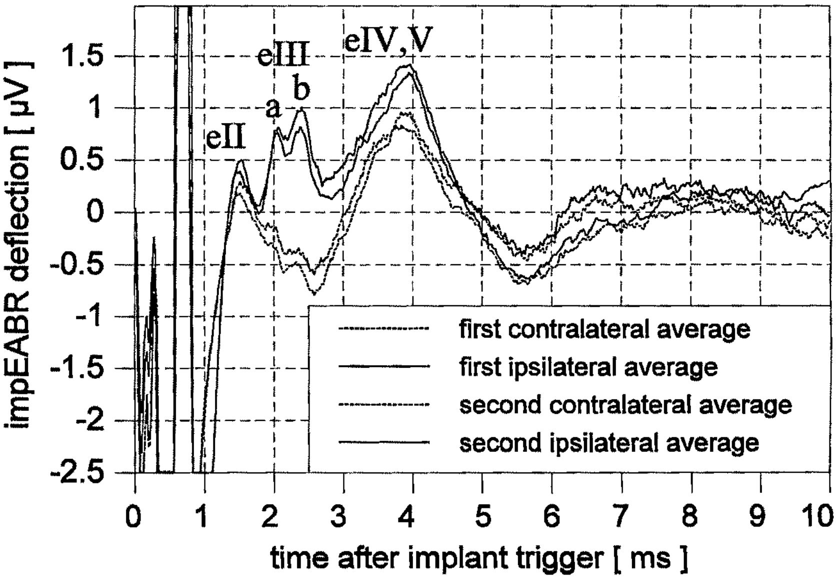

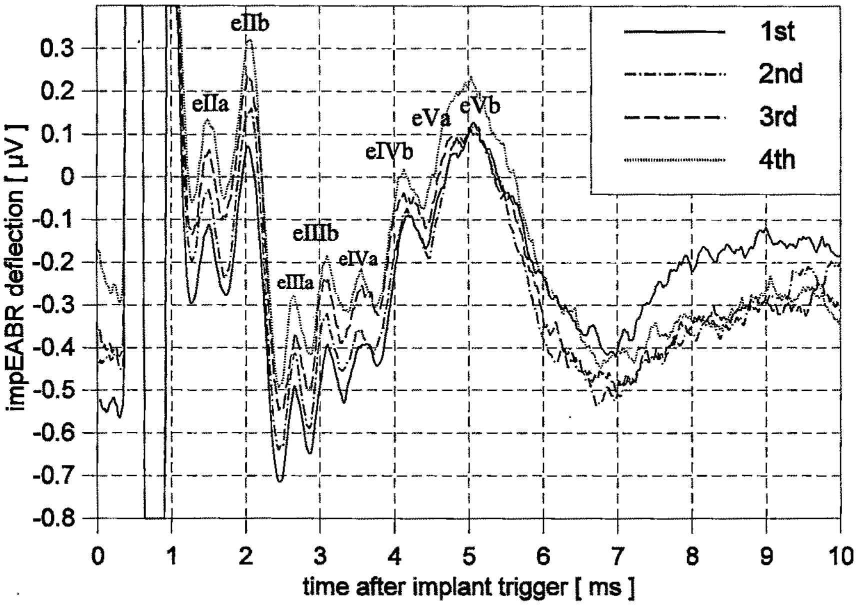

Fig 3. Characteristic basal contralateral impEABR waveforms with stimulation of channel 1. Four successive averages, 512 sweeps per trace. Stimulus mode level 192, pulse duration 206 µs, amplitude 969 µA per phase. Low-frequency band edge 100 Hz.

thetized and paralyzed, tested a few weeks after implantion. Records were made from 81 children with various prototype preamplifiers, and from 28 children with the present preamplifier. The records shown here were made with the new preamplifier, except that Fig 2 was made with a prototype preamplifier.

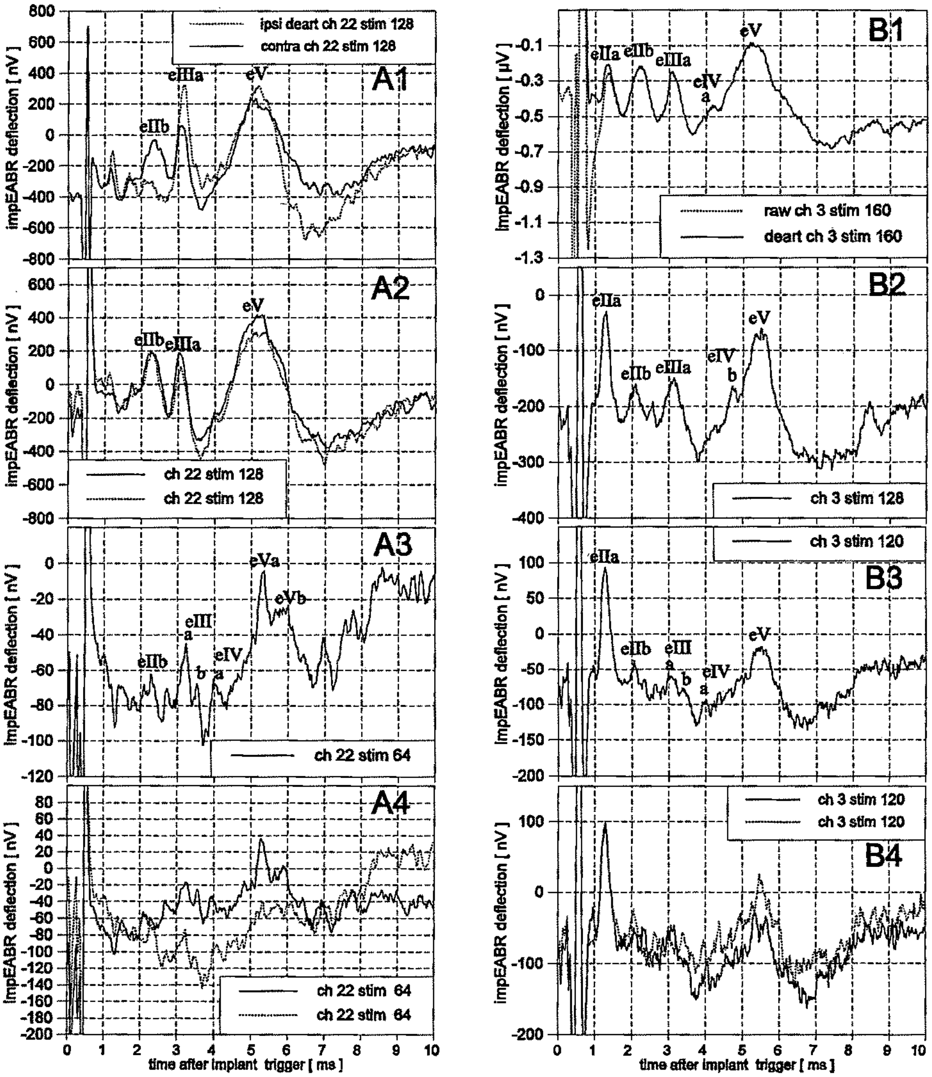

Fig 4. Preservation of waveform detail, but differential decrease of waveform components, as stimulus strength descends. Stimulus: apical (A) channel 22 and basal (B) channel 3; stimulus levels in stimulus mode are marked in Figure. Except in A1, all records are contralateral. A1: identification of eIIb and eIIIa by comparison between simultaneous ipsilateral and contralateral records (256 sweeps per trace). A2: two further contralateral averages (256 sweeps per trace), to show reproducibility. B1: distinct eIIa and eIIb; shown are the raw trace, and its deartifacted version, assuming a single-exponential polarization artifact (512 sweeps). B2: combined average (2,048 sweeps), to show differential decrease of components. A3, B3: combined averages of traces in A4 and B4, showing waveform detail at small stimulus strength. A4, B4: averages of 2,048 sweeps per trace to show reproducibility of waveform detail. Low-frequency band edge 100 Hz, two-coincident-pole analog filter. Critically damped exponential tail effect of this filter has been mathematically removed from A1 ipsilateral record.

RESULTS

From a child 81 months old, Fig 1 shows simultaneously recorded averages of 256 sweeps of ipsilateral and contralateral impEABRs and stimulus artifacts. The impEABR waves are labeled as described below. The different sizes of waves eII and eIII are as described below. The stimulus current artifacts can be seen to be skew-symmetrical.

The impEABR waveforms vary among children, stimulus channels, and stimulus strengths. There is a basic likeness to the waves of the acoustically stimulated auditory brain stem response, and often it is useful to label the waves eII, eIII, eIV, and eV, where the e reminds us that the stimulus is electrical. For the electrically evoked responses, however, one often needs extra labels, here chosen as eIIa, eIIb, eIIIa, eIIIb, eIVa, eIVb, eVa, and eVb. The letters a and b signify apparent components of the roman numeral–labeled peaks. Also (not labeled) in the waveforms, there are at least two distinct nadir components; the first of these is most often between eIII and eIV, sometimes between eIIIa and eIIIb, and sometimes between eII and eIII; the second of these is after eVb. It appears that superposition interference makes components distinctly visible only in some conditions. In many cases not all the a and b labels are needed at once. Each of the apparent wave components has its own growth curve. Wave component latencies depend on age.

Waves eII and eIII are so labeled here because they are like acoustically evoked responses, in that wave eII is less tall ipsilaterally than contralaterally; while wave eIII is taller ipsilaterally than contralaterally. Figure 2 shows distinct waves eIIIa and eIIIb recorded from a child 60 months of age. The taller eIIIa and eIIIb are seen in the ipsilateral record; the size of wave eII is not measurable in this Figure. When it is not distinctly split into eIIIa and eIIIb, wave eIII often has a characteristic flat top lasting 350 microseconds or more.

All of the extra labels are needed at once in some cases, for example, in Fig 3, recorded from a child 33 months of age. This is a characteristic record.

Wave eIIa is more often visible in responses to stimulation of basal (eg, channel 1) than apical (eg, channel 22) channels. Figure 4 shows an example, from a child 23 months of age. Figure 4 shows the preservation of waveform detail, but differential decrease of waveform components, as stimulus strength descends towards threshold. In Fig 4 A1, as in Fig 1, there is a deeper second great nadir in the ipsilateral record. As is to be expected, the apparent latency of the second great nadir is shortened, and the nadir is made to appear more distinct by recording with analog high-pass filters that reject frequencies below 100 Hz.

DISCUSSION

The impEABR varies among children, among recording leads, and among stimuli. The possible differences between impEABR and acoustically evoked auditory brain stem responses (A-ABR) in young children are not yet fully known to us. Subpeaks are often enough distinct in impEABR, and two deep nadirs with latencies about 2.5 milliseconds and about 6.5 milliseconds are nearly always distinct; but subpeaks, and the two deep nadirs, are also seen in the unfiltered A-ABRs of neonates.[4] Wave eVI is less prominent in young children's impEABRs than in their A-ABRs.

ACKNOWLEDGMENTS — The authors acknowledge the large contribution of the members of the Sydney cochlear implant team, headed by Professor W.P.R. Gibson; and the invaluable anesthetic skill of Dr Richard Bailey.

REFERENCES

1. Game CJA, Gibson WPR, Pauka CK. Electrically evoked brainstem auditory potentials. Ann Otol Rhinol Laryngol 1987;92(suppl 128):94-5.

2. Game CJA, Thomson DR, Gibson WPR. Measurement of auditory brainstem responses evoked by electrical stimulation with a cochlear implant. Br J Audiol 1990;24:145-9.

3. Nordholt EH. Design of high-performance negative-feedback amplifiers. Amsterdam, the Netherlands: Elsevier Scientific Publishing, 1983.

4. McPherson DL, Hirasugi Y, Starr A. Auditory brain stem potentials recorded at different scalp locations in neonates and adults. Ann Otol Rhinol Laryngol 1985;94:236-43.

VOLUME 106 (12) — DECEMBER 1997

– Founded in 1892 –

ANNALS
OF OTOLOGY, RHINOLOGY & LARYNGOLOGY

Official Organ of the
AMERICAN LARYNGOLOGICAL ASSOCIATION
AMERICAN BRONCHO-ESOPHAGOLOGICAL ASSOCIATION

TELESCOPIC LARYNGEAL AND PHARYNGEAL SURGERY

LARYNGOTRACHEOESOPHAGEAL CLEFTS

COMPARISON OF CO_2 AND ND:YAG LASERS IN SURGERY OF THE INFERIOR TURBINATE

ENLARGEMENT OF THE VESTIBULAR AQUEDUCT

REDUCTION OF INNER EAR INFLAMMATION BY TREATMENT WITH ANTI–ICAM-1 ANTIBODY

ANNALS
PUBLISHING CO.
ST. LOUIS

LEVAQUIN

Overpowers

key gram-positive, gram-negative, and atypical pathogens

Proven Effective in Mild-to-Severe Community-Acquired Pneumonia, Acute Maxillary Sinusitis, and Acute Bacterial Exacerbations of Chronic Bronchitis*

In an In Vitro Study, 100% of *Streptococcus pneumoniae* Isolates Were Susceptible to LEVAQUIN

	% Susceptible
S pneumoniae (n=209)	**100%**

- The first once-a-day anti-infective indicated for all three common atypical pathogens *Mycoplasma pneumoniae, Chlamydia pneumoniae,* and *Legionella pneumophila* in community-acquired pneumonia
- 96% eradication rate of gram-negative and gram-positive pathogens in patients with mild-to-severe community-acquired pneumonia

The safety and efficacy of levofloxacin in children, adolescents (under 18), pregnant women, and nursing mothers have not been established. Levofloxacin is contraindicated in persons with a history of hypersensitivity to levofloxacin, quinolone antimicrobial agents, or any other components of this product. Serious and occasionally fatal hypersensitivity and/or anaphylactic reactions have been reported in patients receiving therapy with quinolones. These reactions often occur following the first dose. The drug should be discontinued at the first appearance of a skin rash or any other sign of hypersensitivity.

Antacids containing magnesium or aluminum, as well as sucralfate, metal cations such as iron, and multivitamin preparations with zinc should be taken at least 2 hours before or 2 hours after levofloxacin administration.

For information on Warnings, Precautions, and additional Adverse Reactions that may occur, regardless of drug relationship, please see full Prescribing Information.

Please see brief summary of Prescribing Information at the end of this advertisement.

ANNALS OF OTOLOGY, RHINOLOGY & LARYNGOLOGY

— Founded in 1892 —

Editor

BRIAN F. McCABE, MD
Iowa City, Iowa

Associate Editors

CHARLES D. BLUESTONE, MD
Pittsburgh, Pa

GEORGE A. GATES, MD
Seattle, Wash

LAWRENCE W. DeSANTO, MD
Scottsdale, Ariz

LEE A. HARKER, MD
Omaha, Neb

Board of Editors

JOHN G. BATSAKIS, MD	Traverse City, Mich
POUL BRETLAU, MD, DMSc	Copenhagen, Denmark
RICHARD A. BUCKINGHAM, MD	Park Ridge, Ill
JACK D. CLEMIS, MD	Chicago, Ill
CHARLES W. CUMMINGS, MD	Baltimore, Md
PATRICK J. DOYLE, MD	Vancouver, Canada
ALFIO FERLITO, MD	Padua, Italy
UGO FISCH, MD	Zurich, Switzerland
BRUCE GANTZ, MD	Iowa City, Iowa
JEFFREY P. HARRIS, MD, PhD	San Diego, Calif
GERALD B. HEALY, MD	Boston, Mass
WILLIAM F. HOUSE, MD	Los Angeles, Calif
STEVEN K. JUHN, MD	Minneapolis, Minn
TIMOTHY T. K. JUNG, MD, PhD	Loma Linda, Calif
JEROME O. KLEIN, MD	Boston, Mass
FRANK E. LUCENTE, MD	New York, NY
JOSEF MILLER, PhD	Ann Arbor, Mich
WILLIAM W. MONTGOMERY, MD	Boston, Mass
EUGENE N. MYERS, MD	Pittsburgh, Pa
YASUYA NOMURA, MD	Tokyo, Japan
LORNE S. PARNES, MD	London, Canada
FRANK N. RITTER, MD	Ann Arbor, Mich
ROBERT J. RUBEN, MD	Bronx, NY
JAI H. RYU, PhD	Winston-Salem, NC
JACOB SADÉ, MD	Tel Aviv, Israel
ISAMU SANDO, MD	Pittsburgh, Pa
CLARENCE T. SASAKI, MD	New Haven, Conn
RICHARD J. H. SMITH, MD	Iowa City, Iowa
JAN E. VELDMAN, MD, PhD	Utrecht, The Netherlands
T. J. YOO, MD	Memphis, Tenn

Software Review and Computer Applications Editor

KEVIN T. KAVANAGH, MS, MD	Somerset, Ky

Imaging Editor

YUTAKA SATO, MD	Iowa City, Iowa

Book Review Editor

DENNIS G. PAPPAS, MD	Birmingham, Ala

Emeritus Board Members

WESLEY H. BRADLEY, MD	Albany, NY
D. THANE CODY, MD	Jacksonville, Fla
SEYMOUR COHEN, MD	Los Angeles, Calif
ARNDT J. DUVALL III, MD	Minneapolis, Minn
JOHN M. FREDRICKSON, MD	St Louis, Mo
RICHARD R. GACEK, MD	Syracuse, NY
JEROME C. GOLDSTEIN, MD	Alexandria, Va
SIR DONALD F. N. HARRISON, MD PhD	London, England
SAM E. KINNEY, MD	Cleveland, Ohio
JOHN A. KIRCHNER, MD	New Haven, Conn
DAVID J. LIM, MD	Los Angeles, Calif
FRED H. LINTHICUM, Jr, MD	Los Angeles, Calif
MICHEL PORTMANN, MD	Bordeaux, France
LORING W. PRATT, MD	Waterville, Me
GUNNER O. PROUD, MD	Kansas City, Kan
WILLIAM H. SAUNDERS, MD	Columbus, Ohio
F. BLAIR SIMMONS, MD	Palo Alto, Calif
RUEDIGER THALMANN, MD	St Louis, Mo
HARVEY M. TUCKER, MD	Cleveland, Ohio
PAUL H. WARD, MD	Los Angeles, Calif

ANNALS OF OTOLOGY, RHINOLOGY & LARYNGOLOGY

— Founded in 1892 —

ANNALS
PUBLISHING CO.
ST LOUIS

EDITOR'S OFFICE

Brian F. McCabe, MD
Department of Otolaryngology –
Head & Neck Surgery
University Hospitals & Clinics
Iowa City, IA 52242
(319) 356-2310

BUSINESS OFFICE

Annals Publishing Company
4507 Laclede Avenue
St Louis, MO 63108
(314) 367-4987
Fax (314) 367-4988

STAFF

Managing Editor
Michol L. Sheridan

Business Manager
Kenneth A. Cooper, Jr

Chief Copyeditor
Edna Hayes Harrison

Copyeditor
Kirsten K. Novak

Circulation Manager
Michelle M. Steuerwald

Editorial Assistant
Brian H. Aldredge

ADVERTISING REPRESENTATIVES

— East & Midwest —
Cunningham Associates
180 Old Tappan Rd
Old Tappan, NJ 07675
(201) 767-4170
Fax (201) 767-8065

— West —
Charles B. Healy
PO Box 5213
Palm Springs, CA 92263
(619) 320-0118
Fax (619) 325-5473

EDITORIAL CONTENT

The *ANNALS* publishes original manuscripts of clinical and research importance in otolaryngology – head and neck medicine and surgery, bronchoesophagology, head and neck oncology and surgery, plastic and reconstructive surgery, pediatric otolaryngology, audiology, speech pathology, and related specialties. In-depth studies (supplements), papers of historical interest, computer software reviews and applications in otolaryngology are also published, as well as imaging, pathology, and clinicopathology studies, book reviews, and letters to the editor. All papers and supplements are peer-reviewed. The *ANNALS* is the official journal of the American Laryngological Association and the American Broncho-Esophagological Association.

SUBSCRIPTIONS

1997 Annual Subscription Rates	*USA*	*International Surface Mail (All Regions)*
Institution*	$174.00	$198.00
Individual†	119.00	143.00
Resident/Student†	68.00	85.00

*Institutional (multiple-reader) subscription rates apply to public and private libraries, hospitals, and clinics; city, county, state, provincial, and national government bureaus and departments; and commercial and private institutions and organizations.

†Individual, resident, and student subscriptions must be in the individual's name and must be billed to and paid for by the individual.

Airmail rates are available upon request.

CLAIMS

Claims for missing issues must be received within 60 days of the month of publication for the United States and Canada, and 180 days for other countries. Single copy prices will be charged on missing issues claimed after that date.

BACK ISSUES

A comprehensive inventory of back issues and supplements is available. Prices are furnished on request.

CHANGE OF ADDRESS

Address changes must be received 45 days prior to the effective date so that the subscription will be received without interruption.

MICROFILM

The *ANNALS* is available in microform from University Microfilms International, 300 North Zeeb Road, Ann Arbor, MI 48106.

ANNALS OF OTOLOGY, RHINOLOGY & LARYNGOLOGY (ISSN 0003-4894) is published monthly by Annals Publishing Company, 4507 Laclede Avenue, St Louis, MO 63108. Periodicals postage paid at St Louis, Mo. POSTMASTER: Send address changes to *ANNALS OF OTOLOGY, RHINOLOGY & LARYNGOLOGY*, c/o Annals Publishing Company, 4507 Laclede Avenue, St Louis, MO 63108.

Printed on acid-free paper

COPYRIGHT© 1997, ANNALS PUBLISHING COMPANY

ANNALS OF OTOLOGY, RHINOLOGY & LARYNGOLOGY

VOLUME 106 **DECEMBER 1997** **NUMBER 12**

CONTENTS

FROM THE AMERICAN BRONCHO-ESOPHAGOLOGICAL ASSOCIATION

Endoscopic Laryngotracheoplasty and Graft Soldering With the Carbon Dioxide Laser. An Animal Study
Zhi Wang, MD; Mark S. Volk, MD, DMD; Stanley M. Shapshay, MD 989

Telescopic Laryngeal and Pharyngeal Surgery
William J. Richtsmeier, MD, PhD; Richard L. Scher, MD 995

Laryngotracheoesophageal Clefts
Greetha Moungthong, MD; Lauren D. Holinger, MD 1002

FROM THE AMERICAN LARYNGOLOGICAL ASSOCIATION

Efficacy of Repeated Botulinum Toxin Injections as a Function of Timing
Katsuhide Inagi, MD; Charles N. Ford, MD; Arthur A. Rodriquez, MD;
Edward Schultz, PhD; Diane M. Bless, PhD; Dennis M. Heisey, PhD 1012

Utility of Helical Computed Tomography in the Study of Arytenoid Dislocation and Arytenoid Subluxation
Albert E. Alexander, Jr, MD; George D. Lyons, MD; Mary A. Fazekas-May, MD;
Peter L. Rigby, MD; Daniel W. Nuss, MD; Lisa David, MD; Kevin Williams 1020

Basaloid Squamous Cell Carcinoma of the Larynx and Hypopharynx
Alfio Ferlito, MD; Giuseppe Altavilla, MD;
Alessandra Rinaldo, MD; Claudio Doglioni, MD 1024

INDEPENDENT CONTRIBUTIONS

Comparison of Carbon Dioxide and Neodymium:Yttrium-Aluminum-Garnet Lasers in Surgery of the Inferior Turbinate
Burkard M. Lippert, MD; Jochen A. Werner, MD 1036

Algorithm Analysis of Lectin Glycohistochemistry and Feulgen Cytometry for a New Classification of Nasal Polyposis
Sergio Hassid, MD; Christine Decaestecker, PhD; Christine Hermans, MD;
Isabelle Salmon, MD; Jean Lambert Pasteels, MD; André Danguy, PhD; Robert Kiss, PhD 1043

Statistical Evaluation of Hearing Screening by Distortion Product Otoacoustic Emissions
Pierre Bonfils, MD, PhD; Paul Avan, MD, PhD; Paul Landais, MD;
Manuel Erminy, MD; Bernard Biacabe, MD 1052

Three Familial Cases of Hearing Loss Associated With Enlargement of the Vestibular Aqueduct
Satoko Abe, MD; Shin-Ichi Usami, MD; Hideichi Shinkawa, MD 1063

Reduction of Inner Ear Inflammation by Treatment With Anti–ICAM-1 Antibody
Tsuyoshi Takasu, MD, PhD; Jeffrey P. Harris, MD, PhD 1070

Changes in Myosin Expression in Denervated Laryngeal Muscle
John M. DelGaudio, MD; James J. Sciote, DDS, PhD 1076

Transection and Occlusion of Lateral Semicircular Canal in Guinea Pigs
Boo Hyun Nam, MD; Seong Ki Yoon, MD; Chan Il Park, MD 1082

Auditory Evoked Responses Under Total Spinal Anesthesia in Rats
Katsushi Yamada, MD; Kimitaka Kaga, MD; Hideaki Sakata, MD;
Akira Uno, PhD; Toshihiro Tsuzuku, MD 1087

IMAGING CASE STUDIES OF THE MONTH

Iatrogenic Pseudoaneurysm of the Internal Carotid Artery
Karen S. Caldemeyer, MD; Paul D. Righi, MD; Vincent P. Mathews, MD 1093

Imaging Diagnosis of Buckled Innominate Artery
Toshishige Kido, MD; Masahiro Takahashi, MD 1097

Ethmoid and Sphenoid Mucoceles Viewed by Helical Scanning Computed Tomography With Sagittal Reconstruction
Takeo Fuse, MD; Hiroo Inamura, MD; Masaru Aoyagi, MD;
Morio Nagahata, MD; Takaaki Hosoya, MD 1100

ANNUAL INDEX

Authors 1104

Subjects 1107

MISCELLANEOUS

Information for Subscribers 4a

Index to Advertisers 16a

Ann Otol Rhinol Laryngol 106:1997

ENDOSCOPIC LARYNGOTRACHEOPLASTY AND GRAFT SOLDERING WITH THE CARBON DIOXIDE LASER

AN ANIMAL STUDY

ZHI WANG, MD

MARK S. VOLK, MD, DMD STANLEY M. SHAPSHAY, MD

BOSTON, MASSACHUSETTS

Laryngotracheoplasty (LTP) has had considerable success for treatment of selected cases of subglottic stenosis in children. However, certain complications have been associated with an open approach. Our study explores the possibility of decreasing these complications by means of a minimally traumatic endoscopic laser cricoid split and graft transplantation technique. In an in vivo study of six dogs, LTP was performed with a carbon dioxide laser. The gap between the divided cricoid cartilage was either left with no coverage or filled by autogenous mucosa or cartilage grafts through a laser-assisted soldering technique. Compared to LTP without coverage, autogenous grafts, with either mucosa or cartilage, resulted in improved healing. The cartilage graft seems to offer the best result for expansion of the subglottic space. The results show that the new intraluminal approach, a combination of an endoscopic cartilage split and graft transplantation, may be an alternative to standard LTP. The advantage of this technique is that it is less traumatic than the open procedure, with the potential for less morbidity.

KEY WORDS — anterior cricoid split, carbon dioxide laser, endoscopic approach, graft soldering, laryngotracheoplasty, subglottic stenosis.

INTRODUCTION

The anterior cricoid split (ACS) operation has been a successful treatment in infants who have good pulmonary function but have failed extubation. With increased experience, a number of reports have highlighted the expanded indications for the ACS to include both older children, without a definable upper age limit, and also those with fibrous subglottic stenosis in whom relief of upper airway obstruction is expected from widening the subglottic space.[1,2] The technique of the ACS involves division of the lower portion of the thyroid cartilage as well as the cricoid and first two tracheal rings through an open approach. The patient is then left intubated for 10 to 14 days to allow the endotracheal tube (ETT) to act as a stent. Some of the complications that have been encountered with the ACS have been avoided by performing a one-stage laryngotracheoplasty (LTP). This procedure involves the placement of a cartilage interposition graft to close the defect made by the ACS incision. However, this procedure still requires an open operative technique with an ETT as a postoperative stent. This indwelling ETT often necessitates a longer hospitalization and increases the potential for complications, such as subcutaneous emphysema, neck wound infection, and scarring.[3] Our study explored the possibility of minimizing morbidity by using an endoscopic laser approach to both perform the "split" incision and place and solder autologous graft material in place.

MATERIALS AND METHODS

Six beagle dogs weighing 11 to 13 kg were used for the in vivo study in accordance with institutional guidelines for the care and use of animals. One half hour prior to surgery, each animal was given an intramuscular dose of antibiotics (acepromazine maleate, 0.5 mg/kg). After the intravenous administration of a general anesthetic (pentobarbital sodium, 15 to 20 mg/kg), the dogs were allowed to breathe spontaneously, and exposure was obtained with a suspension microlaryngoscope (Dedo-Jako laryngoscope, Pilling Co, Philadelphia, Pa) that was modified in our laboratory for better visualization of the subglottic space. Through an operating microscope (OPMI 1, Carl Zeiss, Thornwood, NY) with a 400-mm objective lens, a carbon dioxide (CO_2) laser with a micromanipulator (Unilase, IL Med, Walpole,

---

From the Otolaryngology Research Center for Advanced Endoscopic Applications, Department of Otolaryngology–Head and Neck Surgery, New England Medical Center and Tufts University School of Medicine, Boston, Massachusetts. This study was performed in accordance with the PHS Policy on Humane Care and Use of Laboratory Animals, the NIH *Guide for the Care and Use of Laboratory Animals*, and the Animal Welfare Act (7 U.S.C. et seq.); the animal use protocol was approved by the Institutional Animal Care and Use Committee (IACUC) of the New England Medical Center.

Presented at the meeting of the American Broncho-Esophagological Association, Orlando, Florida, May 6-7, 1996.

CORRESPONDENCE — Stanley M. Shapshay, MD, Dept of Otolaryngology–Head and Neck Surgery, New England Medical Center #185, 750 Washington St, Boston, MA 02111.

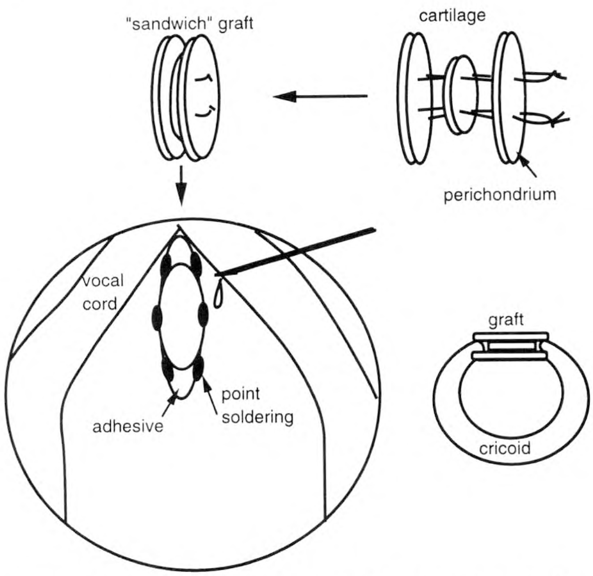

Fig 1. Schematic drawing of "sandwich" cartilage graft.

Mass) delivering a spot size of 0.3 mm at 1.5 to 2.5 W in continuous mode was used to produce a vertical midline incision. This incision was made endoscopically through the lower third of the thyroid cartilage, the cricoid cartilage, and the first and second tracheal rings. At the completion of the laser incision, the wound was checked endoscopically to ensure that all of the involved cartilages had been incised completely. The six animals were then divided into three groups for operative management of the endoscopic incision.

Control Group. The control animals received no graft after the ACS.

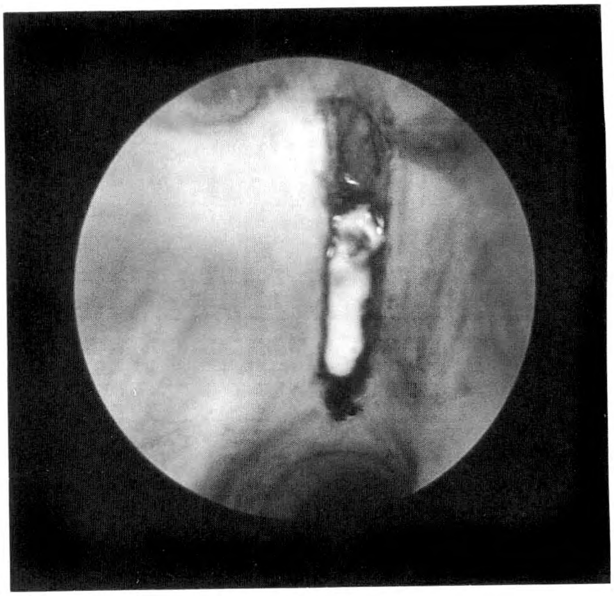

Fig 3. Mucosal graft placed in cricoid gap.

Cartilage Graft Group. In this group, the auricular cartilage was harvested through a preauricular incision while preserving perichondrium on one side of the graft. From this, three pieces of cartilage of appropriate size and shape were sutured together with a 4-0 Prolene suture to form a three-layered structure resembling a sandwich. The sandwich graft was transplanted into the ACS wound, which was filled with 25% human albumin (Public Health Biologic Laboratory, Boston, Mass). A CO_2 laser at 0.5 W of power (7.1 W/mm^2), at continuous exposure for 3 to 4 seconds, was then used with a 0.3-mm spot size to endoscopically solder the graft into place. Every effort was made not to irradiate the wound or graft directly. The end point for the laser soldering was blanching of the albumin (Figs 1 and 2).

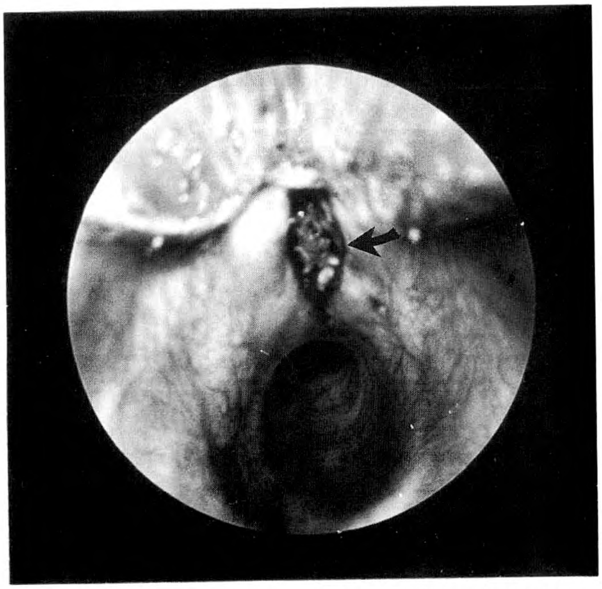

Fig 2. Cartilage graft (arrow) embedded in cricoid gap, which was filled with solder.

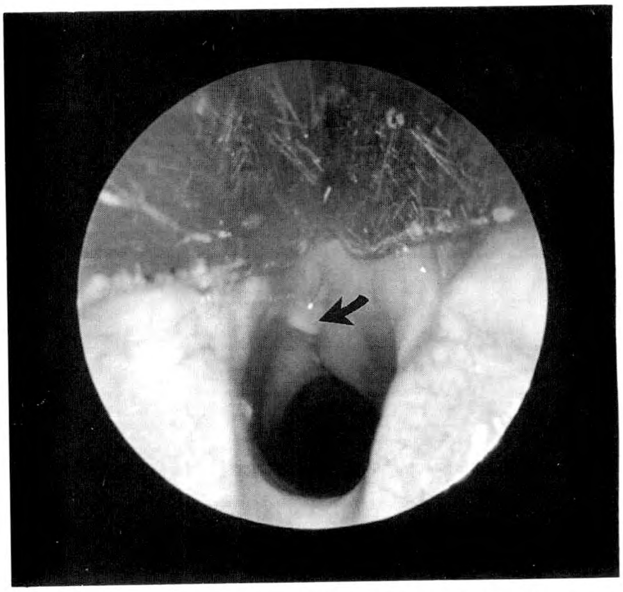

Fig 4. Wound shrinkage with some granulation tissue (arrow) in control animals at 6 weeks.

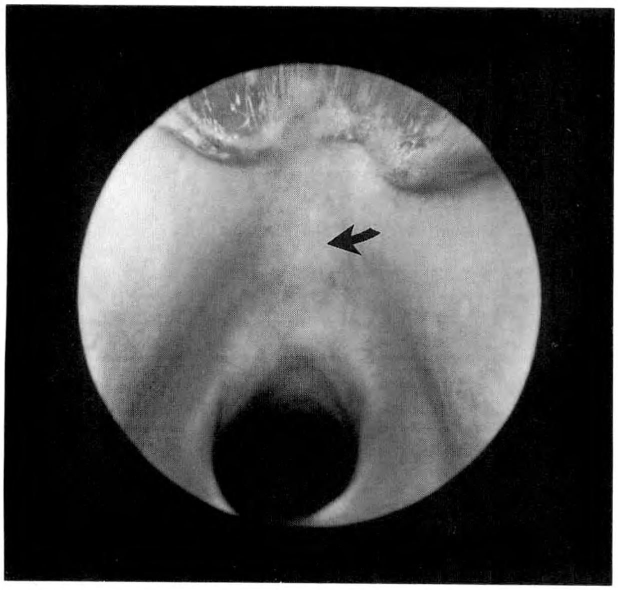

Fig 5. Smooth surface (arrow) on mucosal graft wound at 6 weeks.

Mucosal Graft Group. In this group, a piece of full-thickness buccolabial mucosa was obtained with a surgical blade. This material was then transplanted and soldered into place in the ACS wound by a technique similar to the one outlined above (Fig 3).

After the operative procedure, the animals were awakened and given routine postoperative wound care. In the sixth postoperative week, the animals underwent an endoscopic examination of their subglottic wounds and then were painlessly sacrificed. The larynges were processed for routine light microscopy. The histologic findings and the dimensions of the subglottic spaces were compared.

RESULTS

All animals recovered with near-normal intake of food and water on the first postoperative morning. Five of the animals went on to recover uneventfully until sacrifice during the sixth postoperative week. One of the control animals developed subcutaneous emphysema 15 hours after the surgery. This was treated by making a small incision in the neck. The emphysema resolved, with return to normal appearance in 3 days.

During the endoscopic examination at 6 weeks, the intraluminal wounds showed good healing in all of the animals. Granulation tissue with possible local wound contraction was seen in the two control animals (Fig 4). The subglottic area in the cartilage and mucosal graft groups had smooth mucosal coverage (Figs 5 and 6). However, the lumen in the cartilage graft group appeared larger than the lumen in the mucosal graft group. Histopathologic examination of the horizontal sections showed scar tissue formation between the ends of the native cricoid cartilage in the control and mucosal graft groups and viable-appearing cartilage grafts in the cartilage graft group (Fig 7). There was increased distraction of the cricoid ends in the cartilage graft group (2.0 to 2.5 mm) versus the mucosal graft and control groups (0.5 to 0.75 mm). These differences were not statistically significant because of the small number of animals involved.

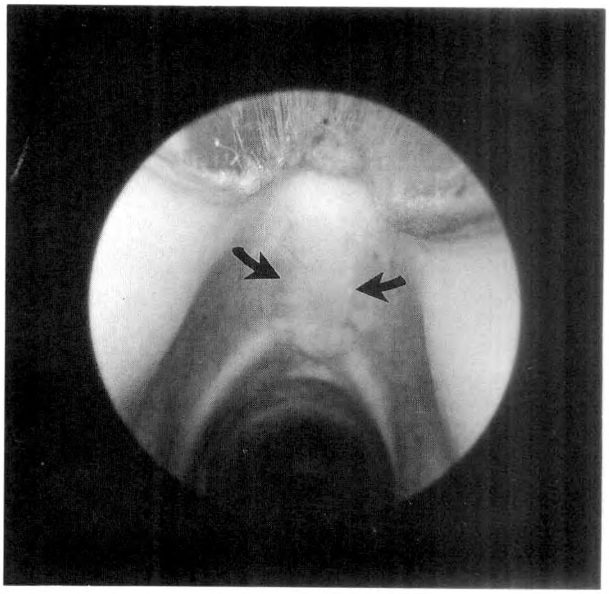

Fig 6. Wider gap (arrows) of cricoid cartilage seen in cartilage graft animal at 6 weeks.

DISCUSSION

Surgical treatment of laryngotracheal stenosis has conceptually advanced along at least two different paths. One type of technique in use has been endoscopic laser incision with mucosal preservation. Endoscopic laser lysis of stenosis with dilation has offered some advantages over open procedures. It is relatively noninvasive, requires minimal recovery time, and can be performed in an outpatient setting. This technique has been useful in adults. However, it has failed to reliably correct subglottic stenosis in the pediatric population.

The other type of technique has utilized open procedures to expand the framework of the subglottis (cricoid cartilage) without scar excision. These techniques have involved three goals. The first is to expand the airway. The second is to fix the airway in the expanded position. The last goal is to isolate the airway from the outside environment.

The ACS was developed as an alternative to tracheotomy in young children who fail extubation.[4,5] The procedure itself is easily performed. It involves

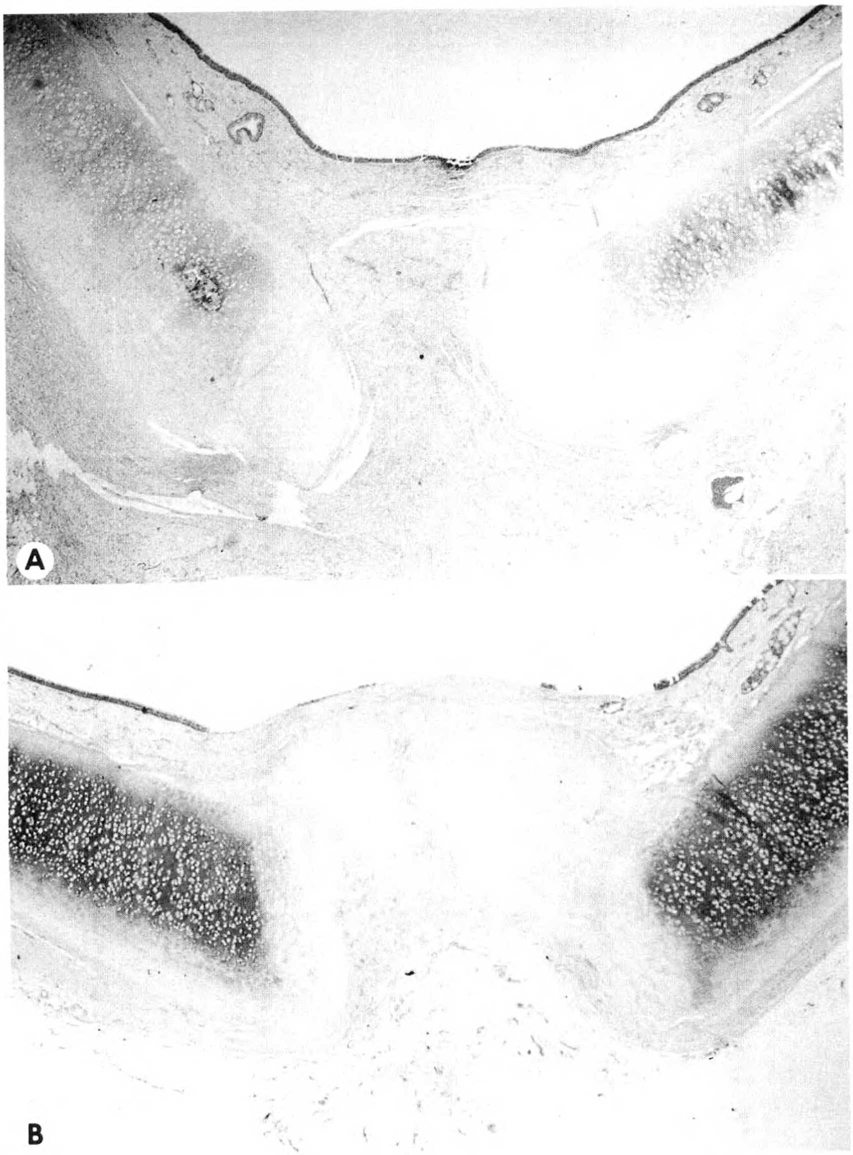

Fig 7. Histopathologic examination of both grafting groups at 6 weeks. A) Nearly closed cricoid gap in mucosal graft group. B) Wider space between cut ends of cricoid in cartilage graft group.

opening the anterior subglottic airway and placing an appropriate-sized ETT as a stent. The ETT is kept in place for 7 to 14 days postoperatively while the anterior airway wound fills in with soft tissue. Several mechanisms have been proposed to explain the success of the ACS procedure. Possible reasons include lysis of occult subglottic cysts or relief of subglottic edema due to the expanded cricoid cartilage.[6-8] Intuitively, it would seem that the most successful ACS operations would be those that bring about the greatest degree of stable expansion of the subglottic airway. However, postmortem histologic examination of the larynx in patients who died after an ACS showed no significant separation at the site of the cricoid split.[2] Additionally, a high level of postoperative intensive care is required to prevent a myriad of potential postoperative complications. These complications have included plugging and malposition of the ETT, and accidental extubation. Most of these complications are secondary to the need for postoperative stenting of the open airway with an indwelling ETT, with the concomitant requirement for mechanical ventilation.[9] While the ACS is able to fulfill the initial goal of expanding the subglottic space, it relies on healing by secondary intention for stabilization and sealing of the expanded airway.

Newer techniques have been developed to improve the success rate and decrease the complication rate of the ACS. The most notable has been one-stage LTP utilizing either rib or auricular cartilage. In this technique, expansion of the airway by an anterior incision is made in the same fashion as with the ACS. However, instead of obtaining the goals of fixation and sealing of the airway by secondary intention, these are acquired more reliably by suturing an autologous cartilage graft into the open subglottic wound. This has resulted in earlier closure of the airway and a higher success rate.[10,11] However, ETT stenting (and ventilatory support) for 4 to 10 days is still often required.

In an attempt to further decrease postoperative ETT stenting with these techniques, endoscopic laser LTP and graft soldering was developed. This technique utilizes new means of achieving the three goals of LTP.

The first goal of expanding the airway is accomplished by making the anterior airway incision via an endoscopic CO2 laser technique. This can be performed with low laser power settings, thereby causing minimal damage to surrounding structures. Without an open neck incision, there is minimal disturbance of tissue planes and blood supply.

The second goal, fixation of the airway in the expanded position, is achieved by endoscopically placing a three-layer "sandwich" of auricular cartilage into the anterior airway incision. In this study, the auricular cartilage was chosen mainly for its accessibility and low morbidity. This multilayered cartilage has the advantage of having increased rigidity compared to a single layer of cartilage. It is also fashioned in such a way that it forms flanges that allow the cricoid and tracheal cartilages to fit into it in a fixed manner. This configuration allows for the graft to be placed endoscopically in a secure fashion that will resist dislodgement. One may infer from this initial study that placement of the cartilage sandwich graft does improve the dimensions of the airway compared to the placement of a mucosal graft or no graft at all.

The third and final goal of LTP is accomplished by using 25% human albumin and the CO2 laser to solder the cartilage graft into place. Because of the configuration of the cricoid and tracheal cartilages inserted into the graft, it is more than likely that the soldering technique produces an airtight seal rather than providing much actual increased stabilization of the graft itself.

As mentioned above, endoscopic LTP may provide a number of advantages over open LTP. These include the potential for decreased tissue trauma, less disruption of blood supply to the area around the operative site, and less need for prolonged postoperative intubation, all of which may result in an overall decrease in morbidity and an improvement in the success rate.

Despite these possible benefits, there are a number of potential problems with the technique that need to be explored. First, the canine model was utilized in this study in order to develop the endoscopic LTP technique in a relatively large airway, which approaches the dimensions of an adult human airway. Thus, it is technically feasible that this procedure could be done on adults. Whether the endoscopic technique can be performed in a pediatric population remains to be seen. Additional studies using a smaller animal model such as rabbits will be necessary to determine if this technique will be of benefit in young children. Second, while auricular cartilage has the advantage of being harvested much more readily and with less morbidity than rib cartilage, it may not be obtained in a large enough quantity in humans to construct the "sandwich." If this is the case, using rib cartilage and fashioning it so that it has the appropriate-shaped flange may be the solution. Third, unlike in similar previous studies, the change in the postoperative airway was measured microscopically by the amount of distraction of the cartilage edges 6 weeks after the procedures. It was felt that this was the best means of directly comparing the results of the various procedures in a small study population. The expense of operating and housing dogs for 6 weeks necessitated using a smaller than optimal number of animals in this pilot study. This study's significance is limited by this small number of animal subjects. Determining the feasibility of using endoscopic LTP in adults and children will require additional studies utilizing a larger number of an animal model with a smaller airway.

REFERENCES

1. Cotton RT, Myer CM, Bratcher GO, Fitton CM. Anterior cricoid split, 1977-1987. Evolution of a technique. Arch Otolaryngol Head Neck Surg 1988;114:1300-2.

2. Berkowitz RG, Zalzal GH, Chandra R. Expansion of the infant subglottis by external cricoid distraction: an animal model. Otolaryngol Head Neck Surg 1990;103:710-2.

3. Seid AB, Pransky SM, Kearns DB. One-stage laryngotracheoplasty. Arch Otolaryngol Head Neck Surg 1991;117: 408-10.

4. Cotton R. Management of subglottic stenosis in infancy and childhood. Review of a consecutive series of cases managed by surgical reconstruction. Ann Otol Rhinol Laryngol 1978;87:649-57.

5. Evans JNG, Todd GB. Laryngotracheoplasty. J Laryngol Otol 1974;88:589-97.

6. Palasti S, Respler DS, Fieldman RJ, Levitt J. Anterior cricoid split for subglottic stenosis: experience at the Children's Hospital of New Jersey. Laryngoscope 1992;102:997-1000.

7. Holinger LD, Stankiewicz JA, Livingston GL. Anterior cricoid split: the Chicago experience with an alternative to tracheotomy. Laryngoscope 1987;97:19-24.

8. Senders CW, Tinling SP. The intrinsic response of the cricoid cartilage to vertical division. Int J Pediatr Otorhinolaryngol 1993;28:33-9.

9. Grundfast KM, Coffman AC, Milmoe G. Anterior cri-

coid split: a "simple" surgical procedure and a potentially complicated care problem. Ann Otol Rhinol Laryngol 1985;94: 445-9.

10. Richardson MA, Inglis AF Jr. A comparison of anterior cricoid split with and without costal cartilage graft for acquired subglottic stenosis. Int J Pediatr Otorhinolaryngol 1991;22: 187-9.

11. Lusk RP, Kang DR, Muntz HR. Auricular cartilage grafts in laryngotracheal reconstruction. Ann Otol Rhinol Laryngol 1993;102:247-54.

≈

ADVANCES IN OTOLARYNGOLOGY–HEAD AND NECK SURGERY

The Fifth Annual Seminar Advances in Otolaryngology–Head and Neck Surgery will be held in Barton Creek (Austin), Texas, March 4-8, 1998. For information, contact Conference Coordinator, Virginia Merrill Bloedel Hearing Research Center, University of Washington, Box 357923, Seattle, WA 98195-7923; telephone (206) 685-2962; fax (206) 616-1828; e-mail: sullivan@u.washington.edu.

Ann Otol Rhinol Laryngol 106:1997

TELESCOPIC LARYNGEAL AND PHARYNGEAL SURGERY

WILLIAM J. RICHTSMEIER, MD, PHD RICHARD L. SCHER, MD

DURHAM, NORTH CAROLINA

Surgery of the hypopharynx and larynx has traditionally been performed with either direct, unaided vision or the operating microscope. We proposed to extend the surgical capability provided by angled Hopkins telescopes to the larynx and hypopharynx. Forty-eight cases in which rigid telescopes were employed primarily for intervention were reviewed. We found significant advantages of the telescopic system when performing procedures on surfaces that were not 90° from the observer, such as the walls of the hypopharynx, the petiole of the epiglottis, the ventricle, and the posterior commissure. Both 30° and 70° telescopes were found useful, but required complementary instruments. The potassium titanyl phosphate laser's flexible fiber provided a distinct advantage in resecting lesions that presented on vertical surfaces. Telescopes also permitted the use of large instruments designed for intraperitoneal and intrathoracic surgery that blocked the view of the operating microscope. Telescopic pharyngeal and laryngeal visualization allowed surgical procedures complementary to more traditional forms of endoscopic surgery.

KEY WORDS — Hopkins telescope, laryngoscopy, potassium titanyl phosphate laser, squamous cell carcinoma of larynx, Zenker's diverticulum.

INTRODUCTION

Telescopic laryngoscopy has been used to diagnose and document a wide variety of disorders and conditions.[1,2] Microscopic surgery of the hypopharynx and larynx had its infancy following the invention of suspension laryngoscopy. This was further refined by the introduction of the operating microscope, which provided magnification, enhanced illumination, and a hands-free environment for surgical intervention, and has led to such surgical advances in laryngeal surgery as the development of the microflap technique.[3] Our familiarity with endoscopic sinus surgery, particularly with surgery in the frontal sinus recess and maxillary sinus using angled telescopes, encouraged us to investigate telescopic laryngeal and pharyngeal surgery to determine in what circumstances this approach augments treatment of laryngopharyngeal disease. This technique, when applied to the larynx and pharynx, utilizes the advantages of angled telescopes, providing a perspective in many cases that cannot be achieved with the operating microscope.

METHODS

We retrospectively reviewed the records and photographic imaging data of patients having laryngeal or pharyngeal surgery between October 1994 and March 1996. We identified 48 procedures performed on 46 patients in which telescopes were critically important in the surgical management of disorders in the hypopharynx or larynx. For our telescopic system, we use both sinus and pediatric bronchoscopic telescopes with a three-chip television camera for viewing. All images were stored as digital recordings giving the same views that the operating surgeon had during the procedure.

The types of surgical procedures fell under three broad categories, outlined in Table 1. The first were situations in which diagnosis of the lesion was enhanced with the telescope as compared with the microscope, but because of limitations in the available instrumentation, the microscope was used for

TABLE 1. CATEGORIES OF LARYNGEAL AND PHARYNGEAL PROCEDURES

Category	*No. of Patients*
Diagnosis only	
Anterior commissure or glottic lesions	6
Subglottic lesions	2
Supraglottic lesions	2
Subtotal	10
Telescope-facilitated procedure	
KTP laser vestibulotomy	7
KTP laser lesion excision	5
Glottic or subglottic biopsies and excisions	9
Subtotal	21
Telescope-unique procedure	
Telescopic-visualized laryngeal injection	1
Biopsies and excisions	5
Stapler-assisted Zenker's diverticulotomy	11
Subtotal	17
Total	48

KTP — potassium titanyl phosphate.

From the Division of Otolaryngology–Head and Neck Surgery, Duke University Medical Center, Durham, North Carolina.

Presented at the meeting of the American Broncho-Esophagological Association, Orlando, Florida, May 6-7, 1996.

CORRESPONDENCE — William J. Richtsmeier, MD, PhD, Division of Otolaryngology–Head and Neck Surgery, Duke University Medical Center, Box 3805, Durham, NC 27710.

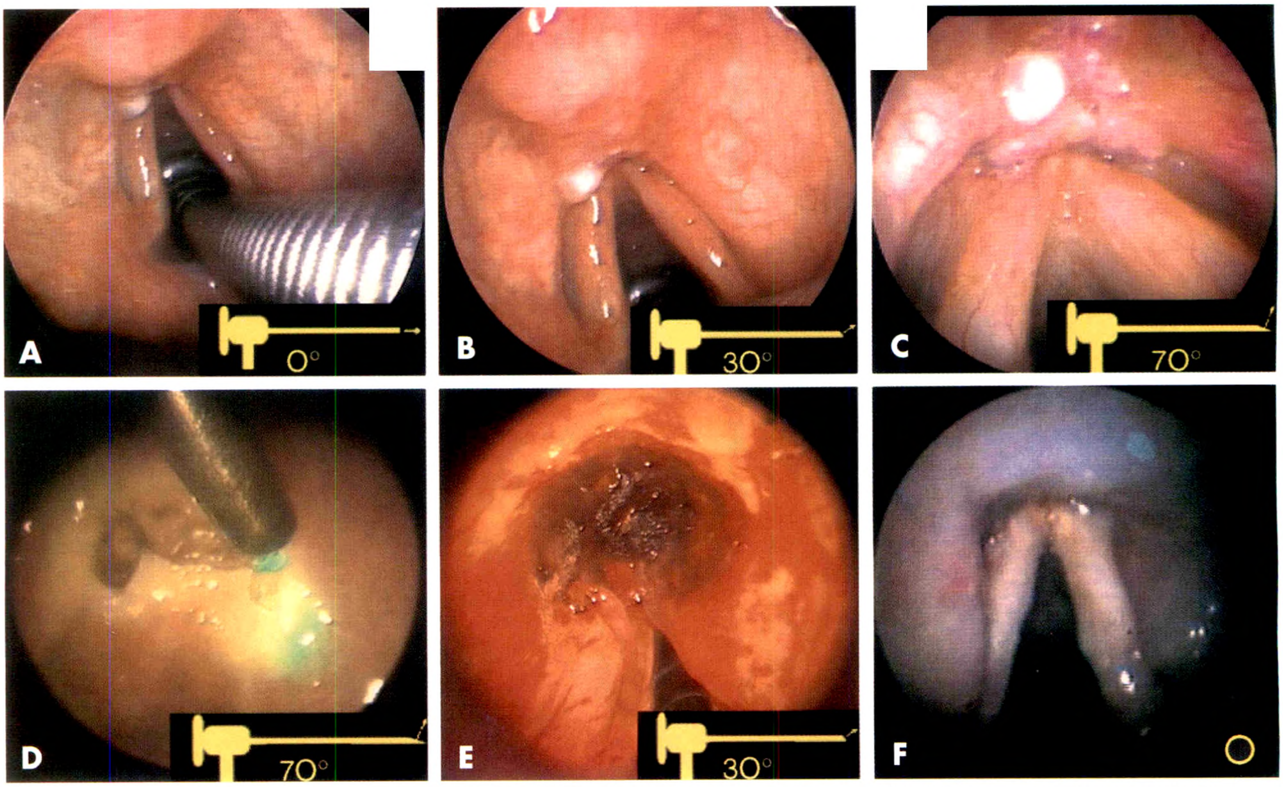

Fig 1. (Case 1) Squamous cell carcinoma of petiole of epiglottis. A) Zero-degree telescopic view. B) Thirty-degree telescopic view. C) Seventy-degree telescopic view. D) View during potassium titanyl phosphate (KTP) laser excision. E) Postexcision 30° telescopic view. F) Fourteen-month fiberoptic laryngoscopy appearance of larynx, with patient showing no evidence of disease.

the definitive surgical treatment. Examples of this were lesions requiring use of the carbon dioxide (CO_2) laser when available instruments could not provide adequate ability to manipulate or engage the lesion requiring treatment. For the most part, increased experience led to greater adaptation and application of presently available instruments. The second category involved circumstances in which we discovered significantly better visualization of the lesions with the telescopes than we could obtain with the operating microscope, and we did have instrumentation available for completion of the procedure. The third circumstance was that in which the telescope offered such an advantage that it was the only instrument that could be used to adequately visualize the lesion during the procedure. In many of these cases, the direct laryngoscope could not be positioned adequately because of patient anatomy, and the telescope provided the means to visualize and treat the lesion.

RESULTS

The numbers and categories of the three types of cases are summarized in Table 1. Patient ages ranged between 18 and 81 for the 23 men and 23 women. One patient was found to have a second lesion that was not seen with fiberoptic, laryngostroboscopic, or conventional microscopic laryngoscopy, but was easily seen in the laryngeal ventricle with a 70° telescope. A second patient returned for a second telescopic procedure when the first conventional microscopic procedure failed (see case 1). The following cases are presented as examples of the types of problems for which we found telescopic instrumentation important.

CASE REPORTS

Case 1. A 70-year-old man presented with a squamous cell carcinoma of the petiole of the epiglottis (Fig 1A). The tumor was barely visible in the view with a 0° telescope, which was essentially the same view as with the operating microscope (not shown). More of the lesion could be visualized with a 30° telescope, and a biopsy was obtained (Fig 1B). The view with a 70° telescope showed the inferior extent of the tumor (Fig 1C). Consent had been obtained only for CO_2 laser excision. With the limitation of the viewpoint imposed by the microscope, the lesion was excised with a pathologically positive inferior margin. The lesion was subsequently excised with a pathologically free margin in a second procedure using a potassium titanyl phosphate (KTP) laser presented through a curved fiber viewed with the 70° telescope (Fig 1D). The postexcision 30° view is shown in Fig 1E. The patient is now 30 months postexcision, with no evidence of recurrence on fiber-

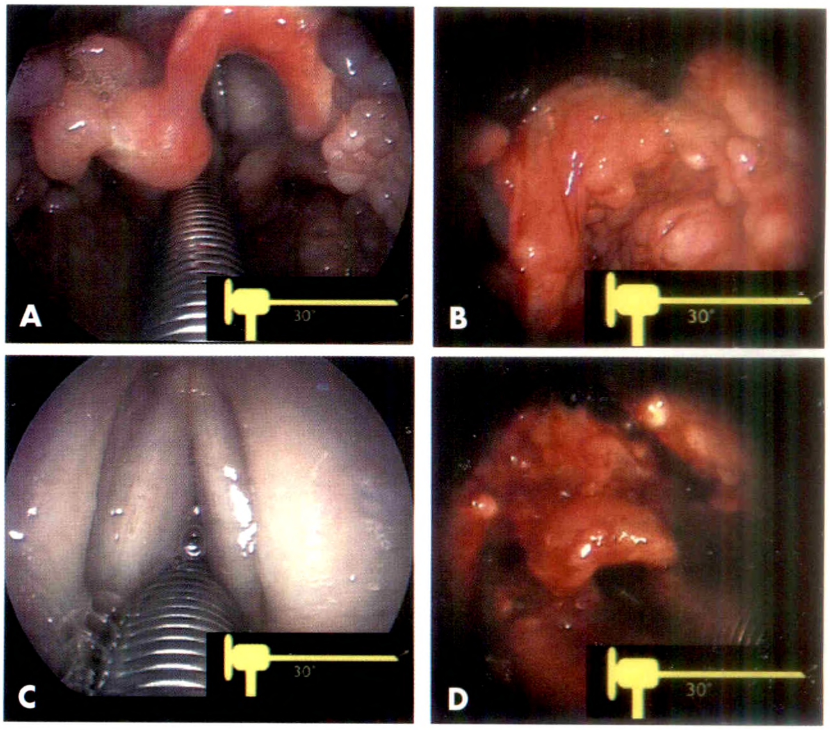

Fig 2. (Case 2) Paralaryngeal and pharyngeal lymphoid hyperplasia. A) Thirty-degree view demonstrating lymphoid tissue in left pyriform sinus and left aryepiglottic fold. B) Lymphoid tissue present in right pyriform sinus visualized with 30° telescope. C) Normal-appearing endolarynx. D) Immediate postexcision appearance.

optic laryngoscopy in which the full anterior commissure can be seen (Fig 1F).

Case 2. A 50-year-old woman presented with dysphagia and weight loss. She was observed to have nodules of mucosal-associated lymphoid tissue involving the vallecula, supraglottis, and pyriform sinus that had the histologic appearance of normal tonsil. Cultures for aerobic and anaerobic (including *Actinomyces*) bacteria, fungi, and mycobacteria were all negative. The patient could not tolerate systemic steroids due to psychiatric effects; therefore, an endoscopic removal was undertaken. Figure 2A,B shows the telescopic appearance of the lesions involving the vallecula, left aryepiglottic fold, and right and left pyriform sinuses, while Fig 2C shows the normal

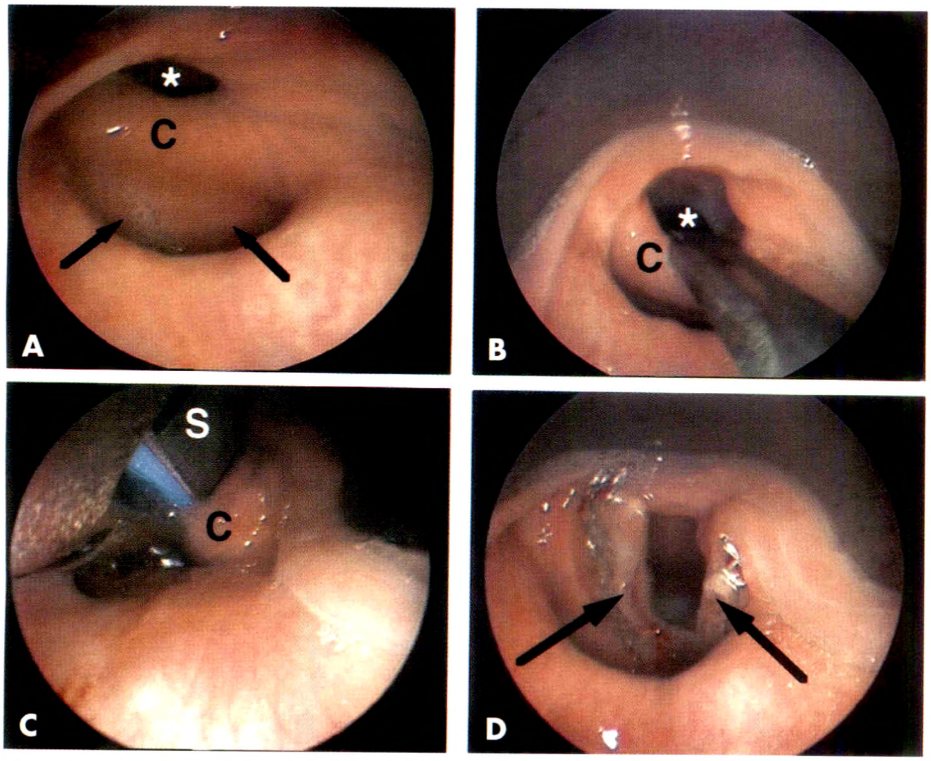

Fig 3. (Case 3) Endoscopic staple-assisted diverticulostomy for Zenker's diverticulum. All views are 30° telescopic views. A) Telescopic appearance of pouch (arrows), esophagus (asterisk), and cricopharyngeal band (C). B) Probe placed in esophagus (asterisk), confirming correct anatomic position. C) Telescopic view, confirming correct placement of stapler (S). D) Arrows show immediate postdiverticulostomy appearance.

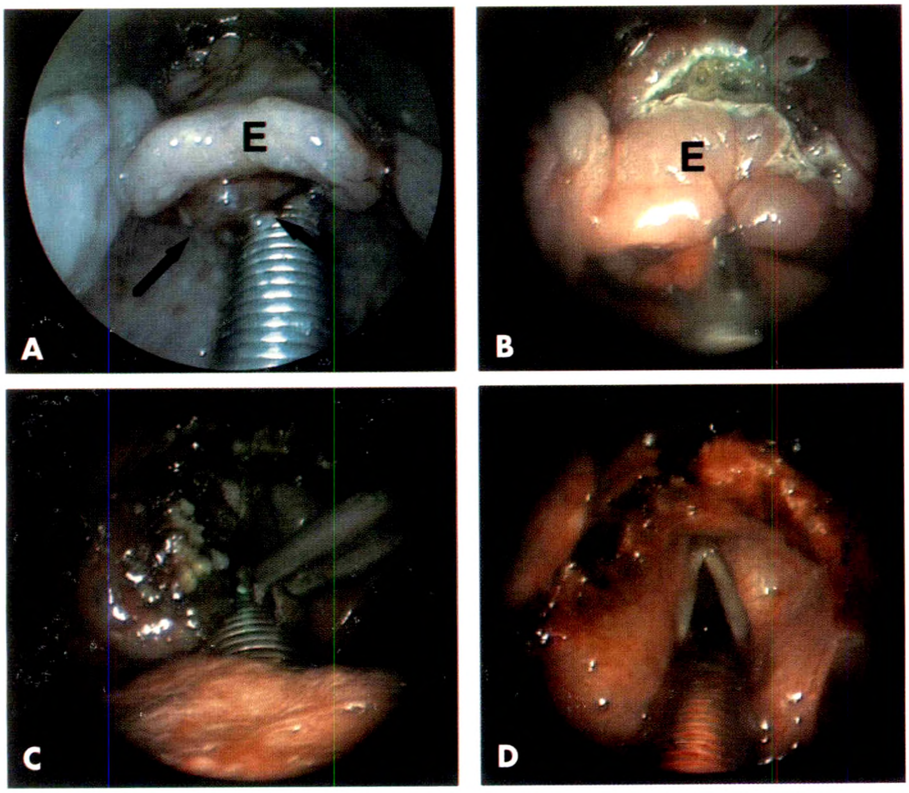

Fig 4. (Case 4) Medullary carcinoma of thyroid metastatic to epiglottis. All views are 0° telescopic views. A) Lesion (arrows) metastatic to epiglottis (E). B) Initial stages of KTP laser excision. C) View after partial resection. D) Appearance of larynx after excision of epiglottis and lesion. Patient remains free of disease.

appearance of her endolarynx. The nodules were successfully removed with telescopic visualization using the KTP laser presented through a curved fiber allowing presentation of the laser beam perpendicular to the plane of dissection over a wide range of surfaces. The immediate postexcision appearance is seen in Fig 2D. The patient recovered uneventfully, and her dysphagia resolved, with weight gain back to her preillness state.

Case 3. A 69-year-old woman presented with a several-month history of increasing dysphagia and mild regurgitation of solid food. Evaluation with barium swallow demonstrated a Zenker's diverticulum arising off the posterior pharyngoesophageal segment. Treatment of the diverticulum was performed with endoscopic staple-assisted esophagodiverticulostomy. Under general anesthesia, the patient was positioned for a laryngoscopy. The diverticulum and esophageal lumen were visualized telescopically with 0° and 30° endoscopes (Fig 3A,B). The same telescopes were then used to confirm appropriate placement of the GIA-30 endostapler around the common diverticular and esophageal wall (Fig 3C). An extended description of this procedure is discussed elsewhere.[4] With direct visualization with the 30° telescope, the common wall was divided and stapled, creating an open passage between the diverticular pouch and the esophageal lumen (Fig 3D).

Case 4. A 50-year-old woman who was found in 1992 to have a medullary carcinoma of the thyroid had undergone total thyroidectomy and a left modified radical neck dissection. Four months prior to recent evaluation, she had the onset of persistent cough, dysphagia for solids and liquids, and hoarseness. The patient had also noted a breast mass, which biopsy demonstrated to be metastatic medullary thyroid carcinoma. Flexible fiberoptic laryngoscopy demonstrated an exophytic, black epiglottic mass arising from the left laryngeal surface and extending to the left aryepiglottic fold. There was normal vocal fold mobility and no evidence of a mass within the vallecula or on the lingual surface of the epiglottis. A presumptive diagnosis of metastatic medullary thyroid carcinoma was made, and the patient was scheduled for direct laryngoscopy with planned excision.

During direct laryngoscopy, 0°, 30°, and 70° telescopes were used to visualize the larynx and the epiglottic tumor (Fig 4A). This evaluation demonstrated the lesion to be completely confined to the supraglottis involving the left aryepiglottic fold and epiglottis. With 0° and 30° telescopic visualization, the epiglottis and left aryepiglottic fold were completely excised with the KTP laser (Fig 4B,C). After excision of the mass, the telescopes were again used to visualize the larynx, with no other gross tumor seen (Fig 4D). Pathologic analysis of the excised specimen showed metastatic medullary thyroid carcinoma. The patient has subsequently recovered well, with complete epithelialization of the resection site and no further evidence of disease.

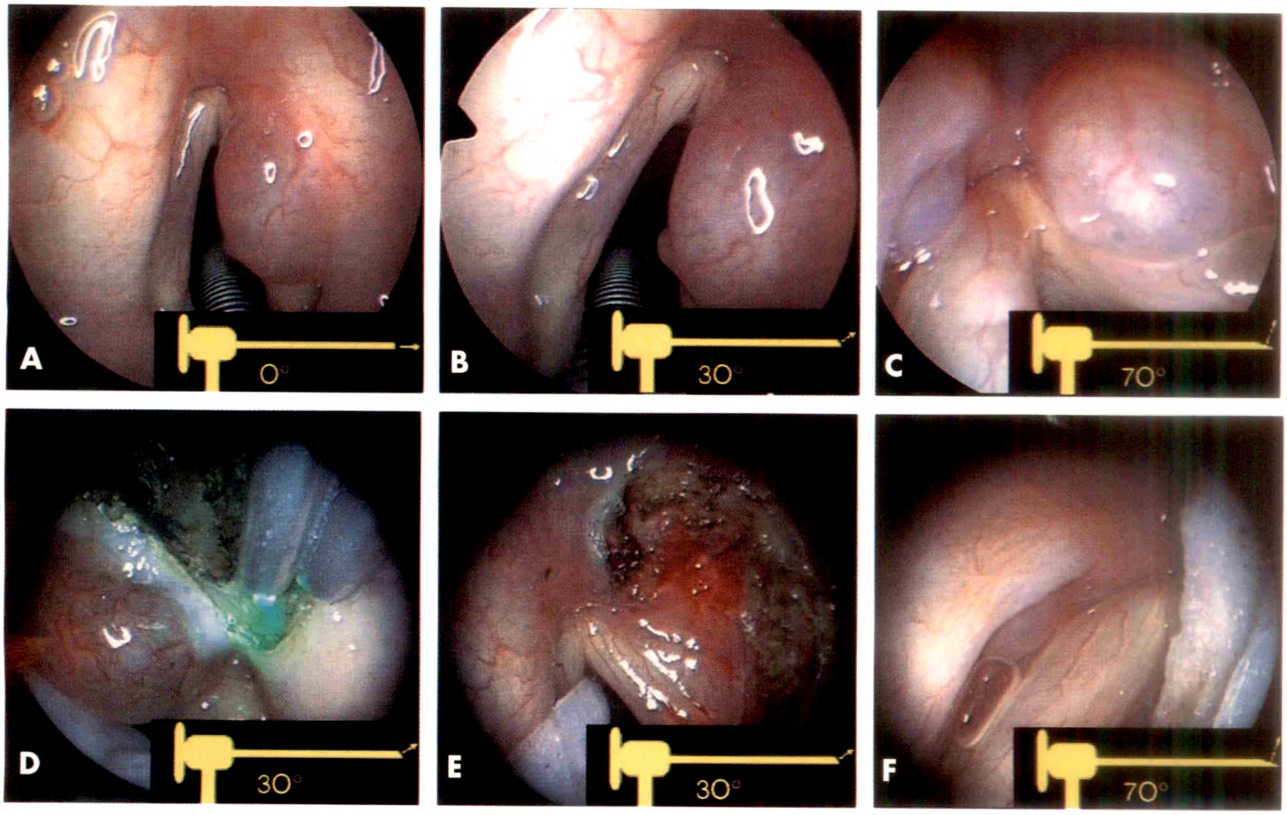

Fig 5. (Case 5) Bilateral laryngeal cysts. A) Zero-degree telescopic view of right ventricular cyst. B) Thirty-degree telescopic view of right ventricular cyst. C) Seventy-degree telescopic view demonstrating bilateral cysts. D) Thirty-degree view during KTP laser excision of right cyst. E) Appearance of larynx after KTP laser excision. F) Seventy-degree view used to excise smaller left laryngeal cyst.

Case 5. A 68-year-old woman presented with a long history of intermittent hoarseness, and a mass protruding from the right ventricle was identified on examination with fiberoptic laryngoscopy. The mass, which proved to be a laryngeal cyst, appeared similar under both the 0° and 30° telescopic views (Fig 5A,B). The 70° telescope view was strikingly different when the telescope was inserted to the level of the true vocal folds, and a second laryngeal cyst was observed in the left ventricle that was not appreciated preoperatively (Fig 5C). The larger cyst in the right ventricle was excised with the 30° telescope for visualization and the KTP laser for excision (Fig 5D,E). This was accomplished with a ventriculectomy approach as described by Kashima et al.[5] The smaller cyst was then precisely removed under visualization with the 70° telescope (Fig 5F). The patient is now 22 months postexcision, with resolution of her hoarseness and no evidence of recurrence of her laryngeal cyst.

TABLE 2. COMPARISON OF TELESCOPIC VERSUS MICROSCOPIC LARYNGOSCOPY

Telescopic	*Microscopic*
View is two-dimensional unless moving	View is three-dimensional
Light moves with telescope	Less light at high magnification
Can use for patients that cannot be visualized with standard equipment	Light travels in straight lines (ie, shadow effect)
Visualizes lesions in ventricle or undersurfaces	Requires retraction or mirror to see undersurfaces
Easily uses curved laser	Provides laser platform
Telescope requires use of one hand	Both hands are free
Requires video magnification	Is self-contained
Adjusts with distance	Fixed-step magnification

COMPARISON OF TECHNIQUES

A comparison of conventional suspension microlaryngoscopy and telescopic laryngoscopy reveals some important differences (Table 2). It should be noted that the telescope provides only a two-dimensional (2-D) image; however, motion of the telescope in and out of the operative field gives the illusion of a three-dimensional (3-D) view by noting the changing relationships between anatomic structures. This 2-D–3-D phenomenon has been noted by endoscopic sinus surgeons. The operating microscope provides a 3-D perspective. The telescope provides light that moves with the scope so that the closer one gets to an

TABLE 3. INSTRUMENTS THAT SUPPORT TELESCOPIC ANGULATED SURGERY

- Potassium titanyl phosphate and carbon dioxide laser fibers
- Angled carbon dioxide laser fiber tip
- Angled suction
- Lindholm laryngoscope
- Weerda laryngoscope
- Kantor/Berci video microlaryngoscope
- Pediatric bronchoscopes
- High-resolution video cameras
- Endoscopic staplers

object, the higher the magnification and the brighter the light. In contrast, with the operating microscope, there is less light with higher magnifications, and in certain circumstances, shadow effects limit visualization due to the distance between the microscope and the larynx.

The telescope allows visualization in certain cases that cannot be visualized with the standard equipment. The best example of this in our series was the staple-assisted endoscopic diverticulostomy for Zenker's diverticulum, in which the stapler takes up so much of the laryngoscope that it would be impossible to ensure that the stapler is in correct position without using some type of imaging apparatus, either a rigid telescope or a flexible fiberoptic laryngoscope. The telescopes' angled views can be simulated with mirrors with the operating microscope; however, illumination of the area is not as good as it is with the angled telescopes. The telescopes easily allow utilization of curved or angled laser fibers with a broad spot size, and the operating microscopes provide the laser-based platform with a micromanipulator. Additionally, use of the 30° and 70° telescopes allows angled instrumentation to be used to approach lesions that are not readily visualized by the direct-line-of-sight view provided by the operating microscope (Table 3).

With the exception of the Kantor/Berci laryngoscope (Karl Storz), telescopes have to be held with one hand. In case 4, an alternative method of treatment could have been the use of the operating microscope, the CO_2 laser, and retraction of the supraglottis with the free hand. If the telescope is fixed in position, one loses the 3-D effect of the telescope motion. By comparison, the microscope allows for 3-D, two-handed surgery.

TABLE 4. INSTRUMENTS REQUIRED FOR TELESCOPIC LARYNGEAL AND PHARYNGEAL SURGERY ADVANCEMENT

- Angled forceps
- Staplers and scissors
- Telescope holders
- Telescope with universal joint prisms connecting to video monitor

DISCUSSION

In reviewing these 48 cases, we find that the use of the rigid telescope augments laryngeal and pharyngeal surgery in many cases, and often offers the unique opportunity to perform certain types of endoscopic procedures that are simply impossible with the conventional operating microscope. We still feel that the operating microscope, with or without the mounted CO_2 laser, will remain the mainstay of sophisticated operative laryngology. Nevertheless, we have performed 48 cases using video-monitored telescopic laryngoscopy as the primary visualization technique. This same type of visualization has proven very satisfactory for surgery in locations such as the peritoneal cavity and sinuses and, in our experience, has proven extremely useful in the larynx and pharynx as well.

Serious current limitations to the use of telescopes for pharyngeal and laryngeal surgery exist. The foremost is the telescope eyepiece and camera occupying the field of vision immediately in line with the lumen of the laryngoscope. This position limits movement of other endoscopic instruments in and out of the laryngoscope. This problem is partially solved by the Kantor/Berci laryngoscope. A variable view for angled telescopes would be preferable. Advancement of telescopic laryngeal and pharyngeal surgery also requires additional angled instrumentation (Table 4).

The fixed perspective of the microscope has limited the advancement of endoscopic oncologic surgery.[6,7] We feel that the advantages of telescopic surgery, including excision performed perpendicular to the laryngeal wall, adequate visualization in the laryngeal ventricle, and use of hemostatic endoscopic devices such as staplers and angled lasers, can initiate a new enthusiasm for endoscopic excision and reconstruction of laryngeal tumors. Telescopic-monitored techniques are advancing in virtually every area of surgery. We feel that they will become an important part of surgery of the hypopharynx and larynx, as they have in the nose and paranasal sinuses.

REFERENCES

1. Kleinsasser O. Microlaryngoscopy and endolaryngeal microsurgery. 3rd ed. Philadelphia, Pa: Mosby-Hanley & Belfus, 1990:3-16.

2. Andrea M, Dias O. Atlas of rigid and contact endoscopy in microlaryngeal surgery. Philadelphia, Pa: Lippincott-Raven, 1995:7-12.

3. Courey MS, Gardner GM, Stone RE, Ossoff RH. Endoscopic vocal fold microflap: a three-year experience. Ann Otol

Rhinol Laryngol 1995;104:267-73.

4. Scher RL, Richtsmeier WJ. Endoscopic staple-assisted esophagodiverticulostomy for Zenker's diverticulum. Laryngoscope 1996;106:951-6.

5. Kashima HK, Lee DJ, Zinreich SJ. Vestibulectomy in early vocal fold carcinoma. In: Johnson JT, Didolkar MS, eds. Head and neck cancer. Amsterdam, the Netherlands: Elsevier Science Publishers, 1993:181-9.

6. Krespi YP, Meltzer CJ. Laser surgery for vocal cord carcinoma involving the anterior commissure. Ann Otol Rhinol Laryngol 1989;98:105-9.

7. Shapshay SM, Hybels RL, Bohigian RK. Laser excision of early vocal cord carcinoma: indications, limitations, and precautions. Ann Otol Rhinol Laryngol 1990;99:46-50.

≈

ENDOSCOPY DAYS IN PEDIATRIC OTOLARYNGOLOGY

International Pediatric Otolaryngology Endoscopy Days of Lyon: The Pediatric Larynx will be held March 2-3, 1998, in Lyon, France. For more information, contact M. C. Duchez, Secretariat, Departement d'ORL, Hopital Ed. Herriot, 69003 Lyon, France; fax 33 4 72 11 05 34.

≈

NEONATAL HEARING SCREENING

The European Consensus Development Conference on Neonatal Hearing Screening will be held in Milan, Italy, May 15-16, 1998. For more information, contact Dr F. Grandori, Centre of Biomedical Engineering, Polytechnic of Milan, Piazza Leonardo da Vinci 32, 20133 Milan, Italy; fax +39-2-23993360; email ecdc@elet.polimi.it.

Ann Otol Rhinol Laryngol 106:1997

LARYNGOTRACHEOESOPHAGEAL CLEFTS

GREETHA MOUNGTHONG, MD
BANGKOK, THAILAND

LAUREN D. HOLINGER, MD
CHICAGO, ILLINOIS

This article reviews laryngeal cleft anomalies from the Laryngeal Development Laboratory at Children's Memorial Hospital in Chicago and includes a discussion of the classification of laryngotracheoesophageal clefts based on previous work and the information presented herein. Of the 115 laryngeal specimens obtained between 1975 and 1995, 11 have laryngeal cleft anomalies. Eight have a submucous laryngeal cleft. There is 1 laryngotracheoesophageal cleft, type II (partial cricoid cleft); and there are 2 laryngotracheoesophageal clefts, type III (complete cricoid cleft). The histopathologic findings are presented in detail and the literature is reviewed. Photomicrographs and drawings illustrate the pathology and classification. Clinical presentation, diagnosis, evaluation, and management are discussed, as is the embryology.

KEY WORDS — cleft larynx, laryngotracheoesophageal cleft, occult laryngeal cleft, submucous laryngeal cleft.

INTRODUCTION

Posterior laryngeal cleft (PLC) and laryngotracheoesophageal cleft (LTEC) are rare congenital anomalies first described and recognized by Richter in 1792. The PLC is characterized by an absence of fusion of the posterior cricoid lamina that effects an abnormal communication between the larynx and hypopharynx. In the more extensive form of LTEC, absence of all or part of the tracheoesophageal septum effects an abnormal communication between the trachea and esophagus as well.

The condition varies in anatomic extent and clinical severity. In its mildest form (type I), the only abnormality is the absence of the interarytenoid muscle above the superior margin of the cricoid cartilage. Affected patients may survive into adulthood with nothing more serious than hoarseness and recurrent respiratory tract infections. In more severe forms (types III and IV), in which the cricoid and posterior tracheal wall are completely cleft, death due to severe aspiration pneumonia and respiratory failure may be inevitable.[1]

MATERIALS AND METHODS

All specimens from the Laryngeal Development Laboratory at Children's Memorial Hospital, Chicago, were reviewed to identify those with LTEC. Specimens are acquired at postmortem examination and include the hyoid bone superiorly, two or more tracheal arches inferiorly, and the hypopharyngeal mucosa posteriorly. In the Laboratory, which was established by Gabriel F. Tucker, Jr, in 1975, specimens are prepared according to the method of Tucker et al.[2] The block of tissue obtained is kept intact, unsplit, and fixed in 10% formalin. After decalcification and fixation, it is embedded in parlodion (pyroxylin), then serially sectioned at 28 µm in the horizontal plane from top to bottom. Every 20th section is mounted and stained with hematoxylin and eosin. The remaining sections are numbered and stored in 80% alcohol for later staining if necessary. The histopathology of each specimen is studied in detail. Patients' medical records are reviewed for clinical presentation and associated anomalies.

RESULTS

Eleven cases of laryngeal cleft anomalies were identified among the 115 laryngeal specimens acquired between 1975 and 1995 by the Laryngeal Development Laboratory. Eight have a submucous ("occult") laryngeal cleft. The collection also contains 1 LTEC, type II (partial cricoid cleft), and 2 LTECs, type III (total cricoid cleft; see Table).

Submucous ("Occult") Laryngeal Cleft. Six of the 8 cases of submucous ("occult") laryngeal cleft were found in preterm infants who had an average gestational age of 26.2 weeks and an average birth weight of 783 g. The other 2 infants were term. All 8 had been intubated at birth for treatment of respiratory distress due to bronchopulmonary dysplasia, upper airway obstruction, and apneic episodes. All devel-

---

From the Division of Pediatric Otolaryngology, Children's Memorial Hospital, and the Department of Otolaryngology–Head and Neck Surgery, Northwestern University Medical School, Chicago, Illinois. The Laryngeal Development Laboratory at Children's Memorial Hospital is supported by the Lillian Shedd Wells Foundation and the Children's Surgical Foundation. Dr Moungthong is currently in the Department of Otolaryngology, Pramongkutklao College of Medicine, Bangkok, Thailand.

Presented at the meeting of the American Broncho-Esophagological Association, Scottsdale, Arizona, May 12-13, 1997.

CORRESPONDENCE — Lauren D. Holinger, MD, Division of Pediatric Otolaryngology, Children's Memorial Hospital, 2300 Children's Plaza, Box 25, Chicago, IL 60614.

CASES OF SUBMUCOUS LARYNGEAL CLEFT AND LARYNGOTRACHEOESOPHAGEAL CLEFT

Case	*Age*	*Sex*	*Birth Weight (g)*	*Status of Birth*	*Respiratory Presentation*	*Diagnosis*	*Histopathology*	*Associated Anomalies*
1	2 y	F	850	Preterm (26 wk)	Bronchopulmonary dysplasia, bronchospasms	Subglottic stenosis	Submucous cleft, elliptical cricoid	Pulmonary valvular stenosis
2	14 mo	F	620	Preterm (28 wk)	Apneic episode, seizure	Subglottic stenosis, tracheomalacia	Submucous cleft, submucous cyst, submucous gland hyperplasia	Aberrant innominate artery, congenital blindness
3	5 y	F		Term	Recurrent pneumonia, respiratory distress	Subglottic stenosis	Submucous cleft, submucous fibrosis	
4	1 y	M	890	Preterm (27 wk)	Bronchopulmonary dysplasia	Subglottic stenosis	Submucous cleft, submucous gland hyperplasia, distortion of cricoid	Patent ductus arteriosus
5	7 mo	F		Term	Upper airway obstruction	Subglottic stenosis, tracheal stenosis	Submucous cleft, submucous fibrosis, submucous cyst	
6	6 mo	M	773	Preterm (24 wk)	Bronchopulmonary dysplasia	Subglottic stenosis	Submucous cleft, distortion of cricoid, tracheal complete ring	Aortic valvular stenosis
7	4 mo	F		Term	Upper airway obstruction	Subglottic stenosis	Submucous cleft, submucous fibrosis, obliterated subglottic lumen	
8	20 d	M		Preterm	Respiratory distress	Tracheal stenosis	Submucous cleft	Ventricular septal defect, patent ductus arteriosus, right lung agenesis
9	1 d	F		Term	Respiratory distress	Laryngeal cleft, tracheal agenesis	Laryngotracheoesophageal cleft type II	Bronchoesophageal fistula, patent ductus arteriosus, rudimentary uterus
10	21 mo	M		Term	Respiratory distress, feeding difficulty	Laryngeal cleft	Laryngotracheoesophageal cleft type III	Tracheoesophageal fistula, gastroesophageal reflux
11	9 mo	F			Respiratory distress	Laryngeal cleft, subglottic stenosis	Laryngotracheoesophageal cleft type III, submucous fibrosis	

oped subglottic stenosis; case 8 also had tracheal stenosis. Most of the patients had other congenital anomalies such as a pulmonary valvular stenosis (case 1), an aberrant innominate artery and congenital blindness (case 2), a patent ductus arteriosus (case 4), an aortic valvular stenosis (case 6), and right pulmonary agenesis with a ventricular septal defect (case 8). Of the cases reported herein, the diagnosis of submucous cleft was never made during life; the clefts were identified at postmortem pathologic examination (Figs 1[3,4] and 2).

Partial Posterior Laryngeal Cleft. The 1 patient (case 9) with a partial PLC (type II; Fig 3[3]) was a term female infant with tracheal agenesis who had severe respiratory distress at birth. She had a bronchoesophageal fistula through which she ventilated until she died, shortly after birth. Her other congenital anomalies included a patent ductus arteriosus and a rudimentary uterus.

Complete Posterior Laryngeal Cleft. Two patients (cases 10 and 11) with a complete PLC (LTEC type III) developed respiratory distress after birth and required airway intervention. Associated anomalies included a tracheoesophageal fistula (TEF, case 10, Fig 4[3]) and congenital subglottic stenosis (case 11, Fig 5).

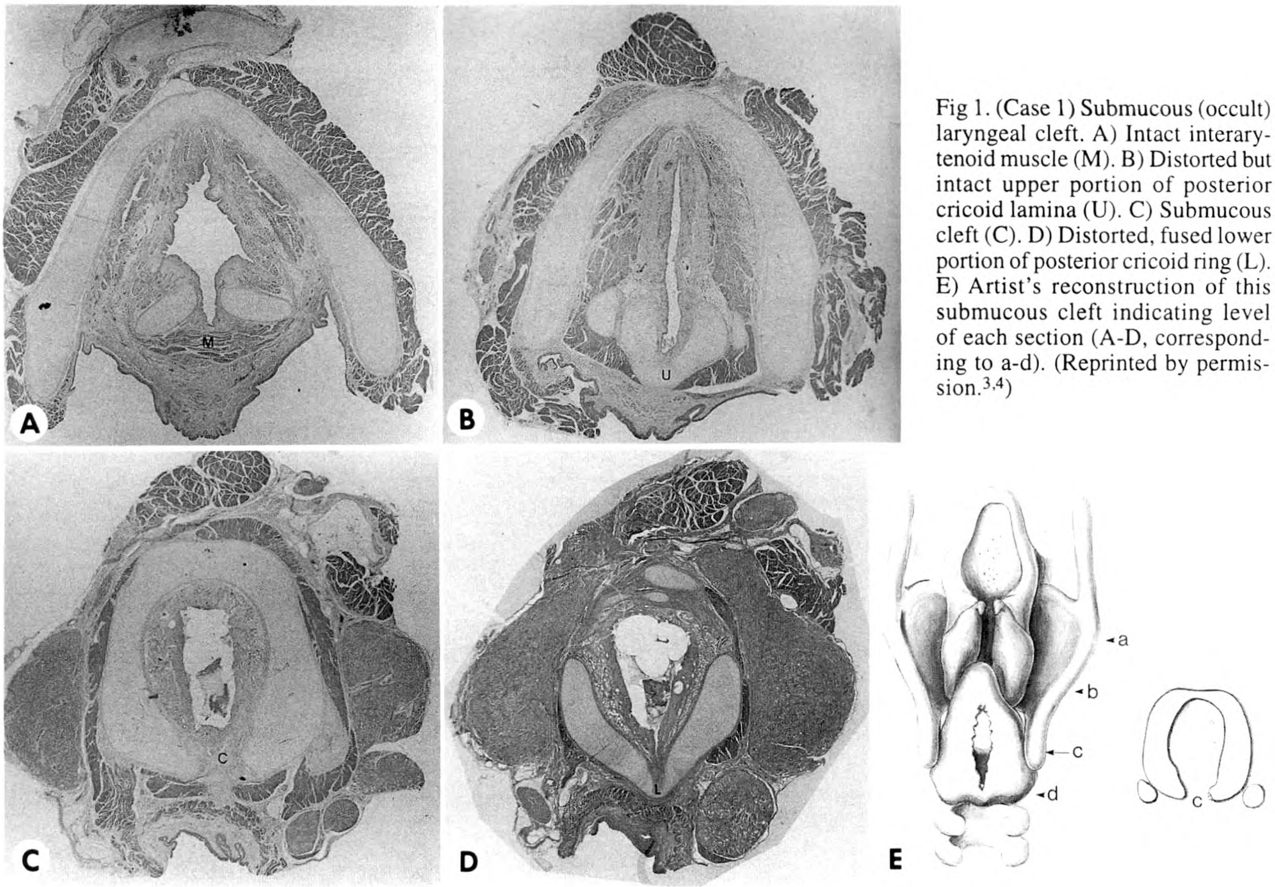

Fig 1. (Case 1) Submucous (occult) laryngeal cleft. A) Intact interarytenoid muscle (M). B) Distorted but intact upper portion of posterior cricoid lamina (U). C) Submucous cleft (C). D) Distorted, fused lower portion of posterior cricoid ring (L). E) Artist's reconstruction of this submucous cleft indicating level of each section (A-D, corresponding to a-d). (Reprinted by permission.[3,4])

DISCUSSION

Incidence. The PLC has been considered to be rare among congenital anomalies of the larynx, especially LTEC types III and IV, in which the septum between the trachea and esophagus fails to develop.[5] Evans[6] found only 2 cases (0.5%) of PLC in 427 children referred for direct laryngoscopy. In the Division of Pediatric Otolaryngology at Children's Memorial Hospital, Chicago, from 1990 to 1995, only 7 cases (0.3%) of PLC were diagnosed clinically of the 2,338 patients who underwent diagnostic direct laryngoscopy during this period. However, there is a higher incidence of these anomalies among the 115 specimens in the Laryngeal Development Laboratory: 8 cases (7%) of submucous laryngeal cleft and 3 cases (2.6%) of LTEC.

Anatomy. At the level of the epiglottis, the aerodigestive tract divides into the airway anteriorly (larynx) and the hypopharynx posteriorly (Fig 6). The PLC communicates between the larynx and the hypopharynx (not the larynx and trachea). The inferior anatomic limit of the larynx and hypopharynx is the inferior margin of the cricoid cartilage. The trachea and esophagus begin at the inferior margin of the cricoid cartilage (Fig 6).

Embryology. According to the Carnegie staging system, the embryonic period has 23 stages of development. At stage 10, the embryo is 2 to 3.5 mm long and 21 to 23 days old, and the first sign of respiratory system development is seen as a laryngotracheal sulcus that begins development of the respiratory system at its caudal end. During stage 11 (2.5 to 4.5 mm and 23 to 25 days), the laryngotracheal groove is lengthening and the pulmonary primordium divides into right and left lobes. By stages 12 and 13 (3 to 6 mm and 25 to 28 days), the tracheoesophageal septum makes its appearance. Any vascular compromise or failure of union in forming this septum may result in some degree of TEF or cleft. In stages 14 to 16, there is further pulmonary development and the primitive laryngeal structures appear. In stage 18, the cricoid cartilage develops from two lateral centers of chondrification that fuse ventrally at about days 40 to 44, and dorsally at about days 50 to 55 (stage 19).

The specific defect of each LTEC depends on the timing of the damage. Blumberg et al[5] postulated that the formation of an LTEC is caused by an arrest of the cranial advancement of the tracheoesophageal septum and the septal defect's effects on the fusion of the cricoid lamina. Formation of a PLC without a cleft of the tracheoesophageal septum is probably due to defective closure of the cricoid arch.[7]

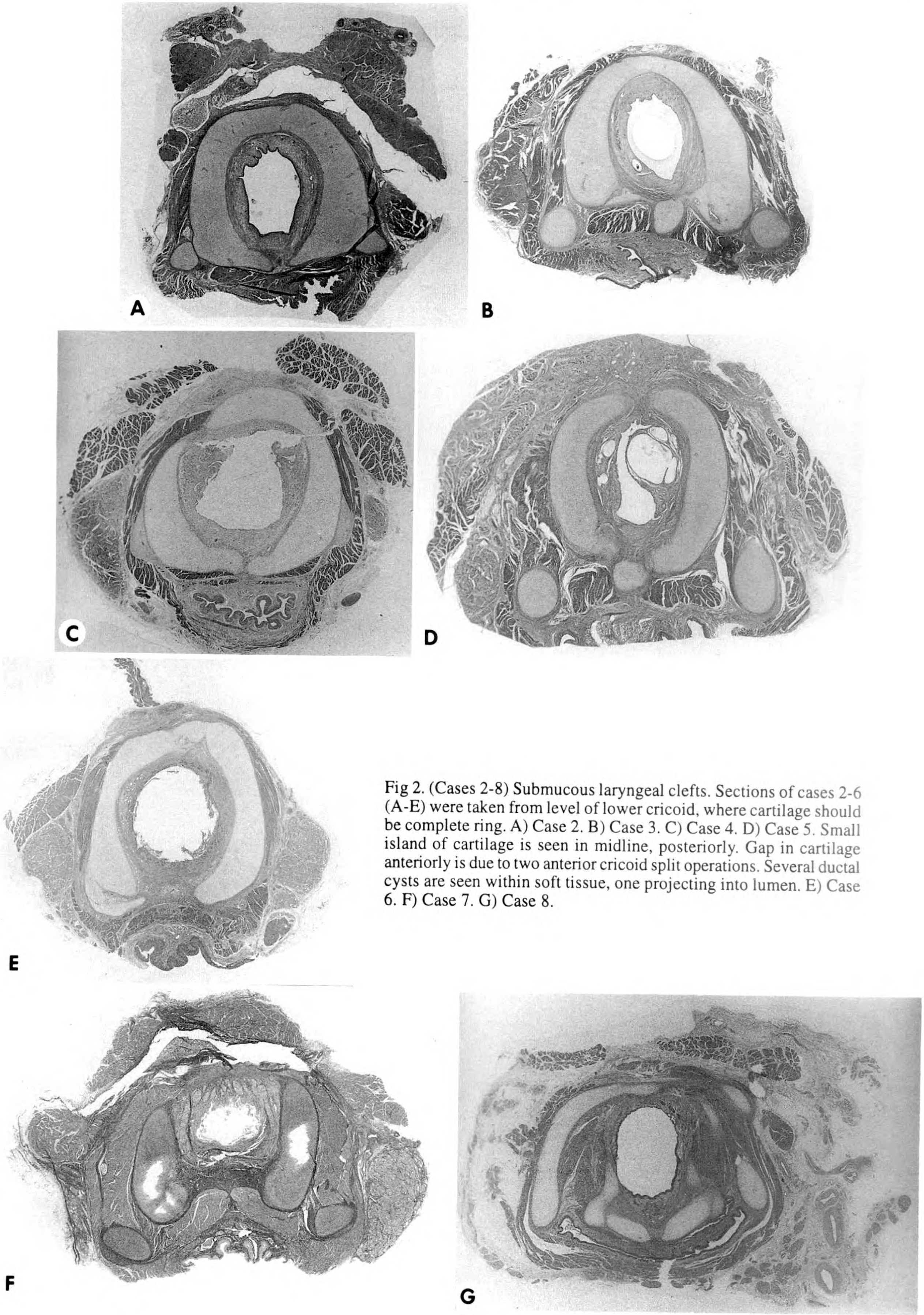

Fig 2. (Cases 2-8) Submucous laryngeal clefts. Sections of cases 2-6 (A-E) were taken from level of lower cricoid, where cartilage should be complete ring. A) Case 2. B) Case 3. C) Case 4. D) Case 5. Small island of cartilage is seen in midline, posteriorly. Gap in cartilage anteriorly is due to two anterior cricoid split operations. Several ductal cysts are seen within soft tissue, one projecting into lumen. E) Case 6. F) Case 7. G) Case 8.

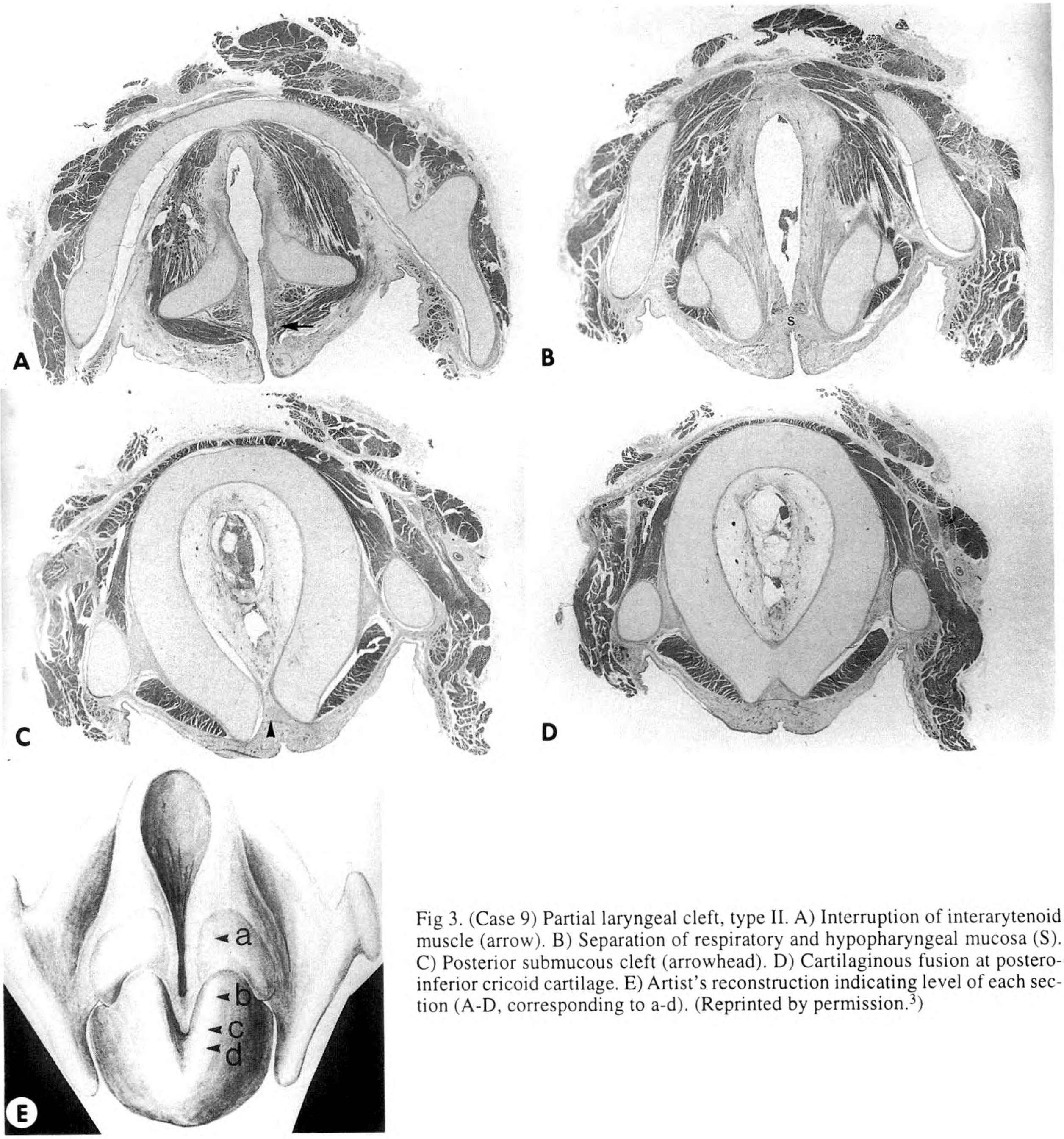

Fig 3. (Case 9) Partial laryngeal cleft, type II. A) Interruption of interarytenoid muscle (arrow). B) Separation of respiratory and hypopharyngeal mucosa (S). C) Posterior submucous cleft (arrowhead). D) Cartilaginous fusion at postero-inferior cricoid cartilage. E) Artist's reconstruction indicating level of each section (A-D, corresponding to a-d). (Reprinted by permission.[3])

Classification. Two basic systems of classification of LTECs have been proposed: anatomic and clinical. Petterssen[8] distinguished three types of LTECs based on anatomy (Fig 7[8-10]). Armitage,[1] an anesthesiologist, introduced a modification in 1984 on the basis of 3 cases. Evans[9] proposed a clinically based classification of PLCs and LTECs in 1985 (Fig 7). In his system, type I is confined to the interarytenoid region above the level of the vocal folds and does not involve the cricoid cartilage. Type II includes the cricoid cartilage and extends caudally to involve the cervical trachea. Type III extends to the thoracic trachea.

Benjamin and Inglis[10] offered a modification of Evans' classification in 1989 and proposed four types of LTECs (Fig 7). Type I is a supraglottic interarytenoid cleft that extends inferiorly no further than the level of the vocal folds. Type II is a partial cricoid cleft that extends below the level of the vocal folds. Type III is a total cricoid cleft that extends completely through the cricoid cartilage with or without further extension into part of the cervical tracheoesophageal wall. Type IV involves a major part of the intrathoracic tracheoesophageal wall; a complete extension to the carina leaves a common esophageal and tracheal lumen.

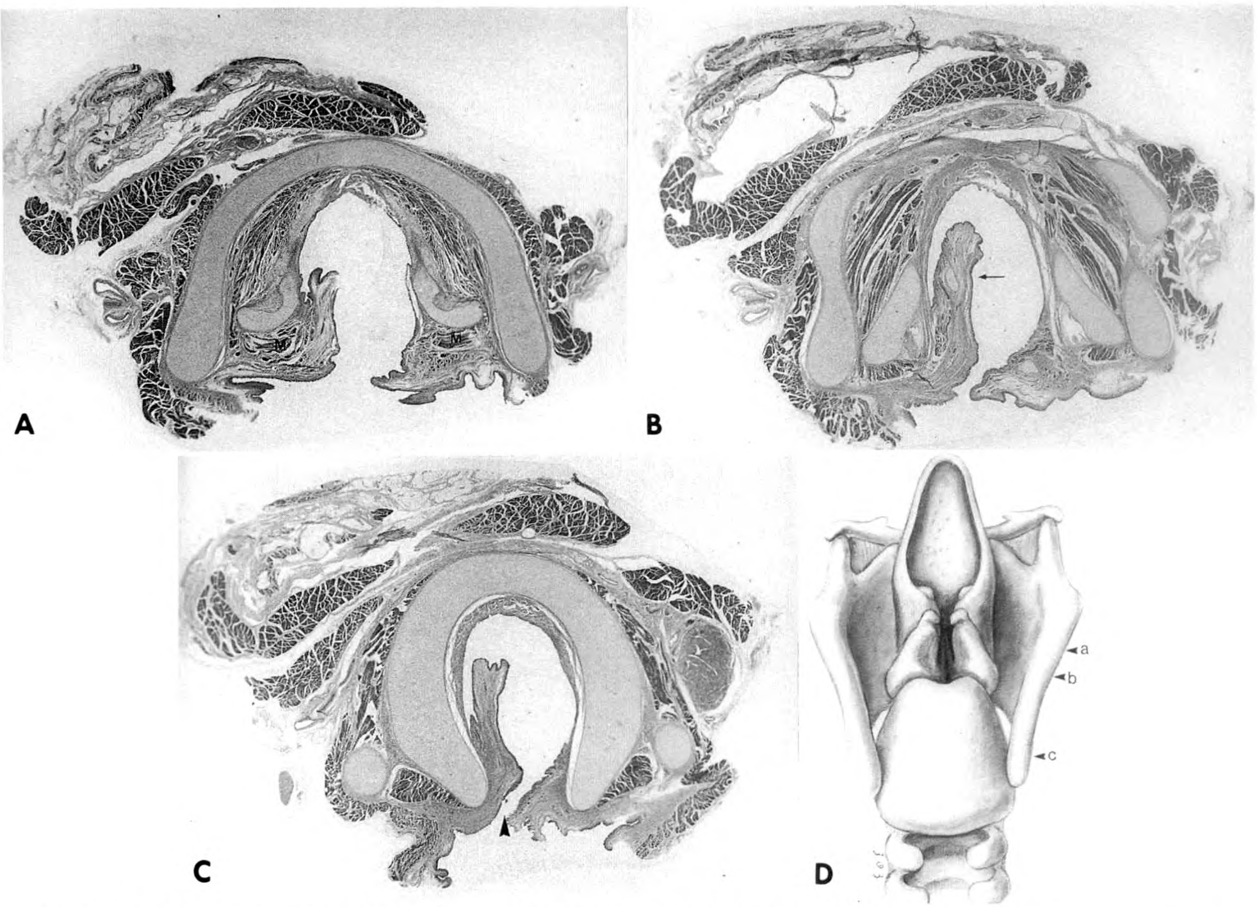

Fig 4. (Case 10) Complete laryngeal cleft, type III. A) Interruption of interarytenoid muscle (M). B) Intraluminal pedunculated hamartomatous mass with small island of cartilage (arrow). C) Cricoid cleft (arrowhead). D) Level of each section is shown (A-C, corresponding to a-c). (Reprinted by permission.[3])

Benjamin and Inglis'[10] classification is probably the most useful. Not only is their proposal well supported, but it is most compatible with the information provided herein regarding the partial cricoid clefts, specifically the submucous ("occult") laryngeal cleft. Technically, submucous clefts might be considered variants of the type II cleft. However, to maintain a classification that is clinically relevant, submucous laryngeal clefts are placed in a category of their own, because they are clinically significant only when they are associated with another cricoid cartilage anomaly. Such an anomaly — for example, the elliptical cricoid cartilage — may cause symptoms of airway obstruction. This classification is illustrated in Fig 8.[9,10]

Submucous ("Occult") Laryngeal Cleft. Submucous laryngeal clefts were first reported by Tucker and Maddalozzo.[4] Only 2 cases have been reported to date; the 8 reported herein include the 2 previously reported.[4] All except 1 had associated subglottic stenosis. The submucous laryngeal cleft consists of a posterior midline submucous cartilage defect (cleft) with intact soft tissue including mucosa and interarytenoid muscle. When viewed on horizontal cross section, the edges of the cleft cartilage are rounded, smooth, and covered with perichondrium (Fig 1). Sections taken superior to the cartilage defect demonstrate a fused, distorted cartilage or absent cartilage. Sections inferior to the cleft demonstrate an intact cartilaginous ring. Deformities of the cricoid cartilage associated with submucous laryngeal cleft include the elliptical cricoid cartilage (Figs 1C and 3C,D).

Partial Posterior Laryngeal Cleft. The partial laryngeal cleft is distinct from the submucous cleft in that the posterior larynx is cleft through to the hypopharynx.

Of the cases reported herein, one demonstrates a partial laryngeal cleft anomaly. A type II cleft (partial cricoid cleft, case 9, Fig 3), the cleft is continuous through the upper part of the cricoid cartilage, ending below the vocal folds. The lower part of the cricoid cartilage is an intact cricoid ring. The interarytenoid muscle shows partial agenesis and a fibrous end at the interface of the cleft (Fig 3).

Complete Posterior Laryngeal Cleft. Delahunty

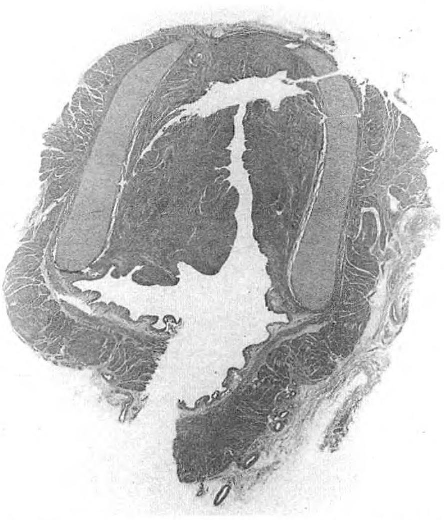

Fig 5. (Case 11) Complete laryngeal cleft, type III, shows several anomalies: absence of arytenoid cartilages, absence of interarytenoid muscle, and deformed cricoid cartilage with thick submucous fibrosis.

and Cherry[11] reported 2 cases of complete PLC and noted atrophic changes of interarytenoid muscle and lateral subluxation of the cricoarytenoid joint. Lim et al[12] reported a case of LTEC extending to the sixth tracheal arch and noted splaying of the posterior cricoid plate, partial agenesis of interarytenoid muscle, and incomplete fusion of the tracheal rings. Zachary and Emery[13] reported a complete LTEC extending to the carina and noted squamous epithelium extending into the tracheal lumen.

A type III LTEC (total cricoid cleft, case 10, Fig 4), the cleft is continuous through the entire cricoid cartilage, ending at an intact membranous posterior tracheal wall. Redundant tissue is present on both sides of the cleft; the tissue on the left is larger than that on the right and prolapses into the laryngeal lumen (Fig 4). Similar redundant tissue may account for symptoms of upper airway obstruction in some patients with laryngeal cleft.[14] The second case of complete laryngeal cleft (case 11, Fig 5) is a severe anomaly with no arytenoid cartilage or interarytenoid muscle and a deformed cricoid cartilage with thick submucous fibrosis that caused subglottic stenosis (Fig 5).

Symptoms. The type I laryngeal cleft deformity may be difficult to diagnose. A triad of husky voice, feeding difficulties, and aspiration pneumonia alerts the clinician to the possibility of a cleft larynx.[15] Patients may present with various degrees of respiratory distress, exacerbated or precipitated by attempts at feeding. Symptoms of upper airway obstruction were the most common presenting symptoms of the cases described herein. Stridor may be due to anterior collapse of the posterior supraglottic structures, especially the cuneiform cartilages or redundant mucosa in the posterior glottic and supraglottic larynx, as in case 10. Coughing, choking, and cyanotic episodes are characteristic.

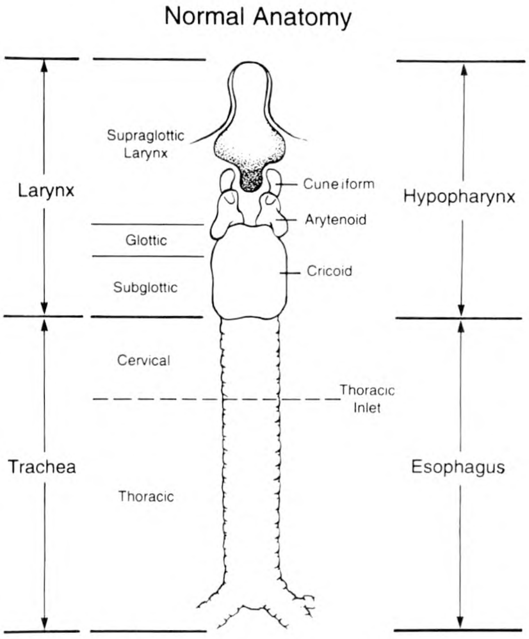

Fig 6. Normal anatomy of larynx and trachea observed from posterior aspect. Inferior anatomic limit of larynx and hypopharynx is inferior margin of cricoid cartilage.

The severity of symptoms is generally in proportion to the inferior extent of the cleft. Infants with type III or IV LTECs present with more severe symptoms than those with types I and II. The former patients have severe aspiration and cyanosis from birth and develop respiratory distress that is likely to require endotracheal intubation and emergency surgi-

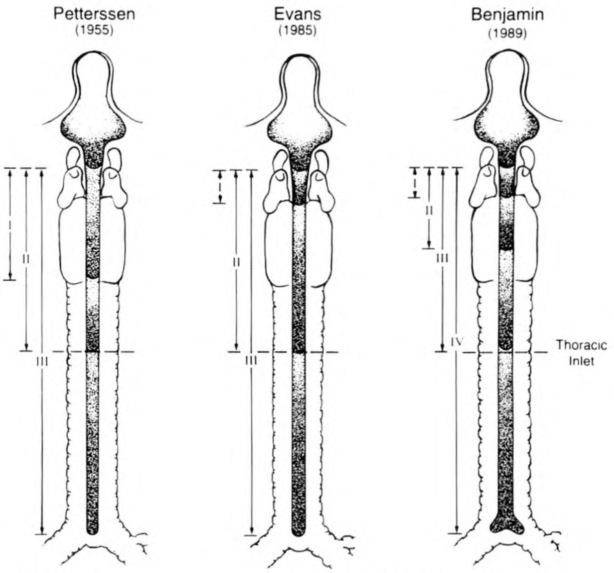

Fig 7. Three most commonly used classifications of laryngotracheoesophageal clefts: Petterssen,[8] Evans,[9] and Benjamin and Inglis.[10]

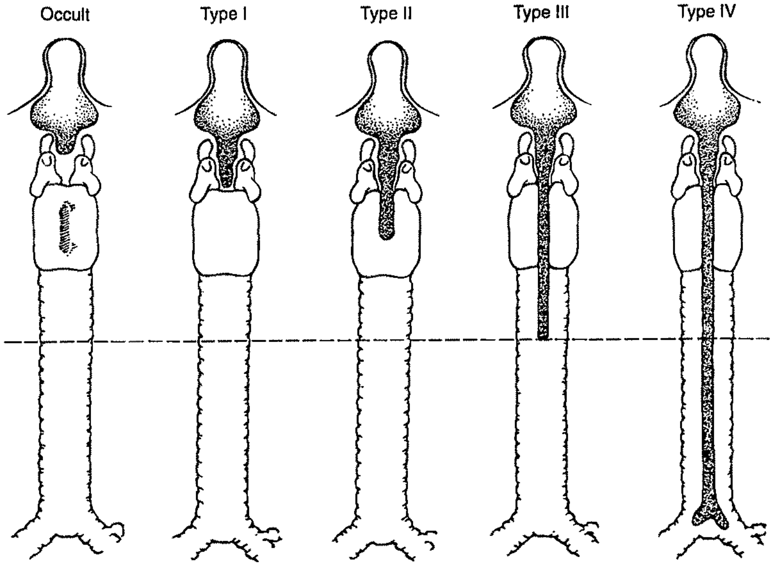

Fig 8. Classification of posterior laryngeal cleft (laryngopharyngeal cleft) and laryngotracheoesophageal clefts based on Benjamin and Inglis'[10] modification of Evans'[9] classification and data contained herein.

cal intervention. Roth et al[7] reviewed symptoms of 85 reported cases and found aspiration and cyanosis after feeding (53%), postpartum asphyxia (33%), increased production of mucus (23%), voiceless crying (16%), recurrent pneumonia (16%), stridor (10%), and impaired swallowing (5%).

Diagnosis. In evaluating a newborn with problems of choking during feeding, aspiration, increased pharyngeal secretions, and intermittent airway obstruction, the differential diagnosis must include TEF, because the symptoms closely mimic those of an LTEC. Other anomalies of the aerodigestive tract such as bilateral choanal atresia, neuromuscular incoordination of deglutition, vocal fold motion impairment, and gastroesophageal reflux (GER) are also considered.[16]

Infants and children with a history of aspiration and its sequelae lead the clinician to suspect an LTEC. Careful neurologic examination helps to exclude neuromuscular incoordination. Passing a catheter through the nasal passages may rule out choanal atresia, while passing a nasogastric (NG) tube into the stomach rules out esophageal atresia.

Chest radiographs often demonstrate aspiration pneumonia. An abnormal anterior position of the NG tube on lateral projection may also suggest the diagnosis.[7,12,14] Lateral airway films may demonstrate the absence of the usual soft tissue density between the larynx and hypopharynx, trachea and esophagus. Barium swallow may fail to demonstrate a cleft if the radiologist looks only for a TEF. Careful review may demonstrate a spill into the larynx and rule out a TEF. Pharyngeal incoordination can also simulate these findings.[17]

Careful direct laryngoscopy (with operating microscope and suspension) and bronchoscopy can make a definitive diagnosis and rule out other anomalies of the trachea and larynx that occur with an LTEC. At endoscopy, the lesion is easy to overlook. This may be due to the clinician's inexperience or failure to use specific laryngoscopic techniques. Even the experienced endoscopist may miss the diagnosis unless there is a high index of suspicion and a posterior cleft is looked for specifically. The laryngeal cleft may have the appearance of laryngomalacia. There is often an inward collapse of the posterior supraglottic structures, as well as redundant hypertrophic soft tissue in the posterior glottis.

Type I or II LTECs can be suspected by observing the failure of closure of the posterior glottis during phonation without anesthesia. A cleft is best demonstrated with suspension microlaryngology by advancing an anterior commissure laryngoscope between the vocal folds and abducting them widely. A type I LTEC requires a right-angle probe or an interarytenoid notch height (IANH)–measuring caliper for accurate assessment.[18] In types III and IV, a bronchoscope and an esophagoscope are necessary for diagnosis and to determine the inferior extent of the cleft.[14] Twenty percent of patients with laryngeal clefts also have a TEF.[12]

Management. The newborn with an LTEC may initially require emergency endotracheal intubation or tracheostomy for respiratory distress. With a type III or IV LTEC, the clinician must be alert to the possibility of displacement of the endotracheal tube posteriorly into the esophagus. Control of GER is critically important. An NG tube or gastrostomy may be necessary to decompress the stomach, prevent aspiration, and feed the infant. Most type I cases improve with growth and may be managed by conservative treatment consisting of upright positioning, thickening of formula, and swallowing rehabilitation.[19] Some will require surgical intervention. An endoscopic approach is usually satisfactory.[7] Type II clefts are almost certain to require surgical correction.[16]

Petterssen[8] reported the first successful repair of a laryngeal cleft in 1955. Armitage,[1] Roth et al,[7] and Lim et al[12] suggested surgical repair when the infant is symptomatic with recurrent episodes of aspiration or failure to thrive after a trial of NG or gastrostomy tube feeding and if thickened oral feedings are not tolerated. Surgical repair of laryngeal clefts can be approached via an open anterior or lateral approach. The anterior approach is suitable for type I, II, and III LTECs, as it provides excellent direct exposure of the cleft and avoids injury to the recurrent laryngeal nerve.[16,20] Some surgeons advise a lateral approach to prevent anterior weakening of the laryngeal cartilages, which may cause an unstable airway.[19,21] Evans[9] suggests the lateral approach for the small cleft with less than 2 cm of cervical tracheal involvement. With more extensive involvement of the cervical trachea, he suggests the anterior approach and a two-layer closure. Roth et al[7] recommend an endoscopic approach in the type I cleft using an operating microscope and endoscopic instruments. Nakahara et al[22] attempted injection of collagen into the submucosal space of the arytenoids for closure of the type I laryngeal cleft.

Successful treatment of the type IV LTEC depends on early diagnosis, securing the airway, protection from GER and aspiration, adequate nutrition, and early surgical repair. Surgical repair through a lateral thoracotomy is combined with a lateral cervical approach. Sternocleidomastoid muscle is used in the upper cleft, in order to decrease the chances of postoperative recurrence. In the lower cleft, likewise, pleura is interposed between the trachea and esophagus.[23]

CONCLUSIONS

Congenital laryngeal clefts are rare anomalies.[24] Of 11 cases reported herein, 8 were submucous clefts (posterior clefts of the cricoid cartilage under intact mucosa). All had associated subglottic stenosis and were not identified as laryngeal clefts until postmortem examination.

Three cases of LTEC that are not submucous clefts are reported. A history of aspiration pneumonia, choking, coughing during feeding, and symptoms of airway obstruction are keys to diagnosis. Morbidity and mortality are minimized by early diagnosis and prompt surgical intervention.

With the addition of the submucous cleft, the Benjamin and Inglis[10] modification of Evans' classification[9] is anatomically correct and the most clinically relevant classification system for laryngeal clefts (Fig 8).

REFERENCES

1. Armitage EN. Laryngotracheoesophageal cleft. Anaesthesia 1984;39:706-13.

2. Tucker GF, Tucker JA, Vidic B. Anatomy and development of the cricoid. Serial-section whole organ study of perinatal larynges. Ann Otol Rhinol Laryngol 1977;86:766-9.

3. Chen J-C, Holinger LD. Congenital laryngeal lesions: pathology study using serial macrosections and review of the literature. Pediatr Pathol 1994;14:301-25.

4. Tucker GF Jr, Maddalozzo J. "Occult" posterior laryngeal cleft. Laryngoscope 1987;97:701-4.

5. Blumberg JB, Stevenson JK, Lemire RJ, Boyden LA. Laryngotracheoesophageal cleft, the embryologic implications: review of the literature. Pediatr Surg 1965;57:559-66.

6. Evans JNG. Laryngotracheoplasty. Otolaryngol Clin North Am 1977;10:119-23.

7. Roth B, Rose KG, Bohn GB, Gunter H. Laryngotracheoesophageal cleft. Eur J Pediatr 1983;140:41-6.

8. Petterssen G. Inhibited separation of the larynx and the upper part of the trachea from the esophagus in a newborn: report of a case successfully operated upon. Acta Chir Scand 1955; 10:250-4.

9. Evans JNG. Management of the cleft larynx and tracheoesophageal clefts. Ann Otol Rhinol Laryngol 1985;94:627-30.

10. Benjamin B, Inglis A. Minor congenital laryngeal clefts: diagnosis and classification. Ann Otol Rhinol Laryngol 1989; 98:417-20.

11. Delahunty JE, Cherry J. Congenital laryngeal cleft. Ann Otol Rhinol Laryngol 1969;78:96-106.

12. Lim TA, Spanier SS, Kohut RI. Laryngeal clefts. A histopathologic study and review. Ann Otol Rhinol Laryngol 1979;88:837-45.

13. Zachary RB, Emery JL. Failure of separation of larynx and trachea from the esophagus: persistent esophagotrachea. Pediatr Surg 1961;49:525-9.

14. Holinger LD, Tansek KM, Tucker GF Jr. Cleft larynx with airway obstruction. Ann Otol Rhinol Laryngol 1985;94: 622-6.

15. Pillsbury HC, Fischer ND. Laryngotracheoesophageal cleft: diagnosis, management, and presentation of new diagnostic device. Arch Otolaryngol 1977;103:735-7.

16. Evans KL, Courteney-Harris R, Bailey M, Evans JNG, Parsons DS. Management of posterior laryngeal and laryngotracheoesophageal clefts. Arch Otolaryngol Head Neck Surg 1995;121:1380-5.

17. Cohen SR. Cleft larynx. A report of seven cases. Ann Otol Rhinol Laryngol 1975;84:747-56.

18. Bent JP III, Bauman NM, Smith RJH. Endoscopic re-

pair of type IA laryngeal clefts. Laryngoscope 1997;107:282-6.

19. Wolfson PJ, Schloss MD, Guttman FM, Nguyen L. Laryngotracheoesophageal cleft. Arch Surg 1984;119:228-30.

20. Cotton RT, Schreiber JT. Management of laryngotracheoesophageal cleft. Ann Otol Rhinol Laryngol 1981;90:401-5.

21. Donahoe PK, Gee PE. Complete laryngotracheoesophageal cleft: management and repair. J Pediatr Surg 1984;19:143-8.

22. Nakahara S, Tayama N, Tsuchida Y. A minor laryngeal cleft (type I-a) diagnosed in infancy. Int J Pediatr Otorhinolaryngol 1995;32:191-7.

23. Ryan DP, Muehrcke DD, Doody DP. Laryngotracheoesophageal cleft (type IV) management and repair of lesion beyond the carina. J Pediatr Surg 1991;26:962-70.

24. Holinger LD, Volk MS, Tucker GF Jr. Congenital laryngeal anomalies associated with tracheal agenesis. Ann Otol Rhinol Laryngol 1987;97:505-8.

≈

HEAD-NECK SURGERY AND ONCOLOGY

The Second Israeli International Symposium on Head-Neck Surgery and Oncology will be held in Jerusalem, Israel, November 1-5, 1998. For more information, please contact the Symposium Secretariat, PO Box 1931, Ramat-Gan 52118, Israel; telephone 972-3-6133340; fax 972-3-6133341.

≈

FIRST WORLD CONGRESS OF OTORHINOLARYNGOLOGIC ALLERGY, ENDOSCOPY AND LASER SURGERY

The First World Congress of Otorhinolaryngologic Allergy, Endoscopy and Laser Surgery will be held in Athens, Greece, June 25-27, 1998. For more information, contact Nereus Tours, Congress & Conference Department, 2 Afentouli Street, 185 36 Piraeus, Greece; telephone 1-4524842; fax 1-4182308.

Ann Otol Rhinol Laryngol 106:1997

EFFICACY OF REPEATED BOTULINUM TOXIN INJECTIONS AS A FUNCTION OF TIMING

KATSUHIDE INAGI, MD
CHARLES N. FORD, MD
ARTHUR A. RODRIQUEZ, MD
EDWARD SCHULTZ, PHD
DIANE M. BLESS, PHD
DENNIS M. HEISEY, PHD

MADISON, WISCONSIN

This pilot study was designed to determine if the interval between repeated botulinum toxin injections influenced physiologic and histologic effects on laryngeal muscles in a rat model. The physiologic measurements included digitized videomicroscopic recording of vocal fold movement and electromyography. The histologic measurements included muscle fiber size and digitized optical density of laryngeal muscles after glycogen depletion by electrical stimulation. The results demonstrated that the effect of timing of the second injection was strongly correlated to laryngeal changes. Most notable were results in the subjects that underwent injections 6 weeks apart. We hypothesize that these findings might be related to terminal axonal sprouting with reinnervation. The results from this study help confirm and expand the validity of using the rat laryngeal model to understand the effect of botulinum toxin. Moreover, we believe that the data might be extrapolated to prove useful in predicting human responses to botulinum toxin treatment for functional dystonias such as spasmodic dysphonia.

KEY WORDS — botulinum toxin, dystonia, electromyography, glycogen depletion, larynx, muscle fiber, rat, spasmodic dysphonia, thyroarytenoid muscle.

INTRODUCTION

Spasmodic dysphonia (SD) is a focal dystonia characterized by dysrhythmic contraction of the laryngeal musculature that often results in severe voice disturbance and impaired communication. Since the cause of this disorder remains in doubt, a definitive cure is unknown. Symptomatic control has been achieved with various medications, behavioral therapy, psychotherapy, recurrent laryngeal nerve resection, thyroplasty techniques, chronic nerve stimulation, and partial thyroarytenoid myomectomy. Periodic injection of botulinum toxin (BT) has proven to be effective in temporarily relieving the symptoms of adductor SD. Unfortunately, the therapeutic effect of BT is transient, and the injection does not always correct the disturbance. The exact BT dosage, site of injection, and timing of repeat injections are decided on an empirical basis guided by patient demands and clinician preference, for there is little scientific basis for those decisions in the treatment of SD.

Clinical studies have demonstrated the efficacy of large[1,2] and small doses of BT,[3-5] and have assayed whether bilateral[6,7] or unilateral[8,9] injection produced the most sustained voice improvement. Our most recent study[10] suggests the importance of precise placement of injectate in the larynx for prolonging the effect. It remains unclear how the spacing of intervals between injections influences efficacy. There is also little objective data describing the measured effects of various treatments. One approach to addressing these issues would be an animal model in which physiological assays could be employed to determine efficacy as a function of repeated BT injections into the larynx.

Most of the studies of BT injection in different volumes and dosages have been limited to studying the effect of a single dose in an animal model. Cohen and Thompson[11] worked out an effective dosage based on dose-response curves from dog larynges. George et al[12] mapped the affected muscle fibers using glycogen depletion techniques in the canine thyroarytenoid muscle. In our rat laryngeal model,[13,14] we demonstrated the relationships between effect and both dosage and volume using videomicroscopic and electromyography (EMG) response measurements; in these preliminary studies, we established suitable dosages and volumes to inject in rat

---

From the Department of Surgery, Division of Otolaryngology–Head and Neck Surgery (Inagi, Ford, Bless), and the Departments of Rehabilitation Medicine (Rodriquez), Neurology (Rodriquez), Anatomy (Schultz), and Surgery (Heisey), University of Wisconsin Medical School, Madison, Wisconsin. This work was supported by the National Center for Voice and Speech through grant P6000976 from the National Institute on Deafness and Other Communication Disorders. This study was performed in accordance with the PHS Policy on Humane Care and Use of Laboratory Animals, the NIH *Guide for Care and Use of Laboratory Animals*, and the Animal Welfare Act (7 U.S.C. et seq.); the animal use protocol was approved by the Institutional Animal Care and Use Committee (IACUC) of the University of Wisconsin.

Presented at the meeting of the American Laryngological Association, Orlando, Florida, May 4-5, 1996.

CORRESPONDENCE — Katsuhide Inagi, MD, University of Wisconsin Clinical Science Center H4/310, 600 Highland Ave, Madison, WI 53792.

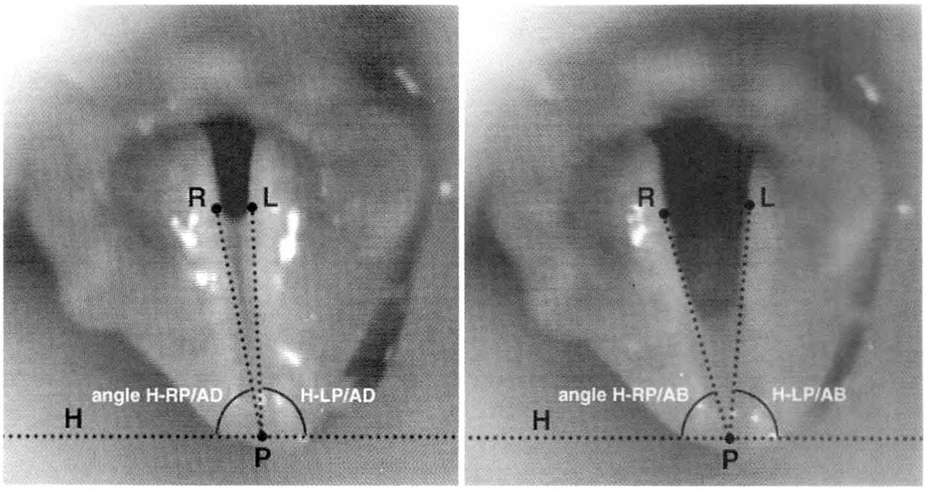

Fig 1. Digitized glottal images of videostroboscopic recordings. Angle H-RP/AD was 81.2, angle H-LP/AD was 91.5, angle H-RP/AB was 71.9, and angle H-LP/AB was 85.6. Movement angle of right vocal fold was 9.3, and that of left vocal fold was 5.9.

larynges. The use of a rat laryngeal model has greatly improved our ability to investigate the efficacy of BT therapy. This convenient animal model should prove helpful in developing a rational basis for treatment decisions in humans.

MATERIALS AND METHODS

This pilot study was designed to determine if the interval between repeated BT injections influenced the physiologic and histologic effects on laryngeal muscles. The physiologic measurements included digitized videomicroscopic recording of vocal fold movement and EMG. The histologic measurements included muscle fiber size and digitized optical density of laryngeal muscle after glycogen depletion by electrical stimulation. These studies evaluated both morphological and functional changes induced by BT injection.

Animals. Nine adult male Sprague-Dawley rats weighing between 425 and 534 g (458.8 ± 31.1 g) were used for this study. Rats were anesthetized with ketamine hydrochloride (48 mg/kg) and xylazine hydrochloride (4 mg/kg) by intraperitoneal injection each experimental day (three times per week: Monday, Wednesday, and Friday). They were grouped by the time interval between the initial injection and the second injection; the groups were control (no second injection, n = 1), 1-week (7 days after initial injection, n = 2), 2-week (n = 2), 4-week (n = 2), and 6-week (n = 2).

Botulinum Toxin Injection Method. Freshly prepared crystalline complex (30 units per nanogram) BT (type A) was diluted with sterile saline to a dosage of 0.007 unit in a volume of 0.4 μL. Diluted toxin was precisely injected unilaterally into the region of the thyroarytenoid muscle at the middle portion of the vocal fold by means of a 5-μL syringe with a 26-gauge, 50-mm needle by a microlaryngoscopic technique. The side (left, right) of initial injection was randomly chosen. The second injection was given via the same methods and same side as the initial injection. For the control rat, 0.4 μL saline was injected in the right vocal fold on the initial injection day only.

Laryngoscopy and Videoendoscopy. Each anesthetized rat was secured on a custom-designed operating platform in a nearly vertical position with the mouth secured open. The customized laryngoscope was inserted orally and adjusted to provide the best view of the larynx obtainable via an operating microscope (Zeiss, Thornwood, NY). The operating microscope was connected to the video equipment with a C-mount and a microcamera (Circon Zimmer, Santa Barbara, Calif) that allowed us to view and record the larynx simultaneously. All rat vocal fold movements were recorded at the same magnification (21×). Recordings were made at the time of each injection, and objective measurements were obtained from digitized glottal images of videostroboscopic recordings (Fig 1). Two glottal frames, selected for each rat, consisted of the images of full adduction and full abduction of respiration. Four reference points were determined for each glottal frame: the posterior commissure (point P), an absolutely horizontal line (line H) at point P, and the edges of the right (point R) and left (point L) vocal folds at 2 mm from point P. The lateral angles between line H and line RP (angle H-RP) or LP (angle H-LP) in each glottal frame (adduction and abduction) were measured. "Movement angles" of the right and left vocal folds were calculated by measuring the difference between angle H-RP in the adduction frame and angle H-RP in the abduction frame, and between angle H-LP in the adduction frame and angle H-LP in the abduction frame. All measurements were performed with Image 1.59 software (US Department of Health and Human Services, National Institutes of Health, Be-

TABLE 1. RATING CRITERIA OF INTERFERENCE PATTERN

	Interference Pattern	
Grade	*Gaps*	*Amplitude*
0	None	0
1	Many	Much reduced
2	Few	Little reduced
3	None	Good (equal to that of intact side)

Interference pattern was graded on scale of 0 to 3.

thesda, Md) and a Macintosh II fx computer (Apple, Cupertino, Calif). The number of days required to return to preinjection movement was calculated.

Electromyography. Electromyographic sampling of the thyroarytenoid muscle was performed on a Nicollet Viking electromyograph (Mound, Minn) with a 50-mm, 26-gauge monopolar needle electrode and a monopolar subcutaneous reference electrode. Filter settings of 20 Hz to 10 kHz and a sweep speed of 10 milliseconds per division were used. Display sensitivity of 50 µV per division was used for interference pattern analysis. The most complete interference pattern from the thyroarytenoid muscle was obtained by manipulation of the electrode within the muscle to maximize high-frequency content and amplitude. Samples were taken before the first injection, then every 2 to 3 days until 70 days after the second injection. The time required to return to preinjection levels of interference was calculated. Interference pattern measurements were made by two judges. One was blinded to the injected dosage and volume. Interference patterns were semiquantitatively graded from 0 to 3 (Table 1). Judgments of EMG measurements were made by comparing measurements made prior to injection and measurements made on the contralateral side. A greater interference response indicated greater muscle fiber activity.

Histology. All surviving rats underwent surgery under anesthesia to isolate both recurrent laryngeal nerves on day 70 after the second injection. The isolated nerves were stimulated by bipolar stimuli for 20 minutes at 700 µA and 10 Hz, to achieve glycogen depletion in the intrinsic laryngeal muscles. Tracheotomy was performed to preserve ventilation during this procedure. All rats were then painlessly sacrificed by intracardiac injection of 7.5% chloral hydrate. Their larynges were immediately excised and frozen in liquid nitrogen. The frozen larynges were sectioned in the coronal plane continuously by cryostat at a thickness of 40 µm from the anterior edge of the thyroid cartilage to the posterior surface of the cricoid cartilage. The frozen block was then remounted to slice the posterior cricoarytenoid muscle transversely. Sections were air-dried for 20 minutes. They were fixed in Histochoice (Amresco, Solon, Ohio) for 5 minutes and washed in double-distilled water for 30 seconds.

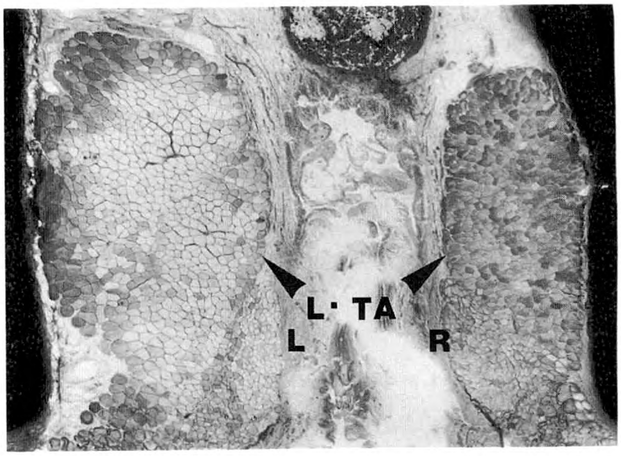

Fig 2. Mean actual optical density of lateral thyroarytenoid (L-TA) muscle was 64.5 pixels on right (R) and 33.0 pixels on left (L) side after glycogen depletion and periodic acid–Schiff staining in 6-week group. Right lateral thyroarytenoid muscle was smaller than left.

Muscle fiber size was determined as the area and perimeter of the lateral thyroarytenoid muscle on both the injected and uninjected sides. The lateral thyroarytenoid muscle was divided into five parts: superior, median, inferior, lateral, and central. Measurement areas that were limited by the microscopic objective magnification (10×) were randomly chosen in each part. All muscle fibers in the field were measured and their areas and perimeters digitized.

The optical density of the muscles was determined on samples immediately adjacent to sections used to measure fiber size. Fibers were stained by the periodic acid–Schiff (PAS) method. Sections washed of fixation solution were incubated in 1% periodic acid solution for 10 minutes and then washed with double-distilled water for 5 minutes with a water change after the first 2 minutes. Then the sections were stained with Schiff reagent (Fisher Scientific, Fair Lawn, NJ) for 10 minutes and washed in 0.5% sodium metabisulfite three times for 2 minutes each. Slides were dehydrated and covered. Optical densities as gray scales ranging from 0 to 256 pixels (Fig 2) were digitized with a microscope (Leitz Wetzlar, Germany) connected to the computer (Macintosh II fx) with software (Image 1.59) with a C-mount and a CCD camera (CCD 72, Dage MTI, Michigan City, Ind). The whole area of the lateral thyroarytenoid muscle in coronal section at the level of the anterior third of the muscle was selected for measurements, and each measurement was performed three times under the same magnification (2.5×) and same power

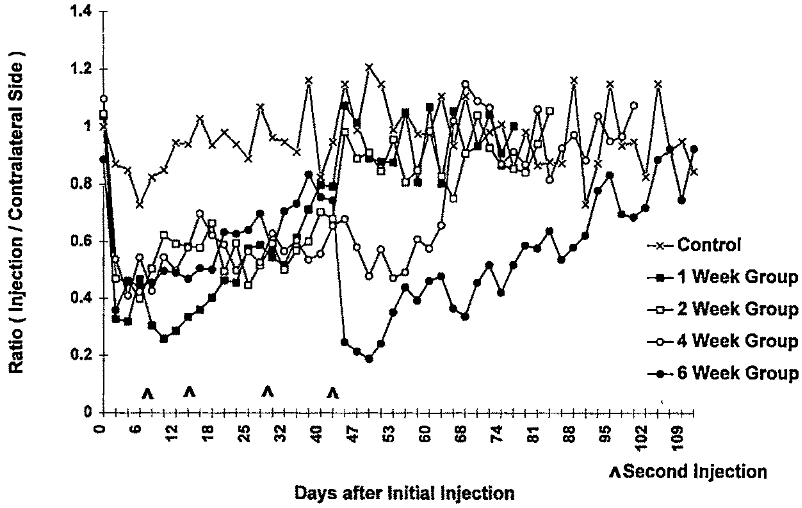

Fig 3. Longitudinal observation of mean vocal fold movement ratio in each subject group. Reductions of vocal fold movement induced by botulinum toxin with repeated injection in 1-week and 6-week groups were evident.

of the light source. To minimize error due to the light source, we calibrated the source by absolute optical density using Photographic Step Tablet No. 2 (Kodak, Rochester, NY) before and after each measurement.

Data Analysis. Of the nine rats, one in the 4-week group died on day 39 after the initial injection (day 11 after second injection), apparently from an anesthesia-related cause. The remaining eight rats were all observed for 70 days following the second injection.

Measurements of vocal fold movement, muscle fiber area and perimeter, and optical density were analyzed as ratios of the injection side to the contralateral side. Use of these ratios reduced errors due to associated confounding factors such as the anesthetic condition of the rats, recurrent laryngeal nerve stimulation conditions, histologic stain variability, and artifacts.

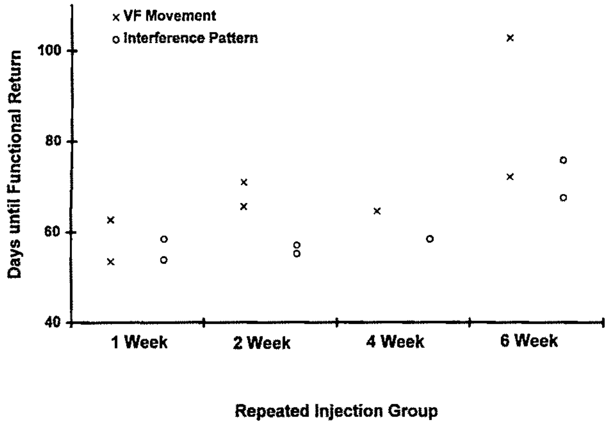

Fig 4. Duration of effect (objective vocal fold [VF] movement and interference pattern). Subject groups were positively correlated with time to recover function of vocal fold movement (p = .012). Overall ANOVA was not quite significant (p = .073). Significant pairwise differences were shown between 6-week group and 1-week group (p = .030) and between 6-week group and 2-week group (p = .030).

The duration of the BT effect was defined as the time required to recover 100% of the preinjection status for the measurements of interference pattern and vocal fold excursion, as predicted from linear regression.

The cross-product ratio of the change after the second injection (postinjection divided by preinjection) to the change after the initial injection (postinjection divided by preinjection) of the vocal fold movement ratio was used for assessing the effect of BT. Preinjection data for the initial injection were obtained on the day before injection. All data gathered within 7 days before the second injection were used as second preinjection data. All measurements made within 7 days after the initial and second injections were used for the postinjection data.

Spearman rank correlation analysis was used to examine the relation between all measurements and the second injection groups. A correlation (rs) was considered significant at $p < .05$. If the Spearman rank correlation analysis for any group was significant, that group was further examined by comparing all pairs of means with Fisher's Protected Least Significant Difference Procedure.[15] All testing was done at the nominal 5%, and the reported p values control the comparison-wide type I error rate within each dependent variable. Interjudge agreement on subjective assessments of change was evaluated.

RESULTS

Vocal Fold Movement. The longitudinal observations of the mean vocal fold movement ratio in each group are shown in Fig 3. The length of time needed to recover preinjection vocal fold movement ranged from 53.4 days in the 1-week group to 102.7 days in the 6-week group (Fig 4). The time needed to re-

TABLE 2. CROSS-PRODUCT RATIO OF PREINJECTION AND POSTINJECTION CHANGES OF VOCAL FOLD MOVEMENT RATIO

	Repeated-Injection Groups			
Rat	*1-Week*	*2-Week*	*4-Week*	*6-Week*
1	0.505	0.385	0.374	1.23
2	0.972	0.470	0.463	2.00

Only 6-week group showed that effect of botulinum toxin induced by second injection was stronger than effect induced by initial injection.

cover function was positively correlated (p < .012) with the group. The 6-week group needed over 19 days on average more than any other group to recover preinjection vocal fold movement, but this was not significant. The cross-product ratio of the change in the vocal fold movement ratio between preinjection and postinjection periods is shown in Table 2. Only the 6-week group showed an effect of the second injection that was stronger than that of the initial injection. Although the overall ANOVA was not significant (p = .056), significant pairwise differences were shown between the 6-week group and the 2-week group (p = .020) or the 4-week group (p = .020).

Electromyography. Time needed to recover to preinjection interference activity of muscle fibers ranged from 55.1 days in the 2-week group to 75.8 days in the 6-week group. Both rats in the 6-week group needed longer to recover muscle fiber function than rats in any other group. Although the overall ANOVA was not significant (p = .073), significant pairwise differences were shown between the 6-week group and the 1-week group (p = .030) or the 2-week group (p = .030; Fig 4).

Muscle Fiber Size. The ratio of the mean muscle fiber area of the lateral thyroarytenoid muscle ranged from 0.995 in the 4-week group to 0.801 in the 6-week group (Fig 5). The mean muscle fiber area ratio was negatively correlated (p = .046) to the interval between injections. The mean muscle fiber perimeter ratio also showed a negative correlation; there was a stronger (p = .01) correlation between the perimeter ratio and the subject groups than between the area ratio and the groups (Fig 5). Although the overall ANOVA was not significant (p = .11), some groups showed significant pairwise differences. The perimeter ratio of the 6-week group was significantly smaller than those of the 1-week (p = .04) and 2-week (p = .04) groups.

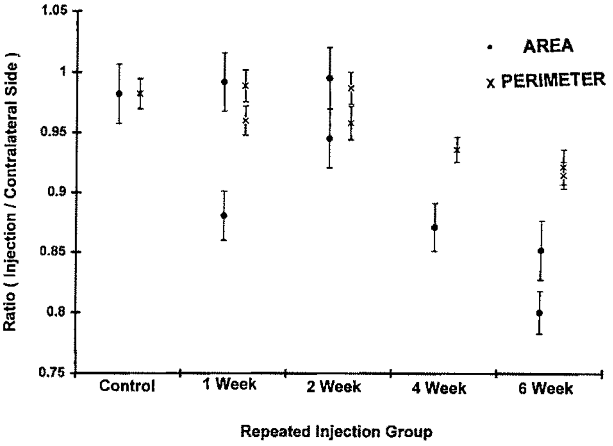

Fig 5. Muscle fiber area and perimeter ratio (lateral thyroarytenoid muscle). Intervals between repeated injections were significantly correlated to mean muscle fiber area ratios (p = .046) and mean muscle fiber perimeter ratios (p = .01). Although overall ANOVA was not quite significant (p = .11), perimeter ratio of 6-week group was significantly smaller than those of 1-week (p = .04) and 2-week (p = .04) groups.

Optical Density. The ratios of the injection side to the contralateral side for optical density measurements of the lateral thyroarytenoid muscle were significantly correlated (p < .01) to the interval between injections (Fig 6). The optical density ratios of the two rats in the 6-week group were 1.55 and 1.75 — higher than those of any other rats. Although the overall ANOVA was not significant (p = .099), some

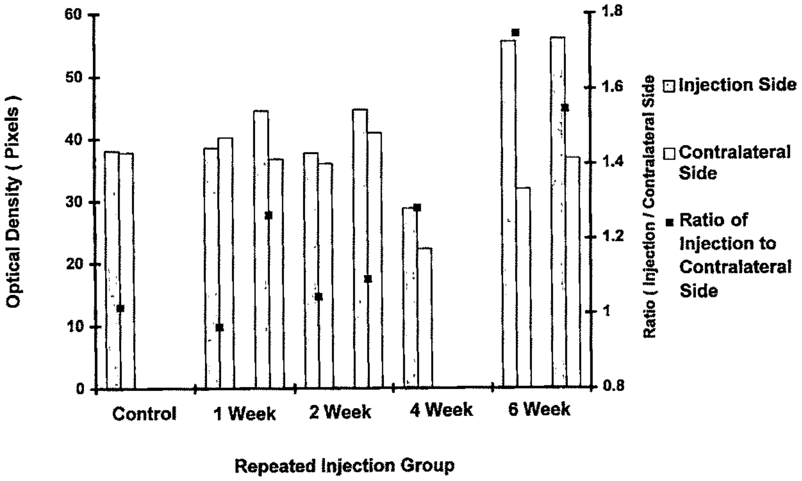

Fig 6. Ratios of injection side to contralateral side regarding optical density measurements of lateral thyroarytenoid muscle were significantly (p < .01) correlated to injection intervals of subject groups. Although overall ANOVA was not quite significant (p = .099), 6-week group had significantly higher optical density ratios than 1-week group (p = .037) and 2-week group (p = .030). Actual measurements of mean optical density of injection side revealed significant (p = .044) differences between groups. Mean optical density of 6-week group was significantly higher than those of other groups.

TABLE 3. COMPARISON BETWEEN SINGLE AND REPEATED INJECTIONS IN TIME TO 100% FUNCTIONAL RETURN

		Repeated Injection			
Functional Measure	*Single Injection*	*1-Week*	*2-Week*	*4-Week*	*6-Week*
Vocal fold movement	52.7	55.7	54.5	60.6	82.1
Interference pattern	57.0	56.1	56.0	58.4	71.7

Time (in days) needed to recover preinjection status for measurements of interference pattern and vocal fold movement were compared between single botulinum toxin injection (preliminary study[14]) and subject groups.

groups showed significant pairwise differences. The 6-week group had significantly higher optical density ratios than the 1-week group (p = .037) or the 2-week group (p = .030). Actual measurements of the mean optical density of the injection side revealed significant (p = .044) differences between the groups. The mean optical density in the 6-week group was 55.8 — significantly higher than the 38.1 in the control group (p = .031), the 41.5 in the 1-week group (p = .032), the 41.2 in the 2-week group (p = .030), or the 28.8 in the 4-week group (p = .010).

Inter-rater Agreement. Exact agreement was 88.6% (636/718), and agreement within one unit was 99.9% (717/718). Spearman rank correlation revealed significant interjudge correlation (r_s = .82, p = .001). These results indicate a fairly high degree of interjudge agreement.

DISCUSSION

This study was designed to investigate one of the variables that appears to have an impact on the efficacy of BT injections used in the treatment of SD. Although BT injection provides an effective means of symptom control in many patients with SD, the results are transient, and repeated injections are required to achieve adequate control of symptoms. Selection of appropriate dosage, volume, and placement of injectate is usually empirical, and based on the clinician's experience and subjective patient responses. The timing of intervals between injections varies, but decisions are usually patient-driven, with some patients waiting until symptoms are severe and others seeking treatment preemptively before symptoms recur. To develop a scientific basis for prescribing BT injection parameters, there is a need for an animal model that can be used to demonstrate the physiological and morphological consequences of altering treatment variables. Although dogs have been used extensively for laryngeal studies, the canine larynx is anatomically quite different from the human one, and in our ongoing comparative studies of larynges from other species, there does not appear to be an ideal model. We have found the rat convenient and useful in preliminary studies[13,14] investigating the effect of dosage, volume, and placement of BT on the magnitude and duration of effect. In this study, the same model is used to establish pilot data on the effect of the interval between injections on the physiologic and histologic changes induced by laryngeal injection of BT.

The methods employed are largely based on our prior BT studies[13,14] in the rat. *The dosage of 0.007 units in a volume of 0.4* µL was chosen because we had demonstrated that it was the lowest dosage and volume that produced the maximal duration of functional paresis without inducing complete paralysis or airway obstruction in the rat. The selection of the dosage was also an attempt to simulate the incomplete paresis that is typically achieved in the human for effective symptom control and minimal side effects. *The lateral thyroarytenoid muscle site for injection* was chosen because it is relatively constant, a large muscle in the rat, and composed of type II fibers. Further, in the human, the thyroarytenoid is the muscle most typically injected for control of adductor SD. *The intervals between the initial and repeated injections* were selected on the basis of linear regression analysis of our pilot data measuring the length of functional ablation from a single BT injection. We found that function was maximally reduced at 1 week postinjection; measurable recovery began to be noticed at 2 weeks, 50% return was noted at 4 weeks, and 75% to 80% at 6 weeks. Full return of vocal fold movement was evident at 52.7 days, and a complete return to preinjection interference patterns was noted on EMG at 57 days (Table 3[14]). We chose to study intervals in the period between maximal functional ablation and the recovery of 75% to 80% of function.

Our preliminary studies indicated a need to control for the mechanical effect of needle insertion in addition to other variables associated with the procedures in this experiment. It also was apparent that repeated insertion of the EMG electrodes caused some scar formation in the laryngeal muscles of the rat. Longitudinal observations of vocal fold excursion revealed some decrease bilaterally that might be ascribed to such changes. To prevent such factors from affecting the data in this study, we elected to employ the concept of ratios. The injected side was compared to the noninjected side, and the difference expressed as a ratio. In this fashion, the common events occurring due to repeated anesthesia inductions and bilateral needle insertions were accounted for by having each rat serve as its own control.

The results of this study indicate a relationship between the interval between injections and the magnitude of the BT injection effect. Although there was little difference noted among the 1-week, 2-week, and 4-week groups, the 6-week interval group demonstrated a distinctly prolonged time to recovery as shown by measurements of vocal fold movement and interference pattern. This difference was corroborated by the prolonged absence of glycogen depletion capability evident on the significantly greater optical densities of the PAS-stained 6-week group compared to all other groups and the controls. Histologic studies also showed a much greater degree of morphological alteration in the 6-week group, as reflected in reduced muscle fiber area and perimeter ratios.

It is not possible to extrapolate these data directly to provide a formula for treating humans with BT. These findings, however, provide a segment of the scientific matrix that might be used in developing a more rational approach to treatment. It appears that short intervals between injections (before evidence of 50% functional recovery) may not produce as prolonged a functional BT effect as somewhat longer intervals. However, as we did not study injection intervals longer than 6 weeks (at which time functional recovery was about 80%), it is possible that the optimal interval is even longer.

The relative ineffectiveness of short interinjection intervals in producing a prolonged functional ablation might be due to the relative efficacy of BT in blocking acetylcholine release at the neuromuscular junction of muscles that have progressed further in the reinnervation process.[16,17] The association of terminal axonal sprouting with reinnervation was evident in our studies (unpublished) using rat gastrocnemius muscle, wherein we observed sprouting beginning 2 weeks after BT injection. More time is probably required for these sprouts to develop functional end plates and thus end the myoneural blockade of the muscle fiber. The resumption of myoneural junction function should be associated with a decrease in fibrillations and improvement of the interference pattern. In a previous study,[14] we found that after a single BT injection of the rat thyroarytenoid muscle using the same dosage as in this study, fibrillations were maximally present within 1 week and were absent after 3 weeks. The interference pattern was maximally depressed at 1 week and returned to baseline by approximately 7 weeks. These data suggest that many axonal sprouts have established functional reconnection between 3 and 7 weeks postinjection. It is possible that BT injected within a short interval after the initial injection might be metabolized or denatured without binding to the target axon because the binding sites are occupied. After the axonal sprouts have established functional reconnection or, alternatively, when the BT is metabolized within the presynaptic axon terminal, the neuromuscular junctions might be more vulnerable to a second injection. Repeating the injection at shorter intervals might not create a greater effect than would simply combining the dosage of the two injections into a single injection.

In addition to the restoration of myoneural junction function, the reestablishment of muscle fiber diameter and strength may play a role in determining the optimal interval. In order to maximally prolong the desired weakness in patients receiving multiple BT injections, it may be important to reinject the muscle after myoneural junction function has been restored, but before muscle atrophy has been reversed. In this study, muscle fiber circumference was smallest in the group reinjected at 6 weeks. Further study using longer interinjection intervals will be needed to determine the optimal interval.

One of the problems with this study is the small number of rats used in each experimental group. This is largely due to our inability to garner sufficient funding to support more comprehensive studies, for there is scientific skepticism about the use of the rat for such studies. Such skepticism is in part methodological, but should be dispelled by this study and our other pilot experiments demonstrating the feasibility of assessing the effects of BT injection in the rat larynx by means of customized videoendoscopy, digitized measures of vocal fold excursion, EMG assessment of interference patterns, and quantification of glycogen depletion with PAS staining and optical density determinations. The other issue is whether this physiological and morphological information is valid in the human. Clearly, there is not an anatomic correlation. That, however, can also be said of canine experiments, which have gained acceptance largely because of the convenience of working with a larger animal model. Increasing numbers of studies with the rat larynx have improved our understanding of its anatomy and physiology; some analogies in fiber types of the different muscle groups and functional correlates are intriguing. We propose that further use of this rat laryngeal model might shed light on basic questions about BT metabolic action in laryngeal muscles and provide an approach to correlating our knowledge about the role of sprouting and morphological changes with neuromuscular functional changes induced by intralaryngeal BT injections.

CONCLUSION

It appears that the interval between initial and subsequent BT injections does affect the physiological and morphological changes induced by the toxin. These changes include decreased vocal fold excursion, loss of the normal EMG interference pattern, and failure to deplete glycogen stores with prolonged stimulation as measured by the optical density of poststimulation PAS-stained lateral thyroarytenoid muscle. There was little enhancement of effect when repeat injections were given at 1 to 4 weeks, but those rats receiving their second injection at 6 weeks exhibited a markedly heightened response. Further study with this rat laryngeal model would be useful in achieving a greater understanding of the mechanisms of action of BT in the larynx and in developing methods to enhance laryngeal denervation and delay undesirable reinnervation.

ACKNOWLEDGMENTS — The authors thank Celeste Kirk for editorial assistance, Joan Kozel for illustrations, and the staff of the University of Wisconsin vocal function laboratory, including Bridget Berning, Kelly Cavanaugh, Kelle Hasenberg, Darin Johnson, Carrie Nachtwey, Linda Suckow, Jennifer Waldron, and Jane Zernicke, for their continuous help throughout this project.

REFERENCES

1. Miller RH, Woodson GE, Jankovic J. Botulinum toxin injection of the vocal fold for spasmodic dysphonia. Arch Otolaryngol Head Neck Surg 1987;113:603-5.

2. Ludlow CL, Naunton RF, Sedory SE, Schulz GM, Hallett M. Effect of botulinum toxin injections on speech in adductor spasmodic dysphonia. Neurology 1988;38:1220-5.

3. Brin MF, Blitzer A, Fahn S, Gould W, Lovelace RE. Adductor laryngeal dystonia (spastic dysphonia): treatment with local injections of botulinum toxin (Botox©). Mov Disord 1989; 4:287-96.

4. Blitzer A, Brin MF, Fahn S, Lovelace RE. Localized injections of botulinum toxin for the treatment of focal laryngeal dystonia (spastic dysphonia). Laryngoscope 1988;98:193-7.

5. Truong DD, Rontal M, Rolnick M, Aronson AK, Mistura K. Double-blind controlled study of botulinum toxin in adductor spasmodic dysphonia. Laryngoscope 1991;101:630-4.

6. Ludlow CL, Bagley J, Yin SG, Koda J. A comparison of injection techniques using botulinum toxin injection for treatment of the spasmodic dysphonias. J Voice 1992;6:380-6.

7. Maloney AP, Morrison MD. A comparison of the efficacy of unilateral versus bilateral botulinum toxin injections in the treatment of adductor spasmodic dysphonia. J Otolaryngol 1994;23:160-4.

8. Adams SG, Hunt KG, Charles DA, Lang AE. Unilateral versus bilateral botulinum toxin injections in spasmodic dysphonia: acoustic and perceptual results. J Otolaryngol 1993;22: 171-5.

9. Zwirner P, Murray T, Woodson GE. A comparison of bilateral and unilateral botulinum toxin treatments for spasmodic dysphonia. Eur Arch Otorhinolaryngol 1993;250:271-6.

10. Inagi K, Ford CN, Bless DM, Heisey D. An analysis of factors affecting botulinum toxin results in spasmodic dysphonia. J Voice 1996;10:306-13.

11. Cohen SR, Thompson JW. Use of botulinum toxin to lateralize true vocal cords: a biochemical method to relieve bilateral abductor vocal cord paralysis. Ann Otol Rhinol Laryngol 1987;96:534-41.

12. George EF, Zimbler M, Wu B-L, Biller HF, Sanders I. Quantitative mapping of the effect of botulinum toxin injections in the thyroarytenoid muscle. Ann Otol Rhinol Laryngol 1992;101:888-92.

13. Inagi K, Schultz E, Ford CN. An anatomical study of the rat larynx: establishing the rat model for neuromuscular function. Otolaryngol Head Neck Surg (in press).

14. Inagi K, Rodriquez AA, Ford CN, Heisey DM. Transoral electromyographic recordings in botulinum toxin–injected rat larynges. Ann Otol Rhinol Laryngol 1997;106:956-64.

15. SAS/STAT User's Guide Version 6. 4th ed. Vol 2. Cary, NC: SAS Institute Inc, 1989.

16. Borodic GE, Ferrante RJ, Pearce LB, Alderson K. Pharmacology and histology of the therapeutic application of botulinum toxin. 1st ed. New York, NY: Marcel Dekker, 1994:119-57.

17. Cichon JV, McCaffrey TV, Litchy WJ, Knops JL. The effect of botulinum toxin type A injection on compound muscle potential in an in vivo rat model. Laryngoscope 1995;105:144-8.

Ann Otol Rhinol Laryngol 106:1997

UTILITY OF HELICAL COMPUTED TOMOGRAPHY IN THE STUDY OF ARYTENOID DISLOCATION AND ARYTENOID SUBLUXATION

ALBERT E. ALEXANDER, JR, MD
GEORGE D. LYONS, MD
MARY A. FAZEKAS-MAY, MD
PETER L. RIGBY, MD
DANIEL W. NUSS, MD
LISA DAVID, MD
KEVIN WILLIAMS
NEW ORLEANS, LOUISIANA

Conventional computed tomography (CT) has been considered a mainstay in the evaluation of the larynx. A major difficulty with utilizing this modality, especially in the study of the arytenoid, is the time necessary to perform a thin-slice examination through a structure that has a propensity to move with respiration and swallowing. Helical CT not only significantly reduces the time necessary to study the larynx, but enables one to perform multiple high-resolution multiplanar reconstructions. Eleven patients with arytenoid abnormalities documented by strobovideolaryngoscopy or direct laryngoscopy were imaged with helical CT. A comprehensive radiographic examination illustrating the cricoarytenoid relationship in all of the subjects was completed in less than 20 seconds by using axial reconstructions in 2-mm-thick slices at 1-mm intervals, with subsequently derived sagittal and coronal reconstructions. Helical CT may be a useful adjunct in the diagnosis of arytenoid subluxation or dislocation.

KEY WORDS — arytenoid cartilage, helical computed tomography.

INTRODUCTION

The purpose of this study is to demonstrate the extensive radiographic examination of the cricoarytenoid relationship that is possible with helical computed tomography (HCT) and to show that a better three-dimensional conceptualization of arytenoid subluxation (AS) or arytenoid dislocation (AD) can be made by utilizing multiplanar image reconstruction algorithms.

An abnormal cricoarytenoid relationship can result from intubation or neck trauma and is probably more common than is generally recognized.[1,2] A timely evaluation of the status and cause of cricoarytenoid joint disease has tremendous implications for treatment and prognosis of voice restoration.

MATERIALS AND METHODS

Eleven adult patients with abnormalities of the cricoarytenoid joint diagnosed or suspected by strobovideolaryngoscopy (SVL) or direct laryngoscopy (DL) were imaged with HCT (Somatom Plus, Siemens Medical Systems, Erlangen, Germany) to confirm or clarify the disorder. Additional subject characteristics are found in the Table. Patients were in-

PATIENT CHARACTERISTICS

Patient	*Age*	*Sex*	*Cause*	*Chief Complaint*	*SVL or DL*	*Arytenoid Position*	*Side*
1	55	M	Cerebrovascular accident requiring intubation	Hoarseness	SVL, DL	Anterior	R
2	51	M	Intubation for cervical disc surgery	Dysphonia	SVL, DL	Posterior	L
3	46	M	Intubation for anterior cervical fusion	Hoarseness	SVL, DL	NR	R
4	54	F	Intubation for anterior cervical fusion	Hoarseness	DL	NR	R
5	55	F	Tracheotomy	NR	DL	Anterior	L
6	53	M	Intubation for back surgery	Dysphonia	SVL, DL	Vertical	L
7	NR	F	Intubation for cervical fusion	NR	SVL	Posterior	R
8	49	M	Intubation	Hoarseness	SVL, DL	Posterior	R
9	26	F	Intubation for cervical fusion	Hoarseness	SVL, DL	Posterior	R
10	63	F	Intubation for appendectomy	Dysphonia	SVL, DL	Posterior	L
11	69	M	Intubation for coronary artery bypass graft	Hoarseness	SVL, DL	NR	R, L

SVL — strobovideolaryngoscopy, DL — direct laryngoscopy, NR — not recorded.

From the Departments of Otolaryngology (all authors) and Radiology (Alexander), Louisiana State University Medical Center of New Orleans, New Orleans, Louisiana.

Presented at the meeting of the American Laryngological Association, Scottsdale, Arizona, May 10-11, 1997.

CORRESPONDENCE — Albert E. Alexander, Jr, MD, 1542 Tulane Ave, Rm 212, New Orleans, LA 70112.

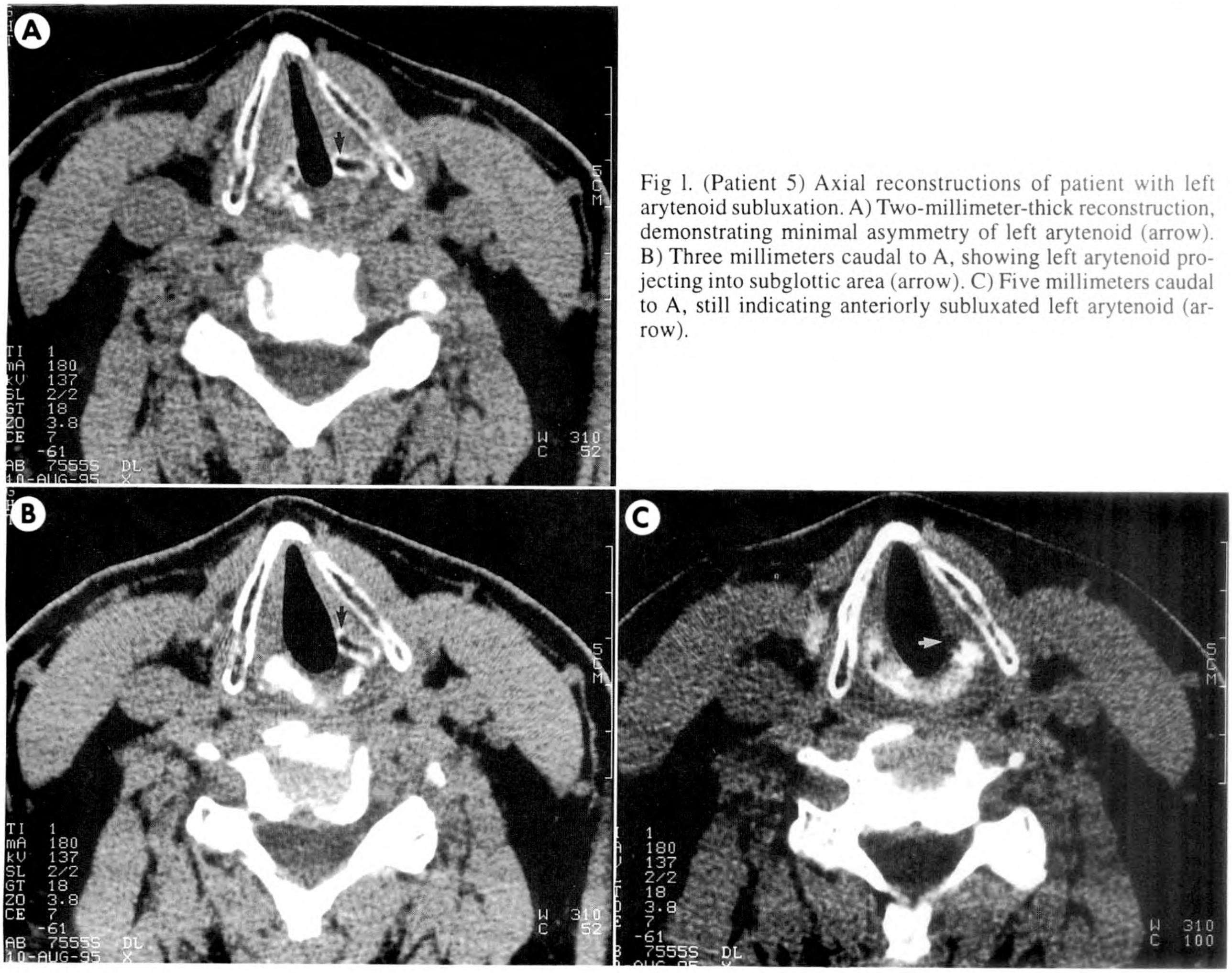

Fig 1. (Patient 5) Axial reconstructions of patient with left arytenoid subluxation. A) Two-millimeter-thick reconstruction, demonstrating minimal asymmetry of left arytenoid (arrow). B) Three millimeters caudal to A, showing left arytenoid projecting into subglottic area (arrow). C) Five millimeters caudal to A, still indicating anteriorly subluxated left arytenoid (arrow).

structed to breathe quietly during the study and not to swallow or cough during data acquisition. Helical data were acquired by using 2-mm collimation with a table feed of 2 mm/s for a pitch of 1.0 at 120 kV at 250 milliampere seconds. Each subject examination took approximately 16 to 20 seconds to complete. Two-millimeter-thick axial images were then reconstructed at 1-mm intervals. Nine sagittal and 9 coronal images were then generated from these axial data. This information was correlated with the findings of SVL or DL in all patients.

RESULTS

The arytenoids and the cricoarytenoid joint were consistently demonstrated on several of the overlapping thin axial reconstructions in each of the 11 patients. Asymmetry, as measured by bilaterally comparing the angles formed between the arytenoid and the back of the cricoid at the level of the vocal process, was noted on axial images in 9 of the 11 subjects. The minimal difference between right and left joints was 15°.

Occasionally, anterior tipping of the vocal process could be inferred from the axial data (Fig 1), as was the case in the 2 patients in whom axial asymmetry was not noted. High-quality sagittal (Fig 2) and coronal (Fig 3) reconstructions often were helpful in confirming or clarifying the complex arytenoid orienta-

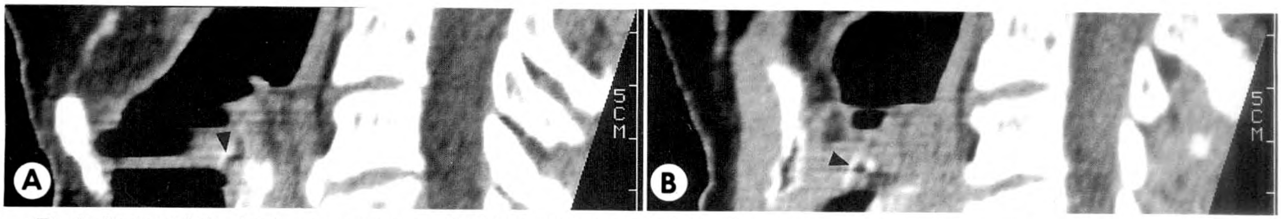

Fig 2. (Patient 5) Sagittal reconstructions. A) Illustrating normal right cricoarytenoid relationship and edge of true vocal cord (arrowhead). B) Demonstrating relative anterior tilting of abnormal left arytenoid (arrowhead). Compare with A.

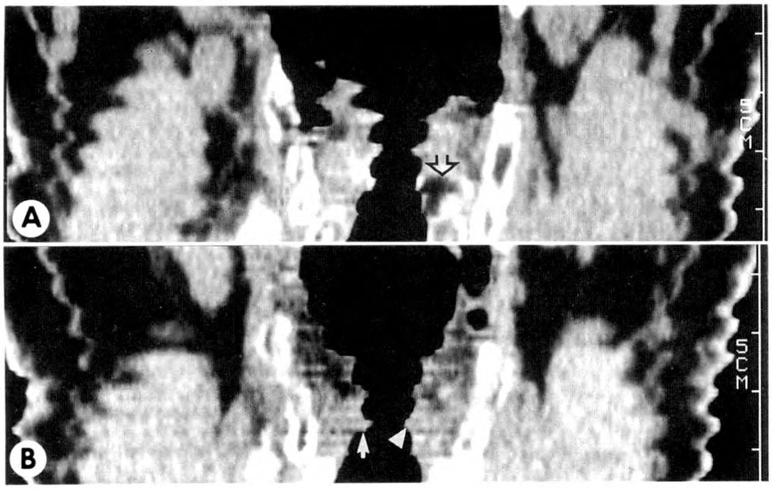

Fig 3. (Patient 5) Coronal reconstructions. A) Showing anteriorly positioned left arytenoid (open arrow). B) Anterior to A, demonstrating normal right subglottic configuration (arrow) and fullness in left subglottis (arrowhead) that represents caudally displaced true vocal cord.

tions possible in AS or AD.

DISCUSSION

The position of the arytenoid has been reported to be consistent on computed tomography (CT) as well as cadaveric specimens,[3,4] and although some authors suggest that small variations of the cricoid facet do exist from person to person and occasionally between the right and left joints,[5,6] these differences may be too small to detect endoscopically or with CT. Any visualized asymmetry of the cricoarytenoid joints, therefore, should be viewed with suspicion and may be the result of AS or AD, or may be secondary to recurrent laryngeal nerve (RLN) apraxia or RLN palsy.

The term AS is probably best used to refer to an abnormal relationship of the arytenoid to the cricoid when joint surfaces still make contact. Arytenoid dislocation is used to describe complete separation of the arytenoid and cricoid joint surfaces.[7] The vocal cord of the anteriorly subluxated or dislocated arytenoid is typically described as being placed inferior to the normal cord and medially rotated. Posterior AD or AS usually results in a superiorly positioned cord that is laterally rotated.[1] However, because the arytenoid is normally capable of sliding, rocking,[8] and some rotation,[1,6] the final position of the displaced arytenoid may involve a variety of configurations.

The configuration of the cricoarytenoid joint, glottis, and supraglottic regions in RLN palsy has been described.[3,9] Typically, there are various degrees of cord atrophy that may be associated with dilation of the ipsilateral pyriform sinus and a shallow, wide ventricle. The position of the arytenoid is usually described as paramedian.[3] However, the final position of the involved vocal cord may vary, depending on the cause of disease and its site along the course of the vagus nerve or its recurrent branch.[9] The arytenoid, therefore, may be seen in fixed adduction or abduction and may be tilted anteromedially.[3]

The spectrum of positions the arytenoid may take in AS or AD, and the overlapping appearances that are possible with RLN dysfunction, make the task of describing and assigning a cause for an asymmetric vocal process daunting. This is especially true when AS or AD coexists with an RLN apraxia or palsy.

Strobovideolaryngoscopy, laryngeal electromyography (EMG), and conventional CT have been described as major tools for evaluation of the cricoarytenoid relationship.[1,10] The subjects in this study all had SVL or DL and HCT instead of conventional CT.

Helical CT differs significantly from conventional CT in that the x-ray source-detector array of helical CT continuously circles the patient as he or she is moved through the gantry for a predetermined distance and at a predetermined speed. The x-ray tube, therefore, proscribes a helix relative to the patient.

Scanning time through the larynx is substantially reduced with helical CT, because x-ray attenuation data are collected continuously rather than in the "stop-and-shoot" fashion of conventional CT. Short scan times, in turn, reduce the possibility of motion contamination and resulting spatial misregistration that would occur if the patient swallowed or coughed during the critical imaging process. An additional advantage of helical scanning is that because the attenuation data are collected as a volume through the area of interest, one is able to arbitrarily and retrospectively reconstruct two-dimensional images in any position, at any interval, with or without overlap, ensuring a complete pictorial display of small anatomic parts, including the arytenoids. Overlapping axial two-dimensional images are in turn utilized to reconstruct high-quality sagittal and coronal projections.[11,12]

The intensive interrogation of the cricoarytenoid relationship in the axial plane is the greatest advantage of HCT. Some asymmetry of the arytenoid, whether it was medial-lateral rotation or anterior-posterior tilting, was ultimately detected in all of the subjects in this study by evaluating and comparing the patient's two vocal processes on multiple axial images.

In conclusion, the arytenoid may assume a large variety of positions in AS, AD, RLN apraxia, and palsy. The status and cause of an abnormal cricoarytenoid relationship can usually be ascertained by SVL and EMG. Helical CT may provide an alternate and inexpensive way to evaluate this area if the clinical evaluation of the larynx is compromised by swollen tissue, or if expertise or availability of SVL and EMG is limited. Serial HCT imaging of arytenoid abnormalities may help quantify therapy and provide additional follow-up documentation of this complex entity.

REFERENCES

1. Sataloff RT, Bough ID Jr, Spiegel JR. Arytenoid dislocation: diagnosis and treatment. Laryngoscope 1994;104:1353-61.

2. Roberts D, McQuinn T, Beckerman RC. Neonatal arytenoid dislocation. Pediatrics 1988;81:580-2.

3. Agha FP. Recurrent laryngeal nerve paralysis: a laryngographic and computed tomographic study. Radiology 1983; 148:149-55.

4. Mave WM, Dickson DR. Cartilages and ligaments of the adult human larynx. Arch Otolaryngol 1971;94:432-9.

5. Sellars IE, Dip TP, Keen EN. The anatomy and movements of the cricoarytenoid joint. Laryngoscope 1978;88:667-74.

6. Sellars I, Sellars S. Cricoarytenoid joint structure and function. J Laryngol Otol 1983;97:1027-34.

7. Close LG, Merkel M, Watson B, Schaefer SD. Cricoarytenoid subluxation, computed tomography and electromyography findings. Head Neck Surg 1987;9:341-8.

8. von Leden H, Moore P. The mechanics of the cricoarytenoid joint. Arch Otolaryngol 1961;73:63-72.

9. Jacobs CJM, Harnsberger HR, Lufkin RB, Osborn AG, Smoker WRK, Parkin JL. Vagal neuropathy: evaluation with CT and MR imaging. Radiology 1987;164:97-102.

10. Hoffman HT, Brunberg JA, Winter P, Sullivan MJ, Kileny PR. Arytenoid subluxation: diagnosis and treatment. Ann Otol Rhinol Laryngol 1991;100:1-9.

11. Brink JA, Heiken JP, Wang G, McEnery KW, Schlueter FJ, Vannier MW. Helical CT: principles and technical considerations. Radiographics 1994;14:887-93.

12. Kalender WA. Technical foundations of spiral CT. Semin Ultrasound CT MR 1994;15:281-9.

≈

17TH UICC INTERNATIONAL CANCER CONGRESS

The 17th UICC International Cancer Congress will be held August 24-28, 1998, in Rio de Janeiro, Brazil. For information, contact CERTAME, Av. Presidente Wilson, 164/9° andar, CEP 20030-020, Rio de Janeiro, RJ, Brasil; telephone (021) 220-3386; fax (021) 240-8195.

Ann Otol Rhinol Laryngol 106:1997

BASALOID SQUAMOUS CELL CARCINOMA OF THE LARYNX AND HYPOPHARYNX

ALFIO FERLITO, MD
UDINE, ITALY
ALESSANDRA RINALDO, MD
PADUA, ITALY

GIUSEPPE ALTAVILLA, MD
PADUA, ITALY
CLAUDIO DOGLIONI, MD
BELLUNO, ITALY

Basaloid squamous cell carcinoma (BSCC) is a recently described bimorphic variant of squamous cell carcinoma with distinct morphological and biological features. We describe the clinicopathological findings, along with immunohistochemical and ultrastructural investigations, in 15 new cases of BSCC of the larynx or hypopharynx observed and treated at the otolaryngology department of the University of Padua between 1989 and 1995. The world literature is also reviewed in order to develop a more accurate clinicopathological profile of the tumor. Patient records and histologic slides were reviewed in all of our 15 cases. The patient group consisted of 13 men (86.67%) and 2 women with a mean age of 63.33 years (median 69 years; range 44 to 84 years). Nine patients presented with cervical lymph node metastases. Surgical treatment was the therapy of choice; radiotherapy and chemotherapy have been applied in different combinations. Follow-up was available on all 15 cases. Local recurrence was described in 3 cases. Five of the 9 patients with cervical lymph node metastases developed distant metastases. Distant spread of the tumor without lymph node involvement was observed during follow-up in 4 cases. Nine patients died of disease, 2 are alive with widespread metastases, 2 are alive with no evidence of disease, and 2 have died of other causes. The determined 5-year survival was estimated to be 17.5% by the Kaplan-Meier method. In conclusion, BSCC is a distinctive carcinoma that is important to recognize, because it has a more aggressive biological behavior than conventional squamous cell carcinoma.

KEY WORDS — basaloid squamous cell carcinoma, electron microscopy, immunohistochemistry, laryngeal neoplasms, pathology, prognosis.

INTRODUCTION

Basaloid squamous cell carcinoma (BSCC) is a bimorphic variant of squamous cell carcinoma (SCC) with distinct morphological and biological features. The term was first used by Wain et al[1] in 1986. They reported 10 cases occurring in the tongue, hypopharynx, and larynx and stressed that this tumor was a distinct, previously undescribed histopathological entity. The World Health Organization has recognized this tumor.[2] It has a predilection for the upper aerodigestive tract, though it has been described in other locations such as the esophagus,[3] trachea,[4] lung,[5-7] uterine cervix,[8] and anal canal.[9] This report describes the clinicopathological findings in 15 new cases of BSCC of the larynx and hypopharynx and evaluates the behavior and natural history of this recently recognized neoplasm.

MATERIALS AND METHODS

Fifteen cases of BSCC from laryngeal and hypopharyngeal sites were observed and treated at the otolaryngology department of the University of Padua between 1989 and 1995. The available medical records on each patient were reviewed for the following data: age at diagnosis, sex, site of origin, stage at presentation, evidence of nodal or distant metastasis, therapy, recurrence, and disease status at last

TABLE 1. SPECIFICITY, SOURCE, AND WORKING DILUTION OF ANTIBODIES USED IN THIS STUDY

Specificity	*Antibodies*	*Source*	*Dilution*
CK 8	Cam 5.2	Becton-Dickinson	1/20
CK 1-8, 10, 14, 15, 16, 19	AE1/AE3	Ortho	1/200
Vimentin	V9	Dako	1/10
Vimentin	VIM 9	Sanbio	1/10
Vimentin	VIM 13-2	Progen	1/50
Chromogranin A	LK10H2	Hybritec	1/100
Synaptophysin	SY38	Boehringer	1/20
S-100 protein	S100	Dako	1/5,000
Alpha smooth muscle actin	1A4	Sigma	1/5,000
Collagen IV	CIV22	Dako	1/100
Epidermal growth factor receptor	31G7	Triton	1/10
p53	DO7	Dako	1/200
Ki-67	MIB1	Immunotech	1/300
c-erbB-2	CB11	Novocastra	1/200

From the Departments of Otolaryngology (Ferlito, Rinaldo) and Pathology (Altavilla), University of Padua, Padua, and the Division of Pathology, Belluno Hospital, Belluno (Doglioni), Italy. Supported by The Laryngeal Cancer Association, Italy.

Presented at the meeting of the American Laryngological Association, Scottsdale, Arizona, May 10-11, 1997.

CORRESPONDENCE — Alfio Ferlito, MD, Dept of Otolaryngology–Head and Neck Surgery, University of Udine, Policlinico Città di Udine, Viale Venezia 410, 33100 Udine, Italy.

TABLE 2. CLINICOPATHOLOGICAL FINDINGS IN FIFTEEN NEW CASES OF BASALOID SQUAMOUS CELL CARCINOMA OF LARYNX OR HYPOPHARYNX

Patient	*Age*	*Sex*	*Site*	*Stage at Presentation*	*Cervical Lymph Node Metastases*	*Distant Metastases*	*Treatment*	*Recurrence*	*Follow-up*	*Remarks*
1	61	M	Pyriform sinus, aryepiglottic fold, true and false vocal cords	IV	No	Lungs	Pharyngolaryngectomy, hemithyroidectomy, right RND, left FND, RT	No	DOD 17 mo	Presence of distant metastases without cervical lymph node metastases
2	70	F	Pyriform sinus, aryepiglottic fold, epiglottis	IV	Yes	Lungs	Pharyngolaryngectomy	Yes	DOD 11 mo	Lymph node involvement after surgery
3	84	M	Epiglottis, aryepiglottic folds	III	Yes	No	Supraglottic laryngectomy, right FND	No	DOC 53 mo	Patient died of acute myocardial infarction
4	75	F	Pyriform sinus, epiglottis, glottic region	IV	Yes	No	Pharyngolaryngectomy, right FND, RT, CT	No	DOD 33 mo	
5	51	M	Pyriform sinus, aryepiglottic fold, arytenoid	IV	Yes	No	Pharyngolaryngectomy, right RND, left MND, RT	No	DOD 24 mo	
6	51	M	Retrocricoid region	IV	Yes	Lungs, thrombosis of superior vena cava	Pharyngolaryngectomy, right RND, left FND, RT, CT	No	DOD 14 mo	Synchronous squamous cell carcinoma of epiglottis and vallecula
7	74	M	Pyriform sinus, arytenoid	IV	Yes	Lungs, liver, bones	Pharyngolaryngectomy, left RND, RT	No	DOD 10 mo	
8	45	M	Epiglottis	III	No	Lungs, mediastinal lymph nodes	Supraglottic laryngectomy, bilateral FND, RT, total laryngectomy	Yes	AWD 60 mo	Presence of distant metastases without cervical lymph node metastases Patient underwent pulmonary excision for lung metastases and CT + RT for mediastinal lymph node metastases
9	70	M	Hemilarynx	II	No	No	Hemilaryngectomy, RT	No	DOC 12 mo	Metachronous squamous cell lung carcinoma (diagnosed and treated 18 mo before) Patient died of intestinal occlusion
10	69	M	Epiglottis	II	No	Lungs	Supraglottic laryngectomy, left FND	No	DOD 5 mo	Presence of distant metastases without cervical lymph node metastases
11	72	M	Hemilarynx	II	No	No	Total laryngectomy, RT	No	NED 37 mo	
12	66	M	Epiglottis, false vocal cord, anterior commissure	IV	Yes	Lungs, liver, brain	RT, left RND, total laryngectomy	No	DOD 49 mo	
13	70	M	Vocal cord, ventricular band, ventricle, anterior commissure, subglottis	IV	No	Lungs	RT, total laryngectomy, bilateral FND	Yes	DOD 55 mo	Synchronous adenocarcinoma of lung and metachronous rectal adenocarcinoma Presence of distant metastases without cervical lymph node metastases Patient was treated with RT + CT for neck recurrence Stomal recurrence was present
14	48	M	Epiglottis, pharyngoepiglottic fold, aryepiglottic fold, vallecula	IV	Yes	No	Supraglottic laryngectomy, right RND, left MND, RT	No	NED 21 mo	
15	44	M	Epiglottis, tongue base, vallecula	IV	Yes	Lungs	Excision of tongue base, supraglottic laryngectomy, left RND, right FND, RT, CT	No	AWD 21 mo	

RND — radical neck dissection, FND — functional neck dissection, RT — radiotherapy, DOD — dead of disease, DOC — dead of other causes, CT — chemotherapy, MND — modified neck dissection, AWD — alive with disease, NED — no evidence of disease.

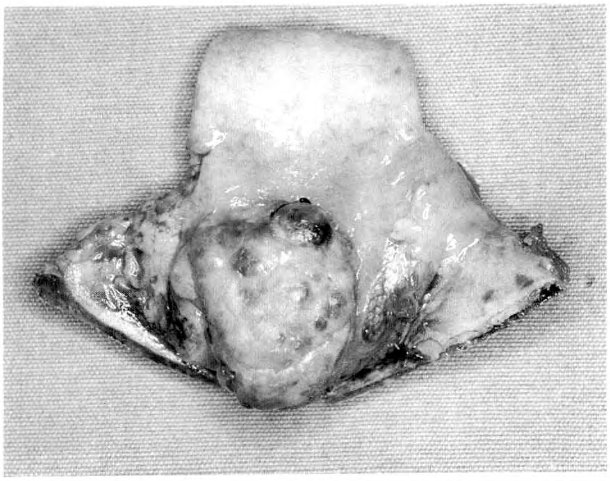

Fig 1. Supraglottic basaloid squamous cell carcinoma. Note exophytic lesion.

follow-up. Light microscopy and immunohistochemical investigations were used to review all cases that were classified as adenoid cystic carcinoma (ACC), poorly differentiated or undifferentiated carcinoma, neuroendocrine carcinoma, or BSCC.

The hematoxylin-eosin–stained sections of both biopsy material and surgical specimens were reviewed to confirm the diagnosis of BSCC. In all cases, formalin-fixed, paraffin-embedded tissue sections were studied with a panel of antibodies (Table 1) by the avidin-biotin-peroxidase complex (ABC-peroxidase) method. Rehydrated histological sections were predigested with 0.025% trypsin in 0.05 mol/L Tris pH 7.8 with 0.1% calcium chloride at 37°C for 20 minutes prior to immunostaining with Cam 5.2, AE1/AE3, and VIM 9 antibodies. The antigen retrieval method[10] was used for V9, VIM 13-2, MIB1, 31G7, SY38, DO7, and CIV22 immunolabeling. Briefly, deparaffinized and rehydrated sections were immersed in a Coplin jar filled with 0.01 mol/L sodium citrate buffer pH 6.0 and incubated in a microwave oven for two 7-minute cycles, each at 700 W. The slides were left to cool and then rinsed in two phosphate-buffered saline (PBS) washes (pH 7.6) prior to immunostaining. Overnight incubation with primary antibodies was performed in all cases. Biotinylated secondary antibodies and avidin-biotinylated horseradish peroxidase complex (Vector ABC Elite Kit) were obtained from Vector Laboratories (Burlingame, Calif). Four cases were studied with serial sections in order to ascertain the topographical relationships in the expression of S-100 protein, smooth muscle actin, and collagen type IV. The primary antibody was replaced with buffer and appropriate nonimmune immunoglobulins for negative case control purposes.

In 6 cases, tissue fragments were processed for ultrastructural observation and were fixed in 2.5% glutaraldehyde in PBS 0.2 mol/L pH 7.2 for 6 to 8 hours, post-fixed in 1% osmium tetroxide in PBS for 4 hours, and then dehydrated and embedded in Epon. Ultrathin sections were stained with uranyl acetate and lead citrate and observed with the Hitachi HS-7000. Three of these cases were not included in the present series, because they were only recently diagnosed and consequently lack sufficient follow-up.

CLINICAL FEATURES

The clinical features are detailed in Table 2. The

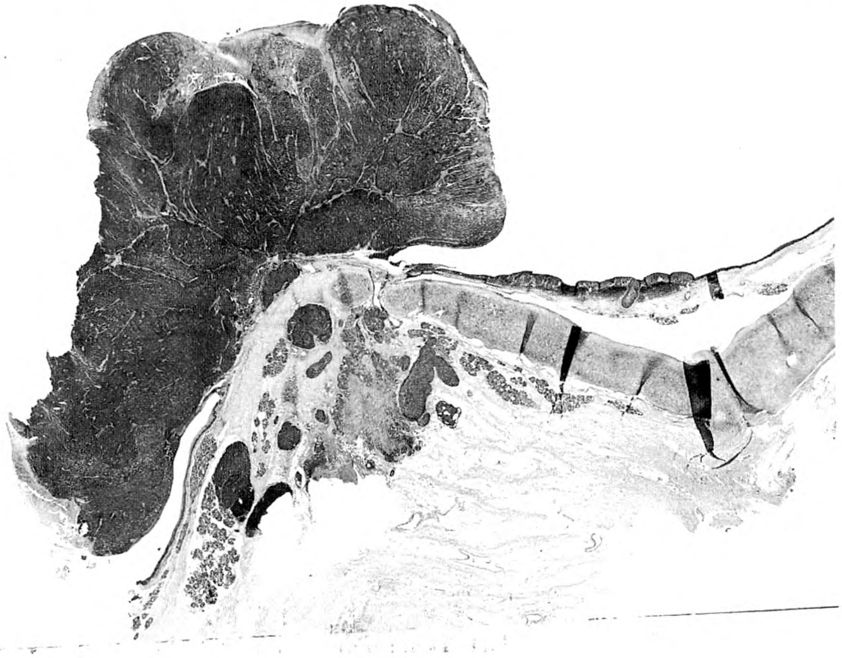

Fig 2. Transverse section of specimen in Fig 1 showing exophytic and infiltrating tumor.

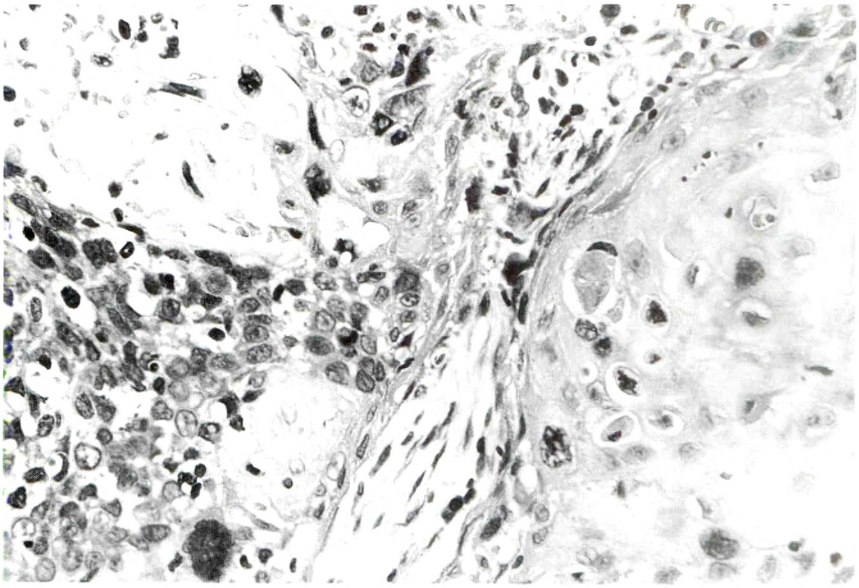

Fig 3. Basaloid squamous cell carcinoma of larynx showing conventional squamous cell carcinoma and basaloid component (H & E, original ×100).

patients included 13 men and 2 women, all white. Their mean age at diagnosis was 63.33 years (median 69 years; range 44 to 84 years). All the male patients were heavy smokers and admitted to being heavy drinkers of alcohol. Most patients presented with multiple complaints. The most common, in descending order of frequency, were dysphonia, dysphagia, and otalgia.

The tumor originated from the larynx in 9 cases and from the hypopharynx in 6 (5 from the pyriform sinus and 1 from the retrocricoid region). Ten patients presented with stage IV, 2 with stage III, and 3 with stage II disease.

Eight patients (Nos. 3-7, 12, 14, and 15) revealed cervical lymph node metastases at presentation; 4 of these developed distant metastases — to the lungs in 1 case, and to multiple sites in 3. During follow-up, metastasis to the cervical lymph nodes occurred in 1 case (No. 2), and lung metastases were also found in the same patient. Distant spread of the tumor without lymph node involvement was observed during follow-up in 4 cases (Nos. 1, 8, 10, and 13).

The primary neoplasm and regional lymph nodes were surgically excised in 12 cases (Nos. 1, 3-8, 10, and 12-15). Eight of these (Nos. 1, 4-8, 14, and 15) received postoperative radiotherapy, and radiotherapy was used preoperatively in 2 cases (Nos. 12 and 13). Chemotherapy complementary to surgery and irradiation was administered in 3 cases (Nos. 4, 6, and 15). One patient (No. 2) underwent surgical excision of the primary tumor alone. In the other 2 cases (Nos. 9 and 11), surgery of the primary lesion was associated with postoperative radiotherapy. One patient (No. 8) underwent pulmonary excision for the lung metastases and a combination of radiotherapy

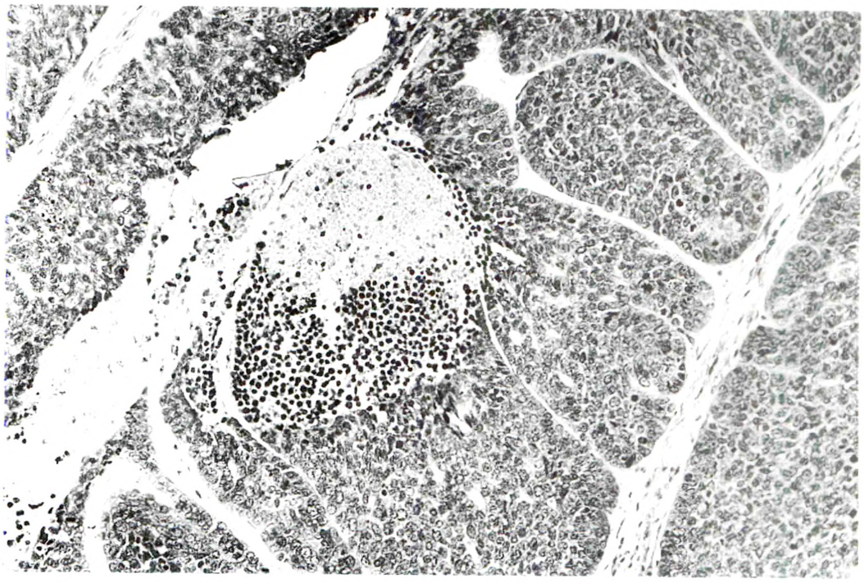

Fig 4. Solid lobular pattern with peripheral palisading and central comedo-type necrosis (H & E, original ×40).

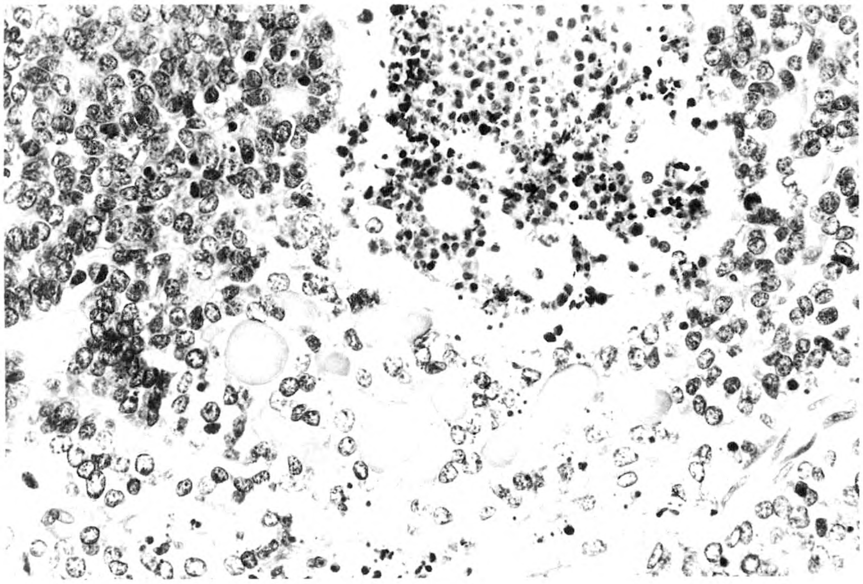

Fig 5. Hyaline material displaying pericellular arrangement (H & E, original ×100).

and chemotherapy for mediastinal lymph node metastases. Another patient (No. 13) was treated with radiotherapy and chemotherapy for a neck recurrence. Three patients (Nos. 2, 8, and 13) experienced local recurrence, one of whom (No. 13) presented also stomal recurrence.

Follow-up was available on all 15 cases and ranged from 5 to 60 months (mean 28.1 months; median 21 months). Nine patients died of disease at 5, 10, 11, 14, 17, 24, 33, 49, and 55 months; 2 are alive with disease at 21 and 60 months; 2 are alive with no evidence of disease at 21 and 37 months; and 2 died of other causes (acute myocardial infarction at 53 months and intestinal occlusion at 12 months).

In 3 patients, BSCC was associated with other primary neoplasms: in 1 case a synchronous SCC was found in the epiglottis and vallecula; in another case a metachronous SCC of the lung had been diagnosed and treated 18 months previously; and in the last case a synchronous adenocarcinoma of the lung and a metachronous adenocarcinoma of the rectum were diagnosed.

PATHOLOGICAL FEATURES

Gross examination revealed firm to hard, poorly defined, exophytic, polypoid, and often centrally ulcerated masses (Figs 1 and 2). Microscopically, these were composed of a carcinoma with a basaloid pattern, associated with in situ and/or invasive SCC (Fig 3). The basaloid pattern consisted of small, crowded cells with hyperchromatic nuclei, scant cytoplasm, small cystic spaces containing material resembling mucin that stained with periodic acid–Schiff (PAS) stain and/or Alcian blue, foci of coagulative necrosis within the central areas of the tumor

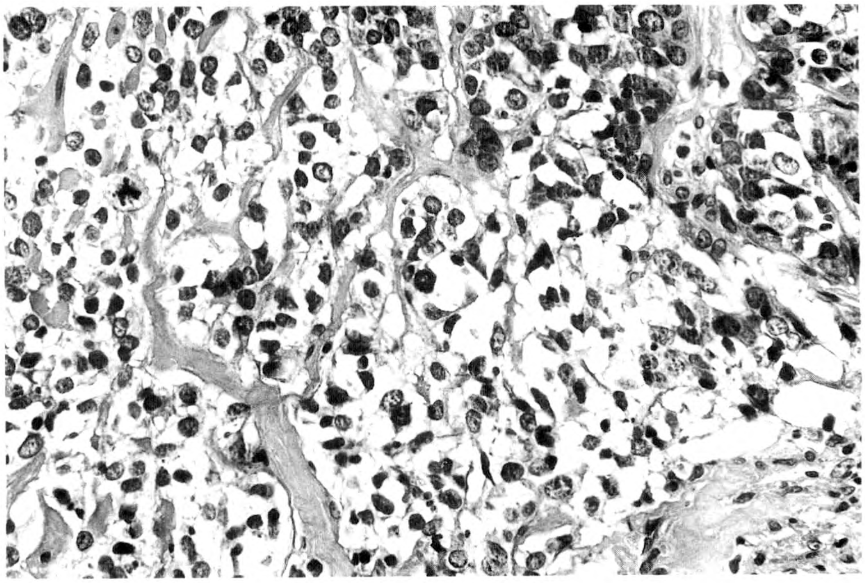

Fig 6. Clear cells in basaloid squamous cell carcinoma (H & E, original ×100).

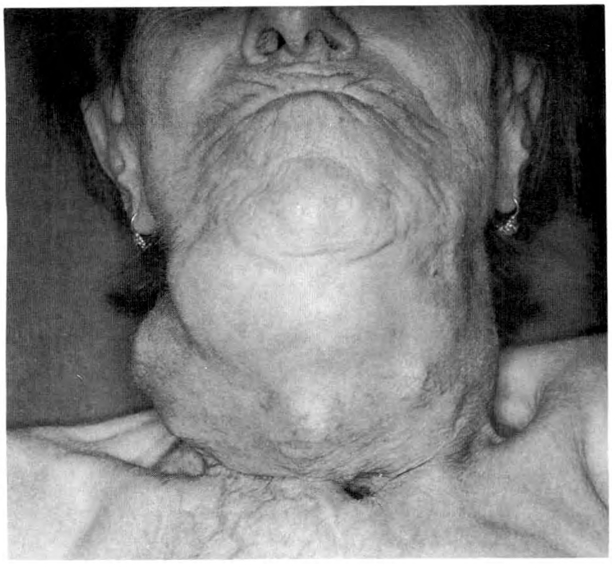

Fig 7. Clinical appearance of very large cervical lymph node metastases.

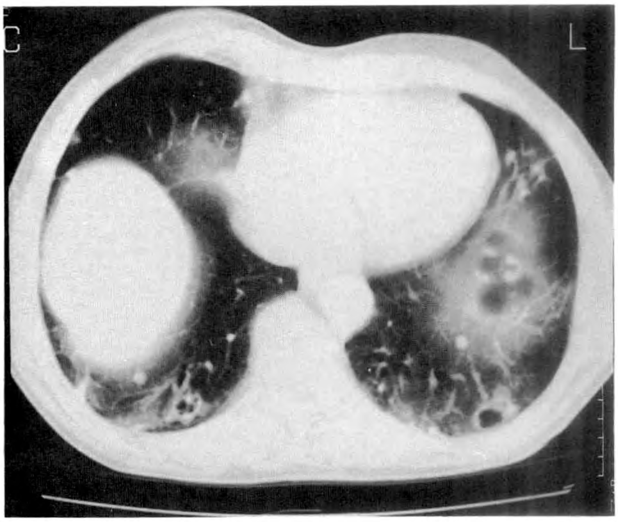

Fig 8. Computed tomography scan showing multiple metastases to lungs.

lobules (comedonecrosis), peripheral palisading (Fig 4), and focal areas of stromal hyalinization (Fig 5). A small cell carcinoma component was occasionally present. Lymphovascular permeation was common. Clear cell changes were seen in some cases (Fig 6). Perineural involvement was also present. The squamous carcinoma was usually well or moderately differentiated and could be superficially invasive. Areas of dysplasia were sometimes present. An abrupt transition between the basaloid component and the keratin pearls was also observed. A spindle cell component was occasionally found associated with osteoclastlike giant cells. Metastatic tumor to the regional lymph nodes (Fig 7) and lungs (Fig 8) was identified, and was composed of squamous or basaloid components or both (Fig 9), but was usually basaloid in composition.

Immunohistochemistry. In all the cases studied, cytokeratin immunoreactivity was observed in the basaloid component with Cam 5.2 and AE1/AE3; the reaction was diffuse in 5 cases, heterogeneous in 8, and focal in 2. All the cases displayed vimentin immunostaining as a delicate perinuclear ring and/or perinuclear dot (Fig 10). This reaction was observed with all antivimentin antibodies and was found in various proportions of basaloid cells, ranging from 20% to 60%. The squamous component in these cases, and also in a series of 10 cases of conventional SCC (data not shown), was devoid of vimentin immunoreactivity. S-100 protein displayed two patterns of reaction: in most cases, numerous S-100 protein–positive dendritic cells were interspersed in the tumor cell population. These dendritic cells were further characterized as Langerhans cells with a CD1a-positive reaction (data not shown). In 5

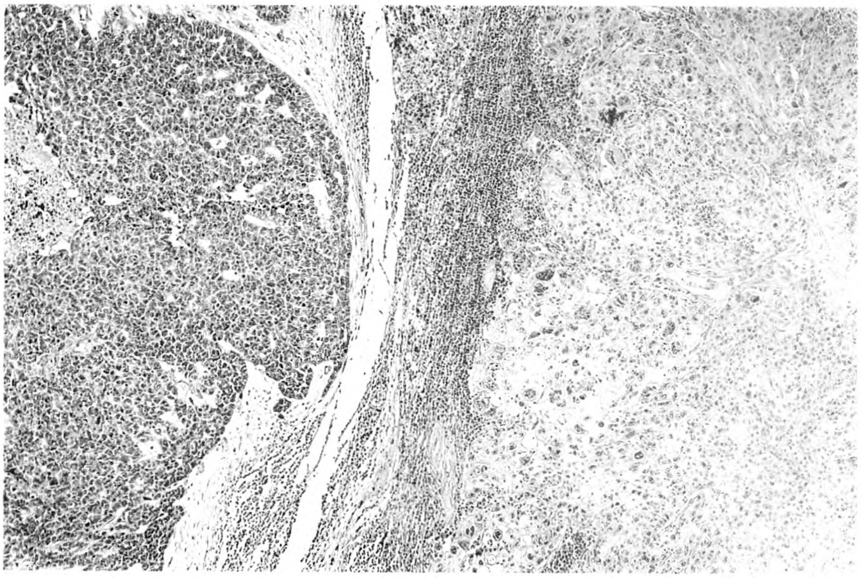

Fig 9. Cervical lymph node showing squamous and basaloid neoplastic components (H & E, original ×40).

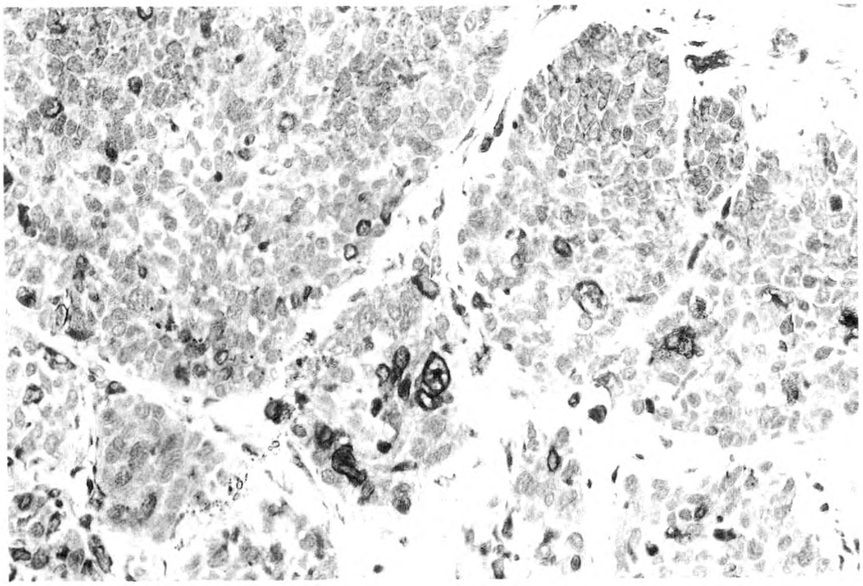

Fig 10. Tumor showing positivity for vimentin immunostaining (H & E, original ×100).

cases, on the other hand, a limited proportion of basaloid cells (10% to 20%) showed S-100 immunoreactivity. Focal actin staining was observed in 4 cases. Collagen IV decorated the basal lamina surrounding neoplastic nodules; it was also present inside some basaloid nodules in 5 cases, in which single cells were delineated by collagen IV antibody. Serial sections demonstrated coexpression of S-100 protein, smooth muscle actin (Fig 11), and collagen IV in the same areas. Intense membrane staining with anti–epidermal growth factor receptor antibody was observed in all cases in both the basaloid and the squamous components. Nuclear p53 immunostaining was present in the majority of cells (>60%) in 10 of the 15 cases of BSCC; an identical pattern of immunoreaction was observed in the squamous component in the same cases. The proliferation marker MIB1/Ki-67 labeled more than 50% of the cells in all cases. Neuroendocrine markers (chromogranin and synaptophysin) and the oncogene product c-erbB-2 were negative in all cases.

Electron Microscopy. Ultrastructurally, the basaloid cells were prevalently polygonal, with a round, centrally located nucleus. Nuclear chromatin was dispersed in dense granules concentrated in the innermost part of the nuclear membrane; a voluminous nucleolus was occasionally seen. The cytoplasm generally contained a few organelles that resembled undifferentiated or immature cells. Free ribosomes, polyribosomes, and strands of rough endoplasmic reticulum, elongated mitochondria, and small aggregates of intermediate filaments were observed. In all cases, the cells were connected by desmosomelike junctions. These belt junctions showed inconstant short annexed tonofilament bundles. Tonofilaments

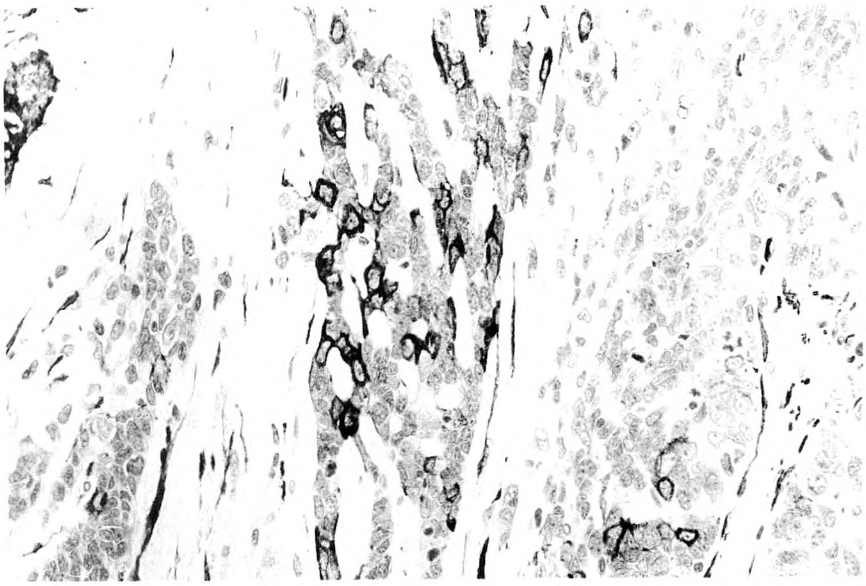

Fig 11. Another area of tumor showing positivity for smooth muscle actin (H & E, original ×100).

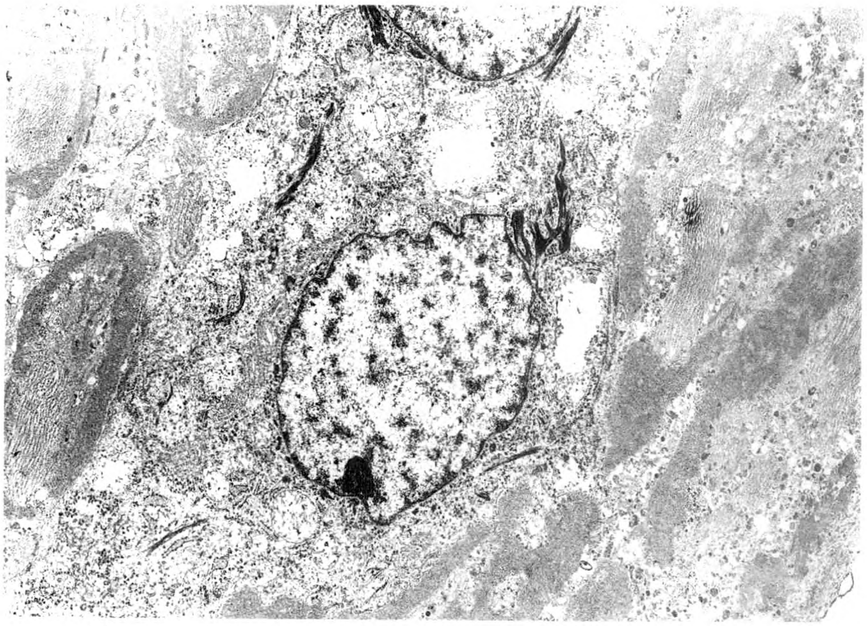

Fig 12. Tumor cells with squamous differentiation containing tonofibrils in cytoplasm (uranyl acetate–lead citrate, original ×9,000). Thick reduplication of basal lamina is clearly evident, also forming irregular round deposits in stroma.

were more evident in the cytoplasm of the differentiated squamous tumor cells. The basal lamina was constantly present and was generally distinctly replicated, frequently forming round deposits with a lamellar architecture lined by tumor cells (Fig 12). Some cells contained hemidesmosomes, but others lacked any basal lamina, and in these, the cytoplasmic membrane was in direct contact with the stromal collagen fibrils. In 2 cases, the intercellular spaces were abnormally dilated, with an irregular outline of the cytoplasmic membrane containing thin filopodia; rare short microvilli were also observed.

DISCUSSION

The natural history of BSCC is characterized primarily by an aggressive biological behavior with a propensity to metastasize widely and a potential for local recurrence. We have identified 158 cases of BSCC of the head and neck reported in the literature.[1,11-43] The large series reported by Banks et al[17] probably included the 16 cases reported by Larner et al[18] and 9 cases reported elsewhere by Banks et al.[19] The cases of BSCC reported by Catalano et al[30] and previously by Coppola et al[31] are the same as the ones described by Coppola et al[29] in 1993. Muller and Barnes[40] mentioned 30 cases of BSCC from the files of the Department of Pathology, Presbyterian University Hospital and The Eye and Ear Institute, Pittsburgh, Pennsylvania, and reported 2 cases located in the tonsil and in the larynx. This large series included 10 cases previously reported from the same department.[41] The case of BSCC described by de Araújo et al[44] has not been included in this review, because the illustrations are not convincing, as already pointed out by Raslan et al.[41] Among these cases, 69 BSCCs occurred in the larynx and hypopharynx.[1,11-17,21,22,24,25,28,32,33,35,37,40,43] The clinicopathological features of the cases reported in this study are very similar to those documented in the literature.[41]

In our series, the lesion mainly affected men (13/15 or 86.67%) in their sixties and seventies (7/13 or 53.84%). The tumor is considered rare, but the reported incidence may be significantly lower than its actual occurrence. Most of our patients had a history of heavy smoking and alcohol abuse. Symptoms depended on the location of the neoplasm, but cervical lymph node metastases were often recognized on presentation. This tumor is typically detected at an advanced stage.

Macroscopically, BSCC appeared as an exophytic, polypoid, firm, but poorly defined mass with surface ulceration. Microscopically, it was a carcinoma composed of a dual population of cells with a basaloid pattern and a squamous component. The basaloid cells appeared small, with hyperchromatic nuclei, sometimes with nucleoli, and scant cytoplasm, forming lobules with cystlike spaces containing material similar to mucin that stained with PAS stain and/or Alcian blue, and with areas of central coagulative necrosis (comedonecrosis). Foci of stromal hyalinization and, sometimes, perineural invasion were also present. The squamous component exhibited either high-grade dysplasia or carcinoma in situ of the superficial mucosa, but it could also be invasive and present as well- or moderately differentiated SCC. Basaloid SCC may also exhibit a malignant spindle cell component very like spindle cell carcinoma.[40] Metastases revealed either basaloid or squamous components or both.

TABLE 3. COMPARISON OF PATHOLOGICAL AND CLINICAL FINDINGS BETWEEN BASALOID SQUAMOUS CELL CARCINOMA AND ADENOID CYSTIC CARCINOMA IN LARYNX AND HYPOPHARYNX

Features	*Basaloid Squamous Cell Carcinoma*	*Adenoid Cystic Carcinoma*
Sex	Male predominance	No significant sex predominance
Age	50-70 years	40-60 years
Sites of predilection	Supraglottis, pyriform sinus	Subglottis
Classic cribriform pattern	Absent	Present
Mitoses	Abundant	Scarce
Nuclear pleomorphism	Prominent	Rare
Squamous component	Present	Absent
Perineural growth	Inconstant	Prominent
Osseous or chondroid metaplasia	May be present	Absent
Cervical lymph node metastases	Usually present	Absent
Necrosis	Frequent	Rare
Clear cells	May be present	Absent
Vimentin positivity	Perinuclear rim and dot	Diffuse cytoplasmic
Actin positivity	Focal	Diffuse
S-100 positivity	Focal; dendritic cell present	Diffuse; dendritic cell absent
Collagen IV	Focal	Abundant
Ki-67/MIB1	High	Low
Presentation	High-stage	Low-stage
Clinical course	Very aggressive	Slow, indolent
Short-term therapeutic results	Unfavorable	Favorable

Modified from Ferlito.[47]

TABLE 4. HISTOLOGICAL DIAGNOSIS

Patient	*Diagnosis on Biopsy*	*Diagnosis on Surgical Specimen*	*Review of Slides*
1	ACC	ACC	BSCC
2	ACC	ACC	BSCC
3	SCC	BSCC	BSCC
4	SCC	SCC	BSCC
5	SCC	BSCC	BSCC
6	SCC	BSCC	BSCC
7	SCC	BSCC	BSCC
8	SCC	BSCC	BSCC
9	SCC	BSCC	BSCC
10	SCC	BSCC	BSCC
11	SCC	BSCC	BSCC
12	SCC	BSCC	BSCC
13	SCC	BSCC	BSCC
14	BSCC	SCC	BSCC
15	BSCC	BSCC	BSCC

ACC — adenoid cystic carcinoma, BSCC — basaloid squamous cell carcinoma, SCC — squamous cell carcinoma.

Ultrastructurally, BSCC cells showed characteristic patterns similar to those of undifferentiated or immature cells (reserve cells), though there was a strong tendency (4/6 or 66.67%) toward squamous differentiation (ie, the presence of junctions and tonofibrils); abortive glandular differentiation was detectable in 2 cases. Moreover, these neoplastic cells constantly revealed the ability to secrete and accumulate basal lamina components. Multiple foci of amorphous eosinophilic or mucinous material among the basaloid tumor cells were recently observed by Hewan-Lowe and Dardick[39] and indicate deposits of basal lamina substance.[45] No secretory granules were identified.[3]

Although clinical and pathological data from this and previous series delineate a specific histological type, several immunohistochemical investigations have failed to identify a common and specific phenotype for this lesion. Furthermore, some common phenotypic markers have been reported in previous series, with strikingly contrasting results; for example, Tsang et al[16] reported vimentin immunoreactivity in 3 of 9 BSCCs, whereas none of the 12 cases reported by Klijanienko et al[32] were positive with this antibody. The same can be said for S-100 protein and for muscle-specific actin, with some series indicating a large proportion of positive cases and other series being totally negative. A difference in the sensitivity of different immunohistochemical protocols may account for these discrepancies. In our series, we used the heat-induced retrieval method in order to obtain a consistently high sensitivity of the ABC-peroxidase reaction, especially for antigens such as vimentin, which suffers from prolonged formalin fixation. In fact, we suggest that vimentin immunoreactivity, in this context, is peculiar to the basaloid cells in BSCC. Other significant features of BSCC are the patterns of immunoreactivity for S-100 protein and muscle-specific actin; coupled with the morphological and electron microscopic findings, this reactivity — albeit limited in the number of cases and the number of stained cells involved — suggests an origin from totipotential cells. Superficial biopsy specimens may not be representative of the whole of a lesion, so an initial diagnosis may prove erroneous. The lesion may be confused with ACC, small cell neuroendocrine carcinoma, basal cell adenocarcinoma, adenosquamous carcinoma, SCC, spindle cell squamous carcinoma, muco-

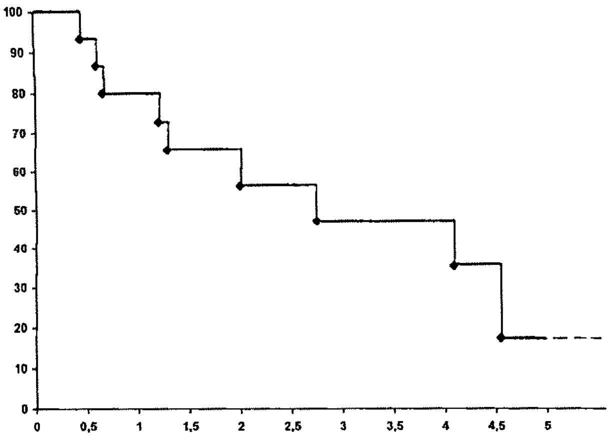

Fig 13. Survival curve of basaloid squamous cell carcinomas of larynx and hypopharynx (Kaplan-Meier).

epidermoid carcinoma, or adenoid SCC. A more comprehensive discussion of the differential diagnosis of laryngeal BSCC is available elsewhere,[46] but the most difficult differential diagnosis is from ACC of the solid type and from small cell neuroendocrine carcinoma. Adenoid cystic carcinoma is not associated with smoking or alcohol, and occurs in younger individuals. It is also less aggressive. Table 3[47] summarizes the differential pathologic and clinical aspects of the two tumors. Before this new phenotype was recognized, these tumors were classified as undifferentiated or poorly differentiated SCCs. As a matter of fact, of 115 cases of poorly differentiated carcinoma of the lung, 37 with sufficient clinical data were reclassified as primary BSCC.[6] This situation occurred in our series, too (Table 4): diagnosis on biopsy originally indicated SCC in 11 cases (73.33%), ACC in 2 (13.33%), and BSCC in only 2 patients (13.33%). Sometimes, the diagnosis on surgical specimens was also wrong: in our series, 11 cases of BSCC were correctly diagnosed (73.33%), for 2 cases the initial diagnosis of ACC was reiterated (13.33%), and 2 cases were classified as SCC (13.33%). However, a careful and meticulous review of all the slides proved that these tumors all had the pathological features of BSCC. All these findings confirm the difficulty that persists in reaching a histological diagnosis of this particular neoplasm. The case reported by McKay and Bilous[11] was also initially diagnosed as ACC.

Immunohistochemistry also plays an important part in distinguishing BSCC from neuroendocrine carcinomas and ACC, with which it has frequently been confused in the past. Unlike neuroendocrine carcinoma, BSCC never expresses neuroendocrine markers. With respect to ACC, BSCC displays actin, S-100, and collagen IV only focally and in a limited number of cases; a proliferation marker such as MIB1/Ki-67 easily separates these two entities, clearly reflecting their different biological behavior, which is slowly progressive for ACC and highly aggressive for BSCC.

Basaloid SCC is considered a biologically high-grade malignancy with a tendency for locally aggressive behavior and early regional and distant metastases (such as to the lung, liver, bone, brain, skin, and subcutaneous tissue). Metastases (regional and/or distant) were found in 86.67% of our series (13/15), with a high incidence of cervical lymph node metastases and lung metastases. In particular, nodal metastases were detected at presentation in 8 of 15 cases (53.33%). Only in 1 case did they occur after surgery. Distant metastases (to lungs, liver, bones, and brain, with thrombosis of the superior vena cava) were found in 9 patients (60%), all of whom developed lung metastases. Two patients presented neither regional nor distant metastases (13.33%); the lesion involved the endolarynx in both cases. A local recurrence occurred in 3 patients (20%), and in 1 of these a stomal recurrence was present. Two patients are alive with no evidence of disease (13.33%), 2 are alive with disease (13.33%), and 9 died of their disease. All 6 patients with BSCC of the hypopharynx and 3 with BSCC of the larynx died of disease. Determined 5-year survival was estimated to be 17.5% by the Kaplan-Meier method (Fig 13).

Tumor ploidy contributes no further prognostic information beyond the data emerging from routine histological evaluation.[41]

Distant metastases with no cervical lymph node involvement were found in 4 of our cases and in some of the cases reported in the literature,[14,41] so the fact that cervical lymph nodes are free of metastasis cannot be considered such a favorable prognostic sign in this tumor as it is in SCC. In fact, 3 of our 9 patients who died of BSCC (33.33%) showed distant spread without nodal involvement.

The propensity of BSCC to metastasize widely justifies an extensive metastatic workup, including endoscopic examination of the upper aerodigestive tract, chest radiography, whole lung tomography, bone scintigraphy, neck and liver echography, computed tomography of the brain, and laboratory investigations.

This tumor shows a tendency for the development of second primary malignant tumors, especially in the upper aerodigestive tract. We found 3 such cases (20%); 1 of these had 3 primary malignancies (Table 2). In a review of the literature, 8 cases of BSCC of the head and neck were reportedly associated with a second primary tumor.[11,15,17,25,27]

The present consensus on treatment is surgery followed by radiotherapy. In the absence of distant metastases, surgical eradication of the neoplasm may be accomplished by partial or total laryngectomy. Neck dissection is recommended because of the high likelihood of cervical lymph node metastases. In consideration of the very aggressive nature of the disease, postoperative radiotherapy is recommended. The combination of surgery and radiotherapy affords good rates of local control, considering that these tumors are often detected in an advanced stage, but the control of distant metastases is a major problem. Adjuvant chemotherapy may also be warranted.[11,13]

This unique phenotype of tumor should be differentiated from conventional SCC and is often associated with an aggressive biological behavior. The aggressive pattern shown in the current study has been seen in BSCC in other locations, too, such as the head and neck[29,41] and the lung.[6] Moro et al[6] noted that median and overall survival differed between BSCC and poorly differentiated SCC in the lung, especially for stage I and II patients: the 5-year actuarial survival in the BSCC group was 15%, whereas that in the poorly differentiated SCC group was 47% ($p = .004$). The median survival of stage I and II patients was 1,218 days (40-month median survival time) for poorly differentiated SCC and 606 days (20-month median survival time) for the BSCC group. The differences are significant in both cases.[6] In conclusion, BSCC is a new morphological and phenotypic entity with distinct prognostic significance.

CONCLUSIONS

This study shows that BSCC of the larynx and hypopharynx has the following characteristics:

1. It occurs in an older population, with a mean age of 63.33 years.

2. It has a male predominance (86.67%).

3. It is usually detected at an advanced stage.

4. It has an aggressive biological behavior characterized by metastases (regional and/or distant) in 86.67%.

5. It has a high rate of regional (60%) and distant metastases (60%). The lungs were always involved when distant metastases were present.

6. Distant metastases may also be present in the absence of lymph node involvement.

7. Differential diagnosis with ACC may be difficult.

8. It shows reactivity for cytokeratin, epithelial membrane antigen, carcinoembryonic antigen, and vimentin. Positivity is focally observed for S-100 protein, muscle-specific actin, and collagen IV.

9. Ultrastructurally, the basal lamina is generally distinctly replicated.

10. There is a tendency for the patient to develop a second primary malignant tumor (synchronous or metachronous) in the upper aerodigestive tract.

11. Surgery and radiotherapy afford good rates of local control. The high incidence of distant metastases suggests that adjuvant chemotherapy may also be warranted.

12. The prognosis is usually worse than that of conventional SCC.

REFERENCES

1. Wain SL, Kier R, Vollmer RT, Bossen EH. Basaloid-squamous carcinoma of the tongue, hypopharynx, and larynx. Report of 10 cases. Hum Pathol 1986;17:1158-66.

2. World Health Organization. Histological typing of tumours of the upper respiratory tract and ear. Berlin, Germany: Springer-Verlag, 1991.

3. Abe K, Sasano H, Itakura Y, Nishihira T, Mori S, Nagura H. Basaloid-squamous carcinoma of the esophagus. A clinicopathologic, DNA ploidy, and immunohistochemical study of seven cases. Am J Surg Pathol 1996;20:453-61.

4. Saltarelli MG, Fleming MV, Wenig BM, Gal AA, Mansour KA, Travis WD. Primary basaloid squamous cell carcinoma of the trachea. Am J Clin Pathol 1995;104:594-8.

5. Brambilla E, Moro D, Veale D, et al. Basal cell (basaloid) carcinoma of the lung: a new morphologic and phenotypic entity with separate prognostic significance. Hum Pathol 1992;23: 993-1003.

6. Moro D, Brichon P-Y, Brambilla E, Veale D, Labat F, Brambilla C. Basaloid bronchial carcinoma. A histologic group with a poor prognosis. Cancer 1994;73:2734-9.

7. Lin O, Harkin TJ, Jagirdar J. Basaloid-squamous cell carcinoma of the bronchus. Report of a case with review of the literature. Arch Pathol Lab Med 1995;119:1167-70.

8. Ferry JA, Scully RE. "Adenoid cystic" carcinoma and adenoid basal carcinoma of the uterine cervix. A study of 28 cases. Am J Surg Pathol 1988;12:134-44.

9. Stearns MW, Quan SH. Epidermoid carcinoma of the anorectum. Surg Gynecol Obstet 1970;131:953-7.

10. Cattoretti G, Becker MHG, Key G, et al. Monoclonal antibodies against recombinant parts of the Ki-67 antigen (MIB1 and MIB3) detect proliferating cells in microwave-processed formalin-fixed paraffin sections. J Pathol 1992;168:357-63.

11. McKay MJ, Bilous AM. Basaloid-squamous carcinoma of the hypopharynx. Cancer 1989;63:2528-31.

12. Weiss LM, Movahed LA, Butler AK, et al. Analysis of lymphoepithelioma and lymphoepithelioma-like carcinomas for Epstein-Barr viral genomes by in situ hybridization. Am J Surg Pathol 1989;13:625-31.

13. Luna MA, El-Naggar A, Parichatikanond P, Weber RS, Batsakis JG. Basaloid squamous carcinoma of the upper aerodigestive tract. Clinicopathologic and DNA flow cytometric analysis. Cancer 1990;66:537-42.

14. Shvili Y, Talmi YP, Gal R, Kessler E, Kolkov Z, Zohar Y. Basaloid-squamous carcinoma of the larynx metastatic to the skin of the nasal tip. J Craniomaxillofac Surg 1990;18:322-4.

15. Seidman JD, Berman JJ, Yost BA, Iseri OA. Basaloid squamous carcinoma of the hypopharynx and larynx associated with second primary tumors. Cancer 1991;68:1545-9.

16. Tsang WYW, Chan JKC, Lee KC, Leung AKF, Fu YT. Basaloid-squamous carcinoma of the upper aerodigestive tract and so-called adenoid cystic carcinoma of the oesophagus: the same tumour type? Histopathology 1991;19:35-46.

17. Banks ER, Frierson HF Jr, Mills SE, George E, Zarbo RJ, Swanson PE. Basaloid squamous cell carcinoma of the head and neck. A clinicopathologic and immunohistochemical study of 40 cases. Am J Surg Pathol 1992;16:939-46.

18. Larner JM, Malcolm RH, Mills SE, Frierson HF, Banks ER, Levine PA. Radiotherapy for basaloid squamous cell carcinoma of the head and neck. Head Neck 1993;15:249-52.

19. Banks ER, Frierson HF Jr, Covell JL. Fine needle aspiration cytologic findings in metastatic basaloid squamous cell carcinoma of the head and neck. Acta Cytol 1992;36:126-31.

20. Cadier MA, Kelly SA, Parkhouse N, Brough MD. Basaloid squamous carcinoma of the buccal cavity. Head Neck 1992; 14:387-91.

21. Gartlan MG, Goetz SP, Graham SM. Basaloid-squamous carcinoma (BSC) of the larynx. Pathologic quiz case 1. Arch Otolaryngol Head Neck Surg 1992;118:1000-1.

22. Guarino M, Micoli G. Basaloid-squamous carcinoma of the upper aerodigestive tract. Histopathology 1992;20:462.

23. Lovejoy HM, Matthews BL. Basaloid-squamous carcinoma of the palate. Otolaryngol Head Neck Surg 1992;106: 159-62.

24. O'Malley BW Jr. Basaloid-squamous carcinoma of the right piriform sinus. Pathologic quiz case 2. Arch Otolaryngol Head Neck Surg 1992;118:215.

25. Puxeddu R, Barezzani MG, Nicolai P, Antonelli AR, Agostini C, Facchetti F. Basaloid squamous carcinoma of the laryngo-pharyngeal region. 2nd Eur Cong Otorhinolaryngol Cerv-Fac Surg, Monduzzi, Bologna, 1992;II:415-8.

26. Tsang WYW, Chan JKC. Basaloid-squamous carcinoma of the upper aerodigestive tract. Histopathology 1992;20:462.

27. Wan SK, Chan JKC, Tse KC. Basaloid-squamous carcinoma of the nasal cavity. J Laryngol Otol 1992;106:370-1.

28. Zamecnik M, Patrikova J. Bazaloidne-squamozny karcinom hypofaryngu a laryngu [Basal-squamous carcinoma of the hypopharynx and larynx]. Cesk Patol 1992;28:158-62.

29. Coppola D, Catalano E, Tang C-K, Elfenbein IB, Harwick R, Mohr R. Basaloid squamous cell carcinoma of floor of mouth. Cancer 1993;72:2299-305.

30. Catalano E, Coppola D, Huston G. Basaloid squamous cell carcinoma (BSCC) of floor of mouth: ultrastructural and oncogene analysis [Abstract]. Patologia 1992;25:145A.

31. Coppola D, Catalano E, Tang C-K, Harwick R, Mohr R. Basaloid squamous cell carcinoma of the floor of mouth [Abstract]. Lab Invest 1991;64:63A.

32. Klijanienko J, El-Naggar A, Ponzio-Prion A, Marandas P, Micheau C, Caillaud J-M. Basaloid squamous carcinoma of the head and neck. Immunohistochemical comparison with adenoid cystic carcinoma and squamous cell carcinoma. Arch Otolaryngol Head Neck Surg 1993;119:887-90.

33. Ma TK-F. Fine needle aspiration cytodiagnosis of basaloid-squamous cell carcinoma metastatic to a cervical lymph node [Letter]. Acta Cytol 1993;37:977-9.

34. Campman SC, Gandour-Edwards RF, Sykes JM. Basaloid squamous carcinoma of the head and neck. Report of a case occurring in the anterior floor of the mouth. Arch Pathol Lab Med 1994;118:1229-32.

35. Ereño C, Lopez JI, Sanchez JM, Toledo JD. Basaloid-squamous cell carcinoma of the larynx and hypopharynx. A clinicopathologic study of 7 cases. Pathol Res Pract 1994;190: 186-93.

36. Hellquist HB, Dahl F, Karlsson MG, Nilsson C. Basaloid squamous cell carcinoma of the palate. Histopathology 1994; 25:178-80.

37. Akyol MU, Seçkin S, Akbayrak L, Özdem C. Basaloid squamous cell carcinoma of the larynx. Eur Arch Otorhinolaryngol 1995;252:485-7.

38. Flaitz CM, Nichols CM, Adler-Storthz K, Hicks MJ. Intraoral squamous cell carcinoma in human immunodeficiency virus infection. A clinicopathologic study. Oral Surg Oral Med Oral Pathol 1995;80:55-62.

39. Hewan-Lowe K, Dardick I. Ultrastructural distinction of basaloid-squamous carcinoma and adenoid cystic carcinoma. Ultrastruct Pathol 1995;19:371-81.

40. Muller S, Barnes L. Basaloid squamous cell carcinoma of the head and neck with a spindle cell component. An unusual histologic variant. Arch Pathol Lab Med 1995;119:181-2.

41. Raslan WF, Barnes L, Krause JR, Contis L, Killeen R, Kapadia SB. Basaloid squamous cell carcinoma of the head and neck: a clinicopathologic and flow cytometric study of 10 new cases with review of the English literature. Am J Otolaryngol 1994;15:204-11.

42. Wan S-K, Chan JKC, Lau W-H, Yip TTC. Basaloid-squamous carcinoma of the nasopharynx. An Epstein-Barr virus–associated neoplasm compared with morphologically identical tumors occurring in other sites. Cancer 1995;76:1689-93.

43. Santamaria Mifsut R, Sanchez Gonzalez F, Limon M, et al. Carcinoma basaloide escamoso de laringe: aportación de un nuevo caso. Acta Otorrinolaringol Esp 1996;47:243-5.

44. de Araújo VC, Biazolla ER, Moraes NP, Furuse TA, Melhado RM. Basaloid squamous carcinoma of the oral cavity. Report of a case. Oral Surg Oral Med Oral Pathol 1993;75: 622-5.

45. Takubo K, Mafune K, Tanaka Y, Miyama T, Fujita K. Basaloid-squamous carcinoma of the esophagus with marked deposition of basement substance. Acta Pathol Jpn 1991;41: 59-64.

46. Barnes L, Ferlito A, Altavilla G, MacMillan C, Rinaldo A, Doglioni C. Basaloid squamous cell carcinoma of the head and neck: clinicopathological features and differential diagnosis. Ann Otol Rhinol Laryngol 1996;105:75-82.

47. Ferlito A. Unusual forms of squamous carcinoma. In: Ferlito A, ed. Surgical pathology of laryngeal neoplasms. London, England: Chapman and Hall, 1996:143-71.

Ann Otol Rhinol Laryngol 106:1997

COMPARISON OF CARBON DIOXIDE AND NEODYMIUM: YTTRIUM-ALUMINUM-GARNET LASERS IN SURGERY OF THE INFERIOR TURBINATE

BURKARD M. LIPPERT, MD JOCHEN A. WERNER, MD

KIEL, GERMANY

At the Department of Otorhinolaryngology–Head and Neck Surgery of the University of Kiel, 533 patients with hyperplastic inferior turbinates were treated between 1987 and 1994 with various carbon dioxide (CO2) and neodymium:yttrium-aluminum-garnet (Nd:YAG) laser techniques. We report on the therapeutic results of both types of laser turbinectomy and compare their long-term results with those of submucosal diathermy. Among the different techniques, we preferred the following approaches. The CO2 laser technique involved the application of a few laser spots (laser energy density 6,100 J/cm^2 per lesion) to the head of the turbinate under the operating microscope. In the Nd:YAG laser procedure, diffuse, low-power irradiation (laser energy density < 53 kJ/cm^2) of the entire concha was performed under endoscopic control. The CO2 laser procedure involved little bleeding and hardly any pain. It produced a positive effect after only a few days and required no follow-up treatment. The success of Nd:YAG laser treatment, by contrast, only became evident after weeks or months, due to the slow scarring process. Compared to submucosal diathermy, both laser methods produced better long-term results. Two years postoperatively, the overall success rate, as defined by patient satisfaction, was 79.6% for the CO2 laser, 68.3% for the Nd:YAG laser, and 36% for submucosal diathermy.

KEY WORDS — carbon dioxide laser, intranasal laser surgery, neodymium:yttrium-aluminum-garnet laser, submucosal diathermy, turbinate dysfunction, turbinectomy.

INTRODUCTION

A variety of surgical procedures are used for reduction of hyperplastic inferior nasal turbinates, including submucosal diathermy,[1] cryotherapy,[2] inferior turbinoplasty,[3] submucosal turbinectomy,[4] vidian neurectomy,[5] total inferior turbinectomy,[6] conchotomy,[7] and inferior turbinate outfracture.[8] The multiplicity of procedures reflects the lack of a single ideal method.

Since the advent of intranasal laser surgery in the 1970s, a number of laser procedures have been introduced for nasal turbinate reduction. By far the greatest experience has been gained with the argon laser.[9] Among other types of lasers successfully applied are the carbon dioxide (CO2) laser,[10,11] the potassium titanyl phosphate (KTP) laser,[12] the holmium:yttrium-aluminum-garnet laser,[13] the magnet laser,[14] and the neodymium:yttrium-aluminum-garnet (Nd:YAG) laser.[15,16] Laser surgical procedures have the advantage of causing minimal blood loss and minimal trauma to surrounding tissues.

Since 1987, the Department of Otorhinolaryngology–Head and Neck Surgery of the University of Kiel has performed laser surgical turbinate reduction using both CO2 and Nd:YAG laser techniques. We report here on the indications, methods, and therapeutic results of both laser procedures and compare their long-term consequences with those of submucosal diathermy.

PATIENTS AND METHODS

There were 1,116 laser turbinectomies performed on 533 patients (217 women, 316 men; mean age 39.5 ± 10.3 years) at the Department of Otorhinolaryngology–Head and Neck Surgery of the University of Kiel between April 1, 1987, and June 30, 1994. The CO2 laser was used in 674 procedures, the Nd:YAG laser in 442. All patients suffered from chronic nasal airway obstruction with enlarged inferior nasal turbinates. None of the patients had any other pathologic causes of airway obstruction, such as a deviated septum or nasal polyps. A minimum 2-year follow-up was accomplished for 142 patients treated with the CO2 laser and 60 patients treated with the Nd:YAG laser.

Preoperative Diagnosis. All patients were examined endoscopically to assess the degree of inferior turbinate enlargement and to exclude other pathologic changes. Rhinomanometry was performed to quantify the extent of nasal obstruction and to verify that it was due to hyperplastic mucosa and not to an enlarged turbinal bone. Following the initial rhinomanometry, an α-mimetic vasoconstrictive naphazoline nitrate solution (1:1,000) was used for detumescence of the mucosa of the superior, middle, and inferior parts of the turbinates. Rhinomanometry was then performed 10 minutes after shrinkage of each section, and patients were asked to report their subjective impression of nasal airflow.

Anesthetic Procedures. In the majority of patients,

From the Department of Otorhinolaryngology–Head and Neck Surgery, University of Kiel, Kiel, Germany.

CORRESPONDENCE — Burkard M. Lippert, MD, Dept of Otorhinolaryngology–Head and Neck Surgery, University of Kiel, Arnold-Heller-Straße 14, D-24105 Kiel, Germany.

TABLE 1. TECHNIQUES OF CARBON DIOXIDE LASER SURGERY FOR REDUCTION OF HYPERPLASTIC NASAL TURBINATES

Technique	*Micro-manipulator*	*Laser Power (W)*	*Approximate Exposure Time (s)*	*Mean Laser Energy Density (J/cm^2)*	*No. of Pts*	*No. of Turbinate Reductions*
Vaporization of anterior third of turbinate	Microslad	20	10	62,200	10	20
		30	10	93,300	10	20
	Acuspot	5	8	81,500	10	20
		8	8	130,400	10	20
Three linear incisions of 2-cm length	Microslad	10	4/incision	12,400	10	20
		20	4/incision	24,800	10	20
	Acuspot	3	4/incision	24,500	10	20
		5	4/incision	51,000	10	20
Single-spot technique on head of turbinate (7 to 12 spots)	Microslad	5	5/lesion	9,330	20	40
		1	5/lesion	1,860	15	30
	Acuspot	5	3/lesion	30,600	20	40
		1	3/lesion	6,100	184	404

inferior turbinate reduction using the CO2 or Nd:YAG laser was performed on an outpatient basis under local anesthesia. Only in children or at the express wish of the patient was the procedure performed under general anesthesia. Local anesthesia consisted of a combination of topical (lidocaine hydrochloride 4%) and infiltration (lidocaine hydrochloride 1%) anesthesia.

CO2 Laser Technique. A variety of CO2 laser (Sharplan 1050, Sharplan Lasers, Freising, Germany, and OPMILAS CO2 50, Zeiss, Oberkochen, Germany) techniques were used to perform 674 turbinate reductions in 319 patients (Table 1). By means of a micromanipulator, the laser beam was applied under microscopic visualization (OPMI-1, Zeiss) at a working distance of 400 mm. Because of the straight laser beam, only the anterior third of the inferior nasal turbinate could be treated. Between 1987 and 1991, the Microslad 719 micromanipulator (Sharplan Lasers) with a focal diameter of 0.64 mm was used, and after 1991, the Acuspot 711 micromanipulator (Sharplan Lasers) with a focal diameter of 0.25 mm was used. The laser energy densities varied depending on the micromanipulator employed and the chosen laser power, and the application time (Table 1). At the end of the operation, carbonization debris was removed with a damp swab to avoid a foreign body reaction. In some cases, a nasal tampon was applied and left in place for approximately 24 hours.

Nd:YAG Laser Technique. The Nd:YAG laser (mediLas 40N, MBB-Dornier, Germering, Germany) was applied under endoscopic control except in procedures involving the head of the turbinate, in which a micro-

TABLE 2. TECHNIQUES OF NEODYMIUM:YTTRIUM-ALUMINUM-GARNET LASER SURGERY FOR REDUCTION OF HYPERPLASTIC NASAL TURBINATES

Technique	*Localization*	*Laser Power (W)*	*Approximate Exposure Time (s)*	*Mean Laser Energy Density (J/cm^2)*	*No. of Pts*	*No. of Turbinate Reductions*
Diffuse (noncontact)	Turbinate tip	20-30	8	56,600-84,900	15	30
		5-10	8	14,200-28,300	15	30
	Entire turbinate	20-30	15	106,200-159,200	20	40
		5-10	15	26,500-53,100	89	192
Interstitial	Anterior two thirds of turbinate	10	8	28,300	35	70
Excision or vaporization (contact)	Turbinate tip	30	8	84,900	20	40
	Entire turbinate	30	15	159,200	20	40

TABLE 3. TIME COURSE OF NASAL BREATHING AFTER LASER TREATMENTS

Nasal Breathing	*CO2 Laser*	*Nd:YAG Laser*
Deteriorated		Up to 1 wk
Satisfactory	After 1 wk	After 4-6 wk
Maximum effect	After 2-4 wk	After 5-6 mo

scope was used. To steer the flexible laser fiber (focal diameter 0.6 mm), a specially designed laser rhinoscope (Storz, Tuttlingen, Germany) was employed under optical control.[16] Different techniques and laser energies were used on the head of the turbinate and on the entire turbinate (Table 2). The diffuse, "noncontact" technique, in which the beam does not strike the turbinate mucosa, was used at a low power setting (5 to 10 W). The laser light was applied till the mucosa of the turbinate turned pale. High power (20 to 30 W) was applied if denaturation with carbonization was desired. An anterior nasal pack was applied at the end of the procedure and left in place for 2 days.

Postoperative Follow-up. The patients were examined at weekly intervals for 6 weeks and every 3 months thereafter for a minimum follow-up period of 2 years. Each follow-up examination involved both nasal endoscopy and rhinomanometry. Patients were also asked to fill out a standardized questionnaire similar to those employed by von Haacke and Hardcastle[17] and Warwick-Brown and Marks.[4] The following questions were asked:

1. Do you feel the operation was a success?
2. How long has the success lasted?
3. Did you experience any postoperative complications such as nasal dryness or crusting, nosebleeds, or unpleasant odors in your nose?
4. Would you agree to undergo the same operation again?

Comparison With Submucosal Diathermy. To compare the long-term results of intranasal laser surgery with those of submucosal diathermy, retrospective examinations were conducted on 25 patients (13 men, 12 women; mean age 29.8 ± 11.7 years) who had undergone 53 electrocoagulation procedures between 1985 and 1987. In all patients, nasal endoscopy and rhinomanometry were carried out. Here, too, patients were asked to complete the questionnaire.

RESULTS

The postoperative course varied widely depending on the type of laser and technique used (Table 3). Carbon dioxide laser surgery resulted in improved nasal breathing by 1 week postoperatively, with marked improvement after 2 weeks. Depending on the type of postoperative treatment, the final therapeutic result was attained after 2 to 6 weeks (Fig 1). Vaporization of the entire head of the turbinate and linear incision of the mucosa required intensive postoperative treatment with nasal ointment and saline solution for 3 to 6 weeks. Procedures employing the Microslad micromanipulator at high power settings did more severe damage to the mucosa with consequent crusting than those using the Acuspot. Following application of the single-spot technique with the large–spot size micromanipulator, which was used till 1991, postoperative care lasted for 14 to 22 days. Use of the narrower spot size since 1992 reduced the length of postoperative care in over 90% of cases to between 8 and 10 days.

Treatment with the Nd:YAG laser, by contrast, was followed by a marked worsening of nasal breathing

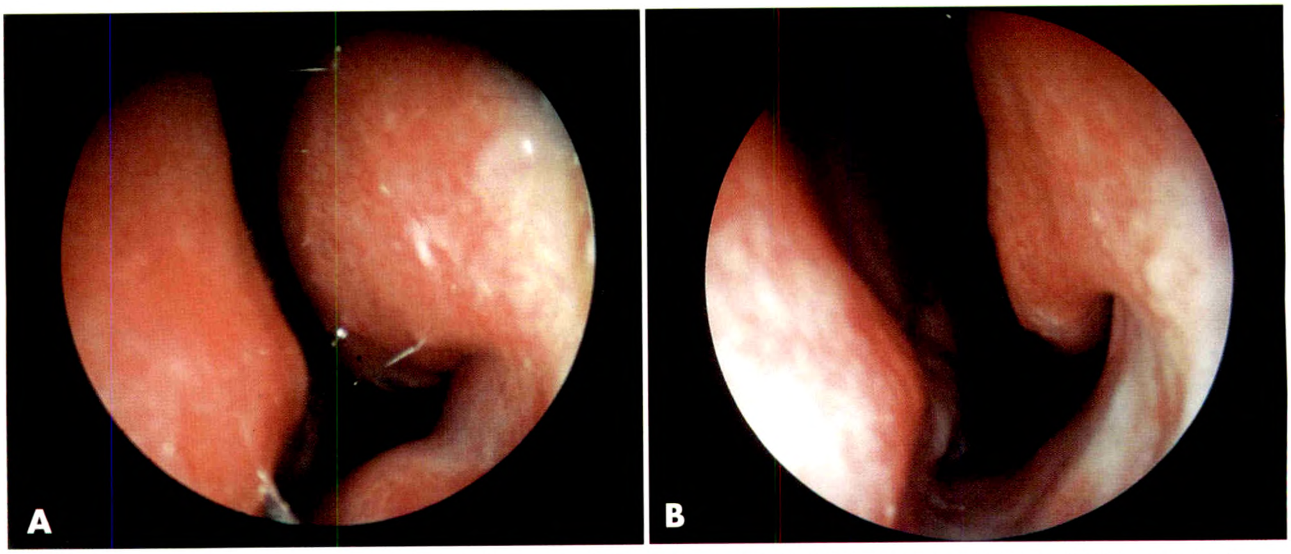

Fig 1. Hyperplastic inferior nasal turbinate A) before and B) 6 weeks after carbon dioxide laser therapy. Volume of turbinate is clearly reduced.

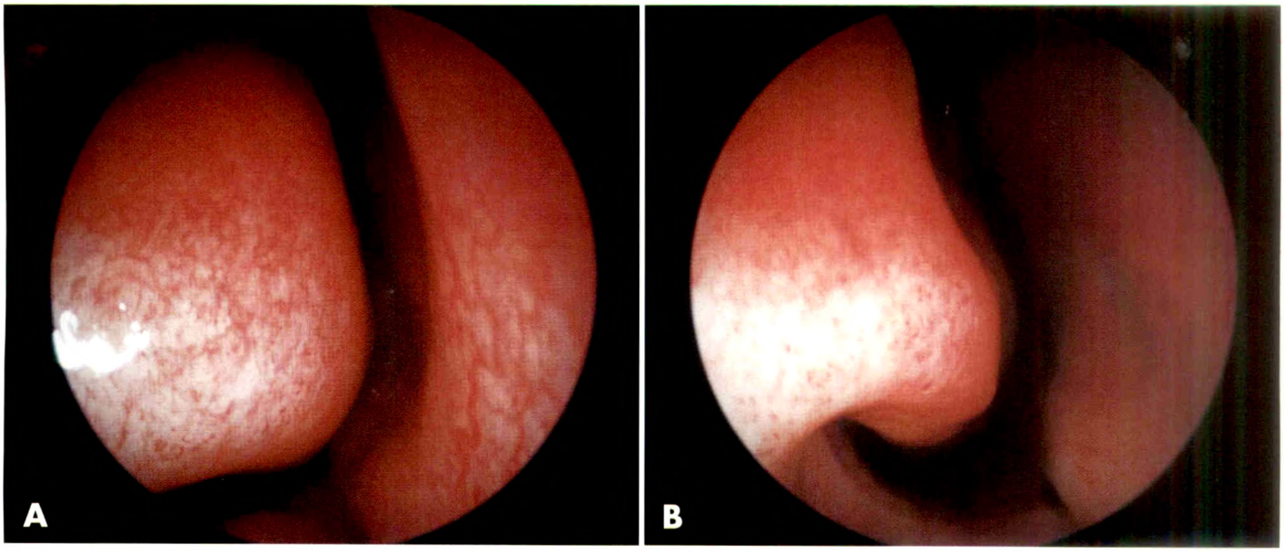

Fig 2. Endoscopic images taken A) before and B) after low-dose neodymium:yttrium-aluminum-garnet laser therapy.

immediately postoperatively. After the first postoperative week, the nasal airways were almost completely obstructed; preoperative values were not reached until after the second postoperative week. Six weeks after Nd:YAG laser therapy, nasal breathing showed a clear improvement over preoperative values. The final therapeutic result was not attained until 5 to 6 months postoperatively (Fig 2 and Table 3). Therapeutic success depended little on the technique employed, but large differences were noted in the type of postoperative care and the rate of complications. Turbinate surgery with the Nd:YAG laser was regularly followed by fibrin deposits, whose severity depended on the laser energy applied and the technique used. The fibrin deposits were especially pronounced following Nd:YAG laser treatment in the contact mode at high energy densities, which required intensive nasal care for 7 to 10 weeks postsurgery. An almost identical course was seen after the interstitial procedure. The length of postoperative care was shortest after noncontact treatment at low energy densities, with wound healing being complete after 4 to 5 weeks.

The long-term success rates for CO_2 and Nd:YAG laser varied markedly, regardless of the technique applied. At 6 months postoperatively, 122 of 142 (85.9%) patients who had undergone CO_2 laser treatment were free of complaints. After 1 year, 116 (81.7%) reported they were still satisfied with the operative results, and after 2 years, 113 (79.6%). For Nd:YAG laser therapy, 39 of 60 (65.0%) patients reported markedly improved nasal breathing at 6 months postoperatively, 43 (71.7%) patients after 1 year, and 41 (68.3%) after 2 years. The therapeutic success of submucosal diathermy was worse than that of either of the two types of laser. Seventeen of the 25 (68%) patients were satisfied with the therapeutic results after 6 months, but only 12 (48%) patients reported no complaints after 1 year, and only 9 (36%) patients were satisfied after 2 years (Table 4).

TABLE 4. THERAPEUTIC SUCCESS RATES AT 6, 12, AND 24 MONTHS AFTER TURBINATE REDUCTION

Postoperative Period (mo)	*CO_2 Laser (n = 142)*		*Nd:YAG Laser (n = 60)*		*Submucosal Diathermy (n = 25)*	
	No.	*%*	*No.*	*%*	*No.*	*%*
6	122	85.9	39	65.0	17	68.0
12	116	81.7	43	71.7	12	48.0
24	113	79.6	41	68.3	9	36.0

Of the CO_2 laser group, 80 (56.3%) patients classified their results as excellent and 33 (23.2%) as satisfactory. For the Nd:YAG laser, 29 (48.3%) patients saw an excellent result and 12 (20%) a satisfactory result (Table 5). Table 6 demonstrates the results in unsatisfied patients. The objective results of rhinomanometry correlated with the patients' perception only in 58%.

The complication rate for the laser surgical procedures was low (Table 7). Intraoperative bleeding occurred during CO_2 laser treatment in 9 patients (all of whom underwent high-power vaporization of the entire head of the turbinate), and postoperative bleeding was not observed. There was no formation of intranasal synechiae. The Nd:YAG laser treatment with the con-

TABLE 5. PATIENTS' OPINION ABOUT EFFICACY TWO YEARS AFTER TREATMENT

Patients' Impression	*CO_2 Laser (n = 142)*		*Nd:YAG Laser (n = 60)*	
	No.	*%*	*No.*	*%*
Excellent	80	56.3	29	48.3
Improved	33	23.2	12	20.0
Unsatisfactory	29	20.4	19	31.7

TABLE 6. DURATION OF EFFECT IN UNSATISFIED PATIENTS

Duration of Improvement	*CO2 Laser*	*Nd:YAG Laser*
Never improved	8	10
<3 mo improved	11	5
<6 mo improved	1	3
<12 mo improved	6	1
<24 mo improved	3	

tact technique produced intraoperative bleeding in 11 cases and postoperative bleeding in 3 cases. In 6 cases (3 cases high-power, noncontact technique; 2 cases vaporization contact technique; 1 case low-power, noncontact technique), synechiae requiring intervention formed between the septum and the inferior nasal turbinate. The postoperative complication rate for submucosal diathermy was higher than for both types of laser therapy. Thirteen (52%) of the patients undergoing turbinate cauterization reported marked crusting requiring lengthy postoperative treatment. Postoperative bleeding was reported by 4 patients (16%).

Patients' willingness to undergo the same treatment again varied widely among the three procedures. Of 142 patients treated with the CO2 laser, 131 (92.3%) said they would be willing to undergo the same treatment again; of 60 patients receiving Nd:YAG laser treatment, 46 (76.7%) said they would agree. For electrocoagulation, by contrast, only 9 of the 25 (48%) patients were willing to undergo the same procedure a second time.

DISCUSSION

Impaired nasal breathing caused by vasomotor or allergic rhinitis is a common disorder whose anatomic-pathologic substrate is an enlarged inferior nasal turbinate. Because conservative measures such as decongestants, topical corticosteroids, antihistamines, and desensitization do not always succeed, surgical intervention is often indicated.[18] A variety of surgical procedures have been described for treatment of a hyperplastic inferior nasal turbinate.[19] One disadvantage of all conventional procedures is their tendency to induce intraoperative and postoperative bleeding, which can lead to mucosal damage and jeopardize long-term success.[4,7] Several authors have also reported the development of atrophic rhinitis.[20,21]

In recent years, various laser systems have been successfully applied in the treatment of hyperplastic nasal turbinates.[9,22-24] The principal indication for laser treatment of the turbinate is nasal airway obstruction caused by mucosal swelling.[25] If, instead, the nasal obstruction is due to an enlarged or deviated turbinal bone, conventional surgery is indicated. The majority of therapeutic failures reported in the literature can be attributed to faulty assessment of the indications for laser therapy.[20,26] The findings of the present study show that selection of the type of laser appropriate for turbinate reduction should be based on the site of turbinate enlargement most responsible for airway obstruction. The CO2 laser is indicated when nasal obstruction is caused by a hyperplastic head of the turbinate, as is generally the case.[27] If the entire epiturbinate is hyperplastic, the Nd:YAG delivery system is our method of choice.

TABLE 7. COMPLICATIONS AFTER TREATMENT OF INFERIOR TURBINATE

Complications	*CO2 Laser*	*Nd:YAG Laser*
Intraoperative bleeding	9 (30 W, vaporization)	11 (contact technique)
Postoperative bleeding		3 (contact technique)
Synechiae		3 (30 W, noncontact technique) 2 (30 W, contact technique) 1 (10 W, noncontact technique)

The differences in the treatment concepts behind the two laser types reflect the differences in their effects on the affected tissues.[28] Since the CO2 laser beam is largely absorbed by cell water — thus, its depth of penetration is limited to 1 mm — it is used to reduce the epiturbinate by excision or vaporization. The CO2 laser techniques described in the literature vary considerably. Whereas Selkin[26] uses the CO2 laser to trim the epiturbinate by cross-hatching (laser power 15 to 18 W), the technique employed by Elwany and Harrison[19] involves near-total vaporization of the anterior third of the mucous membrane (laser power 20 to 30 W). Fukutake et al[22] vaporize the entire mucosa of the inferior nasal turbinate (laser power 20 to 25 W; once a week for 5 weeks).

Generally, reports in the literature only deal with the laser power applied. For a valid comparison between different techniques, it is absolutely necessary to correlate the laser power with the focal diameter to calculate the laser power density, which is given in watts per square centimeter. The application time is also crucial for calculating laser energy density, which is the most exact measure of the biophysical effect of the laser beam. In clinical practice, though, the laser energy density can only be calculated for the intermittent pulsed mode, since the duration of continuous wave application depends on the speed of the manual beam guidance system and thus cannot be given precisely.[29]

Of the various CO2 laser procedures we investigated for this report, the single-spot technique proved to be the best. Single laser spots (laser energy density 6,100 J/

cm^2 per lesion) applied to the enlarged head of the turbinate induced mucosal shrinkage with subsequent formation of scar tissue. This leaves sufficient islands of intact mucosa to enable rapid reepithelialization.[20,23] Scar formation is greater, the greater the laser energy applied and the more extensive the mucosal excision.[20] Vast epithelial scar formation produces marked functional impairment of the mucosa, with a subsequent tendency to dryness, crusting, and atrophic rhinitis.[21] Moderate scar formation, on the other hand, is especially desirable when treating allergic rhinitis, in order to achieve lasting elimination of the submucosal allergic reaction.[10,22]

Between 1987 and 1991, we applied a CO_2 laser employing the Microslad 719 micromanipulator with a focal diameter of 0.64 mm at a working distance of 400 mm. Beginning in 1992, we could achieve the same effect at lower laser power using the Acuspot 711 with a focal diameter of 0.25 mm. Carbonization and areas of necrosis were markedly reduced with the low-power, low-focus beam, which caused less tissue damage and left islands of intact mucosa between the laser spots.[11] The clinical correlate of these experimental results was a decline in the length of postoperative care due to a marked reduction in crusting.

A wholly different treatment principle underlies turbinectomy with the Nd:YAG laser. The Nd:YAG laser beam penetrates up to 8 mm into the tissue and is absorbed by the submucosal venous plexus. This absorption induces a vasculitis with subsequent scar formation and secondary shrinkage of the turbinate.[16,24] Macroscopically, the inferior nasal turbinate becomes firmer and less subject to swelling.

A number of procedures have been described for the Nd:YAG laser. While Johnson[25] performed cross-hatching vaporization (laser power 20 to 30 W) of the entire inferior turbinate, Ohyama et al[15] excised the entire epiturbinate by direct contact at very high power (30 to 40 W). Krespi and Slatkine[30] applied the laser interstitially. We employed the Nd:YAG laser beam in a noncontact mode at such a low power setting (<10 W; laser energy density < 53 kJ/cm^2) that it produced no direct visible effect on the mucosa. Following low-power Nd:YAG laser treatment, the ciliated epithelium of the epiturbinate remained largely intact, and mucociliary clearance was only slightly impaired. Production of glycoproteins in the epithelial beaker cells and subepithelial glands remained undiminished, both findings being signs of a functioning mucosa.[31] Our presented results discourage the application of high laser energies leading to denaturation or carbonization of the mucosa or, in the contact mode, to vaporization. The resulting extensive damage to the mucosa can produce marked postoperative fibrinous coating and crusting requiring intensive postoperative treatment lasting weeks or months. The risk of synechia formation also increases dramatically. It must be pointed out, though, that even low-power techniques can precipitate reactive swelling of the epiturbinate lasting up to 3 weeks, causing a transient aggravation of the nasal breathing impairment, especially in the immediate postoperative period.

The postoperative course differed according to the type of laser turbinectomy performed. Whereas CO_2 laser treatment led to a conspicuous improvement in nasal breathing within a matter of days, the beneficial effect of Nd:YAG laser therapy only became apparent after several weeks. This can be explained by the fact that reactive edema diminishes very slowly and scarring processes are in progress for 6 to 12 months.[16,31] The patient must be informed of this prior to the operation.

Of decisive importance in weighing the benefits of laser turbinectomy are the long-term consequences, especially as compared with those of established techniques. Here laser surgical techniques — turbinate reduction with the CO_2 laser (single spot technique) in particular — are clearly superior to submucosal diathermy. The long-term operative success may be explained by the greater scarring of the epiturbinate resulting from laser therapy. In the judgment of long-term results after nasal surgical procedures, the patient's satisfaction should be regarded as more important than clinical findings or rhinomanometric results.[4,17] Our results confirm this fact. Moreover, patients' willingness to undergo the same treatment again was strikingly higher for the laser procedures (single-spot technique CO_2 laser; low-power, noncontact technique Nd:YAG laser) than for submucosal diathermy. This high acceptance of laser techniques can be attributed to their effectiveness and low rate of complications, combined with the fact that they are carried out at little discomfort to the patient, who can be treated quickly and without pain on an outpatient basis.

CONCLUSION

The CO_2 and Nd:YAG lasers are both useful tools for the reduction of hyperplastic inferior nasal turbinates. The main indication for laser turbinectomy is turbinate hyperplasia, due primarily to swelling of the epiturbinate. If nasal obstruction is caused by bony hypertrophy, conventional surgical techniques are indicated. The CO_2 laser is especially suited for reduction of an enlarged head of the turbinate; a marked positive effect, however, does not become apparent until several days postoperatively. The procedure can be performed on outpatients under local anesthesia, causes minimal pain and bleeding, and produces almost no crusting, thus obviating the need for intensive postoperative care.

The Nd:YAG laser technique is indicated if the entire nasal turbinate is enlarged, since its flexible optical fiber system can deliver energy directly over the entire turbinate. The principal disadvantage to the Nd:YAG procedure is that final therapeutic success often does not occur until several months postoperatively, due to the slow formation of scar tissue. Moreover, the postoperative care after Nd:YAG laser therapy takes considerably longer than that following CO2 laser techniques. The long-term results of laser turbinate reduction surgery, especially with the CO2 laser, are clearly superior to those of submucosal diathermy.

REFERENCES

1. Talaat M, El-Sabawy E, Baky FA, Raheem AA. Submucous diathermy of the inferior turbinates in chronic hypertrophic rhinitis. J Laryngol Otol 1987;101:452-60.

2. Moore JRM, Bicknell PG. A comparison of cryosurgery and submucous diathermy in vasomotor rhinitis. J Laryngol Otol 1980;94:1411-3.

3. Mabry RL. Inferior turbinoplasty: patient selection, technique, and long-term consequences. Otolaryngol Head Neck Surg 1987;98:60-6.

4. Warwick-Brown NP, Marks NJ. Turbinate surgery: how effective is it? A long-term assessment. ORL J Otorhinolaryngol Relat Spec 1987;49:314-20.

5. El-Guindy A. Endoscopic transseptal vidian neurectomy. Arch Otolaryngol Head Neck Surg 1994;120:1347-51.

6. Ophir D, Shapira A, Marshak G. Total inferior turbinectomy for nasal airway obstruction. Arch Otolaryngol 1985;111:93-5.

7. Carrie S, Wright RG, Jones AS, Stevens JC, Parker AJ, Yardley MPJ. Long-term results of trimming of inferior turbinates. Clin Otolaryngol 1996;21:139-41.

8. Thomas P, John LDG, Carlin WV. The effect of inferior turbinate outfracture on nasal resistance to airflow in vasomotor rhinitis assessed by rhinomanometry. J Laryngol Otol 1988;102:144-5.

9. Lenz H. Acht Jahre Laserchirurgie an den unteren Nasenmuscheln bei Rhinopathia vasomotorica in Form der Laserstrichkarbonisation. HNO 1985;33:422-5.

10. Kawamura S, Fukutake T, Kubo N, Yamahita T, Kumazawa T. Subjective results of laser surgery for allergic rhinitis. Acta Otolaryngol Suppl (Stockh) 1993(suppl 500):109-12.

11. Lippert BM, Werner JA. Reduction of hyperplastic turbinates with the CO2 laser. Adv Otorhinolaryngol 1995;49:118-21.

12. Levine HL. Endoscopy and the KTP/532 laser for nasal sinus disease. Ann Otol Rhinol Laryngol 1989;98:46-51.

13. Oswal VH, Bingham BJG. A pilot study of the holmium:YAG laser in nasal turbinate and tonsil surgery. J Clin Laser Med Surg 1992;10:211-6.

14. Mamedov AF. Clinical effectiveness of magnetolaser therapy of vasomotor rhinitis. Vestn Otorinolaringol 1991;3:60-3.

15. Ohyama M, Yamashita K, Furuta S, Nobori T, Daikuzono N. Applications of the Nd:YAG laser in otorhinolaryngology. In: Joffe SN, Oguro Y, eds. Advances in Nd:YAG laser surgery. Berlin, Germany: Springer, 1988:156-65.

16. Werner JA, Rudert H. Der Einsatz des Nd:YAG-Lasers in der Hals-, Nasen-, Ohrenheilkunde. HNO 1992;40:248-58.

17. von Haacke NP, Hardcastle PF. Submucosal diathermy of the inferior turbinate and the congested nose. ORL J Otorhinolaryngol Relat Spec 1985;47:189-93.

18. Mittelman H. CO2-laser turbinectomies for chronic, obstructive rhinitis. Lasers Surg Med 1982;2:29-36.

19. Elwany S, Harrison R. Inferior turbinectomy: comparison of four techniques. J Laryngol Otol 1990;104:206-9.

20. Hoffmann JF, Parkin JL. Rhinologic applications of laser surgery. Otolaryngol Clin North Am 1990;23:19-28.

21. Simpson GT, Shapshay SM, Vaughan CW. Rhinologic laser surgery. Otolaryngol Clin North Am 1983;16:829-37.

22. Fukutake T, Yamashita T, Tomoda K, Kumazawa T. Laser surgery for allergic rhinitis. Arch Otolaryngol Head Neck Surg 1986;112:1280-2.

23. Levine HL. The potassium-titanyl phosphate laser for treatment of turbinate dysfunction. Otolaryngol Head Neck Surg 1990;104:247-51.

24. Lippert BM, Werner JA. CO2 laser surgery of hypertrophied inferior turbinates. Rhinology 1997;35:33-6.

25. Johnson LP. Nasal and paranasal sinus applications of lasers. In: Davis RK, ed. Lasers in otolaryngology–head and neck surgery. Philadelphia, Pa: Saunders, 1990:145-55.

26. Selkin SG. Pitfalls in intranasal laser surgery and how to avoid them. Arch Otolaryngol Head Neck Surg 1986;112:285-9.

27. Lenders H, Pirsig W. Diagnostic value of acoustic rhinometry: patients with allergic and vasomotor rhinitis compared with normal controls. Rhinology 1990;28:5-16.

28. Lippert BM, Werner JA, Rudert H. Laser tissue effects with regard to otorhinolaryngology. Otolaryngol Pol 1994;48:505-13.

29. Werner JA, Lippert BM, Rudert H. Untersuchungen zu einem neuen Mikromanipulator in der CO2-Lasermikrochirurgie. In: Waidelich W, Waidelich R, Hofstetter A, eds. Laser in medicine. Berlin, Germany: Springer, 1993:343-4.

30. Krespi YP, Slatkine M. Neodymium:YAG fiber delivery system for submucosal interstitial photocoagulation of the nasal turbinates. Lasers Surg Med Suppl 1994;15(suppl 5):34.

31. Lippert BM, Werner JA. Nd:YAG-laserinduzierte Nasenmuschelreduktion. Laryngorhinootologie 1996;75:523-8.

Ann Otol Rhinol Laryngol 106:1997

ALGORITHM ANALYSIS OF LECTIN GLYCOHISTOCHEMISTRY AND FEULGEN CYTOMETRY FOR A NEW CLASSIFICATION OF NASAL POLYPOSIS

SERGIO HASSID, MD
CHRISTINE DECAESTECKER, PHD
CHRISTINE HERMANS, MD
ISABELLE SALMON, MD
JEAN LAMBERT PASTEELS, MD
ANDRÉ DANGUY, PHD
ROBERT KISS, PHD
BRUSSELS, BELGIUM

The aim of this study is to present a new classification of nasal polyps. This classification is based both on morphologic criteria relating to morphonuclear features from isolated Feulgen-stained nuclei and on glycohistochemical characteristics from histologic slides submitted to three lectins (peanut, wheat germ, and gorse seed agglutinins) and one neoglycoconjugate glycohistochemical stain. While the morphonuclear features (including 30 variables) relate essentially to chromatin pattern, the glycohistochemical stains (including 16 variables) are linked to the presence of specific carbohydrate moieties in cell membranes and cytoplasm. Forty-nine nasal polyps, including single polyps, diffuse polyposis, cystic fibrosis–related polyposis, and aspirin idiosyncracy–related polyposis associated with asthma, were thus characterized. All the variables were obtained quantitatively by means of computer-assisted microscopy. Two complementary methods of data classification were used to determine the actual diagnostic value contributed by each quantitative variable, namely, discriminant analysis, which forms part of multifactorial statistical analysis, and the decision tree technique, which is an artificial intelligence–related algorithm. The data so obtained show that our morphologic classification of nasal polyps fits in with the classification of nasal polyps defined on the basis of clinical criteria.

KEY WORDS — diagnosis, Feulgen stain, glycohistochemistry, image cytometry, lectins, nasal polyps.

INTRODUCTION

Nasal polyps are a common disease that remains poorly understood. They are the manifestation of unstable respiratory mucosa[1] and, probably, of different clinical and etiopathogenetic entities. Further identification of such subtypes is needed to improve treatment strategy.[2]

Nasal polyps are known to occur in association with other diseases of the respiratory tract such as rhinitis,[3] asthma,[4] aspirin idiosyncracy,[5] cystic fibrosis,[6] and Kartagener's syndrome.[7]

From a histologic point of view, a distinction is made between acute and chronic inflammatory polyps. The former present a mucosal surface with many goblet cells, a thickened eosinophilic basement membrane, and a myxomatous stroma with an inflammatory infiltrate varying from predominantly neutrophils to practically all eosinophils, leading to the conventional allergic origin of nasal polyps. However, systemic allergy or allergies localized in the nasal mucosa are still under debate as the underlying causes of nasal polyps.[8,9] In the chronic disease, the mucosa may reveal a certain degree of squamous metaplasia, while the stroma is usually fibrous with scattered vascular structures.[10]

According to Larsen and Tos,[11] nasal polyps are probably a manifestation of different clinical and etiopathogenic entities, and further identification of these entities is needed to improve treatment strategy.

The aim of this study was to identify specific biological subgroups of nasal polyps and to investigate whether there is any correlation between the morphologic characteristics and the clinical behavior of nasal polyp subgroups. The morphologic characteristics of 49 nasal polyps, including single polyps, diffuse polyposis, cystic fibrosis–related polyposis, and aspirin idiosyncracy–related polyposis associated with asthma (ASA triad), were determined. The morphologic characterization of nasal polyps was carried out by means of computer-assisted methods combining the image cytometric analysis of Feulgen-stained nuclei[12] and the glycohistochemical characterization of the surface epithelium. While the cytometric analysis of Feulgen-stained nuclei made it possible to quantitatively describe the chromatin pattern and nuclear distribution of the DNA content (DNA ploidy level),[12] the glycohistochemical-related part of the study included the quantitative

---

From the Departments of Otorhinolaryngology (Hassid) and Pathologic Anatomy (Hermans, Salmon), Cliniques Universitaires de l'Hôpital Erasme, the Institute of Interdisciplinary Research and Development in Artificial Intelligence (Decaestecker), and the Histology Laboratory, Faculty of Medicine (Pasteels, Danguy, Kiss), Free University of Brussels, Brussels, Belgium. This work was supported by grants from the Fonds de la Recherche Scientifique Médicale (Belgium) and the Fondation Anticancer ROSE (Belgium).

CORRESPONDENCE — Robert Kiss, PhD, Laboratoire d'Histologie, Faculté de Médecine, Université Libre de Bruxelles, 808 route de Lennik, 1070 Brussels, Belgium.

measurements of endogenous ligands (ie, specific sugar moieties detailed in Materials and Methods) for peanut agglutinin (PNA), wheat germ agglutinin (WGA), and gorse seed agglutinin (*Ulex europaeus*; UEA-I). In addition, we characterized the presence of an endolectin acting as a receptor for a neoglycoconjugate carrying a Gal(β1-3)GalNAc glycan residue. The potential use of lectin-related glycohistochemistry[13] and the cytometric image analysis of Feulgen-stained nuclei[14] for diagnostic purposes in nasal polyposis has been emphasized previously. The actual diagnostic value contributed by the cytometric- and glycohistochemical-related data was determined by means of an artificial intelligence–related algorithm in the shape of the decision tree (DT) technique.[15]

MATERIALS AND METHODS

HISTOPATHOLOGIC DIAGNOSIS AND CLINICAL DATA

The medical records and samples of nasal polyps were obtained for 49 patients between January 1993 and September 1995. The diagnosis of polyposis was made with a rigid endoscope. This technique enabled us to differentiate between single polyps (group I; n = 17), typically found between the lateral nasal wall and the middle turbinate, and diffuse polyposis (group II; n = 16), which involves the entire nasal cavity. Group IIIB (n = 7) included nasal polyps from patients with acetylsalicylic acid intolerance established by history. Provocation tests were not performed. The cystic fibrosis group (group IIIA; n = 9) included patients with well-documented disease and a positive sweat test. The histologic slides of all the cases were reviewed by the same pathologist on the basis of the criteria described by Hyams et al.[10]

SPECIMEN PREPARATION

The nasal polyp cases came from archival materials, ie, formalin-fixed, paraffin-embedded tissues. One paraffin block was available for each case. Twelve slides were cut from each block. Slides 1, 3, and 12 (5-µm thickness) were hematoxylin-eosin–stained for histologic diagnosis. Slide 2 (80-µm thickness) was subjected to a method that enables cell suspensions to be obtained (after pronase digestion), and these were cytocentrifuged onto glass slides and submitted to the Feulgen reaction.[12]

The other 8 slides (5-µm thickness) served for glycohistochemical staining. Slides 4, 6, 8, and 10 were PNA–, WGA–, UEA-I–, and Gal(β1-3)GalNAc–BSA–stained, respectively. Slides 5, 7, 9, and 11 served as negative controls (absence of biotinylated probe) for slides 4, 6, 8, and 10, respectively. All the glycohistochemical probes were purchased from Vector Laboratories Inc (Burlingame, Calif). The glycohistochemical procedures were identical to those previously described in detail.[13,16]

The three lectins used included *Arachis hypogaea* ([PNA, which binds to the T-antigen, Gal(β1-3)-GalNAc]), *Triticum vulgare* (WGA, which binds to GlcNAc and neuraminic acid residues), and *U europaeus* (UEA-I, which binds to L-fucose). The neoglycoconjugate was obtained by a chemical grafting of Gal(β1-3)GalNAc (T-antigen) on a glycohistochemically inert core (bovine serum albumin; BSA).

COMPUTER-ASSISTED MICROSCOPY

The computing of the variables deriving from the Feulgen-stained nuclei and quantitative glycohistochemical measurements was carried out by means of a SAMBA 2005 cell image processor (Alcatel-TITN, Grenoble, France) with 100× (aperture 1.30) and 20× (aperture 0.50) magnification lenses, respectively.

The nuclear images of the Feulgen-stained nuclei were digitized at a 540-nm wavelength, evaluated by light microscopy, and accepted by the observers on the same basis as those previously described.[12,14,15] Only epithelial cell nuclei (from both glandular and surface epithelium) were selected for analysis. The Feulgen-stained nuclei images of between 200 and 400 cells were digitized for each of the 49 cases under study. The way in which the cell nuclei were selected for analysis and then digitized is detailed elsewhere.[12,14,15] For each nucleus, 30 variables were determined that described the geometric, densitometric, and textural features of the cell nuclei.[12] These 30 morphonuclear variables related to the mean and standard deviation of each of the 15 specific morphonuclear features described below. The morphonuclear features were divided into four sets, each of which included a specific class of morphologic cell nucleus characteristics. The first set was reduced to 1 cytometric feature, ie, the nuclear area (NA, P1 feature), which determines cell nucleus size. The second set included 5 features describing the cell nuclei densitometrically. These 5 features were the integrated optical density (IOD; P2), the mean optical density (MOD; P3), the kurtosis (P6) and skewness (P4) indices, and the variance of optical density (P5). The third set included 5 features describing chromatin texture by means of a specific algorithm related to the run length matrix.[12] These 5 features were the short (P7) and long (P8) run length frequencies, their relative distributions (P10) and percentages (P11), and the gray level distribution (P9). Finally, the last set included 4 features describing the chromatin texture by means of a specific algorithm related to the co-occurrence matrix.[12] These 4 features were the local mean (P12), energy (P13), the coefficient of variance (P14) of the co-occurrence matrix, and contrast (P15).

The standard deviations of the above features (SDP1 to SDP15 variables) were used to describe the heterogeneity levels of the morphologic characteristics in each of the nasal polyp groups under study.

With respect to the quantitative glycohistochemical measurements, the tissue IOD relating to the hematoxylin counterstaining and the specific glycohistochemical staining was computed on 256 densitometric levels on each pixel and in two distinct color channels. The glycohistochemical positivity for slides 4, 6, 8, and 10 was defined by their integrated optical values in excess of the mean plus two standard deviations of the corresponding negative control slides (ie, slides 5, 7, 9, and 11). Ten fields in the surface epithelium and 10 in the glandular epithelium were assessed for each polyp. The computer-assisted microscope analysis of these fields led to the quantitative description of glycohistochemical patterns in 40,000 to 120,000 μm^2 per tissue in each polyp. The MOD, which relates to staining intensity, was calculated for each area and was obtained by dividing the IOD for the staining by the area of tissue covered by this staining. The calculation of the percentage of positive fields out of the 10 assessed in each of the 40,000 to 120,000 μm^2 analyzed for each type of tissue enabled a labeling index (LI) to be determined for each of these areas.

The MOD and LI values were computed for the four markers. Because of the absence of glandular tissue in several of the polyps, only the values relating to markers in the lining epithelium were used in the present study (suffix R in the feature labels MODR and LIR).

DATA ANALYSIS

CONVENTIONAL STATISTICAL ANALYSIS

Discriminant analysis, a multivariate statistical analysis whose principle is detailed elsewhere,[17] was used to evaluate the actual values contributed by quantitative morphonuclear feature description and lectin expressions to the discrimination between the four groups of polyps defined above. Discriminant analysis enables data to be described in terms of "separability" between different a priori–defined groups, also named "classes." Discriminant analysis is therefore able to generate a description of data as a function of discriminant factors that give prominence to the differential features of cases from distinct classes. As discriminant factors give the best representation for separating data into the different classes, discriminant analysis uses these factors to allocate a case to one of them. Briefly, the allocation rule consists of attributing a case to its nearest class-centroid in the discriminant factor space. This rule produces linear separating surfaces that are (in the factorial space) the median hyperplanes between the centroids of the different classes. This rule has the implicit hypothesis that the prior probabilities of the classes are equal, and is easily adapted if this is not the case.

In view of the large set of candidate variables (a total of 38), we used a stepwise discriminant analysis procedure, the purpose of which is to identify the variables that are the most useful in describing differences among possible groups.[18]

In the present study, we used the stepwise discriminant analysis program from the Statistica/DOS (Statsoft, Tulsa, Okla) package.

ARTIFICIAL INTELLIGENCE–RELATED CLASSIFICATION OF DATA (DECISION TREE ANALYSIS)

Principle. A DT algorithm is a supervised inductive learning technique that is used to produce logical classification rules.[19] These rules express causal relations detected in data between some feature values and preassigned classes. A DT constructs classification rules in the form of trees in which each terminal node (leaf) is labeled as a class and each intermediate node tests a feature of a case, the outcome of which specifies the branch to be followed in the tree (Fig 1). Each path from the root to a leaf thus corresponds to a logical rule characterizing cases belonging to the same class, ie, the one labeling the leaf.

Decision tree algorithms generally use a two-phase scheme, namely, 1) the growing phase for the construction of the classification rules and 2) the pruning phase, which simplifies trees to avoid overfitting the training data. A specific algorithm, ie, C4.5,[20] is used in this paper. This algorithm uses an entropy criterion (labeled the gain ratio criterion) based on Shannon's information theory to select a test at each node of the tree (in the growing phase). It then prunes the tree from the bottom up by means of an error-based criterion with a binomial error approximation (for statistical details, see Quinlan[20]). For our study, we used the default values of the different options included in the C4.5 algorithm.

Production Rules. A rule-generating mechanism is also available with the C4.5 algorithm. A production rule classifier generates logical classification rules with the form "IF (the test on variable *Xi* is satisfied) and (the test on variable *Xj* is satisfied) and (the test on variable *Xk* is satisfied), the class will be *Cx*." In C4.5, a set of rules is generated from a DT. The aim of this rule generation is to be as accurate as a pruned tree, but more easily understood. This rule generation is carried out in two steps. First, initial rules are directly translated from an unpruned tree: every path from the root to a leaf generates a rule whose conditional part contains all the tests along the path, and whose conclusive part specifies the class at the leaf. Second, these initial rules are submitted to a simplification (or generalization) process (eg, some tests can be removed from the conditional part of a rule, some rules can be eliminated, etc).

```
Decision Tree:

SDP11 > 18.1 : IIIB (2.0)
SDP11 ≤ 18.1 :
| SDP2 ≤ 137 : IIIA (3.0)
| SDP2 > 137 :
| | SDP9 ≤ 5.3 : IIIA (2.0)
| | SDP9 > 5.3 :
| | | PNAMODR ≤ 12.12 : IIIA (2.0)
| | | PNAMODR > 12.12 :
| | | | WGALIR ≤ 53.48 :
| | | | | P1 ≤ 2140 : I (2.0/1.0)
| | | | | P1 > 2140 : IIIA (2.0)
| | | | WGALIR > 53.48 :
| | | | | P4 > 0 : I (7.0)
| | | | | P4 ≤ 0 :
| | | | | | UEAMODR > 24.95 : IIIB (2.0)
| | | | | | UEAMODR ≤ 24.95 :
| | | | | | | |SDP13≤ 1.2 : I (4.0)
| | | | | | | |SDP13> 1.2 :
| | | | | | | | PNAMODR ≤ 26.74 : II (11.0)
| | | | | | | | PNAMODR > 26.74 :
| | | | | | | | | UEALIR > 42.08 : I (6.0/1.0)
| | | | | | | | | UEALIR ≤ 42.08 :
| | | | | | | | | | SDP1 ≤ 556 : IIIB (2.0)
| | | | | | | | | | SDP1 > 556 : II (4.0)

 (a)  (b)  (c)  (d)     <-classified as
 ---- ---- ---- ----
 17                     (a): class I
       16               (b): class II
  1         8           (c): class IIIA
  1              6      (d): class IIIB
```

```
Pruned Decision Tree:

SDP11 > 18.1 : IIIB (2.0/1.0)
SDP11 ≤ 18.1 :
| SDP2 ≤ 137 : IIIA (3.0/1.1)
| SDP2 > 137 :
| | SDP9 ≤ 5.3 : IIIA (2.0/1.0)
| | SDP9 > 5.3 :
| | | PNAMODR ≤ 12.12 : IIIA (2.0/1.0)
| | | PNAMODR > 12.12 :
| | | | P4 > 0 : I (8.0/1.3)
| | | | P4 ≤ 0 :
| | | | | UEAMODR > 24.95 : IIIB (2.0/1.0)
| | | | | UEAMODR ≤ 24.95 :
| | | | | |SDP13 ≤ 1.2 : I (4.0/1.2)
| | | | | |SDP13 > 1.2 :
| | | | | | | PNAMODR ≤ 26.74 : II (12.0/1.3)
| | | | | | | PNAMODR > 26.74 :
| | | | | | | | UEALIR > 42.08 : I (8.0/4.5)
| | | | | | | | UEALIR ≤ 42.08 :
| | | | | | | | | SDP1 ≤ 556 : IIIB (2.0/1.0)
| | | | | | | | | SDP1 > 556 : II (4.0/1.2)

 (a)  (b)  (c)  (d)     <-classified as
 ---- ---- ---- ----
 17                     (a): class I
       16               (b): class II
  2         7           (c): class IIIA
  1              6      (d): class IIIB
```

```
Evaluation of training data (49 items):

     Before Pruning              After Pruning
---------------------------  ---------------------------------------------
Size        Errors           Size        Errors        Estimate
 25         2( 4.1%)          21         3( 6.1%)      (31.6%)
```

Fig 1. Decision tree results. SD — standard deviation, P11 — relative percentages, P2 — integrated optical density, P9 — gray level distribution, PNA — peanut agglutinin, MODR — mean optical density in lining epithelium, WGA — wheat germ agglutinin, LIR — labeling index in lining epithelium, P1 — nuclear area, P4 — skewness index, UEA — *Ulex europaeus* agglutinin, P13 — energy of co-occurrence matrix.

In the final system, the rules are organized according to an order of priority, and the first rule that covers a case (ie, the "IF" part of the rule is satisfied by the case description) is taken as the operative one. A default class is determined for the cases not covered by any final rules (Fig 2).

Stability of Selected Features. We studied the stability of the different variables selected by a DT, following a process described elsewhere.[21] This stability study aims to detect the most important variables that may characterize preassigned classes of polyps. Briefly, the stability of the variables was measured by the selection frequency of each one over the DTs generated during a leave-one-out (also called the jackknife) process (Fig 3). This process consists of training a classifier with all the data set except one case, and of using the omitted case to test the classifier performance in classifying new data.[18] This process is reiterated for each case in the data set. The selection frequency of each of the variables over the DTs generated by the leave-one-out process gives information on the importance of the features chosen to describe the data. Hence, if a subset of features appears regularly in the DTs produced by the leave-one-out process, these features can be considered as important (or even indispensable) for the realization of the classification task, because they bring to the fore some regularities in the data. In contrast, some features may rarely appear (or do not appear at all) in the DTs produced. These features can be ignored for data classification purposes.

RESULTS

DISCRIMINANT ANALYSIS RELATING TO FOUR PREDEFINED GROUPS OF POLYPS

Discriminant analysis performed on the 38 morphonuclear and lectin-related variables following a stepwise process finally selected 14 variables, including 8 morphonuclear and 6 lectin-related. They were (in the order of selection indicative of their discriminant power) SDP11, P8, WGALIR, UEALIR, PNAMODR, SDP15, UEAMODR, P2, ENDOMODR, WGAMODR, SDP8, P10, SDP2, and SDP9 (data not shown).

Figure 4 shows the data representation generated by this analysis. This representation is made on the factorial plane defined by the first two discriminant factors.

```
Rule 6:  SDP2 > 137                 Rule 1:  SDP2 ≤ 137
         SDP13 ≤ 1.2                         -> class IIIA  (3/0)
         -> class I  (7/0)
                                    Rule 5:  P1 > 2140
Rule 7:  SDP2 > 137                          WGALIR ≤ 53.48
         P4 ≤ 0                              -> class IIIA  (3/0)
         SDP9 > 5.3
         SDP13 > 1.2                Rule 2:  SDP9 ≤ 5.3
         PNAMODR > 12.12                     SDP11 ≤ 18.1
         PNAMODR ≤ 26.74                     -> class IIIA  (2/0)
         -> class II  (12/0)
                                    Rule 3:  PNAMODR ≤ 12.12
Rule 9:  SDP1 > 556                          -> class IIIA  (1/0)
         UEALIR ≤ 42.08
         PNAMODR > 12.12            Rule 13: SDP11 > 18.1
         -> class II  (4/0)                  -> class IIIB  (2/0)

                                    Default class: I  (15/5)

Evaluation of training data (49 items):

Tested 49, errors 5 (10.2%)

        (a)  (b)  (c)  (d)          <-classified as
        ---- ---- ---- ----
        17                          (a): class I
             16                     (b): class II
                  9                 (c): class IIIA
        5              2            (d): class IIIB
```

Fig 2. Rules extracted from tree in Fig 1. For abbreviations, see Fig 1 legend.

The ellipses in Fig 4 represent the 95% confidence intervals around the mean positions, ie, the centroids (the black dots in Fig 4) of the factorial distributions relating to each of the polyp groups. The results show that characteristics, since the corresponding ellipses did not overlap, of the four polyp groups seemed to correspond to distinct biological features.

All of these observations can be confirmed from a statistical point of view by evaluating the degree of significance of the distances between the centroids in the factorial space (of which the first factorial plane is given in Fig 4). Table 1 lists these distances and their significance levels. Hence, each of the four groups appears significantly separate from all the others ($p < .05$), except groups I and IIIA, for which the distance did not really reach the significance threshold ($p = .053$).

Table 2 shows the confusion matrix related to the classifications produced by discriminant analysis. The percentage of correct classifications was 81.3%. The largest number of errors (or cases of confusion) is due to group II, which appeared to be the least "pure."

DECISION TREE ANALYSIS

Figure 1 shows the DT and its pruned version classifying the 49 cases into the different polyp groups. These trees were obtained when the 38 variables under study were submitted to the C4.5 algorithm. The unpruned tree can be read as follows. If the value of the SDP11 variable is larger than 18.1, the polyp group will be IIIB. The number in parentheses (2.0) characterizing this leaf of the tree indicates that 2 of the cases in our series satisfy this condition, and they both belong to the labeled group (IIIB). If this condition is not satisfied (and thus SDP11 < 18.1), the SDP2 variable must be considered. If the value of this variable is below or equal to 137, the polyp group will be IIIA. (Three cases in this group satisfy this sequence of conditions.) The rest of the tree can be read similarly except for the leaves characterized by 2 numbers [see the fifth leaf: I (2.0/1.0)]. For these leaves, the second number indicates the number of classification errors for the cases associated with this leaf (ie, satisfying the sequence of conditions leading to it).

The pruned tree can be read in a similar fashion,

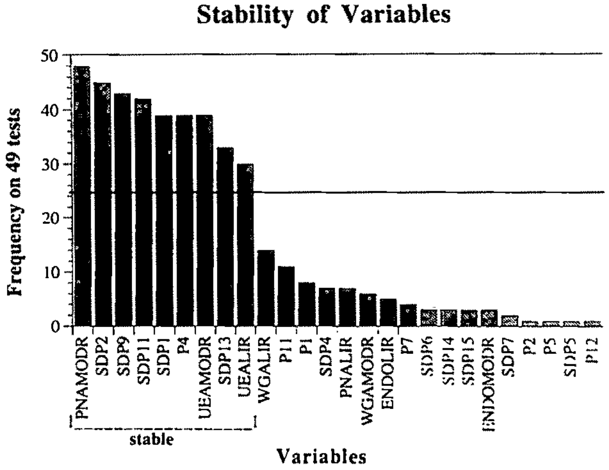

Fig 3. Study of stability of 38 variables for decision tree process. Histogram shows frequencies of occurrence of variables in 49 decision trees generated by leave-one-out process. Nine variables appear with sufficient degree of frequency, as shown by horizontal line (ie, more than 25 times out of 49). P7 — short run length frequency, P6 — kurtosis index, P14 — coefficient of variance of co-occurrence matrix, P15 — contrast, ENDO — endolectin, P2 — integrated optical density, P5 — variance of optical density, P12 — local mean. For remaining abbreviations, see Fig 1 legend.

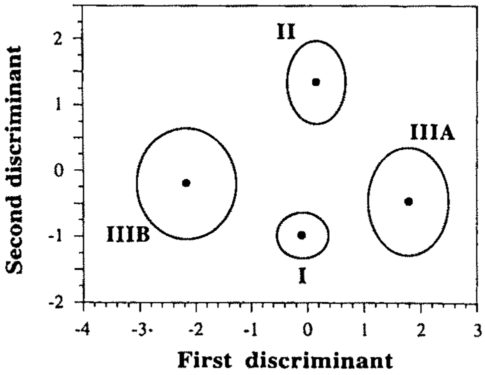

Fig 4. Data sets resulting from discriminant analyses differentiating between four polyp groups, ie, group I (n = 17), group II (n = 16), group IIIA (n = 9), and group IIIB (n = 7). For each polyp group, data show corresponding centroids or means (black points) and 95% confidence intervals around these means (ellipses).

TABLE 1. DISTANCES AND P VALUES RELATED TO CLASS CENTROIDS DEPICTED IN FIGURE 4

Polyp Group	*Polyp Group* II	IIIA	IIIB
I	6.77 p = .0120	8.16 p = .0532	10.34 p = .0281
II	0	9.38 p = .0294	12.12 p = .0127
IIIA		0	21.45 p = .0018

Data represent distances between centroids shown in Fig 4 and significance levels.

TABLE 2. CONFUSION MATRIX RELATED TO CLASSIFICATIONS PRODUCED BY DISCRIMINANT ANALYSIS CARRIED OUT ON POLYP GROUPS

Correct Classification	*Predicted Classification (n = 49)* I	II	IIIA	IIIB	*% Correct*
I	15	0	2	0	88.2
II	2	11	2	1	68.8
IIIA	0	1	7	0	87.5
IIIB	0	1	0	6	85.7
					81.3

except that the second number characterizing a leaf now gives a pessimistically estimated number of errors (upper bound), which are generally positive (Fig 1).

At the bottom of Fig 1, an evaluation of the training data shows that the DT made only 2 errors, and the pruned tree 3 errors. The "size" column indicates the number of nodes in the decision tree. The "estimate" column gives a pessimistic estimation (upper bounds) of the classification error rate. As detailed in the confusion matrices, the classification errors corresponded to cases from groups IIIA and IIIB (the less represented groups) classified as I (one of the most represented groups). The classification rates of the DTs produced by C4.5 were largely better than the discriminant analysis rate (more than 10%). This is due to the relative "flexibility" of the two algorithms in distinguishing between a priori groups. Hence, the boundary constraints are more restrictive for discriminant analysis. Indeed, discriminant analysis is obliged to produce a linear surface to separate one class from all the others. (This surface is principally determined by the class centroids.) In contrast, DTs can generate as many hyperboxes as required to approximate class boundaries. However, hyperbox boundaries have to be perpendicular to the axes (defined by the monovariate tests generated by C4.5) of the multidimensional data space.

STABILITY STUDY OF VARIABLES SELECTED BY DECISION TREES FOR CHARACTERIZING POLYP GROUPS

To evaluate the importance of the variables selected by a DT performed on all the data (Fig 1), we studied the stability of all 38 variables during a leave-one-out process. We established the frequencies with which the variables were chosen in the 49 DTs so produced. (A DT was produced to classify each case of our series; see Materials and Methods.) Figure 2 shows the selection frequency of the variables. It will be seen that only a few did not appear at all in the 49 DTs, and those appearing sufficiently frequently corresponded exactly to the variables used in the pruned tree in Fig 1 (see Fig 3). Between the complete and pruned trees of Fig 1, two conditions related to two variables (P1 and WGALIR) were suppressed. As can be seen in Fig 3, these two variables had a small selection frequency, and were thus adequately suppressed in the pruned tree. The leave-one-out estimate of the classification error rate of DTs (when they tried to classify new cases) showed a significant decrease in the classification error rate after the selection of variables. Indeed, the classification error rate was estimated at 53% after the selection of the variables, against 59% before the selection. The large values of these error rates (even after the selection) can be explained by the small number of available cases in each of the polyp groups. However, these results show that the selection of variables is an efficient strategy to generate more accurate DTs.

LOGICAL RULES CHARACTERIZING POLYP GROUPS

As stated in Materials and Methods, the C4.5 algorithm enables explicit logical classification rules to be extracted from the DT. Figure 2 shows the logical rules that were extracted from the DT given in Fig 1 and that characterize the different polyp groups. Each rule has a number of cases satisfying the conditions given (without satisfying the preceding rules; see Materials and Methods) and a number of classification errors generated by this rule (as for the complete tree in Fig 1). The confusion matrix corresponding to this classification rule system is given at the bottom of Fig 2. As will be seen, no rule generated any errors, except for the default class, which caused 5 IIIB cases to be classified as I. Again, this was due to the difference in distribution between the polyp groups. Hence, only 2 of 7 IIIB cases can be characterized by rule 13, while the others did not satisfy any of the preceding rules and were thus classified into the default class. The default class generally corresponds to one of the most represented groups (such as group I chosen in Fig 2). No error was produced if the cases corresponding to the default rule are considered as unclassified, but only 7 cases in group I and 2 cases in group IIIB were characterized by the corresponding rule system.

All the rules except rule 5 used the stable variables characterized in Fig 3. Rule 5 characterized 3 of 9 cases in group IIIA and used two variables (P1 and WGALIR) that did not appear to enjoy a high level of stability during the leave-one-out process (Fig 3). This rule must therefore be considered with caution.

DISCUSSION

Most diseases have their own classifications that are based mainly on the description of morphologic characteristics from 5-µm-thick hematoxylin-eosin–stained slides. Each pathology type is thus described by one or more classification systems like the various ones proposed by the World Health Organization (WHO) or the Armed Forces Institute of Pathology.

While benign and malignant head and neck tumors have their own WHO classifications,[10] this is not the case for nasal polyps, which are characterized by edematous bulges and composed of a loose edematous mucosal connective tissue covered by respiratory epithelium.[22] Indeed, there is no morphologic nasal polyp classification corresponding to clinical polyp identification. In fact, the development of a nasal polyp classification would improve therapeutic choices for this disorder. Our study thus aims to develop such a classification on the basis of morphologic features only.

It should be emphasized that the major features observed in the epithelium lining nasal polyps are secretory hyperplasia and squamous metaplasia.[10] A distinction is usually made between acute and chronic inflammatory polyps. Another distinction is made between four histologic groups that include the first two types (acute and chronic), a third one showing hyperplasia of the seromucinous glands and an association with a respiratory or metaplastic squamous epithelium, and a fourth one (a polyp with atypical stroma) in which the fibroblasts are reactive and look bizarre.[23] In this case, the polyp may be mistaken for a neoplasm.[23]

In our study, two different groups of morphologic features were used in the development of a nasal polyp classification. The first contained morphonuclear, and the second, histologic features. All the variables belonging to these two groups were quantified by means of computer-assisted microscopy. This aims to produce "objective" measurements. This computer-assisted microscope technology was applied to the morphologic analysis of isolated Feulgen-stained nuclei and the glycohistochemical analysis of histologic slides.

The first group of morphologic features concerns the quantitative description of chromatin patterns in Feulgen-stained nuclei. This first group was used because the notions of anisonucleosis (variation in nuclear sizes), pleomorphism (the morphologic variation of cell nuclei), and hyperchromatism (the significance of dense chromatin areas inside nuclei) are used in most anatomicopathologic classification systems. More precisely, 15 quantitative variables describing chromatin patterns were used, ie, the distribution (as well as the number and size) of dense heterochromatin areas with respect to sparse euchromatin areas inside nuclei. For each of these 15 variables, means and standard deviations were computed on a population between 200 and 400 cell nuclei for each of the 49 nasal polyps being studied. Thirty morphonuclear variables were thus generated by means of computer-assisted microscopy applied to isolated Feulgen-stained nuclei. We have shown previously that this methodology enables efficient morphologic descriptions to be made that are able to discriminate between morphologically similar disorders such as uterine cervical cells both infected and uninfected with various types of human papillomavirus,[24] typical and atypical carcinoid lung tumors,[25] breast cancers both poor and rich in estrogen receptors,[26] and low-grade as opposed to high-grade intraepithelial prostatic neoplasia.[27]

A group of histologic features incorporates glycohistochemical criteria based on measurement of lectin reactions to the presence of specific carbohydrate moieties (the lectins in use were nonimmune, nonenzymatic, and nonhormonal glycoproteins). Several authors have shown that glycohistochemical tracers can aid diagnosis[10] for different disorders of the nervous system[16,28] and the digestive tract.[29]

Four glycohistochemical tracers were retained in our study. There were three lectins reacting to several carbohydrate moieties, ie, the PNA lectin specific to the disaccharide Gal(β1-3)GalNAc, the WGA lectin specific to GlcNAc and neuraminic acid residues, and the UEA-I lectin specific to L-fucose. The fourth tracer was a neoglycoconjugate related to the chemical grafting of Gal(β1-3)GalNAc on a BSA core, and able to bond with an endolectin similar to the PNA lectin. For each of these tracers, we determined the size of the glycohistochemically marked lining epithelium and glandular epithelium areas, as well as the tracing intensity. This glycohistochemical quantification generated 16 variables. Only the 8 variables concerning the lining epithelium were kept for the final morphologic classification of nasal polyps, because some polyps did not have glands.

The computer-assisted microscope technology used here thus made it possible to obtain a large number of quantitative morphonuclear and glycohistochemical variables. To exploit this quantitative information, two data classification methods were used. The first was a traditional multifactorial statistical analysis (ie, discriminant analysis), while the other came from artificial intelligence (ie, a DT technique that forms part of the supervised learning algorithms).

Discriminant analysis enables the data to be described in terms of the separation between different a priori–defined groups. This is done by the construction of discriminant factors determined by the linear combinations of some of the descriptive numeric variables established as the most discriminatory. However, this linear model can be difficult to interpret or explain. In contrast, DT and production rules techniques are not obliged to produce a linear data model and thus have a greater descriptive potential. An advantage of these artificial intelligence techniques is that they produce logical classification rules in terms of subsets of relevant variables selected from the set of descriptive variables. These logical rules detail the biologic characteristics of the different data groups and can be communicated and discussed more easily with specialists in the field. In fact, our study demonstrates that these two data classification methods must be combined in order to obtain better information on the diagnostic value contributed by each quantitative variable.

The data from our study strongly suggest that the four groups are different from a biologic point of view. This fact could partly explain the unexpected clinical behavior of nasal polyps.

Taking into account all the results obtained here, we think that a group I polyp will stay between the middle turbinate and the lateral nasal wall without becoming a group II polyp, while a group II polyp will directly become diffuse polyposis. The same approach can be taken for group IIIB, in which all the patients had aspirin hypersensitivity and asthma. In the Drake-Lee et al series,[1] although nasal polyps are three times more common in males, the sex ratio was inverted in the asthma group (2:1 for women); this finding suggests a subgroup that is likely to develop both polyps and asthma as a result of an underlying condition.[1]

In conclusion, our study shows that a morphologic classification of nasal polyps, including features describing morphonuclear and glycohistochemical characteristics, fit in with the classification set up on the basis of clinical data. We are now increasing our series of cases in order to be able to propose in the near future a reliable classification of nasal polyps based on morphologic characteristics.

REFERENCES

1. Drake-Lee AB, Lowe D, Swanston A, Grace A. Clinical profile and recurrence of nasal polyps. J Laryngol Otol 1984;98: 783-93.

2. Larsen K, Toss M. Origin of nasal polyps. Laryngoscope 1991;101:305-12.

3. Mullarkey MF, Hill JS, Webb DR. Allergic and non-allergic rhinitis: their characterization with attention to the meaning of nasal eosinophilia. J Allergy Clin Immunol 1980;65:122-6.

4. Settipane GA, Chafee FH. Nasal polyps in asthma and rhinitis. A review of 6,037 patients. J Allergy Clin Immunol 1976; 59:17-21.

5. Yamashita T, Tsuji H, Maeda N, Tomoda K, Kumazawa T. Etiology of nasal polyps associated with aspirin-sensitive asthma. Rhinology 1989(suppl 8):15-24.

6. Schwachman H, Kulczycki LL, Mueller HL, Flake CJ. Nasal polyposis in patient with cystic fibrosis. Pediatrics 1962; 30:389-401.

7. Imbrie JD. Kartagener's syndrome: a genetic defect affecting the function of cilia. Am J Otolaryngol 1981;2:215-22.

8. Bernstein J, Gorfien J, Noble B. Role of allergy in nasal polyposis: a review. Otolaryngol Head Neck Surg 1995;113: 724-32.

9. Shatkin JS, Delsupehe KG, Thisted RA, Corey JP. Mucosal allergy in the absence of systemic allergy in nasal polyposis and rhinitis: a meta analysis. Otolaryngol Head Neck Surg 1994;111: 553-6.

10. Hyams VJ, Batsakis JG, Michaels L. Nasal and paranasal polyposis. In: Hyams VJ, Batsakis JG, Michaels L, eds.Tumors of the upper respiratory tract and ear. 2nd ed. Vol 25. Washington, DC: Armed Forces Institute of Pathology, 1988:11-3.

11. Larsen K, Tos M. Clinical course of patients with primary nasal polyps. Acta Otolaryngol (Stockh) 1994;114:556-9.

12. Kiss R, Salmon I, Camby I, Gras S, Pasteels JL. Characterization of factors in routine laboratory protocols which significantly influence the Feulgen reaction. J Histochem Cytochem 1993;41:935-45.

13. Hassid S, Salmon I, Bovin NV, Kiss R, Gabius HJ, Danguy A. Histochemical expression of binding sites for labelled hyaluronic acid and carrier-immobilized synthetic (histo-blood group trisaccharides) or biochemically purified (ganglioside GM1) glycoligands in nasal polyps and other human lesions including neoplasms. Histol Histopathol 1996;11:385-92.

14. Hassid S, Choufani G, El-Kattabi O, et al. Image cytometry characterization of ploidy level, proliferative activity and chromatin pattern in 50 nasal polyps. Int J Oncol 1996;9:137-43.

15. Decaestecker C, Salmon I, Camby I, et al. Identification of high versus lower risk clinical subgroups in a group of adult patients with supratentorial anaplastic astrocytomas. J Neuropathol Exp Neurol 1995;54:371-84.

16. Salmon I, Camby I, Remmelink M, et al. Lectin histochemistry, ploidy level and proliferation indices in meningioma subtypes. Neuropathol Appl Neurobiol 1996;22:68-76.

17. Johnson RA, Wicheren DW. Applied multivariate statistical analysis. 3rd ed. Englewood Cliffs, NJ: Prentice-Hall International Editions, 1992.

18. McLachlan GJ. Discriminant analysis and statistical pattern recognition. New York, NY: Wiley & Sons, 1992.

19. Quinlan JR. Induction of decision trees. Machine Learning 1986;1:81-106.

20. Quinlan JR. C4.5: programs for machine learning. San Mateo, Calif: Morgan Kaufmann Publishers, 1993.

21. Decaestecker C, Remmelink M, Salmon I, et al. Methodological aspects of using decision trees to characterize leiomyomatous tumors. Cytometry 1996;24:83-92.

22. Coste A, Rateau JG, Roudot-Thoraval F, et al. Increased epithelial cell proliferation in nasal polyps. Arch Otolaryngol Head Neck Surg 1996;122:432-6.

23. Davidson A, Hellquist HB. The so-called "allergic " nasal polyp. ORL J Otorhinolaryngol Relat Spec 1993;55:30-5.

24. d'Olne D, Kiss R, Coibion M, et al. Detection of human papillomaviruses 16-18 in cervical cells by molecular hybridization: relationship with morphonuclear cell image analyses. Mod Pathol 1989;2:658-65.

25. Larsimont D, Kiss R, de Launoit Y, Melamed MR. Characterization of the morphonuclear features and DNA ploidy of typical and atypical carcinoids and small cell carcinomas of the lung. Am J Clin Pathol 1990;94:378-83.

26. Larsimont D, Kiss R, d'Olne D, et al. Correlation between nuclear cytomorphometric parameters and estrogen receptor levels in breast cancer. Cancer 1989;63:2162-8.

27. Petein M, Michel P, van Velthoven R, et al. Morphonuclear relationship between prostatic intraepithelial neoplasia and cancers as assessed by digital cell image analysis. Am J Clin Pathol 1991;96:628-34.

28. Wang XC, Kochi N, Tani E, Kaba K, Matsumoto T, Shindo H. Lectin histochemistry of human gliomas. Acta Neuropathol (Berl) 1989;79:176-82.

29. Boland CR, Martin MA, Goldstein IJ. Lectin reactivities as intermediate biomarkers in premalignant colorectal epithelium. J Cell Biochem Suppl 1992(suppl 16G):103-9.

≈

1ST WORLD CONGRESS OF OTORHINOLARYNGOLOGIC ALLERGY, ENDOSCOPY AND LASER SURGERY

The 1st World Congress of Otorhinolaryngologic Allergy, Endoscopy and Laser Surgery will be held in Athens, Greece, June 25-27, 1998. For information, contact Nereus Congress & Conferences, 2 Afentouli Str, 185 36 Piraeus, Greece; telephone ++ 30-1-452 4842; fax ++ 30-1-418 2308; e-mail: nereus@travelling.gr; http://www.travelling.gr/nereuscongress.

Ann Otol Rhinol Laryngol 106:1997

STATISTICAL EVALUATION OF HEARING SCREENING BY DISTORTION PRODUCT OTOACOUSTIC EMISSIONS

PIERRE BONFILS, MD, PHD
PARIS, FRANCE

PAUL AVAN, MD, PHD
CLERMONT-FERRAND, FRANCE

PAUL LANDAIS, MD
PARIS, FRANCE

MANUEL ERMINY, MD
PARIS, FRANCE

BERNARD BIACABE, MD
PARIS, FRANCE

The aim of this study was to provide a statistical evaluation of the screening properties of distortion product otoacoustic emissions (DPOEs) in individuals with clinically normal hearing and in patients with pure sensorineural deafness of various degrees. The main informational parameters used were sensitivity, specificity, positive predictive value (PPV), negative predictive value (NPV), and the analysis of receiver operating characteristic (ROC) curves. For each frequency tested, ears were classified as a function of their audiometric threshold. Two groups were defined relative to an arbitrary reference, the "audiometric criterion." The PPV decreased and NPV increased with increases in the audiometric criterion. Each point of the ROC curve represents the relationship between the false alarm rate and the hit rate for each audiometric criterion ranging between 10 and 75 dB hearing level: the lower the audiometric criterion, the lower the hit rate value, and the lower the false alarm value. The audiometric criterion giving the highest hit rate and the lowest false alarm rate was 55 to 60 dB hearing level for primaries at 60 and 70 dB sound pressure level, or 25 to 30 dB hearing level for primaries at 30, 40, and 50 dB sound pressure level. These two different behaviors of ROC curves are consistent with the hypothesis that DPOEs do not represent activity at a single location along the basilar membrane.

KEY WORDS — audition, cochlea, distortion product otoacoustic emission, hearing screening.

INTRODUCTION

Distortion product otoacoustic emissions (DPOEs) are otoacoustic emissions evoked by two pure tones at f1 and f2 frequencies called primaries. The characteristics of DPOEs are increasingly well established in mammals with thorough reviews.[1-3] In humans, the most prominent DPOE occurs at the 2f1 – f2 frequency. The amplitude of this particular distortion product is much lower than the levels of the primary tones — typically, 60 dB lower in the human ear.

The DPOEs are generated in the cochlear region where the f1 and f2 components both are large and propagate mechanically both toward the distortion frequency location and toward the stapes, through the middle ear and the external ear canal.[4] Moreover, DPOEs are reversibly reduced by exposing the ear to a fatiguing single tone at a frequency near or slightly below the primary frequencies.[5,6] Brown et al[7] recorded DPOEs in guinea pigs before and after treatment with aminoglycosides, and the results were compared in terms of histopathologic features. After such ototoxic treatment, DPOEs can be generated in response to primary intensities of >60 dB sound pressure level (SPL), while DPOEs in response to primary intensities of <60 dB SPL are absent. In these cases, the frequency region in which the primaries achieve their maximum vibration totally lacks outer hair cells. Therefore, DPOEs generated by primary intensities of >60 dB SPL probably have their origin in passive properties of the cochlea. On the other hand, DPOEs elicited by primary intensities of <60 dB SPL probably have their origin in the active mechanical properties of outer hair cells. This fact suggests that several DPOE sources could be present within the inner ear.[7-12]

The DPOEs may have important clinical applications. These possible applications depend on three main factors.[13] First, DPOEs can be easily recorded by means of a small acoustic probe introduced without pain in the external auditory canal either in adults or in infants. Second, DPOEs represent a physiologic and objective test that could prove to be very useful for evaluating auditory function in young children.[14] Third, DPOE seems to be a frequency-selective test.[15]

From the Auditory Research Laboratory (CNRS UMR "Neurobiologie des Systemes Sensorimoteurs") and Formation Associée Claude Bernard, Hospital Boucicaut (Bonfils, Erminy, Biacabe), and the Department of Biostatistics, Hospital Necker (Landais), Faculté Necker-Enfants Malades, Université René Descartes, Paris, and the Biophysics Laboratory, Faculty of Medicine, Université d'Auvergne, Clermont-Ferrand (Avan), France.

This study was supported by Assistance Publique, Hôpitaux de Paris (CRC 920801 and CRC 930803), and by INSERM-CNAM TS 4AIC04.

CORRESPONDENCE — Pierre Bonfils, MD, PhD, Auditory Research Laboratory, ENT Dept, 78 rue de la Convention, F-75015 Paris, France.

In a clinical setting, the amplitudes of DPOE elicited by low primary intensities (<60 dB SPL) are well correlated with pure tone auditory threshold at the mean frequency of the primary tones. Moreover, they appear to be insensitive to the value of auditory thresholds at other frequencies and particularly for higher tones. Thus, these DPOEs do provide frequency-specific information. When higher primary intensities are used, this specificity disappears. These clinical properties of DPOEs also suggest that several DPOE sources could be present within the inner ear.[15]

Several teams have proposed DPOEs as a new screening method for auditory function.[2,3,14] This test could be very useful for evaluating cochlear function in young children, especially in neonates. Evaluating a new diagnostic test is an essential step before its clinical application. The information provided by the test must be considered in terms of diagnostic value and cost. For this purpose, Gorga et al[16,17] were the first to apply to DPOEs an analysis based on decision theory (receiver operating characteristic [ROC] curves). Their goal was to determine DPOE amplitudes that were able to distinguish between normal and impaired ears. The results of Gorga et al allowed the establishment of a quantitative basis to the widespread notion that otoacoustic emission amplitudes are sensitive to a hearing loss of 20 to 30 dB and are, consequently, useful for screening purposes. Alternative approaches might be proposed. An important clinical issue is to separate subjects according to more demanding audiometric criteria. For example, separating a 30-dB from a 40-dB hearing loss may have important practical consequences. Likewise, there is wide acceptance that the level of stimulation tones used for eliciting DPOEs is of prominent significance for the physiological interpretation of responses. It has been hypothesized[7-12] that different cochlear sources of DPOEs exist, so that DPOEs can provide information on the cochlear function in humans, either on the active mechanical status if the stimulation level is low enough, or on the passive mechanical status if the level exceeds 60 to 70 dB SPL. The goal of our experiment was to determine the level of hearing loss for which DPOEs would be present or absent. For this purpose, the level of hearing loss for which presence or absence of DPOEs was assumed to be discriminant was varied, and decision theory was applied to establish the best criterion. We elicited DPOEs by different levels of stimulation tones ranging from 30 to 70 dB SPL (in 10-dB steps) in order to control to what extent they influenced the DPOE properties and, consequently, the diagnostic test properties. Two samples of subjects were recruited: 1) individuals with clinically normal hearing and 2) patients with pure sensorineural hearing losses of various degrees. The goal of evaluating the diagnostic test properties of DPOEs was accomplished by examining these otoacoustic emissions in individuals, but also, the analysis of these results was done from a statistical point of view. The main informational parameters used in this study were the sensitivity, the specificity, the positive predictive value (PPV), and the negative predictive value (NPV) of the test and the analysis of ROC curves.

MATERIALS AND METHODS

Subjects. The DPOEs were measured in 108 subjects. The control group included 34 young adult volunteers (ages 14 to 34 years, mean 23 years). They had normal hearing without any history of otologic disease or exposure to ototoxic agents or noise, and had normal otologic findings (normal otoscopic findings, normal middle ear pressure, and normal acoustic reflex thresholds). All subjects had audiometric pure tone thresholds of 10 dB hearing level (HL) or less at octave frequencies between 0.25 and 1 kHz and at half-octave frequencies between 1 and 8 kHz.

The pathologic group included 74 patients (ages 17 to 92 years, mean 46 years) presenting with hearing impairment. They came to the outpatient otolaryngology clinic for routine evaluation. All patients exhibited a pure sensorineural hearing loss based on audiogram, acoustic reflex thresholds, and auditory brain stem responses. They had normal otoscopic findings and normal middle ear pressure. The sensorineural hearing losses had various causes: acoustic trauma (n = 8), ototoxic drugs (n = 4), and presbycusis (n = 62). Most of the ears exhibited predominantly high-tone hearing losses. The mean auditory thresholds were 26 dB HL (standard error [SE] 1.9), 34.6 dB HL (SE 2), and 52.2 dB HL (SE 2.45) for 1, 2, and 4 kHz, respectively. The reported investigations were performed in accordance with the principles of the Declaration of Helsinki.

DPOE Recordings. The DPOE recordings obtained with a small acoustic probe incorporating two earphones (Etymotic Research ER-2) are characterized by a flat frequency response from 0.2 to 10 kHz, and a linear operation up to 100 dB SPL in the human external auditory canal. A measuring amplifier (Bruël and Kjaër 2609) and a 0.5-in microphone (Bruël and Kjaër 4166) were used to calibrate the probe in a standard 2-cm^3 coupler (Bruël and Kjaër DB138). Acoustic responses were detected by a low-noise microphone (Etymotic ER-10B). All recordings were done in a double-walled, sound-treated booth with the probe sealed into the external auditory canal by an impedance probe without any external support.

TECHNICAL CHARACTERISTICS OF PRIMARY FREQUENCIES

Pure Tones (Primaries, Hz)			*Range of Noise Floor*	*Geometric Mean of*	*Frequency*
f1	*f2*	*f2/f1*	*(dB SPL)*	*f1 and f2 (Hz)*	*of 2f1−f2 (Hz)*
918	1,129	1.23	−7 to −11	1,000	707
1,798	2,211	1.23	−12 to −15	2,000	1,385
3,600	4,440	1.23	−15 to −20	4,000	2,760

The two primary tones, called f1 and f2, were generated by the two earphones (ER-2) connected to a two-channel frequency synthesizer (Hewlett Packard 8904A) and delivered separately to the ear through two small-diameter tubes. The DPOE signal was delivered without amplification to a dynamic signal analyzer (Hewlett Packard 3561A) for extraction of the Fourier components at 1) the 2f1 − f2 frequency and 2) over a 50-Hz frequency span below the 2f1 − f2 frequency that estimated the noise floor. Fast-Fourier transform was done over a frequency span of 1 kHz and a frequency resolution of 2.5 Hz with a Hanning weighting function. The amplitude of 2f1 − f2 and the amplitude of the noise floor were determined from the average of five spectra. Both signal generation and response analysis were automatically controlled by a microcomputer (IBM AT3 with a Hewlett Packard 82304 basic ROM expansion board on a Hewlett Packard 82321 language processor card). For each DPOE measure, the 2f1 − f2 amplitude was statistically compared with the mean noise floor amplitude, estimated as the mean value of 20 points (50-Hz span). If the 2f1 − f2 amplitude was included within the 95% confidence interval (CI) of the noise floor, the DPOE was considered to be nonsignificant. If the 2f1 − f2 amplitude was greater than the upper limit of the 95% CI of the noise floor, the DPOE was considered to be present. Coupler tests showed that instrumental distortions did not exceed −20 dB SPL when primary levels were less than or equal to 70 dB SPL.

Procedures and Statistical Analysis. Audiometric data were available from the same day on which the DPOE measurements were made. But, in all cases, the physicians that recorded the DPOEs were unaware of the audiometric results, which were obtained by another physician. For each subject, the tested ear was selected at random unless there was some indication that an ear would not be appropriate for DPOE testing (eg, external or middle ear disease). The DPOE input-output functions were measured for three 2f1 − f2 DPOEs (ie, 707 Hz, 1,385 Hz, and 2,760 Hz) with a fixed f2/f1 ratio near 1.23 (see Table). For each DPOE input-output function, equilevel stimuli L1 and L2 were delivered from 70 dB SPL to 30 dB SPL in 10-dB steps.

Principles of decision theory[18] have been applied to the problem of evaluating the ability of DPOEs to distinguish normal-hearing subjects from hearing-impaired subjects.[16,17,19] For each frequency tested, two groups of ears were defined relative to an arbitrary reference, the "audiometric criterion." The "audiometric criterion" is the screening limit value separating the two groups. Ears were classified in these two groups as a function of their audiometric threshold. The first group included ears having an audiometric threshold better (lower) than or equal to the audiometric criterion; the second group included ears having an audiometric threshold greater than the audiometric criterion. For example, with an audiometric criterion at 15 dB HL, the first group, including ears with a normal hearing function, had an auditory threshold of <15 dB HL for the frequency tested, and the second group, the diseased ears, had an auditory threshold of >15 dB HL for the frequency tested.

The study attempted to describe the extent to which DPOEs, classified dichotomously as either present or absent, could determine hearing status for audiometric criteria ranging from 10 to 75 dB HL. For each audiometric criterion, two-by-two tables were constructed to determine how normal and impaired ears could be classified on the basis of the presence or absence of DPOEs. The percentages of ears correctly identified as hearing-impaired (hits) on the basis of DPOE absence were estimated, as were the percentages of normal-hearing ears incorrectly identified as hearing-impaired (false alarms). Hits, or true positives, were defined as individuals having hearing thresholds of $>y$ dB HL who would be classified without error if this audiometric criterion value was used. False alarms, or false positives, were defined as individuals having thresholds of $\leq x$ dB HL who would be classified as having an audiometric threshold of $>x$ dB HL if that criterion value was used.

For each tested frequency (ie, 1, 2, and 4 kHz), DPOEs were recorded in response to five different stimulation intensities (ie, 30, 40, 50, 60, and 70 dB SPL). Thus, 15 DPOE recordings were made for 1 tested ear. For each DPOE stimulation intensity, a two-by-two table was constructed for each audiometric criterion. The audiometric criteria ranged from 10 to 75 dB HL in 5-dB steps. Thus, 14 two-by-two tables were constructed for each DPOE stimulation intensity. From each table, the PPV and NPV, with the 95% CI, were estimated. The PPV corresponds to the probability that a subject will have impaired hearing function when the test result is positive. The test was considered positive when DPOEs were absent for a precise frequency and primary stimulation

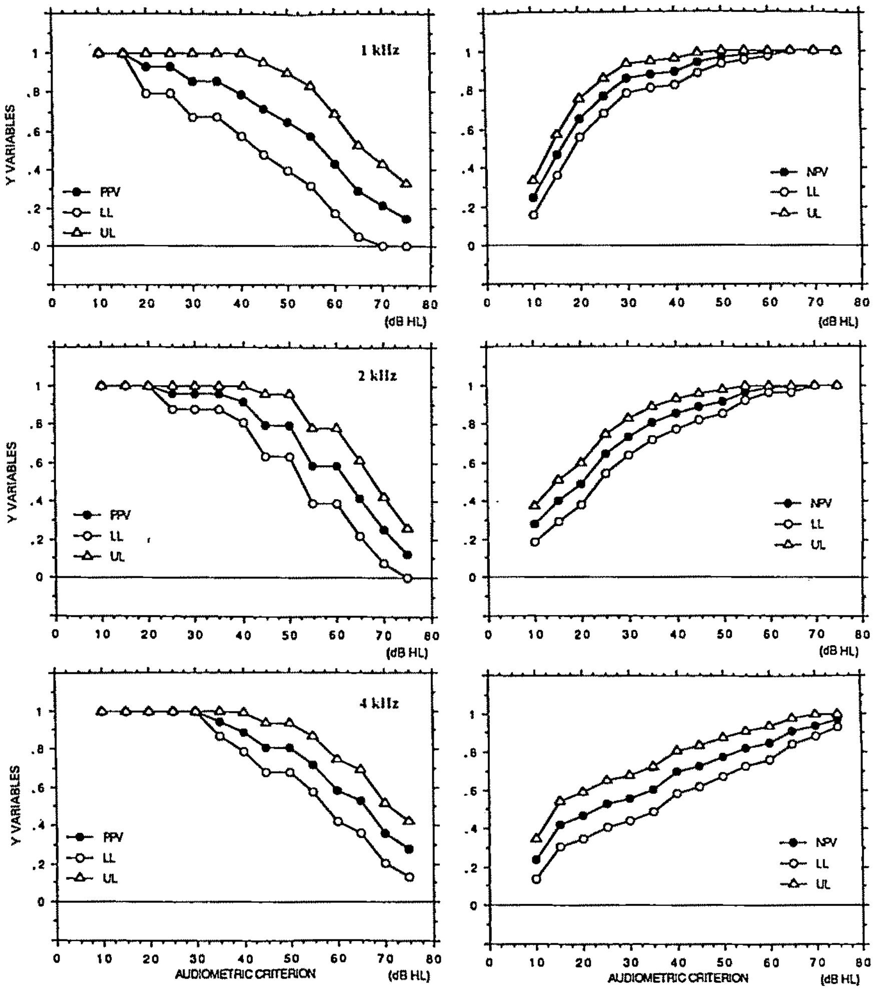

Fig 1. Positive predictive value (PPV; left side of Figure) and negative predictive value (NPV; right side of Figure) (solid circles), with upper limit (UL; open triangles) and lower limit (LL; open circles) of 95% confidence interval (CI) for distortion product otoacoustic emissions (DPOEs) elicited by 70–dB sound pressure level (SPL) equilevel primary stimulation intensity at three frequencies: 1, 2, and 4 kHz. PPV decreases and NPV increases when audiometric criterion increases.

level. The NPV corresponds to the probability that a subject will have normal hearing function when the test result is negative. The test was considered negative when DPOEs were present for a precise frequency and primary stimulation level.

Moreover, the percentages of hits for DPOEs were plotted as a function of false alarms to generate the ROC curves. Each ROC curve point was calculated from hit and false alarm rates corresponding to the presence or absence of a DPOE for precise audiometric criteria ranging from 10 to 75 dB HL in 5-dB steps. Thus, this analysis allows us to determine the optimal audiometric criterion for separating ears according to the presence or absence of DPOEs.

RESULTS

Positive and Negative Predictive Values. The noise floor varied as a function of f2 frequency (see Table). The results summarized in Fig 1 represent the evolution of the PPV and NPV in response to a 70–dB SPL primary stimulation intensity as a function of the audiometric criterion. Three series of curves (ie, curves A, B, and C) were plotted for three different frequencies (1, 2, and 4 kHz, respectively). The upper limit and the lower limit of the 95% CI are represented above and below each PPV or NPV curve.

The main feature of these functions is that the PPV decreased and the NPV increased when the audiometric criterion was increased. With a low audiometric criterion — for example, 15 dB HL (considered the upper limit of normal hearing) — the probability that the ear was impaired was near 1 (for the three frequencies tested) when the test was positive (absence of DPOEs), while the probability that the ear was normal when the test was negative (presence of DPOEs) ranged between .4 and .5, whatever the frequency tested. On the other hand, with an audiometric criterion around 30 dB HL, the probability that the hearing level was ≥30 dB HL ranged between .88 (1 kHz) and 1 (4 kHz) when the test was positive, while the probability that the hearing level was <30 dB HL when the test was negative ranged from .55 (4 kHz) to .85 (1 kHz). With a high audiometric criterion — for example, 60 dB HL (separating moderate versus severe hearing loss) — the probability that the hearing level was ≥60 dB HL (ie, severe or profound hearing loss) ranged between .4 and .6 when the test was positive, while the probability that

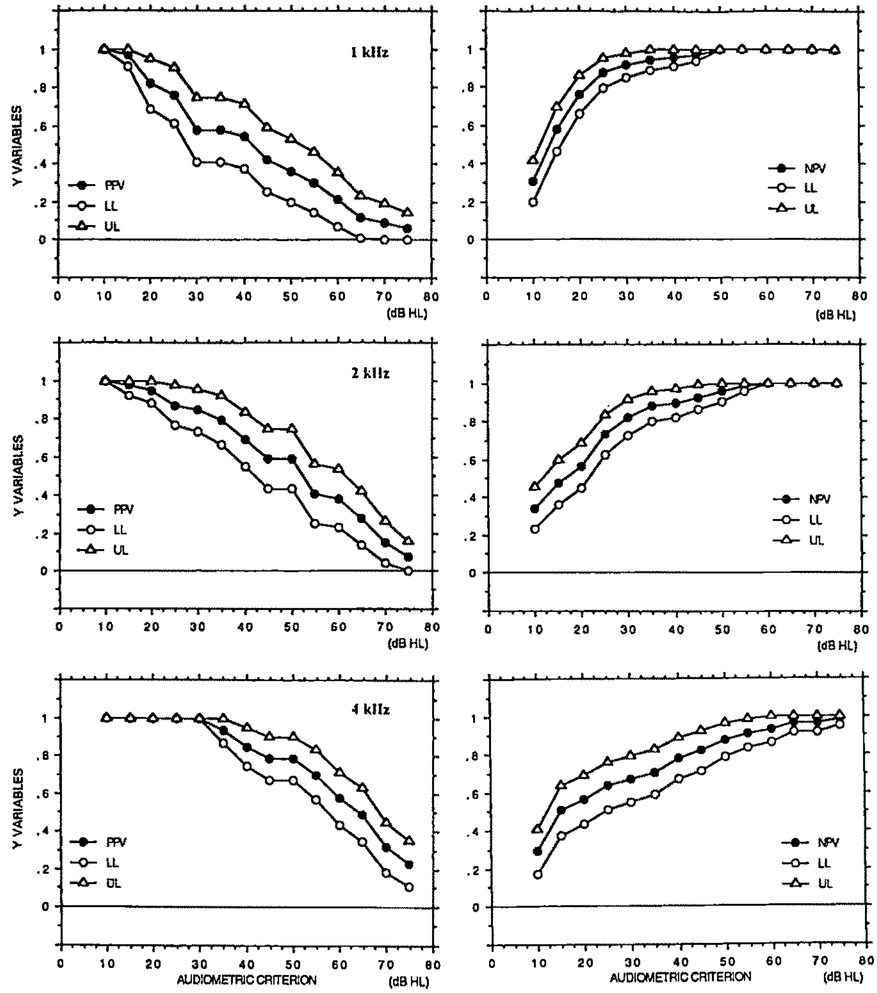

Fig 2. PPV (left side of Figure) and NPV (right side of Figure) (solid circles), with UL (open triangles) and LL (open circles) of 95% CI for DPOEs elicited by 60-dB SPL equilevel primary stimulation intensity at three frequencies: 1, 2, and 4 kHz.

the hearing level was <60 dB HL ranged from .84 to 1 when the test was negative.

Figures 2-5 progressively represent the evolution of the PPV and NPV as a function of the audiometric criterion in response to primary equilevel stimulations ranging from 60 dB SPL (Fig 2) to 30 dB SPL (Fig 5). For each primary stimulation intensity, the PPV decreased and the NPV increased with increases in the audiometric criterion. With a low audiometric criterion — for example, 15 dB HL — the probability that the tested ear was impaired when the test was positive dropped from 1 to .7 with a primary stimulation intensity decreasing from 70 to 30 dB SPL. The probability that the ear was normal when the test was negative ranged between .42 (4 kHz, 70 dB SPL) and .87 (4 kHz, 30 dB SPL).

Receiver Operating Characteristic Curves. The analysis summarized in Fig 6A represents a statistical decision theory approach to selecting appropriate criteria for classifying normal-hearing and hearing-impaired subjects on the basis of DPOEs with equilevel primary stimulation at 70 dB SPL. Each point represents the relationship between the false alarm rate (ie, 1 minus specificity) and the hit rate (ie, sensitivity) for an audiometric criterion used (these ranged from 10 to 75 dB HL by 5-dB steps): the lower the audiometric criterion, the lower the hit rate value, and the lower the false alarm value. For example, with an f2 frequency at 1 kHz, the false alarm rate increased from 0% to 12%, while the hit rate increased from 16% to 100% with an audiometric threshold ranging from 10 to 75 dB HL. An ideal test would have a hit rate value equal to 1 and a false alarm value equal to 0 (upper left corner of each ROC diagram, point A). The audiometric criterion giving the highest hit rate and the lowest false alarm rate was 60 dB HL. Similar results were obtained with a 2-kHz DPOE, but the hit rate decreased and the false alarm value increased at this frequency. At 4 kHz, the maximum hit rate obtained was 83%, while the false alarm value was high (around 25%).

With a primary stimulation intensity at 60 dB SPL, similar results were obtained (Fig 6B). The best hit rates ranged from 100% (1 and 2 kHz) to 90% (4 kHz) with an audiometric criterion around 50 to 55 dB HL. The false alarm rate was around 20% for these three

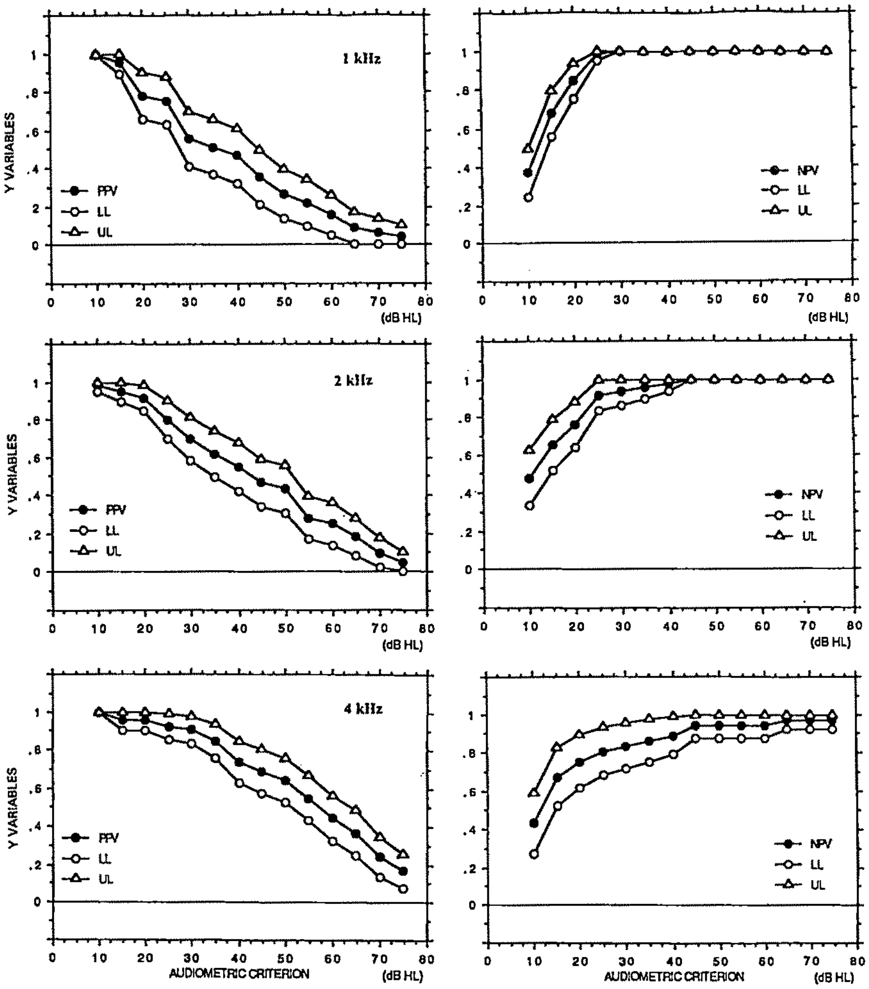

Fig 3. PPV (left side of Figure) and NPV (right side of Figure) (solid circles), with UL (open triangles) and LL (open circles) of 95% CI for DPOEs elicited by 50–dB SPL equilevel primary stimulation intensity at three frequencies: 1, 2, and 4 kHz.

frequencies. Figure 6C summarizes results estimated for primary stimulation intensities of 50 dB SPL. Three important modifications can be observed: 1) maximum hit rates dropped from 100% to 95% when DPOE frequencies decreased from 1 to 4 kHz; 2) in comparison with DPOEs elicited by high primary intensities (70 and 60 dB SPL), false alarm values increased by 20% for best hit rates; and 3) the audiometric criterion giving the highest hit rate and the lowest false alarm rate was around 25 to 30 dB HL, whatever the frequency tested. For the lowest primary stimulation intensities (ie, 40 and 30 dB SPL), the main characteristic was the augmentation of false alarm incidence without any modification of best hit rates (Fig 6D,E). The audiometric criterion giving the highest hit rate and the lowest false alarm rate was around 25 to 30 dB HL, whatever the frequency tested.

DISCUSSION

This work explores the potential of a statistical method to evaluate DPOE measurements in relation to audiometric thresholds at three primary frequencies (f2 frequencies at 1,129 Hz, 2,211 Hz, and 4,440 Hz). The DPOEs were classified as either present or absent, and their amplitudes were not analyzed. We have not analyzed these DPOE amplitude variations because some authors have shown that dramatic changes can occur for DPOE input-output functions obtained with slight primary frequency changes.[11,20,21] Therefore, it was very important to use a reliable decision rule to assess their presence or absence with respect to the noise floor. For this purpose, spectral averaging was used in order to have a more stable estimate of noise. On the other hand, the signal-to-noise ratio would have been improved with temporal averaging. As DPOEs had to be collected in a standard clinical setting, the limitation of the signal-to-noise ratio was mainly the patient's cooperation in being very quiet, and technical improvements in DPOE recording did not seem essential.

Two main points arise from this statistical analysis. The first concerns the interpretation of ROC curves. The second is the analysis of the PPV and NPV as functions of the audiometric criterion.

The aim of this study was to evaluate DPOE test performance. For this purpose, Gorga et al[16] used analyses based on decision theory (ROC curves).

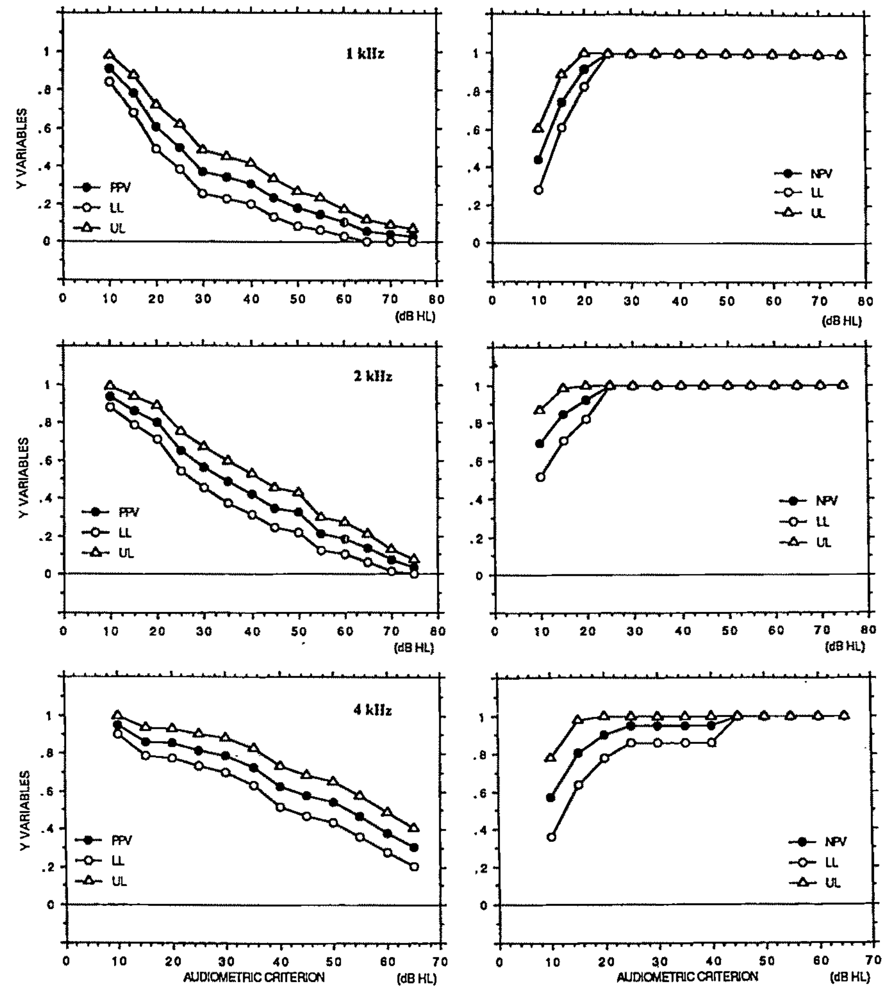

Fig 4. PPV (left side of Figure) and NPV (right side of Figure) (solid circles), with UL (open triangles) and LL (open circles) of 95% CI for DPOEs elicited by 40–dB SPL equilevel primary stimulation intensity at three frequencies: 1, 2, and 4 kHz.

Each ROC curve was constructed for an arbitrarily chosen audiometric criterion (ie, 10 to 40 dB HL in 5-dB steps). For an ROC curve, each point was calculated for a DPOE amplitude (or DPOE/noise) at different frequencies (ie, 500- to 8,000-Hz octave frequencies). Then, their goal was to compare ROC curves for these five frequencies. The DPOE amplitude and DPOE/noise measurements were able to distinguish between normal and impaired ears at >2,000 Hz, but the performance decreased as frequency and audiometric criterion decreased. In another paper, Gorga et al[17] used the same technique in order to compare DPOEs and transient evoked otoacoustic emissions (TEOEs). They also reported better performance for TEOEs at <2,000 Hz.

Our approach is different. Although it is based on ROC curves, their construction differs. Each point was calculated from hit and false alarm rates corresponding to the presence or absence of DPOEs for precise audiometric criteria ranging from 10 to 75 dB HL in 5-dB steps. Therefore, the aim of this analysis was to determine the optimal audiometric criterion for separating ears according to the presence or absence of DPOEs. For both data processing methods, it is not clear whether the conclusions might be generalized to other procedures and equipment. The method of Gorga et al[16] uses DPOE amplitude as a quantitative criterion. However, a recent study by Hall et al[22] showed that DPOE amplitudes in the same ear are variable when the detecting equipment is changed. Allen and Fahey[23] pointed out that the acoustic characteristics of the probe microphone may greatly influence the detection of DPOE. The method we propose eliminates the question of quantitative appreciation of amplitude by merely considering presence or absence of DPOEs with respect to noise floor. However, noise floor levels also depend on technical conditions and on subject cooperation. Thus, none of these methods seems able to provide universal criteria.

The ideal discrimination threshold would allow the separation of all subjects without either false positives or false negatives. In this theoretic case, the sensitivity and the specificity will be equal to 1. In our study, the discrimination threshold used is the audiometric criterion. Thus, the most interesting point of these ROC curves corresponds to the clinical conditions giving the highest hit rate and the lowest false

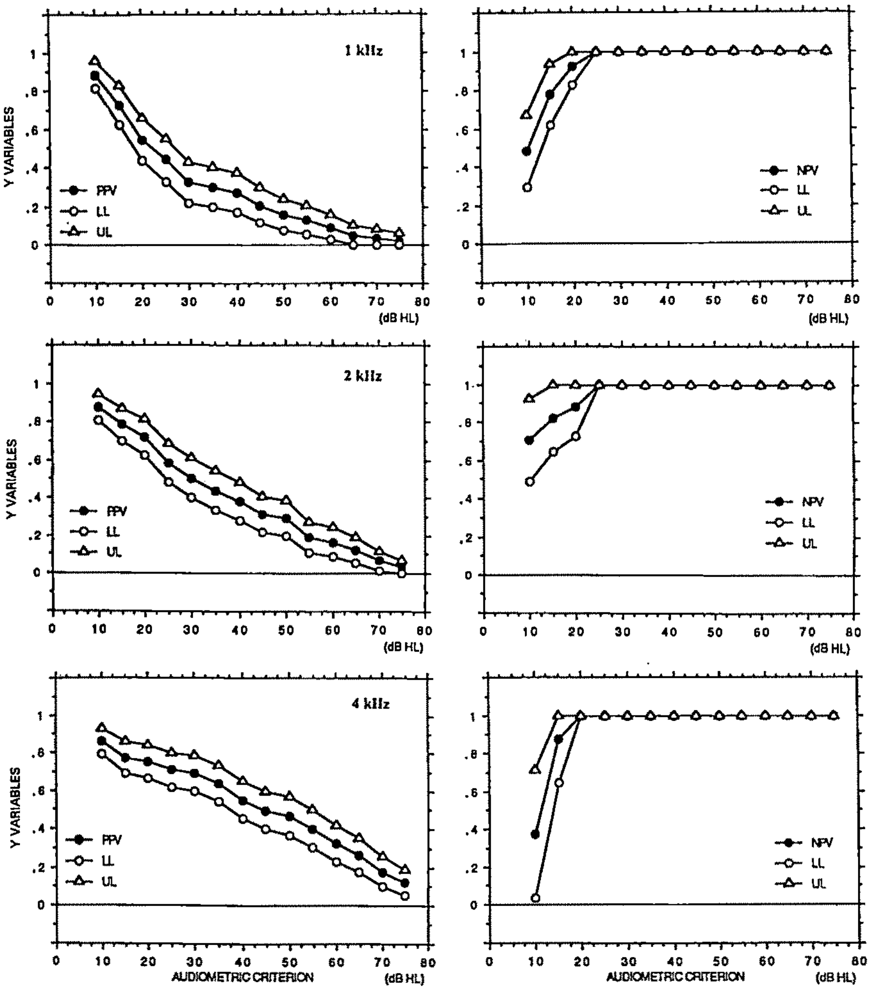

Fig 5. PPV (left side of Figure) and NPV (right side of Figure) (solid circles), with UL (open triangles) and LL (open circles) of 95% CI for DPOEs elicited by 30-dB SPL equilevel primary stimulation intensity at three frequencies: 1, 2, and 4 kHz.

alarm rate. Two different categories of ROC curves were identified in this study. The first one reflects DPOEs elicited by high primary stimulation levels (ie, 70 and 60 dB SPL; Fig 6A,B). In these cases, the best audiometric criterion value, giving a high sensitivity (ie, hit rate) and a low false alarm rate, was >55 dB HL. For example, for a primary stimulation level of 70 dB SPL, this best criterion value was around 60 to 65 dB HL, whatever the frequency tested between 1 and 4 kHz. The second pattern of ROC curves reflects DPOEs elicited by low primary stimulation intensities (ie, ≤50 dB SPL). In these cases, the best audiometric criterion value was <30 dB HL. For example, the best criterion value for 1-kHz DPOEs in response to a 50-dB SPL stimulation level is 30 dB HL. This fact has two main consequences. First, if DPOEs are used for screening auditory function in order to separate subjects with normal versus subnormal hearing function (ie, audiometric threshold of 30 dB HL), the DPOE parameters must include a primary stimulation level of ≤50 dB SPL. On the other hand, if the screening test is used to separate subjects with a profound or severe hearing loss from other subjects, it would be more useful to use DPOEs with a high primary stimulation level, ≥60 dB SPL.

Other clinical circumstances need very high hit rates, whereas high false alarm rates may be tolerated — for example, in assessing individual risk for hearing loss. The ROC curves allow the determination of needed protocol changes. For example (Fig 6C), at 2 kHz, the highest hit rate is obtained for an audiometric criterion of 45 dB HL. The false alarm rate increases by about 20% with respect to the ideal protocol, which was previously chosen with an audiometric criterion of 25 to 30 dB HL. In this case, the hit rate only increases by 8%. Similar features are observed for most frequencies and levels. These modifications of the protocol in order to obtain very high hit rates only produce minor variations of the hit rates, while false alarm rates greatly increase. Thus, it seems that such a practice should not be recommended.

In clinical practice, it is necessary to interpret the result of a test while the real patient status (ie, normal or impaired ear) is unknown. For this purpose, two parameters are defined in diagnostic procedure evaluation theory. First, the PPV corresponds to the prob-

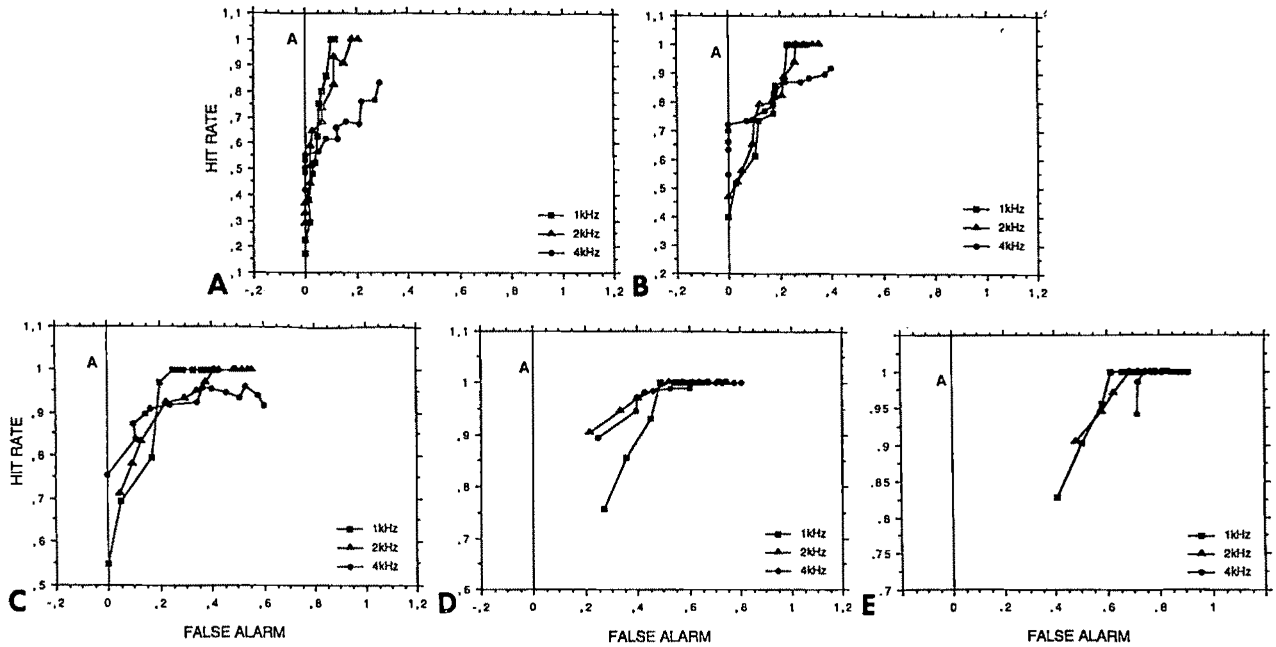

Fig 6. Receiver operating characteristic (ROC) curves for DPOEs elicited by A) 70 dB SPL, B) 60 dB SPL, C) 50 dB SPL, D) 40 dB SPL, and E) 30 dB SPL primary stimulation level at three frequencies: 1 kHz (squares), 2 kHz (triangles), and 4 kHz (circles), with audiometric criterion varying from 10 to 70 dB HL by 5-dB steps. The lower the audiometric criterion, the lower the hit rate value, and the lower the false alarm value. Ideal test would have hit rate value equal to 1 and false alarm value equal to 0 (point A at upper left corner of ROC diagram). Audiometric criterion giving highest sensitivity and lowest false alarm value varied as function of primary stimulation level. It was, respectively, 60 dB HL (A), 50 to 55 dB HL (B), and 25 to 30 dB HL (C-E) for primary stimulation levels of 70 to 30 dB SPL.

ability of a subject's having impaired hearing function when the test result is positive. In the study, the test was considered positive when DPOEs were absent for a precise frequency (1, 2, or 4 kHz) and primary stimulation level (70, 60, 50, 40, or 30 dB SPL). This probability is high when the audiometric criterion is low. This fact is easily understandable: DPOEs are present in normal subjects, and their incidence decreases with increasing audiometric thresholds.[24-26] On the other hand, the absence of DPOEs in patients with a severe or profound sensorineural hearing loss is physiologically reassuring (ie, seems normal on the basis of auditory physiology). These data give the precise probability, with a 95% CI, for each subject to be classified below or above an audiometric criterion as a function of the absence of DPOEs for each frequency and primary intensity tested.

Second, the NPV corresponds to the probability of a subject's having normal hearing function when the test is negative. In the study, the test was considered negative when DPOEs were present for a precise frequency and primary stimulation level. This probability is high when the audiometric criterion is high. This fact is also easily understandable: DPOEs are absent in hearing-impaired subjects, and their incidence increases as audiometric thresholds decrease.[24-26] Most clinical publications on the incidence of DPOEs in ears with sensorineural hearing loss describe the variation in this incidence as a function of the audiometric threshold. Recently, we showed that the incidence of DPOEs in patients with hearing thresholds of ≥30 dB HL ranged between 48% and 53% (as a function of the frequency tested between 1 and 4 kHz) in response to an equilevel primary stimulation level of 72 dB SPL, ranged between 13% and 22% in response to a 62–dB SPL stimulation, and was <7% in response to a stimulation of ≤52 dB SPL.[25] Our results give the precise probability, with a 95% CI, for each subject to be classified below or above an audiometric criterion as a function of the presence of DPOEs for each frequency and primary intensity tested. For example, the probability of a subject's having an audiometric threshold of <30 dB HL and DPOEs in response to a 70–dB SPL primary stimulation intensity is around 88%. This probability is 100%, 93%, 100%, and 100% when DPOEs are present in response to stimulation levels of 60, 50, 40, and 30 dB SPL, respectively. These data provide an estimation of the risk of error when DPOEs are used for screening auditory function in humans.

The study of DPOEs is important because it contributes to a better understanding of cochlear function. The DPOE properties in normal and hearing-impaired ears seem to vary greatly as a function of the primary stimulation intensity. When a high stimulation intensity is used (ie, ≥60 dB SPL), DPOE presence or absence can be useful in discriminating, with good sensitivity and specificity, subjects with an audiometric threshold greater or lower than 55 to 60 dB HL. With a lower audiometric criterion, the sensitivity of the test drops dramatically. Thus, these DPOEs elicited by high stimulation intensities seem to be the marker of some physiological mechanisms whose properties change when cochlear damage is associated with audiometric thresholds around 55 to 60 dB HL. On the other hand, when a lower stimulation level is used (ie, ≤50 dB SPL), DPOE presence or absence can be useful in separating subjects with an audiometric threshold worse than or better than 25 to 30 dB HL with great sensitivity and specificity. Therefore, these DPOEs elicited by low stimulation intensities seem to be associated with other physiological mechanisms whose properties change when audiometric thresholds are around 25 to 30 dB HL. Whitehead et al[27] noted that a notch often existed in the input-output DPOE functions for input levels around 60 to 70 dB SPL. Never was more than one notch observed. Therefore, these observations suggested separating the DPOE input-output function into two parts according to stimulus level. Moreover, in certain input-output functions, an enhancement of the DPOE amplitude was observed that could be explained by the summation of two sources that were in phase.[27] Similar results have been published by Popelka et al.[11]

Most authors consider DPOEs to be made up of two distinct components: an "active" source that is dominant at low and moderate stimulus levels, and a "passive" source. The passive component is observed when the active component disappears after either furosemide intoxication[12,28] or ototoxic aminoglycoside administration.[7,27] The existence of two components in the DPOEs has also been previously suggested on the basis of some other lines of evidence, including changes postmortem and/or after acoustic trauma,[9,29] and changes with development.[30] In our study, the so-called active DPOE component seems to be mainly present in humans when audiometric thresholds are <30 dB HL. The DPOEs elicited by low primary stimulation intensities are produced within the cochlea by nonlinear interactions between the two primary tones,[4,31] and their sensitivity to outer hair cell dysfunction indicates that this nonlinearity is closely related to electromechanical processes in outer hair cells. Hamernik et al[32] have studied the quantitative relationship between sensory cell loss and hearing thresholds on the basis of experimental data obtained from 420 chinchillas with noise-induced hearing loss. For example, at 2 kHz, the percentage of outer hair cell loss changed from 0% to 50% when the threshold shifted from 0 dB to 30 dB. When all outer hair cells disappeared, the threshold shift was around 60 dB. In regions of the cochlea that transduce frequencies of >1 kHz, the three rows of outer hair cells show the same degree of loss for a given threshold shift. This remarkable value of 30 dB HL does not correspond with some drastic cochlear hair cell modification. Moreover, the audiometric limit of 30 dB HL has been found in evoked otoacoustic emissions that are not recordable when the mean audiometric threshold (ie, 1-2-4 kHz) is greater than this value.[24] It seems difficult to strictly associate outer hair cell losses and the variations of DPOE properties at 25 to 30 dB HL (Fig 6C-E). On the other hand, the so-called passive DPOE component seems to be mainly present in humans when audiometric thresholds are <60 dB HL. From a physiological point of view, this audiometric limit of 60 dB HL corresponds to a complete disappearance of the tips of the auditory nerve fibers.[33-35] Histologically, this threshold is associated with a complete disappearance of the three rows of outer hair cells.[32] Thus, outer hair cells probably play a role in the generation of DPOEs elicited by high stimulation intensities. Therefore, it seems excessive to call such DPOEs a passive component.

In conclusion, this evaluation of peripheral auditory function by DPOEs using conditional probability allows a precise description of the statistical risk for a physician to use DPOEs as a screening tool. Moreover, the analysis of ROC curves suggests that two different DPOE components seem to be present in human ears. The properties of these two different components strongly differ in diseased ears.

REFERENCES

1. Gaskill SA, Brown AM. The behavior of the acoustic distortion product, 2f1-f2, from the human ear and its relation to auditory sensitivity. J Acoust Soc Am 1990;89:821-39.

2. Lonsbury-Martin BL, Harris FP, Stagner BB, Hawkins MD, Martin GK. Distortion product emissions in humans. I. Basic properties in normally hearing subjects. Ann Otol Rhinol Laryngol 1990;99(suppl 147):3-14.

3. Probst R, Lonsbury-Martin BL, Martin GK. A review of otoacoustic emissions. J Acoust Soc Am 1991;89:2027-67.

4. Kim DO, Molnar CE, Matthews JW. Cochlear mechanics: nonlinear behavior in two-tone responses as reflected in cochlear-nerve-fiber responses and in ear-canal sound pressure. J Acoust Soc Am 1980;67:1704-21.

5. Mensh BD, Patterson MC, Whitehead ML, Lonsbury-Martin BL, Martin GK. Distortion-product emissions in rabbit. I. Altered susceptibility to repeated pure-tone exposures. Hear Res 1993;70:50-64.

6. Sutton, LA, Lonsbury-Martin BL, Martin GK, Whitehead ML. Sensitivity of distortion-product otoacoustic emissions in humans to tonal over-exposure: time course of recovery and

effects of lowering L2. Hear Res 1994;75:161-74.

7. Brown AM, McDowell A, Forge A. Acoustic distortion products can be used to monitor the effects of chronic gentamicin treatment. Hear Res 1989;42:143-56.

8. Brown AM. Acoustic distortion from rodent ears: a comparison of responses from rats, guinea pigs and gerbils. Hear Res 1987;31:25-38.

9. Johnstone BM, Gleich B, Mavadat N, McAlpine D, Kapadia S. Some properties of the cubic distortion tone emissions in the guinea pig. Adv Audiol 1990;7:57-62.

10. Norton SJ, Rubel EW. Active and passive ADP components in mammalian and avian ears. In: Dallos P, Geisler CD, Mathews JW, Ruggero MA, Steele CR, eds. The mechanics and biophysics of hearing. New York, NY: Springer-Verlag, 1990:219-27.

11. Popelka GR, Osterhammel PA, Nielsen LH, Rassmussen AN. Growth of distortion-product otoacoustic emissions with primary-tone level in humans. Hear Res 1993;71:12-22.

12. Mills DM, Norton SJ, Rubel EW. Development of active and passive mechanics in the mammalian cochlea. Aud Neurosci 1994;1:77-99.

13. Bonfils P, Avan P, Elbez M, Deys S, Erminy M, Francois M. Auditory threshold evaluation by distortion-product otoacoustic emissions using decision support system. Acta Otolaryngol (Stockh) 1994;114:360-5.

14. Bonfils P, Avan P, Francois M, Trotoux J, Narcy P. Distortion-product otoacoustic emissions in neonates: normative data. Acta Otolaryngol (Stockh) 1992;112:739-44.

15. Avan P, Bonfils P. Frequency specificity of human distortion product otoacoustic emissions. Audiology 1993;32:12-26.

16. Gorga MP, Neely ST, Bergman B, et al. Otoacoustic emissions from normal-hearing and hearing-impaired subjects: distortion product responses. J Acoust Soc Am 1993;93:2050-60.

17. Gorga MP, Neely ST, Bergman B, Beauchaine KL, Kaminski JR, Liu Z. Towards understanding the limits of distortion product otoacoustic emission measurements. J Acoust Soc Am 1994;96:2639-48.

18. Weinstein MC, Fineberg HV. Clinical decision analysis. Philadelphia, Pa: WB Saunders, 1980.

19. Prieve BA, Gorga MP, Schmidt AR, et al. Analysis of transient-evoked otoacoustic emissions in normal-hearing and hearing-impaired ears. J Acoust Soc Am 1993;93:3308-19.

20. He NJ, Schmiedt RA. Fine structure of the 2f1-f2 acoustic distortion product: changes with primary level. J Acoust Soc Am 1993;94:2659-69.

21. Sun XM, Schmiedt RA, He NJ, Lam CF. Modeling the fine structure of the 2f1-f2 acoustic distortion product. II. Model evaluation. J Acoust Soc Am 1994;96:2175-83.

22. Hall JW, Hornsby B, Kelly T. Similarities and differences in distortion product otoacoustic emissions (DPOAE) among five commercially-available devices [Abstract]. Abstr Assoc Res Otolaryngol 1996;709:178.

23. Allen JB, Fahey PF. Using acoustic distortion products to measure the cochlear amplifier gain on the basilar membrane. J Acoust Soc Am 1992;92:178-88.

24. Bonfils P, Avan P, Francois M, Trotoux J, Narcy P. Otoacoustic emissions in audiology. A perspective. Ear Hear 1990;11:155-8.

25. Bonfils P, Avan P. Distortion-product otoacoustic emissions. Values for clinical use. Arch Otolaryngol Head Neck Surg 1992;118:1069-76.

26. Martin GK, Ohlms LA, Franklin DJ, Harris FP, Lonsbury-Martin BL. Distortion product emissions in humans. III. Influence of sensorineural hearing loss. Ann Otol Rhinol Laryngol 1990;99(suppl 147):30-42.

27. Whitehead ML, Lonsbury-Martin BL, Martin GK. Evidence for two discrete sources of 2f1-f2 distortion-product otoacoustic emission in rabbit: I. Differential dependence on stimulus parameters. J Acoust Soc Am 1992;91:1587-607.

28. Mills DM, Rubel EW. Variation of distortion product otoacoustic emissions with furosemide injection. Hear Res 1994; 77:183-99.

29. Lonsbury-Martin BL, Martin GK, Probst R, Coats AC. Acoustic distortion products in rabbit ear canal. I. Basic features and physiological vulnerability. Hear Res 1987;28:173-89.

30. Norton SJ, Bargones JY, Rubel EW. Development of otoacoustic emissions in gerbil. Evidence for micromechanical changes underlying development of the place code. Hear Res 1991;51:73-92.

31. Fahey PF, Allen JB. Nonlinear phenomenon as observed in the ear canal and at the auditory nerve. J Acoust Soc Am 1985;77:599-612.

32. Hamernik RP, Patterson JH, Turrentine GA, Ahroon WA. The quantitative relation between sensory cell loss and hearing thresholds. Hear Res 1989;38:199-212.

33. Dallos P, Harris D. Properties of auditory nerve responses in absence of outer hair cells. J Neurophysiol 1978;41:365-83.

34. Kiang NYS, Liberman MC, Levine RA. Auditory-nerve activity in cats exposed to ototoxic drugs and high-intensity sounds. Ann Otol Rhinol Laryngol 1976;85:752-68.

35. Liberman MC, Dodds LW. Single-neuron labelling and chronic cochlear pathology. III. Stereocilia damage and alterations in threshold tuning curves. Hear Res 1984;16:55-74.

Ann Otol Rhinol Laryngol 106:1997

THREE FAMILIAL CASES OF HEARING LOSS ASSOCIATED WITH ENLARGEMENT OF THE VESTIBULAR AQUEDUCT

SATOKO ABE, MD

SHIN-ICHI USAMI, MD HIDEICHI SHINKAWA, MD

HIROSAKI, JAPAN

The present report describes three familial cases of recessive hearing loss associated with enlargement of the vestibular aqueduct (EVA). Six siblings from three families showed EVA. The common characteristic of these patients was the presence of congenital, high-frequency, fluctuating sensorineural hearing loss. These cases suggest that EVA may be a useful discriminator between different types of recessive hearing loss.

KEY WORDS — anomaly, enlargement of vestibular aqueduct, familial disorders, inner ear, recessive hearing loss.

INTRODUCTION

The vestibular aqueduct is the bony canal containing the endolymphatic duct and endolymphatic sac. Enlargement of the vestibular aqueduct (EVA), initially reported by Valvassori and Clemis (1978), has been found in 1% to 1.5% of patients undergoing tomography.[1,2] This deformity has been evaluated by computed tomography (CT),[3-6] and the enlarged endolymphatic duct and sac within the bony otic capsule have been confirmed by magnetic resonance imaging (MRI).[7-10] Enlargement of the vestibular aqueduct is of particular interest, because this anomaly is often associated with characteristic clinical features, including progressive and/or fluctuating sensorineural hearing loss[2,8,9,11-17] and, sometimes, dysequilibrium symptoms.[11,12,18,19]

However, no attention has been paid to genetic backgrounds. Until recently, there had been no detailed reports on EVA associated with hereditary hearing loss, except that of Urman and Talbot,[6] who reported 3 patients with EVA out of 5 siblings. (The other 2

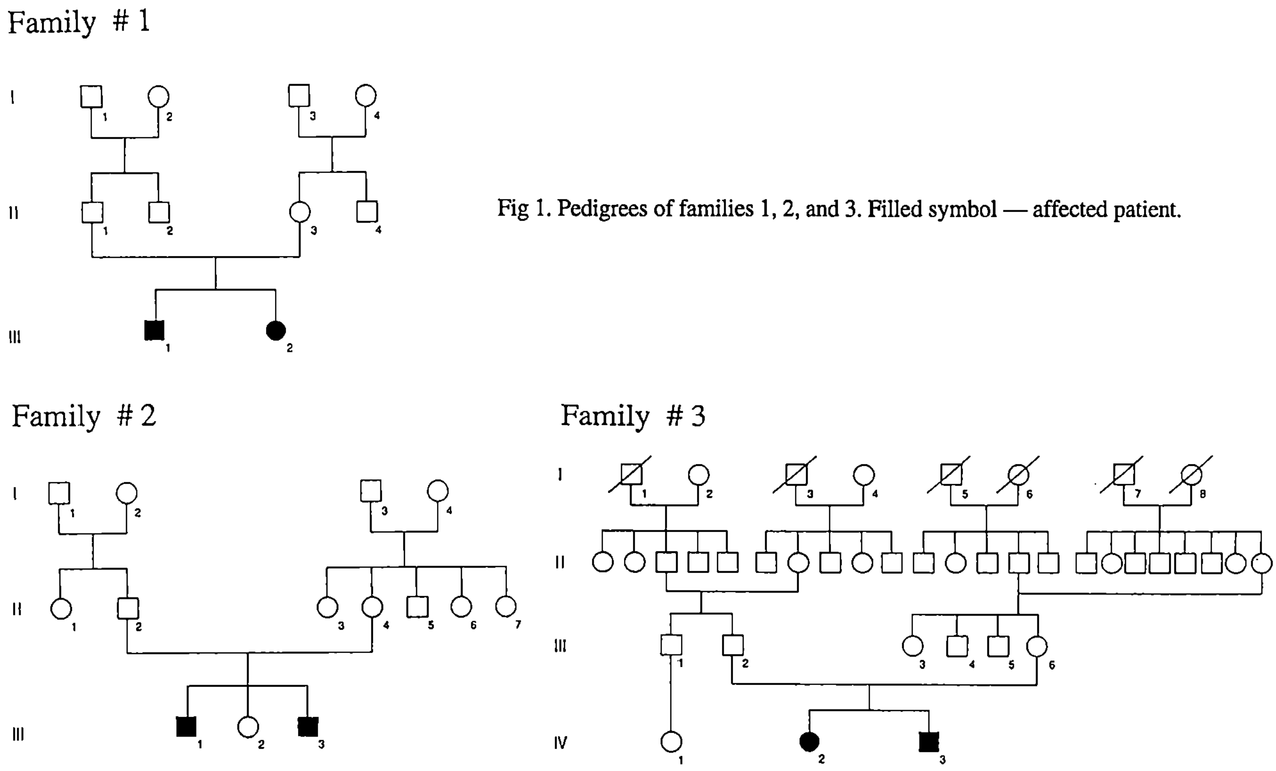

Fig 1. Pedigrees of families 1, 2, and 3. Filled symbol — affected patient.

From the Department of Otorhinolaryngology, Hirosaki University School of Medicine, Hirosaki, Japan.

CORRESPONDENCE — Shin-ichi Usami, MD, Dept of Otorhinolaryngology, Hirosaki University School of Medicine, 5 Zaifu-cho, Hirosaki, 036 Japan.

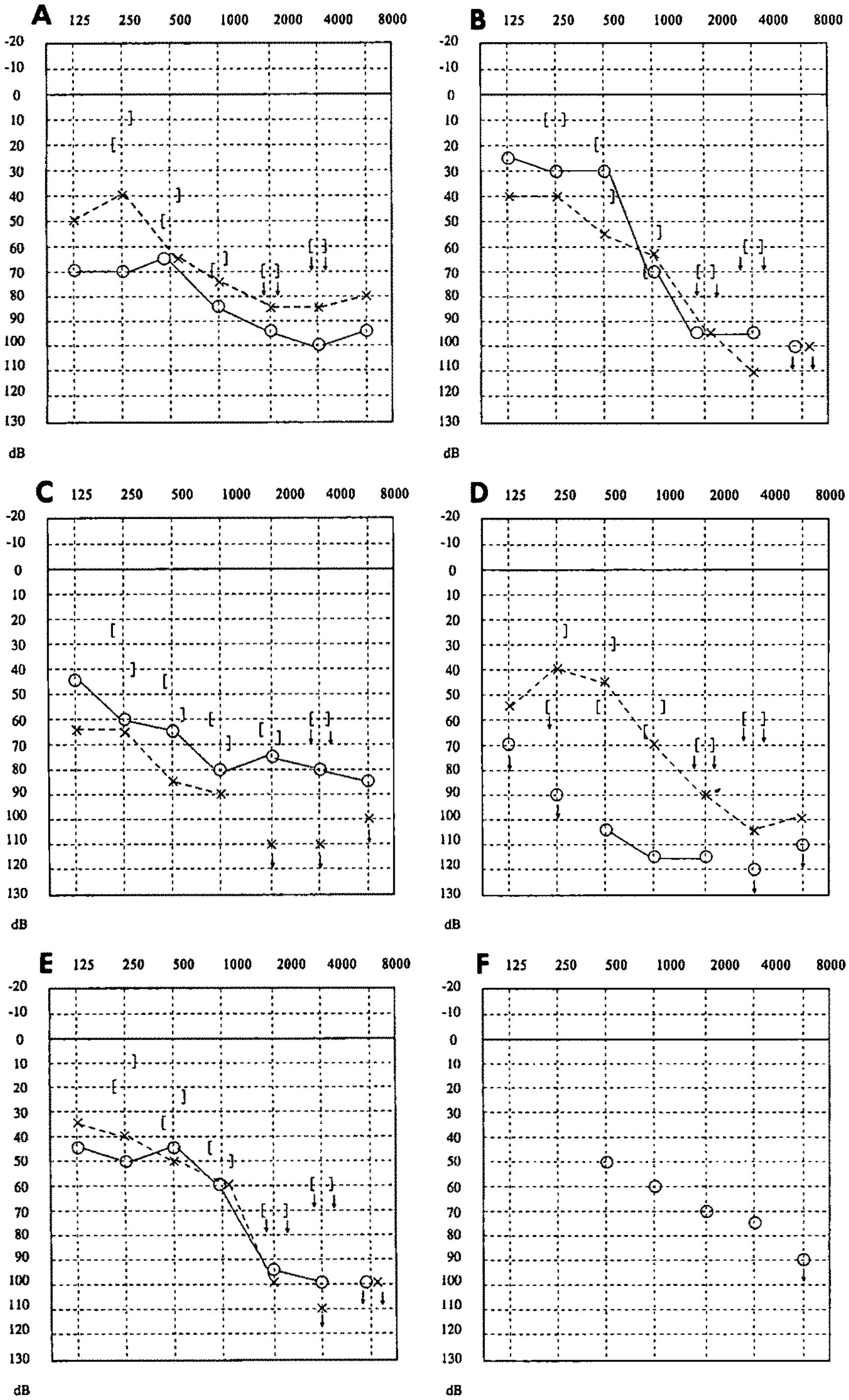

Fig 2. Most recent audiograms of affected siblings in families 1, 2, and 3 (last point of serial examinations shown in Fig 3). A) Family 1, III-1. B) Family 1, III-2. C) Family 2, III-1. D) Family 2, III-3. E) Family 3, IV-2. F) Family 3, IV-3 (conditioned orientation response data). All audiograms show high-frequency sensorineural hearing loss, with conductive components in low frequencies.

siblings had normal hearing and normal appearance of the vestibular aqueduct.) Griffith et al[20] reported 1 familial case of hearing loss associated with EVA. In the present paper, we describe 3 families, in each of which are 2 siblings with congenital hearing loss with EVA that seems to have been inherited in a recessive manner.

SUBJECTS AND METHODS

Six patients (2 siblings each from 3 families; pedigrees are shown in Fig 1; ages ranged from 1 to 8 years at diagnosis) showing EVA on CT scans were clinically evaluated by audiologic and vestibular testing. Gadolinium-enhanced MRI was also performed in 2 cases to confirm enlargement of the endolymphatic duct and sac. For audiometric testing, pure tone audiometry or conditioned orientation response (COR) testing was performed. The audiograms were serially reviewed over a period of 4 to 10 years. In some cases, distortion product otoacoustic emissions (DPOAEs) were measured to determine the status of the mechanical proper-

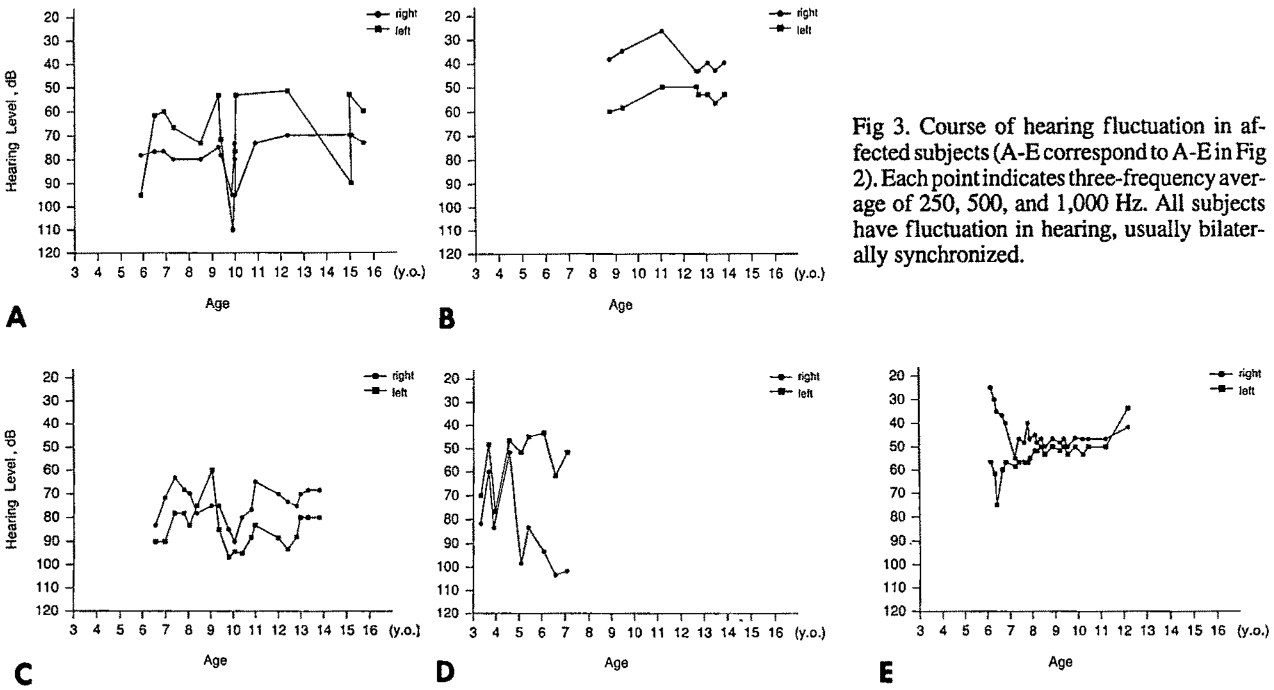

Fig 3. Course of hearing fluctuation in affected subjects (A-E correspond to A-E in Fig 2). Each point indicates three-frequency average of 250, 500, and 1,000 Hz. All subjects have fluctuation in hearing, usually bilaterally synchronized.

ties of the cochlea. For assessment of vestibular function, the eye tracking test (to evaluate smooth pursuit), optokinetic testing, caloric testing, and rotational testing were done in 3 subjects of the 6 (family 1, III-1 and 2, and family 3, IV-2). The 3 families had no known genetic relationships between them.

RESULTS

Pedigrees. That the 3 families had normal hearing in the parents and grandparents (which excludes the possibility of an autosomal dominant trait) and no sexual preference to the hearing loss (which eliminates X-linked inheritance) is indicative of autosomal recessive transmission. The patients had no particular episodes at the time of birth and their mothers did not have any particular problems during pregnancy (infectious disease, etc). None of the families reported any history of consanguinity.

Auditory Findings. Pure tone audiometric data were obtained bilaterally from 125 to 8,000 Hz (Fig 2) for all patients except 1, who was not old enough to undergo this examination. Nine ears showed a high-frequency–involved hearing loss, and 1 ear had profound hearing loss. Two ears, in a 3-year-old boy, could not be classified, but the COR pattern seemed to show high-frequency hearing loss (Fig 2F). In spite of having the sensorineural feature predominating, a conductive component in the lower frequencies was also present in 9 of the 10 ears examined. The degree of conductive loss ranged from 5 to 50 dB. All audiograms indicated somewhat asymmetric patterns. Serial audiometric testing was performed over 4 to 10 years in 5 patients (Fig 3). All ears with pure tone audiograms showed a more or less fluctuating hearing loss. Bilaterally involved ears seemed to be synchronously fluctuating. There were no obvious direct triggers of fluctuation, such as minor head trauma. Most patients recovered their hearing naturally without any special treatment. However, 1 ear presented a progressive hearing loss with fluctuation (Fig 3D).

At the first visit (at 1 to 8 years of age), auditory brain stem response (ABR) and COR testing were performed on 5 of the 6 patients (1 to 4 years old), since pure tone audiograms could not be carried out. The ABR thresholds indicated that hearing loss, at least in the high frequencies, existed at that point. Within the 10 ears examined, the ABR thresholds in wave V were observed at 100 dB in 5 ears, and at 90 dB in 3 ears. The COR data were also collected at the first visit. One example is shown in Fig 2F. The other COR patterns corresponded well to the pure tone audiogram patterns obtained when the patients were older.

The DPOAEs showed no response in the 8 ears (in 4 patients) examined.

Vestibular Function. There were no vestibular symptoms in any of the patients. No abnormal findings were detected in the 3 subjects who were examined by vestibular function testing.

Radiologic Findings. On CT (Figs 4-6), the average size of EVA (at the external aperture) of the present cases was 4.9 mm (range 4 to 6 mm). The EVA was the only anomaly identified in 9 ears. However, 1 ear was associated with another inner ear anomaly (slightly enlarged vestibule; family 1, III-2).

Magnetic resonance imaging (Figs 4-6) was per-

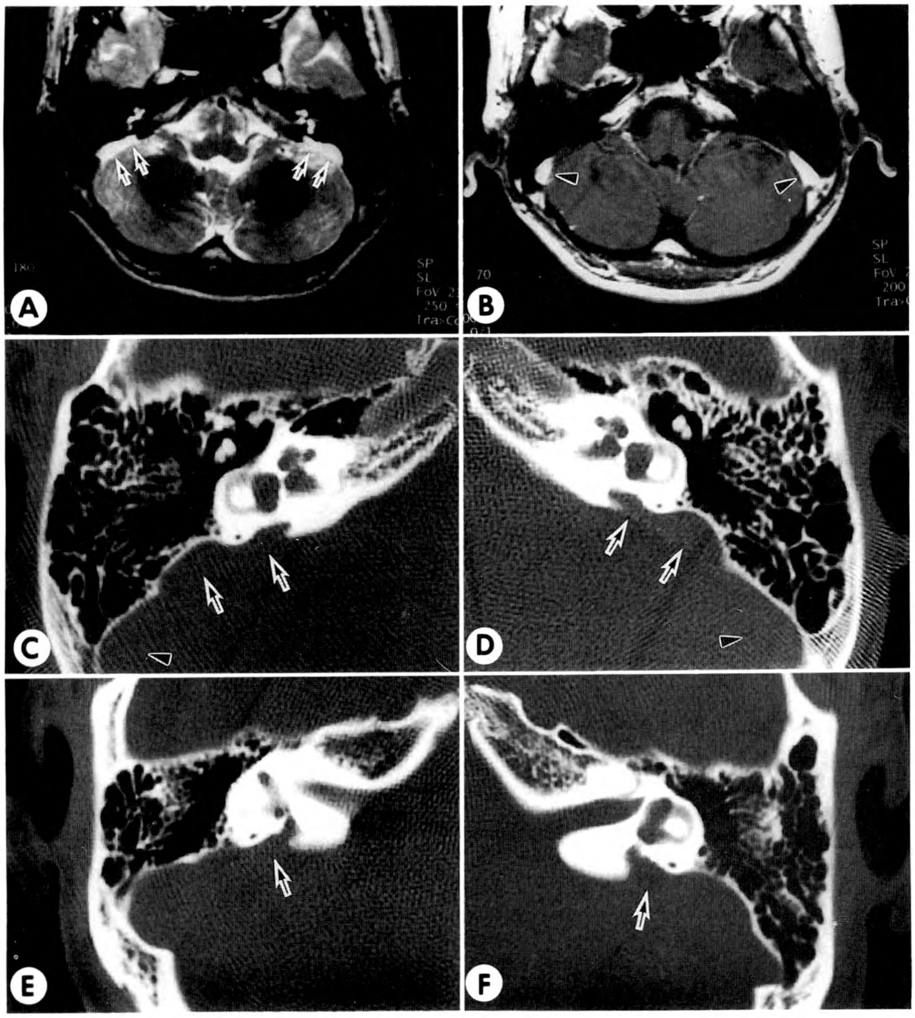

Fig 4. (Family 1) A) T2-weighted magnetic resonance image of 16-year-old boy (family 1, III-1) showing enlarged bilateral endolymphatic sac (arrows). Note that shape of endolymphatic sac complements shape of bony labyrinth shown on computed tomograms (C,D). B) T1-weighted image, after gadolinium. Bilateral sigmoid sinuses (arrowheads) are enhanced, whereas endolymphatic sacs are not. C,D) Computed tomograms of same boy demonstrating enlargement of both vestibular aqueducts (VAs; arrows). Diameter is 4 mm on right and on left at external aperture. Arrowheads — sigmoid sinuses. E,F) Computed tomograms of 14-year-old girl (family 1, III-2). Significant enlargement of VAs is evident (arrows). Diameter is 6 mm on right and left.

formed in 3 patients (family 1, III-1 and III-2, and family 3, IV-2). The endolymphatic sac is located in the posterior fossa adjacent to the sigmoid sinus. In general, the sac is known to show isodensity nearly comparable to that of the sigmoid sinus on T1-weighted images; however, on T2-weighted images, the endolymphatic sac creates higher-density signals than the sigmoid sinus (Figs 4A and 6A,B). Gadolinium-enhanced, T1-weighted images show the sigmoid sinus to be enhanced, but not the sac (Fig 4B).

DISCUSSION

Enlargement of the vestibular aqueduct was originally diagnosed and categorized by polytomography, and was subsequently studied by high-resolution CT. The diagnostic criteria vary according to the author reporting: a diameter greater than 1.5 mm at the midpoint between the common crus and the external aperture has been considered to indicate enlargement,[1,2,11,17,21] whereas other authors have used a measurement of greater than 2 mm at the external aperture[13] or at the midpoint.[12,14] The size of the EVA at the external aperture of the present cases (mean 4.9 mm, range 4 to 6 mm) fulfills the above-mentioned criteria. Magnetic resonance images are known to give more precise imaging of the fluid compartments of the inner ear.[7-10] In the present cases, MRI virtually confirmed a CT diagnosis of EVA, and gadolinium enhancement differentiated the endolymphatic sac from the sigmoid sinus (Fig 4A,B).

Enlargement of the vestibular aqueduct, which is known to be the most common inner ear deformity,[6,7] is sometimes associated with other types of inner ear anomalies, including a hypoplastic lateral semicircular canal, a dilated vestibule, and cochlear hypoplasia.[1,2,7,17] One ear in the present study had another associated anomaly. A study of a large series of inner ear abnormalities suggested that the organs that develop in the later period, such as the lateral semicircular canal and vestibular aqueduct, have more opportunities to be affected.[7]

One of the characteristic features of audiograms of patients with the EVA syndrome is a high-frequency, fluctuating sensorineural hearing loss. The conductive component observed here, hearing loss at the lower

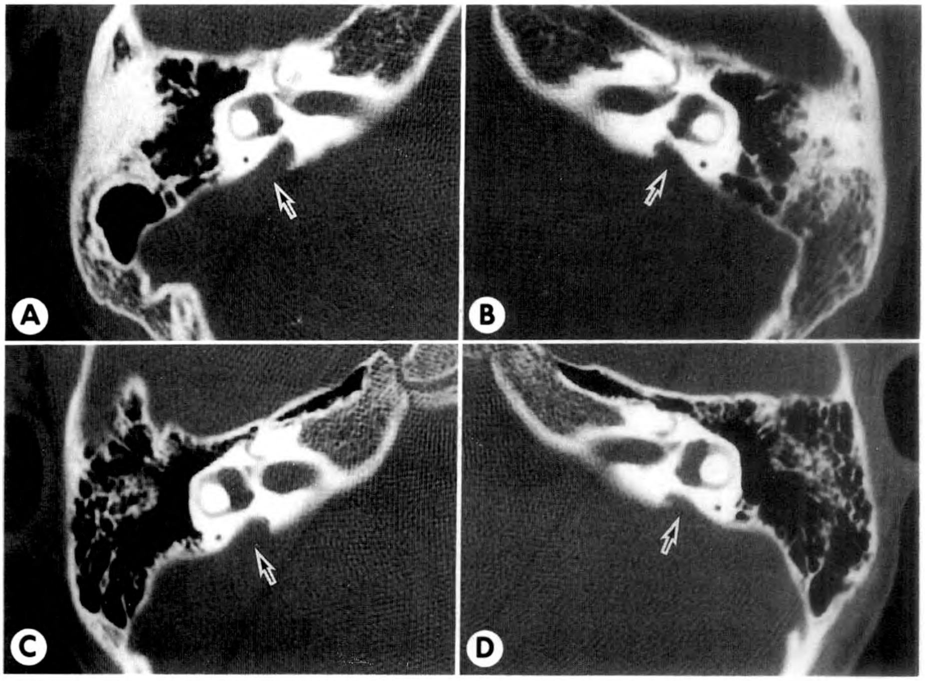

Fig 5. (Family 2) A,B) Computed tomograms of 13-year-old boy (family 2, III-1). Both VAs are markedly enlarged (arrows). Diameter is 5 mm on right and left. C,D) Computed tomograms of 7-year-old boy (family 2, III-2) showing enlarged VAs (arrows). Diameter is 5 mm on right and left.

frequencies,[11,12] has been also reported. According to Valvassori,[11] since no abnormal findings are found at surgical exploration of the middle ear, the conductive component is probably caused by a decreased mobility of the stapes due to increased perilymphatic or endolymphatic pressure.

Fluctuation is one of the characteristic clinical features of the EVA syndrome. All of the present subjects' symptoms fluctuated over the follow-up period. Only 1 ear showed a progressive hearing loss in the present study. This is compatible with other reports stating that the hearing loss was stable in most cases (Emmett[2] 81%, Zalzal et al[17] 61%), but not with the report by Jackler and De La Cruz[12] (35%). The ABR threshold and COR patterns were well correlated with the pure tone audiograms that were performed after 2 to 4 years; this finding suggests that most of the hearing losses were fluctuating, and not progressive (Fig 3). This issue should, however, be reevaluated after a longer period of observation.

Concerning the onset of hearing loss, it has been argued whether this hearing loss is congenital[1] or acquired.[13] Since the endolymphatic duct and sac continue to mature until the age of 4,[22] it has been postulated that hearing loss may be acquired during the development of the endolymphatic duct and sac.[12] Minor head trauma is proposed to be an important factor in progressive and fluctuating hearing loss.[12] Other factors, such as the common cold and exercise, are also reported to be triggers.[16] Rapid changes of intracranial pressure, which are normally buffered by the narrowness of the vestibular aqueduct,[23] may directly affect the inner ear when EVA is present.[12]

Anamnestic information on the present cases, however, provided no evidence for an acquired nature to the hearing loss. Although the possibility cannot be excluded that the patients lost their hearing at a very early age, the good correlation between ABR testing, COR testing (undergone before 4 years of age), and pure tone audiograms (performed several years later) makes it seem unlikely that the hearing loss was acquired and/or progressive. Hearing screening in infants (especially below 2 years old) will be required to resolve the question of the onset of hearing loss.

As far as management of EVA is concerned, surgical procedures involving the endolymphatic sac did not seem to be effective in restoring normal hearing and/or preventing fluctuating hearing.[2,12,13] Since speech audibility is critical for language acquisition, it is important to diagnose hearing loss in early childhood and enhance any residual hearing by means of prescriptive, well-fitted hearing aids. In our cases, the prescriptive hearing aid fitting was started at the ages of 2 to 7, and language acquisition has been successfully begun.

It deserves special emphasis that CT evaluation is required for the early diagnosis of EVA. Immediate habilitation should be started for EVA children with hearing loss. Both ABR testing and COR serve in estimating hearing and in planning medical care and counseling, including hearing aid fitting.

Vestibular dysfunction has been reported as a clinical feature of EVA.[12,18,19] Abnormality shown on vestibular function testing has also been reported.[2] The patients in the present study, however, did not have vestibular complaints or abnormal results on vestibular testing.

There have been only scattered genetic descriptions

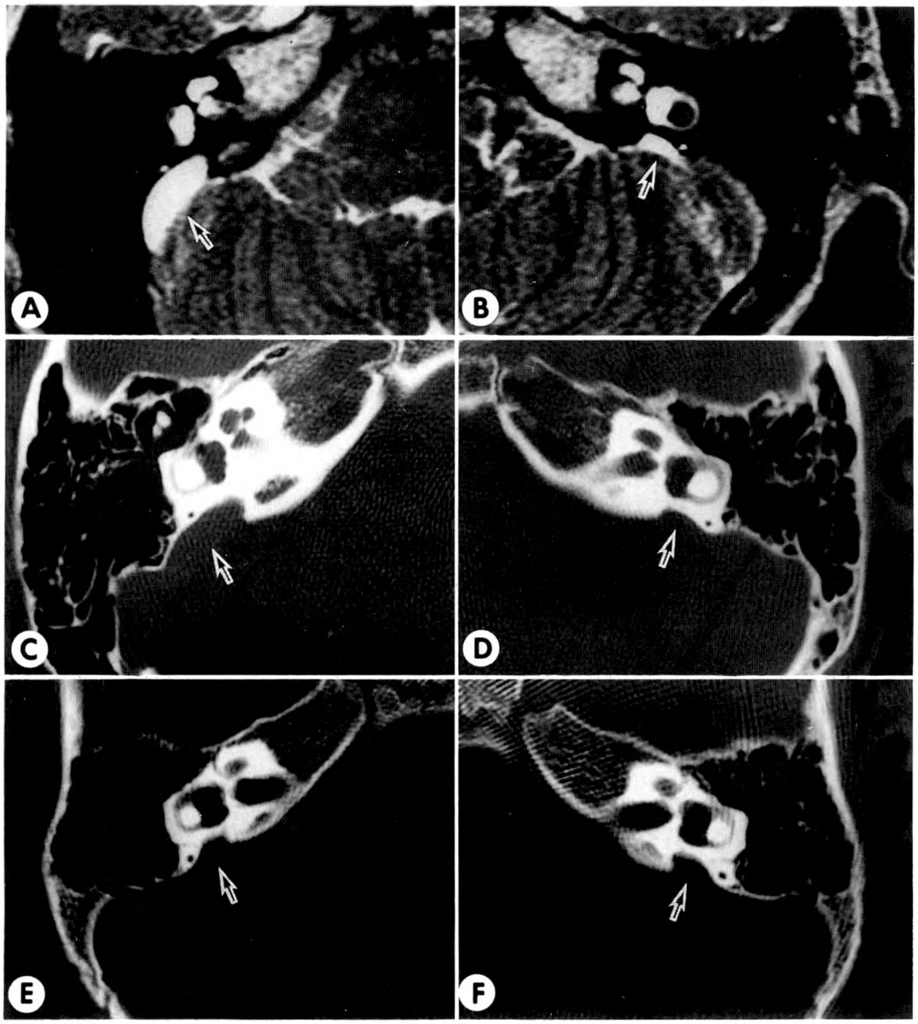

Fig 6. (Family 3) A,B) Magnetic resonance images of 12-year-old girl (family 3, IV-2). T2-weighted images show fluid compartments within membranous labyrinth. Arrows — enlarged VAs. C,D) Computed tomograms of same girl showing enlarged VA (arrows). Diameter is 5 mm on right and left. E,F) Computed tomograms of 3-year-old boy (family 3, IV-3) indicating enlarged VAs (arrows). Diameter is 5 mm on right and 4 mm on left.

concerning EVA. Few EVA patients with a family history (close relatives with hearing loss) have been reported (2 of 14,[1] 0 of 14,[2] 2 of 22,[7] 2 of 17,[12] 0 of 8[15]). The present paper provides a detailed description of cases of recessive hereditary hearing loss associated with EVA, and the clinical entity was consistent with the EVA syndrome reported previously.[13,15,17] If a genetic background is involved in this clinically distinct syndrome, particular attention should be directed toward the discovery of the responsible recessive genes.

ACKNOWLEDGMENTS — We thank Dr William J. Kimberling for his helpful comments. We also acknowledge Dr Miyo Kasai for initiating the collection of data on these families.

REFERENCES

1. Valvassori GE, Clemis JD. The large vestibular aqueduct syndrome. Laryngoscope 1978;88:723-8.

2. Emmett JR. The large vestibular aqueduct syndrome. Am J Otol 1985;6:387-403.

3. Swartz JD, Yussen PS, Mandell DW, Mikaelian DO, Berger AS, Wolfson RJ. The vestibular aqueduct syndrome: computed tomographic appearance. Clin Radiol 1985;36:241-3.

4. Swartz JD, Harnsberger HR. The otic capsule and otodystrophies. In: Swartz JD, Harnsberger HR, eds. Imaging of the temporal bone. 2nd ed. New York, NY: Thieme Medical Publishers, 1992:192-246.

5. Valvassori GE, Buckingham RA. Congenital abnormalities of the temporal bone. In: Valvassori GE, Buckingham RA, Carter BL, Hanafee WN, Mafee MF, eds. Head and neck imaging. Stuttgart, Germany: Georg Thieme Verlag, 1988:44-64.

6. Urman SM, Talbot JM. Otic capsule dysplasia: clinical and CT finding. Radiographics 1990;10:823-38.

7. Mafee MF, Charletta D, Kumar A, Belmont H. Large vestibular aqueduct and congenital sensorineural hearing loss. Am J Neuroradiol 1992;13:805-19.

8. Hirsch BE. Magnetic resonance imaging of the large vestibular aqueduct. Arch Otolaryngol Head Neck Surg 1992;118:1124-7.

9. Harnsberger HR, Dahlen RT, Shelton C, Gray SD, Parkin JL. Advanced techniques in magnetic resonance imaging in the evaluation of the large endolymphatic duct and sac syndrome. Laryngoscope 1995;105:1037-42.

10. Reussner LA, Dutcher PO, House WF. Large vestibular aqueduct syndrome with massive endolymphatic sacs. Otolaryngol Head Neck Surg 1995;113:606-9.

11. Valvassori GE. The large vestibular aqueduct and associated anomalies of the inner ear. Otolaryngol Clin North Am 1983; 16:95-101.

12. Jackler RK, De La Cruz A. The large vestibular aqueduct syndrome. Laryngoscope 1989;99:1238-43.

13. Levenson MJ, Parisier SC, Jacobs M, Edelstein DR. The large vestibular aqueduct syndrome in children. Arch Otolaryngol Head Neck Surg 1989;115:54-8.

14. Arcand P, Desrosiers M, Dube J, Abela A. The large vestibular aqueduct syndrome and sensorineural hearing loss in the pediatric population. J Otolaryngol 1991;20:247-50.

15. Belenky W, Madgy DN, Leider JS, Becker CJ, Hotaling AJ. The enlarged vestibular aqueduct syndrome (EVA syndrome). Ear Nose Throat J 1993;72:746-51.

16. Okumura T, Takahashi H, Honjo I, Takagi A, Mitamura K. Sensorineural hearing loss in patients with large vestibular aqueduct. Laryngoscope 1995;105:289-94.

17. Zalzal GH, Tomaski SM, Vezina LG, Bjiornsti P. Enlarged vestibular aqueduct and sensorineural hearing loss in childhood. Arch Otolaryngol Head Neck Surg 1995;121:23-8.

18. Schessel DA, Nedzelski JM. Presentation of large vestibular aqueduct syndrome to a dizziness unit. J Otolaryngol 1992; 21:265-9.

19. Hill JH, Freint AJ, Mafee MF. Enlargement of the vestibular aqueduct. Am J Otolaryngol 1984;5:411-4.

20. Griffith AJ, Arts A, Downs C, et al. Familial large vestibular aqueduct syndrome. Laryngoscope 1996;106:960-5.

21. Becker TS, Vignaud J, Sultan A, Lachman M. The vestibular aqueduct in congenital deafness; evaluation by the axial projection. Radiology 1983;149:741-4.

22. Kodama A, Sando I. Postnatal development of the vestibular aqueduct and endolymphatic sac. Ann Otol Rhinol Laryngol Suppl 1982;91(suppl 96):3-12.

23. Carlborg BIR, Farmer JC. Transmission of cerebrospinal fluid pressure via the cochlear aqueduct and endolymphatic sac. Am J Otolaryngol 1983;4:273-82.

≈

INTERNATIONAL PEDIATRIC OTORHINOLARYNGOLOGICAL SCHOLARSHIPS

Scholarships to attend the 7th International Congress of Pediatric Otorhinolaryngology (June 7-10, 1998, Helsinki, Finland) are available. For information, contact Pekka Karma, MD, President, or Hans Ramsay, MD, Secretary, 7th International Congress of Pediatric Otorhinolaryngology, ENT Department, Helsinki University Central Hospital, Haarmaninkatu 4 E, FIN-00290 Helsinki, Finland; telephone 358 9 4713019; fax 358 9 4715010; E-mail Hans.Ramsay@muikku.huch.fi.

Ann Otol Rhinol Laryngol 106:1997

REDUCTION OF INNER EAR INFLAMMATION BY TREATMENT WITH ANTI–ICAM-1 ANTIBODY

TSUYOSHI TAKASU, MD, PHD
SAPPORO, JAPAN

JEFFREY P. HARRIS, MD, PHD
SAN DIEGO, CALIFORNIA

The in vivo effect of systemic administration of monoclonal antibody (mAb) against ICAM-1 (αICAM-1) in experimental immune-mediated labyrinthitis was evaluated. The αICAM-1–treated rats showed reduced inflammatory cell infiltration in the scala tympani and the perisaccular tissue of the endolymphatic sac. However, with this experimental paradigm, labyrinthitis could not be completely abolished. These findings suggest that ICAM-1–dependent pathways play an important role in the series of immunologic events occurring in the inner ear, and that the use of ICAM-1 antagonist may be a possible therapeutic approach to labyrinthitis.

KEY WORDS — antibody, ICAM-1, inner ear immunity, intercellular adhesion molecule–1, labyrinthitis, treatment.

INTRODUCTION

The development of pathologic signs in the auditory system in some experimental models of labyrinthitis is known to correlate with immune reaction with the migration of leukocytes.[1] The extravasation of leukocytes through blood vessels at inflammatory sites requires the adhesion of leukocytes to the endothelium, a process mediated by endothelial and leukocyte surface molecules functioning as receptors and ligands.[2] A recent report from this laboratory indicated that during inflammation, the spiral modiolar vein (SMV) transforms into a high endothelial venule (HEV)–like vessel.[3] Additionally, the epithelia of the SMV and collecting venule (CV) show an increase in expression of intercellular adhesion molecule–1 (ICAM-1), one of the cell adhesion molecules, during inflammation.[4] These results suggested that these inflammatory events in the inner ear might correlate with the up-regulation and enhanced expression of ICAM-1 and that the ICAM-1–leukocyte function–associated antigen–1 (LFA-1) adhesion pathways might play a crucial role in them. The interaction between ICAM-1 and LFA-1 is also known to be involved in a variety of other immunologic events, such as antigen presentation during the induction phase of an immune response,[5,6] and antibody production.[7,8]

Recently, successful therapeutic attempts with in vivo administration of antagonists to ICAM-1 or its ligand LFA-1 have been focused on animal models of human diseases.[9] These included diseases that were mediated predominantly by lymphocytes and/or by polymorphonuclear leukocytes (PMNs). In an animal model of immune-mediated labyrinthitis established in our laboratory,[10] the inner ear shows accumulation of PMNs and lymphocytes,[1] and the local production of antibody.[10,11] Therefore, it would be interesting to investigate the potential for antagonists to ICAM-1 to block the accumulation of inflammatory cells in the inner ear.

The present report describes the effect of monoclonal antibody (mAb) against ICAM-1 (αICAM-1) in rats with labyrinthitis immunologically induced by keyhole limpet hemocyanin (KLH). We found that injection of αICAM-1 reduced the severity of inner ear lesions, demonstrating the central role of ICAM-1 receptors in HEV-like vessels of the inner ear.

MATERIALS AND METHODS

Animals. Female Lewis rats weighing 150 to 200 g were purchased from Harlan Sprague-Dawley (Indianapolis, Ind). Prior to auditory brain stem response (ABR) testing, antigen inoculation, blood sampling, and operation, each rat was anesthetized with a mixture of ketamine hydrochloride (Ketaset, 50 mg/kg), xylazine hydrochloride (AnaSed, 5 mg/kg), and acepromazine maleate (PromAce, 0.4 mg/kg) intraperitoneally.

Antigen Preparation. The KLH was purchased from Pacific Biomarine Supply Co (Venice, Calif) as an ammonium sulfate precipitate and then prepared for use according to the following. The slurry was suspended in phosphate-buffered saline (PBS), pH 6.4, dialyzed aseptically against PBS, and then centrifuged for 30 minutes

---

From the Department of Surgery, Division of Otolaryngology–Head and Neck Surgery, University of California, San Diego, and the Research Service, Veterans Affairs Medical Center, San Diego, California. Dr Takasu is currently in the Department of Otolaryngology, NTT Sapporo Hospital, Sapporo, Japan. This work was supported by grant DC00193 from the National Institutes of Health/National Institute on Deafness and Other Communication Disorders and by the Research Service of the Department of Veterans Affairs. This study was performed in accordance with the PHS Policy on Humane Care and Use of Laboratory Animals, the NIH *Guide for the Care and Use of Laboratory Animals*, and the Animal Welfare Act (7 U.S.C. et seq.); the animal use protocol was approved by the Institutional Animal Care and Use Committee (IACUC) of the University of California, San Diego.

CORRESPONDENCE — Jeffrey P. Harris, MD, PhD, Division of Head and Neck Surgery, UCSD, 9350 Campus Point Dr, La Jolla, CA 92093-0970.

at 1,500*g*. The supernatant was recentrifuged for 2 hours at 37,000*g*. The precipitate (associated KLH) was dissolved in PBS to a concentration of 50 mg/mL and used for immunization of animals.

Induction of Labyrinthitis. Animals were immunized subcutaneously in the back with 1 mg of KLH preparation emulsified in Freund's complete adjuvant. Two weeks later, they were boosted subcutaneously with the same dose of KLH in Freund's incomplete adjuvant. At 3 weeks, the scalae tympani were injected with 10 μL of KLH or PBS through a microhole made by a hand drill. The hole was sealed with bone wax after injection.

Antibodies. The hybridoma cell line that produces murine mAb 1A29 (IgG1)[12] directed against rat ICAM-1 was a generous gift of Dr Masayuki Miyasaka (Biomedical Research Center, Osaka University, Japan). Pristane (Sigma, St Louis, Mo)–primed BALB/c mice (Harlan Sprague-Dawley) received a single intraperitoneal injection of the hybridoma cells of 10^7 cells. The mAbs were purified from ascites of the mice by ammonium sulfate precipitation followed by elution through a protein A–Sepharose CL-4B affinity column (Pharmacia, Uppsala, Sweden). Control murine IgG1 of irrelevant specificity from hybridoma cell line P3.6.2.8.1 (American Type Culture Collection, Rockville, Md) was purified in the same manner.

Treatment Schedule. Animals were given intraperitoneal injections of mAb 1A29 or irrelevant IgG1 as a single daily dose of 5 mg/kg every other day beginning 3 days before the induction of labyrinthitis by inner ear KLH inoculations until painlessly sacrificed, with a total dose of 25 mg/kg of mAb administered.

Electrophysiologic Testing. The hearing threshold of each ear was assessed by threshold measurement using ABR recordings before antigen challenge and 6 days later, just prior to sacrifice. Animals were placed in a single-walled acoustic booth (Industrial Acoustics Co, Bronx, NY) on a heating pad. Click stimuli were generated by electrical square waves of 100 microseconds' duration by a Grass S88 signal stimulator (Grass Medical Instruments, Quincy, Mass) at rates of 10/s. They were manually attenuated in 5 to 10 decrements with a Hewlett Packard attenuator (Hewlett Packard, Everett, Wash) and delivered to a Beyer DT 48 200-Ω speaker fitted with an ear speculum for placement in the external auditory meatus. Subdermal electrodes were inserted at the vertex (active electrode), the mastoid (reference), and the back (ground). The potentials were amplified 1,000× with a Parc Model 113 preamplifier (EG&G); 512 responses were averaged by a 3561A dynamic signal analyzer (Hewlett Packard) and plotted on a 7550A graphics plotter (Hewlett Packard).

Histology. Following the second ABR recording on day 6, animals were sacrificed under deep anesthesia by perfusion with phosphate-buffered 4% paraformaldehyde. The temporal bones were dissected and immersed in the fixative at 4°C overnight. After decalcification with 10% ethylenediaminetetraacetic acid, they were processed for paraffin embedding. Sections (5 μm) were cut at 40-μm intervals parallel to the modiolus and stained with hematoxylin and eosin. To assess the severity of inflammatory cell infiltration, the number of inflammatory cells, including PMNs, lymphocytes, and macrophages, was counted as follows. First, cells in the scalae tympani, vestibuli, and media were counted on 10 consecutive sections on both sides of the midmodiolar section. Second, cells in the vestibular labyrinth (saccule, utricle, and ampulla), the modiolus, the perineural tissue of the cochlear nerve, and the perisaccular tissue of the endolymphatic sac were counted in all sections. The data were expressed as cell number per cross section. The severity of fibrotic change in the scalae tympani and vestibuli was assessed on a scale from 0 to +++. Scoring was performed arbitrarily as follows: 0 = none; + = occupying less than one fourth of the volume of the scalae; ++ = occupying one fourth to one half; and +++ = occupying more than one half. The incidence of endolymphatic hydrops in the cochlea was also examined. The measurements of fibrotic change and endolymphatic hydrops were performed in a blinded fashion by two independent observers. These histologic data were compared among KLH-challenged ears in αICAM-1–treated rats (n = 12), KLH-challenged ears in control IgG1-treated rats (n = 9), and PBS-injected ears in control IgG1-treated rats (n = 6).

To gain better insight into the importance of cell-mediated immunity in this model, we estimated the relationship between inflammatory cell counts in the cochlea and hearing threshold shift by correlation analysis using the data from all animals.

Experimental Design. The experimental design is summarized in Fig 1.

RESULTS

Effect of mAbs on Severity of Labyrinthitis. The KLH-challenged ears in irrelevant IgG1-treated (control) animals showed a histopathology on day 6 nearly identical to that reported previously in rats[4]: lymphocytes and macrophages were predominantly present in the scalae tympani and vestibuli and endolymphatic sac lumen, with PMNs being less common; lymphocytes, including plasma cells, were predominant in the modiolar space, vestibular labyrinth, perineural tissue of the cochlear nerve, and perisaccular tissue; inflammatory cells were seen in the scala media of 1 animal; and mild to moderate fibrotic changes in the scala tympani or

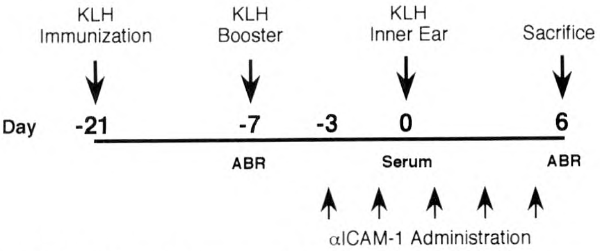

Fig 1. Schema of experimental protocol. Days are indicated as those before or after operation. KLH — keyhole limpet hemocyanin, ABR — auditory brain stem response, αICAM-1 — anti-intercellular adhesion molecule–1 antibody.

scala vestibuli and/or endolymphatic hydrops were also observed in several cochleas. Only a scant number of cells were demonstrated in control PBS-injected inner ears.

Three of 12 KLH-challenged ears in αICAM-1–treated animals showed clear inhibition of inflammatory cell infiltration in every location of the inner ear, but in the remainder of the KLH-challenged ears, the infiltration was not completely inhibited. The composition of inflammatory cells that did enter the inner ear was almost the same as in control animals. To quantitate these results, the numbers of infiltrating cells were counted in both the αICAM-1–treated and irrelevant IgG1–treated (control) animals (see Table). After treatment with αICAM-1 mAb, cell counts were markedly reduced in almost every location of the inner ear examined. These reductions were found to be statistically significant in the scala tympani ($p < .002$, *t*-test), the perineural tissue of the cochlear nerve ($p < .01$, *t*-test), and the perisaccular tissue of the endolymphatic sac ($p < .05$, *t*-test). As shown in the Table, the severity and incidence of fibrosis in the scala tympani and/or scala vestibuli and the incidence of endolymphatic hydrops in the cochlea were not significantly altered by αICAM-1 mAb treatment.

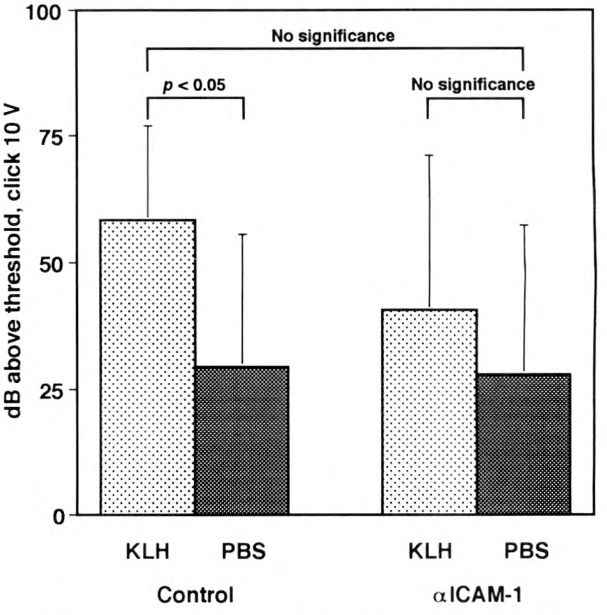

Fig 2. Change in hearing threshold of control and αICAM-1–treated rats. In αICAM-1–treated group, significant elevation in hearing threshold of KLH-challenged ear compared with phosphate-buffered saline (PBS)–injected side was not found. However, there was no statistical difference between αICAM-1–treated KLH ears and nontreated KLH ears. Values are mean + SD.

Effect of mAbs on Hearing Threshold Shift. Averages of hearing threshold shift in KLH- and PBS-injected ears of both αICAM-1–treated and irrelevant IgG1–treated (control) animals are displayed in Fig 2. The PBS-injected ears experienced a 28- to 30-dB threshold shift on average in both αICAM-1–treated and control animals, which was attributed to surgical trauma. While, in control animals, the difference in threshold elevation between KLH-challenged (58.3 dB average) and PBS-injected ears was statistically significant ($p < .05$, *t*-test), in αICAM-1–treated animals, the threshold change caused by KLH challenge in the inner ear (40.5 dB average) was not statistically significant compared with the PBS-injected side. However, there

INNER EAR HISTOPATHOLOGY IN αICAM-1–TREATED AND CONTROL ANIMALS

Histopathologic Parameter	*Location*	*KLH-Challenged Side* Control (n = 9)	*KLH-Challenged Side* αICAM-1 (n = 12)	*PBS-Injected Side* Control (n = 6)
Inflammatory cell counts	Scala tympani	22.13	7.91*	5.90
	Scala vestibuli	23.43	11.70	1.26
	Scala media	0.61	0.05	0.00
	Modiolus	7.07	3.99	2.13
	Cochlear nerve	16.55	3.56†	4.03
	Vestibular labyrinth	15.40	4.44	0.44
	Perisaccular space	96.67	29.40§	25.28
Fibrosis (0/+/++/+++)	Cochlea	(4/4/1/0)	(8/3/1/0)	(6/0/0/0)
Endolymphatic hydrops (incidence)	Cochlea	4/9	4/12	0/6

αICAM-1 — anti-intercellular adhesion molecule–1 antibody, KLH — keyhole limpet hemocyanin, PBS — phosphate-buffered saline.
Statistically significant reduction by *t*-test compared with control animals as follows: *$p < .002$; †$p < .01$; §$p < .05$.

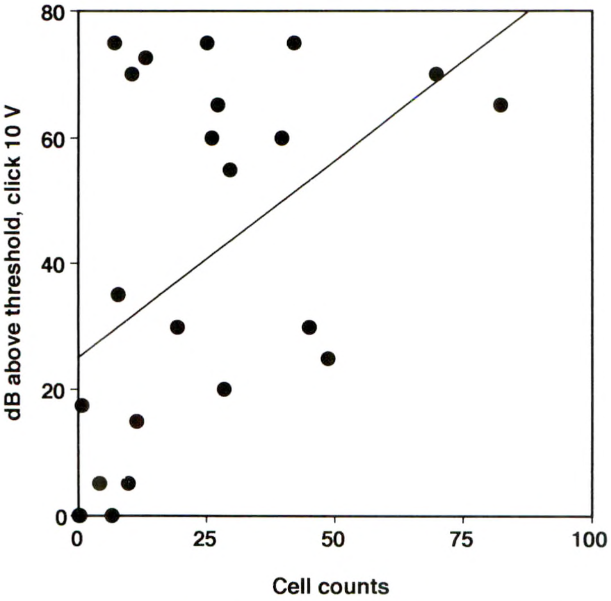

Fig 3. Relationship between inflammatory cell counts in cochlea and hearing threshold shift. Weak but statistically significant correlation was present between them ($r = .485$, $p < .05$, *t*-test). Dots represent individual ears.

was no statistical difference between the αICAM-1–treated KLH ears and the irrelevant IgG1–treated KLH ears.

Correlation Between Inflammatory Cell Counts and Hearing Threshold Shift. The data from all animals are scatter-plotted in Fig 3. A weak correlation ($r = .485$, $p < .05$, *t*-test) was found between cochlear cell counts and hearing threshold shift.

DISCUSSION

The mechanism of inner ear inflammation and dysfunction induced by a secondary immune reaction against KLH in animal models is speculated to consist of a complex series of events. Following KLH challenge in the perilymphatic space, anti-KLH antibody present in perilymph binds to the antigen, and the immune complexes are formed. This presumably triggers a variety of inflammatory processes, including the release of inflammatory mediators, which causes chemotaxis of PMNs and subsequent local tissue damage.[11] Cytokines such as interleukin (IL)-1 released from macrophages that reside in the endolymphatic sac activate lymphocytes and up-regulate adhesion molecules such as ICAM-1.[13] The central role of the endolymphatic sac in antigen processing has been established, and its role may be in the subsequent release of ILs that amplify the inner ear immune response.[14] Antigen binding cells leave the systemic circulation and enter the inner ear via the SMVs and CVs after they have taken on the appearance of HEVs.

The importance of ICAM-1 in the generation and maintenance of inflammation has been elucidated in many experimental systems in which mAbs to ICAM-1 were shown to suppress a variety of inflammatory conditions.[15] In the present in vivo study, we used the mAb against ICAM-1 to assess the functional involvement of ICAM-1–dependent pathways in the experimental labyrinthitis model. We found that systemic administration of the mAb reduced the severity of inflammatory infiltration, especially in the scala tympani and the perisaccular tissue of the endolymphatic sac; this finding suggests that ICAM-1 plays an important role in inner ear immunology. The reduced number of inflammatory cells in the perisaccular tissue also suggests that many of the cells at this site may be derived from the systemic circulation through local postcapillary venules.

While the inflammatory cell infiltration in the inner ear was reduced by the mAb, fibrosis and endolymphatic hydrops were not. The mechanism of fibrosis in the inner ear is not clearly understood, but may be related to the release of local factors, once the inflammation is set up, and not necessarily linearly related to the number of cells. Endolymphatic hydrops in this animal model may be related to the local proliferation of inflammatory cells within the endolymphatic sac that causes absorptive dysfunction of the sac itself. Clearly, under the conditions used in this experiment, αICAM-1 did not ameliorate these events.

The effect of αICAM-1 mAb on experimental labyrinthitis in the present study was not completely suppressive. This may be due to inappropriate timing of the administration of ICAM-1. In vitro and in vivo studies have shown that the inhibition of the ICAM-1–LFA-1 pathway blocks more than just leukocyte trafficking. Lymphocyte adherence to antigen-presenting cells for the generation and elaboration of antigen-specific T cells has also been shown to be dependent on the ICAM-1–LFA-1 pathway.[16] Thus, it is likely that our administration of mAb after systemic immunization and a booster of KLH was not effective in blocking antigen presentation, as this occurred earlier. It is possible that earlier administration of mAb, before and/or during immunization and booster periods, could be more effective in inhibiting inner ear inflammation.

Another possible explanation is that adhesion molecule pathways other than ICAM-1–LFA-1 also play a role in the immune response of the inner ear. Cell adhesion of leukocytes has been elucidated to involve multiple receptor-ligand interactions, such as ICAM-2–LFA-1, vascular cell adhesion molecule–1 (VCAM-1)–very late activated antigen–4 (VLA-4), LFA-3–CD-2, B7–CD28, and CD44 and the selectin family.[17] The detailed distribution of expression of these adhesion molecules in the inner ear has not yet been reported, but it is conceivable that some of these might play reciprocal or functional roles in the inner ear.

By correlation analysis, we found there is a relationship between the number of inflammatory cells in the cochlea and the hearing threshold, which is consistent with several previous studies showing the influence of inflammation on hearing.[18,19] However, the correlation was weak, suggesting that some other immunologic factors may also be involved. The exact role of perilymph antibody concentrations has not been clearly defined, but it is most probable that administration of αICAM-1 did not alter α-KLH perilymph concentrations. The variability between animals can be related to the tremendous variations seen in immunoresponsiveness to KLH sensitization. Wide ranges of anti-KLH titers are routinely seen, and one would expect considerable variability in sensitized immunocompetent cells as well. In addition, the exact concentration of KLH remaining in the inner ear can vary due to some "backwash" into the middle ear during inner ear inoculation. This is minimized by the removal of several microliters of perilymph prior to perfusion; however, this difference in the exact quantity of KLH ultimately delivered to the scala tympani could introduce some interanimal variability.

In summary, this study has demonstrated that prophylactic use of αICAM-1 mAb reduces inner ear inflammation induced by a secondary immune reaction against KLH in the rat, though not completely. Therefore, ICAM-1 appears to be involved in possibly some of several immunologic processes in the inner ear, including cell trafficking. In addition, the nature of the incomplete suppression should be a target for further investigation, and the finding of suppression of inflammation now requires further refinement in the delivery of this antibody to the inner ear. Timing, route, dosage, and antibody structure may all affect the efficiency of this mode of intervention and should be addressed in future studies. These initial results, however, are promising and suggest that the immune response affecting the inner ear, as in other organ systems, may be subject to manipulation of immunoregulatory mechanisms. Furthermore, clinical trials of αICAM-1 therapy have been started in several clinical areas, such as solid organ transplantation[20] and rheumatoid arthritis.[21] The present results suggest the possibility that such a strategy can be applied to patients with inner ear inflammation and immune-mediated inner ear diseases.

ACKNOWLEDGMENTS — The authors thank Masayuki Miyasaka, MD, PhD, for providing the hybridoma cell line 1A29 and Peter B. Billings, PhD, Elizabeth M. Keithley, PhD, Michael J. Ruckenstein, MD, MSc, and Meguru Watanabe, MD, PhD, for their valuable suggestions on these studies.

REFERENCES

1. Takahashi M, Harris JP. Analysis of immunocompetent cells following inner ear immunostimulation. Laryngoscope 1988;98:1133-8.

2. Pober JS, Cotran RS. The role of endothelial cells in inflammation. Transplantation 1990;50:537-44.

3. Stearns GS, Keithley EM, Harris JP. Development of high endothelial venule–like characteristics in the spiral modiolar vein induced by viral labyrinthitis. Laryngoscope 1993;103:890-8.

4. Suzuki M, Harris JP. Expression of intercellular adhesion molecule-1 during inner ear inflammation. Ann Otol Rhinol Laryngol 1995;104:69-75.

5. Dougherty GJ, Murdoch S, Hogg N. The function of human intercellular adhesion molecule–1 (ICAM-1) in the generation of an immune response. Eur J Immunol 1988;18:35-9.

6. Cosimi AB, Conti D, Delmonico FL, et al. In vivo effects of monoclonal antibody to ICAM-1 (CD54) in nonhuman primates with renal allografts. J Immunol 1990;144:4604-12.

7. Charlton B, Guymer RH, Slattery RM, Mandel TE. Intercellular adhesion molecule (ICAM-1) inhibition can induce tolerance in vivo. Immunol Cell Biol 1991;69:89-93.

8. Nishikawa K, Guo YJ, Miyasaka M, et al. Antibodies to intercellular adhesion molecule 1/lymphocyte function–associated antigen 1 prevent crescent formation in rat autoimmune glomerulonephritis. J Exp Med 1993;177:667-77.

9. Bevilacqua MP, Nelson RM, Mannori G, Cecconi O. Endothelial-leukocyte adhesion molecules in human disease. Annu Rev Med 1994;45:361-78.

10. Harris JP. Immunology of the inner ear: response of the inner ear to antigen challenge. Otolaryngol Head Neck Surg 1983;91:18-23.

11. Harris JP. Immunology of the inner ear: evidence of local antibody production. Ann Otol Rhinol Laryngol 1984;93:157-62.

12. Tamatani T, Miyasaka M. Identification of monoclonal antibodies reactive with the rat homolog of ICAM-1, and evidence for a differential involvement of ICAM-1 in the adherence of resting versus activated lymphocytes to high endothelial cells. Int Immunol 1990;2:165-71.

13. Dustin ML, Rothlein R, Bhan AK, Dinarello CA, Springer TA. Induction by IL 1 and interferon-g: tissue distribution, biochemistry, and function of a natural adherence molecule (ICAM-1). J Immunol 1986;137:245-54.

14. Gloddek B, Harris JP. Role of lymphokines in the immune response of the inner ear. Acta Otolaryngol (Stockh) 1989;108:68-75.

15. Rothlein R, Mainolfi EA, Kishimoto TK. Treatment of inflammation with anti-ICAM-1. Res Immunol 1993;144:735-9.

16. Lipsky PE, Rosenthal AS. Macrophage-lymphocyte interaction: II. Antigen-mediated physical interactions between immune guinea pig lymph node lymphocytes and syngeneic macrophages. J Exp Med 1975;141:138-54.

17. Springer TA. Adhesion receptors of the immune system. Nature 1990;346:425-34.

18. Woolf NK, Harris JP. Cochlear pathophysiology associated with inner ear immune responses. Acta Otolaryngol (Stockh) 1986;102:353-64.

19. Darmstadt GL, Keithley EM, Harris JP. Effects of cyclo-

phosphamide on the pathogenesis of cytomegalovirus-induced labyrinthitis. Ann Otol Rhinol Laryngol 1990;99:960-8.

20. Haug CE, Colvin RB, Delmonico FL, et al. A phase I trial of immunosuppression with anti–ICAM-1 (CD54) mAb in renal allograft recipients. Transplantation 1993;55:766-73.

21. Kavanaugh AF, Davis LS, Nichols LA, et al. Treatment of refractory rheumatoid arthritis with a monoclonal antibody to intercellular adhesion molecule 1. Arthritis Rheum 1994;37:992-9.

≈

SAN FRANCISCO OTOLOGY, NEUROTOLOGY & SKULL BASE SURGERY UPDATE

The San Francisco Otology, Neurotology & Skull Base Surgery Update 1998 will be held November 5-7, 1998, in San Francisco, California. For information, contact University of California, Office of Continuing Medical Education, MCB-630, Box 0742, San Francisco, CA 94143-0742; telephone (415) 476-4251; fax (415) 476-0318; e-mail: inquire@ocme.ucsf.edu; web site: http://cme.ucsf.edu.

Ann Otol Rhinol Laryngol 106:1997

CHANGES IN MYOSIN EXPRESSION IN DENERVATED LARYNGEAL MUSCLE

JOHN M. DELGAUDIO, MD
ATLANTA, GEORGIA

JAMES J. SCIOTE, DDS, PHD
PITTSBURGH, PENNSYLVANIA

The effects of chronic denervation on the myosin heavy chain (MyHC) content and muscle fiber type composition of rat laryngeal muscles are described. The posterior cricoarytenoid (PCA) and thyroarytenoid (TA) muscles were removed 3 weeks, 3 months, and 6 months after recurrent laryngeal nerve sectioning. Myofibrillar adenosine triphosphatase staining of cryostat sections was performed, and fiber type percentages were determined. Sodium dodecyl sulfate–polyacrylamide gel electrophoresis was used to separate MyHC isoforms, and densitometry was subsequently used for quantitative analysis. Unoperated animals served as controls. In the PCA muscle, denervation resulted in a progressive reduction in type I MyHC (the slow-contracting isoform) to an almost complete loss at 6 months, with a concomitant increase in type II MyHCs (fast-contracting isoforms, excluding type IIL). Type IIL MyHC (laryngeal-specific isoform) remained relatively constant up to 6 months after denervation. The myosin expression in the TA muscle, which contained only type II MyHCs, remained relatively constant with denervation. Changes in fiber type composition of the muscles described from tissue staining correlated with MyHC content. These findings in laryngeal muscle confirm the dependence of type I MyHC expression upon neural input, as has been found previously in limb skeletal muscles. Since the expression of all MyHCs except the IIL was modified after denervation in the PCA muscle, it is possible that the IIL isoform is maintained by factors that differ from those in the other skeletal myosins.

KEY WORDS — adenosine triphosphatase, ATPase, denervation, laryngeal muscles, larynx, myosin, myosin heavy chains, vocal cord paralysis.

INTRODUCTION

The clinical effects of denervation are well known, including paralysis and atrophy of the affected muscles. In the case of recurrent laryngeal nerve (RLN) injury, this results in a hoarse and/or breathy voice, weak cough, and occasional aspiration. In the case of bilateral RLN paralysis, upper airway obstruction may ensue. Many procedures have been used to treat vocal cord paralysis, including static and dynamic procedures. Despite the fact that much is known about the clinical effects and course of vocal cord paralysis, little is known about the changes that occur in the larynx at the muscle fiber level after denervation.

From histochemical and immunohistochemical staining, several muscle fiber types have been identified in mammalian skeletal muscle, including three fast-contracting fibers (types IIA, IIB, and IIX) and one slow-contracting fiber (type I).[1] Each fiber type homogeneously expresses a distinct myosin heavy chain (MyHC) isoform of the same name. Some fibers, however, coexpress these isoforms, and one example is the type IIC fiber, which contains both type I and IIA MyHCs.[2] Other tissue-specific fiber types have been identified, including type IIM (type II masticatory), found in the jaw-closing muscles of most carnivores and primates.[3] These fiber classifications were first made due to differential reactivity of myosin isoforms for the myofibrillar adenosine triphosphatase (ATPase) histochemical stain,[2] which was followed later by immunohistochemical staining with MyHC-specific antibodies.[4] Concomitantly, MyHC protein species were separated by means of advances in sodium dodecyl sulfate–polyacrylamide gel electrophoresis (SDS-PAGE).[5]

We previously found that the majority of fibers in rat posterior cricoarytenoid (PCA) and thyroarytenoid (TA) muscles stain differently with histochemistry and immunohistochemistry than skeletal fibers from limb muscle. The SDS-PAGE showed these fibers to contain, in addition to other type II isoforms, an unusual MyHC that we termed type IIL (type II laryngeal).[6] It is likely that the IIL isoform is needed for the specialized functions of these muscles, as is the case for the IIM isoform of jaw-closing muscles. While much is known about the effects of denervation in skeletal fibers of limb muscle, there is little information describing denervation in laryngeal muscles, especially given our recent identification of an atypical MyHC. The aim of this study was to de-

---

From the Departments of Otolaryngology–Head and Neck Surgery (DelGaudio) and Anatomy and Cell Biology (Sciote), University of Michigan, Ann Arbor, Michigan. Support for Dr DelGaudio was through National Institutes of Health research grant T32DC00024. This study was performed in accordance with the PHS Policy on Humane Care and Use of Laboratory Animals, the NIH *Guide for the Care and Use of Laboratory Animals*, and the Animal Welfare Act (7 U.S.C. et seq.); the animal use protocol was approved by the Institutional Animal Care and Use Committee (IACUC) of the University of Michigan Medical School.

CORRESPONDENCE — John M. DelGaudio, MD, Dept of Otolaryngology, The Emory Clinic, 1365 Clifton Rd NE, Atlanta, GA 30322.

MYOSIN HEAVY CHAIN COMPOSITION AND FIBER TYPES

	Control Group (4 mo)	Denervated Groups		
		3 wk	3 mo	6 mo
PCA muscle				
II MyHCs	68.44 ± 1.66	68.13 ± 2.64	74.68 ± 2.14	86.52 ± 11.19
IIL MyHC	18.28 ± 2.39	16.01 ± 1.95	14.07 ± 1.32	12.22 ± 10.90
I MyHC	13.28 ± 1.53	15.80 ± 2.29	11.62 ± 1.72	1.26 ± 2.82
TA muscle				
II MyHCs	68.03 ± 2.18	71.4 ± 5.40	70.7 ± 2.03	71.94 ± 5.01
IIL MyHC	31.97 ± 2.18	28.6 ± 5.40	29.3 ± 2.03	28.06 ± 5.01
PCA muscle				
I Fibers	11.5 ± 2.14	9.72 ± 1.55	9.38 ± 0.47	4.35 ± 1.27
II Fibers	88.5 ± 2.14	90.28 ± 1.55	90.62 ± 0.47	95.65 ± 1.27

Data are mean ± SD. For numbers of subjects in groups, and statistical significance, see Fig 1.

PCA — posterior cricoarytenoid, MyHC — myosin heavy chain (type II includes types IIA and/or IIX and type IIB), TA — thyroarytenoid.

scribe the effects of denervation on MyHC composition and muscle fiber types in rat PCA and TA muscles.

METHODS

Male Sprague-Dawley rats weighing approximately 450 g, under ketamine hydrochloride anesthesia, underwent resection of either the left or right RLN, with removal of the portion between the thoracic inlet and the thyroid gland. The proximal stump of the RLN was ligated with a 10-0 nylon suture and buried in the ipsilateral sternocleidomastoid muscle whenever possible to prevent spontaneous regeneration and reanastomosis of the nerve. This was performed with a binocular operating microscope and microsurgical instruments. The animals were then allowed to recover separately for 24 hours.

At intervals of 3 weeks, 3 months, and 6 months, the animal groups underwent a second procedure. With ketamine anesthesia, a transhyoid pharyngotomy was performed to visualize the vocal cords. If necessary, a midline epiglottic split and laryngofissure were performed for better visualization. Vocal cord movement and arytenoid movement were assessed to ensure that reinnervation had not occurred. Vocal cord or arytenoid movement was taken as a sign of reinnervation, and these animals were excluded from the experimental group results. Electromyography (EMG) of the denervated TA muscles was then performed to ensure lack of reinnervation. Supraglottic stimulation was used to elicit glottic closure during performance of the EMG. The EMG of some PCA muscles was performed at 3 and 6 months after denervation by performing a lateral pharyngotomy, entering the pyriform sinus, and rotating the larynx away from the control side. Those muscles with signs of polyphasic potentials were excluded from the results, due to the possibility of reinnervation. In animals with possible signs of reinnervation, no definitive attempt was made to identify the source of reinnervation (ie, RLN stump versus adjacent muscle-to-muscle neurotization). The animals were then painlessly sacrificed with an intracardiac injection of sodium pentobarbital. The PCA and TA muscles were removed, embedded in optimum cutting temperature (OCT) compound (Sakura Finetek, Inc, Torrance, Calif), frozen in isopentane cooled with dry ice, and stored at −60°C. Two groups of nondenervated, age-matched controls were processed as experimental animals at 4 and 6 months to confirm that no age-related changes in myosin expression were present.

Histochemistry. Muscles were sectioned at 10 µm and stained for myofibrillar ATPase activity after preincubation in buffer at pH 10.2, 4.6, and 4.3 as described by Brooke and Kaiser.[2] Muscle sections were evaluated by light microscopy. With a projection microscope, all muscle fibers from each muscle were counted at pH 10.2 or 4.3, and the percentages of type I and II fibers were determined for each muscle.

Myosin Heavy Chain Isoforms. After serial sections were cut from the muscle block, the remainder of the muscle was analyzed by SDS-PAGE as previously described.[6] Gels were stained with silver,[7] and densitometry was performed to determine the relative percentages of myosin isoforms in each muscle. Gels for each muscle were run twice to ensure consistency of the MyHC isoform banding pattern.

RESULTS

Myosin Heavy Chains. The MyHC content was quantitated by densitometric scans of the gels. No age-related changes were found in the control rats. There were progressive reciprocal changes in the

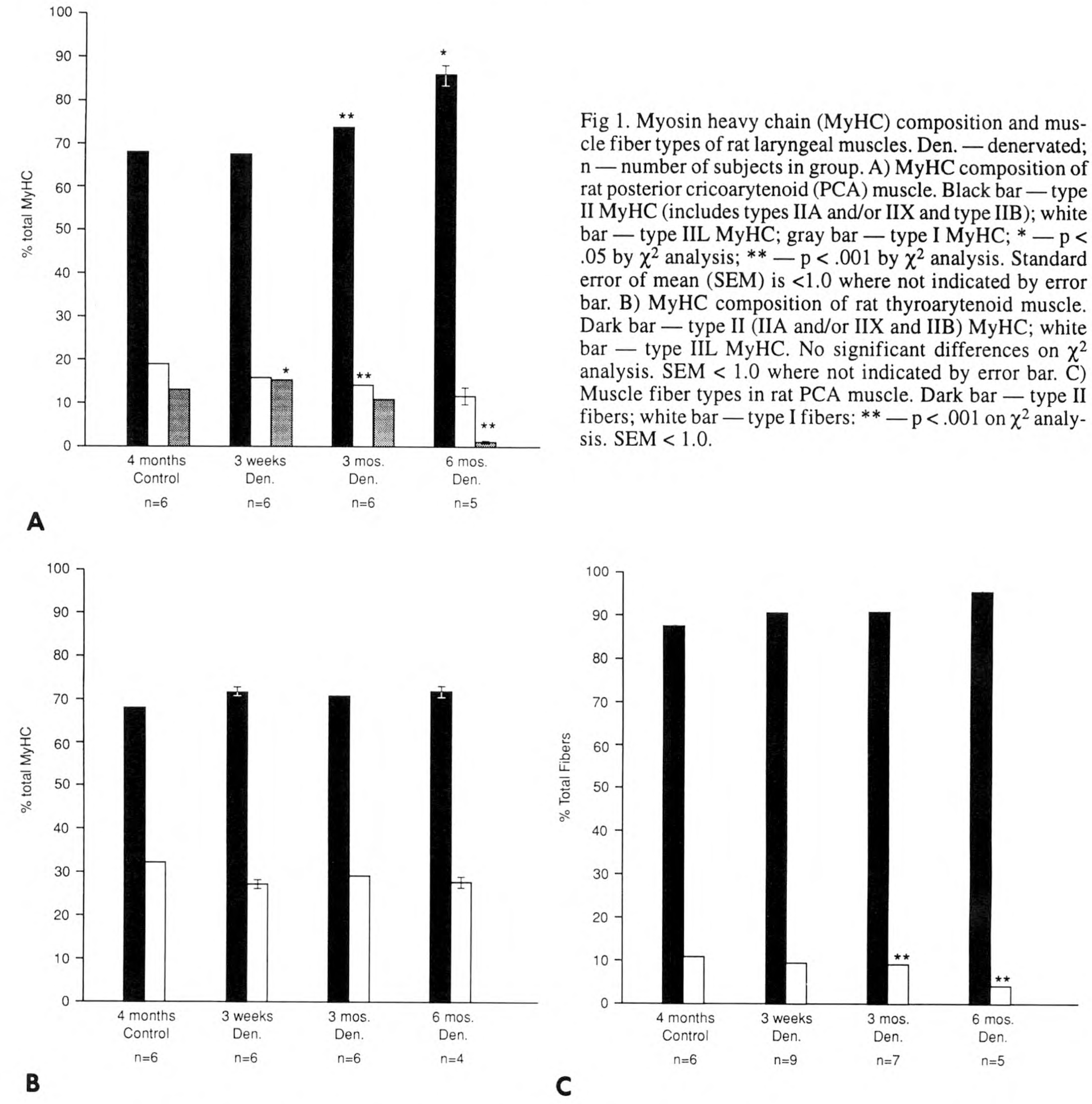

Fig 1. Myosin heavy chain (MyHC) composition and muscle fiber types of rat laryngeal muscles. Den. — denervated; n — number of subjects in group. A) MyHC composition of rat posterior cricoarytenoid (PCA) muscle. Black bar — type II MyHC (includes types IIA and/or IIX and type IIB); white bar — type IIL MyHC; gray bar — type I MyHC; * — $p < .05$ by χ^2 analysis; ** — $p < .001$ by χ^2 analysis. Standard error of mean (SEM) is <1.0 where not indicated by error bar. B) MyHC composition of rat thyroarytenoid muscle. Dark bar — type II (IIA and/or IIX and IIB) MyHC; white bar — type IIL MyHC. No significant differences on χ^2 analysis. SEM < 1.0 where not indicated by error bar. C) Muscle fiber types in rat PCA muscle. Dark bar — type II fibers; white bar — type I fibers: ** — $p < .001$ on χ^2 analysis. SEM < 1.0.

expression of type I and II MyHCs (excluding type IIL) in the denervated PCA muscles, which first became apparent after 3 months, and progressed to almost complete loss of the slow isoform at 6 months (see Table and Figs 1A and 2). This loss was accompanied by an increase in skeletal type II MyHCs. The expression of type IIL MyHC decreased slightly during the experiment, but this change was significant only at 3 months after denervation. In the TA muscle, which does not contain type I MyHC, there were no significant changes in type II isoform content with denervation (see Table and Fig 1B).

Fiber Types. We have described the major fiber in PCA and TA muscles as type IIL. This fiber contains type II MyHCs found in other limb skeletal fibers (IIA and/or IIX, and IIB), as well as the recently identified IIL MyHC.[6] Previously, we confirmed that IIB and IIL MyHCs were present in these fibers, but the relative content of IIA and IIX is still uncertain, since our gel technique does not separate the IIX and IIA isoforms into distinct bands (Fig 2). A further uncertainty exists in that the extraocular muscle–specific myosin heavy chain (EOM MyHC)[6] comigrates to the same position on SDS-PAGE as the IIL MyHC. The similarities and differences between these two protein species have yet to be determined.

The PCA muscle, composed mostly of type IIL fibers with some type I and IIC fibers, expressed fewer type I and IIC fibers over time with denervation. This change was most obvious at 6 months, where only a few darkly stained fibers were apparent with ATPase staining after preincubation at pH

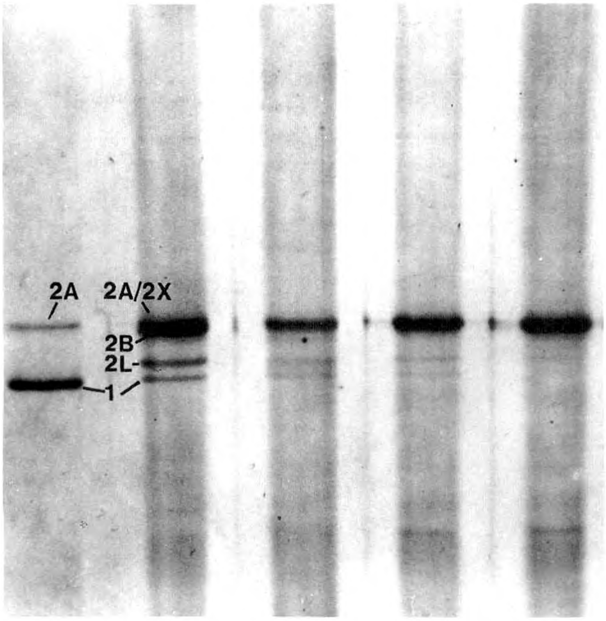

Fig 2. Sodium dodecyl sulfate–polyacrylamide gel electrophoresis of PCA muscles to separate MyHC isoforms (shown with arabic numerals). Lane 1 — soleus muscle; lane 2 — 4-month-old control PCA muscle; lane 3 — 3-week denervated PCA muscle; lane 4 — 3-month denervated PCA muscle; lane 5 — 6-month denervated PCA muscle. Note reduction in type I MyHC band with progressively longer periods of denervation, leading to absence at 6 months.

4.3 (see Table and Figs 1C and 3). There was no change in fiber type composition of the TA muscle with denervation, and no age-related changes were found in the two control groups. A few muscles showed signs of reinnervation on visualization or EMG. Figure 3D shows a PCA muscle that spontaneously reinnervated and is histochemically similar to the control muscles.

DISCUSSION

The phenotypic expression of contractile proteins (ie, the muscle fiber types and related MyHC isoforms) is determined by a complicated interplay of developmental, hormonal, and neurologic factors.[8] Although the frequency of α-motoneuron activity is the principal determining influence on MyHC expression in skeletal fibers, androgenic hormones in jaw-closing muscle and thyroid hormone in cardiac muscle play key roles.[9] The influence of hormonal factors on myosin expression in specialized laryngeal muscles in rats is not known, but has been described in ducks and frogs. Marked sexual fiber type differences in the sternotrachealis muscles in three species of ducks have been demonstrated.[10,11] It is reported that the mean fiber areas of each fiber type are always significantly larger in males, male Pekin ducks have an additional fiber type termed IIIA, and differences in fiber type are related to the effects of androgens on skeletal muscle function in sexual behavior, as the sternotrachealis muscle is involved in vocalization. In the frog, *Xenopus laevis*, laryngeal muscle is sexually differentiated. Male fibers are entirely fast, and female fibers are predominantly slow. This differential sexual phenotype is regulated by androgens. There also exists a laryngeal-specific MyHC expressed in all male fast fiber types.[12] Studies in progress now are looking at sexual differentiation of laryngeal muscles in rats.

The dependence of myosin expression on neural factors is best demonstrated by cross-innervation studies in which the nerves entering predominantly slow-twitch and fast-twitch muscles are crossed, resulting in type II MyHC expression in slow muscles and type I MyHC expression in fast muscles.[13] Evidence also exists to show that the expression of slow (type I) MyHC and fast (type IIB) MyHC is most dependent on neural input for maintenance of expression. For example, with long-term denervation, the rat diaphragm, a muscle of mixed fiber types, expresses a higher proportion of type II fibers relative to type I,[14] and the soleus muscle, composed predominantly of type I fibers, converts to a nearly complete fast fiber–containing muscle.[15] In limb muscles composed predominantly of type II fibers, long-term denervation results in a decrease in type IIB fibers and a proportional increase in IIA fibers.[16]

Similar changes occur in rat PCA and TA muscles after denervation. In the PCA muscle, a decrease in the percentage of type I MyHC was first evident 3 months after denervation, and type I was essentially absent in muscles that were denervated for 6 months. This decrease in type I MyHC was accompanied by an increase in type II MyHCs, but since in this study our gels did not consistently separate the fast isoforms into distinct IIA and/or IIX and IIB bands, we could not determine the relative ratio changes within these isoforms. The IIL isoform, however, was separated from type I and all the other type II MyHCs, allowing us to determine quantitative changes with denervation. Unlike other type II myosins, type IIL MyHC continues to be expressed at similar levels in the PCA muscle after denervation. So, in rat PCA muscle, type I MyHC is almost completely lost, type IIL MyHC remains relatively stable, and other type II MyHCs (as a group) increase.

The fiber type composition change in PCA muscle correlated with the MyHC isoform change. With myofibrillar ATPase histochemical staining, there was an overall decrease in the percentage of type I fibers and an increase in type IIL fibers.

The TA muscle contains only fast MyHC isoforms,

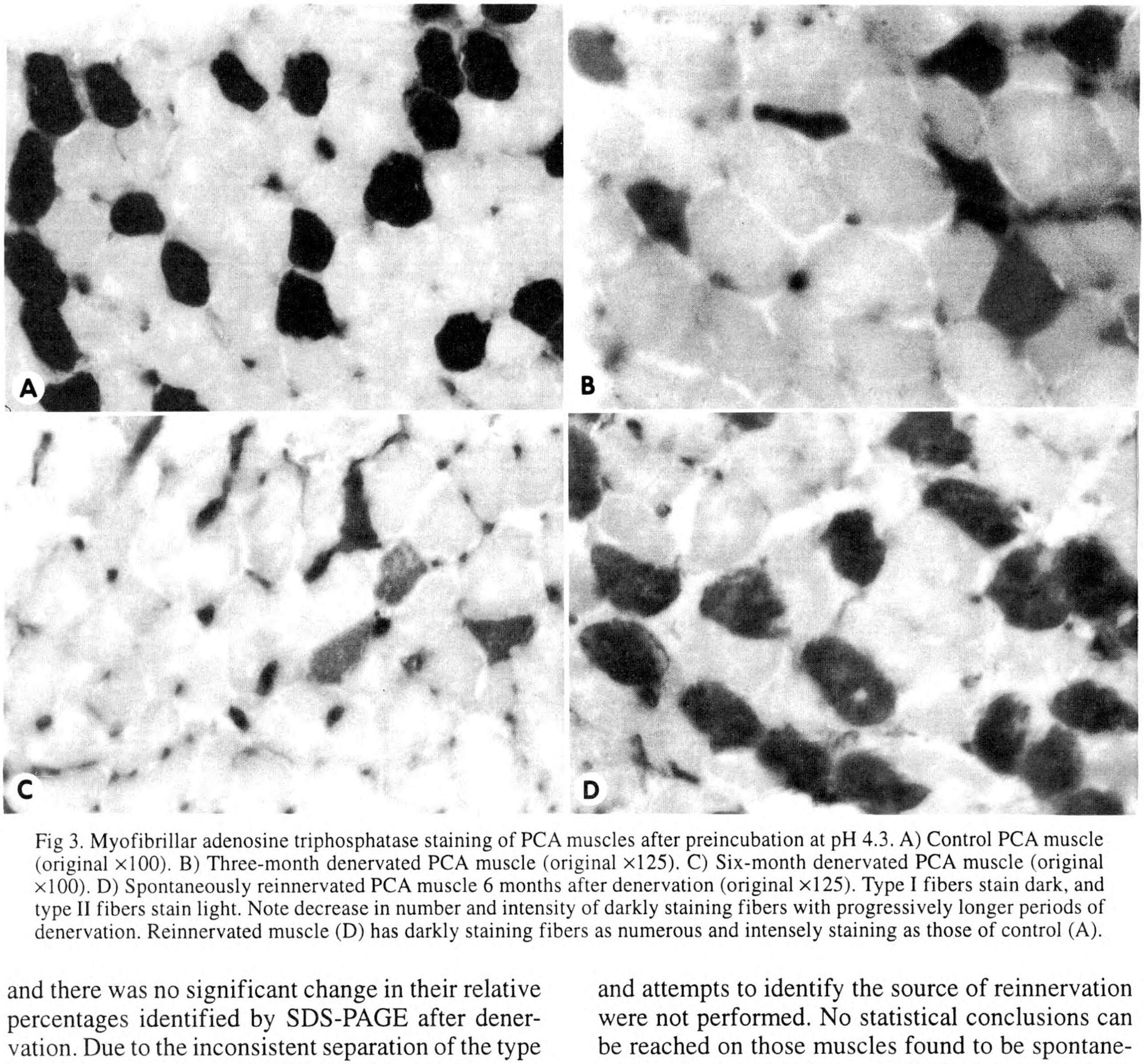

Fig 3. Myofibrillar adenosine triphosphatase staining of PCA muscles after preincubation at pH 4.3. A) Control PCA muscle (original ×100). B) Three-month denervated PCA muscle (original ×125). C) Six-month denervated PCA muscle (original ×100). D) Spontaneously reinnervated PCA muscle 6 months after denervation (original ×125). Type I fibers stain dark, and type II fibers stain light. Note decrease in number and intensity of darkly staining fibers with progressively longer periods of denervation. Reinnervated muscle (D) has darkly staining fibers as numerous and intensely staining as those of control (A).

and there was no significant change in their relative percentages identified by SDS-PAGE after denervation. Due to the inconsistent separation of the type IIA and/or IIX and type IIB MyHC bands, changes in the percentages of these isoforms could not be determined.

These results demonstrate the dependence of type I MyHC on neural input in the rat laryngeal muscles, and are similar to results of previous reports on sheep laryngeal muscles[17] and rat limb skeletal muscle.[18] This is further confirmed by the finding that in the few PCA muscles that became reinnervated spontaneously, there was a conversion back to the pattern of MyHC isoform and fiber type expression found in control muscle (Fig 3D). Since the proximal stump of the RLN was buried in the sternocleidomastoid muscle at the initial procedure, it is probable that reinnervation occurred through neuronal sprouting from adjacent laryngeal muscles (ie, PCA). The possibility of dislodgement and regeneration of the proximal stump cannot be ruled out, but is less likely, and attempts to identify the source of reinnervation were not performed. No statistical conclusions can be reached on those muscles found to be spontaneously reinnervated, due to the limited data, but these muscles appear to revert back to normal (ie, nondenervated) myosin composition. Future studies to evaluate the effect of reinervation of laryngeal muscles are planned.

Although we cannot describe the changes in the ratio of IIA, IIX, and IIB MyHCs in this study, it was demonstrated that type IIL MyHC continues to be expressed at about the same level with or without innervation. The lack of change in type IIL MyHC expression is different from the behavior previously described for the other type II MyHCs in limb skeletal muscle following denervation. Type IIB MyHC usually decreases and type IIA (and possibly IIX) increases, but in rat laryngeal muscles type IIL MyHC is relatively constant. Given these preliminary results, it is possible that non-neuronal factors are principally responsible for the expression of type

IIL MyHC, especially since there are examples of hormonal influence in other specialized branchiomeric muscles. For example, the α-cardiac MyHC in rabbit masseter muscle (an isoform usually found only in cardiac muscle) is regulated by the androgenic hormone testosterone.[9]

The laryngeal muscles carry out the specialized functions of respiration, airway protection, and phonation. As has been found in other specialized muscles, the laryngeal muscles express a unique MyHC that is likely responsible for their unique contractile characteristics. The data presented in this paper support the maintenance of the type IIL MyHC isoform in denervated laryngeal muscles, and the loss of type I MyHC. Maintenance of this isoform in the absence of an innervating nerve is an interesting characteristic, and may indicate that these muscles are genetically coded to express this isoform, contrary to the reliance on neural input for the expression of type I MyHC. This phenomenon would hold promise for improved return of normal laryngeal muscle function after reinnervation of individual muscles with non-native nerves (ie, nerves other than the RLN), if the muscles continue to express type IIL MyHC.

Further studies to determine the effects of changing neural innervation to these muscles, as well as studies on hormonal influences, are needed. In future studies, we plan to investigate how reinnervating the laryngeal muscles with a non-native nerve in both sexes of rats will affect myosin expression, and whether type IIL MyHC remains unchanged in these cases.

REFERENCES

1. Gorza L. Identification of a novel type 2 fiber population in mammalian skeletal muscle by combined use of histochemical myosin ATPase and anti-myosin monoclonal antibodies. J Histochem Cytochem 1990;38:257-65.

2. Brooke MH, Kaiser KK. Muscle fibers. How many and what kind? Arch Neurol 1970;23:369-79.

3. Rowlerson A, Mascarello F, Veggetti A, Carpene E. The fiber type composition of the first branchial arch muscles in carnivora and primates. J Muscle Res Cell Motil 1983;4:443-72.

4. Schiaffino S, Saggin L, Viel A, Ausoni S, Sartore S, Gorza L. Muscle fiber types identified by monoclonal antibodies to myosin heavy chains. In: Benzi G, Packer L, Siliprandi N, eds. Biochemical aspects of physical exercise. Amsterdam, the Netherlands: Elsevier Science, 1986:27-34.

5. Carraro U, Catani C. A sensitive SDS-PAGE method separating myosin heavy chains of rat skeletal muscles reveals the heterogeneous nature of the embryonic myosin. Biochem Biophys Res Commun 1983;116:793-802.

6. DelGaudio JM, Sciote JJ, Carroll WR, Esclamado RM. Atypical myosin heavy chain in rat laryngeal muscle. Ann Otol Rhinol Laryngol 1995;104:237-45.

7. Merril CR, Goldman D, Sedman SA, Ebert MH. Ultrasensitive stain for proteins in polyacrylamide gels shows regional variation in cerebrospinal fluid proteins. Science 1981; 211:1437-8.

8. Gambke B, Lyons GE, Haselgrove J, Kelly AM, Rubinstein NA. Thyroidal and neural control of myosin transitions during development of rat fast and slow muscles. FEBS Lett 1983;156:335-9.

9. d'Albis A, Janmot C, Mira JC, Couteaux R. Characterization of a ventricular V1 myosin isoform in rabbit masticatory muscles. Developmental and neural regulation. Basic Appl Myol 1991;1:23-34.

10. Scapolo PA, Lalatta-Costerbosa G, Barazzoni AM, Lucchi ML, Bortolami R. Sex differences in the histochemical characteristics of the sternotrachealis muscle of the duck. Boll Soc Ital Biol Sper 1988;64:831-3.

11. Lalatta-Costerbosa G, Scapolo PA, Barazzoni AM, Petrosino P, Clavenzani ML, Bortolami R. Analysis of the sternotrachealis muscle fibers in some anseriformes: histochemistry and sex differences. Am J Anat 1990;189:357-64.

12. Catz DS, Fischer LM, Kelly DB. Androgen regulation of a laryngeal-specific myosin heavy chain mRNA whose expression is sexually differentiated. Dev Biol 1995;171:448-57.

13. Buller AJ, Eccles JC, Eccles RM. Interaction between motoneurons and muscles in respect of the characteristic speeds of their responses. J Physiol (Lond) 1965;150:417-39.

14. Carraro U, Morale D, Mussini I, et al. Chronic denervation of rat hemidiaphragm: maintenance of fiber heterogeneity with associated increasing uniformity of myosin isoforms. J Cell Biol 1985;100:161-74.

15. Carraro U, Catani C, Degani A, Rizzi C. Myosin expression in denervated fast and slow-twitch muscles: fiber modulation and substitution. In: Pette D, ed. The dynamic state of muscle fibers. Berlin, Germany: Walter de Gruyter Publishers, 1990:247-62.

16. Jakubiec-Puka A, Kordowska J, Catani C, Carraro U. Myosin heavy chain isoform composition in striated muscle after denervation and self-reinnervation. Eur J Biochem 1990; 193:623-8.

17. Carraro U, Catani C, Saggin L, et al. Isomyosin changes after functional electrostimulation of denervated sheep muscle. Muscle Nerve 1988;11:1016-28.

18. Kelly AM, Rubinstein NA. Patterns of myosin synthesis in regenerating normal and denervated muscles of the rat. In: Pette D, ed. Plasticity of muscle. Berlin, Germany: Walter de Gruyter Publishers, 1980:161-75.

Ann Otol Rhinol Laryngol 106:1997

TRANSECTION AND OCCLUSION OF LATERAL SEMICIRCULAR CANAL IN GUINEA PIGS

BOO HYUN NAM, MD

SEONG KI YOON, MD   CHAN IL PARK, MD

TAEJEON, SOUTH KOREA

Audiologic and histopathologic examinations were made after occlusion of the lateral semicircular canal in eight guinea pigs. The lateral semicircular canal was drilled out, and then the canal lumens were plugged with muscle pieces. After a serial recording of auditory brain stem responses for 2 months, histologic specimens of the temporal bones were prepared in the lateral semicircular canal plane. One animal developed profound hearing loss due to suppurative labyrinthitis. The other seven animals showed no significant threshold elevation during this period. Histopathologic examination revealed that the bone defect on the lateral canal was replaced with newly formed bone; the perilymphatic and endolymphatic spaces maintained their compartmentalization; and the membranous endolymphatic canal healed to form complete blind ducts. These findings suggest that proper management of the injured semicircular canal is important for maintenance of postoperative hearing.

KEY WORDS — auditory brain stem responses, blind ducts, histopathologic examination, lateral semicircular canal, transection and occlusion.

INTRODUCTION

Occlusion of the semicircular canals has been performed in experimental animals and recently in humans for the treatment of benign paroxysmal positional vertigo and of labyrinthine fistula, and for access in skull base surgery (see Table[1-14]). The labyrinth, especially the semicircular canals, once considered inviolable, now can be manipulated without loss of hearing; however, the mechanisms of hearing loss and hearing preservation in membranous labyrinthine injury are poorly understood. In order to understand these mechanisms, histopathologic study may be essential, but there has been a paucity of histopathologic support. The authors observed the histopathologic changes in guinea pig temporal bones in which the lateral semicircular canal had been transected and then occluded.

MATERIALS AND METHODS

Animals. Eight male and female Hartley guinea pigs with normal auditory brain stem responses (ABRs), weighing from 250 to 300 g, were used. The animals were raised and maintained in a conventional facility at Chungnam National University Hospital.

Surgical Technique. The right side of the bulla was exposed laterally under general anesthesia with 50 mg/kg of intraperitoneally injected ketamine hydrochloride. The prominent portion of the lateral semicircular canal, just posterior to the facial canal, was transected by a surgical drill. From both sides of the transected canal lumens, free leakage of the inner ear fluid was observed, and with a pick, the lumens were plugged with harvested temporalis muscle pieces.

Auditory Evaluation. The ABRs were obtained before the operation and at 2, 5, and 10 days and 4 and 8 weeks postoperatively. Sound stimuli (broad-band click, rarefaction phase, 11.29 Hz) were generated and delivered by an audiometer equipped with an insert earphone (Quantum 84, Cadwell Laboratories Inc, Kennewick, Wash). The stimulus intensity at the tip of the sound delivery tube was biologically calibrated on nine healthy young human adults. Rectal temperature and oxygen saturation were monitored throughout the procedure. Thresholds were determined by attenuating the stimulus by 20-dB increments from 70 dB normal hearing level until the waveform was lost and then raising it by 5-dB increments until the waveform appeared.

Histopathology. After the final audiometric assessment, the animals were deeply anesthetized and perfused intravitally with normal saline and Heidenhain-Susa fixative. The right-side temporal bones were removed, fixed, and processed as described by Schuknecht.[15] The specimens were embedded in celloidin and sectioned at 20 µm. A section plane was chosen parallel to the plane of the lateral semicircular canal, because there could be some limitations with an ordinary horizontal or vertical section plane in observing the occluded portion of the canal. Every 10th section was stained with hematoxylin and eosin and examined microscopically.

From the Department of Otolaryngology, Chungnam National University School of Medicine, Taejeon, South Korea.

CORRESPONDENCE — Boo Hyun Nam, MD, Dept of Otolaryngology, Chungnam National University Hospital, 640 Daesa-dong, Jung-ku, Taejeon, 301-040, South Korea.

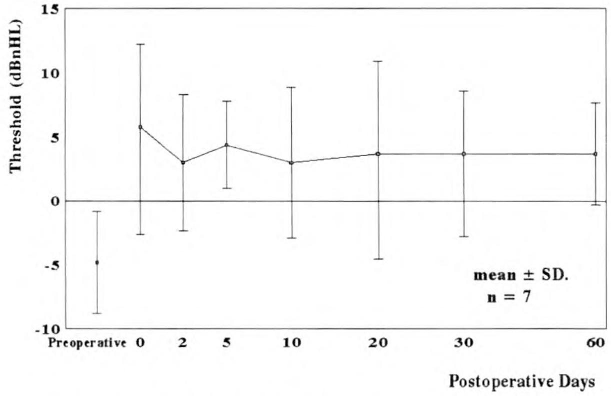

Fig 1. Auditory brain stem response thresholds in experimental animals before and after occlusion of semicircular canal.

RESULTS

On gross inspection, all of the experimental animals demonstrated spontaneous nystagmus and right side–down head-tilt postoperatively. The nystagmus disappeared the next day, but the head posture persisted for 3 to 4 days after surgery.

Auditory Brain Stem Response. After the operation, the thresholds were increased by approximately 10 dB (mean) compared to the preoperative levels in seven animals. The increases were maintained throughout the whole postoperative observation period (Fig 1). The other animal revealed profound hearing loss on the 10th-day ABR, and it was confirmed to have suppurative labyrinthitis on later histopathologic examination.

Histopathology. The surgical defect of the lateral canal produced by drilling was replaced with newly formed bone. The perilymphatic and endolymphatic spaces maintained their compartmentalization without evidence of intercommunication (Fig 2A). The membranous endolymphatic canal formed two blind ducts with a continuous epithelial layer. Necrotic materials

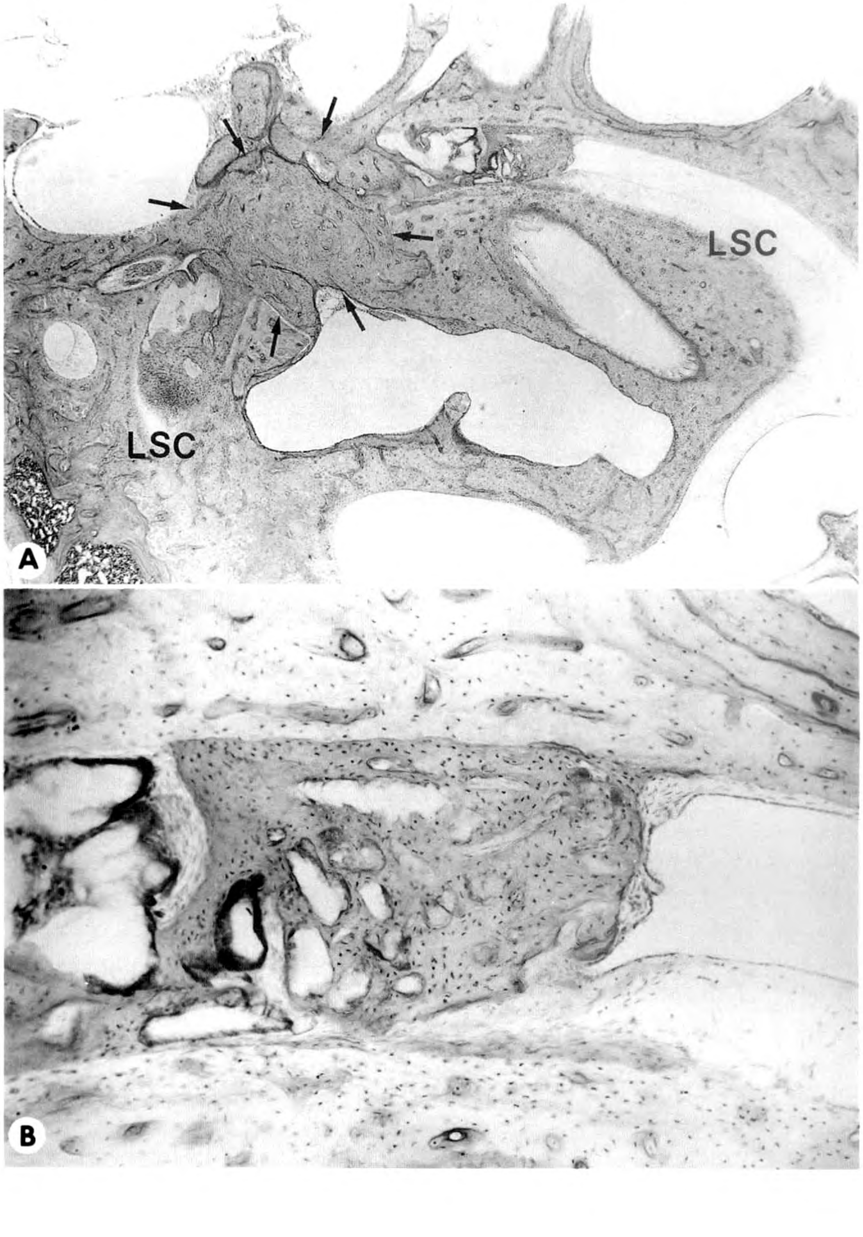

Fig 2. Histologic specimen of guinea pig temporal bone sectioned in lateral semicircular canal plane (H & E). A) Low power (original ×20). Note occluded lateral semicircular canal (LSC) and newly formed bone on surgical defect (arrows). B) High power (original ×100). Note necrotic materials and newly formed bone in occluded canal lumen. Membranous endolymphatic canal forms complete blind duct.

TECHNIQUES OF SEMICIRCULAR CANAL OCCLUSION

Authors	*Date*	*Subjects*	*Techniques and Materials*
Money and Scott[1]	1962	Cats	Transection*
Parnes and McClure[2]	1985	Guinea pigs	Puncture* + bone wax
Palva and Ramsay[3]	1989	Humans†	Fibrin glue and fascia
Parnes and McClure[4]	1990	Humans	Puncture* + fibrin glue and fascia; fenestration + bone paste + bone wax + fascia
Parnes and McClure[5]	1991	Humans	Fenestration + bone paste§ + fibrin glue and fascia
McElveen et al[6]	1991	Humans	Fenestration + bone wax
Pace-Balzan and Rutka[7]	1991	Humans	Fenestration + bone paste§; fenestration + periosteum + bone paste§ + fibrin glue and fascia
Anthony[8]	1991	Humans	Blue-lining + argon laser
Molony et al[9]	1992	Humans	Transection + fascia, or bone wax and fascia
Gjuric et al[10]	1992	Rabbits	Fenestration + perichondrium or fibrin glue; fenestration + fibrin glue + transection + perichondrium; fenestration + bone paste§ + transection
Hirsch et al[11]	1993	Humans	Fenestration + bone paste§ or bone wax
Kobayashi et al[12]	1995	Humans†	Fascia, perichondrium, bone chips, or cartilage
Kartush and Sargent[13]	1995	Humans	Fenestration + CO2 laser + fascia and bone chips + autologous blood
Antonelli et al[14]	1995	Guinea pigs	Fenestration + bone wax + fascia; blue-lining + CO2 laser + bone wax + fascia; blue-lining + CO2 laser + fascia

CO2 — carbon dioxide.
*Simultaneous plugging with bone chips.
†Cholesteatoma with deep labyrinthine fistula.
§Mixed with fibrin glue.

and newly formed bone were observed on both sides of the occluded canal lumen. The larger, smooth, marginated necrotic material appeared to be a muscle piece that had been used for the occlusion. The smaller, multiple materials seemed to come from bone chips that had been produced by drilling during transection of the canal (Fig 2B). The vestibular receptors and cochlea appeared normal. The one animal that had developed profound hearing loss revealed fibro-osseous obliteration of the labyrinth.

DISCUSSION

The mechanism of hearing loss in membranous labyrinthine injury is poorly understood. Cochlear injury in membranous labyrinthine rupture appears to have mechanical and chemical effects.[9,16] The mechanical effect is attributable to a widespread disruption of the membranous labyrinth, including capillary rupture, hemorrhage, and direct cellular damage. The chemical effect is one of massive perilymph-endolymph contamination that first occurs at the vestibule and spreads into the cochlea.

Most occlusion techniques have been concerned with minimizing the risk of labyrinthine trauma by use of more conservative methods (see Table). Parnes and McClure[5] performed occlusion of the posterior semicircular canal after fenestration of the bony canal to avoid tearing the membranous endolymphatic canal. Gjuric et al[10] attempted perfusion of fibrin glue for occlusion of the perilymphatic and endolymphatic spaces. Anthony[8] tried to avoid mechanical occlusion by partitioning the posterior canal using a laser. Kartush and Sargent[13] and Antonelli et al[14] used a laser prior to mechanical plugging of the canal to obtain atraumatic occlusion. Depending on the surgical techniques and materials used for occlusion, the postoperative hearing was different in each study.

In this study, there was a comparable hearing result with these conservative occlusions in spite of the accompanying membranous labyrinthine rupture. The postoperative nystagmus and head position change, which revealed chemical and mechanical injury of the vestibular labyrinth by transection of the lateral semicircular canal, did not last long. Although these inner ear injuries with membranous endolymphatic canal rupture were predicted to be more serious than those of other conservative occlusions, they should not have significantly affected the cochlear and vestibular receptors. In fact, the interruption of the lateral semicircular canal did not affect the endocochlear DC potential or compound action potentials (CAPs) recorded in the scala media of guinea pigs, or the CAP of humans.[17] This indicated that the labyrinthine fluid system of the cochlea was relatively independent of that of the vestibular labyrinth during transection of the semicircular canals. We feel that the profound hearing loss that follows membranous endolymphatic canal rupture might be a result of permanent fistulization between the endolymph and perilymph,[3] rather than a result of injuries that occur during transection of the canal.

The mechanism of hearing preservation in membranous labyrinthine injury still remains unresolved. Jahrsdoerfer et al[18] addressed the valvular function of the utriculoendolymphatic valve, which could prevent the collapse of the pars inferior (cochlea and saccule) in a sudden decompression of the endolymphatic system by rupture of the pars superior (utricle and semicircular canals). Canalis et al[16] believed that the local changes occurring in the injured semicircular canals were important. The sudden loss of the endolymph and supporting structure collapsed the membranous endolymphatic canal and sealed its torn ends. As an explanation of hearing preservation in acoustic neuroma surgery accompanied with semicircular canal injury, Tatagiba et al[19] proposed that incidental closure of an opened canal by bone fragments may occur during drilling, thereby preventing endolymphatic leakage.

In this study, the ruptured membranous endolymphatic canal healed to form blind ducts. In regard to healing of the membranous labyrinth, there is some evidence that endolymphatic membrane ruptures heal in experimental animals[20,21] and humans.[22,23] Healing may be by epithelial proliferation[22] or fibrous reattachment of the endolymphatic membrane[20]; however, these healing processes may require a long time, waiting until the communication between the perilymphatic and endolymphatic spaces is closed. In this study, it is likely that the ruptured and then collapsed endolymphatic canal (Canalis et al[16]) was externally compressed and sealed off by the introduction of muscle pieces into the bony canal lumens, which thereby formed blind ducts. The immediate interruption of the communication between the endolymphatic and perilymphatic spaces could have prevented a profound hearing loss following the membranous labyrinthine rupture. The functions of the utriculoendolymphatic valve and the hydrodynamic change in the labyrinthine fluid system during transection of the semicircular canal are unclear, and histopathologic studies at various stages of occlusion are now under way.

In summary, we formed blind ducts in a ruptured membranous endolymphatic canal by plugging of the bony semicircular canal lumens. The occlusion of the injured semicircular canal, by preventing fistulization between the endolymph and perilymph, might be an effective method in preserving postoperative hearing. For a better understanding of the mechanism of hearing preservation and the development of safer and more reliable techniques for the treatment of labyrinthine injury, further experimental studies are required.

REFERENCES

1. Money KE, Scott JW. Functions of separate sensory receptors of nonauditory labyrinth of the cat. Am J Physiol 1962; 202:1211-20.
2. Pames LS, McClure JA. Effect of brainstem auditory evoked responses of posterior semicircular canal occlusion in guinea pigs. J Otolaryngol 1985;14:145-50.
3. Palva T, Ramsay H. Treatment of labyrinthine fistula. Arch Otolaryngol Head Neck Surg 1989;115:804-6.
4. Pames LS, McClure JA. Posterior semicircular canal occlusion for intractable benign paroxysmal positional vertigo. Ann Otol Rhinol Laryngol 1990;99:330-4.
5. Pames LS, McClure JA. Posterior semicircular canal occlusion in the normal hearing ear. Otolaryngol Head Neck Surg 1991;104:52-7.
6. McElveen JT, Wilkins RH, Erwin AC, Wolford RD. Modifying the translabyrinthine approach to preserve hearing during acoustic neuroma surgery. J Laryngol Otol 1991;105:34-7.
7. Pace-Balzan A, Rutka JA. Non-ampullary plugging of the posterior semicircular canal for benign paroxysmal positional vertigo. J Laryngol Otol 1991;105:901-6.
8. Anthony PF. Partitioning the labyrinth: application in benign paroxysmal positional vertigo. Am J Otol 1991;12:388-93.
9. Molony TB, Kwartler JA, House WF, Hitselberger WE. Extended middle fossa and retrolabyrinthine approaches in acoustic neuroma surgery: case reports. Am J Otol 1992;13:360-3.
10. Gjuric M, Wigand ME, Housemann W. Selective resection of the semicircular canals of rabbits with preservation of hearing. Acta Otolaryngol (Stockh) 1992;112:907-15.
11. Hirsch BE, Cass SP, Sekhar LN, Wright DC. Translabyrinthine approach to skull base tumors with hearing preservation. Am J Otol 1993;14:533-43.
12. Kobayashi T, Sato T, Toshima M, Ishidoya M, Suetake M, Takasaka T. Treatment of labyrinthine fistula with interruption of the semicircular canals. Arch Otolaryngol Head Neck Surg 1995; 121:469-75.
13. Kartush JM, Sargent EW. Posterior semicircular canal occlusion for benign paroxysmal positional vertigo. CO2 laser–assisted technique: preliminary results. Laryngoscope 1995;105: 268-74.
14. Antonelli PJ, Bouchard KM, Kartush JM. Carbon dioxide laser occlusion of the guinea pig posterior semicircular canal. Otolaryngol Head Neck Surg 1995;113:453-8.
15. Schuknecht HF. Pathology of the ear. 2nd ed. Philadelphia, Pa: Lea & Febiger, 1993:7-13.
16. Canalis RF, Gussen R, Abemayor E, Andrews J. Surgical trauma to the lateral semicircular canal with preservation of hearing. Laryngoscope 1987;97:575-81.
17. Kobayashi T, Shiga N, Hozawa K, Hashimoto S, Takasaka T. Effect on cochlear potentials of lateral semicircular canal destruction. Arch Otolaryngol Head Neck Surg 1991;117:1292-5.
18. Jahrsdoerfer RA, Johns ME, Cantrell RW. Labyrinthine trauma during ear surgery. Laryngoscope 1978;88:1589-95.
19. Tatagiba M, Samii M, Matthies C, Azm ME, Schönmayr R. The significance for postoperative hearing of preserving the labyrinth in acoustic neuroma surgery. J Neurosurg 1992;77:766-84.
20. Lawrence M, Yantis PA. Individual differences in func-

tional recovery and structural repair following overstimulation of the guinea pig ear. Ann Otol Rhinol Laryngol 1957;66:595-621.

21. Simmons FB, Mongeon CJ. Endolymphatic duct pressure produces cochlear damage. Arch Otolaryngol 1967;85:143-50.

22. Gussen R. Sudden hearing loss associated with cochlear membrane rupture. Arch Otolaryngol 1981;107:598-600.

23. Schuknecht HF. Meniere's disease: a correlation of symptomatology and pathology. Laryngoscope 1963;73:651-65.

≈

RECENT ADVANCES IN OTITIS MEDIA

The 7th International Symposium on Recent Advances in Otitis Media will be held June 1-5, 1999, in Fort Lauderdale, Florida. For information, contact David J. Lim, MD, House Ear Institute, 2100 W Third St, Los Angeles, CA 90057.

Ann Otol Rhinol Laryngol 106:1997

AUDITORY EVOKED RESPONSES UNDER TOTAL SPINAL ANESTHESIA IN RATS

KATSUSHI YAMADA, MD

KIMITAKA KAGA, MD
HIDEAKI SAKATA, MD
AKIRA UNO, PHD
TOSHIHIRO TSUZUKU, MD

TOKYO, JAPAN

In order to investigate the function of the auditory pathway from the cochlea to the brain stem under total spinal anesthesia, the auditory brain stem response (ABR), compound action potential of the cochlear nerve (CAP), and cochlear microphonics (CM) were simultaneously recorded in rats. Total spinal anesthesia was induced by infusion of 2% lidocaine hydrochloride at a constant rate of 0.10 mL/min into the cerebrospinal fluid through the rats' skulls. The ABR completely disappeared within 1.5 to 4 minutes. After cessation of the injection, the ABR reappeared, starting from wave I and progressing through waves II and III to wave IV. The latency change of the CAP throughout the recording period was quite similar to that of wave I of the ABR. A reduction in amplitude of the CM was observed, but the CM did not disappear during the recording period. Disappearance of the ABR was due, not to loss of cochlear function, but to anesthetic effects on the acoustic nerve and the brain stem. Monitoring of the ABR provided information on the level of neural activity in the brain stem under total spinal anesthesia.

KEY WORDS — auditory brain stem response, cerebrospinal fluid, cochlear microphonics, compound action potential, lidocaine.

INTRODUCTION

Under spinal or epidural anesthesia, accidental spread of a high dose of the anesthetic to the brain induces loss of consciousness and respiratory arrest. This is called total spinal anesthesia. During this accident, neural activity in the brain stem is severely suppressed. However, no methods to monitor the neural activity of the brain stem under total spinal anesthesia have been available.

Auditory brain stem response (ABR) is one of the most useful tests for evaluating the neural activity of the brain stem. Previously, we studied the ABR in a rat model of total spinal anesthesia.[1] A catheter designed for human epidural anesthesia was inserted to the subarachnoid space through the skull at the top of the rat's head, and 2% lidocaine hydrochloride was injected through the catheter at a constant rate of 0.10 mL/min. The ABR disappeared within 4 minutes, and disappearance started with later waves (eg, wave IV) of the ABR. After cessation of the lidocaine injection, the ABR progressively reappeared and recovered from wave I to wave IV. These results demonstrated that the effect of lidocaine on the ABR was reversible and extended from the acoustic nerve to the midbrain (mesencephalon).

However, the results of our previous study did not clarify whether the disappearance of the ABR was due to neural conduction blocks in the acoustic nerve and the brain stem or to some effect on the cochlea, since a loss of cochlear function results in disappearance of the ABR. Using the same rat model, we therefore monitored the cochlear microphonics (CM) and compound action potential of the cochlear nerve (CAP), as well as the ABR, and studied the effect of lidocaine in the cerebrospinal fluid (CSF) on the auditory pathway from the cochlea to the brain stem.

MATERIALS AND METHODS

Ten male Wistar rats with normal Preyer's reflexes and weighing 200 to 250 g (mean 214 g) were used. Each rat was intraperitoneally anesthetized with 50 mg/kg pentobarbital sodium. After tracheotomy, the rat was artificially respirated. The rat's head was fixed in a stereotaxic holder, a small hole was drilled in the top of the skull, and the dura mater was incised. A catheter designed for human epidural anesthesia was inserted into the subarachnoid space. Leakage of CSF was prevented by bonding. A postauricular incision was made on the right, and the bulla was exposed from the dorsal side. A small Teflon-insulated silver ball electrode was placed in the round window niche through a small hole made in the bulla under a microscope. Needle electrodes were inserted through the skin at the vertex, right mastoid, and neck.

The ABR was recorded through the needle electrode at the vertex, and the CAP and the CM were recorded

---

From the Department of Otolaryngology, Teikyo University School of Medicine (Yamada, Sakata, Tsuzuku), the Department of Otolaryngology, Faculty of Medicine, University of Tokyo (Kaga), and the National Institute of Mental Health, National Center of Neurology and Psychiatry (Uno), Tokyo, Japan.

CORRESPONDENCE — Katsushi Yamada, MD, Dept of Otolaryngology, Teikyo University School of Medicine, Kaga 2-11-1, Itabashi-ku, Tokyo 173, Japan.

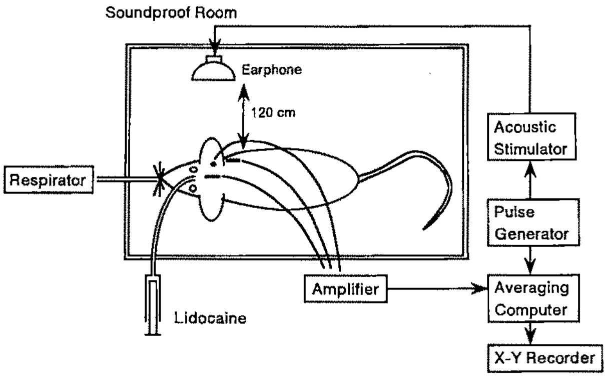

Fig 1. Schematic of experimental setup.

through the silver ball electrode in the round window niche. Needle electrodes at the right mastoid and the neck were used as the reference and ground, respectively.

We performed all recordings of auditory evoked potentials in an electrostatically shielded, soundproof room. An acoustic stimulator (Audible signal controller DA-505, DANA Japan Co), a recorder of evoked potentials (Neuropack 8 MEE-4108, Nihon Kohden Co), and a respirator (model SN-480-7, Shinano Co) were placed outside the room. Auditory stimuli were delivered via an earphone (AD-05, Rion Co) placed 120 cm from the right auricle of the rat (Fig 1).

Auditory stimuli were 3-kHz short tone bursts presented at a rate of 10/s. The rise, fall, and plateau times were 1 millisecond each, with a total duration of 3 milliseconds. The waves of the ABR, CAP, and CM were simultaneously obtained by averaging 200 responses in the following way. During recording, the polarity of the sound was reversed when 100 responses were averaged. Then the remaining 100 responses were averaged. The ABR and CAP were obtained by an addition of the former averaged 100 responses to the remaining averaged 100 responses. The CM was obtained by a subtraction of the two. The filter bandwidth was 100 to 5,000 Hz.

As 2% lidocaine was suitable for injection into rat CSF,[1] 2% lidocaine solution was injected through the catheter at a constant rate of 0.10 mL/min (lidocaine hydrochloride 2.0 mg/min). The ABR was recorded every 30 seconds during the lidocaine injection. We stopped the injection as soon as the ABR disappeared. The time at the end of the injection was defined as time 0. After the lidocaine injection, simultaneous recordings of the ABR, CAP, and CM were taken every 5 minutes until 30 minutes after the injection, and thereafter every 15 minutes until the rat recovered from the total spinal anesthesia. (This took 100 to 145 minutes for the 10 rats.) Rectal temperatures and heart rates were monitored, and the temperature was maintained within 0.5°C throughout the recording period by means of a heat pad. Control waves for each rat were recorded just prior to the lidocaine injection.

No more than 4 major vertex-positive components of the ABR could be consistently and reliably identified in all rats. As in previous reports,[2,3] the positive components were labeled waves I to IV. Amplitudes of waves I to IV and the CAP were measured from a positive peak to the following trough. The amplitude of the CM was measured at the middle of the wave. Statistical differences were evaluated with the paired *t*-test.

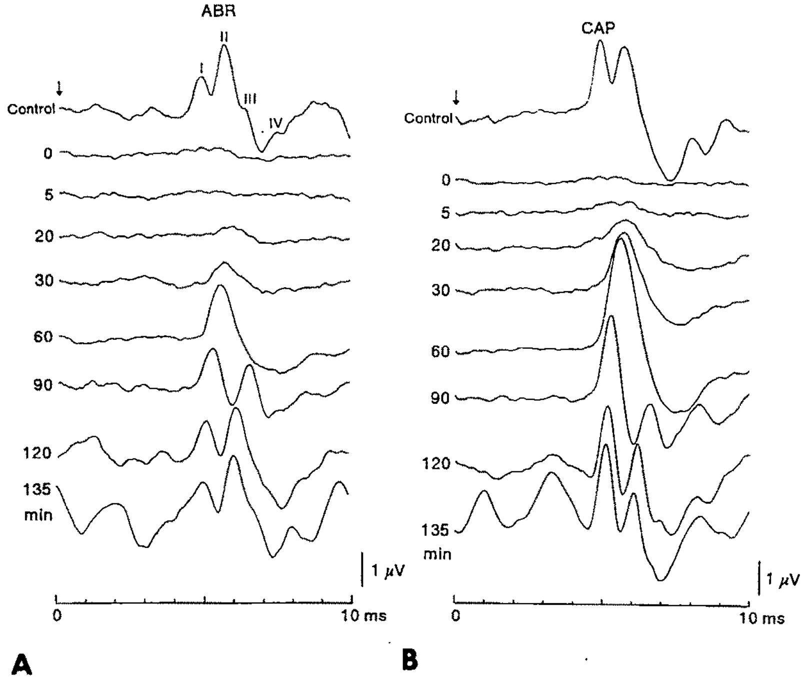

Fig 2. Change in A) auditory brain stem response (ABR) and B) compound action potential (CAP) in rat 1. As earphone was placed 120 cm from auricle, sound reached rat's ear at about 3.5 milliseconds (ms) after start of recording.

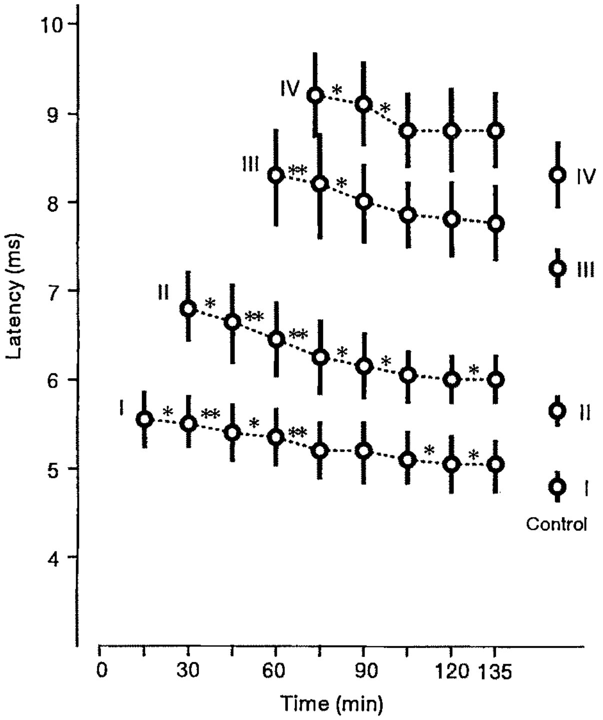

Fig 3. Peak latencies of waves I to IV. Circles represent average values for at least 6 rats. Upper and lower bars represent ±1 SD. Asterisks indicate significant differences in peak latencies between successive recording times: ** — $p < .01$; * — $p < .05$.

After the experiment, the rat was perfused with 10% formaldehyde and the cranial bone was removed. The bone was fixed in 10% formaldehyde, decalcified, and embedded in celloidin. Serial horizontal sections were made at 20 μm, and every 10th section was stained with hematoxylin-eosin. We examined the labyrinth under a light microscope.

RESULTS

In a preliminary experiment, we injected 0.50 mL of saline through the catheter at a constant rate of 0.10 mL/min in 3 control rats. The saline injection failed to induce any changes in peak latencies or amplitudes of waves I to IV and the CAP, or in amplitudes of the CM.

The ABR disappeared on constant injection of 2% lidocaine into the CSF. The dose of the 2% lidocaine solution required to cause total disappearance of the ABR ranged from 0.15 mL (total dose of injected lidocaine hydrochloride 3 mg) to 0.40 mL (8 mg) in the 10 rats, taking from 1.5 to 4.0 minutes for the injection. The total dose of lidocaine hydrochloride per unit weight ranged from 15.0 to 38.1 mg/kg (mean 24.8 mg/kg). Disappearance of the ABR started with wave IV and progressed through waves III and II to wave I. The process of disappearance of the ABR was described and illustrated in our previous report.[1]

After cessation of the injection, the waves of the ABR progressively reappeared and recovered, from wave I to wave IV. The reappearance time and the latency change of the CAP throughout the recording period were quite similar to those of wave I of the ABR. Figure 2 shows the change in the ABR and the CAP

Fig 4. Percent amplitudes of wave II with reference to control values. Circles represent average values for at least 6 rats, and upper and lower bars represent ±1 SD. Asterisks indicate significant differences in amplitudes between successive recording times ($p < .05$).

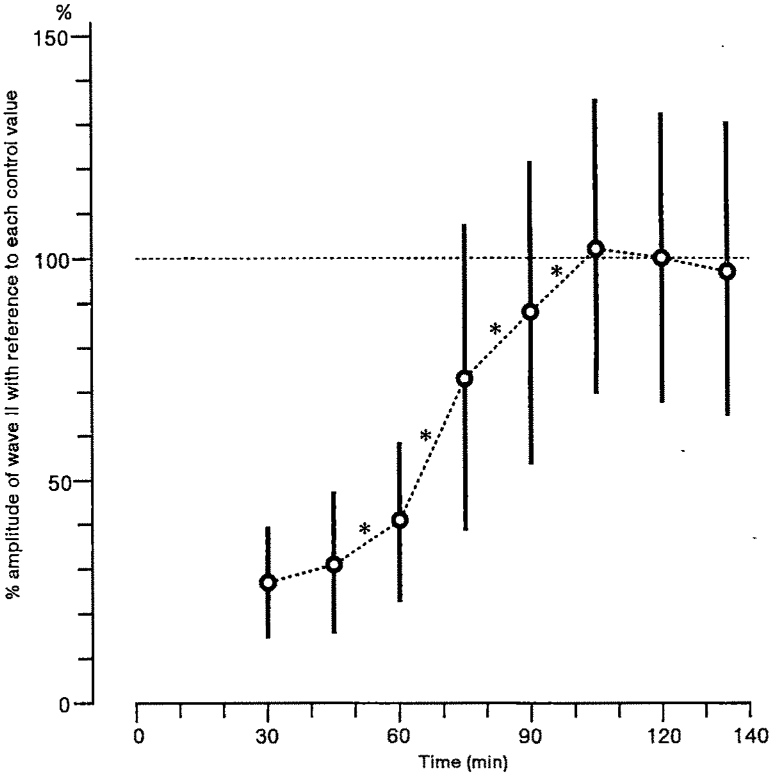

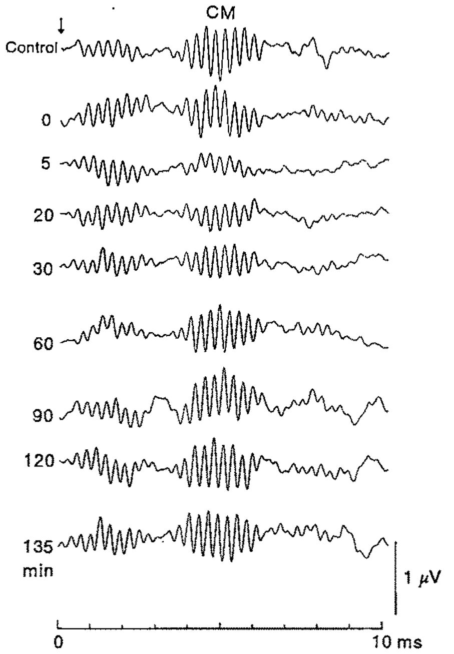

Fig 5. Change in cochlear microphonics (CM) in rat 1. As earphone was placed 120 cm from auricle, sound reached rat's ear at about 3.5 ms after start of recording. Wave during 3.5 to 6.5 ms of recording shows CM. Wave at first 3 ms of recording is electromagnetic wave originating from earphone (stimulus artifact).

throughout the recording period in rat 1. Wave I of the ABR and the CAP reappeared 20 minutes after the end of injection. Thereafter, waves II, III, and IV of the ABR reappeared, in that order. At 135 minutes after the injection, each waveform of the ABR and the CAP approximated those of the controls.

Wave I of the ABR and the CAP reappeared 5 to 20 minutes after injection in all 10 rats. Thereafter, waves II, III, and IV of the ABR reappeared, in that order. The reappearance times in 6 or more rats were 15 minutes for wave I (CAP), 30 minutes for wave II, 60 minutes for wave III, and 75 minutes for wave IV. The averages of the peak latencies of the ABR waves are shown in Fig 3. The latencies of each wave shortened with time, and were close to the control values at the time of the final recording.

The amplitudes of waves I to III and the CAP had a tendency to increase with time, but they varied in the 10 rats. Wave II had the largest amplitude among all the ABR waves, and also showed significant statistical differences in amplitude between successive recording times. Figure 4 shows the mean amplitudes of wave II throughout the recording period. The mean amplitude of wave II increased with time, and was almost the same as that of controls 105 minutes after the injection. The amplitude of wave IV exhibited the widest variation in the 10 rats and showed no tendency to increase with time.

Throughout the recording period, the CM did not disappear in any rat. Figure 5 shows the change in the CM in rat 1. The amplitude of the CM decreased, and the minimal amplitude was observed 5 minutes after the injection. The CM recovered with time. The percent amplitude change of the CM with reference to each control value in 10 rats is shown in Fig 6. The mean percent amplitude of the CM was about 60% that of the control at 0 minute, and was minimal, at about 35%, at 5 minutes. Thereafter, it gradually recovered.

Histologic studies revealed no obvious findings in the cochlea (Fig 7A). Red blood cells were observed in the cochlear aqueduct and the perilymph (Fig 7B).

DISCUSSION

The injection of a lidocaine solution into the CSF results in an elevation of the intracranial pressure that

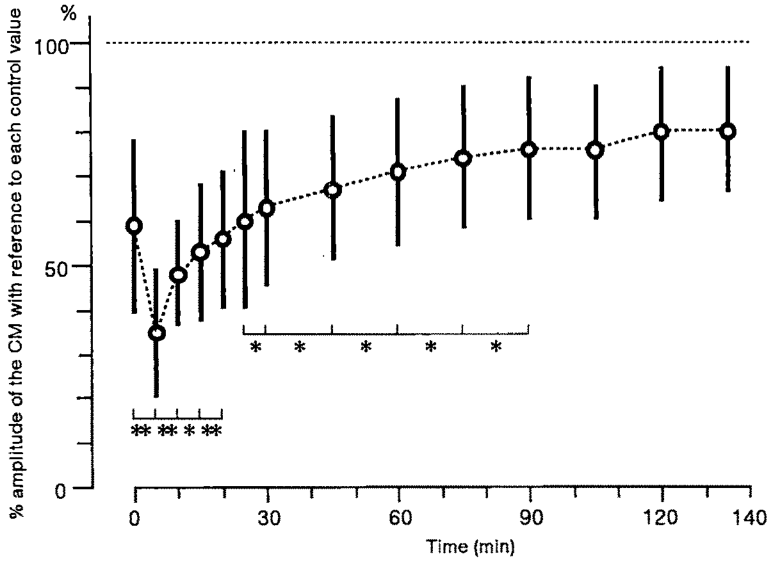

Fig 6. Percent amplitudes of CM with reference to control values. Circles represent average values for 10 rats, and upper and lower bars represent ±1 SD. Asterisks indicate significant differences in amplitudes between successive recording times: ** — $p < .01$; * — $p < .05$.

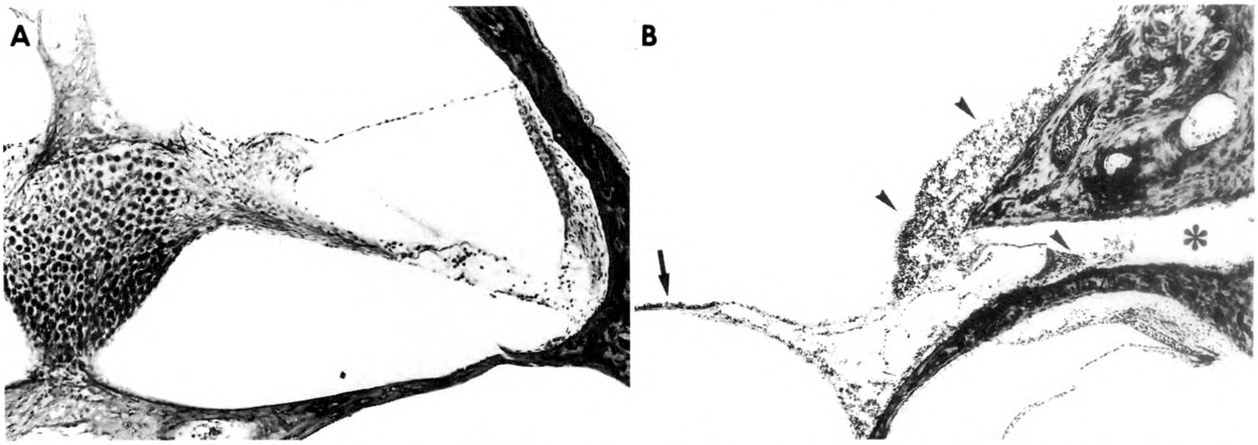

Fig 7. Horizontal sections of temporal bone of rat 1. A) Middle turn of cochlea (original ×150). B) Cochlear aqueduct (asterisk) and perilymph (original ×100). Arrow indicates round window membrane. Arrowheads indicate red blood cells in aqueduct and perilymph.

causes deterioration of the ABR[4] or the CM.[5] Allen et al[6] reported that a decrease in amplitude of the CM observed under conditions of increased intracranial pressure was due to a mechanical effect produced by increased perilymphatic pressure. Results of our previous experiment[1] showed that injection of less than 0.60 mL of saline into the CSF at a constant rate of 0.10 mL/min did not produce intracranial pressure elevation sufficient to cause deterioration of the ABR in rats. A saline injection of 0.50 mL also failed to induce any changes in the amplitude of the CM. Therefore, the changes of the ABR, CAP, and CM in the present study should have been caused by the pharmacologic effects of 2% lidocaine in the CSF.

The change in the ABR evoked by click stimuli and the dose of 2% lidocaine solution required for total disappearance of the ABR in the present study were almost the same as those in the previous study.[1] This consistency indicates that the change in ABR in the rat model of total spinal anesthesia is reliable and almost the same regardless of whether stimuli are clicks or 3-kHz short tone bursts with a rise time of 1 millisecond.

Lidocaine in the CSF may infiltrate the cochlea via one or more of three possible routes: 1) through vessels, 2) through the fundus of the internal auditory meatus and Rosenthal's canals, and 3) through the cochlear aqueduct.

When a therapeutic dose of intravenous lidocaine is injected into the CSF, the CM does not change. In guinea pigs, the amplitude of the CM did not change with a high dose (20 mg/kg) of lidocaine hydrochloride administered intravenously, whereas deterioration of the ABR or the CAP was observed.[7] The dose of lidocaine hydrochloride per weight administered intravenously[7] was almost the same as that injected into the rats' CSF in the present study (24.8 mg/kg). These findings together indicate that the change in the CM in the present study was not due to effects of lidocaine that infiltrated the blood from the CSF.

In human temporal bone studies, red blood cells are sometimes observed in Rosenthal's canals of the modiolus after subarachnoid hemorrhage. These cells enter Rosenthal's canals through the fundus of the internal auditory meatus. Therefore, it is likely that lidocaine in the CSF in the internal auditory meatus infiltrates the area around the spiral ganglion cells. However, it is not certain that lidocaine in the CSF infiltrates the hair cells in the organ of Corti through this route, or that it affects the CM.

The subarachnoid space communicates with the perilymphatic space through the cochlear aqueduct. The cochlear aqueduct of rats is larger than that of humans. In the histologic study, many red blood cells were observed in the cochlear aqueduct (Fig 7B). These cells likely originated from bleeding at the incision of the dura mater. This finding, therefore, indicates that lidocaine injected into the CSF entered the perilymphatic space of the cochlea through the aqueduct.

There have been some reports[8,9] that lidocaine application onto the round window produced a temporary decrease in the amplitude of the CM and the CAP. They suggested that lidocaine entered the perilymphatic space through the round window membrane and directly affected the cochlear function. In the present study, the effect of lidocaine on the CM was also reversible and was maximal 5 minutes after the injection. The change in the CM was very similar to that observed in previous studies of lidocaine application to the round window. This finding suggests that lidocaine entered the labyrinth through the cochlear aqueduct and imperfectly affected the electrophysiologic activities of the cochlea.

The CM did not disappear during the recording period, even when the ABR and the CAP disappeared.

Our result indicate that disappearance of the ABR was due, not to loss of cochlear function, but to anesthetic effects on the acoustic nerve and the brain stem. The results also indicate that lidocaine in the CSF affected the auditory pathway from the cochlea to the brain stem.

Each rat in the present study exhibited transient, regular bradycardia after lidocaine injection. Thereafter, the pulse gradually increased and returned to the preinjection level at 30 to 60 minutes. Each rat recovered from the total spinal anesthesia and began to move by 100 to 145 minutes after the injection. These observations suggest that the depth of anesthesia paralleled the deterioration of the ABR. Moreover, the disappearance of ABR waves from IV to I and the reappearance from I to IV, in that order, suggest that the early component, ie, wave I, was observed at a light level of anesthesia. Monitoring of the ABR, therefore, enables determination of the level of total spinal anesthesia in this model.

For the rat ABR, it has been demonstrated that the origin of wave I is the acoustic nerve and that of wave IV is the inferior colliculi.[2] Changes of waves I to IV in rats correspond with those of waves I to V or VI in humans. But it may be difficult to perfectly apply the present results to clinical total spinal anesthesia, since there are anatomic differences in the subarachnoid space between rats and humans, and because the method of lidocaine injection and the dose of lidocaine administered are different between this model and clinical anesthesia. However, the present results demonstrate that monitoring of the ABR appears to provide information on the level of neural activity in the brain stem under clinical total spinal anesthesia. We hope to monitor ABRs more actively in a clinical situation.

CONCLUSIONS

We injected 2% lidocaine into the subarachnoid space of 10 rats and monitored the ABR, CAP, and CM.

1. The ABR and CAP completely disappeared during the injection, and then reappeared progressively after cessation of the injection.

2. A reduction in amplitude of the CM was observed, but the CM did not disappear when the ABR and the CAP disappeared.

3. The auditory pathway from the cochlea to the mesencephalon was affected by lidocaine, and the effect was reversible.

4. The reduction in amplitude of the CM suggested that lidocaine entered the labyrinth through the cochlear aqueduct and affected the electrophysiologic activity of the cochlea.

5. The disappearance of the ABR was due, not to loss of cochlear function, but to the anesthetic effect on the acoustic nerve.

6. Monitoring of the ABR provided information on the level of neural activity in the brain stem under total spinal anesthesia.

ACKNOWLEDGMENTS — We thank H. Nishida, MD, for his advice on recording the cochlear microphonics; O. Motoyoshi and N. Furuya for their help in setting up the experiment; and E. Saito and M. Baba for their help in the preparation of the serial sections.

REFERENCES

1. Yamada K, Kaga K, Tsuzuku T, Uno A. Analysis of auditory brain stem response with lidocaine injection into the cerebrospinal fluid in rats. Ann Otol Rhinol Laryngol 1994;103:796-800.

2. Jewett DL, Romano MN. Neonatal development of auditory system potentials averaged from the scalp of rat and cat. Brain Res 1972;36:101-15.

3. Burkard R, Feldman M, Voigt HF. Brainstem auditory-evoked response in the rat: normative studies, with observations concerning the effects of ossicular disruption. Audiology 1990; 29:146-62.

4. Jones TA, Weidner WJ. Effects of temperature and elevated intracranial pressure on peripheral and brain stem auditory responses in dogs. Exp Neurol 1986;92:1-12.

5. Allen GW, Habibi M. The effect of increasing the cerebrospinal fluid pressure upon the cochlear microphonics. Laryngoscope 1962;72:423-34.

6. Allen GW, Dallos P, Sakamoto S, Homma T. Cochlear microphonic potential in cats. Arch Otolaryngol 1971;93:388-96.

7. Suzuki M. The effect of intravenous injection of lidocaine on the auditory system. Auris Nasus Larynx 1983;10:25-36.

8. Hughes DW, Yagi T. Lidocaine hydrochloride depression of cochlear microphonics and action potentials in the cat. Auris Nasus Larynx 1975;2:107-16.

9. Laurikainen E, Nuttall AL, Miller JM, Quirk WS, Virolainen E. Experimental basis for lidocaine therapy in cochlear disorders. Acta Otolaryngol (Stockh) 1992;112:800-9.

Ann Otol Rhinol Laryngol 106:1997

IMAGING CASE STUDY OF THE MONTH

IATROGENIC PSEUDOANEURYSM OF THE INTERNAL CAROTID ARTERY

KAREN S. CALDEMEYER, MD
PAUL D. RIGHI, MD
VINCENT P. MATHEWS, MD
INDIANAPOLIS, INDIANA

INTRODUCTION

A mass arising in the carotid space (poststyloid parapharyngeal space) can be neurogenic, vascular, or lymphatic in origin. The most frequent masses are schwannomas, paragangliomas, and lymphadenopathy.[1-3] Aneurysms of the extracranial internal carotid artery (ICA) are rare, but should also be considered in the differential diagnosis of carotid space lesions.[3] We report a case of an ICA pseudoaneurysm and present the interesting computed tomography (CT) and magnetic resonance imaging (MRI) appearance. This lesion presumably occurred as a result of an aspiration to rule out a peritonsillar abscess or as a result of the subsequent tonsillectomy. No ICA pseudoaneurysms have been previously reported in the English-language literature as a complication of these procedures.

CASE REPORT

A 24-year-old woman was referred to the otolaryngology service from an outside institution for evaluation of a densely calcified left neck mass discovered incidentally on facial radiographs obtained after the patient was hit in the jaw by her young son. Neck CT showed a 2-cm densely calcified left carotid space mass. There was no clear distinction between the mass and the adjacent ICA (Fig 1). Then MRI showed the mass directly adjacent to the ICA. The mass was hypointense on T1-weighted images and showed no contrast enhancement. The lesion was hyperintense on T2-weighted images despite the dense calcification (Fig 2). Magnetic resonance angiography did not definitely show an aneurysm. However, there was a stellate appearance of the ICA adjacent to the calcified lesion on the source images that was highly suspicious for a carotid origin of the calcified mass. Subsequent conventional angiography showed the lesion to be a mostly thrombosed pseudoaneurysm arising from the distal cervical ICA (Fig 3).

The patient had been treated at an outside institution for an episode of severe tonsillitis 3 years previously. Peritonsillar aspiration with a needle and syringe, without imaging guidance, was performed at that time to exclude a peritonsillar abscess. The aspirate reportedly did not yield pus or blood. Four weeks later, the patient underwent an uncomplicated tonsillectomy. Her past medical history was also significant for a positive purified protein derivative (PPD) skin test for which she

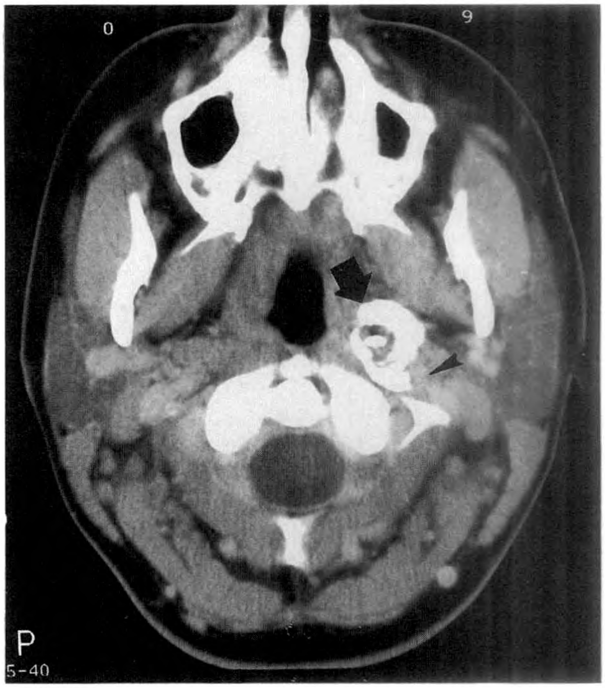

Fig 1. Contrast-enhanced computed tomography shows densely calcified lesion in left parapharyngeal space (arrow) that is not clearly distinct from adjacent internal carotid artery (arrowhead). There was no change in attenuation in lesion between noncontrasted (not shown) and contrasted studies.

From the Division of Neuroradiology, Department of Radiology (Caldemeyer, Mathews), and the Department of Otolaryngology (Righi), Indiana University School of Medicine, Indianapolis, Indiana.

CORRESPONDENCE — Karen S. Caldemeyer, MD, Indiana University School of Medicine, University Hospital, Rm 0279, 550 N University Blvd, Indianapolis, IN 46202-5253.

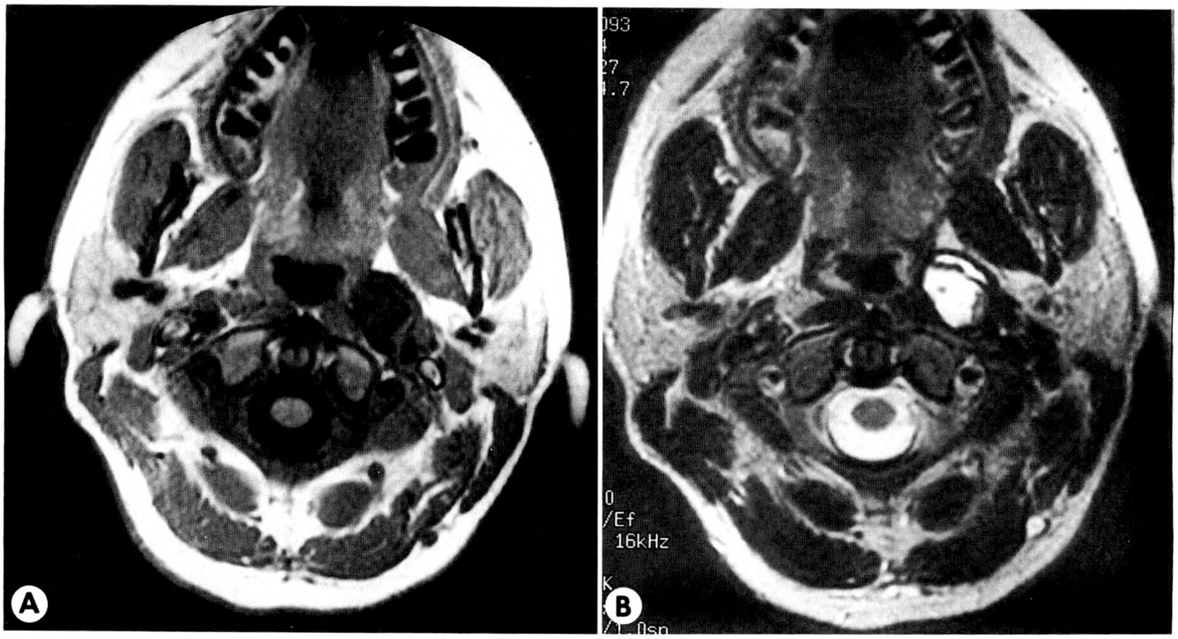

Fig 2. Magnetic resonance imaging. A) T1-weighted (700/11 [repetition time/echo time]) image shows hypointense lesion adjacent to internal carotid artery. B) On fast spin-echo T2-weighted (4,800/102) image, lesion is markedly hyperintense despite dense calcification seen on computed tomography.

had been treated with 6 months of isoniazid. Multiple chest radiographs were normal. The patient denied a history of significant trauma, intravenous drug abuse, history of malignancy, or personal or family history of neurogenic or vascular tumors. Findings of a comprehensive head and neck examination were unremarkable.

The clinical management of this rare problem was determined by multiple factors and involved input from departments of otolaryngology, neurosurgery, and vascular surgery. The patient was neurologically intact and had no evidence of ischemic symptoms due to embolization from the pseudoaneurysm. The patent lumen of the false aneurysm was very small and had a relatively smooth contour. The risk of aneurysm rupture was felt to be low due to the dense calcification. In addition, the location of the lesion near the skull base would require extensive operative exposure and place multiple cranial nerves at risk. In view of the low risk of aneurysm rupture or embolization, the patient was treated with systemic anticoagulation rather than surgery. She remains asymptomatic 1 year after diagnosis.

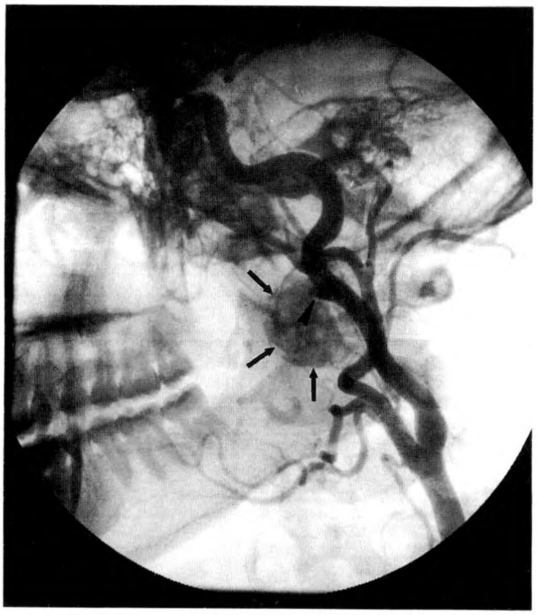

Fig 3. Nonsubtracted view from digital subtraction angiogram confirms that lesion is mostly thrombosed pseudoaneurysm. There is small residual patent lumen projecting from anteromedial aspect of internal carotid artery (arrowhead) into dense calcification (arrows).

DISCUSSION

A false aneurysm, or pseudoaneurysm, is a pulsating hematoma that occurs following injury to all layers of the arterial wall. The center of the hematoma liquefies and contains flowing blood that communicates with the arterial lumen, while the periphery of the hematoma clots, forming the wall of the aneurysm.[4] Pseudoaneurysms may occur due to blunt or penetrating trauma or infection.[4-7] Iatrogenic pseudoaneurysms have been reported after a variety of surgical procedures and may be caused by needle puncture for catheter placement and biopsy.[4,8,9] Nontraumatic extracranial carotid artery aneurysms are extremely rare. Weissman et al[3] reported two patients with carotid sheath masses that were found to be aneurysms at surgery.

Complications of pseudoaneurysms include rupture, local mass effect, embolization, and arteriovenous fistula.[3,4] Pseudoaneurysms may spontaneously thrombose.[9] Treatment of carotid pseudoaneurysms is aimed at maintaining parent vessel flow and preserving neurologic function. Therefore, surgical excision or endovascular thrombosis of the pseudoaneurysm is preferable. Parent vessel occlusion or ligation may be done when repair is not possible due to uncontrollable hemorrhage, if the lesion is in a surgically inaccessible site, or with coexistent infection. Small pseudoaneurysms may be managed by anticoagulation alone.[4-7]

Our patient most likely developed a pseudoaneurysm of the ICA due to inadvertent puncture and injury of the vessel during peritonsillar aspiration. The pseudoaneurysm was directly adjacent to the tonsillar fossa and corresponded to the likely track of needle puncture. Alternatively, the arterial wall could have been damaged during tonsillectomy. Although our patient is PPD-positive, and tuberculosis can cause aneurysms,[7] the patient showed no evidence of pulmonary or systemic tuberculosis at any time; hence, this is a very unlikely cause of the pseudoaneurysm. There was no history of significant blunt or penetrating neck trauma.

Aspiration of the tonsillar region is commonly performed to diagnose and treat a peritonsillar abscess. The procedure is usually performed under local anesthesia, and few serious complications have been reported. Haeggstrom et al[10] proposed that intraoral ultrasound may be useful in increasing the diagnostic accuracy and safety of peritonsillar aspiration. It allows visualization of the carotid artery and can potentially prevent unintended carotid puncture. It may be most practical in guiding peritonsillar aspiration for cases in which the presence of an abscess is uncertain according to clinical examination by an experienced otolaryngologist. To the best of our knowledge, a carotid pseudoaneurysm as a result of diagnostic needle puncture around the tonsil has not been reported in the English-language literature.

The appearance of pseudoaneurysms on CT and MRI depends on the patency of the lesion. On CT, patent aneurysms will appear as spherical, isodense or slightly hyperdense lesions that show intense enhancement after contrast. Partially thrombosed aneurysms may show enhancement of the patent lumen and outer rim of the aneurysm. Completely thrombosed aneurysms are usually hyperdense prior to contrast injection and do not change in attenuation after contrast. Calcification may occur in pseudoaneurysms, most commonly rim calcification along the wall of partially or completely thrombosed pseudoaneurysms. The appearance of pseudoaneurysms on MRI is variable. The patent lumen usually shows high-velocity signal loss on spin echo images. Turbulent flow and thrombosis may create a more heterogeneous appearance. Thrombosis will cause a laminated appearance, with heterogeneous degrees of signal intensity from thrombi of different ages.[3,11]

The differential diagnosis of carotid space masses is relatively limited. The most common lesions are schwannomas arising from cranial nerves IX, X, or XI or the sympathetic chain, paragangliomas, and lymphadenopathy.[1-3] Schwannomas are typically of soft tissue density on CT; calcification is rare. On MRI, they are typically of intermediate signal intensity on T1-weighted images and bright on T2-weighted images. Schwannomas show significant contrast enhancement. Since most schwannomas arise from the vagus or sympathetic chain, schwannomas are typically seen posterior to the carotid artery.[2] Carotid body tumor or vagal paraganglioma may present as a carotid space mass. Carotid body tumors splay the internal and external carotid arteries. Vagal paragangliomas typically arise between the ICA and the jugular vein. On CT, paragangliomas are noncalcified soft tissue–density lesions and show strong contrast enhancement. On MRI, paragangliomas may have a "salt-and-pepper" appearance due to tumor vascularity causing flow voids.[2] Lymphadenopathy can be due to metastatic, lymphomatous, or inflammatory disease. Calcification in lymph nodes may be seen in thyroid and mucin-producing carcinomas, tuberculosis, sarcoidosis, silicosis, scleroderma, amyloidosis, sinus histiocytosis, and previously irradiated metastatic or lymphomatous nodes.[1] Other carotid space masses include ectatic or thrombosed carotid artery, asymmetrically enlarged or thrombosed internal jugular vein, and branchial cleft cyst.[2] Minor salivary gland malignancies may arise from the parapharyngeal space adjacent to the ICA and may occasionally have calcification.[12]

In summary, aneurysm (or pseudoaneurysm) of the cervical ICA is a very rare entity that has a variety of radiologic and clinical manifestations. Aneurysm should always be considered in the differential diagnosis of carotid space lesions, particularly when peripheral or rim calcification is present.

REFERENCES

1. Som PM. Lymph nodes. In: Som PM, Curtin HD, eds. Head and neck imaging. 3rd ed. St Louis, Mo: Mosby–Year Book, 1996:784-92.

2. Weissman JL. Nonnodal masses of the neck. In: Som PM, Curtin HD, eds. Head and neck imaging. 3rd ed. St Louis, Mo: Mosby–Year Book, 1996:806-14.

3. Weissman JL, Johnson JT, Snyderman CH, Steed DL. Thrombosed aneurysm of the cervical carotid artery: avoiding a retrospective diagnosis. Radiology 1994;190:869-71.

4. Batten TF, Heeneman H. Traumatic pseudoaneurysm of floor of mouth treated with selective embolization: a case report. J Otolaryngol 1994;23:423-5.

5. Cogbill TH, Moore EE, Meissner M, et al. The spectrum of blunt injury to the carotid artery: a multicenter perspective. J Trauma 1994;37:473-9.

6. Ramadan F, Rutledge R, Oller D, Howell P, Baker C, Keagy B. Carotid artery trauma: a review of contemporary trauma center experiences. J Vasc Surg 1995;21:46-55.

7. Cross DT, Moran CJ, Brown AP, et al. Endovascular treatment of epistaxis in a patient with tuberculosis and a giant petrous carotid pseudoaneurysm. AJNR Am J Neuroradiol 1995; 16:1084-6.

8. Sahrakar K, Boggan JE, Salamat MS. Traumatic aneurysm: a complication of stereotactic brain biopsy: case report. Neurosurgery 1995;36:842-6.

9. Kent KC, McArdle CR, Kennedy B, Baim DS, Anninos E, Skillman JJ. A prospective study of the clinical outcome of femoral pseudoaneurysms and arteriovenous fistulas induced by arterial puncture. J Vasc Surg 1993;17:125-31.

10. Haeggstrom A, Gustafsson O, Engquist S, Engstrom CF. Intraoral ultrasonography in the diagnosis of peritonsillar abscess. Otolaryngol Head Neck Surg 1993;108:243-7.

11. Osborn AG. Intracranial aneurysms. In: Patterson AS, ed. Diagnostic neuroradiology. St Louis, Mo: Mosby–Year Book, 1994:262-9.

12. Som PM, Brandwein M. Salivary glands. In: Som PM, Curtin HD, eds. Head and neck imaging. 3rd ed. St Louis, Mo: Mosby–Year Book, 1996:879-82.

≈

SURGICAL COURSE ON OTOPLASTY

A Surgical Course on Otoplasty will be held in English in Ulm, Germany, March 13-14, 1998. For more information, contact Prof Dr G. Rettinger, Prittwitzstr 43, D-89075 Ulm, Germany; telephone +731-502-7501; fax +49-731-502-6703.

≈

TWENTIETH ANNUAL MEETING OF THE BÁRÁNY SOCIETY

The Twentieth Annual Meeting of the Bárány Society will be held in Würzburg, Germany, September 20-23, 1998. For more information, contact the Local Organizing Committee, Institute of the 4-G-F, Kurhausstrasse 12, D 97688 Bad Kissingen, Germany; telephone 0049/971-64832; fax 0049/ 971-68637.

Ann Otol Rhinol Laryngol 106:1997

IMAGING CASE STUDY OF THE MONTH

IMAGING DIAGNOSIS OF BUCKLED INNOMINATE ARTERY

TOSHISHIGE KIDO, MD MASAHIRO TAKAHASHI, MD

UBE, JAPAN

INTRODUCTION

Buckling or kinking of the innominate artery is a way of describing elongation, tortuosity, and dilatation of this vessel. Although a buckled innominate artery is seldom encountered in routine clinical examinations, it is of particular radiologic importance, because its radiologic appearance mimics an aneurysm or tumor of the apex of the right lung or superior mediastinum.[1-3] A buckled innominate artery is often manifested clinically as a pulsating mass in the right supraclavicular fossa that may suggest an innominate or carotid artery aneurysm.[2,3] It is possible to avoid unnecessary surgical intervention in patients with a buckled innominate artery by correctly identifying it by imaging studies such as ultrasound, computed tomography (CT), or angiography, because a buckled innominate artery is innocuous and has no serious complications.[1-3] In this report we present the imaging studies that incidentally demonstrated a buckled innominate artery in a patient with a diffuse goiter.

CASE REPORT

A 66-year-old woman was seen in our clinic because of an abnormal sensation in her throat and a nonenlarging anterior cervical mass. She had been on medication for hypertension and cardiomegaly for several years. Physical examination revealed moderate obesity and normal vital signs. A diffuse goiter with an elastic, soft consistency and a pulsating swelling were noted in the anterior part of the neck and the right supraclavicular fossa, respectively. Findings on examination of the pharynx and larynx were unremarkable. A conventional chest radiograph showed left ventricular enlargement, a dilated aorta, and slight widening of the right superior mediastinal shadow. The trachea was normal. Routine laboratory findings were normal, and a serologic test for syphilis was negative. The goiter was thought to represent chronic thyroiditis on the basis of thyroid function tests, thyroid scintigraphy, and fine needle aspiration biopsy guided by ultrasound. The initial diagnosis of the pulsating lesion was a suspected aneurysm of the carotid artery or innominate artery associated with the goiter.

Ultrasound scanning revealed a tortuous, dilated vascular shadow with pulsations on the Doppler view that appeared to coincide with the pulsation of the swelling in the right supraclavicular fossa (Fig 1). Contrast-enhanced CT showed a great vessel shadow that seemed to be located between the enlarged lobes of the thyroid gland in the lower part of the neck (Fig 2A). The shadow of the proximal portion of the innominate artery was seen in front of the trachea, and the shadow of its distal portion in the paratracheal space in the upper thorax (Fig 2B).

Accordingly, we formed a strong suspicion of a buckled innominate artery incidentally found in a

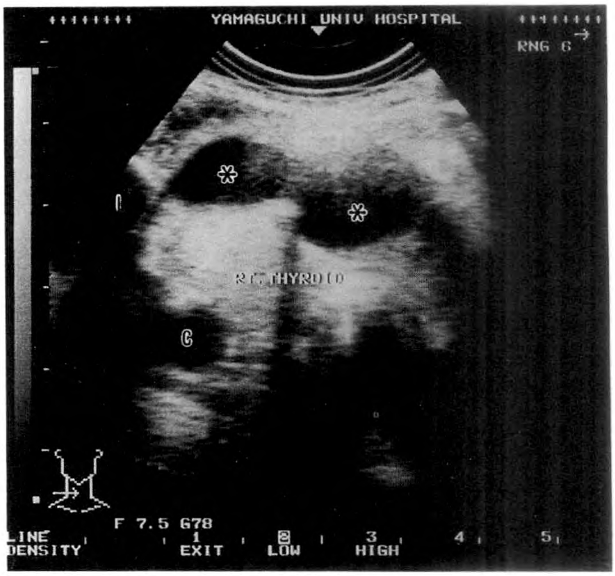

Fig 1. Ultrasound scan of right anterior neck. Transverse scan shows tortuous dilated vascular shadow (asterisks). This shadow showed pulsation on Doppler view and seemed to coincide with pulsating swelling in right supraclavicular fossa. I — internal jugular vein, C — common carotid artery, RT. THYROID — right thyroid gland.

From the Department of Otolaryngology, Yamaguchi University School of Medicine, Ube, Japan.

CORRESPONDENCE — Toshishige Kido, MD, Dept of Otolaryngology, Yamaguchi University School of Medicine, Yamaguchi, Ube 755, Japan.

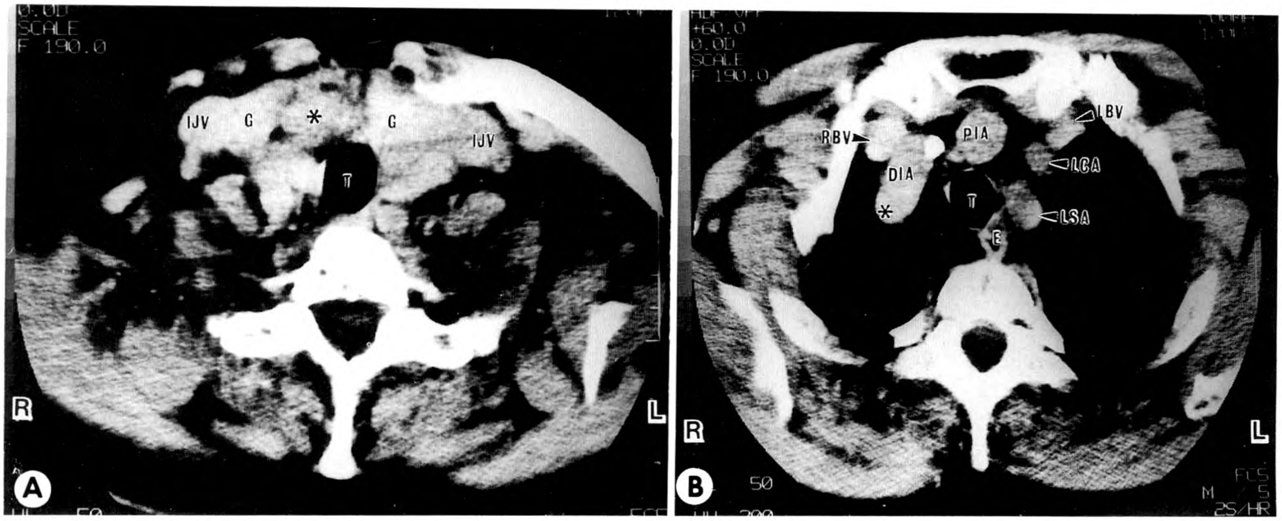

Fig 2. Contrast-enhanced computed tomograms. Enhancement effect was somewhat poor, because patient vomited while being injected with contrast medium, and injection was discontinued. A) Lower level of neck. Shadow of great vessel (asterisk) is seen between lobes of goitrous thyroid gland (G). IJV — internal jugular vein, T — trachea. B) Upper level of thorax. Proximal portion of dilated innominate artery (PIA) is seen in front of trachea (T), following shadow indicated by asterisk in A. Distal portion of dilated innominate artery (DIA) is seen in paratracheal space. Asterisk indicates point at which right common carotid and subclavian arteries bifurcate. RBV — right brachiocephalic vein, LBV — left brachiocephalic vein, LCA — left common carotid artery, LSA — left subclavian artery, E — esophagus.

patient with a diffuse goiter. Since the masses in question were determined to be innocuous, the patient was discharged and scheduled for regular follow-up visits.

DISCUSSION

Elongation, tortuosity, and dilatation of the innominate artery are usually associated with arteriosclerotic and hypertensive lesions of the aortic arch.[1-3] Hypertension produces unfolding and dilatation of the aorta; and arteriosclerosis, which is usually also present, causes simultaneous lengthening.[4,5] On the basis of these findings, Honig et al[1,2] reported that the aortic arch becomes elevated, and that tortuosity of the innominate artery, and secondarily of the right common carotid and subclavian arteries, may result. It should also be pointed out that dilatation and tortuosity of the innominate artery and its branches may occur in syphilitic aortitis.[1,2]

Schneider and Felson[3] reviewed the approximately 125 cases of carotid or innominate artery buckling reported in the literature and found the following interesting facts.

1. Almost all of the patients were over 40 years of age. The few younger patients, particularly those under 30, had coarctation of the aorta.
2. The great majority of patients were women.
3. Most patients were obese and had clinical evidence of arteriosclerosis, hypertension, or both.
4. Cardiomegaly was a frequent finding and was usually due to hypertension, although sometimes it was attributable to aortic insufficiency.
5. A small, pulsating mass was often palpable in the right supraclavicular fossa.
6. The innominate artery was affected far less frequently than the carotid artery.

Buck and Siddiqui[6] reported using ultrasound to investigate the cause of a "cold" nodule on thyroid scintigraphy and found that the thyroid was compressed by a tortuous carotid artery.

Computed tomography can also visualize the great vessels in the upper thorax in transverse section. Tamaki et al[7] reported that CT at the level of a buckled innominate artery revealed a large, unusual "snowman"-shaped mass extending from the right anterior chest wall posteriorly into the lung. In our case, there was strong suspicion of a buckled innominate artery based on the ultrasound and CT findings before it was definitively diagnosed by angiography, which might be avoided in future.

It is common knowledge that the definitive diagnosis of a buckled innominate artery can be made by angiocardiography.[1,2] Although angiography is time-consuming and involves a small risk, it establishes the diagnosis in cases of suspected superior mediastinal lesions.

In conclusion, a buckled innominate artery should be considered in patients with hypertension and arteriosclerotic heart disease who have a pulsating mass in the right supraclavicular fossa. Ultimately, in our patient it was possible to avert unnecessary surgical exploration by performing the imaging examinations, and her prognosis is good with appropriate medication for the abnormal sensation in the throat. Ultrasound and CT are very helpful in detecting buckling of the innominate artery. Angiography may be necessary in selected cases.

REFERENCES

1. Honig EI, Steinberg I, Dotter CT. Innominate artery: angiocardiographic study. Radiology 1952;58:80-7.
2. Honig EI, Dubilier W Jr, Steinberg I. Significance of the buckled innominate artery. Ann Intern Med 1953;39:74-80.
3. Schneider HJ, Felson B. Buckling of the innominate artery simulating aneurysm and tumor. Am J Roentgenol 1961;85:1106-10.
4. Dotter CT, Steinberg I. The angiocardiographic measurement of the normal great vessels. Radiology 1949;52:353-8.
5. Parkinson J, Bedford DE, Almond S. The kinked carotid artery that simulates aneurysm. Br Heart J 1939;1:345-61.
6. Buck RT, Siddiqui AR. Thyroid abnormality secondary to tortuous carotid artery. Eur J Nucl Med 1986;12:51-2.
7. Tamaki M, Tanabe M, Kamiuchi H, Muromoto H, Kurata M. Buckling of the distal innominate artery simulating a nodular lung mass. Chest 1983;83:829-30.

Ann Otol Rhinol Laryngol 106:1997

IMAGING CASE STUDY OF THE MONTH

ETHMOID AND SPHENOID MUCOCELES VIEWED BY HELICAL SCANNING COMPUTED TOMOGRAPHY WITH SAGITTAL RECONSTRUCTION

TAKEO FUSE, MD
HIROO INAMURA, MD
MASARU AOYAGI, MD
MORIO NAGAHATA, MD
TAKAAKI HOSOYA, MD
YAMAGATA, JAPAN

INTRODUCTION

Computed tomography (CT) has been reported to provide much information to surgeons who perform ear and sinus surgery.[1-5] For the presurgical evaluation of nasal surgery, axial and direct coronal CT scans have been used as the standard scan. Recently, endoscopic sinus surgery (ESS) has become a common procedure for nasal surgery, and the lateral sinus images are most helpful in determining the distances between anatomic landmarks in preparation for ESS. Magnetic resonance imaging (MRI) affords sagittal images and has excellent soft tissue contrast, but the bony structures cannot be visualized. In CT, the bone density can be easily visualized, and this provides helpful presurgical information, but it is difficult to obtain lateral images by this means.

We present the sagittal reconstructed CT sinus scans of two patients with ethmoid and sphenoid mucoceles. The axial, coronal, and sagittal CT images are compared, and the advantages of the sagittal CT sinus images for ESS are discussed.

IMAGING TECHNIQUE

Helical scanning was performed with a High-Speed Advantage (General Electric Medical Systems, Milwaukee, Wis) CT scanner on 140-kV and 220-mA settings, with a 25-cm field of view without contrast medium. Three-millimeter collimation was used with 3-mm/s table speed, and scanning was continued for 30 seconds, yielding a total coverage of 9 cm. This allowed complete visualization of the area from the hard palate to the frontal skull base. Axial images were retrospectively reconstructed with a 180° interpolation algorithm, 1.5-mm pitch, and a 16.7-cm display field of view (magnification factor 1.5), producing 59 images that centered on the paranasal sinuses. Sagittal and coronal images were then reconstructed from these 59 axial images by the multiplanar reconstruction (MPR) method. The patient was in the supine position; neck hyperextension, which is necessary in direct coronal CT scanning, was not necessary with this method.

CASE REPORTS

Case 1. A 57-year-old man having a 1-month history of left eye blurriness consulted an ophthalmologist, and an eye CT scan revealed a left ethmoid mucocele. He was referred to our hospital and admitted to undergo ESS. Figure 1 shows the preoperative axial, coronal, and sagittal CT sinus images and the operative findings. The axial and coronal CT images depicted the ethmoid mucocele, but the relationship between the frontal sinus and the anterior ethmoid was unclear. On the sagittal CT images, a clear passage via the frontonasal duct and the wall of the mucocele bordered by the posterior ethmoid were clearly detected. On the ESS findings, the wide ostium of the frontal sinus was seen after resection of the anterior wall of the ethmoid mucocele, and the frontal sinus was filled with mucopurulent fluid.

Case 2. A 56-year-old woman who presented with a 3-month history of right eye blurriness consulted a neurosurgeon, and the brain CT scan obtained at a local clinic revealed a sphenoid mucocele. She was referred to our hospital. Bilateral nasal polyps and right exophthalmos were detected, and she was admitted for ESS. The coronal, axial, and sagittal CT sinus images revealed an ethmoid mucocele and a sphenoid mucocele (Fig 2). Compared with the axial and coronal CT

From the Departments of Otorhinolaryngology (Fuse, Inamura, Aoyagi) and Radiology (Nagahata, Hosoya), Yamagata University School of Medicine, Yamagata, Japan.

CORRESPONDENCE — Takeo Fuse, MD, Dept of Otorhinolaryngology, Yamagata University School of Medicine, 2-2-2 Iida Nishi, Yamagata shi, Yamagata, Japan.

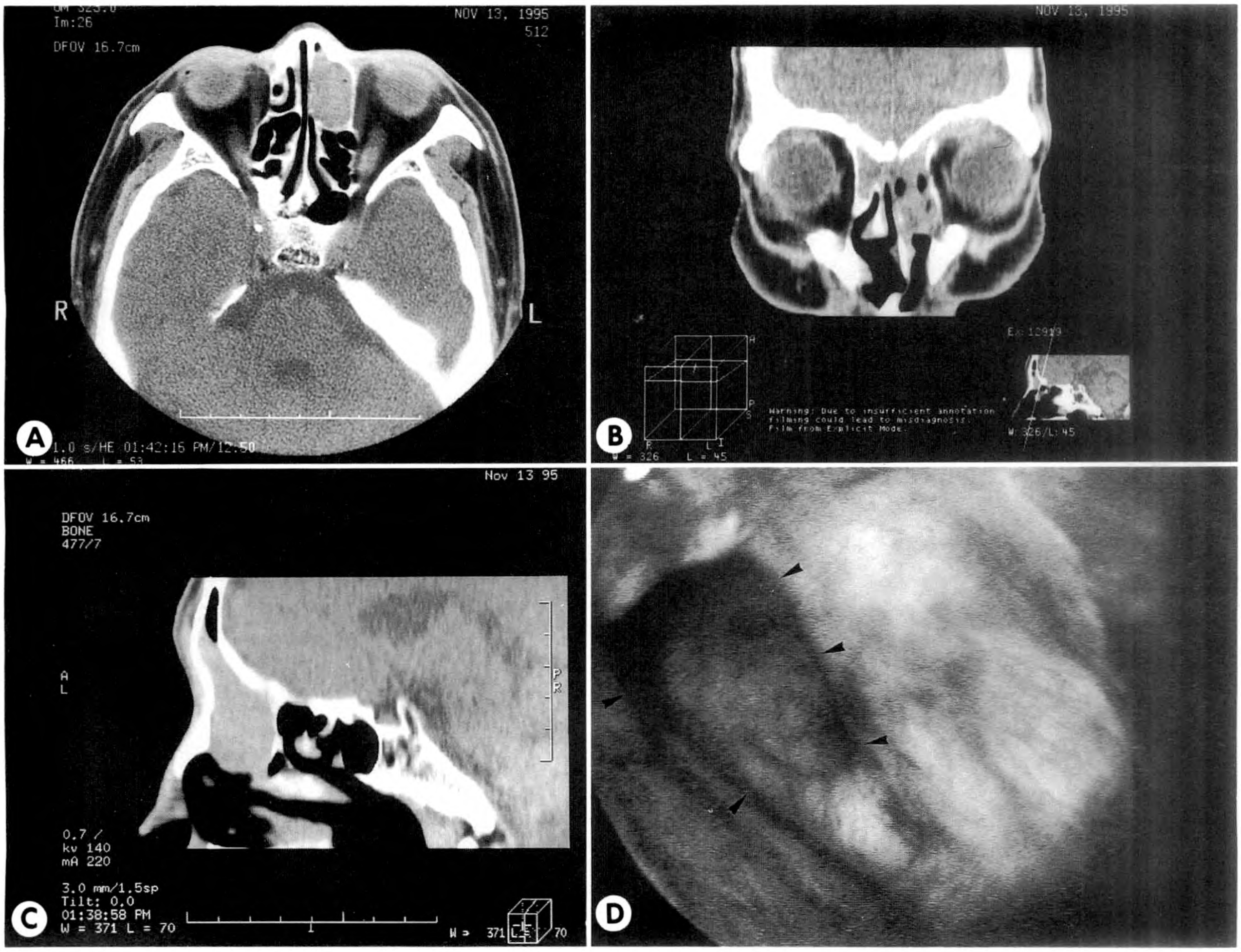

Fig 1. (Case 1) A) Preoperative axial computed tomography (CT) image. B) Coronal CT image. Mucocele of anterior ethmoid is detected. C) Reconstructed sagittal CT image. Beak of frontal sinus is eroded, and passage to frontal sinus is wide. D) Operative findings in endoscopic sinus surgery. Ostium of frontal sinus is widely open (arrowheads).

images, the sagittal CT images revealed more clearly the distribution of the intermediate wall of the two mucoceles that would need to be resected at surgery. At surgery, both mucoceles were seen to be filled with purulent fluid, and the part of the mucocele wall in contact with the nasal cavity was resected for drainage.

DISCUSSION

The paranasal sinus anatomy is complex and shows great variation from patient to patient.[1,2] In a sinus mucocele, important anatomic landmarks are often destroyed by the wall of the mucocele, but detailed information on the anatomic structure is nevertheless needed for presurgical evaluation and planning. On axial and coronal CT scan images, the margin of the wall of the mucocele adjacent to the skull base cannot be imaged on one slice. Useful information is provided by the images when the direction of the CT section coincides with that of the intended surgical procedure. In a previous report,[3] the importance of sagittal CT images was proposed for ESS, but the clinical usefulness was not discussed because of the poor capacity of the conventional sagittal reconstruction scanning equipment.

With the recent development of slip-ring CT technology, helical scanning has been made possible. From the continuous raw data collected with helical scanning, multiple overlapping axial sections at arbitrary intervals can be reconstructed. We use 3-mm X-ray collimation and obtain 3-mm-thick sections reconstructed every 1.5 mm. Because of the reduction of partial volume artifacts, multiple overlapping reconstructed sections can enhance the anatomic resolution within the area imaged. The scanning time is only 30 seconds, and the calculation time is about 15 minutes for the reconstruction of 59 three-mm-thick axial images with 50% of overlap each. Sagittal and coronal reconstruction with the MPR method is completed within seconds. Views in any direction (coronal, sagittal) can be acquired from scanning in a single direction (axial scanning). The reconstructed images can be reviewed as virtual or perspective images. Magnetic resonance imaging has a similar advantage, but the bone is not visualized. The

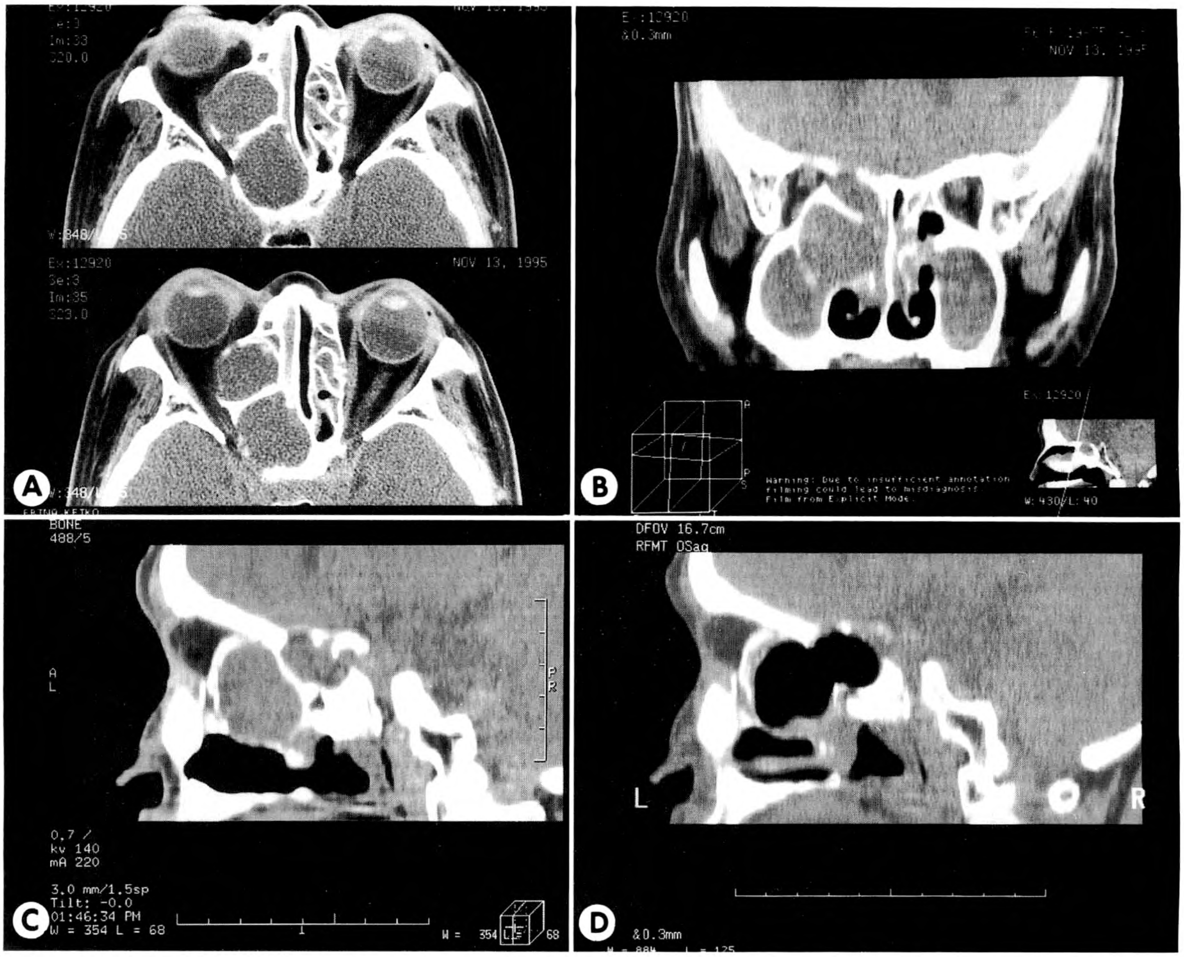

Fig 2. (Case 2) A) Preoperative axial CT images. Mucoceles are seen located in posterior ethmoid sinus and sphenoid sinus. B) Coronal CT images. C) Reconstructed sagittal CT image. Both walls of mucocele are clearly imaged in single slice. D) Reconstructed sagittal CT image (postoperation). Intermediate wall of mucocele has been completely resected, and both sinuses (posterior ethmoid and sphenoid) are well pneumatized.

cost of CT is about 2.5 times less than that of MRI.

The importance of the lateral plane radiograph has been emphasized for ESS, but the real length and angle of the anatomic landmarks are reported to differ from those depicted on the images.[6] On sagittal CT images, the distance and angle for certain anatomic landmarks can be measured directly and more accurately. During the ESS procedure, this anatomic information is of great assistance to the surgeon, who can observe the surgical view on the closed-circuit video monitor in two dimensions. Recognition of anatomic structures has led to the proper performance of the surgical procedure to avoid injury to adjacent normal structures. We think that helical scanning CT is well suited for evaluation of the paranasal sinuses and might be used as a routine examination in the preoperative assessment.

REFERENCES

1. Laine F, Smoker WR. The ostiomeatal unit and endoscopic surgery: anatomy, variations, and imaging findings in inflammatory diseases. AJR Am J Roentgenol 1992;159:849-57.

2. Bolger WE, Butzin CA, Parsons DS. Paranasal sinus bony anatomic variations and mucosal abnormalities: CT analysis for endoscopic sinus surgery. Laryngoscope 1991;101:56-64.

3. Zinreich SJ, Kennedy DW, Rosenbaum AE, Gayer BW, Kumar AJ, Stammberger H. Paranasal sinuses: CT imaging requirements for endoscopic surgery. Radiology 1987;163:769-75.

4. Fuse T, Aoyagi M, Koike Y, Sugai Y. Diagnosis of the ossicular chain in the middle ear by high-resolution CT. ORL J Otorhinolaryngol Relat Spec 1992;54:251-4.

5. Fuse T, Tada Y, Aoyagi M, Sugai Y. CT detection of facial canal dehiscence and semicircular canal fistula: comparison with surgical findings. J Comput Assist Tomogr 1996;20:221-4.

6. Onerci M, Ariyurek M, Tacal T, Aydingoz U. Shortcomings of lateral sinus radiography in the preoperative determination of the extent of endonasal endoscopic sinus surgery. Laryngoscope 1995;105:843-6.

ANNALS OF OTOLOGY, RHINOLOGY & LARYNGOLOGY

— Founded in 1892 —

Volume 106
January-December 1997
Issues 1-12, Supplements 168-171

Published by

ANNALS PUBLISHING COMPANY
4507 LACLEDE AVENUE
ST LOUIS, MISSOURI 63108

Copyright© 1997, Annals Publishing Company

ANNUAL INDEX

AUTHORS

Abe S, 1063
Achilli V, 370
Acquadro MA, 305; 358 (letter to editor)
Aerts R, 329
Ağrali N, 471
Akbulut UG, 471
Akyol MU, 787
Alavi S, 589
Albers FWJ, 329
Alexander AE Jr, 1020
Ali MK, 952
Al-Khader AA, 391
Almadori G, 522
Almeida VF, 823
Alper CM, 422
Al-Shaikh AM, 391
Al Shareef Z, 649
Altavilla G, 1024
Amin MR, 887
Amirali A, 297
Andrews JC, 838
Andrews RJ, 261
Ankerstjerne JKP, 182
Anniko M, 414
Annino DJ, 563
Aoyagi M, 1100
Ar A, 314
Araki M, 27
Araújo MF, 823
Aust MR, 943
Avan P, 1052
Aviv JE, 87
Aydogan B, 182
Ayuso A, 863

Backer CL, 914
Badr-El-Dine M, 139, 934
Bakon M, 75
Balaban C, 182, 662
Balkany T, 608
Ball SS, 633
Barbet JP, 357 (letter to editor)
Baredes S, 705
Barnes DE, 519
Barnes L, 437
Batsakis JG, 170
Bedrin L, 435
Beizai P, 594
Benayam A, 649
Ben-David J, 859
Bendet E, 75
Benjamin B, 770
Berke GS, 261, 594
Berkowitz RG, 167, 714, 897
Bezerra RL, 823
Biacabe B, 1052
Blaugrund SM, 544
Bless DM, 1012
Blinder G, 252
Bloch I, 445
Blondeel PN, 175
Böhmer A, 61
Bollen BA, 869
Bonfils P, 1052
Bongers V, 432
Boss JH, 226
Boucherat M, 854
Bouckaert S, 329
Bowen B, 608
Brasnu D, 159, 291, 364
Brasseux CO, 830
Brook I, 751
Brown K, suppl 168:59
Brown SDM, suppl 168:59
Bunting GW, 533
Burgess R, 123
Burkey BB, 271
Butler-Browne GS, 357 (letter to editor)
Bykhovskaya Y, 320

Cable J, suppl 168:59
Cadoni G, 522
Calcaterra TC, 261
Caldarelli DD, 445
Caldemeyer KS, 1093
Canalis RF, 589
Carbone A, 437
Cardinaal RM, 432
Carenfelt C, 359
Carlborg BIR, 495
Cass SP, 182
Castellanos PF, 451
Catalano P, 244
Çekiç A, 787
Çelikkanat S, 787
Cernea CR, 927
Chaljub G, 976
Chalmers J, 897
Chang S-Y, 783
Chapelin C, 854
Chapnik JS, suppl 171
Charous SJ, 271
Chawla P, 445
Chen J, 279
Chen JC, 240
Chen N, 552
Chen W-X, 326
Cheney ML, 733
Chevalier D, 364
Chiba T, 599
Chong VFH, 979
Chu P-Y, 783
Clerico DM, 799
Close LG, 87
Cohen AF, 640
Cohen NL, 657
Cole P, suppl 171
Conley SF, 310
Coon JS, 445
Corio RL, 399
Coste A, 854
Costen JB, 805 (*Annals* Classic)
Cotanche DA, suppl 168:9
Cotton RT, 891
Crawford MR, 721
Cremers CWRJ, 575
Cui P-C, 326
Cummings CW, 399
Cunningham MJ, 163
Curtin HD, 163
Czaja JM, 909

Dahm JD, 902
Dais CGD, 633
Dallos P, suppl 168:16
Danckwardt-Lillieström N, 190
Danguy A, 1043
da Silva M, 129
Davamony D, 604
David L, 1020
Dayan SH, 914
Decaestecker C, 1043
DeGirolami U, 357 (letter to editor)
de Klerk JMH, 432
Delaere PR, 175
Delaey B, 15
DelGaudio JM, 1076
Dellsperger KC, 869
Del Ninno M, 522
De Rossi G, 522
Devaney KO, 79, 254, 437, 526, 801, 878, 983
Diamond B, 87
Dobie RA, 693
Doglioni C, 1024
Dohse A, 310
Doyle WJ, 422
Driscoll BP, 976
Duinslaeger L, 15
Dunham ME, 914

Eckstein R, 770
Egusa K, 69
Elahi MM, 733
Elidan J, 873
El-Naggar AK, 170
Erminy M, 1052
Erpek G, 875
Esclamado RM, 237
Escudier E, 854
Ézsiás A, 135

Farmer JC Jr, 495
Fazekas-May MA, 1020
Fee WE Jr, 117
Feenstra L, 175
Ferlito A, 79, 254, 348, 437, 526, 611, 716, 801, 878, 983, 1024
Feroah TR, 310
Fetter M, 61
Fink AM, 167
Fischel-Ghodsian N, 320
Fitzgerald DC, 830
Fleming J, suppl 168:59
Flint PW, 399
Foote RL, 943
Ford CN, 956, 1012

Foyt D, 568
Fradis M, 226, 478, 859
Frankel SS, 611
Franko DL, 286
Friberg U, 190
Friedman EM, 199
Friedman M, 445
Friedman RA, 320
Fuchs C, 37
Fujimori I, 571
Fujita S, 33, 310
Fujiwara Y, 380
Fukushima K, 123
Furman JM, 182
Fuse T, 1100
Fyfe B, 244

Gagne A, 286
Ganbo T, 662
Gardner GM, 151
Gardner PA, 710
Garretsen AJTM, 575
Gates GA, suppl 168(ed); 729
Gatt N, 252
Gerber ME, 891
Gerken GM, 139, 934
Getson P, 830
Gibson F, suppl 168:59
Glock MS, suppl 169
Gluckman JL, 909
Goding GS Jr, 920
Goffinet DR, 117
Goldman SA, 461
Gomori M, 873
Goode RL, 117
Goto R, 571
Govaerts P, 15
Grabo DJ Jr, 799
Graham RI, 129
Gray P, 445
Grénman R, 22
Guelinckx PJ, 175

Haginomori S-I, 27
Hagiwara H, 338
Hague K, 244
Halmagyi GM, 129
Hans S, 291
Hanson DG, 279
Hara A, 343
Har-El G, 301, 965
Harell M, 314
Harley EH, 714
Harris JP, 1070
Harris JR, 624
Harris NJ, 357 (letter to editor)
Hartnick CJ, 640
Hartog B, 759
Harvey D, suppl 168:59
Hassid S, 1043
Haughey BH, 506
Heisey DM, 956, 1012
Hejtmancik JF, 123
Hellström S, 513
Hemlin C, 359
Hengesteg A, 552
Hergils L, 743
Hermans C, 1043
Hermans R, 175
Hiller N, 252
Hillman RE, 533
Hirano M, 44, 490
Hirose H, 41
Hisamatsu K-I, 571
Ho WK, 779
Hoffman HT, 869
Hoffman LF, 838
Hokanson JA, 869
Holinger LD, 914, 1002
Hombergen GCJH, 653
Hong WP, 101
Hordijk G-J, 759
Hosoya T, 1100
Howard BK, 248
Hug GA, 210
Hunter BC, 983
Hunter DA, 506
Huraib SO, 391
Huygen PLM, 575
Hwang EG, 688

Ibekwe AO, 649
Ikui A, 33, 583
Imamura M, 674, 746
Imamura S, 674, 746
Inagi K, 956, 1012
Inamura H, 1100
Inwards CY, 94
Isaacson G, 887
Ishida T, 338
Ito Z, 343
Iurato S, 79
Iwamoto Y, 338

Jacobson GP, 210
Jacobson I, 770
Jeon SY, 688
Jerger J, suppl 168:23
Jiang JJ, 279
Johnson JT, 869
Joseph MP, 305
Jung TTK, 604

Kacker A, 544
Kaga K, 971, 1087
Kakinoki Y, 483, 848
Kakitsuba N, 380
Kakoi H, 414
Kallinen J, 22
Kam Z, 859
Kanai R, 380
Kantu M, 301
Kantu S, 965
Kapur TR, 767
Karavus A, 471
Kashima HK, 556
Kass ES, 109
Kato A, 848
Kaufman RS, 5 (*Annals* Classic)
Kawakami M, 27
Kaye GM, 705
Khan A, 739
Kido T, 1097
Kikushima K, 571
Kim HY, 101
Kim JP, 688
Kim K-M, 101
Kim Y-H, 101
Kim Y-M, 594
King JM, 753
Kinnefors A, 190
Kirchner JA, 700
Kirk KI, suppl 168:35
Kiss R, 1043
Kitamura K, 338, 643
Kizilay A, 875
Kobayashi T, 599
Koç C, 787
Kojima H, 544
Konrádsson KS, 495
Kosko JR, 790
Koufman JA, suppl 169
Koyama S, 838
Kreiman J, 261
Kronenberg J, 75, 435
Kumazawa H, 795
Kurokawa H, 795
Kurosaki Y, 343
Kusakari J, 343
Kvaerner KJ, 624
Kwong D, 779

Lacau St Guily J, 357 (letter to editor)
Laccourreye H, 291, 364
Laccourreye L, 159
Laccourreye O, 159, 291, 364
Lai JP, 680
Lai M-T, 69
Laippala P, 22
Lam LK, 779
Landais P, 1052
Lang S, 669
Laszig R, 884 (letter to editor)
Laurikainen E, 22
Lawrence V, 693
Leach JL, 248
Lee CH, 215
Lee EJ, 589
Lee MS, 215
Lee SY, 240
Lee WC, 767
Lerner PK, 560
Levy D, 314
Lewis JE, 94, 943
Li J, 838
Li KK, 163
Lim JW, 560
Linder TE, 619
Linthicum FH, 385, 466
Lippert BM, 1036
Little JP, suppl 169
Liu XZ, 220
Long SA, 604
Lough R, 297
Loughlin CJ, suppl 169
Lucas JG, 519
Lucente FE, 301
Luis M, 863
Luntz M, 314, 608
Lyon MJ, 145, 753
Lyons GD, 1020

Mack B, 669

Mackinnon SE, 506
MacMillan C, 437
Magnus P, 624
Magnuson B, 743
Mahony M, suppl 168:59
Maier W, 478
Makimoto K, 27
Manning MB, 886 (book review)
Mansuri NA, 391
Marcus DC, 599
Marder H-P, 619
Marietta J, 123
Marklund SL, 513
Martin JH, 87
Masterton RB, suppl 168:31
Masuda Y, 69
Matas M, 252
Mathews VP, 1093
Matos C, 544
Matthews BL, suppl 169
Mattsson C, 513
Mavroudis C, 914
Mazzoni A, 370
Mburu P, suppl 168:59
McCabe BF, 2 (preface to obituary), 79, 885 (editor's reply to letter)
McCaffrey TV, 230
McGuirt WF Jr, suppl 169
McKenna MJ, 733
Meara JG, 163
Medina dos Santos LR, 927
Megerian CA, 733, 739
Meland NB, 943
Mens LH, 653
Merchant SN, 49
Messias CI, 823
Meyerhoff WL, 139, 934
Meza MP, 461
Michael LA, 820
Millepied M-C, 854
Miller MR, 385
Milroy CM, 79, 801
Min Y-G, 215
Misselevich I, 226
Miyamoto RT, suppl 168:35
Montgomery SK, suppl 170
Montgomery WW, 109; 358 (letter to editor); suppl 170
Moore JK, 385
Moore KC, 123
Moungthong G, 1002
Mover-Lev H, 314
Munzinger J, 619
Murai K, 408, 643
Murai S, 643
Murakami Y, 571, 674, 746
Murofushi T, 129

Nadol JB Jr, 2 (obituary)
Naficy S, 237
Nagahata M, 1100
Nakai Y, 483, 848
Nakajima S, 503
Nakamura A, 795
Nakao Y, 503
Nam BH, 1082
Nanney LB, 271
Nascimento AG, 943
Nasri S, 594
Naudo P, 291
Nelis HJ, 329
Nerlich A, 669
Netterville JL, 271
Newman B, 461
Newman CW, 210
Newman JP, 117
Newton VE, 220
Ni L, 123
Niimi S, 41
Niparko JK, 385
Nishizawa M, 338
Nozawa I, 571, 674, 746
Nuss DW, 1020

Ofer A, 435
Offeciers E, 15
Oh SH, 215
Ohashi Y, 483, 848
Ohinata Y, 27
Ohmichi T, 69
Ohno Y, 483, 848
Ohta Y, 41
Ohyama K, 599
Okamoto H, 483
Olds MJ, 145
Oliveira CA, 823
Olofsson J, 716
Olopade CO, 474
Olsen KD, 94, 943
Omori K, 544
Oostendorp TF, 653
Ottaviani F, 522
Otto RA, 693
Ouvrier RA, 129
Özdem C, 787

Paltieli Y, 859
Paludetti G, 522
Paniello RC, 902
Panje WR, 775
Papatziamos G, 359
Pappas DG, 86, 358, 720, 886 (book reviews)
Park CI, 1082
Park Y-S, 604
Parker GD, 129
Parks TN, suppl 168:37
Parnes SM, 151
Parsons LS, 320
Pasteels JL, 1043
Pauloski BR, 279
Pearce A, suppl 168:59
Perazzo LM, 385
Pernell KJ, 920
Pillsbury HC, 633
Pilowsky PM, 897
Pinto HA, 117
Piquet J-J, 364
Podoshin L, 226, 859
Pollack GD, suppl 168:44
Poron F, 854
Pratt MF, 790
Prazma J, 633
Prins LC, 759
Putzi MJ, 526

Quiñónez RE, 721

Rabinov CR, 589
Ramsden WN, 767
Rask-Andersen H, 190
Rassekh CH, 869
Ravicz ME, 49
Reboussin DM, suppl 169
Reinert P, 854
Reiss M, 885 (letter to editor)
Remon J-P, 329
Ress B, 608
Rhee C-K, 604
Rhee C-S, 215
Richardson BE, 920
Richter B, 478
Richtsmeier WJ, 995
Rigby PL, 1020
Righi P, 710, 1093
Riley A, suppl 168:35
Rimell FL, 461
Rinaldo A, 79, 437, 526, 716, 801, 878, 983, 1024
Robbins AM, suppl 168:35
Robinson KS, 934
Rodriquez AA, 956, 1012
Roithmann R, suppl 171
Rong Y, 599
Rosen A, 775
Rosen CA, 552
Rosowski JJ, 49
Ross U, 478
Roth Y, suppl 171
Rothschild M, 244
Rothstein SG, 560
Rubel EW, suppl 168(ed)
Ruben RJ, suppl 168:55
Rubin PAD, 109
Rubinstein I, 474
Rubinstein JT, 739

Saah D, 873
Sacco RL, 87
Sadaoka T, 380
Sadé J, 37, 314
Saito T, 338
Sakai C, 693
Sakakura Y, 683
Sakamoto H, 483, 848
Sakata H, 1087
Sakihama N, 503
Sala X, 863
Saleh E, 370
Salman S, 109, 305
Salmon I, 1043
Sánchez J, 863
Sando I, 33, 583, 662
Sandridge SA, 210
Sanna M, 370
Sapçi T, 471
Sato K, 44, 490
Saydam L, 875
Scher N, 775
Scher RL, 995
Schiff NF, 563
Schilling V, 669

Schlosser RJ, 230
Schuknecht HF, 5 (*Annals* Classic)
Schultz E, 1012
Sciote JJ, 1076
Seely DR, 729
Sekosan M, 474
Self T, suppl 168:59
Sercarz JA, 261, 594
Seroky JT, 422
Sewall SR, 310
Shah SS, 163
Shahbahrami PB, 710
Shaheen FAM, 391
Shapiro J, 286; 357 (letter to editor)
Shapshay SM, 563, 989
Sheikh IA, 391
Shilo S, 252
Shimizu T, 683
Shinkawa H, 1063
Shiti H, 859
Singh B, 301
Siqueira MG, 927
Sisti M, 568
Slattery W III, 466
Slavit DH, 544
Smith RJH, 123
Smith RV, 640
Snyderman CH, 869
Soda Y, 41
Somers T, 15
Steel KP, suppl 168:59
Steiniger JR, 151
Stern Y, 891
Strasberg SR, 506
Strauchen J, 244
Straumann D, 61
Streitmann MJ, 952
Stricklin GP, 271
Suarez P, 170
Sudo M, 33, 583, 662
Sugar AW, 135
Suman VJ, 943
Sun Q-J, 897
Suzuki C, 583, 662
Suzuki M, 971
Svirsky M, suppl 168:35
Szwarc BJ, 556

Tabari R, 422
Tabuchi T, 503
Tadmor R, 75
Takahashi H, 27, 380
Takahashi K, 343
Takahashi M, 1097
Takahashi Y, 683
Takasaka T, 599
Takasu T, 1070
Talbot JM, 320
Talmi YP, 75, 435
Tamagawa Y, 338, 643
Tambs K, 624
Tanaka A, 483, 848
Tanaka Y, 394
Tandon R, 87
Tao ZD, 680
Tarasidis G, 506
Teixeira GV, 927
Telischi F, 608
Terr LI, 884 (letter to editor)
Terris DJ, 117
Thompson LDR, 86 (book review)
Thomson J, 87
Tian Q, 466
Tian YQ, 680
Todd S, suppl 168:35
Traserra J, 863
Triana RJ, 633
Tsuiki T, 643
Tsunoda K, 41
Tsuta Y, 795
Tsuzuku T, 1087
Tu G, 320
Turner CW, 885 (editor's reply to letter)

Uğur G, 471
Ulewicz DE, 297
Uno A, 1087
Usami S-I, 1063

van Benthem P-PG, 759
van den Biezenbos AR, 432
van den Broek P, 653
Vanhalle S, 15
van Rijk PP, 432
van Weissenbruch R, 329
Varela A, suppl 168:59
Vasef MA, 348
Vaughn T, 533
Vellutini EAS, 927
Venkatesan TK, 445
Verbeken G, 15
Volk MS, 989
Vrabec JT, 976

Walner DL, 891
Walsh J, suppl 168:59
Walters KS, 123
Wang Z, 989
Watanabe K, 394
Watanabe O, 506
Wax MK, 297
Wazen JJ, 568
Weber AL, 109
Wei WI, 779
Weinstein G, 159, 291
Weiss LM, 348, 437
Welling DB, 519
Wenig BM, 79, 611
Wenig B, 474
Werner JA, 1036
West C, 733
Williams K, 1020
Williams PB, 790
Wilson DF, 320
Wollenberg B, 669
Woo P, 563
Woodson BT, 310
Woodson GE, 552
Wright CG, 934

Xiao JY, 680

Yamada K, 1087
Yamashita T, 795
Yang B, 230
Ye M, 261, 594
Yeh TH, 240
Yetiser S, 182
Yeung D, 552
Yoon SK, 1082
Yorizane S, 69
Yuen APW, 779

Zagzag D, 657
Zakkar M, 474
Zazgornik J, 391
Zbar RIS, 739
Zeitels SM, 533
Zeitouni AG, 657
Zhao SP, 680
Zhou H-M, 326
Zorowitz RD, 705

SUBJECTS

Acoustic measurement
  Acoustic measurement of change in voice quality with treatment for chronic posterior laryngitis, 279
Acquired immunodeficiency syndrome
  Kaposi's sarcoma of larynx, 563
Action potential
  Summating potential and action potential gradients on and in vicinity of round window in guinea pig, 139
Acute hearing loss
  Clinical observations on acute low-tone sensorineural hearing loss. Survey and analysis of 137 patients, 746
Adenoid
  Role of adenoids in pathogenesis of otitis media: bacteriologic and immunohistochemical analysis, 619
Adenoma
  Recurrent pleomorphic adenoma of parotid gland involving osseous external auditory canal. With note on foramen of Huschke, 589
Aging
  Age-related changes of elastic fibers in superficial layer of lamina propria of vocal folds, 44
  Aging rat vestibular ganglion: II. Quantitative electron micro-

scopic evaluation, 753
Hearing loss (in nonoperated ears) in relation to age in osteogenesis imperfecta type I, 575

Airflow
Laryngeal adjustment in whispering. Magnetic resonance imaging study, 41

Airway
Measurement of airway patency. Manual for users of Toronto Systems and others interested in nasal patency measurement, suppl 171

Allergy
Effect of immunotherapy on serum levels of eosinophil cationic protein in perennial allergic rhinitis, 848
Increase in expression of IL-4 and IL-5 mRNA in nasal mucosa of patients with perennial allergic rhinitis during natural allergen exposure, 215
Significant correlation between symptom score and IgG4 antibody titer following long-term immunotherapy for perennial allergic rhinitis, 483

Anastomosis
Partial cricotracheal resection with primary anastomosis in pediatric age group, 891

Anemia
Reversible uremic deafness: is it correlated with degree of anemia? 391

Anesthesia
Auditory evoked responses under total spinal anesthesia in rats, 1087
Effects of anesthetic technique on hemodynamic response to microlaryngeal surgery, 863
Local and regional anesthesia for functional endoscopic sinus surgery, 767
Prevention of flash fires during facial surgery performed under local anesthesia, 248

Angiosarcoma
Angiosarcomas of head and neck: clinical and pathologic characteristics, 943

Annals Classic
A syndrome of ear and sinus symptoms dependent upon disturbed function of temporomandibular joint [1934], 805
Reparative granuloma following stapedectomy: clinical entity [1967], 5

Annulus
Postnatal change in angle between tympanic annulus and surrounding structures. Computer-aided three-dimensional reconstruction study, 33

Antibiotics
Effects of indomethacin, dexamethasone, and erythromycin on endotoxin-induced intraepithelial mucus production of rat nasal epithelium, 683

Anticoagulant
Sudden deafness: comparison of anticoagulant therapy and carbogen inhalation therapy, 22

Antidiuretic hormone
Syndrome of inappropriate antidiuretic hormone secretion associated with head and neck cancers: review of literature, 878

Aplasia
Maxillary sinus aplasia, 799
Monolateral aplasia of parotid gland, 522

Apnea
Posterior cephalometric radiographic analysis in obstructive sleep apnea, 310

Artery
Blood flow in common carotid and vertebral arteries in patients with sudden deafness, 27
Iatrogenic pseudoaneurysm of internal carotid artery, 1093
Imaging diagnosis of buckled innominate artery, 1097

Arthritis
Cricoarytenoid joint effusion secondary to rheumatoid arthritis, 976

Arytenoid
Changes in length and spatial orientation of vocal fold with arytenoid adduction in cadaver larynges, 552
Utility of helical computed tomography in study of arytenoid dislocation and arytenoid subluxation, 1020

Aspiration
Method and clinical results of new transthyrotomy closure of supraglottic larynx for treatment of intractable aspiration, 451
Role of flexible laryngoscopy in evaluating aspiration, 705

Asymmetry
Functional asymmetries in auditory system, suppl 168:23

Atelectasis
Chronic maxillary atelectasis, 109
Middle ear gas composition in pathologic conditions: mass spectrometry in otitis media with effusion and atelectasis, 743

Atrophy
Effect of adult-onset deafness on human central auditory system, 385
Peculiar snoring in patients with multiple system atrophy: its sound source, acoustic characteristics, and diagnostic significance, 380
Vocal fold atrophy: quantitative glottic measurement and vocal function, 544

Audiometry
Investigation of 4,000-Hz dip by detailed audiometry, 408

Auditory brain stem response
Auditory evoked responses under total spinal anesthesia in rats, 1087
Electrophysiologic changes in preterm neonates: auditory brain stem response and distortion product otoacoustic emissions, 721

Auditory canal
Meningioma of internal auditory canal, 657

Auricle
Sonography in preauricular pilomatrixoma of childhood, 167

Axonal regeneration
End-to-side neurorrhaphy resulting in limited sensory axonal regeneration in rat model, 506

Bacteria
Anaerobes and fungi in chronic suppurative otitis media, 649
Bacterial flora of stethoscopes' earpieces and otitis externa, 751
Interaction between oral alpha-streptococci and group A streptococci in patients with tonsillitis, 571
Role of adenoids in pathogenesis of otitis media: bacteriologic and immunohistochemical analysis, 619

Barrier
  Barrier between supraglottis and glottis: myth or reality? 716
  Glottic-supraglottic barrier: fact or fantasy? 700

Basaloid squamous cell carcinoma
  Basaloid squamous cell carcinoma of larynx and hypopharynx, 1024

Basement membrane
  Effect of cisplatin on basement membrane anionic sites in ampulla, macula, and stria vascularis of guinea pigs, 971

Bcl-2
  Prognostic significance of Bcl-2 expression in localized squamous cell carcinoma of head and neck, 445

Beta-blockers
  Effects of anesthetic technique on hemodynamic response to microlaryngeal surgery, 863

Betamethasone
  Single dose of betamethasone in combined medical treatment of secretory otitis media, 359

Blood
  Blood flow in common carotid and vertebral arteries in patients with sudden deafness, 27

Bone
  Parosteal osteogenic sarcoma of mastoid bone, 729
  Repair of thyroid cartilage defect with bone morphogenetic protein, 326

Book Reviews
  Bailey BJ, Calhoun KH, Coffey AR, Neely JG. *Atlas of Head and Neck Surgery–Otolaryngology*, 886
  Chasin M. *Musicians and the Prevention of Hearing Loss*, 886
  Davis PJ, Fletcher NH, eds. *Vocal Fold Physiology. Controlling Complexity and Chaos*, 886
  Ferlito A, ed. *Surgical Pathology of Laryngeal Neoplasms*, 86
  Lucente FE, Lawson W, Novick NL. *The External Ear*, 720
  Morata TC, Dunn DE. *Occupational Hearing Loss*, 86
  Salvi RJ, Henderson D, Fiorino F, Colletti V, eds. *Auditory System Plasticity and Regeneration*, 358
  Sanna M, Saleh E, Russo A, Taibah A. *Atlas of Temporal Bone and Lateral Skull Base Surgery*, 720

Botulinum toxin
  Efficacy of repeated botulinum toxin injections as function of timing, 1012
  Transoral electromyographic recordings in botulinum toxin–injected rat larynges, 956

Brain stem
  Superior laryngeal nerve brain stem evoked response in cat, 101

Bronchus
  Diagnosis and management of left main stem bronchus compression, 461

Brown tumor
  Brown tumor in cricoid cartilage: unusual manifestation of primary hyperparathyroidism, 252

Calcification
  Prevertebral calcification masquerading as hypopharyngeal foreign body, 435
  Rhinolith: unusual case and update, 135

Capillary
  Horseradish peroxidase permeation from capillaries of stria vascularis after inoculation of endotoxin into middle ear, 394

Carbogen inhalation
  Sudden deafness: comparison of anticoagulant therapy and carbogen inhalation therapy, 22

Carcinoma
  Basaloid squamous cell carcinoma of larynx and hypopharynx, 1024
  Expression of matrix metalloproteinases and tissue inhibitor of metalloproteinases in head and neck squamous cell carcinoma, 271
  Surgical management of early-stage hypopharyngeal carcinoma, 909

Carcinomatosis
  Clinicopathologic study of leptomeningeal carcinomatosis involving temporal bone, 674

Cartilage
  Cartilaginous tumors of larynx: clinicopathologic review of 47 cases, 94
  Repair of thyroid cartilage defect with bone morphogenetic protein, 326

Cell
  Auditory epithelial migration. III: Immunohistologic study using anti-BrdU antibody on tympanic membrane in mouse, 414

Cemento-ossifying fibroma
  Juvenile cemento-ossifying fibroma of maxilla, 75

Central auditory system
  Effect of adult-onset deafness on human central auditory system, 385
  Functional asymmetries in auditory system, suppl 168:23
  Neurobehavioral studies of central auditory system, suppl 168:31

Central nervous system
  Effect of antagonism at central nervous system M3 muscarinic receptors on laryngeal chemoresponse, 920

Cervical necrotizing fasciitis, 965

CHARGE association
  Vestibular abnormalities in CHARGE association, 129

Chemoresponse
  Effect of antagonism at central nervous system M3 muscarinic receptors on laryngeal chemoresponse, 920

Cholesteatoma
  Congenital cholesteatoma isolated to mastoid, 608
  Ear cholesteatoma versus cholesterol granuloma, 79
  Giant cholesteatoma of external auditory canal, 471
  Localization of transforming growth factor–β–expressing cells and comparison with major extracellular components in aural cholesteatoma, 669

Chondrogenesis
  Effect of intraoperative ischemia on chondrogenesis by vascularized auricular perichondrium grafted in airway, 237

Chondroma
  Cartilaginous tumors of larynx: clinicopathologic review of 47 cases, 94

Chondrosarcoma
  Cartilaginous tumors of larynx: clinicopathologic review of 47 cases, 94

Cilia
  In vivo measurement of human nasal mucociliary motility using laser light scattering instrument, 859

- Incidence of primary ciliary dyskinesia in children with recurrent respiratory diseases, 854
- Mucociliary clearance of stented laryngotracheal tract in guinea pigs in vivo, 240
- Signal transduction pathways in modulation of ciliary beat frequency by methacholine, 230

Cisplatin
- Effect of cisplatin on basement membrane anionic sites in ampulla, macula, and stria vascularis of guinea pigs, 971

Cleft
- Laryngotracheoesophageal clefts, 1002

Clinicopathological Consultation
- Barrier between supraglottis and glottis: myth or reality? 716
- Ear cholesteatoma versus cholesterol granuloma, 79
- Head and neck Langerhans cell histiocytosis, 526
- Human immunodeficiency virus–1 infection of lymphoid tissues of Waldeyer's ring, 611
- Lymphoepithelial carcinoma of larynx, hypopharynx, and trachea, 437
- Nasopharyngeal carcinoma, with emphasis on its relationship to Epstein-Barr virus, 348
- Pretreatment pathologic prognostic factors in head and neck squamous cell carcinoma, 983
- Role of DNA measurements of head and neck tumors, 801
- Syndrome of inappropriate antidiuretic hormone secretion associated with head and neck cancers: review of literature, 878
- Yolk sac tumors (endodermal sinus tumors) of extracranial head and neck regions, 254

Closure
- Surgical closure of persisting failed tracheoesophageal voice fistula, 775

Cochlea
- Electrical impedance of cochlear implant lubricants hyaluronic acid, oxycellulose, and glycerin, 653
- Ototoxic effect of erythromycin on cochlear potentials in guinea pig, 599
- Selective cochlear neurectomy for debilitating tinnitus, 568

Communicative disorders
- Eradication of communicative disorders: preventive medicine in 21st century, suppl 168:55

Complications
- Complications associated with 327 foreign bodies of pharynx, larynx, and esophagus, 301
- Iatrogenic pseudoaneurysm of internal carotid artery, 1093
- Intracranial complications of otitis media, 873
- Posttransplant lymphoproliferative disease presenting as sudden respiratory arrest in three-year-old child, 244
- Prevention of flash fires during facial surgery performed under local anesthesia, 248
- Treatment of chronic postoperative otorrhea with cultured keratinocyte sheets, 15

Compression
- Diagnosis and management of left main stem bronchus compression, 461

Costen's syndrome
- A syndrome of ear and sinus symptoms dependent upon disturbed function of temporomandibular joint [*Annals* Classic, 1934], 805
- Jaws revisited: Costen's syndrome, 820

Craniofacial procedures
- Indications for, contraindications to, and interruption of craniofacial procedures, 927

Cricoid
- Cricoarytenoid joint effusion secondary to rheumatoid arthritis, 976
- Cricohyoidoepiglottopexy for glottic carcinoma with fixation or impaired motion of true vocal cord: 5-year oncologic results with 112 patients, 364
- Epiglottic position after cricothyroidotomy: comparison with tracheotomy, 560
- Functional outcome and prognosis factors after supracricoid partial laryngectomy with cricohyoidopexy, 291
- Partial cricotracheal resection with primary anastomosis in pediatric age group, 891

Cross-innervation
- Cross-innervation of thyroarytenoid muscle by branch from external division of superior laryngeal nerve, 594

Crystalline deposits
- Intracellular crystalline deposits in lymphoplasmacellular disorders, 170

Dark cell region
- Immunohistochemical localization of manganese superoxide dismutase in rat vestibular dark cell regions, 69

Deafness
- Effect of adult-onset deafness on human central auditory system, 385
- Effects of early deafness on development of brain stem auditory neurons, suppl 168:37
- Molecular analysis of POU3F4 gene in patients with clinical and radiographic evidence of X-linked mixed deafness with perilymphatic gusher, 320
- Unravelling genetics of deafness, suppl 168:59

2-Deoxyglucose
- Glucose utilization of rat vestibular end organs: quantitative 2-deoxyglucose study, 145

Detailed audiometry
- Investigation of 4,000-Hz dip by detailed audiometry, 408

Development
- Effects of early deafness on development of brain stem auditory neurons, suppl 168:37
- Marrow-mesenchyme connections in fetal and newborn tympanum. New entity, 466
- Postnatal change in angle between tympanic annulus and surrounding structures. Computer-aided three-dimensional reconstruction study, 33

Dip
- Investigation of 4,000-Hz dip by detailed audiometry, 408

Dissection
- QT interval changes following neck dissection. Stratified prospective study, 869
- Role of suprahyoid neck dissection in treatment of squamous cell carcinoma of lower lip, 787
- Surgical morbidity of neck dissection after chemoradiotherapy in advanced head and neck cancer, 117

Distortion product emissions
- Distortion product emissions in normal-hearing and low-frequency hearing loss carriers of genes for Waardenburg's syndrome, 220
- Statistical evaluation of hearing screening by distortion product otoacoustic emissions, 1052

DNA
- Audiologic findings in patients with point mutation at nucle-

otide 3,243 of mitochondrial DNA, 338
  Role of DNA measurements of head and neck tumors, 801

Double tumor
  Salivary gland double tumor: synchronous ipsilateral pleomorphic adenoma and acinic cell carcinoma of parotid gland, 226

Dyskinesia
  Incidence of primary ciliary dyskinesia in children with recurrent respiratory diseases, 854

Dysphagia
  Phagophobia: form of psychogenic dysphagia. New entity, 286
  Silent laryngopharyngeal sensory deficits after stroke, 87

Edema
  Reinke's edema: phonatory mechanisms and management strategies, 533

Elastic fibers
  Age-related changes of elastic fibers in superficial layer of lamina propria of vocal folds, 44

Electrical impedance
  Electrical impedance of cochlear implant lubricants hyaluronic acid, oxycellulose, and glycerin, 653

Electrocochleography
  Electrocochleography evaluation of guinea pig model of endolymphatic hydrops, 934

Electromyography
  Transoral electromyographic recordings in botulinum toxin–injected rat larynges, 956

Endoderm
  Yolk sac tumors (endodermal sinus tumors) of extracranial head and neck regions, 254

Endolymph
  Electrocochleographic evaluation of guinea pig model of endolymphatic hydrops, 934
  "Endolymphatic sacitis" in case of active Meniere's disease. Ultrastructural histopathologic investigation, 190
  Transection and occlusion of lateral semicircular canal in guinea pigs, 1082

Endoscopy
  Analysis of pain and endoscopic sinus surgery for sinusitis, 305
  Endoscopic laryngotracheoplasty and graft soldering with carbon dioxide laser. Animal study, 989
  Endoscopic management of combined laryngocele, 556
  Safety of esophagoscopy in irradiated esophagus, 297
  Telescopic laryngeal and pharyngeal surgery, 995

Endotoxin
  Horseradish peroxidase permeation from capillaries of stria vascularis after inoculation of endotoxin into middle ear, 394

Eosinophil cationic protein
  Effect of immunotherapy on serum levels of eosinophil cationic protein in perennial allergic rhinitis, 848

Epiglottis
  Cricohyoidoepiglottopexy for glottic carcinoma with fixation or impaired motion of true vocal cord: 5-year oncologic results with 112 patients, 364
  Epiglottic position after cricothyroidotomy: comparison with tracheotomy, 560

Epithelium
  Auditory epithelial migration. III: Immunohistologic study using anti-BrdU antibody on tympanic membrane in mouse, 414
  Lymphoepithelial carcinoma of larynx, hypopharynx, and trachea, 437

Epstein-Barr virus
  Nasopharyngeal carcinoma, with emphasis on its relationship to Epstein-Barr virus, 348

Erythromycin
  Ototoxic effect of erythromycin on cochlear potentials in guinea pig, 599

Esophagus
  Complications associated with 327 foreign bodies of pharynx, larynx, and esophagus, 301
  Safety of esophagoscopy in irradiated esophagus, 297

Eustachian tube
  Magnetic resonance imaging of development of otitis media with effusion caused by functional obstruction of eustachian tube, 422
  Narrowest (isthmus) portion of eustachian tube: computer-aided three-dimensional reconstruction and measurement study, 583

Evoked response
  Superior laryngeal nerve brain stem evoked response in cat, 101

External auditory canal
  Giant cholesteatoma of external auditory canal, 471

Extracellular fluid
  Extracellular fluid pathway inside facial nerve fascicles, 503

Extracellular matrix
  Localization of transforming growth factor–β–expressing cells and comparison with major extracellular components in aural cholesteatoma, 669

Facial nerve
  Extracellular fluid pathway inside facial nerve fascicles, 503

Fascia
  Cervical necrotizing fasciitis, 965
  Use of composite fascial carrier for laryngotracheal reconstruction, 175

Fat suppression
  Value of fat suppression magnetic resonance imaging in diagnosis of lipomas of internal auditory canal, 343

Fibroma
  Juvenile cemento-ossifying fibroma of maxilla, 75

Fire
  Prevention of flash fires during facial surgery performed under local anesthesia, 248

Fistula
  Magnetic resonance imaging of vocal failure in patients undergoing laryngectomy with tracheoesophageal fistula, 795
  Perilymphatic fistula: Washington, DC, experience, 830
  Surgical closure of persisting failed tracheoesophageal voice fistula, 775

Flap
  Correlation of neutrophil activation and skin flap survival in pharmacologically altered pigs, 790

Flexible laryngoscopy
  Role of flexible laryngoscopy in evaluating aspiration, 705

Foreign body
  Complications associated with 327 foreign bodies of pharynx, larynx, and esophagus, 301

Knife blade as facial foreign body, 710
Prevertebral calcification masquerading as hypopharyngeal foreign body, 435

Free radical
Application of oxygen free radical scavengers to diminish occurrence of myringosclerosis, 513

Functional endoscopic sinus surgery
Efficacy of sinus irrigation versus sinus irrigation followed by functional endoscopic sinus surgery, 759
Local and regional anesthesia for functional endoscopic sinus surgery, 767

Fungus
Calcified mucor fungus ball of sphenoid sinus: unusual presentation of sinoorbital mucormycosis, 875
Chemoprophylaxis of fungal deterioration of Provox silicone tracheoesophageal prosthesis in postlaryngectomy patients, 329

Gas
Dependence of middle ear gas composition on pulmonary ventilation, 314
Middle ear gas composition in pathologic conditions: mass spectrometry in otitis media with effusion and atelectasis, 743

Gastroesophageal reflux
Extraesophageal pediatric reflux: 24-hour double-probe pH monitoring in 222 children, suppl 169

Genetics
Audiologic features of hearing loss due to 1,555 mutation of mitochondrial DNA, 643
Audiologic findings in patients with point mutation at nucleotide 3,243 of mitochondrial DNA, 338
Distribution and heritability of recurrent ear infections, 624
Meniere's syndrome and migraine: incidence in one family, 823
Molecular analysis of POU3F4 gene in patients with clinical and radiographic evidence of X-linked mixed deafness with perilymphatic gusher, 320
Unravelling genetics of deafness, suppl 168:59
Usher's syndrome type 1C: clinical studies and fine-mapping disease locus, 123

Giant cholesteatoma
Giant cholesteatoma of external auditory canal, 471

Gland
Salivary gland double tumor: synchronous ipsilateral pleomorphic adenoma and acinic cell carcinoma of parotid gland, 226

Glottis
Barrier between supraglottis and glottis: myth or reality? 716
Glottic-supraglottic barrier: fact or fantasy? 700
Vocal fold atrophy: quantitative glottic measurement and vocal function, 544

Glucose
Glucose utilization of rat vestibular end organs: quantitative 2-deoxyglucose study, 145

Graft
Effect of intraoperative ischemia on chondrogenesis by vascularized auricular perichondrium grafted in airway, 237
Endoscopic laryngotracheoplasty and graft soldering with carbon dioxide laser. Animal study, 989
Use of composite fascial carrier for laryngotracheal reconstruction, 175

Granuloma
Ear cholesteatoma versus cholesterol granuloma, 79
Reparative granuloma following stapedectomy: clinical entity [*Annals* Classic, 1967], 5

Hair cell
Hair cell regeneration in avian cochlea, suppl 168:9
Outer hair cells: inside story, suppl 168:16

Handicap
Perceived hearing handicap of patients with unilateral or mild hearing loss, 210

Head and neck neoplasms
Angiosarcomas of head and neck: clinical and pathologic characteristics, 943
Role of DNA measurements of head and neck tumors, 801

Headache
Migraine-related vestibulopathy, 182

Hearing
Clinical observations on acute low-tone sensorineural hearing loss. Survey and analysis of 137 patients, 746
Distortion product emissions in normal-hearing and low-frequency hearing loss carriers of genes for Waardenburg's syndrome, 220
Frontiers in hearing research, suppl 168
Hearing loss (in nonoperated ears) in relation to age in osteogenesis imperfecta type I, 575
Perceived hearing handicap of patients with unilateral or mild hearing loss, 210
Statistical evaluation of hearing screening by distortion product otoacoustic emissions, 1052
Three familial cases of hearing loss associated with enlargement of vestibular aqueduct, 1063

Helical computed tomography
Ethmoid and sphenoid mucoceles viewed by helical scanning computed tomography with sagittal reconstruction, 1100
Utility of helical computed tomography in study of arytenoid dislocation and arytenoid subluxation, 1020

Hemangiosarcoma
Angiosarcomas of head and neck: clinical and pathologic characteristics, 943

Hemodynamic response
Effects of anesthetic technique on hemodynamic response to microlaryngeal surgery, 863

Histiocytosis
Head and neck Langerhans cell histiocytosis, 526

Histology
Fine three-dimensional structure of pericytes in vocal fold mucosa, 490

History
Jaws revisited: Costen's syndrome, 820

Hormone
Syndrome of inappropriate antidiuretic hormone secretion associated with head and neck cancers: review of literature, 878

Human immunodeficiency virus
Human immunodeficiency virus–1 infection of lymphoid tissues of Waldeyer's ring, 611

Hydrops
Electrocochleographic evaluation of guinea pig model of endolymphatic hydrops, 934

Hypobaric pressure
Pressure gradients affecting labyrinth during hypobaric pressure. Experimental study, 495

Hypopharynx
  Surgical management of early-stage hypopharyngeal carcinoma, 909

Idiopathic subglottic stenosis
  Idiopathic subglottic stenosis: diagnosis and endoscopic laser treatment, 770

Imaging
  Invisible culprit: intralabyrinthine schwannomas that do not appear on enhanced magnetic resonance imaging, 739
  Magnetic resonance imaging of development of otitis media with effusion caused by functional obstruction of eustachian tube, 422
  Utility of helical computed tomography in study of arytenoid dislocation and arytenoid subluxation, 1020

Imaging Case Study of the Month
  Brown tumor in cricoid cartilage: unusual manifestation of primary hyperparathyroidism, 252
  Calcified mucor fungus ball of sphenoid sinus: unusual presentation of sinoorbital mucormyosis, 875
  Congenital cholesteatoma isolated to mastoid, 608
  Cricoarytenoid joint effusion secondary to rheumatoid arthritis, 976
  Ethmoid and sphenoid mucoceles viewed by helical scanning computed tomography with sagittal reconstruction, 1100
  Iatrogenic pseudoaneurysm of internal carotid artery, 1093
  Imaging diagnosis of buckled innominate artery, 1097
  Intracranial complications of otitis media, 873
  Juvenile cemento-ossifying fibroma of maxilla, 75
  Knife blade as facial foreign body, 710
  Magnetic resonance imaging of vocal failure in patients undergoing laryngectomy with tracheoesophageal fistula, 795
  Masticator space in nasopharyngeal carcinoma, 979
  Maxillary sinus aplasia, 799
  Melanoma of petrous apex of temporal bone, 519
  Monolateral aplasia of parotid gland, 522
  Odontogenic keratocyst in young child, 163
  Osteoma of middle ear, 714
  Prevertebral calcification masquerading as hypopharyngeal foreign body, 435
  Sonography in preauricular pilomatrixoma of childhood, 167
  Value of fat suppression magnetic resonance imaging in diagnosis of lipomas of internal auditory canal, 343
  Value of technetium-99m pertechnetate imaging in differential diagnosis of salivary gland lesions, 432

Immunity
  Decrease in immunoreactive neutral endopeptidase in uvula epithelium of patients with obstructive sleep apnea, 474
  Effect of immunotherapy on serum levels of eosinophil cationic protein in perennial allergic rhinitis, 848
  Reversible sensorineural hearing loss after renal transplant immunosuppression with OKT3 (Muromonab-CD3), 640
  Significant correlation between symptom score and IgG4 antibody titer following long-term immunotherapy for perennial allergic rhinitis, 483

Implant
  Comparison of soft tissue response in rabbits following laryngeal implantation with hydroxylapatite, silicone rubber, and Teflon, 399
  Montgomery® Thyroplasty Implant System, suppl 170
  Speech intelligibility of children with multichannel cochlear implants, suppl 168:35

Indications
  Indications for, contraindications to, and interruption of craniofacial procedures, 927

Inflammation
  "Endolymphatic sacitis" in case of active Meniere's disease. Ultrastructural histopathologic investigation, 190
  Reduction of inner ear inflammation by treatment with anti–ICAM-1 antibody, 1070

Inheritance
  Distribution and heritability of recurrent ear infections, 624
  Three familial cases of hearing loss associated with enlargement of vestibular aqueduct, 1063

Inner ear
  Effect of cisplatin on basement membrane anionic sites in ampulla, macula, and stria vascularis of guinea pigs, 971

Interleukin
  Increase in expression of IL-4 and IL-5 mRNA in nasal mucosa of patients with perennial allergic rhinitis during natural allergen exposure, 215
  Role of tumor necrosis factor and interleukin-1 in endotoxin-induced middle ear effusions, 633

Internal auditory canal
  Meningioma of internal auditory canal, 657

Interruption
  Indications for, contraindications to, and interruption of craniofacial procedures, 927

Irradiation
  Safety of esophagoscopy in irradiated esophagus, 297

Irrigation
  Efficacy of sinus irrigation versus sinus irrigation followed by functional endoscopic sinus surgery, 759

Ischemia
  Effect of intraoperative ischemia on chondrogenesis by vascularized auricular perichondrium grafted in airway, 237

Jugular foramen
  Lower cranial nerve schwannomas involving jugular foramen, 370

Kaposi's sarcoma
  Kaposi's sarcoma of larynx, 563

Keratin
  Odontogenic keratocyst in young child, 163
  Treatment of chronic postoperative otorrhea with cultured keratinocyte sheets, 15

Kidney
  Reversible uremic deafness: is it correlated with degree of anemia? 391

Labyrinth
  Aging rat vestibular ganglion: II. Quantitative electron microscopic evaluation, 753
  Invisible culprit: intralabyrinthine schwannomas that do not appear on enhanced magnetic resonance imaging, 739
  Middle ear pressure and dysfunction of labyrinth: is there a relationship? 478
  Pressure gradients affecting labyrinth during hypobaric pressure. Experimental study, 495
  Reduction of inner ear inflammation by treatment with anti–ICAM-1 antibody, 1070
  Transection of occlusion of lateral semicircular canal in guinea pigs, 1082

Lamina propria
  Age-related changes of elastic fibers in superficial layer of lamina propria of vocal folds, 44

Langerhans cell histiocytosis
  Head and neck Langerhans cell histiocytosis, 526

Larynx
  Acoustic measurement of change in voice quality with treatment for chronic posterior laryngitis, 279
  Endoscopic management of combined laryngocele, 556
  Functional outcome and prognosis factors after supracricoid partial laryngectomy with cricohyoidopexy, 291
  Impact of laryngectomy on quality of life: perspective of patient versus that of health care provider, 693
  Laryngotracheoesophageal clefts, 1002
  Morbidity of combined therapy for treatment of supraglottic carcinoma: supraglottic laryngectomy and radiotherapy, 151
  Reversibility of medialization laryngoplasty. Experimental study, 902
  Role of flexible laryngoscopy in evaluating aspiration, 705
  Ruptured pexis after supracricoid partial laryngectomy, 159
  State-dependent laryngomalacia, 887
  Surgical management of early-stage hypopharyngeal carcinoma, 909
  Vocal function following vertical hemilaryngectomy: comparison of four reconstruction techniques in canine, 261

Laser
  Comparison of carbon dioxide and neodymium:yttrium-aluminum-garnet lasers in surgery of inferior turbinate, 1036
  Effect of photodynamic therapy on selected laboratory values of patients with nasopharyngeal carcinoma, 680
  Endoscopic laryngotracheoplasty and graft soldering with carbon dioxide laser. Animal study, 989
  Endoscopic management of combined laryngocele, 556
  Excision of rhinophyma with carbon dioxide laser: ten-year experience, 952
  Idiopathic subglottic stenosis: diagnosis and endoscopic laser treatment, 770
  In vivo measurement of human nasal mucociliary motility using laser light scattering instrument, 859
  Telescopic laryngeal and pharyngeal surgery, 995

Lectin
  Algorithm analysis of lectin glycohistochemistry and Feulgen cytometry for new classification of nasal polyposis, 1043

Leptomeningeal carcinomatosis
  Clinicopathologic study of leptomeningeal carcinomatosis involving temporal bone, 674

Letters to the Editor, 357, 358, 884, 885

Life expectancy
  Impact of laryngectomy on quality of life: perspective of patient versus that of health care provider, 693

Lipoma
  Value of fat suppression magnetic resonance imaging in diagnosis of lipomas of internal auditory canal, 343

Lubricant
  Electrical impedance of cochlear implant lubricants hyaluronic acid, oxycellulose, and glycerin, 653

Lung
  Dependence of middle ear gas composition on pulmonary ventilation, 314

Lymph
  Immunohistochemistry of lymphocytes and macrophages in human celloidin-embedded temporal bone sections with acute otitis media, 662
  Intracellular crystalline deposits in lymphoplasmacellular disorders, 170
  Lymphoepithelial carcinoma of larynx, hypopharynx, and trachea, 437
  Posttransplant lymphoproliferative disease presenting as sudden respiratory arrest in three-year-old child, 244

Macrophage
  Immunohistochemistry of lymphocytes and macrophages in human celloidin-embedded temporal bone sections with acute otitis media, 662

Manganese superoxide dismutase
  Immunohistochemical localization of manganese superoxide dismutase in rat vestibular dark cell regions, 69

Marrow
  Marrow-mesenchyme connections in fetal and newborn tympanum. New entity, 466

Masticator space
  Masticator space in nasopharyngeal carcinoma, 979

Mastoid
  Congenital cholesteatoma isolated to mastoid, 608
  Parosteal osteogenic sarcoma of mastoid bone, 729
  Secretory otitis media in adults: II. Role of mastoid pneumatization as prognostic factor, 37

Maturation
  Electrophysiologic changes in preterm neonates: auditory brain stem response and distortion-product otoacoustic emissions, 721

Maxilla
  Chronic maxillary atelectasis, 109

Measurement
  Narrowest (isthmus) portion of eustachian tube: computer-aided three-dimensional reconstruction and measurement study, 583

Medialization
  Comparison of soft tissue response in rabbits following laryngeal implantation with hydroxylapatite, silicone rubber, and Teflon, 399
  Reversibility of medialization laryngoplasty. Experimental study, 902

Melanoma
  Melanoma of petrous apex of temporal bone, 519

Meniere's disease
  "Endolymphatic sacitis" in case of active Meniere's disease. Ultrastructural histopathologic investigation, 190

Meniere's syndrome
  Meniere's syndrome and migraine: incidence in one family, 823
  Middle ear pressure and dysfunction of labyrinth: is there a relationship? 478

Meningioma
  Meningioma of internal auditory canal, 657

Mesenchyme
  Marrow-mesenchyme connections in fetal and newborn tympanum. New entity, 466

Metalloproteinase
  Expression of matrix metalloproteinases and tissue inhibitor of metalloproteinases in head and neck squamous cell carcinoma, 271

Metastasis
  Clinicopathologic study of leptomeningeal carcinomatosis involving temporal bone, 674

Role of suprahyoid neck dissection in treatment of squamous cell carcinoma of lower lip, 787

Methacholine
  Signal transduction pathways in modulation of ciliary beat frequency by methacholine, 230

Microbiology
  Anaerobes and fungi in chronic suppurative otitis media, 649

Middle ear
  Mechanics of type IV tympanoplasty: experimental findings and surgical implications, 49
  Osteoma of middle ear, 714

Migraine
  Meniere's syndrome and migraine: incidence in one family, 823
  Migraine-related vestibulopathy, 182

Monoclonal antibody
  Reduction of inner ear inflammation by treatment with anti–ICAM-1 antibody, 1070

Montgomery® Thyroplasty Implant System, suppl 170

Morbidity
  Morbidity of combined therapy for treatment of supraglottic carcinoma: supraglottic laryngectomy and radiotherapy, 151
  Surgical morbidity of neck dissection after chemoradiotherapy in advanced head and neck cancer, 117

Mucocele
  Ethmoid and sphenoid mucoceles viewed by helical scanning computed tomography with sagittal reconstruction, 1100

Mucociliary clearance
  Mucociliary clearance of stented laryngotracheal tract in guinea pigs in vivo, 240

Mucor
  Calcified mucor fungus ball of sphenoid sinus: unusual presentation of sinoorbital mucormycosis, 875

Mucosa
  Effects of platelet activating factor on vascular permeability of middle ear mucosa, 604
  Fine three-dimensional structure of pericytes in vocal fold mucosa, 490

Multiple system atrophy
  Peculiar snoring in patients with multiple system atrophy: its sound source, acoustic characteristics, and diagnostic significance, 380

Muscarinic receptor
  Effect of antagonism at central nervous system M3 muscarinic receptors on laryngeal chemoresponse, 920

Muscle
  Changes in myosin expression in denervated laryngeal muscle, 1076
  Cross-innervation of thyroarytenoid muscle by branch from external division of superior laryngeal nerve, 594
  Efficacy of repeated botulinum toxin injections as function of timing, 1012
  Respiratory activity of rat posterior cricoarytenoid muscle, 897

Mutation
  Audiologic findings in patients with point mutation at nucleotide 3,243 of mitochondrial DNA, 338

Myringosclerosis
  Application of oxygen free radical scavengers to diminish occurrence of myringosclerosis, 513

Neck
  QT interval changes following neck dissection. Stratified prospective study, 869
  Role of suprahyoid neck dissection in treatment of squamous cell carcinoma of lower lip, 787
  Surgical morbidity of neck dissection after chemoradiotherapy in advanced head and neck cancer, 117

Necrotizing fasciitis
  Cervical necrotizing fasciitis, 965

Nerve
  Auditory evoked responses under total spinal anesthesia in rats, 1087
  Changes in myosin expression in denervated laryngeal muscle, 1076
  Cross-innervation of thyroarytenoid muscle by branch from external division of superior laryngeal nerve, 594
  End-to-side neurorrhaphy resulting in limited sensory axonal regeneration in rat model, 506
  Extracellular fluid pathway inside facial nerve fascicles, 503
  Lower cranial nerve schwannomas involving jugular foramen, 370
  Neurobehavioral studies of central auditory system, suppl 168:31
  Origin and distribution of NADPH diaphorase–positive nerves in rat nasal mucosa, 688
  Selective cochlear neurectomy for debilitating tinnitus, 568
  Silent laryngopharyngeal sensory deficits after stroke, 87
  Superior laryngeal nerve brain stem evoked response in cat, 101
  Trigeminal neo-neurotization of paralyzed face, 733

Neutrophil
  Correlation of neutrophil activation and skin flap survival in pharmacologically altered pigs, 790

Nitric oxide
  Origin and distribution of NADPH diaphorase–positive nerves in rat nasal mucosa, 688

Nose
  Algorithm analysis of lectin glycohistochemistry and Feulgen cytometry for new classification of nasal polyposis, 1043
  Comparison of carbon dioxide and neodymium:yttrium-aluminum-garnet lasers in surgery of inferior turbinate, 1036
  Effect of photodynamic therapy on selected laboratory values of patients with nasopharyngeal carcinoma, 680
  Effects of indomethacin, dexamethasone, and erythromycin on endotoxin-induced intraepithelial mucus production of rat nasal epithelium, 683
  Excision of rhinophyma with carbon dioxide laser: ten-year experience, 952
  In vivo measurement of human nasal mucociliary motility using laser light scattering instrument, 859
  Masticator space in nasopharyngeal carcinoma, 979
  Measurement of airway patency. Manual for users of Toronto Systems and others interested in nasal patency measurement, suppl 171
  Nasopharyngeal carcinoma, with emphasis on its relationship to Epstein-Barr virus, 348
  Origin and distribution of NADPH diaphorase–positive nerves in rat nasal mucosa, 688
  Rhinolith: unusual case and update, 135

Nystagmus
  Three-dimensional analysis of spontaneous nystagmus in peripheral vestibular lesions, 61
  Vestibular and optokinetic function in normal guinea pig, 838

Obituaries
  Prentice Bloedel, suppl 168:5

Virginia Merrill Bloedel, suppl 168:7
Harold F. Schuknecht, 1

Obstructive sleep apnea
  Decrease in immunoreactive neutral endopeptidase in uvula epithelium of patients with obstructive sleep apnea, 474
  Posterior cephalometric radiographic analysis in obstructive sleep apnea, 310

Optokinetic function
  Vestibular and optokinetic function in normal guinea pig, 838

Osteogenesis imperfecta
  Hearing loss (in nonoperated ears) in relation to age in osteogenesis imperfecta type I, 575

Osteoma
  Osteoma of middle ear, 714

Otitis externa
  Bacterial flora of stethoscopes' earpieces and otitis externa, 751

Otitis media
  Anaerobes and fungi in chronic suppurative otitis media, 649
  Distribution and heritability of recurrent ear infections, 624
  Immunohistochemistry of lymphocytes and macrophages in human celloidin-embedded temporal bone sections with acute otitis media, 662
  Intracranial complications of otitis media, 873
  Magnetic resonance imaging of development of otitis media with effusion caused by functional obstruction of eustachian tube, 422
  Middle ear gas composition in pathologic conditions: mass spectrometry in otitis media with effusion and atelectasis, 743
  Role of adenoids in pathogenesis of otitis media: bacteriologic and immunohistochemical analysis, 619
  Role of tumor necrosis factor and interleukin-1 in endotoxin-induced middle ear effusions, 633
  Secretory otitis media in adults: II. Role of mastoid pneumatization as prognostic factor, 37
  Single dose of betamethasone in combined medical treatment of secretory otitis media, 359

Otoacoustic emissions
  Electrophysiologic changes in preterm neonates: auditory brain stem response and distortion product otoacoustic emissions, 721
  Statistical evaluation of hearing screening by distortion product otoacoustic emissions, 1052

Otorrhea
  Treatment of chronic postoperative otorrhea with cultured keratinocyte sheets, 15

Ototoxicity
  Audiologic features of hearing loss due to 1,555 mutation of mitochondrial DNA, 643
  Ototoxic effect of erythromycin on cochlear potentials in guinea pig, 599
  Reversible sensorineural hearing loss after renal transplant immunosuppression with OKT3 (Muromonab-CD3), 640

Outer hair cell
  Outer hair cells: inside story, suppl 168:16

Oxygen
  Application of oxygen free radical scavengers to diminish occurrence of myringosclerosis, 513

Pain
  Analysis of pain and endoscopic sinus surgery for sinusitis, 305

Paralysis
  Changes in length and spatial orientation of vocal fold with arytenoid adduction in cadaver larynges, 552
  Changes in myosin expression in denervated laryngeal muscle, 1076
  Comparison of soft tissue response in rabbits following laryngeal implantation with hydroxylapatite, silicone rubber, and Teflon, 399
  Cricohyoidoepiglottopexy for glottic carcinoma with fixation or impaired motion of true vocal cord: 5-year oncologic results with 112 patients, 364
  Role of ultrasound in assessment of vocal cord function in infants and children, 199
  Transoral Teflon injection under flexible laryngovideostroboscopy for unilateral vocal fold paralysis, 783
  Trigeminal neo-neurotization of paralyzed face, 733

Parotid gland
  Monolateral aplasia of parotid gland, 522
  Recurrent pleomorphic adenoma of parotid gland involving osseous external auditory canal. With note on foramen of Huschke, 589

Pathology Consultation
  Intracellular crystalline deposits in lymphoplasmacellular disorders, 170

Pericyte
  Fine three-dimensional structure of pericytes in vocal fold mucosa, 490

Perilymph
  Molecular analysis of POU3F4 gene in patients with clinical and radiographic evidence of X-linked mixed deafness with perilymphatic gusher, 320
  Perilymphatic fistula: Washington, DC, experience, 830

Peripheral vestibular lesions
  Three-dimensional analysis of spontaneous nystagmus in peripheral vestibular lesions, 61

Petrous apex
  Melanoma of petrous apex of temporal bone, 519

Pexis
  Ruptured pexis after supracricoid partial laryngectomy, 159

pH
  Extraesophageal pediatric reflux: 24-hour double-probe pH monitoring in 222 children, suppl 169

Phagophobia
  Phagophobia: form of psychogenic dysphagia. New entity, 286

Photodynamic therapy
  Effect of photodynamic therapy on selected laboratory values of patients with nasopharyngeal carcinoma, 680

Pilomatrixoma
  Sonography in preauricular pilomatrixoma of childhood, 167

Platelet activating factor
  Effects of platelet activating factor on vascular permeability of middle ear mucosa, 604

Pleomorphic adenoma
  Recurrent pleomorphic adenoma of parotid gland involving osseous external auditory canal. With note on foramen of Huschke, 589

Pneumatization
  Secretory otitis media in adults: II. Role of mastoid pneumatization as prognostic factor, 37

Polyp
  Algorithm analysis of lectin glycohistochemistry and Fuelgen cytometry for new classification of nasal polyposis, 1043

Posterior cricoarytenoid muscle
  Respiratory activity of rat posterior cricoarytenoid muscle, 897

Potential
  Summating potential and action potential gradients on and in vicinity of round window in guinea pig, 139

Pressure
  Middle ear pressure and dysfunction of labyrinth: is there a relationship? 478
  Pressure gradients affecting labyrinth during hypobaric pressure. Experimental study, 495

Prevention
  Eradication of communicative disorders: preventive medicine in 21st century, suppl 168:55

Primary ciliary dyskinesia
  Incidence of primary ciliary dyskinesia in children with recurrent respiratory diseases, 854

Processing
  Roles of GABAergic inhibition for binaural processing of multiple sound sources in inferior colliculus, suppl 168:44

Prognosis
  Functional outcome and prognosis factors after supracricoid partial laryngectomy with cricohyoidopexy, 291
  Pretreatment pathologic prognostic factors in head and neck squamous cell carcinoma, 983
  Prognostic significance of Bcl-2 expression in localized squamous cell carcinoma of head and neck, 445

Prosthesis
  Chemoprophylaxis of fungal deterioration of Provox silicone tracheoesophageal prosthesis in postlaryngectomy patients, 329

Protein
  Repair of thyroid cartilage defect with bone morphogenetic protein, 326

QT interval
  QT interval changes following neck dissection. Stratified prospective study, 869

Quality of life
  Impact of laryngectomy on quality of life: perspective of patient versus that of health care provider, 693

Questionnaire
  Perceived hearing handicap of patients with unilateral or mild hearing loss, 210

Reconstruction
  Use of composite fascial carrier for laryngotracheal reconstruction, 175
  Vocal function following vertical hemilaryngectomy: comparison of four reconstruction techniques in canine, 261

Recurrence
  Results of surgical salvage of locoregional recurrence of carcinoma of tongue after radiotherapy failure, 779

Reflux
  Extraesophageal pediatric reflux: 24-hour double-probe pH monitoring in 222 children, suppl 169

Regeneration
  End-to-side neurorrhaphy resulting in limited sensory axonal regeneration in rat model, 506
  Hair cell regeneration in avian cochlea, suppl 168:9

Reinke's edema
  Reinke's edema: phonatory mechanisms and management strategies, 533

Respiration
  Respiratory activity of rat posterior cricoarytenoid muscle, 897

Reversibility
  Reversibility of medialization laryngoplasty. Experimental study, 902

Rhinitis
  Significant correlation between symptom score and IgG4 antibody titer following long-term immunotherapy for perennial allergic rhinitis, 483

Rhinolith
  Rhinolith: unusual case and update, 135

Rhinomanometry
  Measurement of airway patency. Manual for users of Toronto Systems and others interested in nasal patency measurement, suppl 171

Rhinophyma
  Excision of rhinophyma with carbon dioxide laser: ten-year experience, 952

RNA
  Increase in expression of IL-4 and IL-5 mRNA in nasal mucosa of patients with perennial allergic rhinitis during natural allergen exposure, 215

Rupture
  Ruptured pexis after supracricoid partial laryngectomy, 159

Salivary gland
  Salivary gland double tumor: synchronous ipsilateral pleomorphic adenoma and acinic cell carcinoma of parotid gland, 226
  Value of technetium-99m pertechnetate imaging in differential diagnosis of salivary gland lesions, 432

Salvage
  Results of surgical salvage of locoregional recurrence of carcinoma of tongue after radiotherapy failure, 779

Sarcoma
  Kaposi's sarcoma of larynx, 563
  Parosteal osteogenic sarcoma of mastoid bone, 729

Schwannoma
  Invisible culprit: intralabyrinthine schwannomas that do not appear on enhanced magnetic resonance imaging, 739
  Lower cranial nerve schwannomas involving jugular foramen, 370

Semicircular canal
  Transection of occlusion of lateral semicircular canal in guinea pigs, 1082

Sensorineural hearing loss
  Clinical observations on acute low-tone sensorineural hearing loss. Survey and analysis of 137 patients, 746

Signal transduction
  Signal transduction pathways in modulation of ciliary beat frequency by methacholine, 230

Silicone
  Chemoprophylaxis of fungal deterioration of Provox silicone tracheoesophageal prosthesis in postlaryngectomy patients, 329

Sinus
  Analysis of pain and endoscopic sinus surgery for sinusitis, 305

  Chronic maxillary atelectasis, 109
  Efficacy of sinus irrigation versus sinus irrigation followed by functional endoscopic sinus surgery, 759
  Local and regional anesthesia for functional endoscopic sinus surgery, 767
  Maxillary sinus aplasia, 799

Skin flap
  Correlation of neutrophil activation and skin flap survival in pharmacologically altered pigs, 790

Sleep apnea
  Posterior cephalometric radiographic analysis in obstructive sleep apnea, 310

Slide tracheoplasty
  Slide tracheoplasty in management of congenital tracheal stenosis, 914

Snoring
  Peculiar snoring in patients with multiple system atrophy: its sound source, acoustic characteristics, and diagnostic significance, 380

Sound localization
  Roles of GABAergic inhibition for binaural processing of multiple sound sources in inferior colliculus, suppl 168:44

Spasmodic dysphonia
  Efficacy of repeated botulinum toxin injections as function of timing, 1012

Speech
  Speech intelligibility of children with multichannel cochlear implants, suppl 168:35

Squamous cell carcinoma
  Basaloid squamous cell carcinoma of larynx and hypopharynx, 1024
  Pretreatment pathologic prognostic factors in head and neck squamous cell carcinoma, 983
  Prognostic significance of Bcl-2 expression in localized squamous cell carcinoma of head and neck, 445

Stapes
  Mechanics of type IV tympanoplasty: experimental findings and surgical implications, 49
  Reparative granuloma following stapedectomy: clinical entity [*Annals* Classic, 1967], 5

Stenosis
  Idiopathic subglottic stenosis: diagnosis and endoscopic laser treatment, 770
  Partial cricotracheal resection with primary anastomosis in pediatric age group, 891
  Slide tracheoplasty in management of congenital tracheal stenosis, 914

Stent
  Mucociliary clearance of stented laryngotracheal tract in guinea pigs in vivo, 240

Steroids
  Effects of indomethacin, dexamethasone, and erythromycin on endotoxin-induced intraepithelial mucus production of rat nasal epithelium, 683
  Single dose of betamethasone in combined medical treatment of secretory otitis media, 359

Stethoscope
  Bacterial flora of stethoscopes' earpieces and otitis externa, 751

Streptococcus
  Interaction between oral alpha-streptococci and group A streptococci in patients with tonsillitis, 571

Streptomycin
  Audiologic features of hearing loss due to 1,555 mutation of mitochondrial DNA, 643

Stria vascularis
  Horseradish peroxidase permeation from capillaries of stria vascularis after inoculation of endotoxin into middle ear, 394

Stridor
  Role of ultrasound in assessment of vocal cord function in infants and children, 199
  State-dependent laryngomalacia, 887

Stroke
  Silent laryngopharyngeal sensory deficits after stroke, 87

Sudden deafness
  Blood flow in common carotid and vertebral arteries in patients with sudden deafness, 27
  Sudden deafness: comparison of anticoagulant therapy and carbogen inhalation therapy, 22

Summating potential
  Summating potential and action potential gradients on and in vicinity of round window in guinea pig, 139

Supraglottis
  Barrier between supraglottis and glottis: myth or reality? 716
  Glottic-supraglottic barrier: fact or fantasy? 700
  Method and clinical results of new transthyrotomy closure of supraglottic larynx for treatment of intractable aspiration, 451
  Morbidity of combined therapy for treatment of supraglottic carcinoma: supraglottic laryngectomy and radiotherapy, 151

Swallowing
  Phagophobia: form of psychogenic dysphagia. New entity, 286

Syndromes
  Usher's syndrome type 1C: clinical studies and fine-mapping disease locus, 123
  Vestibular abnormalities in CHARGE association, 129

Technetium-99m
  Value of technetium-99m pertechnetate imaging in differential diagnosis of salivary gland lesions, 432

Teflon
  Transoral Teflon injection under flexible laryngovideostroboscopy for unilateral vocal fold paralysis, 783

Telescope
  Endoscopic laryngotracheoplasty and graft soldering with carbon dioxide laser. Animal study, 989

Temporomandibular joint
  A syndrome of ear and sinus symptoms dependent upon disturbed function of temporomandibular joint [*Annals* Classic, 1934], 805
  Jaws revisited: Costen's syndrome, 820

Three-dimensional reconstruction
  Narrowest (isthmus) portion of eustachian tube: computer-aided three-dimensional reconstruction and measurement study, 583

Thyroid
  Brown tumor in cricoid cartilage: unusual manifestation of primary hyperparathyroidism, 252

Thyroplasty implant
  Montgomery® Thyroplasty Implant System, suppl 170

Tinnitus
  Selective cochlear neurectomy for debilitating tinnitus, 568

Tissue inhibitor of metalloproteinase
  Expression of matrix metalloproteinases and tissue inhibitor of metalloproteinases in head and neck squamous cell carcinoma, 271

Tongue
  Results of surgical salvage of locoregional recurrence of carcinoma of tongue after radiotherapy failure, 779

Tonsil
  Interaction between oral alpha-streptococci and group A streptococci in patients with tonsillitis, 571

Tooth
  Odontogenic keratocyst in young child, 163

Trachea
  Epiglottic position after cricothyroidotomy: comparison with tracheotomy, 560
  Laryngotracheoesophageal clefts, 1002
  Slide tracheoplasty in management of congenital tracheal stenosis, 914

Transforming growth factor–β
  Localization of transforming growth factor–β–expressing cells and comparison with major extracellular components in aural cholesteatoma, 669

Transoral electromyography
  Transoral electromyographic recordings in botulinum toxin–injected rat larynges, 956

Transplant
  Posttransplant lymphoproliferative disease presenting as sudden respiratory arrest in three-year-old child, 244
  Reversible sensorineural hearing loss after renal transplant immunosuppression with OKT3 (Muromonab-CD3), 640

Transthyrotomy closure
  Method and clinical results of new transthyrotomy closure of supraglottic larynx for treatment of intractable aspiration, 451

Trauma
  Knife blade as facial foreign body, 710
  Perilymphatic fistula: Washington, DC, experience, 830

Trigeminal nerve
  Trigeminal neo-neurotization of paralyzed face, 733

Tumor necrosis factor
  Role of tumor necrosis factor and interleukin-1 in endotoxin-induced middle ear effusions, 633

Turbinate
  Comparison of carbon dioxide and neodymium:yttrium-aluminum-garnet lasers in surgery of inferior turbinate, 1036

Tympanic membrane
  Auditory epithelial migration. III: Immunohistologic study using anti-BrdU antibody on tympanic membrane in mouse, 414
  Mechanics of type IV tympanoplasty: experimental findings and surgical implications, 49
  Postnatal change in angle between tympanic annulus and surrounding structures. Computer-aided three-dimensional reconstruction study, 33

Ultrasound
  Role of ultrasound in assessment of vocal cord function in infants and children, 199

Uremia
  Reversible uremic deafness: is it correlated with degree of anemia? 391

Usher's syndrome
  Usher's syndrome type 1C: clinical studies and fine-mapping disease locus, 123

Uvula
  Decrease in immunoreactive neutral endopeptidase in uvula epithelium of patients with obstructive sleep apnea, 474

Vascular system
  Diagnosis and management of left main stem bronchus compression, 461
  Effects of platelet activating factor on vascular permeability of middle ear mucosa, 604
  Imaging diagnosis of buckled innominate artery, 1097

Ventilation
  Dependence of middle ear gas composition on pulmonary ventilation, 314

Vestibule
  Aging rat vestibular ganglion: II. Quantitative electron microscopic evaluation, 753
  Glucose utilization of rat vestibular end organs: quantitative 2-deoxyglucose study, 145
  Immunohistochemical localization of manganese superoxide dismutase in rat vestibular dark cell regions, 69
  Migraine-related vestibulopathy, 182
  Three-dimensional analysis of spontaneous nystagmus in peripheral vestibular lesions, 61
  Three familial cases of hearing loss associated with enlargement of vestibular aqueduct, 1063
  Vestibular abnormalities in CHARGE association, 129
  Vestibular and optokinetic function in normal guinea pig, 838

Vibration
  Laryngeal adjustment in whispering. Magnetic resonance imaging study, 41

Video
  State-dependent laryngomalacia, 887
  Transoral Teflon injection under flexible laryngovideostroboscopy for unilateral vocal fold paralysis, 783

Vocal fold
  Changes in length and spatial orientation of vocal fold with arytenoid adduction in cadaver larynges, 552
  Vocal fold atrophy: quantitative glottic measurement and vocal function, 544

Voice
  Acoustic measurement of change in voice quality with treatment for chronic posterior laryngitis, 279
  Magnetic resonance imaging of vocal failure in patients undergoing laryngectomy with tracheoesophageal fistula, 795
  Reinke's edema: phonatory mechanisms and management strategies, 533
  Surgical closure of persisting failed tracheoesophageal voice fistula, 775

Vocal function following vertical hemilaryngectomy: comparison of four reconstruction techniques in canine, 261

Waardenburg's syndrome

Distortion product emissions in normal-hearing and low-frequency hearing loss carriers of genes for Waardenburg's syndrome, 220

Waldeyer's ring

Human immunodeficiency virus–1 infection of lymphoid tissues of Waldeyer's ring, 611

Whispering

Laryngeal adjustment in whispering. Magnetic resonance imaging study, 41

Yolk sac tumor

Yolk sac tumors (endodermal sinus tumors) of extracranial head and neck regions, 254

CLINICAL AND RESEARCH FELLOWSHIP IN OTOLOGY AND NEUROTOLOGY

MASSACHUSETTS EYE AND EAR INFIRMARY

A three-year Fellowship is offered for individuals who aspire to an academic full-time career. In the first two years, 80% of the time will be devoted to basic research; in the third year, 80% of the time will be devoted to clinical otology. The start date will be July 1. Board-eligibility or certification is required.

For more information, contact:

Michael J. McKenna, MD
Dept of Otolaryngology
Massachusetts Eye and Ear Infirmary
243 Charles Street
Boston, MA 02114
(617) 573-3654

A2

WAKE FOREST UNIVERSITY BAPTIST MEDICAL CENTER

CHAIR, DEPARTMENT OF OTOLARYNGOLOGY

Wake Forest University (Bowman Gray) School of Medicine is seeking candidates for Chair, Department of Otolaryngology. Located in Winston-Salem, North Carolina, Wake Forest University School of Medicine is a large multispecialty academic medical center affiliated with North Carolina Baptist Hospital and Brenner Children's Hospital. Existing areas of faculty clinical practice, research, and education include skull base surgery, laryngology, rhinology, otology, head/neck oncology, pediatric otolaryngology, and temporal bone pathology. The Department has an accredited residency training program. AA/EOE.

Letter of inquiry and curriculum vitae should be sent to:

Edward G. Shaw, MD
Chair, Department of Otolaryngology Search Committee
c/o Department of Radiation Oncology
Wake Forest University Baptist Medical Center
Medical Center Boulevard
Winston-Salem, NC 27157-1030
Phone: (910) 716-4647 Fax: (910) 716-5972
E-mail:eshaw@bgsm.edu

A141

ANNALS OF OTOLOGY, RHINOLOGY & LARYNGOLOGY

ANNOUNCEMENT RATES

Quarter page	$175
Half page	300
Full page	520

Material must be received 30 days prior to the month of issue, eg, for the February issue the due date is January 1.

CHANGE OF ADDRESS

Address changes must be received **45 days** prior to the effective date so that your subscription will be received without interruption.

CLAIMS

Claims for missing issues must be received within **60 days** of the month of publication for the United States and Canada, and **180 days** for other countries.

Annals Publishing Company
4507 Laclede Avenue
St Louis, MO 63108
(314) 367-4987
FAX (314) 367-4988

Laryngoscopes from Karl Storz

For all anatomic situations

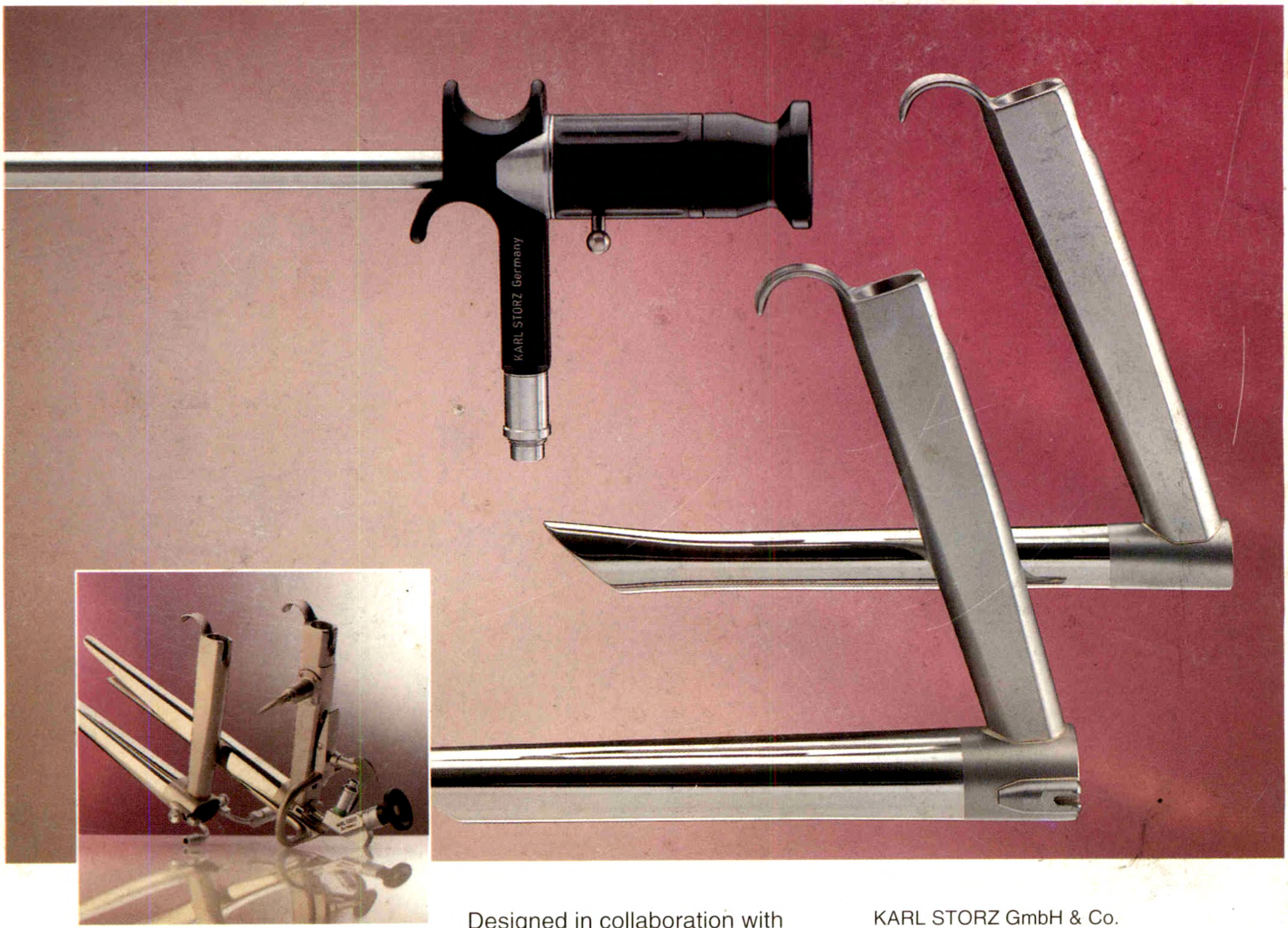

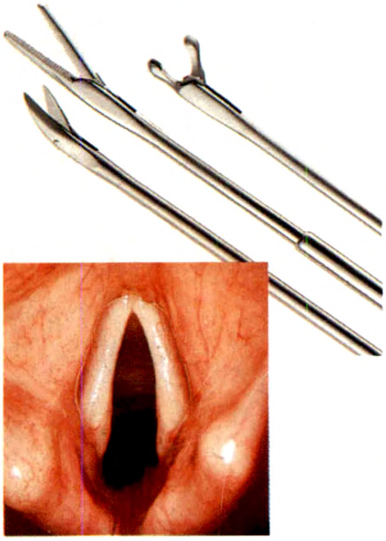

Designed in collaboration with leading authorities, Karl Storz laryngoscopes provide optimal site specific or panoramic visualization for even the most difficult anatomic situations. From neonate to adult, these lightweight stainless steel laryngoscopes have a unique handle for easy introduction. The Kantor-Berci Video Laryngoscope provides a distal telescopic view and allows unobstructed bi-manual manipulations from the monitor image. HOPKINS rod-lens telescopes from 0° to 120° enhance the diagnostic capability of direct laryngoscopy.

For more information or a demonstration, please contact your local Karl Storz representative, or call Karl Storz directly at **(800) 421-0837.**

KARL STORZ GmbH & Co.
Mittelstraße 8, D-78532 Tuttlingen, Germany
Postfach 230, D-78503 Tuttlingen, Germany
Telegramm: Endoskopie
Telefon: (07461) 70 80, Telex: 762 656 storz d
Telefax: (07461) 70 81 05

KARL STORZ Endoscopy-America, Inc.
600 Corporate Pointe
Culver City, CA 90230-7600
Telephone: (310) 558-1500
(800) 421-0837
Telefax: (310) 410-5530

KARL STORZ Endoscopy-Canada, Inc.
438 University Avenue, Suite 1800
Toronto, Ontario, Canada M5G 2K8
Telephone: (416) 596-9900
(800) 268-4880 (English)
(800) 361-7388 (Francais)
Telefax: (416) 596-9333

KARL STORZ Endoscopia Latino America
815 N.W. 57th Ave., Ste. No. 480
Miami, FL 33126-2042, USA
Telefono: (305) 262-8980
Telefax: (305) 262-8986

STORZ
Karl Storz Endoscopy